

# CubeSat Handbook

# CubeSat Handbook

From Mission Design to Operations

*Edited by*

***Chantal Cappelletti***  
***Simone Battistini***  
***Benjamin K. Malphrus***



**ACADEMIC PRESS**

An imprint of Elsevier

Academic Press is an imprint of Elsevier  
125 London Wall, London EC2Y 5AS, United Kingdom  
525 B Street, Suite 1650, San Diego, CA 92101, United States  
50 Hampshire Street, 5th Floor, Cambridge, MA 02139, United States  
The Boulevard, Langford Lane, Kidlington, Oxford OX5 1GB, United Kingdom

Copyright © 2021 Elsevier Inc. All rights reserved.

No part of this publication may be reproduced or transmitted in any form or by any means, electronic or mechanical, including photocopying, recording, or any information storage and retrieval system, without permission in writing from the publisher. Details on how to seek permission, further information about the Publisher's permissions policies and our arrangements with organizations such as the Copyright Clearance Center and the Copyright Licensing Agency, can be found at our website: [www.elsevier.com/permissions](http://www.elsevier.com/permissions).

This book and the individual contributions contained in it are protected under copyright by the Publisher (other than as may be noted herein).

#### Notices

Knowledge and best practice in this field are constantly changing. As new research and experience broaden our understanding, changes in research methods, professional practices, or medical treatment may become necessary.

Practitioners and researchers must always rely on their own experience and knowledge in evaluating and using any information, methods, compounds, or experiments described herein. In using such information or methods they should be mindful of their own safety and the safety of others, including parties for whom they have a professional responsibility.

To the fullest extent of the law, neither the Publisher nor the authors, contributors, or editors, assume any liability for any injury and/or damage to persons or property as a matter of products liability, negligence or otherwise, or from any use or operation of any methods, products, instructions, or ideas contained in the material herein.

#### Library of Congress Cataloging-in-Publication Data

A catalog record for this book is available from the Library of Congress

#### British Library Cataloging-in-Publication Data

A catalogue record for this book is available from the British Library

ISBN 978-0-12-817884-3

For information on all Academic Press publications visit our website at <https://www.elsevier.com/books-and-journals>

*Publisher:* Matthew Deans  
*Acquisitions Editor:* Carrie Bolger  
*Editorial Project Manager:* Ana Claudia A. Garcia  
*Production Project Manager:* Prasanna Kalyanaraman  
*Cover Designer:* Matthew Limbert

Typeset by Spi Global, India



## About the editors

**Chantal Cappelletti** is currently an Assistant Professor at University of Nottingham (the United Kingdom), where she is affiliated with the Nottingham Geospatial Institute. She is the cofounder of the Italian company GAUSS Srl. She has led six satellite projects in Italy (UNISAT program and others) and in Brazil (SERPENS, TuPOD). She was PI on two missions concerning the behavior of cancer cells in space. She was an Italian Space Agency delegate at the Inter-Agency Space Debris Coordination Committee.

**Simone Battistini** is a senior lecturer in Aerospace Engineering at Sheffield Hallam University (the United Kingdom). He has been working in the field of Aerospace Engineering both at academic and industrial level, having served on the faculty of the University of Brasília (Brazil) and on the staff of MBDA Italy. In 2017 he was a visiting professor at the University of Vigo (Spain). He was the principal or coprincipal investigator on four projects concerning aerospace systems funded by Brazilian public institutions. His main research interests are related to guidance, navigation, and control of aerospace systems.

**Benjamin K. Malphrus** directs Morehead State University's Space Science Center and has served on the scientific staff of the National Radio Astronomy Observatory and on the faculty of universities including the University of South Carolina and West Virginia University. He has served as Principal Investigator on several nanosatellite missions including Lunar IceCube, KySat-1, KySat-2, the Cosmic X-Ray Background Nanosatellite (CXBN), CXBN-2, and DM-7. Dr. Malphrus led the effort to design a dedicated R&D center for space science and to establish a 21-meter ground station at Morehead State, evolving it into NASA's affiliated Deep Space Station-17. Dr. Malphrus has published research on topics ranging from extragalactic astrophysics to instrumentation in radio astronomy, to space systems engineering. In the late 1990s he was part of a research team that developed a theory of galaxy formation that has gained wide acceptance among the astronomical community.

# Contributors

**Kira Abercromby** Department of Aerospace Engineering, California Polytechnic State University, San Luis Obispo, CA, United States

**Fernando Aguado Agelet** Signal Theory and Communications Department and AtlanTTic, University of Vigo, Vigo, Spain

**José Miguel Lago Agra** Alén Space, AIV & Ground Segment, Nigrán, Spain

**Krisjani Angkasa** Jet Propulsion Laboratory, California Institute of Technology, Pasadena, CA, United States

**Alessandra Babuscia** Jet Propulsion Laboratory, California Institute of Technology, Pasadena, CA, United States

**James Barrington-Brown** NewSpace Systems, Somerset West, South Africa

**Simone Battistini** Department of Engineering and Mathematics, Sheffield Hallam University, Sheffield, United Kingdom

**Jacob Beningo** Beningo Embedded Group, LLC, Linden, MI, United States

**Chantal Cappelletti** Department of Mechanical, Materials and Manufacturing Engineering, University of Nottingham, University Park, Nottingham, United Kingdom

**Mengu Cho** Laboratory of Spacecraft Environment Interaction Engineering, Kyushu Institute of Technology, Kitakyushu, Japan

**James W. Cutler** University of Michigan, Ann Arbor, MI, United States

**Pedro Luiz Kaled Da Cás** Signal and Telecommunication Department, University of Vigo, Vigo, Spain

**Nathan D. Fite** Morehead State University, Space Science Center, Morehead, KY, United States

**David C. Folta** NASA/Goddard Space Flight Center, Navigation and Mission Design Branch, Greenbelt, MD, United States

**Arno Formella** Computer Science Department, University of Vigo, Ourense, Spain

**Anthony Freeman** Jet Propulsion Laboratory, California Institute of Technology, Pasadena, CA, United States

**Jose L. Garcia** Morehead State University, Space Science Center, Morehead, KY, United States

**Alessandro Golkar** Skolkovo Institute of Science and Technology, Center for Entrepreneurship and Innovation, Moscow, Russia

**Filippo Graziani** GAUSS Srl, Rome, Italy

**Kyle Hughs** Jet Propulsion Laboratory, California Institute of Technology, Pasadena, CA, United States

**Santiago Iglesias Cofán** Computer Science Department, University of Vigo, Ourense, Spain

**Shigeru Imai** Manned Space Systems Engineering Department, Japan Manned Space Systems Corporation (JAMSS), Chiyoda-ku, Tokyo, Japan

**Danil Ivanov** Space Systems Dynamics Department, Keldysh Institute of Applied Mathematics of Russian Academy of Sciences, Moscow, Russia

**Andrew T. Klesh** Jet Propulsion Laboratory, California Institute of Technology, Pasadena, CA, United States

**Mary Knapp** Massachusetts Institute of Technology, Haystack Observatory, Westford, MA, United States

**Naomi Kurahara** Infostellar Inc., Network Operations, Shinagawa City, Tokyo, Japan

**Benjamin K. Malphrus** Morehead State University, Space Science Center, Morehead, KY, United States

**Alberto González Muíño** Alén Space, CTO, Nigrán, Spain

**Yuichiro Nogawa** ISS Utilization and Operations Department, Japan Manned Space Systems Corporation (JAMSS), Chiyoda-ku, Tokyo, Japan

**Chris Ostrom** HX5—Jacobs JETS Contract, Orbital Debris Research & Science Operations, Houston, TX, United States

---

**Mikhail Ovchinnikov** Space Systems Dynamics Department, Keldysh Institute of Applied Mathematics of Russian Academy of Sciences, Moscow, Russia

**Khary I. Parker** NASA/Goddard Space Flight Center, Propulsion Branch, Greenbelt, MD, United States

**Antonio J. Ricco** NASA Ames Research Center, Moffett Field, CA, United States

**Daniel Robson** Department of Mechanical, Materials and Manufacturing Engineering, University of Nottingham, University Park, Nottingham, United Kingdom

**Sergio R. Santa Maria** NASA Ames Research Center, Moffett Field, CA, United States

**Robert Staehle** Jet Propulsion Laboratory, California Institute of Technology, Pasadena, CA, United States

**Sergey Trofimov** Space Systems Dynamics Department, Keldysh Institute of Applied Mathematics of Russian Academy of Sciences, Moscow, Russia

**Ricardo Tubío-Pardavila** Infostellar Inc., Network Operations, Shinagawa City, Tokyo, Japan

**Joost Vanreusel** European Space Agency, ESTEC, Strategy Department, Noordwijk, The Netherlands

**Andrés Eduardo Villa** Aerospace Group, UARX Space S.L., Nigrán, Spain

**Roger Walker** European Space Agency, Noordwijk, The Netherlands

**Boris Yendler** YSPM LLC, Saratoga, CA, United States

**Luis Zea** BioServe Space Technologies, University of Colorado, Boulder, CO, United States

# Preface

A new space age has emerged, often referred to as Space 2.0, owing to an increased access to space made possible by new launch service providers, new launch vehicles, new space systems technologies, and international partnerships. Advances in small satellite (SmallSat) technologies and miniaturized science instruments have coupled with this new accessibility to space to accelerate change in the way space business is conducted. SmallSats, in particular, are considered “disruptive technology” by the aerospace industry because they can provide many of the same services as conventional satellites at a fraction of the cost and with short development times. These small satellites can range from the size of loaf of bread to a small suitcase and orbit the Earth in formations. They have evolved to the point where they are used by governments worldwide, universities, and private aerospace companies for a variety of applications ranging from Earth remote sensing to biomedicine, to astrophysics, to space physics, to planetary science research.

Since the beginning of the CubeSat in the early 2000s, these miniature satellites have played an important role in this evolution. A “democratization” of space has occurred based on the low cost of access to space and the low cost of CubeSat systems, allowing previously non-space-faring countries fly their first satellites. A generation of scientists and engineers has received unprecedented training on space-related projects with a hands-on focus. Constellations of CubeSats have been flown by innovative companies like Planet and Spire. A new era of solar system exploration has been ushered in by the MarCO mission and the 13 Artemis 1 CubeSats. CubeSat missions are underway in countries across the world that utilize CubeSats and CubeSat constellations that have the potential to revolutionize Earth remote sensing, asset tracking, communications and data delivery, astrophysics, space science, and robotic solar system exploration.

To assist CubeSat developers in realizing these missions, several documents currently exist that serve as valuable references. Among these are the NASA State of the Art in SmallSat Technology Report, the National Academies of Sciences, Engineering and Medicine report, *Achieving Science with CubeSats: Thinking Inside the Box* and a host of online resources including NASA’s CubeSat 101 Basic Concepts and Processes for First-Time CubeSat Developers, NASA’s Small Spacecraft Systems Virtual Institute, and Cal-Poly’s CubeSat Design Specification documents. NASA maintains an online version of the State of the Art in SmallSat Technology Report that documents current CubeSat technologies in detail. The report provides a comprehensive summary of the current state of SmallSat spacecraft technologies categorized by power, propulsion, guidance navigation and control, structures, materials and mechanisms, thermal control, command and data handling, communications, integration, launch and deployment, ground data systems and operations, and passive deorbit devices. The report



provides an excellent reference for CubeSat developers, especially when combined with CubeSat 101. The state of the art in SmallSat Technology is a comprehensive and valuable resource, which is regularly updated.

The CubeSat Handbook is intended to complement these excellent reference documents by providing in-depth background information for mission designers to develop and evaluate the parameters upon which design decisions can be made. CubeSat 101 and other references can be utilized alongside the CubeSat Handbook to inform trade studies related to system and subsystem decisions. The CubeSat Handbook is intended to provide a foundation for developers that will allow them to optimize the use of the existing resources.

The CubeSat Handbook is divided into six parts that reflect the different stages of a CubeSat mission. The first part is dedicated to the principles of system engineering applied to CubeSats. The second part deals with the aspects of mission analysis and design: astrodynamics concepts, missions and applications, and innovative concepts like interplanetary missions, distributed architectures, and scientific missions. The third part is an overview of the subsystems of a CubeSat, giving an insight into the main design processes and solutions for each subsystem. The fourth part is concerned with the assembly, integration, testing, and verification activities. The fifth part deals with the mission operation, covering both the ground and the space segment. Finally, the sixth part gives an overview of many important aspects related to the launch of the satellite into space, from the rules related to international laws to the choice of the launcher and the deployers.

To produce the CubeSat Handbook, experts from all around the world came together to share their expertise, lessons learned, and thoughts on available and evolving technologies. The nearly limitless potential of the CubeSat will no doubt be realized by the next generation of CubeSat mission designers. The editors and authors hope that the CubeSat Handbook will serve as an inspiration and a guide to unlock this potential and that it will serve as a valuable resource for CubeSat mission designers as they continue to drive the evolution of space utilization and exploration.

**Chantal Cappelletti**  
**Simone Battistini**  
**Benjamin K. Malphrus**

# Introduction: The history of the CubeSat by Bob Twiggs and Jordi Puig-Suari

## 1 The CubeSat standard

The CubeSat came about from a project at the Aeronautics and Astronautics Department that Stanford University had with DARPA and the Aerospace Corporation in 1998. The Aerospace Corporation wanted to launch a little satellite (picosat) the size of Klondike ice cream bar as part of a Defense Advanced Research Projects Agency (DARPA) program. The graduate engineering students at Stanford that had been working on microsats since 1995 decided that it would be challenging to build a launcher for this little picosatellite. They designed a deployer that fit inside one of our microsattelites. The launcher was built like the cartridge holder for a gun. The cartridges were pushed down into the holder where a collapsed spring is ejected when needed. The students designed and built a rectangular device that would hold the picosats. The microsat was called Orbiting Picosat Automated Launchers (OPAL) and with the mission to deploy the picosats when in Earth orbit. OPAL and the picosats were launched in 2000. The little picosats from DARPA worked as planned. OPAL and the picosats demonstrated the feasibility for students to work on smaller satellites like picosats. With the existing student microsatellite program, it was difficult to get the students to finish a design because there was too much room and they kept adding to the satellite experiments.

After the OPAL launch, we were working on a project with Jordi Puig-Suari at Cal Poly at San Louis Obispo, CA. We had an opportunity to launch a small satellite on a Russian rocket if we could design a very small satellite like the picosats. It turned out that launch opportunity was canceled. We then started thinking about picosat-sized satellites as a standard. The idea that evolved from this led to the CubeSat. The design challenge was to make something like this little picosat that was like the size of an ice cream bar and a launcher that could launch several of them at once. But, to make them useful, we needed to put more solar cells on them than could only be mounted on the flat sides of the picosat. That need led to the thought of making the picosat in a cube shape. Using some solar cells that were donated from JPL, we tried these  $2 \times 4$  cm cells to see how many solar cells could be put on the square surface like a cube and still have a method of holding the cube in the launcher. Laying these cells out to get a reasonable voltage string took about a square of 4 in. To find a model, we went to the local plastic shop where a 4-in. cube was selected. At that time, beanie babies were the rage, so the cube selected was a display case for the beanie babies.

We purchased several 4-in. beanie baby cubes and began to design a way to contain them in a deployer. The method of holding the picosats was by the corners that were chamfered. In the picosat, they were secured in the launcher only by the force of the launcher door. It had worked for the picosats, so this same method was used with the CubeSat deployer. Being held by the corners with 10 one-thousandths clearance, it would not move significantly during vibration. A quarter inch was allowed on the edges for the rails. To have multiple CubeSats in a launcher, it would require some way to separate the cubes. We bought quarter inch plastic cubes that were put on the ends of the 4-in. cubes to keep the adjacent cube faces from contacting. These were later called separation feet.

We were using the standard English units in our engineering programs. The aerospace industry uses metric units so we decided that the students should learn metrics. The 4-in. cube is roughly equivalent to 10 cm, so even though the model was based on a 4-in. cube, we changed the design to a 10-cm cube. At that time in the late 1990s, Lockheed and Martin Marietta had built a satellite, the Mars Climate Orbiter that went to Mars and it failed. The reason it failed was because one team was working in English units and one was working in metric units. That was a Mars mission that burned up in the Martian atmosphere because of a mix up. We decided that US engineering students should learn the metric system and changed the CubeSat standard to 10cm. The accepted aerospace definition for a picosat was 1 kg. If a 10-cm cube is filled with water, it weighs a kilogram. The mass allocation became 1 kg. That was how the CubeSat standard was determined.

## 2 The PPOD

After the initial model cube was selected, I built a plastic deployer that held three CubeSats with the rails and that included feet on the CubeSats. This model was given to Jordi Puig Suari at Cal Poly. They had a reputation as an innovative mechanical engineering program and I believed that they could come up with a deployer design for the CubeSats. Jordi's students came up with all sorts of ideas and finally settled on the one that I had sent to them based on the OPAL design, basically a Jack-in-the-Box. Cal Poly then wrote specs that were the key factor in making the CubeSat form factor successful in being adopted by the space industry. The deployer was named the Poly Picosat Orbiting Deployer (PPOD).

The size of the PPOD was defined by the only secondary launch accommodation specification available at the time: the Delta II secondary payload specification CubeSats. The dimensions of that location are the reason for the PPOD holding three 1 U CubeSat. It is interesting that CubeSats were never launched using that Delta II specification, even when they were launched later on the Delta II rocket.

The key function of the PPOD was to protect the launch vehicle and the primary payload from any mechanical failure of the CubeSats. This eliminated one of the main concerns that launch providers had about including university payloads in their launches. As a result, the PPOD was an enclosed box with very strong walls, not a traditional mass optimized space system.

### 3 The first CubeSat launches

Cal Poly took on the task as the integrator for launching the first CubeSat. At that time the Russians were the only people that would even talk about launching these things because they needed the money. The cost for first launch was \$30,000 for a 1U CubeSat. There were several PPODs with CubeSats that were launched on Russian rockets that comprised the early CubeSat launches.

The first group of CubeSats was launched in June of 2003 from Plesetsk, Russia, on a Eurokot, utilizing the Russian Multiple Mission Orbit Service. Several CubeSats were put into a Sun-synchronous orbit. These were the Danish AAU CubeSat and DTUSat, the Japanese XI-IV and CUTE-1, the Canadian Can X-1, and our Quakesat. QuakeSat was a collaboration between Stanford and a small company in Palo Alto called Quake Finder. They were looking for earthquakes, and they were looking for the energy that is emitted from an earthquake right before they occur. They had a number of low-frequency ground sensors that they had put out around California. With these sensors, they found some evidence that before the Loma Prieta earthquake in the Bay Area there were definite low-frequency signals emitted. They built this satellite with a pop-out low-frequency antenna, and we flew it on the Russian rocket. After the fact, they picked up some signals from an earthquake that was near Lompoke in California. There was a satellite built by the Danish Technical University (DTUSat) and a Japanese satellite from the University of Tokyo (CUTE-1). CUTE-1 had a camera on board. We got the CubeSats launched and were successful. The QuakeSat group put a ground station up in Alaska to make contact with their CubeSat. Several of these first missions were very successful.

It should be noted that QuakeSat was the first 3U CubeSat and opened the door for the most popular form factor in the CubeSat world and required the modification of the standard after the first launch.

The Japanese students asked me if a camera would work on a CubeSat. I said, well I don't know if they could get an image that shows you very much. They went ahead and built it anyway. After it was launched in 2003, the students started sending me pictures that the satellite had taken. For years, they kept sending me pictures. The Japanese CubeSat, CUTE-1, lasted for years, becoming the longest-lived CubeSat, and may still be working. This first group of CubeSats that was launched was very successful.

The next Cubesat launch did not happen until July 26, 2006. Again a Russian vehicle, in this case a Dnepr, was selected since Russia was the only country willing to fly CubeSats. The launch included 14 CubeSats from 11 organizations from around the world. Unfortunately the launch was a failure, and all the CubeSats were lost. This failure had a surprising result since the space community rallied around the students who saw their hard work crash into a field in Kazakhstan. The efforts to find US launch opportunities for university CubeSats increased dramatically, and after a second Dnepr launch in 2007, the Cal Poly team changed their focus to US launch vehicles, and within a few years had successfully launched CubeSats on most major US launch vehicles.

## 4 CanSat—The proto-history of the CubeSat

In 1998 at a joint US and Japanese student conference, I proposed the idea of launching a spacecraft the size of a soda (Coke) can into space. This initial idea would later evolve into other nanosatellite projects and influenced the idea for the CubeSat. The idea at that time was to take a Coke can, put some electronics in it, put it on a high-power amateur rocket, fly it, and eject it out on a parachute. Professor Shinichi Nakasuka and his students from the University of Tokyo began developing the CanSat. There is now an annual event with the high amateur rocket Aero Pac group in Northern California going to the Black Rock desert in Nevada in September every year to launch CanSats and rovers.

### 4.1 Use of amateur radio frequencies

When we proposed the CubeSat, we wanted to use the amateur radio frequencies, and the AMSAT guys were not in favor of us using these amateur radio frequencies. The AMSAT guys had launched several successful amateur satellites, and they had a table of the frequencies allocated to them, so I asked them if they would give me a frequency, and they said we were not qualified to use these frequencies, even though we had the proper amateur licenses.

Because of the years of experience of AMSAT members building and launching small satellites, we were told that we did not have the technical capability to build satellites. They had an Internet blog at the time where they put some less than favorable comments on new proposals for the use of space like their program. There were unfavorable comments about student university projects using those frequencies. It was, however, legal for other licensed amateur to use them. So we then picked a frequency band to use at Stanford and suggested to other university CubeSat developers the frequencies they could use. We all then applied to the FCC and got them approved, without the blessing of the AMSAT group. It took several years for the AMSAT international group to help coordinate amateur frequencies for University satellites and to accept the concept of the CubeSat.

## 5 NASA and NSF get in the game

Initially the scientific side of the aerospace community and NASA paid no attention to the CubeSats. In 2008, that changed, when Terese Jorgensen at the National Science Foundation organized a CubeSat conference to explore the possibility of using CubeSats for atmospheric research. Dr. Jorgensen saw the potential and convinced NSF to offer contracts to support the first CubeSat science missions.

I caught Dr. Jorgensen right at the end of the conference to talk to because I thought it was ironic that she had not become interested in CubeSats before 2008, 5 years after the first launch. I asked her why NSF waited so long since we announced this initiative in 2003. Dr. Jorgensen said that NSF was waiting to see if it worked before committing. Dr. Jorgensen went to NASA before committing to sponsor the conference, since

satellites in the past had been managed by NASA. When Dr. Jorgensen contacted one of Chief Directors at NASA that builds satellites and asked, “should NASA build CubeSats?”. He said, “we build real satellites like Ferraris; we don’t build those Hot Wheel type satellites.” But once NSF committed to CubeSat programs, other aerospace companies started to consider them.

I had predicted that CubeSats would have an exponential growth with the students building them and that the innovation would really grow when there was an acceptance of failure if the students had built them. In my opinion, NASA had become extremely conservative, building bigger and more expensive satellites. Failure was not an option for NASA. It is hard to innovate if you don’t take chances. I thought that the CubeSat could be a stepping-stone to new technology. In the late 2000s, things started opening up, and it is amazing what you see today.

NASA got involved in around 2010. It was after NSF had launched satellites. In a way, I’m glad NASA did not say I’m here to help you. They did not pay attention, and their biggest complaint was that it was too small for their instruments. Everybody thought that the CubeSat was a dumb idea. Now with small instruments being developed and with the support of NASA and NSF, CubeSats have evolved to become an important platform for space-based research.

## 6 The PocketQube

The main purpose of the CubeSat initiative was to educate students. One of the big factors in CubeSat missions is the launch price. When CubeSats became popular, the launch price went up because the big guys could afford to pay it. So in about 2005, I said I don’t like this, so I started thinking about ways to start making a little satellite and launch those in place of the CubeSat. So, I looked at the CubeSat design and said: “well if we slice this thing up, we can make eight PocketQubes in the space of a CubeSat in the PPOD.” I was trying to figure out how to put small satellites together to be like a CubeSat and how to separate them after they are deployed. I made model after model trying to figure out how to do it. The final design is a 5-cm cube and has a mass of 250 g (one PQU). When the PocketQube design was finalized, I set about trying to find a launch for it.

Beginning in 2009, I had moved to the Space Science Center at Morehead State University (MSU) where we worked with an organization called Kentucky Space to develop the PocketQube specifications. The team at Morehead State University, led by Ben Malphrus, had a long-term relationship with the Italian group from the University of Rome. I had introduced Ben to Filippo Graziani, Dean of the Aerospace Engineering School and founder of the Group of Astrodynamics for the Use of Space Systems company (GAUSS) in around 2004. The GAUSS team had a relationship with the Russians and had flown several times on the Dnepr rockets. We worked out an arrangement to launch the first round of PocketQubes on a Dnepr launch. They were deployed from UniSat-5, a microsat built by the Italians, in much the same way that OPAL had deployed the first picosats. The first four PocketQube Satellites were launched on November 21, 2013. They included T-LogoQube/Eagle-1 (Morehead

State University and Sonoma State), QubeScout-S-1 University of Maryland, \$50Sat/Eagle-2 (An Amateur Radio group and Morehead State University), and WREN (Stadoko UG). T-LogoQube/Eagle-1 and \$50Sat were successful. The \$50Sat worked over 2 years, and T-LogoQube led by Garrett Jernigan launch worked for about 6 months. But one of the interesting technologies used was that the radio in both were RFM-22B that cost \$15, and they worked. A number of people said that these inexpensive radios would not work in space.

Since the successful launch of the first PocketQubes, many others have been in development. Workshops have been held at NASA Ames and at TU Delft (the Netherlands) and are now an annual event. At least 30 PocketQubes are in development. While most of them come from academia, several companies build PocketQubes, such as GAUSS Srl, Fossa Systems KSF Space Foundation, and Alba Orbital. PocketQube projects have even been the subject of Kickstarter campaigns and are popular with amateur radio satellite groups.

## 7 The ThinSat

In about 2015, I was at a SmallSat conference and attended a NASA Town Hall Meeting. I asked why we can't put CubeSats in the trunk of the Dragon capsule. They said it's all filled up with stuff, but if you want to put something on the second stage, there may be room. You will only get a short orbit life—maybe 4 or 5 days. I said I will take it! But I couldn't find anybody that would consider using this second stage for small satellite launches. The next year at the SmallSat conference I met a guy from Orbital Sciences Corporation, and I asked how about getting this on the second stage of your Antares? I had a PocketQube ready to launch. I had asked him for a launch for years, and he had laughed at me. This time he said that I might have something here; his name was Warren Frick. A few weeks later, he had talked to some people at Orbital ATK, and they said we might have a launch for you. Sometimes, things happen quickly!

We started looking at deployers. I found out that Orbital-ATK would prefer to use the Canisterized Satellite Dispenser (CSD) developed by Planetary Systems Corporation. I contacted Walter Holemans at Planetary Systems, and he met with me and Dale Nash from Virginia Space at an Orbital ATK meeting. They showed a manifest with PocketQubes. That was 1 month from the first time I met Warren Frick at the Utah Conference.

I then met with Hank Voss from Near Space Launch, whom I had known for many years. Hank was using a Globalstar radio that allowed you to send your data from your CubeSat to the Globalstar Network of satellites and then to the ground using their Internet network. So, it was not necessary to have your own ground station. The GlobalStar radio would fit in the little PocketQube. Using GlobalStar would solve the problem of communicating with large numbers of PocketQubes on a single launch.

Hank helped us design the next generation of PocketQubes. A couple of months later, Hank came back, and we had a meeting at Morehead State. Hank presented a different design for the PocketQube. Rather than a cube, he proposed satellites with the size of slices of a bread. Everybody talked about how PPOD is like a bread box.

Other people had also proposed a slice of bread satellite. It would allow us to eliminate all these little tedious circuit boards and use one big circuit board. We proposed this to Dale Nash at Virginia space and Orbital-ATK, and it was accepted. We decided that we wanted to tether them together and that got everyone excited. We thought about putting a stiff wire in between the ThinSats rather than using a loose tether. Ultimately, we came up with these folding panels and everything looked good.

We got our first launch of the ThinSats in April of 2019. The ThinSats, as we called them, didn't operate quite as we had expected. Depending on the altitude they were released at and the ballistic coefficient, everybody predicted they might last 5 days to 2 weeks. But they only lasted 1 day and a half. What we figured is that when they came out, they were spinning which did not leave them all face on which represents the minimum ballistic coefficient. We ended up launching 64 of them, and I think that out of the 64 we got data out of probably over half of them. So, the first generation of ThinSats was a success.

To me the value of the ThinSat program is in the STEM activity in the schools. It is very difficult to get a satellite launched, and you go through a lot of pain to do that. What is the education that you get if you build a satellite and don't launch it? To me, you get 95% of the value because you get most of the of the education. The idea that I'm going to launch something into space inspires students. So, we can work with the students and instill in them the idea that they don't necessarily have to launch a satellite to get all this education. And the learning that they achieve translates to a variety of areas beyond aerospace because of the diversity of the satellite systems.

## 8 CubeSats take off

The two things that made the CubeSat successful were the size and the containment. The small size made the launches affordable, and the containment relieved the fear of the launch provider that the CubeSats would damage the launch vehicle or the primary satellite. In the beginning the launch costs and containment did not do us any good in the United States because none of the US launchers would give us a ride. We talked to Lockheed Martin and Martin Marietta at the time about launching these things, and they said: "well if you give us a half a million dollars to study it, we will consider it." That's kind of funny now because Lockheed Martin has announced its own CubeSat program. Everybody that I got in contact with declined. Nobody would give us an opportunity except the Russians—they were hungry at the time.

This whole thing has become a worldwide industry. The mistake that I made is that I should have somehow patented the CubeSat so I could have gotten a dollar for each one that was launched. The initial intent was education for the students. Sending something to space is cool. I liked it because of all the technologies—you have the computers, you have the radio, and you have to talk with payloads; there are many challenges to solve.

When we first started working on satellites, I really got intrigued. With CubeSats, we have this little thing that we can get launched cheaper, and it doesn't cost a lot to



get it built, and we could do it quickly. That is another key thing; it doesn't take 20 years to build a satellite from inception to launch. That was the whole intent of it. Because of these reasons, I hoped that we would see a lot of them in the Universities, but I did not anticipate the commercial applications that would come along. They are overwhelming.

I never anticipated the commercial applications, but the thing that is kind of interesting is that the CubeSat really had some role in stimulating the space program. It has to be a factor in ushering in the new space era and a significant factor at that. I always thought it was the same as what Apple did with the computer industry. Apple started a whole generation believing that everybody can have and work with computers—you don't have to be a technical student or an engineer. If you look at the apps that are on a cell phone now, you never would have thought about doing something like that because people that create those apps are not necessarily the people that know the technology in the cell phones. I hope this does the same thing that is to spawn a whole new generation of people that are looking for apps on satellites, but more than that, expanding the application of the technology more widely.

I never envisioned that the commercial application would be what it is now. Was this the thing that will reinvigorate the space program? When we built the first CubeSats, everybody said we can't put our instrument in it because they are too little. But we came along at the right time—the miniaturization of the electronics for commercial applications like for the cell phone coincided at the time. If we had been earlier, it might not have worked. But now, miniaturized instruments have come a long way and can support interesting science and a variety of practical applications. And I can raise the TRL level of my technology so I can use it with other missions. That has really sparked a lot of activity. Who would have ever thought that you would send CubeSats to Mars or have constellations of hundreds of CubeSats monitoring the Earth? It has really been very satisfying from that standpoint, but I worry that the education end is getting shorted—we need to keep students involved in CubeSats because it was really designed for them.

# Part One

## Systems engineering applied to CubeSats

*Fernando Aguado Agelet<sup>a</sup> and Andrés Eduardo Villa<sup>b</sup>*

<sup>a</sup>Signal Theory and Communications Department and AtlanTTic, University of Vigo, Vigo, Spain, <sup>b</sup>Aerospace Group, UARX Space S.L., Nigrán, Spain

### 1 Introduction

For years, national and international space agencies, as well as large corporations have applied similar systems engineering definitions and approaches to large space projects, characterized to be interdisciplinary, complex, costly, and with long life-cycle programs. Examples of these systems engineering approaches include:

- The INCOSE Systems Engineering Handbook: “Systems engineering is an interdisciplinary approach and means to enable the realization of successful systems. Successful systems must satisfy the needs of its customers, users, and other stakeholders.”
- The NASA Systems Engineering Handbook: “at NASA, ‘systems engineering’ is defined as a methodical, multidisciplinary approach for the design, realization, technical management, operations, and retirement of a system. A ‘system’ is the combination of elements that function together to produce the capability required to meet a need. The elements include all hardware, software, equipment, facilities, personnel, processes, and procedures needed for this purpose.”
- ESA ECSS E-10 Part 1B: “Systems engineering is the interdisciplinary approach governing the total technical effort to transform a requirement into a system solution.”

A practical definition of systems engineering is the technical management of product design and development. In recent years, an increasing number of countries have shown a growing interest in developing their indigenous space capacity through national small satellite programs. The satellites produced through these efforts, which were initially focused on educational and training missions, currently are now more oriented toward scientific research and operational systems. Thus, small satellite missions are considered not only educational tools, but also technological demonstrators or, even, mature enough for commercial and scientific missions. The initial educational CubeSat missions were characterized by high infant mortality, caused, among other factors, by the lack of the application of an adequate system engineering approach for this kind of projects, especially during mission definition and the assembly, integration, and test (AIT) phases on ground. Nevertheless, the application of the systems engineering methodologies and associated documentation and tests used in large space projects are not directly applicable to small satellite programs. It is

necessary to downsize and tailor these standards to the size, organization, complexity, and cost of a typical CubeSat project. This chapter presents an overview of how systems engineering can be applied to CubeSats projects, including a review of the most important standards, requirements definition, and an example of the mission phases and its associated documentation, as well as a cost analysis methodology that can be used for a CubeSat mission.

### ***1.1 Engineering vs. systems engineering***

A significant difference exists between pure engineering and systems engineering. The former is centered only on engineering processes and implementation to solve a specific problem. The focus of this section is systems engineering that deals with systems and the associated boundaries as well. Ultimately, systems engineering is a balance between “systems” and “engineering,” but without proposing a specific implementation to solve a problem, initially. It is a process to conduct engineering to solve a given problem systematically.

Furthermore, systems engineering intends to describe the interactions between different systems in a broader way than just a specific field of engineering. Ultimately systems engineering brings multiple specialists from different areas together to analyze a problem from different perspectives to find a balanced solution to meet the objective.

## **2 Systems engineering standards overview**

Before introducing the existing systems engineering standards, it is important to understand why standards are essential. It is now well known that CubeSats started as a standard educational program to allow students have hands-on experience with satellites. The initial standard defined the dimensions, mass, and mechanical interface of a small satellite with a deployer. At the same time, the deployer was standardized using the corner rails as the touching interface between the spacecraft and the deployer. This standard interface ultimately allowed CubeSats to succeed. In that way, the interface with the launch vehicle was already defined, allowing developers to focus just on the spacecraft problem. Without the standard, each CubeSat would have needed to work on a custom interface with specific launchers, increasing the time, cost, and complexity of the whole project.

Another example is the standardized interface between a spacecraft and a ground segment. In 1982, the Consultative Committee for Space Data Systems (CCSDS) was formed to define a standard between the two segments. This standard allowed the reuse of the existing ground stations, used for previous missions, not only for nominal operations but also for contingencies. Without the standardized interface, for example, at the beginning of the space race, if a mission required a ground station, it was developed from scratch. If a different mission required a ground station, they needed to develop it following the new requirements. This process was not only expensive and time consuming, but also increased the risk to the mission. Ultimately, the CCSDS standard has allowed the creation of distributed networks of ground stations capable of operating multiple diverse spacecraft that implement the standard.

## 2.1 *A couple of lessons learned*

The Japanese Aerospace Exploration Agency (JAXA) experienced a series of failures in 2003, including a Mars orbiter, a spacecraft, and their primary launch vehicle, the H-IIA. JAXA partially attributed the failure to a lack of or inadequate use of systems engineering, forcing them to conduct enhancement activities on the subject [1]. Since then, JAXA puts a great effort into formally following systems engineering best practices.

In 2013, during the process of designing the Mars Science Laboratory, as part of the development of the Curiosity rover, NASA/Caltech Jet Propulsion Laboratory (JPL) found that the team was not following the systems engineering process accordingly, for which they released a lessons-learned document [2]. A redesign in one part of the robotic arm was conducted out of schedule, which derived into a new development that replaced the initially designed catalog component. This problem ultimately affected schedule control, risk management, and the cost of the mission.

## 2.2 *Systems engineering standards*

For space systems engineering, there are specific standards that were created by NASA and ESA. In the case of NASA, the standard is defined in the NASA Systems Engineering Handbook and can be accessed through the NASA Online Directives Information Service. In the case of ESA, the standard is defined in the E-ST-10 Engineering Standard [3] created by the European Cooperation for Space Standardization (ECSS). The ECSS is an organization founded by ESA in 1993 to create a coherent and single set of space standards for European space activities [4]. Both systems engineering standards are intended to be tailored by the end user according to their needs and are actively used by many countries outside the boundaries of North America and Europe. Fig. 1 shows how systems engineering relates to other activities, as defined in the ECSS standard.

Although these are domain-specific standards that were created within the context of the space industry, others are fed by industries with high-quality requirements too, like the medical and automotive industries. Many international organizations, like the International Council on Systems Engineering (INCOSE), the International Organization for Standardization (ISO), the International Electrotechnical Commission (IEC), and the Institute of Electrical and Electronics Engineers have been working on aligning the definitions used in the standards. Some of the results are described in ISO/IEC/IEEE 24748 (Systems and software engineering—life cycle management—Part 1: Guidelines for life cycle management), which is publicly available [5]. More specific information about the application of systems engineering and software systems engineering in different contexts is presented in Parts 2 and 3 of the same standard. These standards define a generic meaning and generic definitions that can be used in conjunction with another more specific standard. It is important to note that, in opposition to space-related standards, these do not define the process of systems engineering, but rather give an overview of typical life cycle definitions.

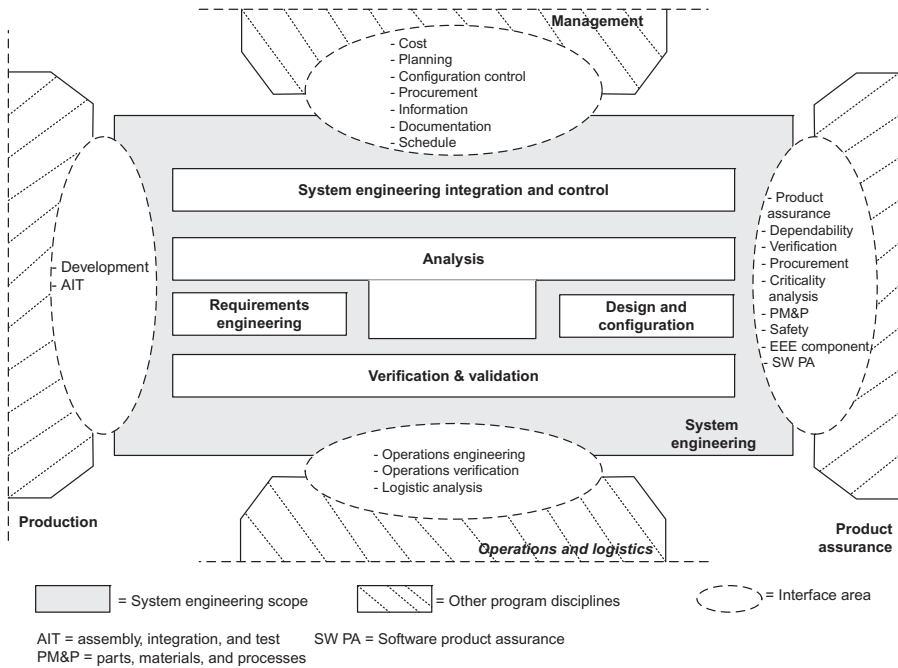


**Fig. 1** Systems engineering functions and boundaries.

Source: ECSS-E-ST-10C.

### 2.3 Model-based systems engineering vs. document-based systems engineering

Traditionally, the practical application of systems engineering to space projects has been based on the elaboration of a set of documents that follow a logical workflow. They use the output of other documents as inputs for the documentation. In large and complex projects, information and control management is not trivial. Thus, complex management document systems are required to guarantee the access and use of the correct and updated information for all analyses, designs, and documentation workflows during all the phases of the project.

Nowadays, model-based systems engineering (MBSE) is becoming more popular within the industry, including CubeSat missions, as an alternative to the traditional document-based information exchange. This trend is probably because, in MBSE, the communication of the information is based on visual modeling, which is easier to follow. MBSE eliminates the transmission of unnecessary information by relying on abstract models that keep only the relevant data. Available MBSE software iterates the workflow automatically with the updated information, facilitating the analysis of the impact of the design changes.

The System Modeling Language (SysML) was proposed to provide a standard way to define the models. SysML is a dialect of the Unified Modeling Language (UML 2.x), which is driven technology for MBSE [6]. SysML is an open standard

that provides a general-purpose architecture modeling language for systems engineering applications. It supports the specification, from analysis to validation, going through design and verification of system and system of systems.

Conclusively, the objective of using MBSE is to provide a system engineering team with a tool to find errors in the simplest automatic way, facilitate iterations in system design, as well as provide scalability for complex projects. MBSE practical application in CubeSat projects is still very nascent but is expected to be used more and more in the following years.

## 2.4 Which standards to use?

Ultimately, all the standards mentioned have many things in common because their goal is the same: propose an organized method to get things done in the right way. If the project is space-related and located in Europe, then the program should follow the ECSS standard. However, if it is located in the United States, then it should follow the NASA standard. Also, other space agencies like the Canadian Space Agency have their own tailored standard, citing as reference NASA and ESA standards.

As can be seen, there is no easy answer to the question. Indeed, it depends on different factors: who is your client, where is your business located, or if the project is an element of a more significant project. Often companies impose constraints on the choice of standard to be used to make the project compatible with other parts.

Often, bearing the cost of acquiring a set of standards may be a problem for small projects. However, many resources can be downloaded and tailored to the project needs without any cost. This is an invaluable resource that space agencies and organizations make available to the community to encourage their adoption.

The following are some formal document-based and model-based systems engineering standards:

- European Cooperation for Space Standardization (ECSS): ECSS-E-ST-10C [3]
- The National Aeronautics and Space Administration (NASA): Systems Engineering Handbook [7]
- International Council on Systems Engineering (INCOSE): Guide to the Systems Engineering Body of Knowledge (SEBoK) [8]
- ISO/IEC/IEEE 15288: Systems and software engineering
- Model-Based Systems Engineering Wiki [9]

## 3 Phases, documentation, and project reviews

The objective of this section is to provide an organization baseline for the deliverables during all phases of a CubeSat project. It includes a downsizing of the ECSS standards (ECSS-M-ST-10C Rev. 1), selecting the most relevant documents for each phase. This ECSS tailoring example has been used in Xatcobeo, the first Spanish CubeSat, the HUMSAT Project, including HumSat-D and Serpens CubeSats, which was selected by the Space Office of the United Nations within the Basic Space Technology

Initiative Program, having the sponsorship of the European Space Agency (ESA) through the Program GEOID (Genso Experimental Orbital Initial Demonstration) and the Fly Your Satellite initiative promoted by ESA, and finally in LUME-1, a 2U CubeSat developed for the SUDOE FIRE-RS project [10]. The HumSAT project generated the documentation using this tailored standard [11].

The phases of a satellite project, according to ECSS, and its associated reviews are shown in Fig. 2, which mostly coincide with NASA phases and reviews. For a CubeSat mission, only a few formal reviews are usually carried out, typically PRR, PDR, CDR, and AR.

Phases 0, A, and B are focused mainly on the elaboration of system functional and technical requirements and identification of system concepts to comply with the mission statement, taking into account the technical and programmatic constraints identified by the project initiator and top-level customer. Phases C and D comprise all activities to be performed to develop and qualify the space and ground segments and their products. Phase E comprises all activities to be performed to launch, commission, utilize, and maintain the orbital elements. Phase F comprises all activities to be performed to dispose of the different segments according to the national and international regulations.

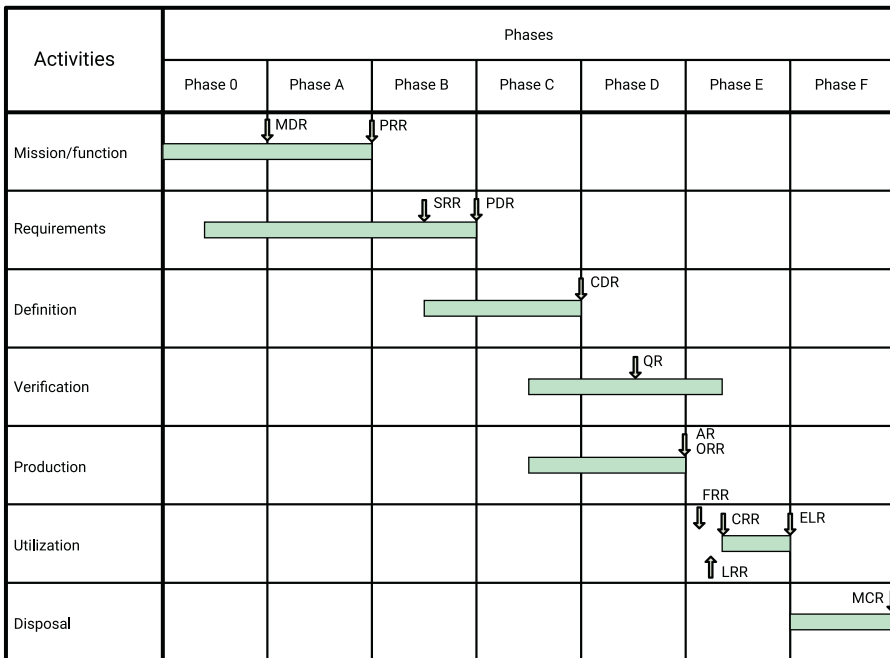


**Fig. 2** Typical project life cycle for a space project, including activities and formal reviews to be carried out during the different phases.

Source: ECSS-M-ST-10C.

The following sections include a possible adaptation of ECSS standards to a CubeSat project, which was used during the HumSAT project [12].

### **3.1 Phase A**

#### **3.1.1 Objectives of phase A**

The objectives of phase A are as follows:

1. Establish the preliminary project plan
  - Issue the initial master baseline schedule for the whole project, following the main milestones, product deliveries, and documentation releases.
  - Establish the preliminary systems engineering management plan.
2. Propose the preliminary architecture for the system
3. Propose the preliminary concept of operations
4. Elaborate the functional analysis for segment-level elements of the proposed architecture
5. Initiate predevelopment activities for critical technologies
6. Propose first model philosophy and verification approach to be further elaborated along phase B
7. Elaborate on the initial risk assessment

#### **3.2 Review at the end of phase A: Preliminary requirements review**

This is the first milestone for every CubeSat project where the documentation should be delivered. The objectives of these documents are as follows:

- Release of preliminary Project Organization. This document includes, among others, an organizational structure and information reporting methods.
- Release of the preliminary requirements specifications.
- Confirmation of the feasibility of the system. This technical feasibility covers all the project aspects, among others, funds, time, and human resources.
- Selection of system technical solutions, including model philosophy and verification approach, to be carried forward into phase B.

#### **3.3 Documentation in phase A**

The documentation issued during phase A of a CubeSat project is summarized in [Table 1](#). This phase ends with the approval of the preliminary requirements review (PRR).

Budget analysis might be a compilation of the following documents:

- Preliminary link budget analysis
- Preliminary power budget analysis
- Preliminary mass budget analysis
- Preliminary space environment analysis
- Preliminary data budget
- Preliminary pointing budget



**Table 1** Minimal documentation requirements for phase A.

Phase	Meeting	Name	Document status
A	PRR	Project Organization Plan <sup>a</sup>	New
A	PRR	Mission Requirements Document	New
A	PRR	Mission Operation Concept Document	New
A	PRR	System Architecture Definition	New
A	PRR	System Requirements Document	New
A	PRR	Budget Analysis	New

<sup>a</sup> Include Project Management Plan and Configuration and Documentation Control Plan.

Source: HumSAT Project website, 2013, <https://www.humsat.org/>.

### 3.4 Phase B

#### 3.4.1 Objectives of phase B

The objectives of phase B are as follows:

1. Finalize the project management plan
2. Finalize engineering management plans
3. Prepare the specification to be released for the segment-level components of the system
4. Select the preferred technical solutions for the system and establish a preliminary design
5. Identify and define external interfaces
6. Initiate long-lead item procurement required to meet project schedule needs

#### 3.4.2 Review at the end of phase B: Preliminary design review

At the end of phase B, a preliminary design review (PDR) is conducted with the following objectives:

- Verification of the preliminary design and technical solutions against the project and system requirements set in the previous phase
- Release of final engineering management plans
- Release of product tree and work breakdown structure (WBS)
- Release of the technical specifications according to the phase A requirements
- Release of the verification plan

#### 3.4.3 Documentation in phase B

The documentation issued during phase B of a CubeSat project is summarized in [Table 2](#).

The budget analysis mentioned in [Table 2](#) might be a compilation of the following documents:

- Updated link budget analysis
- Updated power budget analysis
- Updated mass budget analysis
- Updated space environment analysis
- Updated pointing budget

**Table 2** Minimal documentation requirements for phase B.

Phase	Meeting	Name	Document status
B	PDR	Project Organization Plan	Updated
B	PDR	Mission Requirements Document	Finalized
B	PDR	Mission Operation Concept Document	Updated
B	PDR	System Architecture Definition	Updated
B	PDR	System Requirements Document	Finalized
B	PDR	Spacecraft Technical Specification	New
B	PDR	Ground Segment Technical Specification	New
B	PDR	Budget Analysis	Updated
B	PDR	AIV Plan	New
B	PDR	Frequency Request Submission	New and finalized

Source: HumSAT Project website, 2013, <https://www.humsat.org/>.

- Updated data budget analysis
- Thermal budget analysis

### 3.5 Phase C

#### 3.5.1 Objectives of phase C

The objectives of phase C are as follows:

1. Completion of the detailed definition of the system
2. Production and development testing of engineering models as required by the verification approach
3. Finalization of the AIV plan

#### 3.5.2 Review at the end of phase C: Critical design review

At the end of phase C, a critical design review (CDR) is conducted with the following objectives:

- Assess the qualification and validation status of the spacecraft and ground segment
- Confirm compatibility with the identified external interfaces
- Release the final design related to the spacecraft and ground segment
- Release the final AIV plan
- Release the verification control document. This document comprises the spacecraft and ground segment requirements and its state of verification

#### 3.5.3 Documentation in phase C

The documentation issued during phase C of a CubeSat project is summarized in [Table 3](#).

**Table 3** Minimal documentation requirements for phase C.

Phase	Meeting	Name	Document status
C	CDR	Project Organization Plan	Finalized
C	CDR	Mission Operation Concept Document	Updated
C	CDR	System Architecture Definition	Finalized
C	CDR	Spacecraft Technical Specification	Finalized
C	CDR	Ground Segment Technical Specification	Finalized
C	CDR	Budget Analysis	Finalized
C	CDR	AIV Plan and Procedures	Finalized
C	CDR	Verification Control Document	New
C	CDR	Frequency Request Acceptation	New
C	CDR	Mission Operation Procedures	New

Source: HumSAT Project website, 2013, <https://www.humsat.org/>.

## 3.6 Phase D

### 3.6.1 Objectives of phase D

The objectives of phase D are as follows:

1. Complete qualification testing and associated verification activities
2. Complete the interoperability testing between the space and the ground segment

### 3.6.2 Review at the end of phase D: Acceptance review

At the end of phase D, an acceptance review (AR) is conducted with the following objectives:

- Confirm that the verification process has demonstrated that the design meets the applicable requirements
- Verify that the verification reports are complete and meet the applicable requirements
- Verify readiness of the operational procedures and readiness of the ground segment
- Release the ground segment for operations

### 3.6.3 Documentation in phase D

The documentation issued during phase D of a CubeSat project is summarized in [Table 4](#).

**Table 4** Minimal documentation requirements for phase D.

Phase	Meeting	Name	Document status
D	AR	Test Reports	New/finalized
D	AR	Verification Control Document	Finalized
D	AR	Mission Operation Concept Document	Finalized
D	AR	Mission Operation Procedures	Finalized

Source: HumSAT Project website, 2013, <https://www.humsat.org/>.

## 4 Requirements definition: User, mission, and system

The Oxford Dictionary defines the term “requirement” as something that you want or need or something that you must have to do something else [13]. For any space project and for a CubeSat mission, in particular, it is essential to define correctly, formally, quantifiable, and verifiable needs that the final users are expected to meet. Therefore, the requirements will allow us to validate if the manufactured system will meet the customer’s actual needs.

Typically, CubeSat university projects are mainly focused on educational and technological missions. The requirements are usually defined by the same institution that designs, integrates, and operates the satellite. On many occasions, the mission statement is quite open, and the user needs are not very well defined.

Currently, CubeSat-based scientific and commercial missions are becoming more popular. They are led by space agencies or commercial industries, focused on technological demonstrations complementary to large scientific missions, as well as offering services based on the data collected or transmitted by the CubeSats. In this case, the user and mission objectives are well defined.

### 4.1 Requirements definition and the V-model

NASA (NPR 7123.1B [14]) and ECSS standards (ECSS-E-ST-10C [3] and ECSS-E-ST-10-06C [15]) provide a detailed explanation of how to define and manage the requirements for a traditional space mission. According to ECSS-E-ST-10C, requirements engineering includes requirement statement, allocation, validation, and maintenance.

Fig. 3 shows the two levels into which a space project can be divided: the user level, including “stakeholders,” where the needs and expectations of the mission results are identified, and the engineering level, where the space system is designed, manufactured, integrated, verified, and put into operation. Whatever, commercial, scientific, or educational, be nature of the mission, the end user of the system expects to receive the data and products that meet their expectations. The space system is a “black box” for the end user, who is fundamentally interested in the data generated provided it meet their needs.

The first phase of any CubeSat project must be focused on defining the needs (requirements) of the satellite (end user), regardless of which technical solution will be finally implemented. The first CubeSats projects were eminently academic, whose objectives were educational or technological demonstrations. Currently, thanks to the technology being more mature, CubeSats missions have been extended to scientific and commercial projects.

In many university projects, the mission has been defined by the same team that later will design, manufacture, integrate, and operate its satellite. This is the main reason why an adequate definition of requirements has probably not been traditionally elaborated for this kind of missions.

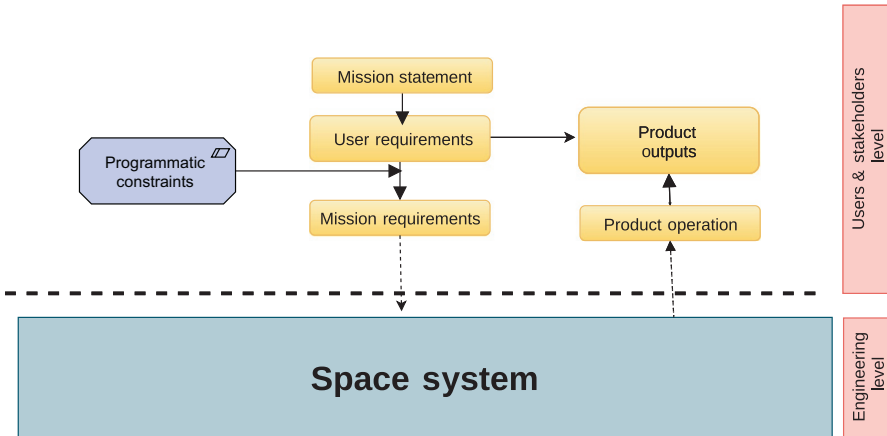


**Fig. 3** User and engineering levels in a space project.

*Source:* Original content.

The requirements at the user and mission level can be seen as a contract signed between the system user and the engineering team. Correct and defect-free definitions of the top-level requirements will allow systems engineers to identify the technical specifications accurately. Based on these requirements, the design and manufacture of the system can be carried out, which, once integrated, will allow its validation against the requirements, verifying that a correct development has been achieved.

The modification or inclusion of new user or mission requirements, once have been initially frozen, might dramatically impact the project. It could impose a partial or complete redesign of individual parts or even the entire system, with their corresponding impact being at the budgetary level as of calendar.

Every requirement must have the following key characteristics:

- Function: define “what” is to be done
- Quantified performance: define “how well” it has to be done
- Verifiable: define “how” the requirement should be confirmed
- Feasible: the need shall be technically possible
- Indispensable: define a necessary need of the system

From a formal point of view, the requirements must be written using the verbal form “shall.” Each requirement must identify a single need, self-contained, positively formulated, concise, and straightforward, as well as grammatically correct, numbered, and labeled.

A requirement stated by the verbal forms “should,” “may,” “might,” or “may” is not really a requirements since it identifies a “nice to have” that is not really necessary for the system, but rather something that would be desirable to achieve, but in the case that it is not implemented, the system would be equally valid for the user.

Other terms to avoid in formulating the requirements are adequate, best effort, easy, robust, user-friendly, optimize, minimize, high data rate, enough, sufficient, plenty, stable, and reliable.

#### 4.1.1 *Examples of requirements for a CubeSat mission*

ESA Education Office has recently released an updated version of the “Fly Your Satellite Design Specification” (FDS). FDS is not publicly available, but is made available based on a request to ESA Education Office, in particular to teams preparing an application to the third edition of Fly Your Satellite.

The FDS defines the technical requirements for CubeSats participating in the Fly Your Satellite! Program and the set of requirements comprises, according to the meet-or-exceed principle, Fly Your Satellite program-specific requirements as well as requirements from:

- The CubeSat Design Specification
- The NanoRacks CubeSat Deployer Interface Control Document
- The JAXA JEM Payload Accommodation Handbook
- ESA Space Debris Mitigation Requirements, ECSS-U-AS-10C
- ITU Radio Regulations
- NASA Crewed Space Vehicle Battery Safety Requirements
- ISO 17770-Space Systems Cube Satellites Standards
- NASA’s General Environmental Verification Standard

The specification is tailored, but not limited, to launch opportunities from the ISS, and it targets CubeSats for which the CubeSat Deployer and launch vehicle may not yet have been selected. Fig. 4 shows how system and subsystem technical requirements are defined in the first phase of the project and could be iterated based on system budget and analysis results.

Top-level, and system and subsystem requirement definitions are included in the user requirements document, mission requirements document, and system and subsystem requirements document. Examples can be found in [11].

#### 4.1.2 *User requirements document*

The user requirements documents (URD) comprise the requirements for defining the products and services provided for the mission, how users can access them, and which performance they shall expect. The user requirements are part of the mission requirements document. In a CubeSat mission, the user requirements are typically included in the mission requirements document as a section.

#### 4.1.3 *Mission requirements document*

The mission requirements document (MRD) captures the requirements that shall be met by the proposed mission. It describes the externally observable behaviors that the mission must exhibit and the performance that the system shall achieve.

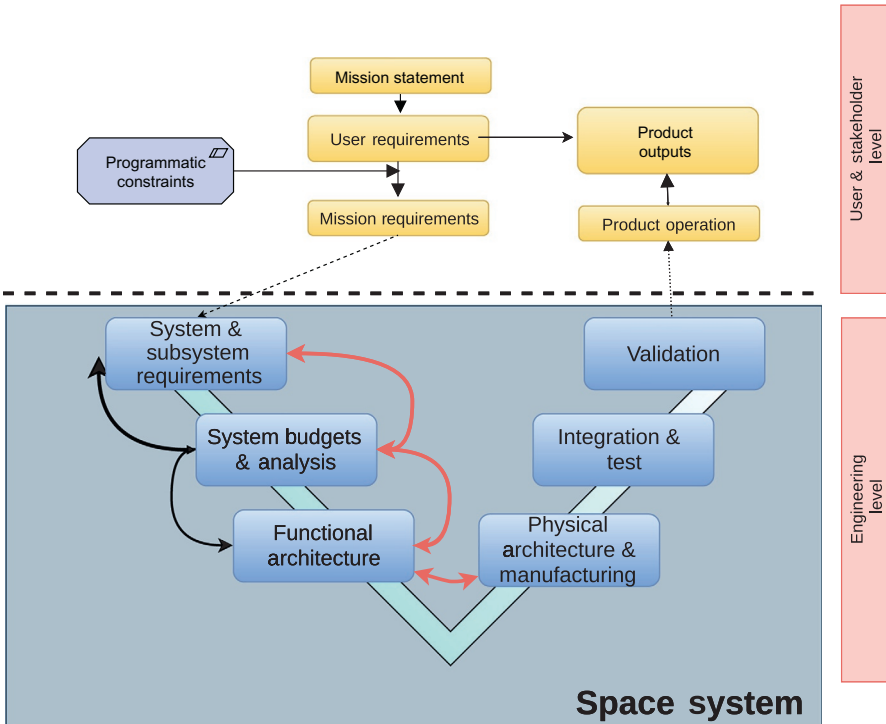


**Fig. 4** System engineering V-model, including requirements definition, design, manufacturing, and AIV activities at engineering level.

Source: Original content.

MRD typically includes the following sections [16]:

- general requirements
- user requirements
- availability and performance requirements
- service requirements
- implementation requirements
- mission protection requirements
- operational requirements

#### 4.1.4 System requirements document

The system requirements document (SRD) establishes a set of requirements that shall define the components of the system at the system level and, therefore, shall determine the framework of development to be used by any team willing to design parts for the CubeSat system. The key elements are as follows [17]:

1. General system requirements
  - general requirements
  - services definition

- performance requirements
  - system scalability requirements
2. Space segment
    - constellation requirements
    - spacecraft requirements
    - general requirements
    - payload requirements
  3. Ground segment
    - general requirements
    - per-facility requirements
    - ground station facilities
    - satellite control facilities
    - payload control facilities
    - user data distribution facilities
  4. User segment requirements

#### 4.1.5 *Subsystem requirements document*

The subsystem requirements document establishes a set of requirements that shall define the components of each subsystem at this level and, therefore, shall determine the framework of development to be used by any team willing to design any element for the CubeSat subsystems.

## 5 **Mission cost analysis**

Planning how to manage the cost is essential for any project. The cost management plan should, at least, determine how it must be estimated and scheduled, how it must be managed, and how it must be monitored and controlled. For estimating the cost, a commonly used technique is to break down the costs and create what it is called a cost breakdown structure (CBS). Then, it is possible to estimate each subdivision using different methods. The choice of which technique to use depends on the amount of information available at a given point in time. Traditional mission cost estimation methods are based on the experience of previous projects of national space agencies or prime contractors. However, using this approach in the private industry would bring unrealistic cost estimations because the industry expense is not even close to the resulting cost. An excellent example of the difference in costs in the New Space Era has been proven by SpaceX. If a space agency or a prime contractor had developed the Falcon 9, the cost would have been prohibitive for the industry to access it. The industry optimizes costs because ultimately their profit is based on their cost schemes. Cost planning or scheduling, also known as “determine budget” for the Project Management Institute (PMI), is essential to determine when the money is needed. This information is crucial to decide on the financial cash flow required for the project. Cost estimation gives an idea of how much money is necessary for the project, and cost planning provides a sense of when the funds are required. The cost management plan should incorporate details on how the cost must be estimated. Also, it must include techniques



to use, as well as enumerate identified assumptions and risks. Then, it should establish different indicators that help the project manager, during the execution of the project, to monitor and control the cost. A hypothetical mission of a CubeSat to Low Earth Orbit, named LEON-I, is used throughout this section to provide a practical example.

## 5.1 Cost breakdown structure

Because of the magnitude of space projects, breaking down the costs into categories should be the first step. Also, the resulting categories could be broken down further to make a more detailed cost estimation along the lifetime of the project.

Often the CBS does not correspond to the WBS because cost categories are transversal to many different work packages. However, the WBS is a valuable input to estimate the costs of the project. Once the definition of cost categories is complete, the cost estimation of each one of the work packages must be done, considering these categories. Usually, not all work packages have imputable items to each group.

Top-level categories often include human resources, facilities, external contracts, indirect costs, materials and supplies, transportation, and mission operations, among others. For example, to be compliant with the ECSS-M-ST-60 standard, CBS should have at least the top-level categories listed in [Table 5](#). For the LEON-I mission, let us consider ECSS-M-ST-60 proposed CBS, as shown in [Fig. 5](#).

**Table 5** Cost breakdown structure top-level categories according to ECSS-M-ST-60C.

Category	Description
Direct human power	Includes all the human power that is required directly for the project. This category can be split down into different types to account for different hourly rates
Internal special facilities	Includes computer facilities, integration facilities, test environments, among others. A work unit is often used to define the cost per unit of work
Supplies and other direct costs	These are supplies that are incorporated directly into the work, either modified or unmodified. This category may also include subcontracts or services required for other jobs. This category is also broken down by the ECSS standard in seven additional subcategories: materials, parts, major products, external services, transport and insurance, missions and travels, and miscellaneous
Subcontracts	These are subcontracts other than those required for internal work to be performed. They are contracts with external suppliers that are supported by a statement of work, or technical specification
Nonproduction expenses	Includes all nonproduction expenses that apply to the project. These are usually the indirect cost of work

Adapted from ECSS, Space project management: cost and schedule management, Tech. Rep. ECSS-M-ST-60C, European Cooperation for Space Standardization, 2008.

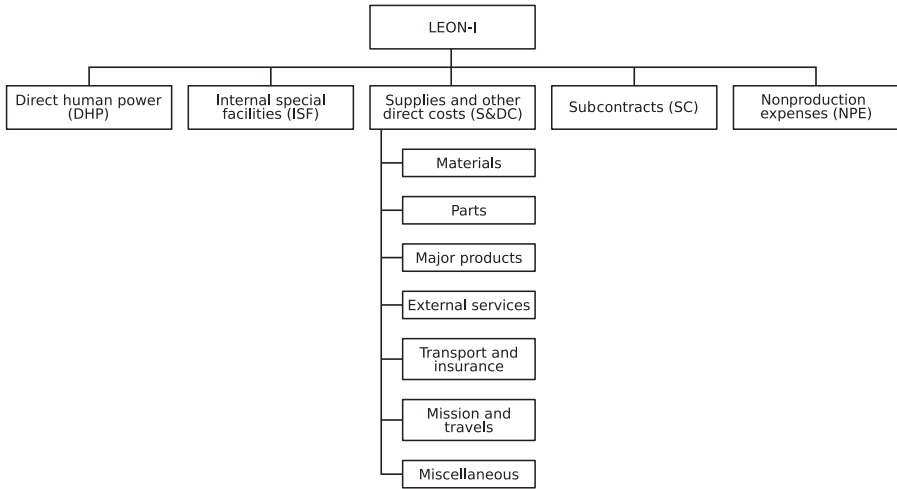


**Fig. 5** Cost breakdown structure for the LEON-I mission. Adapted from ECSS-M-ST-60.

## 5.2 Cost estimation

The first step when performing a mission cost analysis is to estimate the cost of each leaf of the CBS.

The following are some of the techniques used to estimate costs, according to the PMBOK [18]:

- Expert judgment, where a person or a group of persons who have worked in similar projects have enough expertise to estimate the cost.
- The analogous estimation that uses a known project cost, with similar characteristics, to estimate the expenses for this project.
- Parametric estimating that uses statistical information to create models for estimation. For example, when extrapolating the cost of 1U CubeSat to LEO to the cost of a 6U CubeSat.
- The bottom-up estimation consists of determining the cost of each work package. In this case, the activities are taken from the WBS and can include more than one category of the CBS already in the estimation.
- Three-point estimating, which is used to account for uncertainty and risk. Three different estimations are considered: most likely, optimistic, and pessimistic. Then, the expected cost is obtained by using a formula that depends on the desired distribution model.
- Software estimation tools that are specific to different areas of expertise.

Space projects are complex, so there are always uncertainties on the scope and schedule in the early phases. Depending on the phase where the cost estimation is made, a margin of uncertainty should be included to account for possible variances. Uncertainty margins used are subject to the area of expertise on which the

project is developed. As a rule of thumb, for space-related projects, the cost can be expressed as follows:

- Phase 0: estimated cost  $-20\%$   $+40\%$
- Phases A and B: estimated cost  $-15\%$   $+35\%$
- Phase C: estimated cost  $-10\%$   $+15\%$
- Phase D and subsequent: estimated cost  $-5\%$   $+10\%$

The more mature the project is, the more accurate the estimates will be. In any case, it is essential to document and communicate the uncertainties associated with the estimate. According to NASA Cost Estimating Handbook [19], areas of uncertainty can be: “pending negotiations; concurrency; schedule risk; performance requirements that are not yet firm; appropriateness of analogies; the level of knowledge about support concepts; critical assumptions; among others.”

To account for the occurrence of known risks, the estimator should consider the project risk registry as an essential input to conduct the cost estimation. The fact that any risk occurs undoubtedly creates a gap in the estimated schedule and cost.

There is another expense the estimator should consider, which is known as management reserves. These reserves are preagreed with the company to account for possible unallocated deviations. A 10% should be a reasonable quantity to account for at first stages of a new project. Although the estimator should account for this expense, when controlling the cost, it should not be considered. More information on how to monitor and control the costs is given later in this chapter.

In changing or agile environments like CubeSat projects, where a high degree of uncertainty exists concerning requirements, it would be more challenging to disaggregate and perform precise estimations from the beginning. In those cases, cost estimation and control are also possible, breaking down the whole estimation process in shorter schedule timelines. As an example, if a small team uses Scrum methodology, it would be possible to tune up the cost estimation before starting each sprint. However, at some point during the planning phase of the project, it is necessary to make an estimation. In that sense, the use of budgets is powerful and allows more changing scenarios. For example, it would be possible to assign a budget of \$750,000 for the spacecraft, or \$45,000 for the onboard computer, and during the selection of components to make sure that the chosen parts are within the assigned budget. Alternatively, for noncomponent-based tasks, assign a time box for the required tasks, and keep the work within limits.

Things to remember when making the whole project budget are listed in [Table 6](#).

### 5.2.1 *Software development cost estimation*

Software development is often underestimated, in both time and costs, by CubeSat teams. Estimating the cost of software development deserves a different section because of this and given that there are several tools and models available for calculating it. One very popular model is the COCOMO Model, or Constructive Cost Model, proposed in 1970 and published in 1981 by Barry Boehm. COCOMO is a regression model based on the number of lines of code. Boehm included, in the formulation, three different types of systems: organic, semidetached, and embedded systems.

**Table 6** General concepts to remember when calculating a required budget for a project.

Concept	Description
Engineering process	Following a standard gives already a good sense of the number of deliverables expected as a result of the job done during this process. It is important to reserve time for reviewing documentation, time to conduct internal and external reviews, time for delta reviews, and time to contact possible providers
External revisions	Each project phase requires a review, so it is always a good idea to request the participation of external revisors. These revisions can be done by inviting outer reviewers to the review meetings, or by sending the documentation to a specialized company for reviewing it
Concepts and technology demonstrators	Some time may be required to develop a proof of concept or technology demonstrators, depending on the project type and aversion to risk. Also, some time may be needed to build a structural and thermal model (STM), or a mass model, to validate calculations, or to discard assumptions
Spacecraft	The most commonly used subsystems are always included, but it is crucial to include in the budget those not so obvious. Harnessing and developing a wiring model can be a headache. Design and machine shieldings within tolerances, and the inclusion of thermal protection coatings must be considered
Ground support equipment	Almost every subsystem requires a specific ground support equipment (GSE) to run tests and to validate it works as expected. Also, diverse mechanical GSEs may be needed to integrate the spacecraft, or to carry it to another destination. Moreover, with the satellite completely integrated, a specific GSE is usually necessary to run the final tests
Environmental campaign	Sometimes overlooked, environmental campaigns are time consuming and can be very expensive, depending on the requirements. When calculating their cost, travel expenses and the human power required to prepare and execute the campaigns should be taken into account
Transportation and launch	Certainly, every space mission requires transportation and launch. Extra money should be reserved for shipping or carrying the spacecraft, for possible customs paperwork, travel expenses, and the human power needed to achieve those tasks
Operations phase	The operational phase can be of very different duration, from days to years, depending on the mission. An effort has to be put to predict the required fees for this phase. Are specific antennas or facilities will be needed during operations? Does the company have all the infrastructure to operate the spacecraft? How many human hours are required per day?

*Continued*

**Table 6** Continued

Concept	Description
Indirect costs	All nondirect expenses must be considered when estimating the cost of a task. What is the amortization period set for each piece of equipment or tool required for the job? How are the rent of the office and the services included in the price? How much money is the company paying for the software licenses required to do the job?

Source: Original content.

The purpose of this section is not to describe the model itself, because there are an innumerable number of resources available online free of charge that can be used. However, it is worth mentioning that three different types of models are available. These can be used depending on the level of details available for the estimation: basic, intermediate, and detailed. Ultimately, the COCOMO model gives an estimate of the effort required to develop the software in person-month units.

Although extensively used, the model is based on standard techniques used for software development in those years. An evolution of the original model, formulated by the University of Southern California and led by Barry Bohem, was published in 1995 under the name of COCOMO II [20]. In this case, the model is divided into three submodels used during the life cycle of the project, providing increasing fidelity. These submodels are application composition, early design, and postarchitecture models.

### 5.2.2 Other estimation models

Following the same principles of estimating the cost of a project using a model, Ricardo Valerdi developed a model for estimating the costs of Systems Engineering at the University of Southern California. The model was named the Constructive Systems Engineering Cost Model (COSYSMO) and was initially published in 2002 [21]. This model includes the estimation of both software and hardware for a project. It is also aligned with the phases of a project life cycle, as per ISO/IEC 15288.

COSYSMO is based on several indicators to determine the required effort and risk associated with the development of a system. First, to determine the size of the project, the model requires the user to enter the number of system requirements, system interfaces, algorithms, and operational scenarios, with the option to define the quantities in up to three complexity levels. Then, the user must provide details on 14 different cost drivers, grouped into five groups: personnel factors, environment factors, operational factors, understanding factors, and complexity factors.

Once again, as stated in the study published by Ricardo Valerdi [21], the COSYSMO model has been optimized and calibrated “using data from six aerospace companies in the form of expert opinion and historical project data,” which yields to the same problem as with traditional cost estimation: the data used comes from space agencies or prime contractors. Thus, the generic equation that uses given calibration may not reflect the cost effectively, so a local calibration of the cost drivers is needed on each organization.

**Table 7** Cost estimation for a subset of work packages of the LEON-I mission (in \$).

WP code	DHP	ISF	S&DC	SC	NPE	Total cost
1.1	10,000	5000	3000	–	500	18,500
1.2	2000	–	2500	–	1000	5500
1.3	–	–	–	50,000	–	50,000
2.1	3000	500	20,000	–	500	24,000
2.2	2500	–	–	150,000	2000	154,500
3.1	5000	2000	–	–	3000	10,000
3.2	500	10,000	–	–	2000	12,500
EAC						275,000

Source: Original content.

### 5.2.3 Cost estimation for the LEON-I mission

For the example with LEON-I, let us imagine that some work packages were defined in the WBS, with the estimation of costs (including uncertainty margin) as listed in Table 7. In reality, we should use the WBS Dictionary to understand what is included in the work package while estimating the cost, but this serves for our example.

For each of the work packages listed, the estimated cost of the work to be done is broken down into the classifications defined in the CBS. As mentioned earlier, not necessarily all categories must have a value for each work package. As an example, WP 1.3 only has \$50,000 in the subcontract category, which means that it is an external subcontracted work that does not require any intervention from our side. The final row shows the total cost estimated at completion (EAC).

## 5.3 Cost planning (or cost scheduling)

After completion of the cost estimation of each work package, using the project schedule baseline, the development of the cost planning comes next. The result is a time-phased expenditure requirement, known as the project budget.

Before starting with the execution of the project, the first version of the project budget must be saved as the cost baseline. This initial baseline is used in later stages to monitor and control the costs. Similarly, the scope baseline and the schedule baseline will be used to check the project evolution in those terms.

## 5.4 Cost planning for the LEON-I mission

Continuing with the LEON-I CubeSat mission, the schedule baseline for the work packages presented during the estimation process is shown in Fig. 6. The next control point, shown by shaded region, is scheduled to happen during the first week of July, to control costs up to the end of June. It is essential to have the expected percentage of progress for all tasks at that point (in schedule and cost) to conduct valuable control. This percentage is something that ultimately must be given in advance to the

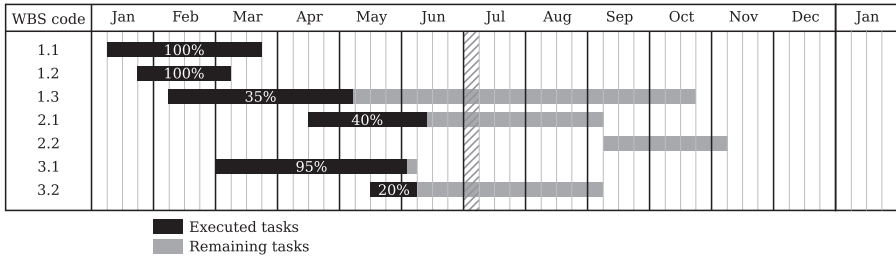


**Fig. 6** Gantt chart with some of the work packages of the LEON-I mission.

Source: Original content.

accountants to plan the finances of the project accordingly. For simplicity, even expenditures per week are considered over the total amount estimated. For example, for WP 1.1, the number of weeks is 10, and the total cost is \$18,500, which means that every week \$1850 will be required. In reality, a more detailed schedule is expected, at least for those work packages that may require an extended amount of money to be expedited at a given point. With this information, it is possible to create a financial planning sheet. In this example, months from January to November must be included. The resulting planning is illustrated in Fig. 6 and Table 8.

The cost baseline distributed over time, considering the cumulative cost, is usually represented graphically in what it is called an S-curve. The name is given because of the similarity to an S, as it can be seen in Fig. 7.

### 5.5 Cost monitoring and control

Different approaches can be used to monitor and control the cost. The method to be used should be defined in the project management plan. Earned value management (EVM) is one of the most used methods in the space industry. However, it requires discipline in the management process to report the performance evolution of what was planned, and here it is where many large projects have had some troubles in the past (as stated in 2009 and 2012 reports generated by the US Government Accountability Office [22, 23]). Still, it provides invaluable information that helps to determine if the project requires preventive actions, corrective actions, or changes in scope, schedule, and cost.

The ESA performs cost control based on the ECSS-M-ST-60, where there is no mention of the earned value. However, the indicators used by this standard, the EAC and the estimate to completion, are both parts of the same analysis.

Important to note is that earned value is not the actual expenses, but the tasks that have been completed at the cost they were planned, compared to the project baseline. At least one is expected to be created during the initial analysis of the project, and subsequent baselines can be created afterward depending on changes in scope, schedule, or cost. Ultimately, the earned value analysis provides a series of performance indicators to tell how healthy the project is when compared to the baseline plan.

**Table 8** Financial planning for some of the work packages of the LEON-I mission (in \$).

<b>WBS code</b>	<b>Jan</b>	<b>Feb</b>	<b>Mar</b>	<b>Apr</b>	<b>May</b>	<b>Jun</b>	<b>Jul</b>	<b>Aug</b>	<b>Sep</b>	<b>Oct</b>	<b>Nov</b>
1.1	5550	7400	5550	–	–	–	–	–	–	–	–
1.2	917	3667	917	–	–	–	–	–	–	–	–
1.3	–	4412	5882	5882	5882	5882	5882	5882	5882	4412	–
2.1	–	–	–	2526	5053	5053	5053	5053	1263	–	–
2.2	–	–	–	–	–	–	–	–	57,938	77,250	19,313
3.1	–	–	3077	3077	3077	769	–	–	–	–	–
3.2	–	–	–	–	1667	3333	3333	3333	833	–	–
<b>Total</b>	<b>6467</b>	<b>15,478</b>	<b>15,426</b>	<b>11,486</b>	<b>15,679</b>	<b>15,038</b>	<b>14,268</b>	<b>14,268</b>	<b>65,916</b>	<b>81,662</b>	<b>19,313</b>
<b>Cumulative</b>	<b>6467</b>	<b>21,945</b>	<b>37,371</b>	<b>48,857</b>	<b>64,535</b>	<b>79,573</b>	<b>93,841</b>	<b>108,109</b>	<b>174,026</b>	<b>255,688</b>	<b>275,000</b>

Source: Original content.



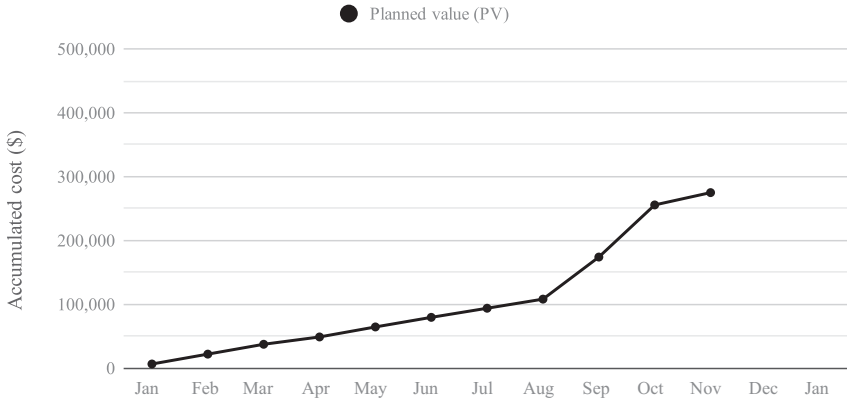


**Fig. 7** Planned value for the LEON-I mission used as a baseline for cost monitoring and control.  
*Source:* Original content.

Some calculations are required to use the EVM method. A simple description of each one is provided in the following. However, further reading is recommended from specialized literature.

### 5.5.1 Budget at completion

The sum of all planned costs required to finish with all tasks, excluding management reserves, is called budget at completion (BAC). It is the total cumulative cost scheduled for the end of the project.

### 5.5.2 Planned value

Planned value (PV) is the planned cost of the planned work at the moment of the measurement. It is also called the performance measurement baseline (PMB). The formula to calculate it is

$$PV = (\text{Expected \% of the job done}) * (\text{Planned cost})$$

### 5.5.3 Earned value

Earned value (EV) is used to measure the actual job done, but considering the cost that was planned. The formula to calculate it is

$$EV = (\text{Real \% of the job done}) * (\text{Planned cost})$$

### 5.5.4 Actual cost

Actual cost (AC) is the real cost of the job done so that it considers the actual cost. It is important to use the actual amount of money expended on the job, even if it was less or

more than planned. There is no formula for the actual cost. Instead it is all the money spent to complete the job done for a particular task.

$$AC = \text{Actual cost of the job done}$$

### 5.5.5 *Schedule variance*

Schedule variance (SV) is used to measure the behavior of the project schedule in terms of planned cost. It provides information to determine if the project is on schedule, ahead of schedule, or delayed. The formula to calculate it is

$$SV = EV - PV$$

### 5.5.6 *Cost variance*

Cost variance (CV) is used to measure how the expenditures of the project evolve compared to what was planned. It provides information to determine if there have been more expenses than planned, exactly as planned, or less than planned. The formula to calculate it is

$$CV = EV - AC$$

### 5.5.7 *Schedule performance index*

Normalization of the indicators is necessary to have a better understanding of them. The schedule performance index (SPI) measures the job done compared to what was planned. If the value is exactly one, the project is on schedule. If it is less than one, the project is delayed, and otherwise, the project is ahead of schedule. The formula to calculate it is

$$SPI = EV/PV$$

### 5.5.8 *Cost performance index*

As with the SPI, the cost performance index (CPI) is a normalized indicator. The CPI compares the cost planned to the actual cost of the job done. If the CPI is exactly one, the project expenses are as planned. If it is less than one, the project expenditures have been higher than expected, and otherwise, the project has spent less money than initially calculated. The formula to calculate it is

$$CPI = EV/AC$$

### 5.5.9 Estimate at completion

Having more information about the actual state of the evolution of expenditure allows the calculation of forecast information. This information provides an update on cost estimation concerning the BAC, originally calculated. There are different ways to calculate the EAC, and the method used depends on each project management plan, or requirements of the company. A description of the three most used ways is provided in the following.

#### Projection at the rate of the original budget

This projection would be the best case, which estimates that the projection remains as it was originally planned. The formula to calculate it is

$$EAC = AC + BAC - EV$$

#### Projection at a rate modified by the CPI

It is possible to use the CPI, which uses information about how the project has been evolving from the beginning. The formula to calculate it is

$$EAC = BAC / CPI$$

#### Projection at a rate modified by the CPI and the SPI

It is possible to use both indexes calculated, which considers that both the CPI and the SPI affect the evolution of the project. The formula to calculate it is

$$EAC = AC + [(BAC - EV) / (CPI * SPI)]$$

### 5.5.10 Estimate at completion time

Estimate at completion time (EACtime) projections provide an idea on the increase in money required to finish the project if nothing changes. However, to estimate the delay in time, a different formula must be used. Similarly, as with the EAC, there are different ways to estimate the delay in time: considering the originally estimated rate; or, considering the rate modified by the SPI.

#### Projection at the rate of the original budget

This case considers that the remaining tasks are going to be done as initially planned. The equation to calculate it is

$$EACtime_{initial} = \text{Actual time} + \text{Remaining tasks duration estimation}$$

### Projection at a rate modified by the SPI

It is possible to estimate the delay by making use of the SPI previously calculated. In that way, the schedule is reestimated, considering the last performance. The formula to calculate it is

$$EACtime_{SPI} = \text{Actual time} + (\text{Remaining tasks duration estimation})/SPI$$

Other techniques exist to forecast the time delay incurred in the project, but they are not analyzed in this book. The most valuable information is ultimately given by the people who are executing the job, so surveys are often handy. Reestimation of the effort required, focusing on those tasks that are in the critical path, provides the required information to reestimate the duration of the project.

After a new schedule and cost estimation is done, the baselines have to be updated and used from that moment as new baselines for monitoring and controlling the evolution in time and costs.

#### 5.5.11 Monitoring and controlling the LEON-I mission

Continuing with the example of LEON-I, and considering that the control point has arrived, it is time to survey the actual numbers of the work packages. Assuming the evolution of the job carried out on each work package as listed in [Table 9](#), the objective is to control the deviation of the project compared to the plan.

The schedule variance at this point is

$$SV = 63,100 - 79,573 = (16,473)$$

which means that the schedule is delayed when compared to the plan.

**Table 9** Evolution of the expenses for the LEON-I mission at the control point.

WBS code	Total planned cost (\$)	Expected completion (%)	Actual completion (%)	PV (\$)	EV (\$)	AC (\$)
1.1	18,500	100	100	18,500	18,500	26,992
1.2	5500	100	100	5500	5500	14,350
1.3	50,000	56	35	27,941	17,500	31,780
2.1	24,000	53	40	12,632	9600	9200
2.2	154,500	0	0	0	0	5000
3.1	10,000	100	95	10,000	9500	16,348
3.2	12,500	40	20	5000	2500	6890
Totals				79,573	63,100	110,560

Source: Original content.

The cost variance is

$$CV = 63,100 - 110,560 = (47,460)$$

which means that more money than what was planned has been spent.

The two performance indexes are

$$SPI = 63,100/79,573 = 0.793$$

$$CPI = 63,100/110,560 = 0.571$$

Having these indicators should mandate to take corrective actions to fix the situation. If nothing changes the cost EAC is, considering the actual CPI,

$$EAC = BAC/CPI = 275,000/0.571 = 481,611$$

However, this change in cost may require the extension of the execution time for the project. It is possible to use the estimated time at completion (EACtime) to obtain the extension in time. Considering the best case, where the schedule is the same from now on as the one initially estimated, the EACtime is

$$EACtime_{initial} = 1st\ of\ July + (65\% \ of\ WP1.3) \approx 16th\ of\ December$$

Alternatively, considering the estimation adjusted by the SPI, the EACtime is

$$EACtime_{SPI} = 1st\ of\ July + (65\% \ of\ WP1.3)/0.793 \approx 31st\ of\ Jan$$

The newly estimated cost and schedule is shown in [Figs. 8](#) and [9](#), respectively.

It is important to note that these are indicators, and never should be considered as a valid estimation tool. They alert the project manager about how the situation is at a specific control point. Actions have to be taken whenever situations like the one in the LEON-I mission occurs to prevent the schedule from diverging.

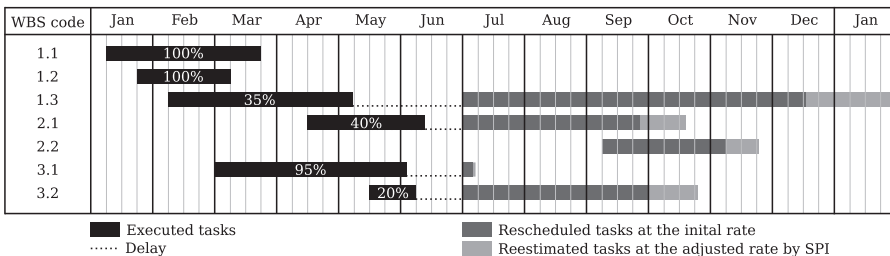


**Fig. 8** Updated Gantt chart at the control point with the newly estimated duration using the initial and adjusted rate, for the LEON-I mission.

Source: Original content.

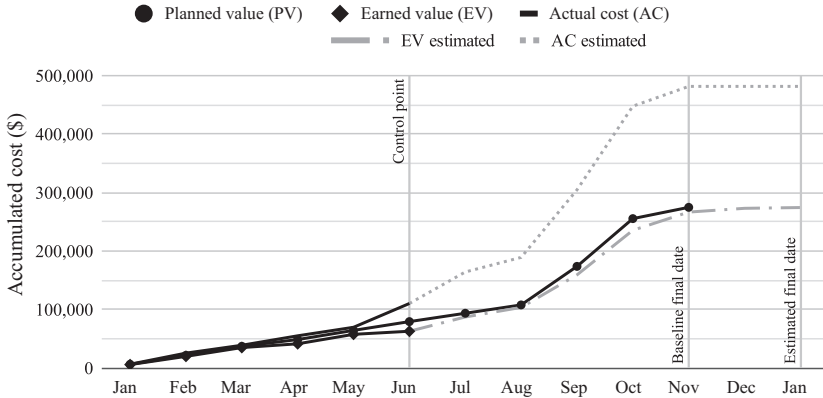


**Fig. 9** Estimation of the actual cost and delay in the schedule for the LEON-I mission considering the actual CPI.

Source: Original content.

## 5.6 Cost estimation conclusions

Cost estimation is a complex task to be performed by systems engineers and project managers, so it is essential to make it an evolving process during the life cycle of the project. While more information is available, more details can be included in the planning. The use of earned value management can help the managers to monitor and keep under control the project, giving information about how healthy it is at each control point.

With a simplified example, the author intended to demonstrate all the considerations required to perform the cost estimation, monitoring, and control that can be applied to a CubeSat mission without a work overhead.

## 6 Summary

In this chapter, the authors have presented some elements considered key to guaranteeing the success of any space mission. They started in [Section I.1](#) with a brief introduction to clarify the difference that exists between simple engineering and systems engineering. This initial explanation allows the reader to understand better [Section I.2](#), where the existing systems engineering standards applied to space projects are presented. Here, the authors also introduced the model-based systems engineering, which allows application of automation during the engineering process.

In [Section I.3](#), the tailoring of one of the available standards is presented with examples of the documentation generated for real projects that have flown. This section also includes the key milestones and the associated documentation expected, including the evolving status of each document over time.

The project life cycle that starts with gathering requirements at the user level and ends with the disposal of the spacecraft is presented in [Chapter I.4](#). Here the authors

present the V-model applied to space missions. Finally, to complete the discussion about the tools needed during the systems engineering process, the authors present in [Chapter I.5](#) how to do a mission cost analysis, through an example with a hypothetical mission named LEON-1. The rest of the book gives the reader essential information about the elements of a mission that must comply with user requirements.

## References

- [1] M. Okada, S. Yamamoto, T. Mukai, Systems engineering enhancement initiative in JAXA. Trans. JSASS Space Technol. Jpn 7 (ISTS26) (2009) 1–6, [https://doi.org/10.2322/tstj.7.Tt\\_1](https://doi.org/10.2322/tstj.7.Tt_1).
- [2] JPL, Lessons Learned: MSL Actuator Design Process Escape, 2014, JPL, Lesson Number 11501, <https://llis.nasa.gov/lesson/11501>.
- [3] ECSS, Space Engineering: System Engineering General Requirements, Tech. Rep. ECSS-E-ST-10C, European Cooperation for Space Standardization, 2009.
- [4] W. Kriedte, ECSS: an initiative to develop a single set of European Space Standards, in: W.R. Burke (Ed.), Spacecraft Structures, Materials and Mechanical Engineering, ESA Special Publication, vol. 386, 1996, p. 321.
- [5] ISO/IEC/IEEE, 24748-1:2018 Part 1: Guidelines for Life Cycle Management, in Systems and Software Engineering-Life Cycle Management, International Organization for Standardization, Geneva, 2018.
- [6] What Is the Systems Modeling Language (SysML)? 2019, <https://sysml.org> (Accessed 24 January 2020).
- [7] NASA, NASA Systems Engineering Handbook, revision second ed., National Aeronautics and Space Administration, 2017.
- [8] Guide to the Systems Engineering Body of Knowledge, 2019, <https://www.sebokwiki.org/> (Accessed 24 January 2020).
- [9] Model Based Systems Engineering Wiki, 2019, <http://www.omgwiki.org/MBSE/> (Accessed 24 January 2020).
- [10] wildFIRE Remote Sensing Website, 2018, <https://www.fire-rs.com/en/>.
- [11] HumSAT Project website, 2013, <https://www.humsat.org/>.
- [12] D. Hermida, R. Tubio, HUMSAT Milestones and Documentation Plan, 2010, <https://www.husmat.org/>.
- [13] OED Online, Requirement, n., 2019, Oxford University Press, <https://www.oed.com/view/Entry/163260>.
- [14] NASA, NASA systems engineering processes and requirements, Tech. Rep. NPR 7123.1B, National Aeronautics and Space Administration, 2013.
- [15] ECSS, Space Engineering: Technical Requirements Specification, Tech. Rep. ECSS-E-ST-10-06C, European Cooperation for Space Standardization, 2009.
- [16] D. Hermida, H. Iglesias, J. Iglesias, R. Tubio, HUMSAT Mission Requirements Document, 2010, <https://www.husmat.org/>.
- [17] A. Vazquez, J. Iglesias, R. Tubio, HUMSAT System Requirements Document, 2010, <https://www.husmat.org/>.
- [18] PMI, A Guide to the Project Management Body of Knowledge (PMBOK Guide), sixth ed., Project Management Institute, Newton Square, PA, 2017.
- [19] NASA, NASA Cost Estimating Handbook Version 4.0, National Aeronautics and Space Administration, 2015.
- [20] J. Baik, COCOMO II Model Definition Manual, University of Southern California, 2008.

- 
- [21] R. Valerdi, The Constructive Systems Engineering Cost Model (COSYSMO) (Ph.D. thesis), University of Southern California, 2005.
  - [22] GAO, Agencies need to improve the implementation and use of earned value techniques to help manage major system acquisitions, Tech. Rep. GAO-10-2, US Government Accountability Office, 2009, <https://www.gao.gov/products/GAO-10-2>.
  - [23] GAO, NASA: earned value management implementation across major spaceflight projects is uneven, Tech. Rep. GAO-13-22, US Government Accountability Office, 2012, <https://www.gao.gov/products/GAO-13-22>.

## Further reading

ECSS, Space project management: cost and schedule management, Tech. Rep. ECSS-M-ST-60C, European Cooperation for Space Standardization, 2008.



# Applied astrodynamics



Filippo Graziani<sup>a</sup>, Sergey Trofimov<sup>b</sup>, and Simone Battistini<sup>c</sup>

<sup>a</sup>GAUSS Srl, Rome, Italy, <sup>b</sup>Space Systems Dynamics Department, Keldysh Institute of Applied Mathematics of Russian Academy of Sciences, Moscow, Russia, <sup>c</sup>Department of Engineering and Mathematics, Sheffield Hallam University, Sheffield, United Kingdom

## 1 Introduction

The discipline dealing with engineering applications of celestial mechanics was defined as astrodynamics by Herrick in his renowned book [1]: “It’s an engineer specific skill, since the orbit designer has to evaluate various solutions both for the implementation of an orbit, and for its variations, as well as to determine it and find out the best out of the possible solutions, through a process of optimization.” Many authors [2–8] agree on emphasizing the typical engineering aspect of astrodynamics, as well as the mathematical: “and mathematical-physical aspects of celestial mechanics closer to the astronomy’s domain.” Kaplan defines astrodynamics as “the study of controlled trajectories of artificial satellites,” thus highlighting the close interrelation that such a discipline has with control and implementation.

Astrodynamics is based on the principles of celestial mechanics. It deals with the study of the dynamics of man-made vehicles, playing with maneuvers and control techniques to achieve specific mission goals. In this way, astrodynamics fulfills the important task of integrating many heterogeneous—yet closely related—elements, such as, for instance, orbit, stability, control, propulsion, and systems. In the past, the definition of space flight dynamics was used, although orbiting bodies move in *free fall* rather than defeating gravitational pull/attraction due to aerodynamic forces. There is still a certain amount of resistance to the name astrodynamics. It is preferable to leave the ascent stage (more properly the subject of launcher flight mechanics) and the reentry phase to the discipline of space flight dynamics, and to assign to astrodynamics the study of dynamics and orbital control and stability/attitude of those vehicles whose sustenance/airworthiness does not necessarily depend on the atmosphere.

The main objectives of astrodynamics are

- Mission analysis, with the study of optimum flight paths and of maneuvers and control techniques, both active and passive, orbital and positioned, to produce them (acquisition and maintenance).
- The study of guidance, navigation, and control systems.
- Orbit and position determination for spacecraft/aerospace vehicles (satellites and probes).
- Orbital propagation for determining the ephemeris of spacecraft/aerospace vehicles.

Moreover, the methodology used to study astrodynamics problems has two different approaches: one is more mathematical and the other is an *engineering approach* that

allows to *see* the practical results besides being able to formulate them. Applied astrodynamics is therefore a transition from theory to practice in the field of astrodynamics. This chapter aims to present both approaches, while keeping an eye on the peculiarities of CubeSat missions. In fact, if the classical formulation of the two-body problem does not change from one kind of satellite to another, other aspects like perturbations can be characterized to the case of CubeSats. Moreover, advanced astrodynamics addressing low-thrust trajectories are gaining more relevance nowadays for the implementation of interplanetary CubeSat missions.

This chapter is organized as follows: the basics of classical astrodynamics, including the two-body problem, and the definition of orbits are presented in [Section 2](#); the effect of the most relevant environmental perturbations for CubeSat missions are summarized in [Section 3](#); and a selection of advanced topics in astrodynamics, such as gravity assist (GA) maneuvers and invariant manifolds, is presented in [Section 4](#).

## 2 Principles and laws of astrodynamics

The motion of the planets was deduced by Kepler through several observations carried out by the Danish astronomer Tycho Brahe. The empirical laws describing the motion of the planets, called Kepler laws, can be summarized as:

1. The orbits of the planets are ellipses and the Sun is at one focus.
2. The areas swept by the vector going from the Sun to a planet are proportional to the time necessary to cover/ride them.
3. The squares of the periods necessary for the planets to go through their orbits are proportional to the cube of the major semiaxis.

Kepler's laws were formulated at the beginning of the 17th century based on astronomical observations. A few decades later, Newton developed the mathematical model that supported Kepler's deductions. The basis of this model are the laws of classical mechanics, which can be summarized in the relation:

$$\vec{F} = m \vec{a} \tag{1}$$

where acceleration is considered as an effect of the force causing motion, contrary to Aristotelic physics. The classical formulation of the two-body problem made by Newton assumes a very simple model for the gravitational field of the Earth, yet it reasonably approximates the main features of the orbital motion of a spacecraft in many circumstances. The trajectories obtained with this model follow Kepler's laws and are periodic and return to the same point every period: they are called orbits.

Taking into account the effects, called perturbations, of the other relevant forces in the orbital model gives a more complete representation of the motion of a spacecraft and, at the same time, allows to better design the mission. In this section, it will be shown how to derive a basic description of orbits from the principles of physics and mechanics.

## 2.1 The two-body problem

The fundamental law of dynamics expressed in Eq. (1), also called law of inertia, is identical in all references and moves by uniform rectilinear motion with respect to the *fixed stars*. Infinite references (Cartesian sets of three) then exist, equivalent to whom the law of inertia is applicable. The force  $\vec{F}$ , which characterizes astrodynamics, is the force due to Newton's law of universal gravitational attraction exchanged by two bodies with masses  $m$  and  $M$  placed at a distance  $r$ :

$$\vec{F} = \frac{GmM}{r^2} \quad (2)$$

where  $G$  is the universal gravitational constant. The constant of proportionality between force and acceleration in Eq. (1) is called inertial mass, while the mass in the expression of the gravitational law Eq. (2) is called gravitational mass. The principle of equivalence states that the ratio between inertial mass and gravitational mass is identical for all bodies, so the inertial mass can be considered equal to the gravitational mass. It follows that the motion of material bodies in free fall is independent of their composition and structure as was highlighted by Galilei through the famous experiments "thought of, but not carried out" throwing different objects (lead and feather) out of Pisa's tower and noticing that they touched the ground at the same moment. Therefore the motion of material bodies subjected only to the gravitational force (Eq. 2) does not depend on their mass.

The so-called two-body or Kepler's problem is the study of the motion of a spacecraft with mass  $m$  around a celestial body with mass  $M$  ( $m \ll M$ ), assuming a spherically symmetric gravitational field centered in the celestial body and no other forces acting on the system. The acceleration  $\ddot{\vec{r}}$  of the spacecraft due to the gravity force  $\vec{F}_g$  is found by Newton's law of gravity in what is called the equation of motion of a spacecraft:

$$\frac{d^2 \vec{r}}{dt^2} = \frac{\vec{F}_g}{m} = -\frac{GM}{r^3} \vec{r} = -\frac{\mu}{r^3} \vec{r} \quad (3)$$

where  $\mu$  is the gravitational parameter (depending on the mass of the celestial body) and  $\vec{r}$  is the vector from  $M$  to  $m$ . Another important quantity to be defined is the angular momentum  $\vec{h} \equiv \vec{r} \times \frac{d\vec{r}}{dt}$  of the orbit, which is constant since

$$\vec{r} \times \frac{d^2 \vec{r}}{dt^2} = \vec{r} \times \frac{d^2 \vec{r}}{dt^2} + \frac{d\vec{r}}{dt} \times \frac{d\vec{r}}{dt} = \frac{d}{dt} \left( \vec{r} \times \frac{d\vec{r}}{dt} \right) = \frac{d\vec{h}}{dt} = 0 \quad (4)$$

This result shows that, at every time instant, the position and velocity vectors lie on the same plane, the *orbital plane*, with the angular momentum being perpendicular to it. Therefore the trajectory of the satellite is planar and lies always in the orbital plane.

The equation of motion can be further managed to obtain an insight into the shape of the orbit. Taking the cross-product with the angular momentum yields

$$\vec{h} \times \frac{d^2 \vec{r}}{dt} = -\frac{\mu}{r^3} \vec{h} \times \vec{r} = -\frac{\mu}{r^3} \left( \vec{r} \times \frac{d\vec{r}}{dt} \right) \times \vec{r} = -\mu \frac{d}{dt} \left( \frac{\vec{r}}{r} \right) \quad (5)$$

Integrating the left- and right-hand site of the equation yields

$$\vec{h} \times \frac{d\vec{r}}{dt} = -\mu \frac{\vec{r}}{r} - A \quad (6)$$

where  $A$  is a vector constant of the integration depending on the initial position and velocity. Taking the scalar product by  $r$  results in

$$\left( \vec{h} \times \frac{d\vec{r}}{dt} \right) \cdot r = -\mu \frac{\vec{r}}{r} \cdot r - A \cdot r \quad (7)$$

Using the property  $(a \times b) \cdot c = -(c \times b) \cdot a$  and defining the *true anomaly*  $\nu$  as the angle on the orbital plane between  $\vec{r}$  and  $A$ , an equation for the position of the satellite is obtained:

$$h^2 = \mu r + A r \cos \nu \quad (8)$$

$$r = \frac{p}{1 + e \cos \nu} \quad (9)$$

where  $p \equiv h^2/\mu$  is a geometrical constant called the semilatus rectum of the orbit and  $e \equiv A/\mu$  is another constant called the eccentricity. This expression of the position of the satellite corresponds to the general equation of a conic section in polar coordinates, suggesting that the orbital trajectory in the two-body problem is always a conic section.

Depending on the value of  $e$ , the orbit will be a closed or an open trajectory. The type of conic section according to the value of  $e$  is described in [Table 1](#).

**Table 1** Conic sections of an orbit.

Eccentricity	Conic section	Open/closed trajectory
$e = 0$	Circle	Closed
$0 < e < 1$	Ellipse	Closed
$e = 1$	Parabola	Open
$e > 1$	Hyperbola	Open

## 2.2 Energy and orbital period

Eq. (4) can be used to find a relationship between the velocity and the radius of the orbit. Dot multiplying Eq. (1) by  $\frac{d\vec{r}}{dt}$  yields

$$\begin{aligned} \frac{d\vec{r}}{dt} \cdot \frac{d^2\vec{r}}{dt^2} &= -\frac{\mu}{r^3} \frac{d\vec{r}}{dt} \cdot \vec{r} \\ \frac{1}{2} \frac{d}{dt} (\dot{\vec{r}} \cdot \dot{\vec{r}}) &= -\frac{\mu}{r^3} (\dot{\vec{r}} + \vec{\omega} \times \vec{r}) \cdot \vec{r} \\ \frac{1}{2} \frac{d}{dt} (v^2) &= -\frac{\mu}{r^2} \dot{r} \\ \frac{1}{2} \frac{d}{dt} (v^2) &= \frac{d}{dt} \left( \frac{\mu}{r} \right) \\ \frac{1}{2} v^2 - \frac{\mu}{r} &= \text{const} \end{aligned} \quad (10)$$

The constant obtained by the integration in the last equation is the specific mechanical energy  $E$  associated with the orbital motion. The two terms, in fact, correspond to the kinetic and potential energy of the satellite, respectively:

$$E = \frac{1}{2} v^2 - \frac{\mu}{r} \quad (11)$$

## 2.3 Keplerian elements

As explained in the previous section, in the two-body problem formulation the orbit of a spacecraft around a celestial body is a planar trajectory completely determined by the position and velocity vectors. Another way of representing orbits is through the use of six quantities, called *Keplerian* or *orbital elements*. Since the dimension of this vector of orbital elements is equal to the dimension of the position and velocity vectors, the two representations are equivalent. The advantage of using the orbital elements is that they allow a prompter visualization of the orbit of a satellite rather than the position and velocity vectors.

There exist different sets of elements, the most classical being composed by

1. *Semimajor axis*  $a$  of the orbit.
2. *Eccentricity*  $e$  of the orbit.
3. *Inclination*  $i$  of the orbital plane with respect to a reference plane, e.g., the equatorial plane.
4. *Longitude of the ascending node*  $\Omega$ , the angle in the reference plane between the intersection with the orbital plane (*line of nodes*) and the first axes of the coordinate system centered in the celestial body.
5. *Argument of periapsis*  $\omega$ , the angle in the orbital plane between the line of nodes and the periapsis point.
6. *Time of periapsis passage*  $t$ .

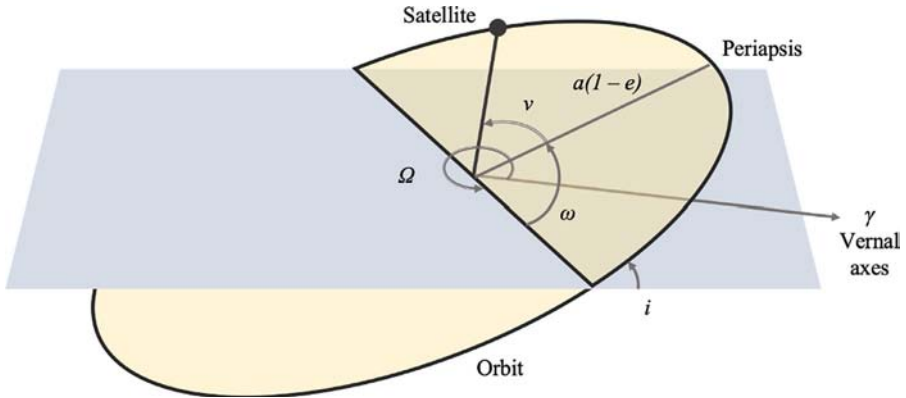


**Fig. 1** Keplerian elements.

The first two parameters define the size and shape of the orbit;  $i$ ,  $\Omega$ , and  $\omega$  define its orientation in space; and the sixth parameter defines the position of the spacecraft along the orbit. While it is always possible to calculate position and velocity vectors from the Keplerian elements, the reverse might not be feasible in some cases. For example, for circular orbits,  $\omega$  is not defined and the calculation of  $e$  might cause numerical problems (Fig. 1).

## 2.4 Orbit classification

The definition of the orbital elements given in the previous section allows a taxonomy for orbits to be defined. In fact, orbits can be classified in accordance with their altitude (related to the semimajor axis  $a$ ), eccentricity, and inclination. The Earth orbits whose maximum distance from the center of mass of the Earth is smaller than 2000 km are called low Earth orbits (LEO); medium Earth orbits (MEO) are between 2000 and 20,000 km; and high Earth orbits (HEO) are those above 20,000 km. Classification according to eccentricity distinguishes among closed and open orbits: circular ( $e=0$ ) and elliptical ( $0 < e < 1$ ) orbits are closed trajectories, while parabolic ( $e=1$ ) and hyperbolic ( $e > 1$ ) orbits are open trajectories that can escape the gravitational pull of the celestial body. Finally, according to the inclination, orbits can be defined as equatorial ( $i = 0$  degrees) or polar ( $i = 90$  degrees).

Combining some of these characteristics yields some of the most important orbits. The orbits with a period equal to a sidereal day are called geosynchronous. Geostationary orbits are geosynchronous circular orbits with zero inclination. A geostationary satellite will appear fixed in the sky to an observer on the Earth and this is why these orbits are used for important telecommunication missions.

CubeSats are not likely to be launched in geostationary orbits, but most of them have been launched in another kind of synchronous orbit, called the Sun-synchronous orbit. In a Sun-synchronous orbit the orbital plane rotates to maintain a constant orientation with respect to the Sun through the year ( $\dot{\Omega} = 360$  degrees/year), as shown in Fig. 2. At every time of the year (points 1, 2, and 3), the spacecraft will pass over the

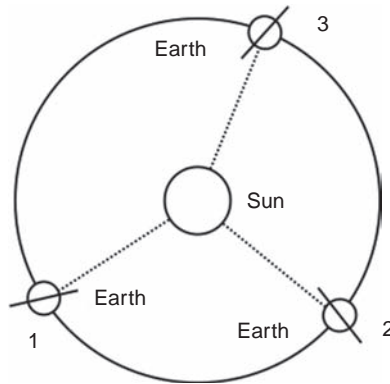


**Fig. 2** Orientation of the orbital plane in a Sun-synchronous orbit.

Earth always at the same local solar time. This is very important for remote sensing missions, because at each passage the Earth surface is in similar lighting conditions. The rotation of the orbital plane (*precession*) can be obtained at no cost by exploiting the  $J_2$  perturbation (see next section). To do so, a precise combination of altitude and inclination is required. For low orbits, the most accessible for CubeSats, the resulting inclination is near 90 degrees. As a result of this, a satellite in a low Sun-synchronous orbit spans across the entire surface of the Earth many times per day, with many opportunities for contact with ground stations. This is fundamental, especially if there is a single station that can operate the spacecraft, as in the case of many university missions.

### 3 Perturbations

A perturbation is a variation of the force model assumed in the unperturbed Keplerian motion. Apart from the gravitational force, in fact, other actions also contribute to determine the motion of a satellite, such as aerodynamic forces and interactions with space radiations. Even the assumptions made on the gravitational field are not adequate to describe the real situation: first of all, the spacecraft and the celestial body are not an isolated system. There are other bodies (e.g., Earth, Sun, Moon, and so on) that contribute to create the gravitational field in which the spacecraft's motion takes place; furthermore, the actual gravitational field of each of these bodies is quite complex, rather than spherically homogeneous.

The perturbed orbits could depend on the mass of the body, therefore a difference between a CubeSat and a larger satellite could exist. This section will deal with the perturbations that are most relevant for CubeSat missions, such as the anomalies of the Earth gravitational field and the atmospheric drag. These actions are typically more relevant at low altitudes, where most of the CubeSat missions take place.

### 3.1 Anomalies of the Earth gravitational field

The Earth is not a perfect sphere and its mass is not homogeneously distributed inside it. Some portions of the Earth are more *massive*, and some are less. This is the reason why the Earth gravitational field is not uniform in intensity and direction. A realistic model for the Earth gravitational field is derived through the gradient of the gravity potential  $\vec{U}$ :

$$\ddot{\vec{r}} = \nabla \vec{U}, \quad \vec{U} = GM \frac{1}{r} \quad (12)$$

Since  $\vec{U}$  depends on the mass density inside the Earth, it can be described as a function  $U(\varphi, \lambda, r)$  of the latitude  $\varphi$ , the longitude  $\lambda$ , and the distance from the center of the Earth  $r$ . The mass  $M$  in the potential can be calculated taking the integral of the density over the entire volume of the Earth by using a series of Legendre polynomials to expand the integral. The result is a sum of elements depending on  $\varphi$ ,  $\lambda$ , and  $r$  multiplied by coefficients depending on the mass distribution. The potential can be written as:

$$U = \frac{GM}{r} \sum_{n=0}^{\infty} \sum_{m=0}^n \frac{R^n}{r^n} P_{nm}(\sin \varphi) (C_{nm} \cos m\lambda + S_{nm} \sin m\lambda) \quad (13)$$

where  $P_{nm}$  is the Legendre polynomial of degree  $n$  and order  $m$ , and  $C_{nm}$  and  $S_{nm}$  are two coefficients that depend on the planet's internal mass distribution.

The gravitational potential is therefore an infinite sum of terms, each one describing a specific mass distribution model for the planet. For example, the first term of the series expansion is the potential associated to a perfectly spherical mass distribution, which is the same gravity acceleration considered in the two-body problem. The other terms of the series expansion represent *zonal* (varying with  $r$  and the latitude  $\varphi$ ), *sectorial* (varying with  $r$  and the longitude  $\lambda$ ), and *tesseral* (varying with  $r$ ,  $\lambda$ , and  $\varphi$ ) harmonics. The most relevant among these harmonics is the zonal harmonics of order 2, associated with Earth's *flattening*  $f$ , i.e., the Earth's radius at the equator being circa 20km wider than the radius at the poles. This corresponds to  $S_{20} = 0$  and a coefficient  $C_{20} = -0.00108$  in the series expansion. This perturbation is also known as  $J_2$ , from the symbol used to identify the zonal coefficient  $J_2 = -3/2C_{20} = 0.00162$ . Other zonal harmonics of higher order are numerically less relevant.

The effects of the  $J_2$  perturbation are mainly on  $\Omega$  and  $\omega$ . The extra mass at the equator produces an extra gravitational pull in the equatorial plane, which causes a precession of the orbit angular momentum. Depending on the altitude and the inclination of the orbit, the ascending node is shifted in the opposite direction of flight. The nodal regression rate caused by  $J_2$  can be used to naturally achieve the necessary  $\dot{\Omega}$  required for a Sun-synchronous orbit without making any maneuver, which is the case of many CubeSat missions. For example, at low altitudes, the orbit shall be almost polar to use the  $J_2$  effect to achieve Sun synchronicity.



The effect of  $J_2$  on  $\omega$  is a shift in the orbit perigee, depending on the altitude and the inclination of the orbit. The apsidal rotation can be in the direction of flight or in the opposite direction, depending on the inclination.

### 3.2 Atmospheric drag

A spacecraft in low altitude orbit experiences an aerodynamic force due to the interaction between the atmosphere and the spacecraft surface. The main component of this force is the aerodynamic drag, while other components like lift force are usually negligible. The atmospheric drag is a force in the opposite direction to the spacecraft velocity  $v$ . The resulting acceleration  $\ddot{\mathbf{r}}_{\text{drag}}$  is defined as:

$$\ddot{\mathbf{r}}_{\text{drag}} = -\frac{1}{2}\rho\frac{A}{m}v^2C_D\hat{\mathbf{v}} \quad (14)$$

where  $\rho$  is the atmospheric density (exponentially decreasing with the altitude),  $A$  is the spacecraft cross-sectional area,  $m$  is the spacecraft mass, and  $C_D$  is the drag coefficient. The primary effect of this perturbation is a decrease in the total energy of the satellite (nonconservative force). The force is opposed to the motion and makes the orbit's semimajor axis decrease. As a consequence, the orbital velocity increases (drag paradox). The increased speed further increases the value of drag, making the spacecraft spiral down. For elliptical orbits, the trajectory first becomes circular and then the orbital radius is reduced. The variation of the semimajor axis is

$$\dot{a} = -\frac{2a^2}{\mu}\ddot{\mathbf{r}}_{\text{drag}}mv \quad (15)$$

The atmospheric drag is very relevant for Earth orbits up to 1000 km, which are the most common for CubeSat missions. Above this altitude, the atmospheric drag can be neglected as other perturbations have more significant effects. Atmospheric drag can also be used in the approach to a generic celestial body with atmosphere to circularize the orbit. This concept, called aerobraking, is further described in [Section 4.1](#).

The main consequence of atmospheric drag on a CubeSat mission is that of reducing the orbit lifetime. This is essential to respect the 25-year rule on spacecraft lifetime, which otherwise will be difficult to meet for CubeSats. Orbital decay due to atmospheric drag can be compensated with on-board propulsion systems. These aspects are dealt with in other chapters of this book and therefore will not be discussed further here.

Nevertheless, it is evident that the effects of atmospheric drag on the orbit need to be estimated during the mission design phase. This might be particularly difficult, because the variation of  $a$  depends on factors like the atmospheric density, the cross-sectional area, and the drag coefficient. The atmospheric density is estimated using atmospheric models, like the Harris-Priester density model [9] or the Jacchia density model [10], which of course are affected by errors and approximations.

The cross-sectional area depends on the attitude of the spacecraft at each instant. Since the time interval to be considered is quite large,  $A$  will vary and in general cannot be a priori predicted. Therefore an average value is used for the computation. The drag coefficient depends on the materials employed in spacecraft realization and the composition of the atmosphere and is therefore difficult to determine too. Even in this case, a reference value (usually around 2.2) can be adopted.

## 4 Leveraging natural dynamics in interplanetary missions

Among the critical challenges for micro- and nanosatellite interplanetary missions, propulsion is probably the most difficult since further technology advancement is physically limited by mass and energy constraints. It is therefore very important to maximally exploit a broad range of natural dynamical effects if a CubeSat-like spacecraft cannot be delivered directly to the nominal orbit around the target celestial body.

All the dynamical effects can be divided into two large groups depending on what type of fundamental interaction, gravitational or electromagnetic, underlies the effect. The first group effects can in turn be roughly split into two subgroups: those primarily based on two-body dynamics (the Oberth effect, GA maneuvers, resonant encounters) and essentially non-Keplerian phenomena commonly described by dynamical systems theory. The mechanisms and techniques of using solar radiation pressure and solar wind—such as solar sailing and electric sailing, respectively—comprise the second group. The gravitational dynamical effects are outlined next, with emphasis on their possible applications in CubeSat interplanetary missions.

### 4.1 GA maneuvers

The mechanism of GA maneuvers to reach a planet or a small body is conventional regardless of the spacecraft mass and size. For an unpowered (i.e., applying no thrust) GA maneuver, the intermediary's gravity field deflects the trajectory of a spacecraft entering its sphere of influence by an angle  $\beta$  related to the hyperbolic excess velocity  $V_\infty$  and the fly-by distance  $r_\pi$  (from the intermediary's center of mass) according to the formula:

$$\beta = 2 \sin^{-1} \frac{\mu}{\mu + V_\infty^2 r_\pi} \quad (16)$$

The magnitude of the change in spacecraft heliocentric velocity after performing a GA maneuver can be calculated as follows:

$$\Delta V = 2V_\infty \sin \frac{\beta}{2} = \frac{2\mu V_\infty}{\mu + V_\infty^2 r_\pi} \quad (17)$$

The maximum velocity value attained is  $V_{\max} = 2\sqrt{\mu/r_\pi}$  if  $V_\infty^2 = \mu/r_\pi$ . The largest achievable  $\Delta V$  amounts to more than 30 km/s as a result of a GA maneuver near Jupiter

for a spacecraft with radiation-hardened components. In a CubeSat mission, however, it can hardly exceed 15 km/s due to safety restrictions on the minimum fly-by distance. To obtain a higher  $\Delta v$  than the one generated by the GA, one could also consider an orbital maneuver performed at the periapsis of the orbit, where the energy gain is maximum. This is a consequence of the fact that the deeper a spacecraft is in the gravity well, the more efficient the propulsive force is. This effect, sometimes called the Oberth effect, is explained in further detail in [Chapter 13](#) dedicated to Orbit Determination and Control.

To determine the feasible chains of intermediate GA maneuvers for multiple GA trajectories to a target celestial body, various analytical and semianalytical techniques have been developed. The most famous one is the Tisserand graph [11, 12]. It is based on the concept of Tisserand's parameter, a specific invariant combination of spacecraft orbital elements remaining constant after close encounter with an intermediary. Assuming the motion is planar, one can plot Tisserand's parameter contour lines on the plane periapsis distance versus orbital period. In some cases, it appears more convenient to use the plane periapsis distance versus apoapsis distance. The contour lines for different intermediaries (planets or moons) are then combined on a single plot—the Tisserand graph. The intersections indicate the potential feasibility of corresponding sequences. For essentially 3D spacecraft motion, the more complicated  $V_\infty$  globe-mapping technique is used [13].

Upon choosing a sequence of GA maneuvers, the trajectory optimization problem is then solved. During the past several decades, many automated trajectory design and/or optimization tools have been developed. Some of the tools have a built-in function of generating the optimal sequence. Various heuristic global optimization procedures are often used. An excellent review of the approved tools with their detailed descriptions can be found in Ref. [14].

The patching of two arcs before and after a GA maneuver can be improved by adding an impulse or a low-thrust arc during the intermediary fly-by. Such a GA maneuver is called “powered.” The resulting hyperbola-to-hyperbola transfer problem was solved by Gobetz [15] who considered both optimal and periapsis single-impulse transfers. The latter, being easily calculated, are usually just slightly less efficient than the former. It is therefore this kind of powered GA maneuver that is available in most of the trajectory design tools. However, it is recommended not to include such an option in a CubeSat mission since it reduces the overall reliability by increasing the influence of GA maneuver execution errors and trajectory determination uncertainties.

It is also worth mentioning another extension of GA maneuvers: aerogravity assist (AGA) maneuvers [16–19]. For high lift-to-drag ( $L/D$ ) ratio spacecraft, such as the so-called waveriders [20], the AGA maneuver gives an opportunity to bypass the otherwise unavoidable constraint on the turn angle resulting from the minimum fly-by distance limitations. This can be achieved by exploiting the negative lift force acting upon a waverider in the planet's atmosphere. Such a mechanism artificially increases the spacecraft weight and allows it to glide in the atmosphere at almost constant altitude for a much longer time as compared to a conventional GA maneuver. Bunches of efficient trajectories to the outer planets [18] and to the main belt asteroids [17] have

been found. Similar to conventional GA maneuvers, AGA maneuvers near Venus can be effectively used for energy pumping, whereas Mars is best suited to perihelion changing [19].

One more promising application of the planet's atmosphere, the aerobraking effect, is available if the planet is the final destination. A spacecraft with low  $L/D$  ratio, being captured by the planet's gravitational field, can transfer from the initial highly elliptical orbit to the target near-circular low orbit by performing a series of fly-bys. The drag force described in the previous section can be exploited near the periapsis to gradually decrease the apoapsis altitude. This technique has been successfully tested in many missions near the Earth (Hiten, 1991), Mars (Mars Global Surveyor, 1997; Mars Odyssey, 2001; Mars Reconnaissance Orbiter, 2006), and Venus (Magellan, 1993; Venus Express, 2014). Unlike the aerocapture maneuver [21, 22] or skip reentry [23], aerobraking does not require superior thermal protection and is theoretically affordable for micro- and even nanosatellites equipped with deployable solar panels or a drag sail. To reduce the navigation-related risk, the use of autonomous closed-loop guidance, navigation, and control algorithms is recommended [24].

## 4.2 Resonant encounters

Consecutive GA maneuvers performed near the same intermediary are called resonant encounters. To ensure a series of resonant encounters near a planet or a moon, mid-course maneuvers (referred to as deep-space maneuvers, DSMs) are inserted into a heliocentric or, respectively, planetocentric arc of the trajectory. The efficiency of resonant encounters with a celestial body well suited for GA maneuvers was first revealed in the mid-1970s when the so-called  $\Delta V$ -EGA maneuver—a series of GA maneuvers near the Earth—was discovered [25]. Later on, the term  $V_\infty$  leveraging maneuver (VILM) was coined for the corresponding DSM, and a solid theory has been developed [26, 27]. VILMs are performed when the spacecraft is at either the apoapsis (an exterior VILM) or the periapsis (an interior VILM) of its orbit. The magnitude of a VILM is relatively small but is enough for a significant increase/decrease in  $V_\infty$ .

Resonant encounters and VILMs are particularly powerful tools in planetary moon tours, including the final phase of any tour, the endgame [28–30]. Basically, the endgame is a transfer to the target low orbit around the final destination moon. The complexity of the endgame phase consists of minimization of the fuel cost required for capture and lowering the orbit. In the patched conic approximation, the purely ballistic endgame with multiple fly-bys cannot lead to the decrease of the arrival speed  $V_\infty$  (the ballistic endgame paradox [29]). Therefore the use of VILMs is essential.

## 4.3 High-altitude fly-bys

The endgame design problem serves as an excellent example of modern trends in astrodynamics where the circular restricted three-body problem (CR3BP) model became dominant and, in many instances, replaced the patched conic approximation. The superiority of the CR3BP approach is explained by the fact that it reveals additional trajectory design opportunities undetectable when considering patched conics.

One of these opportunities is a high-altitude (distant) fly-by. In contrast to a conventional GA maneuver, the spacecraft “encounters” a planet/moon outside its sphere of influence. Such a low-energy encounter is impossible within the patched conic framework because it corresponds to the case  $V_\infty^2 < 0$ . Though a series of high-altitude fly-bys followed by lunar ballistic capture was utilized in the SMART-1 mission implemented as early as in 2003, a comprehensive theoretical basis for this technique was developed several years later [29, 31–36]. When applied to the endgame problem, high-altitude resonant encounters allow the ballistic endgame paradox to be solved. The elegant unified endgame theory extends the classic Tisserand graph to what is called the Tisserand-Poincaré graph [29], a convenient tool for efficient moon tour design [37].

Even more important are high-altitude resonant fly-bys for low-thrust transfers to the Moon similar to the SMART-1 spiral trajectory. Properly adjusted, distant lunar encounters are capable of saving much fuel by significantly increasing the geocentric orbit perigee [38, 39]. This is one of the most promising options for a piggyback CubeSat injected into either a low-Earth or the geostationary transfer orbit [40].

#### 4.4 Weak stability boundaries and ballistic capture

The CR3BP model gives rise to a new type of transfer trajectory: low-energy trajectory. The action of a third body allows a spacecraft to arrive at the destination planet/moon with lower launch energy and fuel expenses. Probably the first example of a low-energy trajectory is the transit trajectory to the Moon suggested by Conley [41]. It terminates with lunar capture that does not require any insertion maneuver: the spacecraft-Moon Keplerian energy naturally changes sign from plus to minus due to the gravitational perturbation of a highly elliptical near-Earth orbit. This is what Belbruno later called ballistic capture [42, 43]. In contrast to capture by means of propulsion, ballistic capture has proved to be temporary. It is therefore also referred to as weak.

To study low-energy trajectories in the three-body or even four-body system (e.g., Earth-Moon-Sun-spacecraft), Belbruno introduced an extension of the sphere of influence concept, termed a weak stability boundary (WSB) [42, 43]. The original algorithmic definition of the WSB as a boundary of the region in the configuration space where the spacecraft motion about one of the massive celestial bodies is stable (i.e., the spacecraft makes at least one revolution about this body) was subsequently supplemented with a more general and rigorous analytic definition [32, 33]: the extended WSB of a body is set in the phase space lying in the intersection of a given Jacobi integral hypersurface and the hypersurface of zero Keplerian energy (relative to the body in hand). In the planar CR3BP case, Poincaré map and Keplerian (periapsis) map analysis reveal the chaotic nature of ballistic capture and its close connection with the WSB and transitions between the resonant orbits. The resonance hopping theory [29, 31–36], mentioned earlier as applied to high-altitude resonant encounters, treats resonant transitions as hops in the chaotic “sea” surrounding the stable resonance “islands.” The intrinsic link between the WSB and the stable invariant manifolds

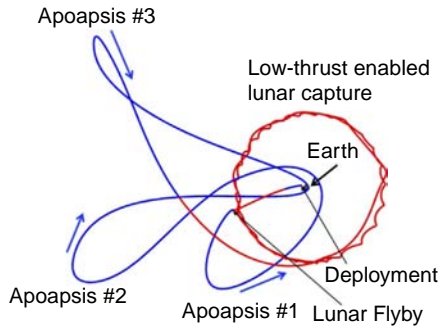


**Fig. 3** The baseline Lunar IceCube trajectory [46]. Coast arcs are indicated by blue (dark gray in print version); low-thrust arcs are red (light gray in print version). The figure is plotted in the Sun-Earth rotating frame. The Sun is from the left.

associated with libration point orbits has also been discovered [44, 45]. A fruitful field of space manifold dynamics will be addressed in the following subsection.

Among the practical achievements of the WSB theory, one can point out two successful missions to the Moon, Hiten (1991) and GRAIL (2011), designed using the algorithmic WSB definition. When launched toward the Sun-Earth  $L_1$  libration point, a spacecraft experiences the Sun's perturbation force, which deflects the trajectory to the Moon's vicinity, where ballistic capture occurs. A similar idea is used in the Lunar IceCube project. Scheduled for 2020, this groundbreaking CubeSat mission to the Moon includes lunar capture preceded by a low-thrust arc and a long WSB-type transfer phase (Fig. 3).

Low-energy trajectories to the Moon and the Solar System planets, especially those ending with ballistic capture, have many useful benefits and have the only drawback of the long duration of the cruise phase. The benefits include

1. The reduction in  $\Delta V$  required (typically from 10% to 30%).
2. The elimination of the orbit insertion maneuver, usually the riskiest and most expensive in terms of fuel maneuver in the whole mission.
3. Significantly larger launch windows. At the same time, the arrival date can often be fixed for any start date from the launch window.

All these advantages become increasingly important for low-cost and medium-cost small spacecraft with limited launch opportunities and propulsion capabilities (particularly for piggyback CubeSats with low-thrust propulsion systems).

#### 4.5 Hyperbolic manifolds and interplanetary transport network

The crucial topological entities in the CR3BP model are periodic and quasiperiodic orbits near the collinear libration points (CLPs) and the hyperbolic invariant manifolds, stable and unstable, associated with these orbits. Among all five relative equilibria in the rotating (synodic) reference frame, the CLPs, denoted by  $L_1$ ,  $L_2$ , and  $L_3$  (Fig. 4), are unstable for any mass ratios  $m_2/m_1$  of the primaries. The phase space in the

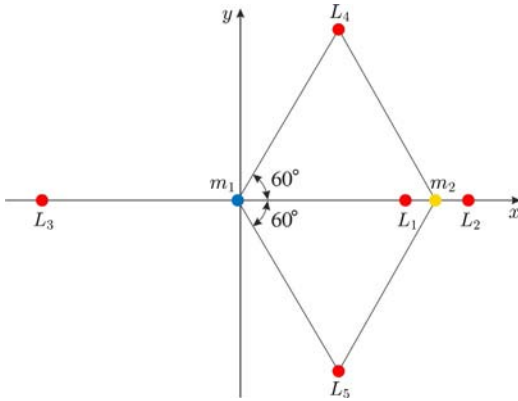


**Fig. 4** Libration points as relative equilibria in the CR3BP dynamical model.

close vicinity of CLPs is of saddle  $\times$  center  $\times$  center type. The 4D center  $\times$  center manifold is formed by (quasi)periodic orbits. The saddle component manifests as two asymptotic trajectories emanating from each point of any unstable (quasi)periodic orbit, one from the stable manifold and another from the unstable manifold (Fig. 5). Hyperbolic invariant manifolds of different libration point orbits in the same

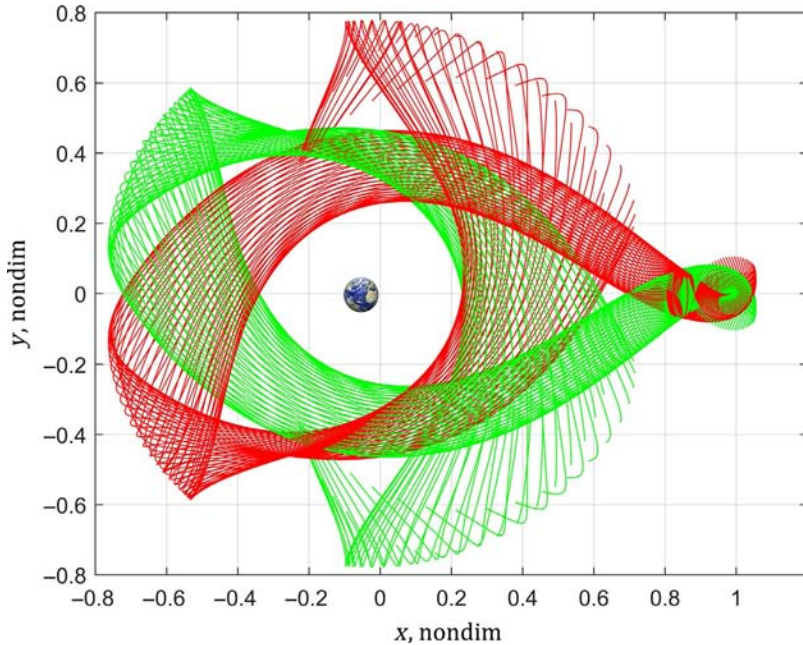


**Fig. 5** Stable [green (light gray in print version)] and unstable [red (dark gray in print version)] invariant manifolds emanating from some  $L_1$  halo orbit in the Earth-Moon system. The Earth is not drawn to scale. The Moon is hidden by hyperbolic invariant manifolds.

three-body system or even different three-body systems can intersect and, similar to ocean currents, serve as a propellant-less deep-space transport mechanism.

A turning point in astrodynamics was marked at the end of the 1990s when, for the first time, dynamical systems theory (in particular, invariant manifold dynamics) was applied to the mission design [47, 48]. Based on early fundamental investigations [41, 49], the space manifold was soon developed and successfully exploited in designing the Genesis mission [50, 51]. The summit of the manifold approach success was probably the proposed idea of the so-called Petit Grand Tour between the Jovian moons [52–54] and the most remarkable discovery—the existence of the vast Solar System network consisting of stable and unstable invariant manifolds of the planets and their moons, called the Interplanetary Superhighway (IPS) [55], or Interplanetary Transport Network (ITN) [56]. Chaotic regions close to collinear libration points play the role of “portals” to the “tunnels” confined by hyperbolic manifold “walls.” For the outer planets, the stable and unstable manifolds of any two neighboring planets intersect, allowing a spacecraft to migrate across the Solar System with little or no fuel.

To the present day, astrodynamists all over the world continue generating a substantial amount of literature related to the design of high-thrust and low-thrust interplanetary transfers augmented with hyperbolic manifold arcs. In the context of CubeSat missions, such trajectories are especially promising provided the short lifetime problem is solved for electronics and propulsion system components.

## References

- [1] S. Herrick, *Astrodynamics*, Van Nostrand Reinhold, New York, 1971.
- [2] V. Szebehely, *Theory of Orbits: The Restricted Problem of Three Bodies*, Yale University, New Haven, 1967.
- [3] P.R. Escobal, *Methods of Orbit Determination*, Wiley, New York, 1965.
- [4] R.H. Battin, *An Introduction to the Mathematics and Methods of Astrodynamics*, Revised ed, American Institute of Aeronautics and Astronautics, Reston, 1999.
- [5] F.T. Geyling, H.R. Westerman, *Introduction to Orbital Mechanics*, Addison-Wesley Aerospace Series, Addison-Wesley, Reading, MA, 1971.
- [6] A.E. Roy, *Astrodynamics*, *Phys. Educ.* 12 (7) (1977) 445–451.
- [7] W.J. Larson, J.R. Wertz, *Space Mission Analysis and Design*, Microcosm, Torrance, 1992.
- [8] M.H. Kaplan, *Modern Spacecraft Dynamics and Control*, John Wiley and Sons, New York, 1976.
- [9] I. Harris, W. Priester, Time-dependent structure of the upper atmosphere, *J. Atmos. Sci.* 19 (4) (1962) 286–301.
- [10] L.G. Jacchia, Revised static models of the thermosphere and exosphere with empirical temperature profiles, SAO Special Report 332, Smithsonian Institution, Astrophysical Observatory, 1971.
- [11] A. Labunsky, O. Papkov, K. Sukhanov, *Multiple Gravity Assist Interplanetary Trajectories*, Earth Space Institute Book Series, Gordon and Breach, London, 1998.
- [12] N.J. Strange, J.M. Longuski, Graphical method for gravity-assist trajectory design, *J. Spacecr. Rocket.* 39 (1) (2002) 9–16.
- [13] N.J. Strange, R.P. Russell, B. Buffington, Mapping the  $V_\infty$  globe, *Adv. Astronaut. Sci.* 129 (2007) 423–446.



- [14] M. Ceriotti, *Global Optimization of Multiple Gravity Assist Trajectories* (PhD thesis), University of Glasgow, Scotland, UK, 2010.
- [15] F. Gobetz, Optimum transfers between hyperbolic asymptotes, *AIAA J.* 1 (9) (1963) 2034–2041.
- [16] L.B. Livanov, Flights to asteroids along energetically optimum courses with perturbational, impulsive, and aerodynamic maneuvers near Venus, the Earth, Mars, and Jupiter, *Kosm. Issled.* 24 (4) (1986) 581–597 (in Russian).
- [17] W.S. Vaning, Mars aeroassist to asteroids (part 1), in: *AAS/AIAA Spaceflight Mechanics Meeting*, Pasadena, CA, USA, 1993.
- [18] J. Sims, J. Longuski, M. Patel, Aerogravity-assist trajectories to the outer planets and the effect of drag, *J. Spacecr. Rocket.* 37 (1) (2000) 49–55.
- [19] W.R. Johnson, J.M. Longuski, Design of aerogravity-assist trajectories, *J. Spacecr. Rocket.* 39 (1) (2002) 23–30.
- [20] M. Lewis, A. McRonald, Design of hypersonic waveriders for aeroassisted interplanetary trajectories, *J. Spacecr. Rocket.* 29 (5) (1992) 653–660.
- [21] S.J. Hoffman, A comparison of aerobraking and aerocapture vehicles for interplanetary missions, in: *AAS/AIAA Astrodynamics Conference*, Seattle, WA, USA, 1984.
- [22] J.L. Hall, M.A. Noca, R.W. Bailey, Cost-benefit analysis of the aerocapture mission set, *J. Spacecr. Rocket.* 32 (2) (2005) 309–320.
- [23] C.W. Brunner, P. Lu, Skip entry trajectory planning and guidance, *J. Guid. Control Dynam.* 31 (5) (2008) 1210–1219.
- [24] M.K. Jah, M.E. Lisano, G.H. Born, P. Axelrad, Mars aerobraking spacecraft state estimation by processing inertial measurement unit data, *J. Guid. Control Dynam.* 31 (6) (2008) 1802–1812.
- [25] G.R. Hollenbeck, New flight techniques for outer planet missions, in: *AAS/AIAA Astrodynamics Conference*, Nassau, Bahamas, 1975.
- [26] S.N. Williams, *Automated Design of Multiple Encounter Gravity Assist Trajectories* (MSc thesis), Purdue University, West Lafayette, IN, USA, 1990.
- [27] J. Sims, J. Longuski, A. Staugler,  $V_\infty$  leveraging for interplanetary missions: multiple-revolution orbit techniques, *J. Guid. Control Dynam.* 20 (3) (1997) 409–415.
- [28] S. Campagnola, R.P. Russell, Endgame problem part 1:  $V_\infty$ -leveraging technique and the leveraging graph, *J. Guid. Control Dynam.* 33 (2) (2010) 463–475.
- [29] S. Campagnola, R.P. Russell, Endgame problem part 2: multibody technique and the Tisserand-Poincaré graph, *J. Guid. Control Dynam.* 33 (2) (2010) 476–486.
- [30] R.C. Woolley, D.J. Scheeres, Application of  $V$ -infinity leveraging maneuvers to endgame strategies for planetary moon orbiters, *J. Guid. Control Dynam.* 34 (5) (2011) 1298–1310.
- [31] S.D. Ross, D.J. Scheeres, Multiple gravity assists, capture, and escape in the restricted three-body problem, *SIAM J. Appl. Dyn. Syst.* 6 (3) (2007) 576–596.
- [32] F. Topputo, E. Belbruno, M. Gidea, Resonant motion, ballistic escape, and their applications in astrodynamics, *Adv. Space Res.* 42 (8) (2008) 1318–1329.
- [33] E. Belbruno, F. Topputo, M. Gidea, Resonance transitions associated to weak capture in the restricted three-body problem, *Adv. Space Res.* 42 (8) (2008) 1330–1351.
- [34] P. Grover, S. Ross, Designing trajectories in the planet-moon environment using the controlled Keplerian map, *J. Guid. Control Dynam.* 32 (2) (2009) 436–443.
- [35] G. Lantoine, R.P. Russell, S. Campagnola, Optimization of low-energy resonant hopping transfers between planetary moons, *Acta Astronaut.* 68 (7–8) (2011) 1361–1378.
- [36] E.M. Alessi, et al., Out-of-plane extension of resonant encounters for escape and capture, in: *Proceedings of the 64th International Astronautical Congress*, Beijing, China, 2013.

- 
- [37] S. Campagnola, B.B. Buffington, A.E. Petropoulos, Jovian tour design for orbiter and lander missions to Europa, *Acta Astronaut.* 100 (2014) 68–81.
- [38] G.D. Racca, et al., SMART-1 mission description and development status, *Planet. Space Sci.* 50 (14–15) (2002) 1323–1337.
- [39] J. Schoenmaekers, Post-launch optimisation of the SMART-1 low-thrust trajectory to the Moon, in: 18th International Symposium on Space Flight Dynamics, Munich, Germany, 2004.
- [40] D. Dichmann, D. Folta, F. Vaughn, J. Parker, Ways to the Moon: trajectory options from Earth GEO transfer orbit to the Moon, in: 2nd International Workshop on LunarCubes, Cocoa Beach, FL, USA, 2013.
- [41] C.C. Conley, Low energy transit orbits in the restricted three-body problem, *SIAM J. Appl. Math.* 16 (4) (1968) 732–746.
- [42] E.A. Belbruno, Examples of the nonlinear dynamics of ballistic capture and escape in the Earth-Moon system, in: AAS/AIAA Astrodynamics Conference, Portland, OR, USA, 1990.
- [43] E.A. Belbruno, J.K. Miller, Sun-perturbed Earth-to-Moon transfers with ballistic capture, *J. Guid. Control Dynam.* 16 (4) (1993) 770–775.
- [44] F. García, G. Gómez, A note on weak stability boundaries, *Celest. Mech. Dyn. Astron.* 97 (2) (2007) 87–100.
- [45] E.A. Belbruno, M. Gidea, F. Topputo, Weak stability boundary and invariant manifolds, *SIAM J. Appl. Dyn. Syst.* 9 (3) (2010) 1061–1089.
- [46] D. Folta, N. Bosanac, A. Cox, K. Howell, The Lunar IceCube mission design: construction of feasible transfer trajectories with a constrained departure, in: 26th AAS/AIAA Space Flight Mechanics Meeting, Napa, CA, USA, 2016.
- [47] B.T. Barden, K.C. Howell, M. Lo, Application of dynamical systems theory to trajectory design for a libration point mission, *J. Astronaut. Sci.* 45 (2) (1997) 161–178.
- [48] M.W. Lo, S. Ross, Low energy interplanetary transfers using invariant manifolds of  $L_1$ ,  $L_2$ , and halo orbits, in: AAS/AIAA Space Flight Mechanics Meeting, Monterey, CA, USA, 1998.
- [49] R. McGehee, Some Homoclinic Orbits for the Restricted Three Body Problem (PhD thesis), University of Wisconsin, Madison, WI, USA, 1969.
- [50] K.C. Howell, B.T. Barden, R.S. Wilson, M.W. Lo, Trajectory design using a dynamical systems approach with application to GENESIS, in: AAS/AIAA Astrodynamics Specialist Conference, Sun Valley, ID, USA, 1997.
- [51] W.S. Koon, M.W. Lo, J.E. Marsden, S.D. Ross, The genesis trajectory and heteroclinic connections, in: AAS/AIAA Astrodynamics Specialist Conference, Girdwood, AK, USA, 1999.
- [52] G. Gómez, W.S. Koon, M.W. Lo, J.E. Marsden, J. Masdemont, S.D. Ross, Invariant manifolds, the spatial three-body problem and space mission design, in: AAS/AIAA Astrodynamics Specialist Conference, Quebec City, Canada, 2001.
- [53] W.S. Koon, M.W. Lo, J.E. Marsden, S.D. Ross, Constructing a low energy transfer between Jovian moons, *Contemp. Math.* 292 (2002) 129–145.
- [54] G. Gómez, W.S. Koon, M.W. Lo, J.E. Marsden, J. Masdemont, S.D. Ross, Connecting orbits and invariant manifolds in the spatial restricted three-body problem, *Nonlinearity* 17 (5) (2004) 1571–1606.
- [55] M.W. Lo, The interplanetary superhighway and the origins program, in: IEEE Aerospace Conference, Big Sky, MT, USA, 2002.
- [56] S.D. Ross, The interplanetary transport network, *Am. Sci.* 94 (3) (2006) 230–237.

# CubeSat missions and applications

2

*Chantal Cappelletti and Daniel Robson*

Department of Mechanical, Materials and Manufacturing Engineering, University of Nottingham, University Park, Nottingham, United Kingdom

## 1 Introduction

The key driving factors behind the worldwide adoption and growth of CubeSats can be approximately summarized as the following:

### 1. Accessibility

Their original intention was to be an educational tool for university student teams; with this platform universities were able to afford the financial costs, development time, and expertise to design, launch, and operate a satellite over the course of a student's degree program. These simplicity and cost-effectiveness factors were achieved by creating a simplified design, using recommended affordable COTS components and accepted specifications and requirements that streamlined various stages of the development cycle such as deployment, structural design, and some verification requirements.

### 2. Standardization

The incidental industry standards came about over time, thanks to CubeSats design specifications such as structural dimensions, deployment mechanisms, and the “stackability” of units. Within the boundary conditions of the design specification, a few engineering solutions became standout options and very quickly became industry standards—such as the PC/104 form factor for electronics and the P-POD common deployment mechanism. These enabled the further streamlining of the development process and mass production of parts and even entire subsystems as COTS products for CubeSats, further reducing costs to developers.

### 3. Entrepreneurship

Over time the result of these net forces led to CubeSats becoming high return-on-investment space platforms, with low start-up or “buy-in” costs (costs referring to monetary costs and resources like time, expertise, equipment, and facilities). This is what enables the CubeSat today to fulfill such a wide variety of roles in such a wide variety of mission scenarios, from a wide variety of developers and customers.

### 4. Technology

Advances in technology have allowed for more miniaturized, distributed autonomous, and higher-performing systems to be flown and more of this flight hardware to become COTS available products. Many areas of this book will detail some of these advances in materials, manufacturing, power, software algorithms, mission architectures (both in space and ground segments), communications, and more besides.

### 5. Community

This spread of experience, technology, facilities, and industry has helped create a boom in services and customers and one that may not have evolved from traditional aerospace industries or practices. Opportunities for customers from less wealthy or less space-invested countries, industries, or research fields have broadened the scope of experiments and

objectives that can be accomplished in space using a CubeSat. A plethora of smaller, more novel, and enterprising companies have formed to fill this niche to support such customers interested in taking their payloads to orbit, regardless of the stage of development—from feasibility consultations to inexpensive launch services. In business terms, this is referred to as a horizontal market (as opposed to “traditional” aerospace vertical markets and industries). This has led CubeSats to sometimes being referred to as a part of NewSpace, Space 4.0, or the “democratization” of Space.

With these key factors driving the spread of CubeSat technology across the world and beyond, we shall explore what was once regarded as an educational “toy” became a dominant force in the NewSpace industry and what roles it may play in the future [1–3].

## 2 Applications

The CubeSat specification by its engineered design and increasingly commonplace use in the space sector has led to CubeSats becoming highly versatile platforms. They can be used to achieve many different mission objectives inexpensively due to their low cost and simple development process and integration into mission architecture. Importantly, their lightweight aspect means they can be assigned as secondary payloads to many different orbits and destinations, and thanks to standardizations such as the P-POD deployment mechanism, with relative ease for the developer and launch service provider [4,5].

Further to this, services, technology, and facilities developed internationally to support this industry—COTS components, CubeSat-specific consultants, and other services—are now enabling opportunities for missions and customers that may have faced difficulty and high costs in developing payloads for traditional spacecraft or platforms or even accessing the space sector at all [1]. To highlight and summarize some of the areas in which CubeSats operate or are under development, the nonexhaustive list in the succeeding text has been compiled:

- **As alternative platforms for space-borne instruments**  
Enhancing traditional satellite roles such as telecommunications, observations of the Earth, and astronomical targets such as the Sun, galaxies, exoplanets, and many more scientific targets.
- **As alternative platforms for space-borne experiments and laboratories**  
Giving life sciences, pharmacology, materials science, radiology, and other fields access to space as an environment.
- **As affordable technology-demonstrator and proof-of-concept platforms**  
Due to their low costs to develop and the possibility to use existing components, CubeSats have found a natural application as in-orbit demonstrators for several kinds of new technologies (solar cells, radio communications systems, and so on) and for demonstrating new mission concepts.
- **As payloads outside of Earth orbit**  
To provide additional measurements or support for mothership spacecraft or to place instruments in advantageous orbits that would otherwise require dedicated launches.

- **The realization of megaconstellations at achievable prices**

The use of universal design specifications and evolved industry standards have encouraged CubeSat components and sometimes entire spacecraft to be easier and cheaper to mass produce, significantly reducing costs in producing many for a constellation. The more spacecraft in a constellation, the more coverage is guaranteed, the greater redundancy is built-in, and the shorter revisit time is available.

## **3 CubeSats enhancing traditional satellite missions and objectives**

This section will analyze how the CubeSats have enhanced the concept of traditional satellite missions related to Earth observation, telecommunications, and astronomy.

### **3.1 Earth remote sensing**

Earth observation (EO) involves the use of either active or passive sensors to collect data related to a variety of different targets on the Earth below, ranging from (quite literally) the depths of the ocean to the highest mountain and beyond to the atmosphere and magnetosphere, as well as the mantle and core. Typically a CubeSat's small size limits the structure available for solar arrays to be mounted, and hence, its power output is limited. This means the majority of EO CubeSats have relied on passive sensors that collect data using the Sun or the Earth itself as the source and observing changes in the spectra received as it interacts with various parts of the atmosphere or surface [1]. As will be discussed later in [Section 7](#), CubeSats' affordability and ease of mass production encourage their use in constellations, which greatly improves the quality of data returned for EO missions.

ExoCube is one example of the CubeSat specification being used as a platform to support dedicated Earth observation science. This 3U launched in January 2015 measured the density of hydrogen, helium, nitrogen, and oxygen in the Earth's exosphere, in addition to characterizing the ion density above various ground stations [6]. As a CubeSat, it was capable of supporting all the instruments required for this and proved that such miniaturization is feasible for a CubeSat-sized platform. Other examples of EO missions are reported in [Table 1](#).

### **3.2 Telecommunications**

CubeSats have taken a prominent role in demonstrating in orbit technologies for telecommunications since their earliest years. Arguably out of necessity, increasingly miniaturized communication technologies are demanded for CubeSats, as it is often the downlink bandwidth that limits the science data return rather than the payload instrument's capability—which typically generates more data than can be downlinked from a CubeSat [1]. CubeSats' affordability and commonplace use of industry standards ensure that any new developments tested on board have a more streamlined

**Table 1** Examples of Earth observation CubeSat missions.

Spacecraft, size, and launch	Organizations involved	Mission description
ExoCube, 3U, 2015	California Polytechnic State University [6]	Uses an Ion and Neutral Mass Spectrometer (INMS) to characterize the densities of various elements and ions in the Earth’s exosphere and ionosphere
ANGELS, 12U, 2019	CNES and Hemeria [7]	Carries the newest version of “Argos” tracking payloads, which currently are on a constellation that locates and tracks beacons tagged onto animals, ships, and weather buoys
RAVAN, 3U, 2016	NASA [1]	Measures reflected solar and emitted thermal energy from the Earth to more accurately determine radiative forcing
RaInCube, 2018	NASA JPL [1]	A technology demonstration mission to enable Ka-band precipitation radar technologies on a low-cost, quick-turnaround platform (see also Table 2)
SathyabamaSat, 2U, 2016	Sathyabama University [1]	Carries an infrared spectrometer for measuring levels of greenhouse gases and pollutants in the atmosphere

route to becoming marketable components in their own right. Further to this, CubeSats’ regular form, components, and design encourage their ability to be mass produced for constellations that are vital for ensuring near-constant coverage of target ground areas. Representative examples of CubeSats that have demonstrated advanced telecommunications technologies are listed in Table 2.

### 3.3 Astronomy

Most astronomical missions require specific objectives and dedicated instruments that provide impeccably precise, restricted data about unique astronomical bodies—the Sun, planets and moons, distant galaxies, black holes, and exoplanets, to name a few. It is often impossible to construct payloads that can be applicable to multiple types of targets; hence, often dedicated satellites are required for each payload or suite of instruments if the customer can afford them. More often a space agency is responsible for operating a larger satellite with a suite of instruments focused on one target type and distributing the data to relevant customers afterward (GAIA, Hubble, SWIFT, Spitzer, etc.). CubeSats however present the opportunity for individual or a consortium of customers to develop a dedicated spacecraft, capable of supporting their unique requirements for specific targets at much lower costs than with previous, larger, standard buses [2].

One such experimental CubeSat dedicated to astronomy was ASTERIA, launched in 2017 by JPL and MIT. ASTERIA was a 6U, exoplanet hunter that operated using

**Table 2** Examples of telecommunications technology related CubeSat missions.

Spacecraft, size, and launch	Organizations involved	Mission description
ISARA, 3U, 2017	NASA/JPL [1]	Proof of concept for a foldable Ka-band reflectarray antenna (integrated into the solar arrays) that would significantly improve downlink bandwidth for small satellites
CQuCoM, 6U, undetermined	University of Strathclyde/ National University of Singapore [8]	An IoD of quantum key distribution for future communication and as a pathfinder for potential future constellations
RaInCube, 6U, 2018	NASA/JPL [1]	Uses the first Ka-band radar from a CubeSat (including deployable antenna dish) that was used to track storm movements
CubeSOTA, 6U, undetermined	NICT/University of Tokyo [9]	This LEO CubeSat seeks to use a GEO satellite as a relay to benefit from its much-improved coverage and link availability while sacrificing some bandwidth
CubeRRT, 6U, 2018	NASA/JPL [10]	IoD of in situ radio frequency interference filtering, which will improve the accuracy of reading microwave radiances from geophysical sources such as soil moisture and sea-surface salinity

the transit method to observe stars several times over a period of a few days and measuring any dips in the light curve due to an exoplanet occulting its star. This impressive accomplishment is testament to the CubeSat community's professionalism, due to its use of COTS components to achieve the accurate pointing control required. Not only did the CubeSat operate successfully for over 2 years (with an original mission lifetime of 90 days), but also it was the first CubeSat to observe a transiting ExoPlanet—55 Cancri e [11,12]. Other notable examples of CubeSats that successfully performed astronomy and astrophysics research are shown in Table 3.

## 4 CubeSats supporting space-borne experiments

The majority of in situ microgravity research conducted today happens aboard the International Space Station (ISS). This platform acts not only as a testament to international collaboration but also as the most sophisticated and well-equipped laboratory in Earth orbit. Outside of the ISS a selection of other platforms and satellites regularly

**Table 3** Examples of CubeSat missions with astronomy science objectives.

<b>Spacecraft, size, and launch</b>	<b>Organizations involved</b>	<b>Mission description</b>
ASTERIA, 6U, 2017	MIT/NASA/JPL [2,11]	First successful exoplanet detecting CubeSat equipped with COTS systems for providing necessary pointing accuracy
HaloSat, 6U, 2018	NASA/GSFC/JHU/Nagoya University of Japan [1,2,12]	Measures x-ray emissions from highly ionized oxygen in the Milky Way’s galactic halo. Galactic halos are theorized to be a possible reservoir of baryons currently “missing” from the observed local universe, compared with cosmic background microwave radiation
MinXSS, 3U, 2015	University of Colorado Boulder [2]	Characterize the solar x-ray spectrum across wavelengths where the largest enhancement of solar flares is expected to occur
CSSWE, 3U, 2012	University of Colorado Boulder [3]	Measures the relativistic energy spectrum of solar energetic particles for studying space weather. Also features a magnetometer. Supports other missions such as VA probes
PicSat, 3U, 2018	Paris Observatory, PSL, CNRS [13]	A dedicated CubeSat for the study of the beta Pictoris system, its circumstellar disk, exocomets, and the transit of the Hill Sphere of exoplanet beta Pictoris b

conduct or have conducted crucial research that can only be achieved in the environmental conditions of space and microgravity. The fields of research that benefit from research experiments in space are numerous and include materials science, crystallography, planetary science, molecular chemistry, fiber optics, pharmacology, and biology.

In addition to the ISS, several of the larger manned platforms include MIR, Tiangong 1 and 2, and STS. However, using humans to operate or install (or even share an enclosed environment with) experiments while in space is a very costly and complex task—but one that has a great many advantages too. At times, it may be more cost-efficient to have an automated system on board a satellite or space station that can be teleoperated from the ground instead; however, the cost of developing a satellite that can simultaneously prepare, operate, monitor, and transmit the results of as wide a variety of experiments that exists or are desired for spaceflight is nearly impossible. Often, these satellites carry suites of payloads involving intersecting areas of science or experiment requirements—for example, Bion-M1 carried a selection of animals that required roughly the same ambient environmental requirements [14].



CubeSats however can be tailor-made to suit specific and unique payloads desired by research groups—often with lower costs and development time than one may need to fly similar payloads on board the ISS or other platforms, manned or otherwise. Although not as fully developed as CubeSat payloads for Earth observation or astronomy, exploiting this niche and market demand will greatly expand the variety and depth of science conducted in space today [2]. These opportunities not only allow long-time space science research groups the chance to have near-full control of their payload and its conditions but also provide industries with no previous relations to space an open door to affordably test any materials or drugs or procedures in space [15].

One field that is likely to see future growth from adopting CubeSats is the study of life sciences in space. While vitally important for preparing for longer-term space missions, both beyond Earth to the Moon or Mars, and further studying the effects of spaceflight in Earth orbit, this research will doubtless be used to benefit surface-dwelling people on Earth too [16,17]. Studies of cancer, pathogens, and age-related diseases and new methods of producing medicine and treatments for these already are an important highlight of ISS science operations and a field that is planned to mature during the commercialization of the ISS, expansion of private spaceflight, and preparation for deep space exploration.

Currently, NASA Ames' Small Satellites Technology Division has been the premier source of CubeSats with biological payloads—although notably SpacePharma launched DIDO 2, and there have been other larger biosatellites that have flown as well [1]. There is even a 6U named BioSentinel on the manifest for interplanetary space on Artemis I. In the future, life sciences in space could be expanded from the ISS and into the CubeSat community in the same way that EO and astronomy are being expanded today. If simple, affordable CubeSat platforms were to be developed to support the wide variety of payloads and instruments that are wanted to be flown, it would revolutionize the way in which science is taken from Earth labs to orbit. Using the CubeSat standard as a template model to support space qualified payloads originally modified from their control experiments in the lab would greatly streamline the process of conducting spaceflight biology research. Table 4 lists representative examples of CubeSats that have flown dedicated space environment experiments.

## 5 CubeSats as technology demonstrators

CubeSats make excellent platforms for technology demonstrations and for proof-of-concept missions. Multiple factors support this, such as their widely accepted industry standards, design specifications, and COTS equipment providing simple and cheap spacecraft buses and structures that can be relatively cleanly built around a more complex, dedicated payload. This “standard packing” is also a useful factor for encouraging streamlined interfacing between a complex and unique satellite and the launch provider/deployment mechanism. The other prime advantages are that of the low cost and buy-in for a CubeSat mission is more practical for early-stage businesses and researchers with less capital to invest in a technology with no flight heritage and also

**Table 4** Examples of CubeSats supporting space-laboratory payloads.

Spacecraft, size, and launch	Organizations involved	Mission description
PharmaSat, 3U, 2009	NASA/AMES [2,16]	Grew “brewer’s yeast” in LEO before dosing it with various concentrations of an antifungal agent to determine its efficacy in orbital conditions
BioSentinel, 6U, Artemis I	NASA/AMES [18]	A secondary payload on Artemis I flying heritage from PharmaSat to test “brewer’s yeast” growth and DNA repair in the radiation environment beyond Earth orbit
Q-PACE, 3U, slated 2020	University of Central Florida [2]	Studies the early stages of protoplanet accretion by observing collision of small, 0.1 mm–1 cm, particle collisions inside the CubeSat’s payload chamber
3Cat-1, 1U, 2018	Universidad Politécnica de Cataluña [19]	Contains seven payloads in a 1U structure, one to categorize the performance of graphene field-effect transistor

for nonspace industries to work with specialized consultants to develop their ideas into flyable payloads in a cost-effective and streamlined manner.

One important quality that may be overlooked regarding CubeSats is that as a relatively, inexpensive platform for space operations, risky in orbit demonstration missions can be seen as more economically viable, as less money and technology is “lost” should the mission fail. Many of these technology demonstrator missions would pose risks deemed uneconomical or downright dangerous had they been carried out aboard larger research satellites or the ISS; however, given the comparatively low investment required for a CubeSat mission, some technology can be demonstrated efficiently and effectively. Notable examples of technology demonstration missions are provided in [Table 5](#).

An example of how CubeSats that can support in-orbit demonstration of new technologies has been a part of the RemoveDEBRIS mission from SSTL and the University of Surrey. During this mission, a mothership measuring  $65 \times 65 \times 72$  cm and two 2U+ CubeSats were deployed together from the ISS (incidentally the largest deployment from the ISS so far), with the first CubeSat, DebrisSat1, deploying an inflatable aluminum balloon to be the target of a net released from the mothership. DebrisSat 2 contained instruments that were used to verify the precision of the mothership’s vision-based navigation experiment and other tests for the validation of the technology [20].

LightSail 1 and 2 were 3U CubeSats designed to test the deployment and operation of solar sailing in LEO. Solar sails had been attempted previously, with the most successful certainly being the JAXA IKAROS mission that used controlled solar sailing to reach and fly past Venus [23].

**Table 5** Examples of CubeSat technology demonstrator missions.

Spacecraft, size, and launch	Organizations involved	Mission description
RemoveDEBRIS, Mothership +2 × 2U, 2018	SSTL/University of Surrey/other industrial partners [20]	Designed to demonstrate four different methods of active space debris removal, including nets, harpoons, drag sails and vision-based navigation for an autonomous satellite. One Cubesat was the target for the harpoon and the other a “target” for the mothership to maneuver around and collect data
STARS flights, 2U, various launches	Kagawa University [21]	Demonstrations of space elevator and tether technology. Each “U” of CubeSat separates and unspools a tether between them to test the movement along it of a “cable car”. While full-size space elevator technology is in its extreme infancy, some examples of it are already now TRL 9 thanks to CubeSats
LightSail 2, 3U, 2019	The Planetary Society [22]	Tested controlled solar sailing in LEO on board a CubeSat. Results are debated although IKAROS achieved solar sailing to Venus in 2010
DIDO-2, 3U, 2017	SpacePharma [15]	Designed to test various biochemical processes in space that are vital for further understanding life sciences in space

## 6 CubeSats as deep space explorers

CubeSat missions are not limited to low Earth orbit (LEO) but can be considered as a tool to improve knowledge of deep space or as support for future manned missions to other planets. In this section, recent missions that have demonstrated the capability of CubeSats to operate beyond Earth orbit will be analyzed: from first successes with the MarCO mission to upcoming launches to the Moon and NEOs that CubeSats will rideshare.

Several critical technology gaps have had to be crossed for successful use of CubeSats in deep space operations. For one the small structure of CubeSat restricts the aperture size of antenna that can be used—similar to solar array size and imaging apertures for astronomical instruments—which presents an issue in possessing a large enough effective area for sufficiently high transmission or reception. Several solutions to this issue have been flown in Earth orbit, including patch and circularly polarized antennas and reflectarrays [18]. Another issue is related to the capabilities that miniaturized propulsion devices can provide, both in terms of total delta-v and thrust, which can be problematic for CubeSats reaching and establishing orbit at their target

destination within a reasonable and cost-effective time frame. Fortunately, however, the ability of CubeSats to be manifested as secondary payloads onto launchers through standardized deployers means that they take advantage of rideshare opportunities on interplanetary missions that larger secondary spacecraft might not be able to afford. With the upcoming renaissance of interplanetary exploration, supported by a renewed space race and new super heavy lift vehicles, it may be more likely that we see CubeSats flying alongside their motherships into the solar system.

As the key driving factors and other sections of this chapter describe, CubeSats have found their place supporting a wide variety of roles and missions across the space sector. The utility of the platform and success of the supporting industry have ensured that developing new prototypes and flight ready pathfinding missions is simple, cost-effective, and easy to facilitate for all involved parties. These benefits encourage mission planners and PIs looking into undertaking deep space missions on a budget (or with a desire to demonstrate relevant technology) to utilize the CubeSat as the desired platform. We have already explored how CubeSats can support miniaturized instruments with a variety of functions—EO, astronomy, telecommunications, etc., so it is unsurprising that these techniques and advantages are desired to be leveraged for interplanetary exploration also. Not only are the support for instrumentation available for interplanetary CubeSat developers one appealing factor, but also is the support available—in terms of COTS products, experience, and facilities available—for other subsystems, launch support, mission analysis, and rideshare opportunities.

A list of the main CubeSat missions beyond Earth orbit is reported in [Table 6](#).

**Table 6** Examples of CubeSat missions beyond Earth orbit.

Spacecraft, size, and launch	Organizations involved	Mission description
MarCO, 2 × 6U, 2018	NASA/JPL <a href="#">[1,18]</a>	The first interplanetary CubeSat mission. Daughter spacecraft to the InSight lander, these relayed critical EDL information to Earth in near real time when the lander or other orbiters such as MRO were unable to (see <a href="#">Chapter 4</a> )
Lunar Exploration from Artemis I, 13 × 6U, NEL 2021	Various/NASA Launch <a href="#">[1,18]</a>	The first launch of SLS to cis-lunar space will allow for these CubeSats to travel beyond Earth orbit and into deep space. Many are focused on studying the Moon
AIDA, 3 CubeSats from two motherships, 2021 and 2024	NASA/ESA <a href="#">[12,24]</a>	Daughter CubeSats to assist with studying a near-Earth object (65,803 Didymos currently) and to analyze the effectiveness of intentional impact by a spacecraft in redirecting its orbit path
NEA Scout	NASA <a href="#">[18]</a>	Solar sail propelled spacecraft from Artemis I. Planned to sail to a near Earth asteroid and perform analysis on flyby.

## 7 CubeSats as distributed instruments in constellations

CubeSats have been implemented to fulfill GNSS and EO roles as individual satellites and constellations. However, in the future, their ability to be mass produced inexpensively and mass deployed safely has led to their being featured prominently in plans for future megaconstellations such as Planet Labs and Spire Global, as well as other upcoming constellations like Kepler Communications. Owing to their cost advantage, more spacecraft can be placed in a constellation for the same price; therefore more coverage is guaranteed, greater redundancy is built-in, and shorter revisit times are made available [1,25].

These advantages become even more crucial and provide more value for cost when they are used in scenarios such as disaster management where up-to-date, high-quality observation data can be vital for directing emergency services, warning populations of imminent danger, and reliably providing satellite-internet communications to workers on the ground in the event of damaged telecom infrastructure. It is for these reasons that emerging space powers, NGOs, and developing countries are increasingly seeking to develop or utilize CubeSat constellations for cost-effective disaster management resources [25]. Table 7 lists representative examples of CubeSat-based megaconstellations.

**Table 7** Examples of CubeSat-based megaconstellations.

Spacecraft, size, and launch	Organizations involved	Mission description
Planet Labs	Planet Labs [1]	A series of “flocks” of various Cube and SmallSats equipped with telescopes to image in high-resolution swathes of Earth within 52 degrees of the equator—a large portion of Earth’s agriculture and population
Spire Global	Spire Global [1]	Over 80 operational CubeSats in a constellation offering space as a service. It measures the atmospheric refraction of radio signals sent from GNSS satellites on the other side of the planet
Kepler Communications	Kepler Communications [26]	An upcoming company planning on using a constellation of CubeSats to provide high-bandwidth links to relay satellites and ground stations, including for polar operations

## 8 Conclusions

The variety of missions and applications that CubeSats can undertake—and very often at significant cost reductions—has led to them being widely regarded as the economical method of operating in space. While initially designed to be a tool for university students to gain experience with real space hardware, they have seen adoption from space agencies, military organizations, nonprofits, and from some of the biggest aerospace industries on Earth today. The CubeSat community has grown into an important sector of the space economy and is responsible for driving the ambition, accessibility, and variety of missions conducted today, thanks to the evolution of common industry standards, COTS products and services for developers, and mass production. The adoption of CubeSats by emerging space powers, NewSpace ventures, professional space agencies, and traditional aerospace industries reaffirms their position as viable and practical platforms for spaceflight and assures their continuing utilization in the future. The future of CubeSat applications largely depends on the creativity and capability of the CubeSat developers to identify and solve interesting new problems using small, innovative satellite solutions.

## References

- [1] A. Poghosyan, A. Golkar, CubeSat evolution: analyzing CubeSat capabilities for conducting science missions. *Prog. Aerosp. Sci.* 88 (2017) 59–83, <https://doi.org/10.1016/j.paerosci.2016.11.002>.
- [2] National Academies of Sciences, Engineering, and Medicine, *Achieving Science with CubeSats*, National Academies Press, Washington, DC, 2016.
- [3] M. Swartwout, The first one hundred CubeSats: a statistical look, *J. Small Satellites* 2 (2) (2013) 213–233.
- [4] A. Chin, R. Coelho, L. Brooks, R. Nugent, J. Puig-Suari, C.P.S.L. Obispo, Standardization promotes flexibility: a review of CubeSats' success, in: 6th Responsive Space Conference, April 28–May 1, Los Angeles, CA, 2008.
- [5] J. Puig-Suari, G. Zohar, K. Leveque, Deployment of CubeSat constellations utilizing current launch opportunities, in: *Small Satell. Conference*, August, 2013.
- [6] S. Jones, et al., ExoCube INMS with neutral hydrogen mode, *AGUFM 2015* (2015). SA32A-06.
- [7] S. Salas, et al., ANGELS SmallSat: demonstrator for new French product line. in: 2018 SpaceOps Conference, 28 May–1 June, Marseille, France, 2018, <https://doi.org/10.2514/6.2018-2731>.
- [8] D.K. Oi, et al., CubeSat quantum communications mission. *EPJ Quantum Technol.* 4 (1) (2017) 1–20, <https://doi.org/10.1140/EPJQT/S40507-017-0060-1>.
- [9] A. Carrasco-Casado, et al., Intersatellite-link demonstration mission between CubeSOTA (LEO CubeSat) and ETS9-HICALI (GEO satellite). in: 2019 IEEE International Conference on Space Optical Systems and Applications (ICSOS), 2020, pp. 1–5, <https://doi.org/10.1109/icsos45490.2019.8978975>.
- [10] S. Misra, et al., CubeSat Radiometer Radio frequency Interference Technology (CubERRT) validation mission: enabling future resource-constrained science missions. in: *International Geoscience and Remote Sensing Symposium (IGARSS)*, July, Vol. 2018, 2018, pp. 6308–6311, <https://doi.org/10.1109/IGARSS.2018.8517477>.

- [11] M.W. Smith, et al., SSC18-I-08 on-orbit results and lessons learned from the ASTERIA space telescope Mission, in: 32nd Annual AIAA/USU Conference on Small Satellites, 2018.
- [12] P. Kretschmar, M. Küppers, R. Walker, et al., *The CubeSat Revolution*, (2018).
- [13] M. Nowak, S. Lacour, A. Crouzier, L. David, V. Lapeyrère, G. Schworer, Short life and abrupt death of PicSat, a small 3U CubeSat dreaming of exoplanet detection, in: *Space Telescopes and Instrumentation 2018: Optical, Infrared, and Millimeter Wave*, 2018.
- [14] J.R. Dennison, G. Wilson, A. Souvall, B. Russon, K. Gamaunt, CubeSat Space Environments Effects Studied in the Space Survivability Test Chamber Survivability Test Chamber, Fig. 4. Video Discharge Monitoring Output, (2017).
- [15] S. Amselem, Remote controlled autonomous microgravity lab platforms for drug research in space. *Pharm. Res.* 36 (12) (2019) 1–15, <https://doi.org/10.1007/s11095-019-2703-7>.
- [16] A.J. Ricco, et al., PharmaSat: drug dose response in microgravity from a free-flying integrated biofluidic/optical culture-and-analysis satellite. in: *Microfluidics, BioMEMS, and Medical Microsystems IX*, Vol. 7929, 2011, p. 79290T, <https://doi.org/10.1117/12.881082>.
- [17] L.S. Stodieck, T. Bateman, R. Ayers, V. Ferguson, S. Simske, Benefits attained from space flight in pre-clinical evaluation of candidate drugs. in: *AIPC*, Vol. 420, 2008, pp. 627–632, <https://doi.org/10.1063/1.54856>.
- [18] A. Freeman, Exploring our solar system with CubeSats and SmallSats: the dawn of a new era. *CEAS Space J.* (2020) 1–12, <https://doi.org/10.1007/s12567-020-00298-5>.
- [19] R. Jove-Casarellas, et al., <sup>3</sup>Cat-1 project: a multi-payload CubeSat for scientific experiments and technology demonstrators. *Eur. J. Remote Sens.* 50 (1) (2017) 125–136, <https://doi.org/10.1080/22797254.2017.1274568>.
- [20] G.S. Aglietti, et al., The active space debris removal mission RemoveDebris. Part 2: in orbit operations. *Acta Astronaut.* 168 (2020) 310–322, <https://doi.org/10.1016/j.actaastro.2019.09.001>.
- [21] STARS Project, [Online]. Available: <http://stars.eng.shizuoka.ac.jp/english.html>, 2020. Accessed 20 March 2020.
- [22] J. Mansell, et al., Orbit and attitude performance of the LightSail 2 solar sail spacecraft. in: *AIAA Scitech 2020 Forum*, 6–10 January, Orlando, FL, 2020, <https://doi.org/10.2514/6.2020-2177>.
- [23] L. Johnson, *Setting Sail for the Sun the NEA Scout & Solar Cruiser Missions*, (2019).
- [24] C. Cheng, P. Michel, S. Ulamec, L.B.R. Cheryl, *AIDA: Asteroid Impact & Deflection Assessment*, (2015).
- [25] G. Santilli, C. Vendittozzi, C. Cappelletti, S. Battistini, P. Gessini, CubeSat constellations for disaster management in remote areas. *Acta Astronaut.* 145 (2018) 11–17, <https://doi.org/10.1016/j.actaastro.2017.12.050>.
- [26] Kepler Communications Inc, [Online]. Available: <https://www.keplercommunications.com/network>, 2020. Accessed 20 March 2020.

# CubeSat science instruments

3

*Anthony Freeman<sup>a</sup>, Benjamin K. Malphrus<sup>b</sup>, and Robert Staehle<sup>a</sup>*

<sup>a</sup>Jet Propulsion Laboratory, California Institute of Technology, Pasadena, CA, United States, <sup>b</sup>Morehead State University, Space Science Center, Morehead, KY, United States

## 1 Introduction to CubeSat science instruments

CubeSats are increasingly being referred to as an example of a “disruptive technology” owing to their rapid development cycles and the fact that they are less expensive to develop, launch, and operate compared to large, conventional satellites. The evolving capabilities of CubeSats are leading to a rapid expansion of their application to a wide variety of mission profiles. New, innovative technologies are enabling fundamental science observations, constellations of Earth remote sensing CubeSats, and, more recently, interplanetary CubeSat missions. A variety of evolving technologies, implementing reduced size, weight, and power (SWaP), has led to miniaturized science instruments that are now being used in applications that were once the realm of large, extremely expensive satellite systems.

The pace of development of these technologies is accelerating. SmallSat form factors allow fast-track infusion of technology for space missions, which amounts to a new paradigm in space exploration and utilization. New technologies and new science instruments being developed under the “NewSpace” umbrella are being rolled out at a pace that has the potential to disrupt planetary science exploration as it has begun to do for Earth remote sensing from Low Earth Orbit (LEO) and in astrophysics and heliophysics.

The National Academies of Sciences undertook a study published in 2016 entitled “Achieving Science with CubeSats.” The study concluded that CubeSats had already produced high-value science and are particularly well suited to targeted investigations that augment the capabilities of larger, more capable spacecraft and enable new types of science measurements [1]. Technological advances that support these science measurements and the CubeSat revolution in general are considered in other chapters. NASA maintains an online version of the state of the art in SmallSat technology report that documents such technologies in detail. The report provides a comprehensive summary of the current state of SmallSat spacecraft technologies categorized by power, propulsion, guidance navigation and control, structures, materials and mechanisms, thermal control, command and data handling, communications, integration, launch and deployment, ground data systems and operations, and passive deorbit devices [2]. The report provides an excellent reference for CubeSat developers, especially when combined with a companion NASA publication, “CubeSat 101: Basic Concepts and Processes for First-Time CubeSat Developers” [3]. The state of the art in SmallSat



technology is a comprehensive and valuable resource, which is regularly updated, and provides a far more in-depth look at CubeSat spacecraft technologies than can be considered here. An overview of these technologies with reference to their impact to specific SmallSat mission profiles has been discussed in previous chapters. These advances in spacecraft technologies facilitate CubeSat science missions, which can target specific measurements or observations. The instruments that are used to make these measurements and observations are considered in this chapter.

## 2 Current and planned CubeSat instruments

For any CubeSat science mission, the point is to make useful, science-grade measurements, whether from Earth orbit or some more exotic destination in the solar system. Consider the latter case, since it is more challenging: not all the instruments needed for deep space exploration can be miniaturized to fit within the constraints of CubeSat or NanoSat volumes. Magnetometers can be made to fit, as seen on INSPIRE [4]; radios can be miniaturized to enable radio science investigations, as seen on both INSPIRE and MarCO; and in situ instruments can, with some effort and ingenuity, be made small and low power enough, as seen in the case of instruments designed for NASA's next Mars rover [5]. Which of these and other instruments can be tailored for CubeSats/NanoSats?

For a first cut at an answer to this question, a survey of Earth observation instruments that was generated in 2012 [6] lends insight. In this study the authors Daniel Selva and David Krejci binned the current state-of-the-art instruments into three categories: feasible, infeasible, and problematic. Their list is summarized and updated for 2020 in Table 1. In the taxonomy used in the 2012 paper, “feasible” meant that a technology or a sensor compatible with the CubeSat standard had already been developed; “infeasible” meant that a technology was seen as clearly incompatible with the CubeSat standard; “problematic” technologies captured instances for which an instrument could be developed to fit the CubeSat standard but at the expense of significantly reduced data quantity and/or quality. This list was recently updated to reflect the progress made by instrument developers by 2019 [7]. It is quite a long list (Table 1) and includes optical/IR cameras; UV/optical spectrometers; IR radiometers and spectrometers, from the Near-IR to Far-IR; microwave radiometers; submillimeter-wave spectrometers; short wavelength radars; GPS radio occultation; and optical communication lasers that can be used for occultation. CubeSat versions of synthetic aperture radars (SARs)—which conventional wisdom has requiring huge apertures and kW's of power to operate from orbit—are under study [8]. Substantial progress has been made in advancing the feasibility of several instrument classes since 2012. In fact, none of the original list from Ref. [6] are now considered infeasible, and only one category (Lidars) can be considered problematic. For planetary science, astronomy, and heliophysics investigations, compact neutron and X-ray spectrometers and mass spectrometers should be added to the list. The NANOSWARM mission concept, for example, proposed to NASA's 2019 Discovery call, included a miniaturized neutron spectrometer and a solar wind ion sensor [9]. Other instruments, such as UV, visible and IR telescopes, and field and particle sensors, are being incorporated into

**Table 1** Examples of science-grade instruments designed for CubeSat form factors.

Technology	Examples
Atmospheric chemistry instruments	PICASSO
Atmospheric temperature and humidity sounders	CIRAS, 3D Winds
Cloud profile and rain radars	RainCube, Cloudcube
Earth radiation budget radiometers	RAVAN, CSIM, PREFIRE
Gravity instruments	Drag Free CubeSat
High-resolution optical imagers	Planet
Imaging microwave radars	Ka-Band 12U design
Imaging multispectral radiometers (Vis/SWIR) and hyperspectral imagers	AstroDigital, SWIS , HyperScout, APEX
Imaging multispectral radiometers (IR, microwave, and millimeter wave)	LunarIceCube, TEMPEST, TROPICS, IceCube
Lidars	Lunar Flashlight, TOMCAT, APEX
Lightning imagers	RaioSat
Multiple angle/polarimeter	HARP Polarimeter
Ocean color spectrometer	SeaHawk
Precision orbit	CanX-4&-5; LEDSat
Radar altimeters	SNoOPI
Scatterometers	GNSS refl. (CyGNSS)
Neutron spectrometers	LunaHMap
UV/Vis/IR telescopes	ASTERIA, SPARCs, GUCI
Field and particle sensors	Dellingr, CuSP, Min-XSS, BurstCube
Radio interferometer	SunRISE
Mass spectrometers	APEX

compelling astrophysics and heliophysics science CubeSat missions. The science community has invested significantly in technology development to miniaturize a broad range of instruments, an effort that is now paying off as instrument concepts mature to the point where they can be incorporated into CubeSat/Nanosat missions for exceptional quality science.

The instrument classes summarized in [Table 1](#) are discussed in some detail in the succeeding text, one at a time:

## 2.1 Remote sensing instruments

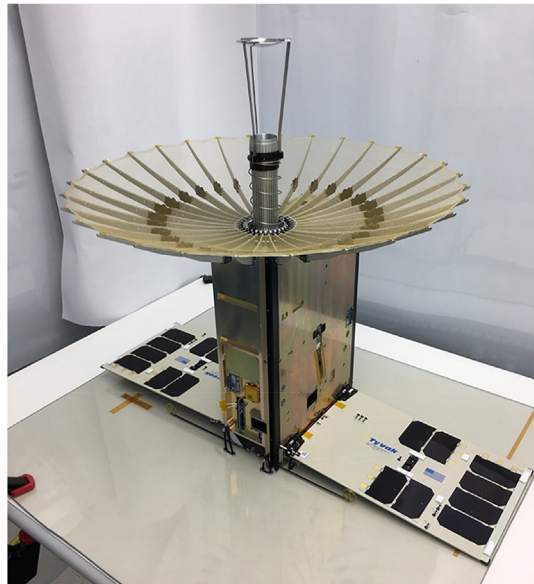
*Atmospheric chemistry instruments*—PICASSO's visible spectral imager for occultation and nightglow (VISION) instrument is designed to obtain vertical profiles of stratospheric ozone via spectral observation of sun occultations in the Chappuis band [10]. Compact for a hyperspectral imager, at less than 1U in size, its spectral range covers the visible and the near-infrared (430–800nm). Spectral band selection is performed by a tunable Fabry-Perot interferometer, which is well suited for compact realizations. As an ESA-funded mission, PICASSO is scheduled to launch in 2020.

*Atmospheric temperature and humidity sounders*—The CubeSat IR atmospheric sounder (CIRAS) is a 4U cryo-cooled grating MWIR spectrometer designed primarily for sounding of atmospheric water vapor and temperature but with sufficient spectral coverage and resolution to resolve some atmospheric constituents such as CO and CO<sub>2</sub> [11]. The new technologies embedded in CIRAS are a compact grating spectrometer and a high operating temperature barrier IR detector (HOT-BIRD), operating at 190K. This relatively high operating temperature is critical for use in CubeSats. Lower temperatures require cryogenic cooling that can create significant thermal management challenges, especially in tightly constrained volumes. HOT-BIRD’s spectral range spans 4.08–5.13  $\mu\text{m}$ , with spectral resolution of 1.3–2.0  $\text{cm}^{-1}$ . CIRAS was funded as a NASA technology development program.

Another atmospheric sounder known as 3D winds has been proposed as a constellation of 12 6U CubeSats, each carrying a passively cooled MWIR hyperspectral FTS sensor, operating in a cross-track scanning mode to cover a 650-km-wide swath at a spatial resolution of  $\sim 5$  km. The spectral range is 5.7–8.2  $\mu\text{m}$ , with spectral resolution 1.26  $\text{cm}^{-1}$ . As an IR sounder, each individual 3D wind sensor can retrieve 3D profiles of atmospheric water vapor. In a constellation, measurements separated in time by a few minutes of changes in the water vapor profiles can be combined to estimate atmospheric winds [12].

*Cloud profile and rain radars*—RainCube proved that a precipitation radar could fit in a CubeSat volume and return high-value science measurements [13]. RainCube’s 35.75-GHz radar payload was designed to fit within a 4U volume inside a 6U CubeSat form factor (Fig. 1). RainCube demonstrated miniaturized radar electronics and an innovative, compact deployable antenna within this tiny volume. Funded by NASA’

**Fig. 1** The 6U RainCube spacecraft in integration and test, with the solar panels and Ka-band radar antenna deployed. Courtesy NASA/JPL/Caltech.



Earth Science and Technology Office, RainCube was delivered to the ISS on the OA-9 resupply mission and deployed from the Nanoracks dispenser in July 2018. The CloudCube radar concept, currently under development, takes the lessons learned from RainCube and folds in a higher frequency W-band measurement capability for cloud profiling [14].

*Earth radiation budget radiometers*—The RAVAN mission used a novel approach to a compact radiometer targeting the Earth’s radiation budget by capturing all outgoing radiation from the UV (200 nm) to the far-IR (200  $\mu\text{m}$ ) with an accuracy of better than  $0.3 \text{ W m}^{-2}$  absolute [15]. This was achieved by demonstrating two new technologies: vertically aligned carbon nanotubes (VACNTs) that have an extremely flat spectral response over a wide wavelength range to absorb this broadband radiation and a gallium fixed-point blackbody calibration source.

The next CubeSat mission to measure a key part of the Earth’s radiation budget will be Polar Radiant Energy in the Far-InfraRed Experiment (PREFIRE)—a miniaturized thermal IR spectrometer operating over the wavelength range 0–45  $\mu\text{m}$  at 0.84- $\mu\text{m}$  spectral resolution [16]. The mission’s objective is to quantify a poorly understood component of the Earth’s radiation budget: spectrally resolved emissivities over the Arctic at wavelengths  $>15 \mu\text{m}$  (Far-IR) that have never before been systematically measured. PREFIRE takes advantage of advances in thermopile detector technology that allow Far-IR measurements in a compact form factor at ambient temperatures without onboard cooling.

*Gravity instruments*—Clearly marking a path toward CubeSats that can measure gravity field variations, a 3U drag-free CubeSat mission has been proposed to demonstrate the feasibility of a gravitational reference sensor (GRS) with an optical read-out. The drag-free CubeSat is designed to shield a 25.4-mm spherical test mass (TM) from external nongravitational forces and to minimize the effect of internal generated disturbances [17]. There is significant potential for gravimetric instruments in Earth remote sensing and planetary exploration.

*High-resolution optical imagers*—The commercial company Planet has deployed hundreds of its 3U Dove satellites, each carrying a multispectral, optical imager capable of 3–5-m spatial resolution [18]. As a constellation, their flock of Doves yields unprecedented global coverage at this spatial resolution on a daily basis. Since the beginning of operations of the Doves, Planet has produced an archive of  $>7$  petabytes of data. The enabling technology is the camera’s use of a line scan technique, which allows for continuous acquisition of high spatial resolution imagery.

*Imaging microwave radars*—It may seem incredible that a synthetic aperture radar (SAR) might fit in a CubeSat volume, but a concept for a Ka-band SAR has been envisioned that fits in a 12U volume [19]. The shorter Ka-Band wavelength allows a smaller antenna to obtain reasonable swath coverage, SNR, and spatial resolution in such a small package. Additionally, Capella Space, Inc., is building a constellation of six SAR-based microsattellites whose goal is to offer hourly coverage of every point on the Earth rendered in submeter resolution [20].

*Imaging multispectral radiometers (Vis/SWIR) and hyperspectral imagers*—Another commercial company Astro Digital has developed and flown the LandMapper-BC satellites, a small constellation of 6U CubeSats each carrying a

three-band (red, green, and NIR) multispectral imager, capable of 22-m spatial resolution [21]. JPL’s Snow and Water Imaging Spectrometer (SWIS) is a compact imaging spectrometer and telescope system designed for integration on a 6U CubeSat platform. It covers the 350–170-nm spectral range with 5.7-nm sampling. The Dyson spectrometer has an innovative single drive onboard calibration system capable of providing radiometric stability and features a new Teledyne CHROMA detector array, optimized for high-temperature operation, with a linear variable antireflection coating to enhance quantum efficiency and minimize backscatter [22]. CoSine’s HyperScout visible/near-IR hyperspectral imager is currently flying on ESA’s GOMX-4 CubeSat platform [23]. This 1.5U instrument is capable of 70-m spatial resolution over a 200-km swath and 15-nm spectral resolution in the 400–1000-nm range.

*Imaging multispectral radiometers (IR, microwave, and millimeter wave)*—Lunar IceCube, led by Morehead State University, partnered with the Busek Company, NASA GSFC, the NASA Independent Verification and Validation (IV&V) Center, and JPL, is one of the most challenging CubeSats undertaken to date. In addition to navigating itself into a lunar orbit after its release from the Artemis 1 SLS rocket, using a state-of-the-art RF ion propulsion drive (developed by the Busek space propulsion company), it will carry the first cryo-cooled thermal imaging radiometer flown in space by a CubeSat—the Broadband infrared compact high-resolution exploration spectrometer (BIRCHES). BIRCHES (Fig. 2) will measure solar reflectance around the 3  $\mu\text{m}$  band with 10-nm spectral resolution to separate OH, liquid water, and ice absorption features on the lunar surface at 10-km spatial resolution.

It is a compact 1.5U instrument, with a Teledyne H1RG focal plane array and a linear variable filter (LVF) detector coating. Cooling is achieved by a tactical AIM SX030 microcryocooler with a cold finger to maintain the detector at  $\leq 115^\circ\text{K}$  [24]. Lunar IceCube and 12 other Artemis 1 interplanetary CubeSats will be launched on the maiden voyage of NASA’s Space Launch System in 2020.

The Temporal Experiment for Storms and Tropical Systems-Demonstration (TEMPEST-D) mission is a 6U CubeSat carrying a cross-track scanning, five-channel passive microwave radiometer with bands in the spectral range 90–200 GHz.

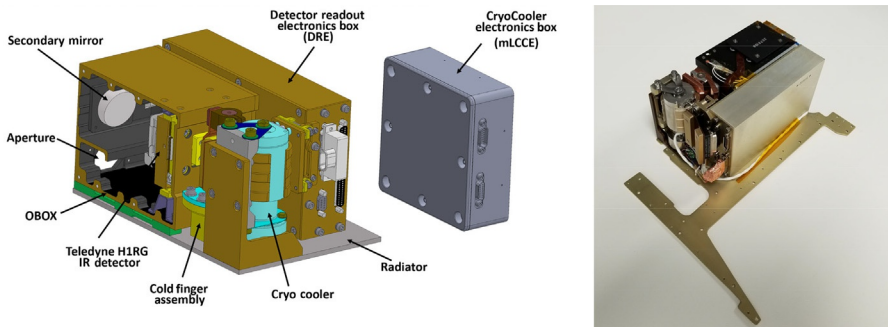


**Fig. 2** Lunar IceCube’s BIRCHES IR spectrometer (CAD model shown on the left and photograph shown on the right).

Courtesy Morehead State University and NASA Goddard Spaceflight Center.

TEMPEST-D is a collaboration between Colorado State University and JPL. TEMPEST-D was launched in May 2018 and deployed from the ISS in July 2018 at nearly the same time as RainCube [25, 26]. TEMPEST-D resolves the time derivative of the scene brightness temperature, primarily due to atmospheric water vapor variations. The sensor design includes high-quality blackbody calibration sources viewed through the antenna, end to end. Data quality is similar to that of more conventional microwave sounders such as the Advanced Technology Microwave Sounder (ATMS) on the NOAA polar satellites [27].

The TROPICS constellation of six 3U CubeSats is being developed by MIT/Lincoln Labs under a NASA contract to study the development of tropical cyclones through rapid-revisit sampling using a multiband millimeter-wave radiometer instrument [28]. The TROPICS sensor is actually two total power radiometers that measure 12 channels altogether: a “WF-band” radiometer with eight channels from 90 to 119 GHz and a “G-band” radiometer with four channels from 183 to 206 GHz. TROPICS will provide high-revisit microwave nearly global observations of precipitation, temperature, and humidity (Fig. 3).

Another passive radiometer instrument was flown on GSFC’s 3U IceCube mission, which carried an 874-GHz submillimeter-wave radiometer for cloud ice observations [29]. At 874 GHz, ice cloud scattering in Earth’s atmosphere produces a larger brightness temperature depression than at lower frequencies, which can be used to retrieve vertically integrated cloud ice water path (IWP) and ice particle size. IceCube’s compact submillimeter radiometer is based on just one channel of the compact scanning submillimeter wave imaging radiometer, a multiband airborne conical and cross-track imager.

*Lidars*—The Lunar Flashlight mission, a collaboration between JPL and MSFC, is manifested to launch with NASA’s Artemis 1 mission to the Moon, and its 6U CubeSat spacecraft will maneuver into a lunar polar orbit and then use near-infrared



**Fig. 3** TROPICS CubeSat.  
Courtesy MIT/Lincoln Laboratories.

lasers to reflect off the surface to distinguish water ices from regolith. The lasers will operate in 1 ms train pulses, though they are more of a reflectometer than a true Lidar [30]. McGill and Yorks [31] have proposed a compact Lidar known as TOMCAT for cloud and aerosol profiling.

*Lightning imagers*—Brazil’s RaioSat project [32] is designed to detect intracloud and cloud-to-ground lightning flashes simultaneously, using an optical sensor and a VHF antenna onboard a 3U CubeSat platform. Lightning detections will be validated by comparison with data from existing ground networks. The sensor payload is a VHF passive antenna (frequency range from 50 to 200 MHz) and a spectral imaging camera (spectral range 700–900 nm) using a CCD with resolution of  $2048 \times 1536$  pixels for surface imaging at 80 m/pixel.

*Multiple angle/polarimeter*—The 3U HARP CubeSat mission, a joint effort by UMBC and Utah State’s Space Dynamics Lab (SDL), targets measurements of the microphysical properties of cloud water and ice particles in the atmosphere using a hyperangular imaging polarimeter [33]. The HARP sensor is a wide field of view visible/NIR imager that splits three spatially identical images into three independent polarizers and detector arrays. This technique achieves simultaneous imagery of three polarization states and is the key innovation to achieve high polarimetric accuracy with no moving parts. HARP’s hyperangular channel has up to 60 viewing angles per pixel at 670 nm, and three additional channels can provide up to 20 viewing angles per pixel at 440, 550, and 670 nm, with 2.5-km spatial resolution at nadir.

*Ocean color spectrometer*—The University of North Carolina’s Seahawk satellites are 3U CubeSats built by AAC Clyde Space that measure ocean color using eight visible/NIR bands in the same range as SeaWiFS (402–885 nm), at spatial resolutions from 75 to 150 m, with SNR comparable with its predecessor SeaWiFS. The ground swath for each ocean color image frame is  $216 \times 720$  km. The Seahawk instrument is a push-broom design, with four linear array CCDs, each containing three rows of detectors, scanning the field of view as the satellite passes overhead. Saturation is avoided on either the land or clouds using a technique called bilinear gain. Seahawk-1 launched in December 2018 and returned its first ocean color image in March 2019 [34].

*Precision orbit*—The University of Toronto’s CanX-4&5 mission was a dual-nanosatellite formation flying demonstration [35]. The mission achieved its objectives in spectacular fashion by proving that satellite formation flying can be accomplished with submeter tracking error accuracy and low  $\Delta V$  capability, achieving submeter control of satellite separation and subcentimeter relative position knowledge. Project LEDsat [36] is a collaborative international project designed to improve the identification and orbit determination of CubeSats in LEO. Multiple methods of measuring positions will be flown on the same spacecraft: GPS, optical tracking, satellite laser ranging (SLR), and radio tracking. These satellites will also be equipped with light-emitting diodes (LEDs) for optical tracking while the satellite is in Earth shadow.

*Radar altimeters*—The NASA-funded SNOPI 6U CubeSat mission, currently under development, will use reflectometry to exploit UHF (P-Band) signals from geostationary communication satellites to retrieve root-zone soil moisture [37]. The technique cross correlates the direct signal received from GEO with the signal reflected

from the ground, using the amplitude and phase of the result to retrieve variations in the reflection coefficient related to subsurface moisture changes. Adding in precision orbit determination to fix the location of the receiver CubeSat allows similar measurements to be used for altimetry, though shorter wavelengths (e.g., Ka-band) are preferred for this type of measurement [38].

*Scatterometers*—Building on a technique first demonstrated using a much larger instrument, the L-band SIR-C radar [39], the Cyclone Global Navigation Satellite System (CyGNSS) mission [40] is the first science mission utilizing a bistatic radar scatterometer to characterize surface ocean winds through GPS reflections, especially under tropical cyclones. CyGNSS was implemented as a partnership between the University of Michigan and the Southwest Research Institute (SwRI). CyGNSS measures the shape and power of the delay-Doppler map in the GPS signals reflected from the ocean surface, which are modulated by roughness induced by near-surface winds [41]. The CyGNSS science team has been very creative in finding broader applications for CyGNSS measurements over land, indicating great promise for future measurements of soil moisture, for example, which compare favorably with those from NASA’s much larger (and costlier) SMAP mission [42]. Each CyGNSS spacecraft in the eight-satellite constellation carries a pair of GPS antennas, mounted on the bottom and facing Earthward, providing high revisit rate observations between  $\pm 35$ -degree latitude. The CyGNSS spacecraft are properly designated as SmallSats, but their GPS reflections instrument could be sized to fit on a 12U CubeSat.

*Neutron spectrometers*—Arizona State University’s Lunar Polar Hydrogen Mapper (LunaH-Map) is another Artemis 1 mission, a 6U CubeSat that will propel itself into a polar orbit around the moon with a low altitude (5–12 km) perilune centered on the lunar South Pole, near the Shackleton crater. LunaH-Map, illustrated in Fig. 4, will carry two neutron spectrometers that can map neutron emissions from near-surface hydrogen (H) at spatial scales of  $\sim 7.5$  km/pixel. This is made possible by an innovative new scintillator technology called an elpasolite, specifically Cs<sub>2</sub>YLiCl<sub>6</sub>:Ce (CLYC), with high neutron detection efficiency across a wide energy range [43].

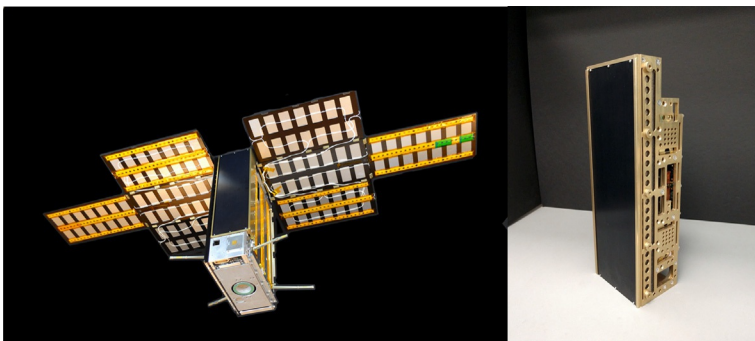


**Fig. 4** LunaH-Map’s Neutron Spectrometer (Mini-NS) left and spacecraft right. Images courtesy Arizona State University.



## 2.2 Instruments for astronomy and heliophysics

Thus far, this chapter has focused on instruments used for remote sensing of planetary surfaces and atmospheres, particularly for Earth. In the following, CubeSat instruments used for astronomy and heliophysics are addressed in the context of the missions on which they are flown.

*UV/Vis/IR telescopes*—ASTERIA was a compact, visible/near-IR (500–900-nm wavelength range) telescope mounted on a 6U CubeSat platform (Fig. 5) and flown in LEO. In a collaboration between MIT, JPL, and Morehead State University, the mission’s objectives were to demonstrate fine pointing and thermal control of the detector array while staring at distant stars to look for exoplanet transits using the technique of precision photometry. The ASTERIA team was successful in achieving all of the mission objectives: demonstrating 0.5 arcsecond pointing by tracking a set of guide stars on the CMOS detector and moving a piezoelectric stage to compensate for residual pointing errors; 0.01 K temperature stability over an observing period of 20 min; and detection of the transit of exoplanet 55 Cancri e across the face of its parent star in 2018 [44]. During operations, Morehead State University tracked the spacecraft, providing the telemetry and control services to the Mission Operations team at JPL, while MIT performed target selection and analysis of stellar photometry data from ASTERIA.

In a collaboration between Arizona State University and JPL, the Star-Planet Activity Research CubeSat (SPARCS) spacecraft will carry a UV telescope (162- and 280-nm wavelength bands) in a LEO orbit to observe time-domain variability in low-mass stars and assess the habitability of those that harbor planetary systems. The enabling technology for SPARCS is the highly sensitive delta-doped

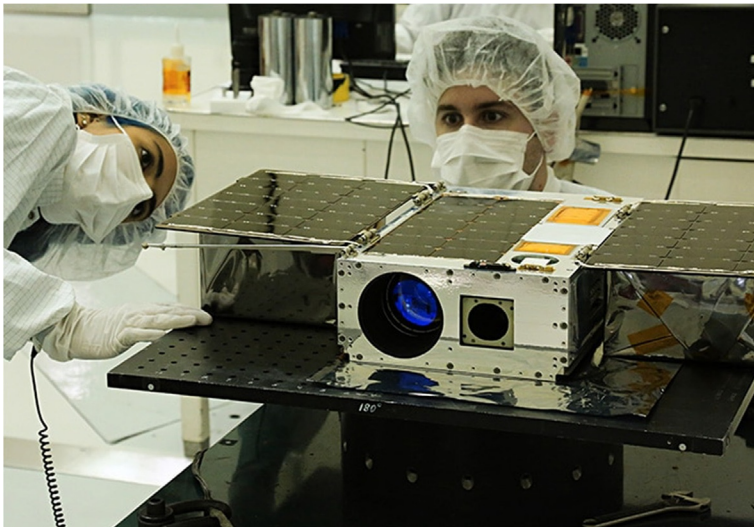


**Fig. 5** The ASTERIA spacecraft in integration and test in JPL’s CubeSat Development Lab. Courtesy NASA/JPL/Caltech.

detectors it uses [45]. This example of time-domain astronomy is a unique use of CubeSats, which can stare at a single bright star for extended periods—unlike larger telescopes that are generally tasked to observe multiple objectives in different locations in the sky.

The Gravitational-wave Ultraviolet Counterpart Imager (GUCl) Mission, led by NASA GSFC, is a time-domain observatory under consideration for flight within the Small Explorer program. GUCl consists of two 12U CubeSats in LEO orbits, each instrumented with a wide-field (50 square degrees) dual-band UV (190–220 and 260–290 nm) imager. The concept of operations for GUCl is to uplink occurrences of binary neutron star mergers detected by ground-based gravitational wave observatories and then scan the sky to localize them via their UV signature within an average of 1 h. Localization of such transient events then allows ground-based telescopes to observe their time-varying signatures at longer wavelengths, as they cool. While not tracking down neutron star mergers, GUCl will study other energetic, transient phenomena, such as accretion around supermassive black holes, and core collapses in supernovae, by conducting a first synoptic survey of the UV transient sky, imaging 1500 square degrees every 3 h to a depth of 19.0 mag (AB) [46].

Another time-domain astronomy mission, GSFC's 6U BurstCube, will detect long gamma ray bursts (GRBs), attributed to the collapse of massive stars and short GRBs (sGRBs), resulting from binary neutron star mergers while monitoring other gamma ray transients in the energy range 10–1000 keV. Models of binary star mergers predict that short GRBs are generated alongside gravitational waves that can now be detected by ground-based observatories such as LIGO. BurstCube will enhance the likelihood of coincident detection and the number of short GRBs that can be correlated with gravitational wave signals. The BurstCube gamma ray detector contains four CsI scintillators coupled with arrays of compact low-power silicon photomultipliers (SiPMs) on a 6U CubeSat. This first BurstCube can be seen as a pathfinder for a future Gamma Ray Observatory—a constellation of up to 10 BurstCubes providing all-sky, time-domain observations for GRBs and localization of their point of origin [47].

*Fields and particles*—NASA and other space agencies fly many space missions to study heliophysics, particularly the interaction of the solar wind with the Earth's magnetosphere and upper atmosphere. The instruments these missions carry measure strong electromagnetic fields and the properties of energetic particles. The intensity of the signals these instruments are designed to observe means that miniaturized versions can still be very effective, even when making measurements over relatively short timescales.

NASA's first science CubeSat was Min-XSS, launched in 2016 and operated for almost a year [48]. In a collaboration between the University of Colorado, Southwest Research Institute, NASA GSFC, and NCAR, this 3U CubeSat was a heliophysics mission, studying soft X-rays generated by the sun and their interaction with Earth's atmosphere, using a miniature solar X-ray spectrometer instrument. Miniaturized silicon drift detectors that can operate in the 0.5-keV (25 Å) to 30-keV (0.4 Å) range with ~0.15-keV FWHM spectral resolution were the enabling technology for Min-XSS measurements.

Another notable heliophysics science mission is NASA GSFC's first 6U CubeSat, *Dellinger* [49]. The measurement made by *Dellinger*'s instrument suite of a gated ion/neutral mass spectrometer, and three fluxgate magnetometers are used to study coupling of the solar wind with the magnetosphere and its effects on Earth's ionosphere.

The CubeSat mission to study Solar Particles (CuSP) is a 6U CubeSat manifested on the Artemis 1 launch of the SLS planned for 2021. CuSP carries three small but capable instruments: the Suprathermal Ion Spectrograph (SIS) from SWRI to detect and characterize low-energy solar energetic particles; GSFC's miniaturized Electron and Proton Telescope (MERIT), which will return counts of high-energy solar energetic particles; and JPL's vector helium magnetometer (VHM). From its vantage point in interplanetary space (away from the influence of Earth's magnetosphere), CuSP will measure variability in the solar wind and solar magnetic fields, as a kind of space weather "sentinel" [50].

*Radio interferometer*—Recently selected for flight by NASA, SunRISE will be the first radio interferometer flown in space. In a collaboration between the University of Michigan and JPL, the SunRISE instrument is a "science swarm" of 6U CubeSats that together form a high-frequency (HF) radio interferometer to observe coronal mass ejections from our sun. This constellation of six CubeSats will fly in a loose formation at separations from 1 to 10 km in a GEO "graveyard" orbit (just above GEO) as a synthetic aperture radio telescope to study a critical problem in solar physics: how solar energetic particles are accelerated and released into interplanetary space [51]. They will be delivered to their orbit as a hosted payload on a Maxar communication satellite via Maxar's Payload Orbital Delivery System (PODS). Once on orbit, each CubeSat is pointed toward the sun and uses an HF receiver (Fig. 6) to measure radio emissions

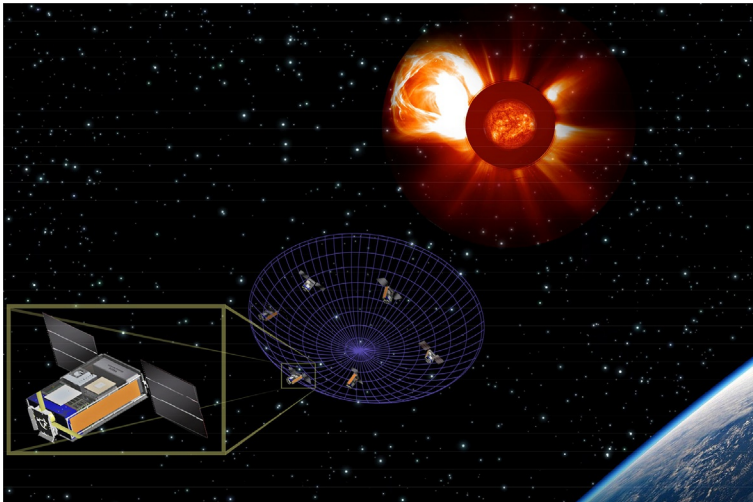


**Fig. 6** The SunRISE mission concept—a constellation of CubeSats that combine to form the first HF radio interferometer in space, studying coronal mass ejections (CMEs) through their radio emissions.

Courtesy NASA/JPL/Caltech.

from 0.1 to 25 MHz—a frequency range not observable from the Earth’s surface due to the ionosphere. Signals collected by the synthetic array will be combined on the ground. Radio frequency emissions generated by coronal mass ejections will be tracked and localized.

### 3 The future of CubeSat instruments

The range of instruments being proven to be viable for the CubeSat form factor, as can be seen from this discussion, is ever increasing. The sensitivity of these instruments, in some cases, approaches that of instruments designed for larger, monolithic spacecraft. Instrument designers have found creative ways to calibrate CubeSat instruments, so the quality of the data they collect can be favorably compared to data acquired by larger, more expensive instruments. As the on-orbit success rate of these instruments trends ever upward, so too will the efforts to further evolve these measurements and to miniaturize other types of instruments, advancing the technological evolution of CubeSat missions.

The enabling technologies described in previous chapters and the miniaturized instruments described herein have ushered in the first generation of science-grade CubeSats for Earth observation and will soon enable true interconnected constellations of MicroSats and CubeSats. Earth observation missions will ultimately also be revolutionized through the implementation of constellations of SmallSats with highly capable, miniaturized instruments. Heliophysics is undergoing a similar revolution. Time-domain astronomy, observing time-varying or transient phenomena such as stellar flares, seems to be a very fruitful niche for CubeSats in astronomy. In the very near future, the Artemis 1 fleet of CubeSats will demonstrate that science quality measurements can be achieved with interplanetary CubeSats. It seems clear that, despite the “tyranny of the rocket equation,” planetary science missions in the future will build on this foundation to go further than they do today, touch more objects in our solar system, return far more information, and be implemented for budgets and schedules that can only be dreamed of today.

In the future, it may be common practice to incorporate CubeSat/NanoSat ride-alongs on Flagship missions to enable science measurements at close range and in environments that would be considered too risky for the primary spacecraft. This future is already on the verge of being realized by the selection of the Italian Space Agency’s LICIAcube CubeSat as a ride along for NASA’s Double Asteroid Redirect Test (DART) mission [52] and the Asteroid Prospection Explorer (APEX) and Juventas CubeSat ride along for ESA’s Hera mission [53]. The science yield of both the DART and Hera primary missions, planned to launch in the early 2020s toward their destination—the Didymos binary asteroid pair—will be significantly enhanced by their CubeSat companions. LICIAcube will carry a camera to observe the larger DART spacecraft as it impacts the smaller of the two Didymos asteroids. The Juventas CubeSat plans to carry a low-frequency radar to probe the interior of the smaller asteroid. The planned payload for APEX is ambitious for a 6U CubeSat: an imaging spectrometer, a magnetometer, a compact mass spectrometer, and a Lidar. As we have seen

in this chapter, ambition is not particularly bounded, given the ingenuity of the CubeSat community.

Projecting a little farther into the future, small landers with instruments demonstrated on CubeSat missions will allow us to explore the surface and even the subsurface of planetary bodies. Science results from these smaller, subsidiary missions may often have a higher profile than results from the primary mission and likely will attract much greater public attention—as Philae did on Rosetta. Recent trends also suggest launch costs/kg will continue to decline and spacecraft capabilities will continue to expand. In all, new eras of space exploration and Earth observation from the high ground of space are being ushered in by CubeSat and SmallSat technologies, particularly science instruments. The space paradigm of the future will no doubt incorporate CubeSats and NanoSats as a central element of the new exploration architecture.

## References

- [1] National Academies of Sciences, Engineering, and Medicine, *Achieving Science With CubeSats: Thinking Inside the Box*, The National Academies Press, Washington, DC, 2016, <https://doi.org/10.17226/23503>.
- [2] B. Yost (Ed.), *State of the Art of Small Spacecraft Technology*, NASA On-line Publication, 2019, <https://sst-soa.arc.nasa.gov/>. (Accessed 29 March 2020).
- [3] NASA CubeSat Launch Initiative, *CubeSat 101: Basic Concepts and Processes for First-Time CubeSat Developers*, Revision October, 2017.
- [4] A. Klesh, et al., *INSPIRE: Interplanetary NanoSpacecraft Pathfinder in a Relevant Environment*, in: *AIAA/USU Conference on Small Satellites*, SSC13-XI-8, 2013.
- [5] NASA/JPL Mars, <https://mars.nasa.gov/mars2020/mission/instruments/>, 2020. (Accessed 29 March 2020).
- [6] D. Selva, D. Krejci, A survey and assessment of the capabilities of Cubesats for Earth observation. *Acta Astronaut.* 74 (2012) 50–68, <https://doi.org/10.1016/j.actaastro.2011.12.014>.
- [7] G. Stephens, A. Freeman, P. Pilewskie, E. Richard, P. Larkin, C. Chew, S. Tanelli, S. Brown, D. Posselt, E. Peral, The emerging technological revolution in Earth observations, *Bull. Am. Meteorol. Soc.* 101 (3) (2020) E274–E285, <https://doi.org/10.1175/BAMS-D-19-0146.1>.
- [8] L. Wye, *SRI CubeSat imaging radar for earth science (SRI-CIRES)*, in: *Earth Science Technology Office Forum*, 2015.
- [9] I. Garrick-Bethel, et al., *NANOSWARM: a Cubesat discovery mission to study space weathering, lunar magnetism, lunar water, and small-scale magnetospheres*, in: *46th Lunar and Planetary Science Conference*, 2015.
- [10] P. Cordoen, J. De Keyser, P. Demoulin, D. Fussen, D. Pieroux, S. Ranvier, *PICASSO—Pico-satellite for atmospheric and space science observations*, in: *6th European CubeSat Symposium*, Estavayer-le-Lac, Switzerland, October 14–16, 2014.
- [11] T.S. Pagano, D. Rider, J. Teixeira, H. Aumann, M. Rud, M. Lane, A. Kummer, D. Johnson, J. Rodriguez, S. Gunapala, D. Ting, D. Rafol, F. Irión, C. Norton, J. Wolfenbarger, J. Pereira, D. Furlong, D. Mamula, *The CubeSat infrared atmospheric sounder (CIRAS), pathfinder for the earth observing nanosatellite-infrared (EON-IR)*, in: *Proceedings of the 30th Annual AIAA/USU SmallSat Conference*, Logan UT, USA, August 6–11, 2016. Paper: SSC16-WK-32.

- [12] R. Glumb, et al., A constellation of Fourier transform spectrometer (FTS) CubeSats for global measurements of three-dimensional winds, in: Proceedings of the 29th Annual AIAA/USU Conference on Small Satellites, Logan UT, USA, August, 2015. Paper: SSC15-XII-04.
- [13] E. Peral, T. Imken, J. Sauder, S. Statham, S. Tanelli, D. Price, N. Chahat, A. Williams, RainCube, a Ka-band precipitation radar in a 6U CubeSat, in: Proceedings of the 31st Annual AIAA/USU Conference on Small Satellites, Logan UT, USA, August 5-10, 2017. Paper: SSC17-III-03.
- [14] S. Tanelli, E. Peral, G. Sadowy, S. Durden, M. Sanchez-Barberty, K. Cooper, R. Rodriguez-Monje, E. Im, Z. Haddad, O. Sy, M. Lebsock, G. Stephens, S. van den Heever, Evolution of radars for spaceborne observations of cloud and precipitation processes at JPL: from CloudSat to RainCube and beyond, in: ESA Living Planet Symposium, Milan, Italy, May 2019.
- [15] W.H. Swartz, S.R. Lorentz, P.M. Huang, A.W. Smith, J. Carvo, D.M. Deglau, E. L. Reynolds, S.J. Papadakis, D.L. Wu, The RAVAN CubeSat mission: a pathfinder for a new measurement of Earth's energy budget, in: Proceedings of the IAA Symposium on Small Satellites for Earth Observation, Berlin, Germany, April 24-28, 2017. Paper: IAA-B11-0902.
- [16] JPL, PREFIRE (Polar Radiant Energy in the Far-InfraRed Experiment), <https://science.jpl.nasa.gov/projects/PREFIRE/>, 2019. (Accessed 25 May 2019).
- [17] C. Zanoni, et al., The design of a drag-free CubeSat and the housing for its gravitational reference sensor, in: 2nd IAA Conference on University Satellites. Proceedings of 2nd IAA Conference on University Satellites, 2013. Paper IAA-CU-13-12-01.
- [18] eoPortal, Planet—Flock Imaging Constellation, <https://directory.eoportal.org/web/eoportal/satellite-missions/f/flock-1>, 2019. (Accessed 25 May 2019).
- [19] A. Freeman, J. Hyon, D. Waliser, The cube-train constellation for earth observation, in: 13th Annual Cubesat Developer's Workshop, San Luis Obispo, 2016.
- [20] Capella Space Website, <https://www.capellaspace.com/>, 2019. (Accessed 29 March 2020).
- [21] Gunter, Gunter's Space Page—Landmapper-BC 1, [https://space.skyrocket.de/doc\\_sdat/landmapper-bc.htm](https://space.skyrocket.de/doc_sdat/landmapper-bc.htm), 2019. Accessed 25 May 2019.
- [22] H.A. Bender, P. Mouroulis, C.D. Smith, C.H. Smith, B.E. Van Gorp, M.L. Eastwood, J. Gross, Snow and Water Imaging Spectrometer (SWIS): Optomechanical and System Design for a CubeSat-Compatible Instrument, vol. 9611, SPIE Optical Engineering + Applications, San Diego, California, 2015, p. 961103, Imaging Spectrometry XX, <https://doi.org/10.1117/12.2190013>.
- [23] M. Esposito, et al., Initial operations and first light from a miniaturized and intelligent hyperspectral imager for nanosatellites, in: Proceedings of the 4S Symposium, Sorrento, Italy, June, 2018.
- [24] P.E. Clark, B.K. Malphrus, D. Reuter, T. Hurford, R. MacDowall, N. Petro, W. Farrell, C. Brambora, D. Patel, S. Banks, P. Coulter, D. Folta, P. Calhoun, B. Twiggs, J. Kruth, K. Brown, R. McNeill, M. Tsay, V. Hruby, Broadband infrared compact high-resolution exploration spectrometer: lunar volatile dynamics for the lunar ice cube mission, in: Proceedings of the 30th Annual AIAA/USU SmallSat Conference, Logan UT, USA, August 6-11, 2016.
- [25] S.C. Reising, T.C. Gaier, S. Padmanabhan, B.H. Lim, C. Heneghan, C.D. Kummerow, W. Berg, V. Chandrasekar, C. Radhakrishnan, S.T. Brown, J. Carvo, An earth venture in-space technology demonstration mission for temporal experiment for storms and tropical systems (Tempest), in: IGARSS 2018—2018 IEEE International Geoscience and Remote Sensing Symposium, Valencia, 2018, pp. 6301–6303, <https://doi.org/10.1109/IGARSS.2018.8517330>.

- [26] S. Padmanabhan, T.C. Gaier, B.H. Lim, R. Stachnik, A. Tanner, S. Brown, S.C. Reising, W. Berg, C.D. Kummerow, V. Chandrasekar, Radiometer for the temporal experiment for storms and tropical systems technology demonstration mission, in: IGARSS 2018-2018 IEEE International Geoscience and Remote Sensing Symposium, Valencia, 2018, pp. 2001–2003, <https://doi.org/10.1109/IGARSS.2018.8517803>.
- [27] E. Kim, C.H. Lyu, K. Anderson, R. Vincent Leslie, W.J. Blackwell, S315 NPP ATMS instrument prelaunch and on-orbit performance evaluation, *J. Geophys. Res. Atmos.* 119 (9) (2014) 5653–5670.
- [28] W. Blackwell, D. Buriának, K. Clark, D. Crompton, A. Cunningham, L. Fuhrman, P. Hopman, S. Michael, The NASA TROPICS CubeSat constellation mission: overview and science objectives, in: Proceedings of the 31st Annual AIAA/USU Conference on Small Satellites, Logan UT, USA, August 5-10, 2017. Paper: SSC17-VI-07.
- [29] D.L. Wu, J. Esper, N. Ehsan, T.E. Johnson, W.R. Mast, J.R. Piepmeier, P.E. Racette, Ice-Cube: spaceflight validation of an 874 GHz submillimeter wave radiometer for cloud ice remote sensing, in: ESTF 2014 (Earth Science Technology Forum), Leesburg, VA, USA, October 28-30, 2014, 2014. [http://esto.nasa.gov/forum/estf2014/presentations/B1P5\\_Wu.pdf](http://esto.nasa.gov/forum/estf2014/presentations/B1P5_Wu.pdf).
- [30] T. Imken, Payload developments on the lunar flashlight mission, in: CubeSat Developer's Workshop, Cal Poly San Luis Obispo, CA, April 2016, 2016.
- [31] M.J. McGill, J.E. Yorks, TOMCAT: a SmallSat lidar for cloud/aerosol profiling and hazard events, in: American Geophysical Union, Fall Meeting, 2018.
- [32] P. Kleber, W.A. Naccarato, A. Santos, M.A. Carretero, C. Moura, A. Tikami, Total lightning flash detection from space: a CubeSat approach, in: 24th International Lightning Detection Conference, San Diego, April, 2016.
- [33] J. Vanderlei Martins, T. Nielsen, C. Fish, L. Sparr, R. Fernandez-Borda, M. Schoeberl, L. Remer, HARP CubeSat—an innovative hyperangular imaging polarimeter for earth science applications, in: Small Sat Pre-Conference Workshop, Logan, UT, 3 August, 2014.
- [34] UNCW, SOCON: Sustained Ocean Color Observations With Nanosatellites, [https://uncw.edu/socon/first\\_image.html](https://uncw.edu/socon/first_image.html), 2019. (Accessed 25 May 2019).
- [35] G. Bonin, N. Roth, S. Armitage, J. Newman, B. Risi, R.E. Zee, CanX-4 and CanX-5 precision formation flight: mission accomplished! in: Proceedings of the 29th Annual AIAA/USU Conference on Small Satellites, Logan UT, USA, August, 2015. Paper: SSC15-I-05.
- [36] J. Cutler, et al., Improved orbit determination of LEO CubeSats: project LEDsat, in: AMOS Technologies Conference, 19–22 September 2017, Maui, Hawaii, 2017.
- [37] J. Garrison, J.R. Piepmeier, Y.C. Lin, R. Rajat, R. Bindlish, B. Nold, M.R. Vega, M. H. Cosh, C.F. Du Toit, P-band signals of opportunity: a new approach to remote sensing of root zone soil moisture, in: Managing Global Resources for a Secure Future, Annual Meeting October 22-25, Tampa, FL, 2017.
- [38] R. Shah, A. Freeman, J.L. Garrison, Constellations of CubeSats to exploit signals-of-opportunity for Earth system science, in: SPIE Optical Engineering + Applications (2018), San Diego, CA, vol. 10769, CubeSats and NanoSats for Remote Sensing II; 107690D, 2018, <https://doi.org/10.1117/12.2319863>.
- [39] S.T. Lowe, J.T. LaBrecque, C. Zuffada, L.J. Romans, L.E. Young, G.A. Hajj, First spaceborne observation of an Earth-reflected GPS signal, *Radio Sci.* 37 (1) (2002) 1–28.
- [40] C.S. Ruf, et al., A new paradigm in earth environmental monitoring with the CYGNSS small satellite constellation, *Nat. Sci. Rep* 8 (2018) 8782, <https://doi.org/10.1038/s41598-018-2712>.
- [41] C.S. Ruf, R. Balasubramaniam, Development of the CYGNSS geophysical model function for wind speed, *IEEE J. Sel. Topics Appl. Earth Obs. Remote Sens.* 12 (1) (2019) 66–77, <https://doi.org/10.1109/JSTARS.2018.2833075>.

- 
- [42] C.C. Chew, E.E. Small, Soil moisture sensing using Spaceborne GNSS reflections: comparison of CYGNSS reflectivity to SMAP soil moisture, *Geophys. Res. Lett.* 45 (2018) 4049–4057, <https://doi.org/10.1029/2018GL077905>.
- [43] E. Johnson, C. Hardgrove, R. Starr, S. Vogel, R. Frank, G. Stoddard, S. West, J. Christian, Development of the LunaH-Map miniature neutron spectrometer, in: *Society of Photo-Optical Instrumentation Engineers (SPIE) Optical Engineering + Applications Conference Presentation*, August 24, 2017.
- [44] M.W. Smith, et al., On-orbit results and lessons learned from the ASTERIA space telescope mission, in: *32nd Annual AIAA/USU Conference on Small Satellites, SSC18-III-08*, 2019.
- [45] D.R. Ardila, et al., The Star-Planet Activity Research CubeSat (SPARCS): a mission to understand the impact of stars in exoplanets, in: *Proceedings of the 32nd Annual AIAA/USU Conference on Small Satellites*, Logan UT, USA, SSC18-WKIV-02, 2018. arXiv:1808.09954.
- [46] S.B. Cenko, The gravitational-wave ultraviolet counterpart imager (GUCl) network, in: *American Astronomical Society Meeting #234*, id. 212.03. *Bulletin of the American Astronomical Society*, vol. 51, No. 4, 2019.
- [47] J. Racusin, et al., BurstCube: a CubeSat for gravitational wave counterparts, in: *35th International Cosmic Ray Conference*, Busan, Korea, 2017. arXiv:1708.09292.
- [48] J.P. Mason, et al., Miniature X-ray solar spectrometer: a science-oriented, university 3U CubeSat, *J. Spacecr. Rocket.* 53 (2) (2016), <https://doi.org/10.2514/1.A33351>.
- [49] L. Klepko, et al., Dellingr: NASA Goddard Space Flight Center’s first 6U CubeSat, in: *31st Annual AIAA/USU Conference on Small Satellites*, Logan UT, SSC17-III-06, 2017.
- [50] E.R. Christian, et al., The Cubesat mission to study solar particles (CuSP), an interplanetary Cubesat, in: *AGU Fall Meeting*, 2015. 2015AGUFMEP53C1035C.
- [51] F. Alibay, J.C. Kasper, T.J.W. Lazio, T. Neilsen, Sun radio interferometer space experiment (SunRISE): tracking particle acceleration and transport in the inner heliosphere, in: *IEEE Aerospace Conference*, Big Sky, MT, 2017, <https://doi.org/10.1109/AERO.2017.7943789>.
- [52] S. Pirotta, et al., LICIAcube, the light Italian CubeSat for imaging of asteroid joining NASA DART mission to Didymos binary system, in: *Geophysical Research Abstracts*, vol. 21, EGU2019-17780, 2019, EGU General Assembly, 2019.
- [53] ESA, [https://www.esa.int/Safety\\_Security/Hera/CubeSats\\_joining\\_Hera\\_mission\\_to\\_asteroid\\_system](https://www.esa.int/Safety_Security/Hera/CubeSats_joining_Hera_mission_to_asteroid_system), 2019. (Accessed 29 March 2020).



# Interplanetary CubeSat missions

4

*Benjamin K. Malphrus<sup>a</sup>, Anthony Freeman<sup>b</sup>, Robert Staehle<sup>b</sup>,  
Andrew T. Klesh<sup>b</sup>, and Roger Walker<sup>c</sup>*

<sup>a</sup>Morehead State University, Space Science Center, Morehead, KY, United States,

<sup>b</sup>Jet Propulsion Laboratory, California Institute of Technology, Pasadena, CA, United States,

<sup>c</sup>European Space Agency, Noordwijk, The Netherlands

## 1 Introduction

A new era of Solar System exploration began on May 5, 2018 with the launch of the twin Mars Cube One (MarCO) CubeSats. The success of the MarCO mission, along with 13 interplanetary CubeSats planned for launch on Artemis 1 in 2021, is establishing a new paradigm of planetary exploration. This new paradigm includes CubeSats and other small satellite platforms in supporting roles like MarCO and in primary roles like the Artemis 1 Lunar Cubes (Lunar IceCube, Lunar Flashlight, and LunaH-Map). Numerous studies are underway in the United States and Europe, in particular, that utilize CubeSats and CubeSat constellations that have the potential to revolutionize robotic Solar System exploration. This chapter examines the missions underway and the upcoming missions and discusses the differences between low Earth-orbiting CubeSats and interplanetary CubeSats. The chapter ends with a projection of future Solar System exploration made possible by this new standard.

Interplanetary CubeSats take advantage of the CubeSat paradigm and of the availability of commercial components developed for low Earth orbit (LEO) missions, but they are specifically designed to explore deep space. As a result, interplanetary CubeSats are essentially very different from low Earth orbit CubeSats in three primary technological areas: propulsion, radiation tolerance, and telecommunications. While fundamental differences exist in these areas, interplanetary CubeSats require changes to almost every satellite subsystem. Interplanetary CubeSats require propulsion systems capable of generating enough  $\Delta V$  to support trajectories from Earth escape or from GEO transfer to interplanetary destinations. Interplanetary CubeSats often need power systems with lower power modes and higher energy storage capabilities since they have a higher level of power requirements than LEO missions, due to the presence of propulsion and due to demanding telecommunication systems. Due to higher power level requirements, more advanced thermal control solutions are often needed to dissipate excess heat to deep space. Interplanetary CubeSats also require strategies for radiation tolerance as they are outside the protection of Earth's magnetosphere. Attitude determination and control systems (ADCS) for interplanetary CubeSats need a combination of traditional control system and propulsion to avoid the issues of wheel saturation outside the Earth's geomagnetic field. In terms of autonomy, interplanetary missions have

less frequent contact with the ground than LEO missions, imposing the need of agile algorithms to facilitate autonomous onboard operations. Finally, one of the most important differences between LEO missions and interplanetary missions is represented by the telecommunication systems. Telecommunication systems for interplanetary CubeSats face harsher environments and longer path distances and have more sophisticated navigation needs than the LEO CubeSats. For this reason the design of telecommunication systems for interplanetary missions is extremely challenging, and significant development is currently ongoing in the areas of radio design, antenna design, and in the design of ground support architectures. Optical communications have also been considered for interplanetary CubeSats, though that technology is less mature. In general, interplanetary CubeSats require different and more complex spacecraft systems architectures and must utilize different and more sophisticated ground station systems than LEO missions [1]. These differences are discussed in this chapter in detail using specific examples from current and planned missions.

Nine years after the idea was first floated in a proposal to NASA's Innovative Advanced Concepts (NIAC) opportunity [2], we are on the threshold of a new era in robotic exploration of our Solar System, one in which CubeSats and SmallSats will play an important role [3,4]. As flight opportunities begin to open up, deep space CubeSats and SmallSats could exhibit exponential growth, as seen for CubeSats in low Earth orbit [5]. Indeed, growing interest has been expressed within the space and Earth science community for such missions [6]. For Earth-orbiting CubeSats and SmallSats, the growth trend is driven by the push toward constellations, which may consist of multiple elements that each yield unique measurements that collectively serve one higher objective [7], or of similar elements that offer significantly enhanced temporal resolution [8,9], consistent with recently expressed requirements from the Earth science community [10]. It is also clear that miniaturization of many key spacecraft technologies across a broad front will have a profound effect on future deep space exploration [11], projecting out into the far future, perhaps even on interstellar exploration [12]. It is these kinds of projections that stimulate interest within the space science community for interplanetary CubeSat and SmallSat missions.

## 2 Destinations

If CubeSats are to be sent out into unexplored corners of our Solar System, where can they reasonably be expected to roam? Fig. 1 illustrates the regions that are most easily accessible and for which SmallSat missions are operating or planned. The inner Solar System is considered reachable with both free-flying and mother-daughter configuration CubeSats/Nanosats, while the outer Solar System is currently compatible with just the mother-daughter or ride-along configuration. Without a suitably compact radioisotope power source, deep space nanosats heading out to Jupiter and beyond will likely have to hitch a ride along with their host spacecraft, run on energy stored in batteries after their release from their storage/hibernation container, and relay data back to Earth through the mother spacecraft. Beyond the CubeSat form factor,

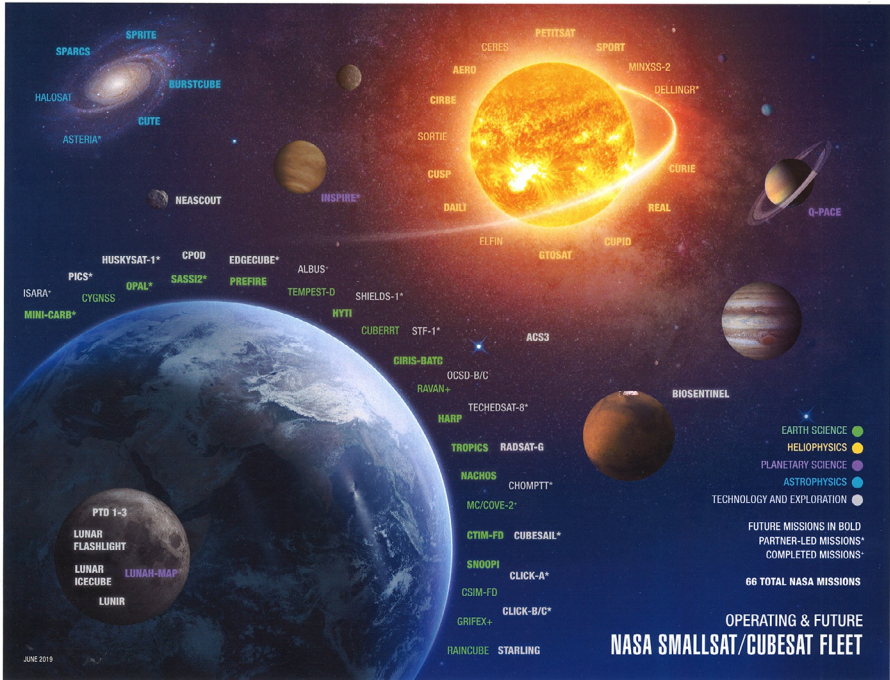


**Fig. 1** Exploring our Solar System with CubeSats and nanosats.  
Image Courtesy of NASA/JPL/Caltech.

but within the capability of a SmallSat on an ESPA ring, a NASA Innovative Advanced Concepts (NIAC) investigation was initiated utilizing an inflatable solar concentrator/telecomm antenna up to 5 m in diameter, low duty cycle operations, very low-power system-on-a-chip (SoC) electronics, and other advancements to enable heliophysics or flyby missions out to the orbit of Neptune or beyond [12a]. These spacecraft might be carried as secondary payloads on launches of primary missions to Jupiter or Saturn.

In recent decades, several deep space missions have used a gravity assist or slingshot maneuver at Venus to provide a boost in velocity to propel them on their way to their primary mission target. These missions include Galileo (Jupiter), MESSENGER (Mercury), Cassini (Saturn), and Solar Probe (the Sun). Venus gravity assists have become an arrow in the mission designer’s quiver that is pulled out whenever we need to save time, money, or propellant to get where we want our primary mission to go. Now imagine that every time a mission executes a gravity assist at Venus, it could drop off a small nanosat probe that could sample and analyze part of Venus’ atmosphere, relaying the data back to Earth via the vehicle that dropped it off. Straight shot, independent trajectories to Venus are also possible for nanosats and could launch as secondaries on a launch vehicle propelling a larger spacecraft on a Venus trajectory or with a hybrid approach involving a number of nanosats being carried on a larger microsat carrier platform that is itself released by the launch vehicle. With its thick

atmosphere, Venus is a good target to demonstrate aerocapture with a nanosat, placing into orbit around our sister planet.

Closer to home, the Moon is an attractive destination for nanosats, since it can be reached in a relatively short time, and communication distances are manageable. Near-Earth asteroids (between 0.98 and 1.3 AU distant from the Sun) represent another rich target set, with their number estimated at over 14,000, and  $\sim 1000$  of them larger than 1 km in diameter. Larger mothercraft carrying several daughter CubeSats could be used for deep in situ multipoint characterization of individual asteroids. Due to cost, however, it is unlikely that with this approach, we will ever visit more than a very few with a NASA Discovery-class mission like NEAR Shoemaker [13] or the Japanese Hayabusa missions [14]. But if these asteroids could be reached with CubeSats, it may become possible to examine hundreds of them close up within a generation, at a price tag comparable with that of a single Discovery mission. As a first step in this direction, the MSFC-JPL Near-Earth Asteroid Scout (NEAScout) CubeSat mission is slated for launch in 2021 aboard the same Artemis launch that will carry the first lunar CubeSats.

Launch periods for energy-efficient Mars transfers occur at intervals of about 26 months, and in recent times, most of these launch periods have had one or more spacecraft inserted onto a trajectory toward the red planet. Nanosats could ride along as ballast to make up the launch mass on larger Mars missions or make their way there as free-flying spacecraft, as the twin MarCO spacecraft did [15]. With a few kilometers per second of  $\Delta V$  capability, free-flying nanosats could be placed into orbit around Mars, opening up the potential for science from orbit at dramatically lower cost and adding to the communications and navigation infrastructure.

The main asteroid belt, situated between 2.2 and 3.2 AU (AU) away from the Sun, contains between 0.7 and 1.7 million objects with a diameter  $> 1$  km. Thus far, spacecraft en route to the outer planets have given us a closer glimpse of only a handful, and the Dawn mission [16] has provided detailed examination of just two of the largest: Ceres and Vesta. This is definitely rich hunting ground for CubeSat missions—the asteroid belt is close enough to the Sun that solar power generation is practical and close enough to Earth that communication distances are not extreme. It can take a long time to get out to the main asteroid belt though—Dawn arrived at its first target, Vesta, nearly 4 years after launch—so reliability and longevity will need to be demonstrated over several years if nanosat missions to the main belt are to succeed.

There are also more than 5000 known comets, whose orbits have taken them close enough to the Sun to be visible from Earth. Again, our spacecraft have visited less than a dozen: Halley's comet, 21P/Giacobini-Zinner, 26P/Grigg-Skjellerup, 107P/Wilson-Harrington, 19P/Borrelly, 81P/Wild, 9P/Tempel, 103P/Hartley, 2P/Encke, and 67P/Churyumov-Gerasimenko, which leaves numerous possibilities for nanosat mission flybys and encounters of future comets. Enough is known about comet trajectories to plan and quickly execute flyby missions, but rendezvous missions take longer and will require a higher standard of reliability: ESA's flagship Rosetta mission took 10 years to catch up with comet 67P/Churyumov-Gerasimenko and match trajectories [17]. Such long mission durations are not unusual when missions are planned to chase the so-called "short-period" comets.

Or a strategy could be implemented to allow the outer Solar System and beyond come to us. CubeSat missions are uniquely positioned to take advantage of the expanding reach of ground-based telescopes that can now detect objects such as Oumuamua [18] and the Oort cloud comet CK 2017 [19] several years before they traverse the inner Solar System. Given sufficient advance warning, fast response missions that offer a close encounter of these objects become feasible. CubeSats can have much shorter development cycles than conventional spacecraft (MarCO was put together and made ready for flight in under 18 months); all we need is to marry that capability with one of the new low-cost launch vehicles, capable of achieving a high C3. These strategies will further accelerate the interplanetary CubeSat paradigm.

### 3 What makes interplanetary CubeSats different?

Succinctly put, interplanetary CubeSats are different because their orbits take them far from home, our mother planet Earth, and its familiar environment. To be successful in low Earth orbit, a CubeSat must be relatively complex in a manner that affords powering and survival of electronics and other equipment, maintaining specified orientations, and responding to commands, all while acquiring and transmitting health status and data to meet mission objectives. Once a CubeSat's orbit leaves Earth's vicinity, all these functions must be provided, but for some of these functions, *how* to do so requires new techniques and complexity. For most CubeSats in Earth orbit, and especially LEO, getting to the mission's destination orbit is fundamentally over within minutes when the CubeSat starts operating. For most interplanetary CubeSats, most of the mission and its complexity will be exercised while transiting from the mission's launch orbit to one or more destination orbits where the CubeSat can perform its intended mission by acquiring data unavailable from elsewhere.

The following topics will all be covered later in this chapter because they represent significant differences from LEO CubeSat missions: (a) operating environment dominated by the need for radiation tolerance, compounded by mission duration; (b) telecommunications, which is driven especially by the distances involved; (c) navigation to a variety of destinations; (d) instrumentation, some of which differs from that common in LEO; (e) onboard data storage and processing often required because telecommunication distance necessitates lower data rates and longer latencies; (f) operations autonomy driven by lack of frequent commanding opportunities and lack of frequent visibility into onboard housekeeping parameters; and (g) transit to a destination as a secondary payload.

Recognizing that every mission is unique, some other aspects of interplanetary spacecraft and missions remain much the same as for any orbit, including (a) structure and mechanical systems, (b) thermal control, (c) some forms of attitude determination and control, and (d) propulsion. With respect to propulsion, some beyond-Earth CubeSat missions have extremely demanding total  $\Delta V$  requirements that put them in a class outside of what may be required for any mission in Earth orbit.

## 4 Historical perspective and the first interplanetary CubeSat developers

By the start of 2011, over 50 CubeSats had been launched, all to low Earth orbit, with 3U being the largest form factor. By 2019, over 1000 CubeSats had been launched [20]. In the early days of the CubeSat initiative, very few rigorous scientific investigations were performed, and the form factor was not generally regarded as being highly useful except as a university tool, and there was no serious discussion of going beyond Earth orbit. A few people suspected that this situation would change. For those who even thought about it, surely there were obstacles. For one thing, no credible telecommunication package existed with the required small size (e.g., a 10-cm cube or one-third of the then-largest CubeSat), mass ( $\sim 1$  kg), and power ( $< 10$ – $20$  W) that could send data or receive commands beyond a few thousand kilometers. For another, the published “CubeSat Standard” prohibited “propulsion” from being aboard CubeSats carried as secondary payloads, because to most people, this term implied the use of stored and potentially unstable chemical energy that without extensive qualification could represent a threat to the primary payload and its launch if something went wrong inside the ride-along CubeSat. So, even if a way to communicate were established, how would the small spacecraft get anywhere interesting? Further, many of the electronic components readily used in low Earth orbit were thought to be intolerant to radiation levels commonly found beyond the shielding cocoon of Earth’s magnetosphere. Radiation-tolerant electronics were well known, but often beyond the budget of most CubeSat implementors.

After 2010, some factors began to converge that inevitably would have led to interplanetary CubeSats at some point. But it would be difficult to overemphasize how preposterous the concept seemed to most space cognoscenti at the time. The most basic enabling factor was that CubeSat size was on a path toward the 6U form factor. Two propulsion techniques were being developed and miniaturized that had high  $\Delta V$  capability without any unusual stored energy during launch: solar sails and electric propulsion not requiring pressurized propellants. At JPL, both optical and RF telecommunication experts were working to dramatically reduce the size of needed electronics.

Robert Staehle at JPL was inspired by the work of longtime colleague Tomas Svitek of Stellar Exploration, Inc. on the solar sail for The Planetary Society’s LightSail[tm]-1 and asked how big a sail might be deployable from 2U of a 6U CubeSat. It turned out that such a sail,  $\sim 9$  m on a side, would be able to impart  $> 1$  km/s of  $\Delta V$  per year of mission duration at 1 AU. Consulting with telecom experts Hammid Hemati, then with JPL, and Courtney Duncan, also at JPL, indicated that they believed they were on technology development paths toward 1U equipment that could provide  $> 1$  kbit/s from Mars using optical and RF links, respectively. Pantazis Mouroulis in JPL’s Instruments Division showed that a new optical layout could reduce the shoebox-sized Moon Mineralogy Mapper that had been provided to India’s Chandrayaan-1 lunar orbiter to 2U with similar performance as an imaging spectrometer covering the visible-to-IR wavelength range 400–3000 nm. Armed with this information at the end of 2010, plus a few back-of-the-envelope calculations, Robert Staehle met with

CubeSat coinventor Jordi Puig-Suari of California Polytechnic University, San Luis Obispo, to show that with 2U for an instrument payload, 2U for propulsion, 1U for telecommunications, and 1U for everything else, meaningful interplanetary CubeSat missions would be possible. Jordi and other team members were assembled, and their 2011 proposal to NASA's just-reestablished Innovative Advanced Concepts (NIAC) was submitted, selected, and funded to define a convergent technology path to enable an example CubeSat mission to visit asteroids riding as a secondary payload to be deployed off a launch to GEO or escape.

At the same time, the NIAC investigation group asserted the feasibility of a wider set of example missions serving different disciplines [21]: (1) Mineral Mapping of Asteroids (*Small Body Science*); (2) Solar System Escape Technology Demonstration (*Tech Demo*); (3) Earth-Sun Sunward of L1 Space Weather Monitor (*Heliophysics and Terrestrial Applications*); (4) Phobos Sample Return (*Planetary Science*) (Fig. 2); (5) Earth-Moon L2 Radio Quiet Observatory (*Astrophysics*); and (6) Out-of-Ecliptic Missions, for example, Solar Polar Imager CubeSat Constellation (*Heliophysics*); (7) Lunar Surface Water Ice Mapper (Lunar Science & Resource Exploration); and (8) Near-Earth Asteroid NanoSat Lander.

Before their study report was complete, the group proposed a more detailed analysis of two particularly difficult missions that just might be possible with CubeSats: a sample return from Phobos using *two* CubeSats suggested by team member Louis Friedman, and observing the Sun's poles from a heliocentric latitude of 45 degrees, attained using an interplanetary superhighway trajectory conceived and later mapped out by coinvestigator Martin W. Lo. Many observers still consider these concepts preposterous.

At the AIAA Space 2012 conference in Pasadena, California, the NIAC group recommended that "NASA could enable dramatic new capability by making launch

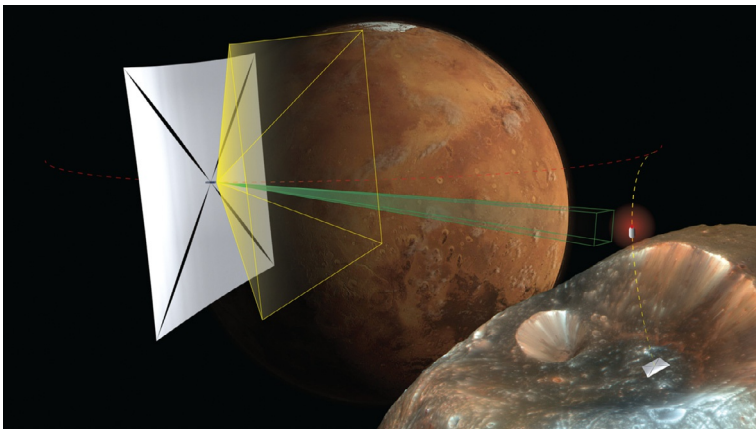


**Fig. 2** Far-out concept: Interplanetary CubeSats retrieving a sample from Phobos or Deimos. Artist's concept by Ryan Sellers/CalPoly-SLO, courtesy of NASA/JPL/Caltech.

slots and funding available to support CubeSats on all launches to C3  $> \sim 0$ , and as hosted riders aboard some fraction of geostationary satellites” [22]. NASA later adopted a similar policy at the heart of their Small Innovative Missions for Planetary Exploration (SIMPLEx) program [23].

In response to lunar Strategic Knowledge Gap goals announced by NASA HEOMD, Robert Staehle, David Eisenman, and Garry Burdick kicked off teams at JPL to propose an asteroid-visiting CubeSat and the Lunar Flashlight mission concept (with MSFC) now slated to fly aboard EM1, recently redesignated as Artemis 1. At the same time, Les Johnson of MSFC formed a team to independently propose a solar sail-propelled multiasteroid mission remarkably similar to the JPL proposal, which HEOMD combined upon selection to create the NEA Scout mission, also slated for EM1. Simultaneously, Ben Malphrus (Morehead State University) formed a team including GSFC to propose Lunar IceCube, also now slated for Artemis 1. A short time after that, Craig Hardgrove of Arizona State University proposed LunaH-Map into NASA’s first SIMPLEx call for proposals also now slated for Artemis 1.

As evidenced by this multiplicity of proposals with broad participation, funded and in various stages of development, the *potential* value of interplanetary CubeSats had been asserted convincingly to enough people with enough influence to secure the necessary resources. It remained only to clearly *prove* the value in flight to complete the transition from nearly total ignorance and skepticism to acceptance, if not full embrace, by the community.

Leadership of that step fell to Andrew Klesh, Joel Krajewski, and the team John Baker helped them to assemble for the Mars CubeSat One (MarCO) mission, which gained quick support from JPL’s director, Charles Elachi, and the Assistant Director at that time, Firouz Naderi. Started in late 2014 when the twin Interplanetary NanoSpacecraft Pathfinder In a Relevant Environment (INSPIRE) mission had been passed up for a near-escape launch opportunity, MarCO was on a fast schedule to meet the launch date for the Discovery InSight mission in early 2016, with which the two MarCOs were to ride on the same launch to Mars. In spite of the rapid schedule, the team secured the resources to leapfrog INSPIRE’s capabilities with new electronics and other innovations to make the design capable of all the fundamental functions of planetary flight found in missions costing hundreds of millions of dollars, all for well less than \$20M [24].

MarCO had to be delayed because the launch of the primary mission to carry it—Interior Exploration using Seismic Investigations, Geodesy and Heat Transport (InSight)—had to be delayed 26 months because *its* payload was not ready on time. Once launched, MarCO succeeded in every way planned at the outset, with the A and B spacecraft both performing their real-time “bent-pipe” relay of communications throughout InSight’s landing and even taking pictures of Mars. Thus in the span from 2010/11 to 2018, MarCO’s success (see [Section 6.1](#)) swept away much of the prior skepticism and outright opposition to using CubeSats and, by extension, SmallSats, for planetary science and exploration. The door to CubeSat exploration of the Solar System was opened.



## 5 Solution paths to uniquely interplanetary challenges

### 5.1 Radiation tolerance and mission duration

Higher single-event upset rates were expected on the first interplanetary CubeSats, dealt with using latchup immune parts (having linear energy transfer [LET]  $> \sim 35\text{--}70\text{ MeV/mg-cm}^2$ ), robust software, and the ability to implement periodic power cycles with the system without disrupting normal operations. In practice, single-event upset rates have proven to be much less than predicted, perhaps because of careful part selection.

For commercial electronics, part-to-part radiation performance variability is a major challenge, because the same parts from different fabrication runs can have very different radiation performance characteristics. Ensuring mission success can imply the need to purchase enough parts from a single manufacturing run to perform radiation testing on some samples and being prepared to reject all parts from that lot in the event of test failure.

Total ionizing dose (TID) tolerance levels are lower for commercial electronics, but simple shielding techniques are sufficient since interplanetary radiation environments are generally more benign than those in GEO. There are, however, some interplanetary environments that experience intense radiation, such as near the orbits of the inner Galilean satellites of Jupiter, where radiation levels will necessitate both heavy shielding and radiation hard parts that are outside the typical CubeSat experience base.

Additional robustness is achievable using asymmetric connections among different CubeSat functions and processors; radiation-tolerant features including triple-mode redundancy, monitoring, and rebooting systems utilizing watchdog timers; the use of FPGA-based processor nodes; spot shielding; and numerous other techniques. New technologies are under development including atomic number (Z) Grade technology that shows promise for radiation shielding that will improve the performance of interplanetary CubeSats.

### 5.2 Propulsion systems for interplanetary CubeSats

The spectacular success of NASA/JPL's MarCO—the first interplanetary CubeSats—has raised expectations for SmallSat missions that can explore our Solar System at much lower cost than a conventional NASA mission. But MarCO only flew to Mars: the 40 m/s  $\Delta V$  provided by its cold gas propulsion system fell far short of the  $\Delta V$  needed to get into the orbit around the red planet (Table 1). The planetary science community's appetite for SmallSat missions will be further whetted by the upcoming Artemis 1 mission, the first launch of the SLS rocket, planned for 2021, which will send a total of 13 CubeSats on a trajectory toward the Moon. Two of them, Lunar Ice-Cube and LunaH-Map, will carry a Busek RF ion propulsion system, imparting enough  $\Delta V$  ( $\sim 0.8\text{ km/s}$ ) to place these 6U CubeSats into highly elliptical lunar orbits.

**Table 1** Nominal  $\Delta V$  in kilometers per second required for some commonly considered deep space CubeSat missions.

Nominal $\Delta V$ values for CubeSat deep space missions (km/s)	From LEO at 250 km	From GTO	From Earth escape
Earth Escape, for example, for Earth-trailing orbit, or L1/L2	3.2	0.7	–
Lunar orbiter at $h=100$ km	4.0	1.5	0.8
Deimos orbiter at $h=1$ km	5.3	2.8	2.1
Mars orbiter at $h=200$ km	5.8	3.3	2.6
Space weather mission at Earth-Sun L5	5.8	3.3	2.6
NEO asteroid rendezvous at 1.2 AU	6.3	3.8	3.1
Mercury flyby	5.6	3.1	2.4
Venus orbiter at $h=400$ km	6.9	4.4	3.7
Main belt asteroid rendezvous at 2 AU	9.5	7.0	6.3

Note that these values are for ballistic trajectories; values for low-thrust missions may be higher.

How far out into the Solar System is it reasonable to expect an independently flying CubeSat to venture? [Table 1](#) provides some  $\Delta V$  values for several examples. The commercially available 1 kg/1U IFM nanotruster from Enpulsion can provide enough total impulse for a 6U CubeSat to achieve 0.8 km/s. The Busek BIT-3 can propel a 14-kg 6U CubeSat to achieve 1.2 km/s of  $\Delta V$  [25]. Clustered into a package of six identical units, this could be increased to stretch to a range of 2.5–3.4 km/s, again for a 6U CubeSat, although for this example the propulsion units would add another 6U to the spacecraft volume, scaling it up to a total of 12U. This range of  $\Delta V$  values puts most of the inner Solar System within reach from an Earth escape trajectory and a few targets within reach from an initial geostationary transfer orbit (GTO-highly elliptical Earth orbit). From an initial LEO orbit at 250 km altitude, it may just about be possible to achieve Earth escape, enabling missions that we may want to go to an Earth-trailing orbit, or to one of the Earth-Moon or Earth-Sun Lagrangian points.

For some segments of some missions, significantly lower  $\Delta V$ s can be effective, at the expense of longer transit times, by utilizing the so-called interplanetary superhighway of multibody gravitational effects, as modeled using LTool software [26–28].

### 5.3 Overcoming telecommunication challenges

Telecommunication issues for interplanetary CubeSats are extreme. Interplanetary CubeSats face harsher environments, have much longer path distances, and have more navigation needs than LEO CubeSats. For this reason the design of telecommunication systems for interplanetary missions is extremely challenging, and significant development is currently ongoing in the areas of radio design, antenna design, and

the design of ground support architectures. All three of these aspects of a space communication system are being addressed, and the success of the MarCO mission shows that the telecommunication challenges faced by interplanetary CubeSats can be overcome with available technologies and proper mission design.

UHF frequencies that are typical of LEO CubeSats can be used, to some extent, at lunar distances, but getting a signal back to Earth at a reasonable data rate, and sending commands up to the spacecraft, generally requires higher frequencies to limit free space losses. While UHF systems may still have value for proximity operations of interplanetary CubeSat constellations, higher frequencies (S-band, X-band, and Ka-band) are more appropriate. To close a telecommunication link over interplanetary distances requires higher Equivalent Isotropic Radiated Power (EIRP) on the spacecraft and the use of large apertures with sensitive electronics on the ground. Since output power of deep space transceivers is limited (typically 4–7 W), the only degrees of freedom related to the communication design are wavelength and antenna dimensions (although effectively higher throughput can be achieved using higher-order modulation schemes, encoding, and advanced techniques like delay tolerant networking). Regarding antennas, typically slotted waveguide, patch or parabolic antennas are used at the higher frequencies, since gain is a function of size. Examples of high-gain antennas flown on CubeSats include the reflectarray antennas on MarCO (0.3 × 0.6 m X-band antenna) and the ISARA 0.34 × 0.24 m Ka-band reflectarray. NASA's RainCube flew a successful deployable 0.5-m-diameter Ka-band parabolic antenna. These missions have proven that the relatively high-gain antennas needed for deep space missions can be adapted to the CubeSat platform [29].

Data rates achieved by large interplanetary spacecraft on deep space missions are a function of distance given that they typically use the most effective technologies (high-gain antennas and the use of the NASA Deep Space Network). NASA's Mars Reconnaissance Orbiter (MRO) achieves a data rate of 4 Mbps from Mars. Juno at Jupiter's distance is reduced to 200 Kbps, while Rosetta at comet 67P/Churyumov-Gerasimenko achieves 20 Kbps. New Horizons at the distance of Pluto achieves only 2 Kbps owing to the extreme range problem. MarCO achieved 16 Kbps at the distance of Mars—a rate that is quite good for a CubeSat in deep space in comparison with these much larger-class missions.

Data rates at the same range could be boosted by a factor of 8 or 9 by switching to Ka-band and by a further factor 6 by using a 1 × 1 m antenna. The trade-off is that the narrower transmit antenna beamwidths (associated with higher frequencies) means that pointing toward Earth can become challenging. Attitude determination and control systems (ADCS) currently available for CubeSats, however, can achieve the platform stability and pointing accuracy needed to support these high-frequency communication systems. Additionally, aggressive use of onboard data compression can achieve high science return, as proven by NASA during the Galileo mission. New Horizons made use of time, taking more than a year after the flyby to send back the highest resolution images from Pluto and Charon. Both mission architectures could well be applicable to CubeSat deep space missions.

On the horizon, optical communications will ultimately be available for the CubeSat platform. A downlink data rate of 600 Mbps was achieved by a CubeSat in LEO,

demonstrating the Optical Communications and Sensor Demonstration (OCSD) flown by the Aerospace Corporation. A data rate of 200Gbps may well be achieved by TBIRD, an upcoming mission by the Massachusetts Institute of Technology (MIT) and Lincoln Laboratories. The Lunar Reconnaissance Orbiter (LRO) achieved 100Mbps using an experimental optical communication system at lunar distances.

Uplink for commanding and ranging typically requires lower data rates and can often be achieved using omnidirectional antennas aboard the spacecraft; to allow for loss of high-gain antenna (HGA) pointing (e.g., in safe mode). Several of the interplanetary CubeSats in development including Lunar IceCube, Lunar Flashlight, and LunaH-Map, utilize the same Iris X-band communication system for uplink and downlink, operating uplink at a much lower data rate. Regardless of the strategy used, a good practical guideline is to have enough bandwidth to allow for spacecraft flight software upgrades in a reasonable timeframe (e.g., one or a few DSN 8-hour passes).

## ***5.4 Deep space navigation and tracking of interplanetary CubeSats***

### ***5.4.1 Deep space navigation and tracking of interplanetary CubeSat ground support***

CubeSats in LEO can be tracked and telemetry downloaded using a ground station comprised entirely of commercially available hardware and operated by anyone with a few hours' training. Add a few thousand-dollars worth more equipment and a licensed amateur radio operator, and commands may be sent to your CubeSat. For most LEO orbits, a ground station may be sited to enable communication no less frequently than every few days. For polar orbits, communications can be enabled nearly every orbit, 90 min apart. Alternatively, equipment and services can be purchased to communicate nearly anytime through orbital relay. Rudimentary navigation services can be set up utilizing the Joint Space Operations Command website. The situation is entirely different for spacecraft going to the Moon and beyond.

While UHF frequencies, in theory, could be used at lunar distances, getting a signal back to Earth, and commands up to the spacecraft, generally requires higher frequencies to limit space losses, for example, S-, X-, and Ka-bands. Obtaining navigation information typically requires measuring Doppler shifts on already weak signals and comparing measured values with predicted values for an estimated orbit, revising the estimate, and driving down differences in an automated, iterative process that proceeds as far as data link noise allows. These functions are readily performed by equipment and people comprising NASA's Deep Space Network (DSN) and smaller networks deployed by ESA, JAXA, RSA, and ISRO. Millions of dollars worth of highly specialized equipment, including sensitive receivers operating at cryogenic temperatures, is required to receive, process, and transmit the signals required to communicate with a world fleet of a few dozen spacecraft, ranging from Voyager 1 and 2 now just barely into interstellar space beyond the Heliopause, to Parker Solar Probe's close approaches to the Sun. To enable interoperability, these networks all adhere to particular Coordinating Committee for Space Data Standards (CCSDS) protocols.

Because of the high cost, these few ground stations are heavily scheduled servicing existing interplanetary missions. While the DSN is making plans to support the 13 CubeSats to be launched with Artemis 1, allocations of time for navigational tracking of each spacecraft, accepting downlinked data and telemetry and commanding, will be minimal and subject to the needs of higher-priority missions, including Artemis 1 itself. It is notable that the DSN is opening itself to the creation of DSN affiliate stations to enable the availability of more apertures to service the anticipated increase in numbers of interplanetary CubeSat and SmallSat missions [29,30].

The first of these, DSS-17, utilizes a 21-m X-band compatible dish at Morehead State University. Other sites may be added around the world to provide greater aperture availability. For trajectories taking a CubeSat beyond a small fraction of 1 AU, data rates no more than a few kbps are viable for the power levels available on a 6U CubeSat. Thus for instruments that produce high data volumes, large onboard storage and a mission plan enabling later playback in small chunks are required. Strategies for mission operations related to interplanetary CubeSats have been developed and proven out on the MarCO mission, and the first steps toward providing tracking, ranging, telemetry, and command services for the impending Armada of deep space CubeSats have been taken [31,32] (Fig. 3).

Given the situation imposed by long distances, interplanetary CubeSats need to be ultimately imbued with significant autonomy software and hardware to (a) process any large data volumes onboard, in some cases elevating the information content per kilobit of data one hundred-fold or one thousand-fold, or more; (b) enable onboard algorithms to detect and respond to abnormal situations and minimize the need to extended “safe modes” that require extensive ground interaction to exit; (c) make decisions as to the highest priority information to return from data stored onboard (see onboard storage and data processing); and (d) (a future possibility) derive much or all of needed navigation information from onboard sources, with only occasional



**Fig. 3** The Morehead State University 21-m ground station has been upgraded with support from NASA’s Advanced Exploration Systems to become the first non-NASA Affiliated node on the DSN. Referred to as DSS-17, the station will support NASA interplanetary CubeSat missions.

updates or checks using Earthbound assets. Automation of interplanetary CubeSats and their associated ground support stations is inevitable.

## **5.5 Navigating CubeSats in deep space**

Deep space navigation enables missions to precisely target distant bodies in the Solar System and to create trajectory and orbit models to explore these targets. Navigation requires the use of trajectory and orbit models, near real-time operation and control, and precise ranging and Doppler techniques. Navigating a spacecraft to deep space locations requires a team of scientists and engineers using sophisticated spacecraft transponders, extremely large ground-based antennas, digital signal processing equipment, and precise timing equipment. These navigation processes and hardware systems needed for interplanetary CubeSats are largely the same as they are for large-scale interplanetary missions.

Navigation and flight dynamics are elements of interplanetary CubeSat missions that do not scale; they require essentially the same resources as other interplanetary missions. Trajectory and orbit modeling tools have been developed by NASA and other organizations for numeric modeling of complicated trajectories for a variety of propulsion systems, including low-thrust solar electric propulsion systems. Low-thrust trajectory design, in particular, has been optimized through a variety of analytic tools that are now available. Precision tracking requires the use of a variety of techniques including Doppler, ranging and Delta-DOR (delta-differential one-way ranging), and PN ranging (pseudonoise ranging). These techniques require a highly capable ranging transponder on the spacecraft and precision timing on the ground (typically a Hydrogen MASER). JPL successfully demonstrated the Iris transponder, a CubeSat X-band transponder system on the MarCO mission. The Iris, combined with DSN assets (including DSS-17), proved that CubeSat technology has evolved to the point of supporting deep space missions.

Future CubeSat missions will build on these successful developments to meet higher performance requirements and allow CubeSat missions to reach deeper into outer space. Future CubeSat missions, like other deep space missions, will rely on an increasing level of autonomy for navigation and will ultimately use optical time transfer (when optical communications are available). Chip-scale atomic clocks, currently under development for space applications, will improve onboard spacecraft timing and therefore facilitate increased precision in tracking and ranging. Ultimately, Pulsars may be used for deep space navigation. What is clear is that technology exists now to support interplanetary CubeSat missions and technology is on the horizon that will support missions that have not been dreamed of today.

## **6 Mission implementation**

### **6.1 Success on (and lessons from) the first try: MarCO A and B**

Early in 2014 the Mars Cube One (MarCO) concept was developed to independently send two small spacecraft to Mars after launching with and separating from the InSight launch vehicle. MarCO's mission, as initially conceived, was to perform

atmospheric observations through radio occultation experiments. NASA's CubeSat Challenge utilized lessons from INSPIRE to develop appropriate competitions that pushed the envelope for deep space CubeSat capability. The MarCO mission, from initial concept through interplanetary flight operations, was a technological demonstration to advance the technology necessary to bring NanoSpacecraft into deep space. While MarCO itself took advantage of the significant developments of INSPIRE (a 3U CubeSat whose intent was to demonstrate the utility of a small spacecraft in deep space, but never flew), it pioneered operational usage and laid the groundwork for many NanoSpacecraft now in development. In the end, MarCO-A and MarCO-B provided a critical real-time communication link to Earth for InSight during its entry, descent, and landing (EDL) on November 26, 2018 when InSight was out of line of sight from the Earth [33].

MarCO A and B, nicknamed Wall-E and Eva by the MarCO team, were 6U CubeSats (Fig. 4). The spacecraft were developed from commercially available components obtained from CubeSat system suppliers. The C&DH and electronics systems were provided by AstroDev of Ann Arbor, Michigan, and Blue Canyon Technologies of Boulder, Colorado, for the attitude control system (ADCS: the XACT). MMA Design LLC, of Boulder, provided solar arrays and Tyvak NanoSatellite Systems Inc., a Terran Orbital Company in San Luis Obispo, California, developed the CubeSat dispenser system. VACCO Industries of South El Monte, California, provided the cold gas micropropulsion system. The propulsion system contains eight thrusters—four canted for attitude control and four for trajectory correction maneuvers (TCMs). The propellant is R-236FA, a cold gas propellant often used in fire extinguishers [34]. The MarCO propulsion system produced 755 Ns of total impulse,

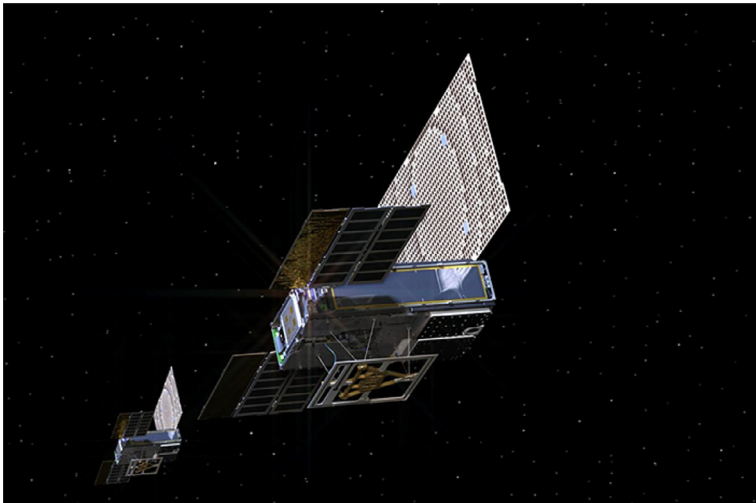


**Fig. 4** Artist's conception of MarCO A and B in flight. Image courtesy NASA/JPL-Caltech.

providing in excess of 40 m/s of TCM  $\Delta V$  capability. All systems were proven to be effective during deep space operations.

During the mission the MarCO spacecraft performed as intended, receiving the UHF telemetry from InSight during its EDL phase and relaying this telemetry at X-band frequencies to NASA's Deep Space Network. In addition to the InSight telemetry, the MarCO spacecraft returned an image of Mars as the spacecraft was passing 6000 km from the planet and images of the Earth–Moon system on the outbound trajectory. In all, the MarCO mission was extraordinarily successful.

MarCO's key lessons stem from the deliberate development of systems with excess capability that could be used in flight operations and the use of a small, multidisciplinary, colocated team. A streamlined governance model served to oversee and review the risks undertaken by the mission, mitigated through extensive end-to-end testing and multiple high-fidelity testbeds. The engineering model spacecraft, serving as a testbed, was critical to mission success and ultimately was used in all aspects of mission operations—checkout, nominal cruise, failure recovery, and EDL planning.

Lessons learned from operating the MarCO mission are being published in a variety of publications—two of the most significant lessons are reported here. These include compensating for a drifting onboard clock and a leaky propulsion system valve that created torques leading to momentum buildup. The MarCO team was able to find innovative solutions to these (and other) problems resulting in a highly successful mission.

Early in the mission the team discovered that the onboard clock was drifting at a significant rate, such that passes were misscheduled by seconds to minutes. Rather than directly adjust the onboard clocks, a calibration function was used to more accurately schedule spacecraft contacts. At each contact the time of carrier acquisition was recorded, along with a telemetry point for the SCLK of radio power on. Together, over multiple passes, these allowed for a simple calibration function to be created to set an onboard wake-up table and provide the DSN with appropriately scheduled contacts.

During the outbound trajectory an excessive momentum buildup was discovered and was found to be increasing over time. The reaction wheels were in danger of becoming saturated, placing the mission at risk. The team suspected that a single external valve was leaking, with the addition of the known tank-to-plenum leak; this provided a direct path for propellant to leave the spacecraft. As the leaky thruster was on a corner, it provided a net torque on the spacecraft in multiple axes, resulting in momentum buildup. The overall rate of momentum buildup was increasing, resulting in rapid and aggressive desaturations (as liquid was being expelled from the full plenum), which were unable to be compensated by the wheels. New sequences were derived to attempt to at least control the impulsive thrusting with the reaction wheels. The team attempted a fix that involved implementing a blow-down sequence every 20 min that was autonomously executed to allow the plenum to empty out of specified thrusters without further opening the tank-to-plenum valve. This would allow for controllable plenum emptying, countering the leaky thruster and keeping internal pressure low (reducing the effect of the leak). The solution worked, reserving adequate propellant, and the burns were executed effectively. The burns were observed in real time with ranging and Doppler due to the healthy power state of the spacecraft, and each segment received execution approvals following a rapid evaluation of telemetry.



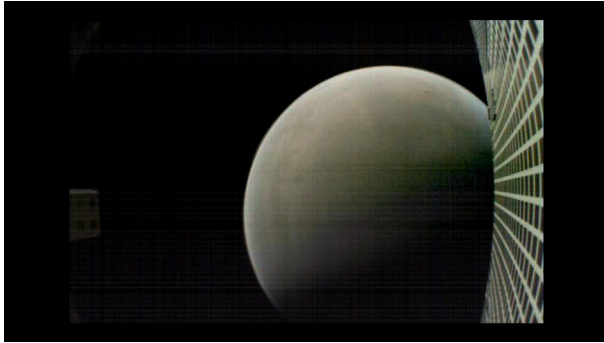


**Fig. 5** By NASA/JPL-Caltech—PIA22833: Farewell to Mars on the NASA Photojournal.

Together, MarCO-A performed 9.2m/s of  $\Delta V$  during TCM-1, and MarCO-B completed 6m/s, bringing both spacecraft to a trajectory with an anticipated close Mars flyby [35] (Fig. 5).

On February 5, 2019, NASA reported that both the CubeSats had gone silent and are unlikely to be heard from again. MarCO, the smallest spacecraft to ever complete an interplanetary mission, has enabled a new class of planetary exploration. At a cost forty times less than most NASA Discovery missions and a schedule of 15 months from concept to first flight article, MarCO demonstrated the feasibility of a constraint-driven interplanetary small spacecraft. The technologies developed for MarCO, including the critical Iris radio, modified commercial hardware, and the flight software, are all available for use from the mission partners and commercial entities. Continued investment from NASA, ESA, JAXA, and others implies a bright future for Solar System exploration with small spacecraft; however, as with MarCO, significant challenges, setbacks, and failures will occur.

MarCO was successful because of a narrow focus, an acceptance of risk, and significant support of its governance council. It built upon technology developed over many missions and was motivated directly from the success of the worldwide CubeSat community. While the mission was never required for InSight success, ultimately over seven million worldwide observers watched the near real-time descent of the lander through the “seven minutes of terror,” with all telemetry relayed through the two MarCO spacecraft. Even InSight’s first image of Mars was sent via MarCO; subsequent media metrics showed more than five billion “impressions” from articles, interviews, social media postings, and replays in the following days. The MarCO mission was a hard-fought success—its choices and subsequent lessons will undoubtedly inform those missions still to come.

## 6.2 Cislunar CubeSats

The 13 secondary payloads to be deployed on Artemis 1, following the success of MarCO, will usher in a new era of Solar System exploration with small satellite platforms. Three of the Artemis 1 lunar orbiter missions, Lunar IceCube (Morehead State

University and Partners), Lunar Flashlight (JPL), and LunaH-Map (Arizona State University and Partners) will contribute to our understanding of the lunar global water cycle and its impact on in situ surface modification processes (degree of interaction with solar wind protons resulting in physical or chemical changes on grain surfaces and the release or generation of volatiles) and on the potential generation or storage of water as a resource [36]. Table 2 describes the impact of each mission on our understanding of sources and sinks for water.

Collectively the Artemis 1 lunar orbiters will provide complimentary observations to be used in understanding volatile dynamics, addressing NASA’s Strategic Knowledge Gaps related to lunar volatile distribution (abundance, location, and transportation physics of water ice). A brief description of each mission follows.

### 6.2.1 Lunar IceCube

Lunar IceCube (L-IC) is a 6U CubeSat designed to prospect for water in solid, liquid, and vapor forms and other volatiles from a low-perigee, highly inclined lunar orbit. The mission was selected by NASA to fly on Exploration Mission-1 (renamed Artemis 1) in 2021. Sponsored by NASA’s Advanced Exploration Systems (AES) Program, the mission is a partnership between Morehead State University, NASA Goddard Spaceflight Center, JPL, the NASA Independent Verification and Validation Center (IV&V), and Busek Space Propulsion Company. Lunar IceCube will be deployed during translunar trajectory by the Space Launch System (SLS) and use an innovative RF ion engine to achieve lunar capture and the science orbit (inertially locked, highly elliptical, 100-km periapsis) to investigate the distribution of water as a function of time of day, latitude, and regolith composition in the context of lunar mineralogy. Lunar IceCube will include the Broadband InfraRed Compact High-Resolution Exploration Spectrometer (BIRCHES), developed by GSFC—a compact version of the successful New Horizons instrument designed with the high spectral resolution (5 nm) and wavelength range (1–4 μm) needed to distinguish forms of

**Table 2** Comparison of volatile mission impacts on understanding the water cycle.

Water source or sink	Solar wind (time of day, latitude, shadowing effects)	Meteorite impact (transients)	Pyroclastics, other bound-water minerals (globally distributed volcanic deposits)	Polar cold traps (shadowed regions, buried ice)	Thermal migration (time of day, latitude, poleward facing slopes)
L-IC	Time of day	Maybe	Yes	No	Yes
LM	Shadowing	Maybe	No	Yes	No
LF	Shadowing	Maybe	No	Yes	No

water, including ice [37]. The mission will complement the scientific work of other missions by focusing on the abundance, location, and transportation physics of water ice on the lunar surface at a variety of latitudes. Lunar IceCube, while primarily a science mission, will demonstrate technologies that will enable future interplanetary exploration with small satellite platforms including radiation-hardened systems and subsystems, the Iris precise ranging transponder/transceiver, a capable attitude determination and control system, a high-power solar array, and an innovative electric propulsion system (EP). The EP (Busek BIT-3 Iodine engine) generates 1.2 km/s of  $\Delta V$  [BIT-3] and, combined with an innovative low-energy manifold trajectory on the interplanetary superhighway, allows the spacecraft to reach lunar orbit from Earth escape with minimal energy.

The primary science objectives of the Lunar IceCube mission are to undertake spectral determination of the composition and distribution of volatiles in the lunar regolith as a function of time, latitude, and regolith age and to provide a geological context for those measurements through spectral determination of mineral components. Lunar IceCube could determine the relationship between adsorbed and bound water, hydroxyl, and ice throughout the diurnal cycle. The mission also has the potential to lend insight into understanding the role of external sources, internal sources, and solar wind proton and micrometeorite bombardment in formation, trapping, releasing of water, and exosphere formation.

Although previous missions (e.g., Clementine, Chandrayaan-1, and LRO/LCROSS) discovered various signatures of OH/H<sub>2</sub>O on the lunar surface, they were not optimized for volatile characterization. BIRCHES is designed with a high spectral resolution (5 nm) and wavelength range (1–4  $\mu\text{m}$ ) needed to fully characterize water and other volatiles and to distinguish forms of water, including ice. Because the emphasis was on maximizing coverage during the nominal mission, LRO was not designed to provide repeated systematic (by time of day) measurements of representative features at higher and lower latitudes. IceCube is designed to provide these systematic measurements [38]. Working together as the first “ad hoc” constellation of interplanetary CubeSats exploring the Moon, Lunar IceCube, Lunar Flashlight, and LunaH-Map have the potential to lend significant insight into the location, depth, cyclic nature, and transport mechanisms of water on the Moon (Fig. 6).

### 6.2.2 Lunar Flashlight

Lunar Flashlight (LF) is a 6U CubeSat mission developed by a team from the Jet Propulsion Laboratory and the Marshall Space Flight Center that was selected by NASA’s Advanced Exploration Systems (AES) program in 2013. Planned to launch on the Space Launch System’s Artemis 1 flight in 2021, this innovative, low-cost CubeSat mission will map the lunar South Pole for volatiles and demonstrate several technological firsts, including being among the first CubeSats to reach the Moon, the first planetary CubeSat mission to use green propulsion, and the first mission to use lasers to look for water ice. Locating ice deposits in the Moon’s permanently shadowed craters addresses one of NASA’s Strategic Knowledge Gaps (SKGs) to detect

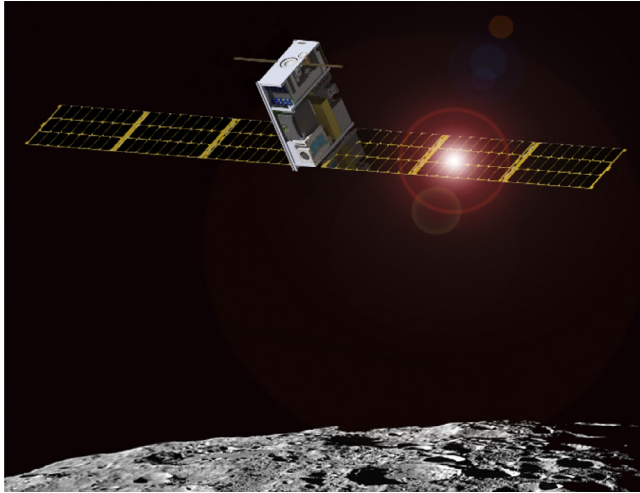


**Fig. 6** The Lunar IceCube mission is designed to prospect for water ice and other lunar volatiles from lunar orbit. Morehead State University is leading the mission in partnership with NASA Goddard Spaceflight Center, JPL, Busek, and the NASA Independent Verification and Validation Center (IV&V).  
Image credit: Morehead State University.

composition, quantity, distribution, form of water/H species, and other volatiles associated with lunar cold traps [39].

The scientific and economic importance of lunar volatiles extends far beyond the question “is there water on the Moon?” Volatile materials including water come from sources central to NASA’s strategic plans, including comets, asteroids, interplanetary dust particles, interstellar molecular clouds, solar wind, and lunar volcanic and radiogenic gases. The volatile inventory, distribution, and state (bound or free, evenly distributed or blocky, on the surface or at depth, etc.) are crucial for understanding how these molecules interact with the lunar surface and for utilization potential [40].

The Lunar Flashlight mission spacecraft maneuvers to its lunar polar orbit and uses its near-infrared lasers to shine light into the shaded polar regions, while the onboard reflectometer measures surface reflection and infers composition from the reflectance ratios between the different laser bands. The Lunar Flashlight 6U spacecraft has heritage elements from predecessor systems including JPL’s Interplanetary NanoSpacecraft Pathfinder in a Relevant Environment (INSPIRE), Mars CubeSat One (MarCO), and JPL’s experience with spectrometers, including the Moon Mineralogy Mapper (M3) [41]. The mission will demonstrate a path where 6U CubeSats could, at a much lower cost than previously thought possible, explore, locate, and estimate size and composition of ice deposits on the Moon. Polar volatile data collected by Lunar Flashlight data could be key to selecting future surface exploration targets, for more expensive lander- and rover-borne measurements, based on its laser reflection measurements of surface ice fraction and areal extent (Fig. 7).

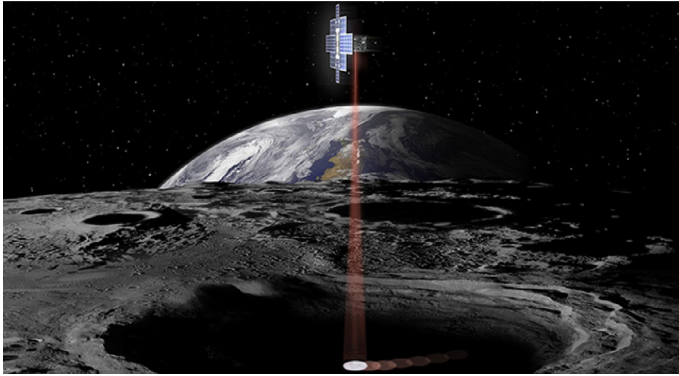


**Fig. 7** Artist's concept showing the Lunar Flashlight spacecraft, a six-unit CubeSat designed to search for ice on the Moon's surface. The spacecraft will use its near-infrared lasers to shine light into shaded polar regions on the Moon, while an onboard reflectometer will measure surface reflection and infer composition.

Image credit: NASA/JPL-Caltech.

### 6.2.3 *LunaH-Map*

The Lunar Polar Hydrogen Mapper (LunaH-Map, or LM) is a 6U+ CubeSat funded through NASA Science Mission Directorate's Small, Innovative Missions for Planetary Exploration (SIMPLEx) program. LunaH-Map will make maps of hydrogen enrichments near the Moon's South Pole at spatial scales smaller than the extent of the neutron suppressed regions detected by the NASA Lunar Prospector (LP) and Lunar Reconnaissance Orbiter (LRO) missions [42]. Like LP and LRO, LunaH-Map will use a neutron spectrometer to create a map of hydrogen abundance; however, LunaH-Map will fly at much lower altitudes over the lunar South Pole to create maps of hydrogen enrichments at finer spatial resolutions than achieved by previous missions. Arizona State University began the development of LunaH-Map after being awarded a contract by NASA in early 2015. LunaH-Map's primary objective is to map the abundance of hydrogen down to 1 m beneath the surface of the lunar south polar region. This information may then be used to improve scientific understanding of how water is initially distributed and spread throughout the Solar System and where water might be found by future manned missions for life support and fuel production. It will be inserted into a polar orbit around the Moon, with its periapsis located near the lunar South Pole, initially passing above Shackleton crater [43].

Planetary nuclear spectroscopy relies on detection of leakage neutrons generated by galactic cosmic rays interacting within the top meter of the body's surface. Fast neutrons produced by the GCR interaction undergo further interactions with the regolith. With a mass roughly equivalent to one neutron, hydrogen is particularly efficient at reducing the energy of neutrons. As such, regions with increased hydrogen abundance will have a depressed flux of epithermal ( $E > 0.3$  eV) neutrons, whereas the flux of thermal ( $E < 0.3$  eV) neutrons will be enhanced. The mission's primary payload, the

Miniature Neutron Spectrometer (Mini-NS), has been designed to use the scintillator material  $\text{Cs}_2\text{YLiCl}_6:\text{Ce}$  and a thin shield of gadolinium (which absorbs thermal neutrons) to measure count rates of epithermal neutrons [44].

### 6.3 Asteroids, Mars, and the outer Solar System

Concepts for interplanetary CubeSat missions have stretched beyond the Moon to include the inner Solar System, asteroids, and ultimately the outer Solar System. The first of these missions likely to be implemented since MarCO is the Near-Earth Asteroid Scout (NEA Scout). NEA Scout, one of the 13 missions selected for Artemis 1, is a 6U CubeSat developed by a partnership between NASA's Marshall Space Flight Center and the Jet Propulsion Laboratory. NEA Scout is a flyby encounter of an asteroid representative of Near-Earth Asteroids (NEAs) that are potential human destinations. Target NEAs are currently being evaluated and are updated based on the dynamic launch date of Artemis 1, on new discoveries and expected performance. The current planned target is 1991VG, a small NEA in a heliocentric orbit that brings it near the Earth (0.0568 AU in 2017), making it a prime target for CubeSat exploration [45].

NEA Scout's science mission is to determine the characteristics of 1991VG including its global shape, spin rate, pole position, regional morphology, regolith properties, and spectral class using an optical imager to capture a series of low- (50 cm/pixel) and high-resolution (10 cm/pixel) images. The mission's concept of operations is unique. SLS will carry the CubeSat to Earth escape and placed on lunar trajectory. Once NEA Scout reaches the lunar vicinity, it will utilize a cold gas propulsion system to provide the initial propulsive maneuvers. NEA Scout will then utilize an 84 m<sup>2</sup> solar sail, leveraging the CubeSat's continual solar exposure for efficient transit to the target asteroid during an approximate 2-year cruise [46]. NEA Scout, along with the other Artemis 1 CubeSats, will prove out innovative enabling technology to support future Solar System exploration utilizing the CubeSat form factor and produce science data that will ultimately support human exploration of the Solar System (Fig. 8).

A recent study conducted jointly by JPL and the Aerospace Corporation looked at microlanders that could be carried to Mars as secondary payload(s) on spacecraft bound for Mars [47]. In the study, each lander (Fig. 9) consists of a 30-cm-diameter probe, carrying a ~1 kg scientific payload. The concept built on the success of Aerospace's small Earth Reentry Breakup Recorder (REBR) vehicle (which was a CubeSat-based technology demonstration) to design a low mass/low ballistic coefficient entry system that allows for subsonic deployment of a steerable parawing hang glider, capable of up to 10 min and more than 10 km of guided flight, which would impact the surface with a 3:1 glide ratio at ~20.5 m/s. The MarsDROP concept would enable scientists to reach areas of Mars that are inaccessible to larger landed missions [47].

In October 2014, JPL selected proposals from 10 universities to study CubeSat concepts that could enhance the Europa Clipper mission currently planned for a 2023 launch opportunity by NASA [48]. As illustrated in Fig. 10, such CubeSats would be carried to Jupiter by the host spacecraft and then released on approach to Europa to execute their assigned mission. In this mother-daughter architecture, the CubeSat

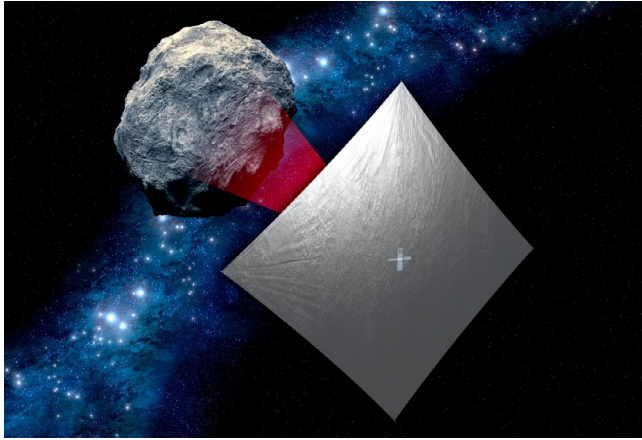


**Fig. 8** Artist’s conception of NEA Scout CubeSat with its solar sail deployed as it characterizes a near-Earth asteroid. Image is courtesy of NASA.

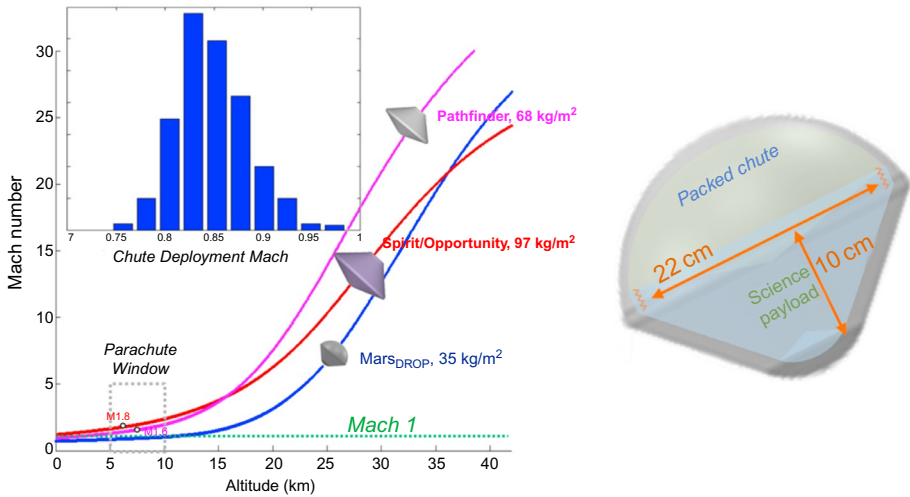


**Fig. 9** MarsDROPS MicroProbe concept.

elements can approach much closer to the surface of Europa than the primary spacecraft, enabling unique science observations. As an example, one CubeSat under study by the University of Michigan proposed to use multifrequency magnetic induction sounding from a compact magnetometer to characterize the subsurface ocean of Europa [49]. At the time of writing, it appears that Europa Clipper will likely not have sufficient mass margin to accommodate any of the 10 concepts, but that does not eradicate the validity and creativity of these mother-daughter concepts, which can be dusted off and revamped for future outer planet missions (Fig. 10).

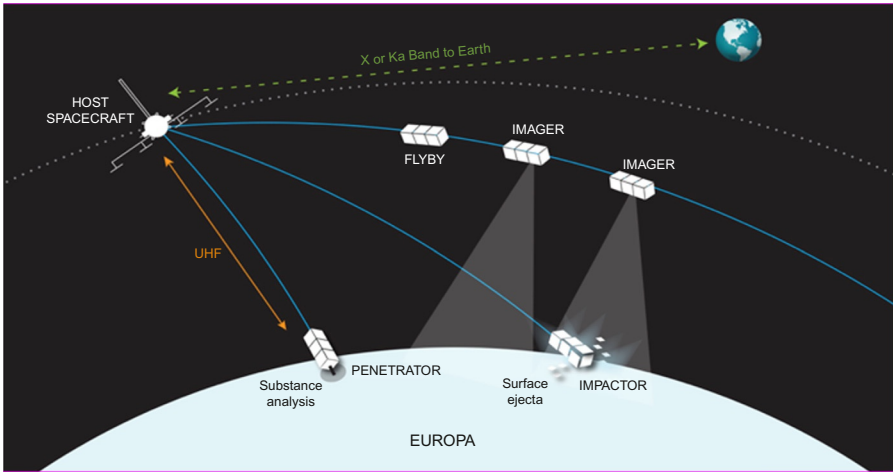


**Fig. 10** Illustration of CubeSats deployed from the Europa Clipper mission.

## 6.4 Venus

Recent mission concept studies continue to push the boundaries of the science that is possible with CubeSats and SmallSats. Another recent study at JPL examined a free-flyer nanosat probe, launched directly from Earth toward Venus [50]. While the probe does not conform strictly to the CubeSat form factor, it is highly derivative of CubeSat systems. The probe targets very high priority science at Venus—the need to measure the relative abundances of Neon, Argon, Helium, Krypton, and other noble gases to understand how Venus’ atmosphere formed and has evolved. To be truly representative of the noble gases and their isotopic ratios, a sample of the atmosphere has to be acquired where the atmosphere is well mixed at an altitude below the homopause, which for Venus is around 120 km.

The study came up with a novel, low-cost, SmallSat architecture for a conceptual stand-alone mission that would sample the noble gases and their isotopic ratios at Venus. Sampling is achieved by a compact ion-trap mass spectrometer incorporated into a small (60 cm diameter) probe that skims through the atmosphere, targeting a closest approach altitude above the surface below the nominal 120 km (Fig. 11). Following acquisition the gas sample is analyzed over a period of  $\sim 60$  min.

The Venus probe and carrier spacecraft are assumed to launch together on a Type II trajectory toward Venus, on a dedicated smaller-class rocket, with a kick stage. The probe and carrier spacecraft both make extensive use of NanoSpacecraft components. The compact mass spectrometer instrument mass is estimated at 8 kg. En route to Venus the carrier spacecraft would execute preplanned TCM maneuvers for a total  $\Delta V$  of about a hundred meters per second. On approach the carrier spacecraft would spin up to rotate at  $\sim 10$  rpm and then release the probe on its path to skim through the atmosphere. The carrier spacecraft would then execute a small maneuver (with a few meters per second of  $\Delta V$ ) to fly past Venus above the atmosphere. Each sample



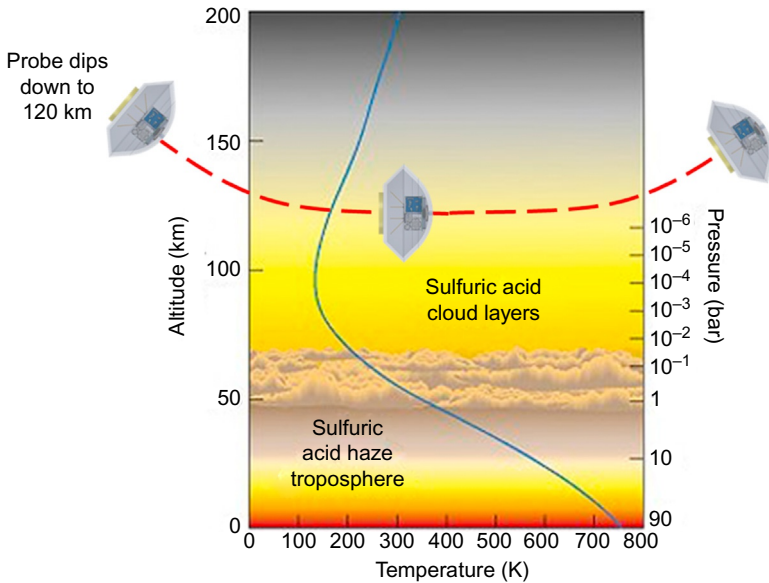


**Fig. 11** Venus atmospheric sampling probe would skim through the atmosphere to sample the noble gases below the homopause at  $\sim 120$  km altitude above the surface. Image courtesy of NASA/JPL/Caltech.

acquired is then analyzed by a miniaturized quadrupole ion trap mass spectrometer (QITMS) developed at JPL (see Fig. 12). A calibrant tank provides a reference for calibration. Data are transmitted to Earth during the long apoapsis segment of the orbit. The current estimate for the mass of the dry probe is 70 kg, including margins. Following the probe skim through and data analysis, results are returned to Earth via a UHF/X-Band relay, similar to that developed for MarCO.

## 7 Planned NASA interplanetary CubeSat missions

Today, Solar System exploration missions are the exclusive domain of space agencies and their scientists and engineers who can muster multi-hundred-million dollar budgets. While their accomplishments are broad, the high cost limits our pace of important discoveries. Interplanetary CubeSats, however, offer an opportunity to conduct focused science investigations around the inner Solar System at a cost 10 times lower than missions mounted today. Adopting this exploration philosophy, NASA has dozens of interplanetary CubeSat missions in various stages of planning and development. Among these are numerous missions planned by JPL, NASA Centers including the Goddard Spaceflight Center, the Marshall Space Center, and a collection of missions funded as studies under the NASA Planetary Science Deep Space SmallSat Studies (PSDS3) program.

## Venus NanoSat probe concept

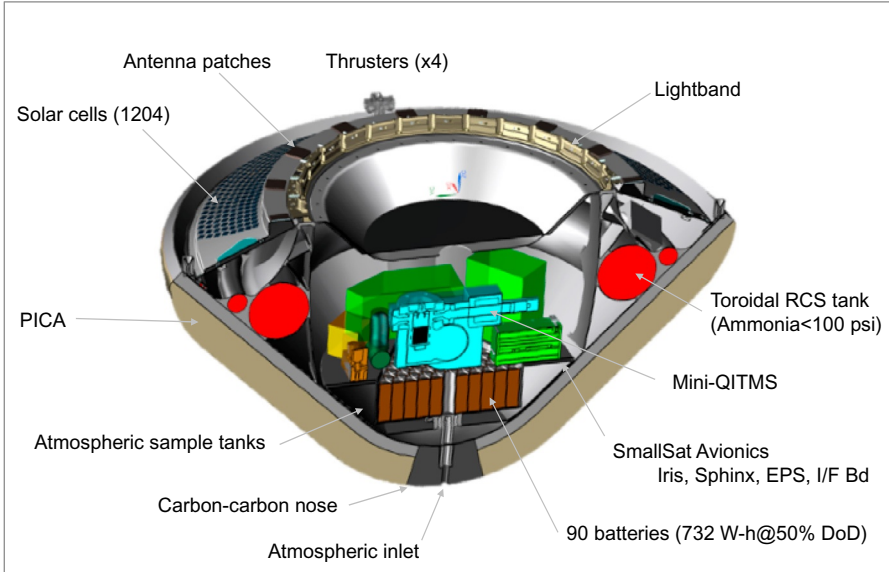


**Fig. 12** Cutout depicting the design of the Cupid’s Arrow Venus atmospheric “skimmer”. Image courtesy of NASA/JPL/Caltech.

Ten studies were selected under the PSDS3 program that utilize SmallSat platforms to explore Venus, Earth’s Moon, asteroids, Mars, and the outer planets. For the purpose of the study, SmallSats were defined as having a mass less than 180 kg [51]. Several of the PSDS3 missions are CubeSats; these are briefly described in the succeeding text, categorized by the Solar System body targeted for exploration.

## 7.1 Venus

### 7.1.1 CubeSat UV Experiment (CUVE)

CUVE is a study undertaken at the University of Maryland, College Park based on a 12-unit CubeSat orbiter that is intended to measure ultraviolet absorption and night-glow emissions to understand Venus’ atmospheric dynamics.

### 7.1.2 Cupid’s Arrow

Cupid’s Arrow is a 70-kg probe proposed by JPL to measure noble gases in the atmosphere of Venus and their isotopes to investigate the comparative geological evolution of Venus and the Earth (described previously).

## **7.2 Earth's Moon**

### **7.2.1 CubeSat X-ray Telescope (CubeX)**

CubeSat X-ray telescope (CubeX) is a study undertaken by the Smithsonian Astrophysical Observatory, Cambridge, Massachusetts. The primary mission of CubeX, a 12-unit CubeSat, is to map the elemental composition of airless bodies such as the moon to understand their formation and evolutionary history.

### **7.2.2 Bisat Observations of the Lunar Atmosphere above Swirls (BOLAS)**

BOLAS is a collaboration between the NASA Goddard Spaceflight Center, Morehead State University, and Tethers Unlimited to perform a study to deploy two 12U CubeSats in lunar orbit tethered by a thin tens of kilometers-long tether allowing them to fly in a gravity gradient formation. The objective is to investigate the hydrogen cycle by investigating the mechanisms and dynamics of lunar hydrogen implantation and their dependence on composition, regolith properties, local topography, plasma conditions, time of day, and crustal magnetic fields [52].

## **7.3 Asteroids**

### **7.3.1 Asteroid Probe Experiment (APEX)**

APEX is a study undertaken by the Johns Hopkins University Applied Physics Laboratory, Laurel, Maryland to develop a SmallSat with a deployable seismometer to rendezvous with the asteroid Apophis and directly explore its interior structure, surface properties, and rotational state.

### **7.3.2 CubeSat Asteroid Encounters for Science and Reconnaissance (CAESAR)**

Lockheed Martin Space Systems Company, Littleton, Colorado led the CubeSat Asteroid Encounters for Science and Reconnaissance (CAESAR) study; CAESAR is a constellation of 6-unit CubeSats designed to evaluate the bulk properties of asteroids to assess their physical structure and to provide constraints on their formation and evolution.

## **7.4 Mars**

### **7.4.1 Chariot to the Moons of Mars**

Purdue University, West Lafayette, Indiana led the Chariot to the Moons of Mars study program. Chariot is a 12-unit CubeSat with a deployable drag skirt designed to produce high-resolution imagery and surface material composition of Phobos and Deimos to lend insight into the formation of these Moons of Mars.

### **7.4.2 *Aeolus***

NASA Ames Research Center, Moffett Field, California led the Aeolus study. The Aeolus mission concept is based on a 24-unit CubeSat intended to directly measure vertically resolved global winds to help determine the planetary-wide energy balance of Mars and to lend insight into Martian climate variability.

## **7.5 *Icy Moons and outer planets***

### **7.5.1 *Small Next-generation Atmospheric Probe (SNAP)***

The SNAP study was led by team at Hampton University, Virginia. SNAP is an atmospheric entry probe intended to measure vertical cloud structure, stratification, and winds of the atmosphere of Uranus. The science goal is to lend insight into the chemical and physical processes that shape the atmosphere of Uranus.

### **7.5.2 *Jupiter Magnetospheric boundary ExploreR (JUMPER)***

The JUMPER concept study was led by Southwest Research Institute, San Antonio, Texas. JUMPER is a SmallSat intended to explore Jupiter's magnetosphere, including characterization of the solar wind upstream of the magnetosphere to providing science context for future missions such as the Europa Clipper.

While the missions described in the preceding text do not represent a comprehensive list of NASA interplanetary CubeSat missions in study and planning, the number and breadth of these missions illustrate the level at which NASA has embraced the interplanetary CubeSat paradigm.

## **8 *Planned ESA interplanetary CubeSat missions***

The European Space Agency has also enthusiastically adopted the CubeSat paradigm for some of its upcoming Interplanetary missions, as described in this section.

### **8.1 *CubeSats on the Hera mission to Didymos***

ESA's Hera mission to the binary near-Earth asteroid Didymos is the agency's contribution to the international Asteroid Impact and Deflection Assessment (AIDA) collaboration with NASA. The NASA Double Asteroid Redirection Test (DART) spacecraft planned to launch in late 2020/early 2021 is targeting to impact the smaller of the two bodies in the Didymos binary system (dubbed "Didymoon") at very high velocity in late 2022. Hera is under development for launch in 2024 and is planned to rendezvous with Didymos in 2026 to perform a detailed characterization of Didymoon postimpact and hence gather important data relevant to the kinetic energy impact technique for asteroid deflection in planetary defense scenarios. As part of its payload, Hera will carry two 6U CubeSats on its interplanetary cruise phase and deploy them upon arrival at Didymos. During the long cruise the CubeSats are stowed inside a CubeSat Deployer specially developed to provide power, data, and thermal interfaces.

Due to the weak gravity field of the asteroid, the Deployer has to be capable of deploying the two CubeSats at very low velocity of only a few cm/s; otherwise they will quickly drift away from the asteroid vicinity. The two CubeSats will be operated via an S-band intersatellite link (ISL) with the Hera mothercraft as a communication relay with Earth ground stations and mission control. Once deployed at the Didymos system, the CubeSats are planned to be navigated in close proximity to the smaller body Didymoon where they will perform close-up measurements with their respective miniaturized instrument suites and eventually attempt a landing. Navigation is enabled by a combination of ranging function over the ISL and visual camera-based center-of-brightness observations relative to Didymain and Didymoon [53].

The first CubeSat is called Juventas, developed by Danish company GomSpace and GMV in Romania. It will measure the gravity field and the internal structure of the two smaller Didymos asteroids. In close orbit around Didymoon, Juventas will line up with Hera to perform satellite-to-satellite radio science experiments and carry out a low-frequency radar survey of the asteroid interior, similar to performing a detailed “x-ray scan” of Didymoon to unveil its interior. The adventure will end with a landing using the dynamics of any likely bouncing to capture details of the asteroid’s surface material, followed by several days of surface operations (Fig. 13). Due to funding constraints, the second CubeSat is currently under consolidation and is planned to start development in the short term.

## 8.2 *Lunar CubeSats for Exploration (LUCE)*

Within the framework of the European Exploration Envelope Programme (E3P), a number of commercial partnerships have been established between ESA and industry. One of these is the Commercial Lunar Mission Support Services partnership with

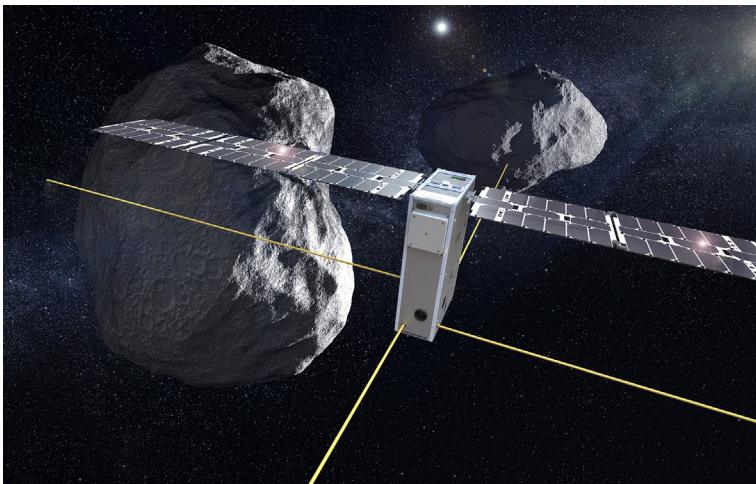


**Fig. 13** The Juventas CubeSat will probe the interior of the Didymos asteroid using a low-frequency radar.

Credit: ESA/Gomspace.

SSTL and Goonhilly Earth Station in the United Kingdom. The definition phase of the partnership is ongoing, and the second phase is proposed to comprise the Lunar Pathfinder mission to demonstrate provision of communication and navigation services to lunar orbiting or lander assets. Lunar Pathfinder is planned to launch in 2023 and during its operational lifetime, is planned to communicate with two 12U CubeSats in lunar orbit. After the CubeSats are deployed, they are planned to be operated by using Pathfinder as a communication data relay to the Goonhilly station interfaced to the two CubeSat mission control centers.

### 8.3 LUMIO

The two CubeSats were selected via an open competitive Request for Information process for Lunar Payloads. The mission concepts were previously joint winners of the ESA SysNova Challenge on “Lunar CubeSats for Exploration (LUCE),” an open competitive Announcement of Opportunity process that downselected four lunar CubeSat concepts for further study.

LUMIO is led by an Italian/Dutch/Norwegian consortium (Politecnico Di Milano, Innovative Solutions In Space b.v., TU Delft, EPFL, S[&]T Norway, Leonardo S.p.A, Uni. Arizona). The mission objective is to perform meteoroid impact flash monitoring of the lunar far side from an Earth-Moon L2 halo orbit using a high-frame rate optical camera. The CubeSat system consists of a single 12U with propulsion for L2 transfer and capabilities of autonomous onboard optical navigation of the lunar disk (Fig. 14).

### 8.4 VMMO

VMMO is led by a Canadian/UK consortium (MPB Communications, Surrey Space Centre, Uni. Winnipeg, and others) and is aimed at measuring the content of water ice deposits in permanently shadowed craters at South Pole, minerals (e.g., ilmenite) on

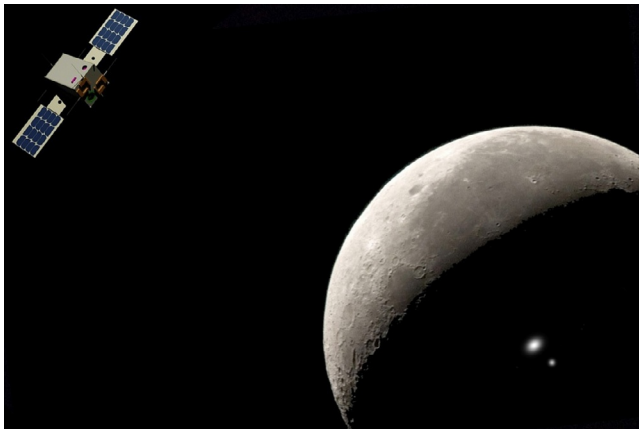


**Fig. 14** Illustration of the LUMIO CubeSat at Earth-Moon L2 Lagrangian point.  
Credit: Politecnico di Milano.

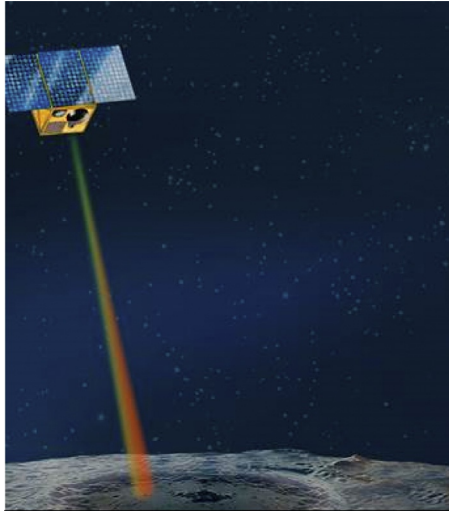


**Fig. 15** Illustration of VMMO CubeSat performing low-altitude observations of lunar ice with active fiber laser spectrometer.  
Credit: MPB Communications.

the day side, and the lunar radiation environment. The payload consists of an Active Fiber Laser spectrometer (1560 and 530nm with 10-m spot size) and a radiation environment sensor. The CubeSat system consists of a single 12U CubeSat with electric propulsion for transfer to very low lunar orbit for conducting the required observations at low altitude (Fig. 15).

### **8.5 Miniaturized Asteroid Remote Geophysical Observer (M-ARGO)**

The M-ARGO mission is proposed as a highly innovative mission to demonstrate critical technologies and operations for stand-alone deep space CubeSats in the relevant environment, rendezvous with a near-Earth object (NEO), and perform physical characterization of the object with a small payload suite for in situ resource exploration purposes. A successful demonstration of M-ARGO would be the world's first CubeSat to independently rendezvous with and study an asteroid over an extended period in close proximity. ESA studies on the M-ARGO mission concept have shown that it is feasible to integrate a number of enabling miniaturized technologies (see Fig. 16) into a 12U CubeSat platform and, based on a piggyback launch to Sun-Earth L2 transfer, have sufficient performance to rendezvous with a near-Earth object while carrying a small payload. Up to 140 different NEOs were found (so far) to be accessible with the current system design. M-ARGO is planned to lower the entry-level cost of deep space exploration by over an order of magnitude. This will enable new system architectures and missions, such as fleets of nanoprobes for in situ resource exploration of NEOs and for other applications such as planetary science, planetary defense,

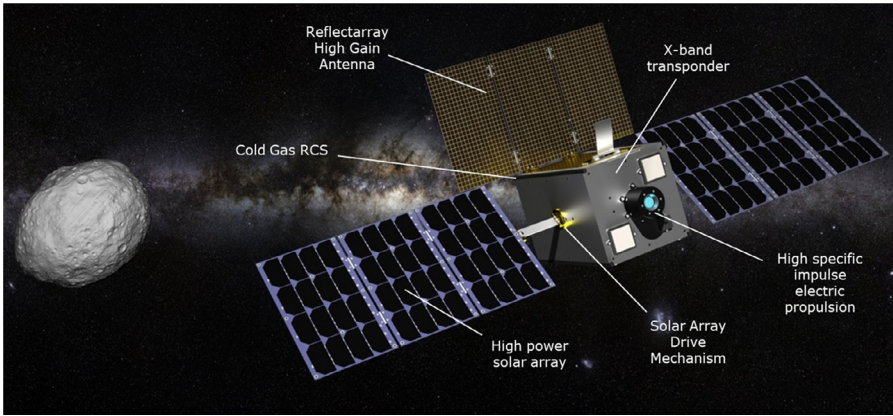


**Fig. 16** M-ARGO stand-alone CubeSat mission for NEA rendezvous.  
Credit: ESA.

and space weather monitoring, for example. Currently all of the critical technologies are under development. The contract for the industrial Phase A study was kicked off with GomSpace Luxembourg and Politecnico di Milano. Flight readiness is targeted for 2023, dependent upon further funding for the implementation phase [54].

## 9 Future opportunities

### 9.1 Daughter spacecraft to larger missions

To get to the outer Solar System, as discussed earlier, CubeSats are going to have to hitch a ride on larger planetary science missions, making good use of excess mass margin. One recent mission, Cassini, made countless discoveries at Saturn furthering our knowledge of the Solar System formation and finding new ocean worlds that might have the possibility of supporting life. But now that the mission has ended, questions remain unanswered, and new ones have arisen. To address this the planetary science community has proposed several follow-on missions. Dragonfly, selected for NASA's next New Frontiers mission opportunity, aims to land a quadcopter on the surface of Titan to study prebiotic chemistry and potential habitability [55]. If the mission, as selected, has ample mass margin, it could accommodate ride-along CubeSats that could accompany the primary spacecraft to Saturn and perform unique and ground-breaking science as well as demonstrate new technologies.

In a recent study [56], 10 “hitch-hiker” CubeSat and SmallSat concepts were studied that could ride along on NASA's next mission to the Saturn system. These concepts included probes similar to Cupid's Arrow but targeting the atmospheres of Venus (en route to Saturn), Saturn, and Titan, orbiting CubeSats to study the magnetosphere, stereo mapping of the South Pole of Enceladus and other phenomena at Titan, and finally a “Ring-Diver” to get the closest possible view of Saturn's famous ring system; see Fig. 17. These concepts for exploring the Saturn system would take



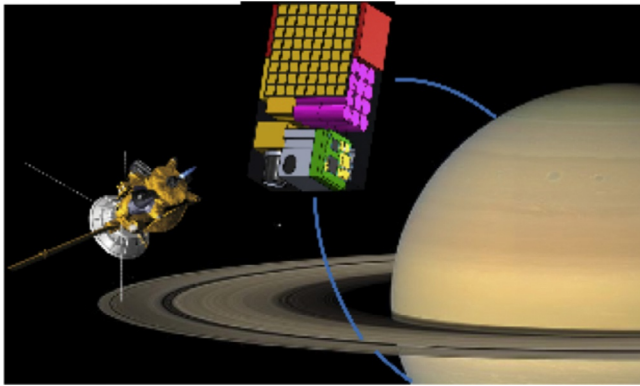


**Fig. 17** The Saturn Ring-Diver CubeSat mission concept.

advantage of advances in Small/CubeSat technology, demonstrating their ability to be used outside the traditional confines of LEO. New technology and instruments would also be demonstrated for use in future missions.

JPL recently proposed seven CubeSat/Nanosat missions as technology demonstrations to augment larger missions proposed to NASA's Discovery program [57]. Each CubeSat or Nanosat was carried in a mother-daughter configuration to its destination in the Solar System, which ranged from Venus to main-belt asteroids, a Jovian comet, and Phobos [58]. Each provided a unique capability that could have augmented the science of the companion (mother) discovery mission. Some were flybys of the target body to offer a closer look than could be risked with the main spacecraft, others provided in situ measurements. None of these concepts were selected for flight, but they remain documented as evidence of the creativity of the CubeSat community, and can easily be pulled off the shelf as the foundation for future Interplanetary CubeSat missions.

One forward-looking mission concept submitted to the recent NASA Discovery call proposed to achieve all of its science using NanoSats. The NANOSWARM mission concept [59] positions a fleet of NanoSats in orbit around the Moon to address science questions on space weathering; the origins of planetary magnetism; the origins, distributions, and migration processes of surface water on airless bodies; and the physics of small-scale magnetospheres. The NANOSWARM concept uses a novel "mother-with-many-children" architecture to place its CubeSat Armada into a low, circular, polar lunar orbit. The mother ship releases some CubeSats on impact trajectories into the hearts of lunar magnetic anomalies to measure magnetic fields and proton fluxes, in real time, up until the last tens of milliseconds. A second set of CubeSats would then be released into a polar orbit with a periapsis over the South Pole to measure neutron fluxes.

In LEO, SmallSats and CubeSats have changed the exploration paradigm, offering a fast and low-cost alternative to traditional space vehicles. These small spacecraft have spawned a revolutionizing industry for performing cutting-edge science. This new mission development philosophy has the potential to significantly change the

economics of interplanetary exploration. A number of missions are in development, which utilize CubeSat class spacecraft beyond Earth orbit, while mind-blowing newer concepts will emerge inspired by the experiences of these first CubeSat Solar System explorers.

## References

- [1] A. Babuscia, K. Angkasa, B. Malphrus, C. Hardgrove, Development of Telecommunications Systems and Ground Support for EM-1 Interplanetary CubeSat Missions: Lunar Ice-Cube and LunaH-Map, IAC-17-B4, 2017.
- [2] R. Staehle, D. Blaney, H. Hemmati, D. Jones, A. Klesh, P. Liewer, J. Lazio, M. Wen-Yu Lo, P. Mouroulis, N. Murphy, P. Pingree, T. Wilson, B. Anderson, C. Channing Chow II, B. Betts, L. Friedman, J. Puig-Suari, A. Williams, T. Svitek, Interplanetary CubeSats: opening the Solar System to a broad community at lower cost, *J. Small Satell.* 2 (1) (2013) 161–186.
- [3] C. Norton, et al., *Small Satellites: A Revolution in Space Science*, KISS Institute for Space Studies Report, July 2014.
- [4] A. Freeman, C. Norton, Exploring our Solar System with Cubesats and nanosats, in: 13th ReInventing Space Conference, Oxford, United Kingdom, 2015.
- [5] A. Freeman, Deep space nanosats – poised for exponential growth, in: Proceedings of the 4S Symposium, Valletta, Malta, 2016.
- [6] T. Zurbuchen, et al., *Achieving Science with CubeSats, Thinking Inside the Box*, National Academies Press, 2016.
- [7] A. Freeman, J. Hyon, D. Waliser, The cube-train constellation for Earth observation, in: 13th Annual Cubesat Developer’s Workshop, San Luis Obispo, CA, 2016.
- [8] A. Freeman, R. Friedl, Time-series measurements for earth system science, in: *Smallsat Symposium*, Logan, UT, 2017.
- [9] A. Freeman, N. Chahat, S-Band Smallsat InSAR Constellation For Surface Deformation Science, in: *Proceedings of Radarcon 2017*, Seattle, WA, 2017.
- [10] National Research Council, *2017-2027 Decadal Survey for Earth Science and Applications from Space*, National Academies Press, 2018.
- [11] A. Freeman, Small is beautiful—technology trends in the satellite industry and their implications for planetary science missions, in: *Planetary Science Vision 2050 Workshop*, NASA HQ, Washington, DC, February, 2017.
- [12] A. Freeman, L. Alkalai, The First Interstellar Explorer: what should it do when it arrives at its destination? in: *Fall AGU Meeting*, New Orleans, LA, 2017.
- [12a] R.L. Staehle, A. Babuscia, J. Bellardo, N. Bonafede, N. Chahat, S. Chien, C. Cochran, K. Crowley, C. Duncan, M. Fernandez, H. Garrett, C. Gillespie, C. Kraver, D. Landau, D. Leon, P. Liewer, L. Mages, L. Martos-Repath, P. Mouroulis, N. Murphy, J. Puig-Suari, S. Retzpath, A. Tang, Thangavelautham, Low-cost SmallSats to explore to our Solar System’s boundaries (interim report), in: *NIAC Symposium*, Alabama, Huntsville, 2019 September 25, 2019.
- [13] J. Veverka, et al., The landing of the NEAR-Shoemaker spacecraft on asteroid 433 Eros, *Nature* 413 (2001) 390–393.
- [14] <http://www.isas.jaxa.jp/e/enterp/missions/hayabusa/>. (Accessed 21 June 2019).
- [15] A. Klesh, J. Krajewski, MarCO: Cubesats to Mars in 2016, in: *29th Annual AIAA/USU Conference on Small Satellites, SSC15-III-3*, 2015.

- [16] M. Rayman, T.C. Fraschetti, C.A. Raymond, C.T. Russell, Dawn: a mission in development for exploration of main belt asteroids Vesta and Ceres, *Acta Astronaut.* 58 (11) (2006) 605–616.
- [17] A. Atzei, ROSETTA and FIRST: two cornerstone missions of ESA, in: 4th Cosmic Physics National Conference, Capri, September, 1988.
- [18] A. Hibberd, A.M. Hein, M. Eubanks, Project Lyra: Catching 1I/'Oumuamua-Mission Opportunities After 2024, 2019.
- [19] <https://www.nasa.gov/feature/goddard/2017/hubble-observes-the-farthest-active-inbound-comet-yet-seen>. (Accessed 1 June 2019).
- [20] <https://www.nanosats.eu/>. (Accessed 2 July 2019).
- [21] R. Staehle, D. Blaney, H. Hemmati, D. Jones, A. Klesh, P. Liewer, J. Lazio, M. Wen-Yu Lo, P. Mouroulis, N. Murphy, P. Pingree, T. Wilson, B. Anderson, C. Channing Chow II, B. Betts, L. Friedman, J. Puig-Suari, A. Williams, T. Svitek, Interplanetary CubeSats: opening the Solar System to a broad community at lower cost, *J. Small Satell.* 2 (1) (2013) 161–186.
- [22] R. Staehle, D. Blaney, H. Hemmati, D. Jones, A. Klesh, P. Liewer, J. Lazio, M. Wen-Yu Lo, P. Mouroulis, N. Murphy, P. Pingree, T. Wilson, B. Anderson, C. Channing Chow II, B. Betts, L. Friedman, J. Puig-Suari, A. Williams, T. Svitek, Interplanetary CubeSat architecture and missions, in: American Institute Aeronautics & Astronautics (AIAA) September, Pasadena, CA, 2012.
- [23] R. Staehle, D. Blaney, H. Hemmati, D. Jones, A. Klesh, P. Liewer, J. Lazio, M. Wen-Yu Lo, P. Mouroulis, N. Murphy, P. Pingree, T. Wilson, B. Anderson, C. Channing Chow II, B. Betts, L. Friedman, J. Puig-Suari, A. Williams, T. Svitek, Interplanetary CubeSats: opening the Solar System to a broad community at lower cost, *J. Small Satell.* 2 (1) (2013) 161–186.
- [24] A. Klesh, et al., INSPIRE: interplanetary NanoSpacecraft pathfinder in a relevant environment, in: AIAA/USU Conference on Small Satellites, SSC13-XI-8, 2013.
- [25] M. Tsay, J. Frogillo, K. Hohman, B. Malphrus, LunarCube: a deep space 6U CubeSat with mission enabling ion propulsion technology, in: 29th Annual AIAA/USU Conference on Small Satellites, SSC15-XI-1, 2015.
- [26] M.W. Lo, The interplanetary superhighway and the origins program, in: IEEE, 0-7803-7231-X/01, 2002.
- [27] M.W. Lo, S. Ross, SURFing the Solar System: Invariant Manifolds and the Dynamics of the Solar System, *JPL IOM* 312/97, 1997.
- [28] [www.gg.caltech.edu/~mwl/LTool/LTool2.htm](http://www.gg.caltech.edu/~mwl/LTool/LTool2.htm). (Accessed 17 June 2019).
- [29] K.M. Cheung, D. Abraham, B. Arroyo, E. Basilio, A. Babuscia, C. Duncan, D. Lee, K. Oudrhiri, T. Pham, R. Staehle, S. Waldherr, G. Welz, J. Wyatt, M. Lanucara, B. Malphrus, J. Bellardo, J. Puig-Suari, C. Corpino, Next-Generation Ground Network Architecture for Communications and Tracking of Interplanetary Satellites, *IPN Progress Report* 42-202, August 15, 2015.
- [30] K.M. Cheung, D. Abraham, B. Arroyo, E. Basilio, A. Babuscia, C. Duncan, D. Lee, K. Oudrhiri, T. Pham, R. Staehle, S. Waldherr, G. Welz, J. Wyatt, M. Lanucara, B. Malphrus, J. Bellardo, J. Puig-Suari, Architecture and CONOPS of next-generation ground network for communications and tracking of interplanetary SmallSats, in: AIAA SpaceOps 2016 Conference, Daejeon, Korea, 16–20 May, 2016.
- [31] B. Malphrus, J. Kruth, T. Pham, J. Wyatt, Enabling university-operated tracking and communications for deep space SmallSat missions, in: CubeSat Developers' Workshop, Cal-Poly, May 2, 2018.
- [32] T. Pham, B. Malphrus, J. Kruth, J. Wyatt, Ground system development at morehead state university for interplanetary smalls missions, in: The 4S Symposium, 2018.

- [33] J. Foust, MarCO success vindicates use of CubeSats on deep space missions, *Space News* (2018). November 26.
- [34] A. Klesh, J. Krajewski, MarCO: CubeSats to Mars in 2016, in: SSC15-III-3, 29th Annual AIAA/USU Conference on Small Satellites, 2015.
- [35] <https://commons.wikimedia.org/w/index.php?curid=74696160>. (Accessed 1 June 2019).
- [36] P.E. Clark, et al., Lunar ice cube mission: determining lunar water dynamics with a first generation deep space CubeSat, in: 47th Lunar and Planetary Science Conference, 2016.
- [37] B.K. Malphrus, et al., The Lunar IceCube EM-1 Mission: Prospecting the Moon for Water Ice, IEEE Aerospace and Electronics Systems SYSAES-201800168R, 2019.
- [38] P.E. Clark, B.K. Malphrus, et al., Lunar IceCube mission: determining lunar water dynamics with a first generation deep space Cubesat, in: Lunar and Planetary Science Conference Proceedings, 2017.
- [39] [http://www.jpl.nasa.gov/cubesat/missions/lunar\\_flashlight.php](http://www.jpl.nasa.gov/cubesat/missions/lunar_flashlight.php).
- [40] P.O. Hayne, B.A. Cohen, et al., Lunar flashlight: illuminating the Moon's south pole, in: 47th Lunar and Planetary Science Conference, March 21, 2016.
- [41] B.A. Cohen, et al., Lunar flashlight: mapping lunar surface volatiles using a Cubesat, in: Annual Meeting of the Lunar Exploration Analysis Group, 3031 2014.
- [42] <https://www.nasa.gov/feature/lunah-map-university-built-cubesat-to-map-water-ice-on-the-moon>. (Accessed 5 July 2019).
- [43] C. Hardgrove, et al., The lunar polar hydrogen mapper (lunah-map) mission: mapping hydrogen distributions in permanently shadowed regions of the moon's south pole, in: Lunar Exploration Analysis Group (2015): n. pag. USRA-Houston. Universities Space Research Association. Web. 18 February, 2016.
- [44] C. Hardgrove, et al., LunaH-Map CubeSat, AIAA, Arizona State University, 2016. <http://neutron.asu.edu/>. (Accessed 20 March 2016).
- [45] <https://www.nasa.gov/content/nea-scout>. (Accessed 4 July 2019).
- [46] L. McNutt, et al., Near-Earth asteroid scout, in: AIAA SPACE 2014, August, 2014.
- [47] R.L. Staehle, S. Spangelo, M. Eby, M.S. Lane, K.M. Aaron, R. Bhartia, J.S. Boland, L. E. Christiansen, S. Forouhar, M. de la Torre Juarez, D.A. Paige, N. Trawny, C. R. Webster, R.M. Williams, Multiplying Mars Lander opportunities with MARS<sub>DROP</sub> Microlanders. in: AIAA/USU Small Satellite Conference SSC15-XI-3, Logan, Utah, August 13, 2015. <https://doi.org/10.13140/RG.2.1.3599.1127>.
- [48] <http://www.nasa.gov/content/jpl-selects-europa-cubesat-proposals-for-study>. (Accessed 30 June 2019).
- [49] B. Bronner, C. Steuer, Europa CubeSat concept study: characterizing subsurface oceans with a CubeSat magnetometer payload, in: Annual AIAA/USU Conference on Small Satellites, 2015.
- [50] A. Freeman, C. Sotin, M. Darrach, J.E. Baker, Sampling Venus' atmosphere with a low-cost, free-flying Smallsat probe mission concept, in: Interplanetary SmallSat Conference, Caltech, April, 2016.
- [51] T. Talbert, NASA Press Release "NASA Selects CubeSat, SmallSat Mission Concept Studies", <https://www.nasa.gov/feature/nasa-selects-cubesat-smallsat-mission-concept-studies>, 2017. (Accessed 22 March 2017).
- [52] T. Stubbs, B. Malphrus, R. Hoyt, M.A. Mesarch, M. Tsay, D.J. Chai, M.K. Choi, M. R. Collier, J.W. Keller, W.M. Farrell, J.R. Espley, J.S. Halekas, A. Zucherman, R. R. Vondrak, P.E. Clark, D. Folta, T.E. Johnson, G.Y. Kramer, S. Fatema, J. Deca, J. R. Gruesbeck, J.L. McLain, M.E. Purucker, Bi-Sat observations of the lunar atmosphere above swirls (BOLAS): tethered SmallSat investigation of hydration and space weathering processes at the moon, in: 49th Lunar and Planetary Science Conference, 2018. LPI Contrib. No. 2083.

- 
- [53] [http://www.esa.int/Our\\_Activities/Space\\_Engineering\\_Technology/Asteroid\\_Impact\\_Mission/CubeSat\\_companions\\_for\\_ESA\\_s\\_asteroid\\_mission](http://www.esa.int/Our_Activities/Space_Engineering_Technology/Asteroid_Impact_Mission/CubeSat_companions_for_ESA_s_asteroid_mission). (Accessed 29 June 2019).
  - [54] <https://www.nanosats.eu/>. (Accessed 2 July 2019).
  - [55] <http://dragonfly.jhuapl.edu/>. (Accessed 17 June 2019).
  - [56] A. Blocher, D. Atkinson, A. Freeman, Saturn swarm study, in: Low Cost Planetary Mission Conference, Pasadena, CA, August, 2017.
  - [57] Discovery 2014 Announcement of Opportunity, NASA Solicitation (Nov 2014) Discovery 2014 Announcement of Opportunity, 2014.
  - [58] B. Sherwood, et al., Planetary cubesats come of age, in: Proceedings of the 66th International Astronautical Congress, Jerusalem, Israel (Oct 2015). Discovery 2014 Announcement of Opportunity, NASA Solicitation, Nov 2014.
  - [59] I. Garrick-Bethel, et al., NANOSWARM: a Cubesat discovery mission to study space weathering, lunar magnetism, lunar water, and small-scale magnetospheres, in: 46th Lunar and Planetary Science Conference, 2015.

# Distributed CubeSat mission concepts

5

*Alessandro Golkar*

Skolkovo Institute of Science and Technology, Center for Entrepreneurship and Innovation, Moscow, Russia

## 1 Introduction

Instead of relying on individual spacecraft, distributed CubeSat systems (DCS) allocate the required mission functionality across multiple flight units. A distribution strategy allows mission designers to enable new mission capabilities such as ubiquitous connectivity at costs compatible with commercial intents or enhance system features of interest such as temporal resolution and interspacecraft-coordinated operations. Distributed spacecraft design strategies are indeed relevant for spacecraft platforms of all sizes, though they are of special interest to CubeSat systems due to their inherent enabling features. Distribution allows CubeSats to achieve mission performance or mission assurance levels that would be more complex or even not possible to achieve by an individual nanosatellite system. It allows for new design approaches to be put in place, such as “fail fast, fail often” strategies that have been historically at odds with the design philosophy of spacecraft systems but that are now being actively experimented in private space ventures. Several spacecraft distribution strategies are possible, each of which offering different opportunities while exhibiting inherent technical challenges. This chapter offers an overview of distributed CubeSat mission concepts and architectures that are presently flying or have been proposed and that could be thus envisioned for future mission implementations. Satellite distribution offers several avenues for innovation, as several distribution strategies and related technologies have not yet been explored in the domain of CubeSats.

This chapter is structured as follows. [Section 2](#) provides a comprehensive analysis of feasible concepts of DCSs and a synthesis of the state-of-the-art distributed CubeSat mission concepts and architectures. [Section 3](#) discusses enabling technologies for DCS in the technical domains related to onboard autonomy and spacecraft coordination. [Section 4](#) discusses conclusions from the analysis of DCS and outlines a potential way forward for the adoption of those concepts in the emerging new space industry worldwide.

## 2 Distributed CubeSat system concepts

### 2.1 State of the art

The notion of DCS encompasses all CubeSat missions that involve more than one spacecraft unit to fulfill mission requirements. As such the notion of DCS is quite broad and includes an array of well-known concepts such as satellite constellations, formation flight missions, and satellite swarms. It also includes innovative concepts that have not flown yet at the time of writing of this chapter, such as fractionated and federated CubeSat systems. While distributed concepts have been implemented in several occasions in “standard” missions employing traditional “large” spacecraft, they are still unexploited in the domain of CubeSats. The most notable examples as of today, in terms of number of spacecraft flown, are the CubeSat constellations operated by Planet [1] and Spire [2], which account for 355 and 103 CubeSats, respectively, that are currently operating in orbit (according to public database sources, at the time of writing [3]).

There are several examples of DCSs that have already been operated in orbit. Referring to previous work by Selva et al. [4], it is possible to classify distributed satellite concepts from an architectural standpoint, referring to five fundamental factors that can either take high (H) or low (L) values for the given concepts. These are *homogeneity*, *size*, *spatial separation*, *functional interdependence*, and *operational independence*. The definition of those factors is provided in Table 1.

Selva’s taxonomy identifies six distributed satellite concepts using the proposed factor classification, mapping them to the known distributed concepts of satellite constellations, swarms, clusters, fractions, trains, and federations (Table 2). It also identifies potential other concepts through morphological analysis, which however do not map to any well-known concept formulation. We analyze each concept individually and discuss challenges and opportunities specific to CubeSat implementations.

**Table 1** DCS classifying factors’ definition.

Homogeneity	The degree of structural similarity of the units
Size	Number of units participating into the DCS
Spatial separation	Maximum physical distance between the units in the DCS
Functional interdependence	The degree to which each unit in the DCS relies on other units to perform basic functions
Operational independence	The degree to which each unit is operated and/or owned by different organizations

From D. Selva, A. Golkar, O. Korobova, I.L. i Cruz, P. Collopy, O.L. de Weck, Distributed earth satellite systems: what is needed to move forward?, J. Aerosp. Inform. Syst. 14(8) (2017) 412–438, doi:10.2514/1.1010497.

**Table 2** Distributed CubeSat system concepts.

Name	Homogeneity	Size	Spatial separation	Functional interdependence	Operational independence
Cluster	H	L	L	H	L
Constellation	H	H	H	L	L
Federation	L	H	H	L	H
Fractionated	L	L	L	H	L
Series	H	L	H	L	H
Swarm	H	H	L	L	L
Train	L	L	L	L	H

### 2.1.1 Constellations

CubeSat constellations are currently being operated in orbit, such as those previously mentioned operated by Planet and Spire. Forty-one additional constellations are planned to be launched or proposed to be developed in the coming years [3]. Fig. 1 provides the most recent statistics of CubeSat constellations. Constellations are distributed systems made of identical flying units.

As for non-CubeSat counterparts, CubeSat constellations find use across a wide range of applications. Such applications benefit from an improved temporal resolutions and ubiquitous availability of service when compared with traditional

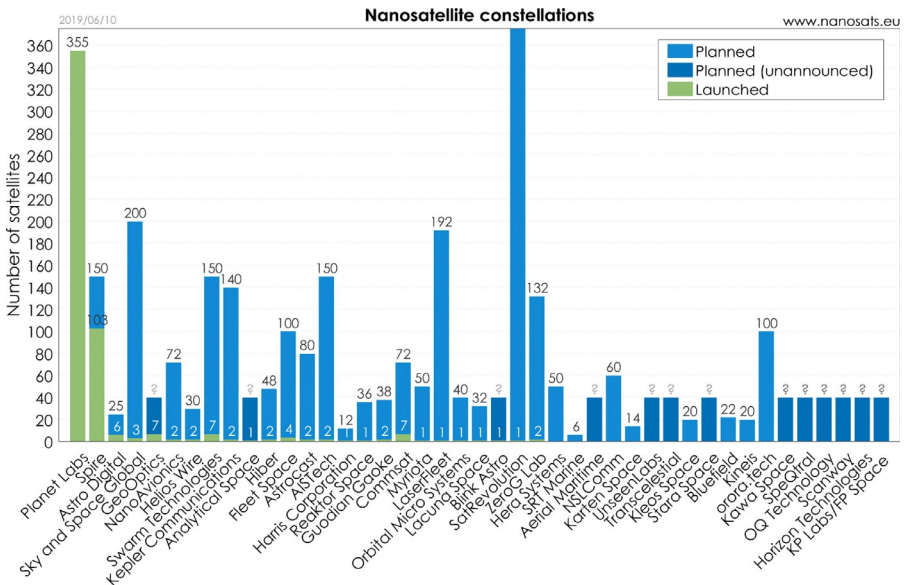


**Fig. 1** Nanosatellite constellations.

From E. Kulu, Nanosats Database. [www.nanosats.eu](http://www.nanosats.eu) (Accessed 4 September 2019).



“monolithic” systems. Applications include Earth imaging, weather data, satellite automatic identification systems (AIS), space-based Automatic Dependent Surveillance-Broadcast (ADS-B), and Internet of Things (IoT) connectivity.

CubeSat constellations are finding increasing commercial relevance due to the advancement in miniaturization of technology and increasing power utilization efficiency of radiofrequency components. Missions that were unconceivable few years past have been now demonstrated on miniaturized platforms. For instance, Sky and Space Global has demonstrated the first voice call routed through a CubeSat-based distributed system [5].

As it can be expected, DCSs will hardly replace large satellite platforms in applications requiring high-end performance or capacity. However, they represent a viable trade-off in terms of value for money and can be seen as complementary assets enhancing services based on data derived from “traditional” larger spacecraft. Such complementary includes the opportunity for fusing low to mid fidelity data acquired at a higher temporal resolution (through DCS) with high-fidelity data from larger platforms for improved mission readiness or quality of service. An example application of such opportunity is represented by coordinated Earth observations, fusing optical and synthetic aperture radar (SAR) data to inform mission scheduling and operations. While institutional constellations of high-fidelity instrumentation cannot be scaled to large numbers for cost reasons, small instrumentation can be scaled and used to improve the utilization efficiency of larger assets. From a commercial perspective, CubeSat constellations provide the opportunity to deliver space-based services at a cost per unit service that is one or two orders of magnitude lower compared with legacy systems.

Challenges in the development of future CubeSat constellations are twofold: economic and technical. From an economic perspective, CubeSat operators are still to demonstrate the long-term financial viability of their value proposition. While 43 CubeSat constellation proposals have appeared over the last decade, only Planet and Spire have delivered major constellations that are currently operational in orbit. All other operators have launched minimum viable technology demonstrators made of one to seven flying units. Those demonstrators are typically designed to retire technical, financial, and other types of risks in the project and to secure funding in successive fundraising rounds. A consolidation of CubeSat constellation proposals is therefore likely to be expected in the coming 5-year timeframe. From a technical point of view, a major challenge to overcome is the saturation of the radiofrequency spectrum due to exponentially larger utilization. The emergence of CubeSat constellations increased the number of orbiting spacecraft to unprecedented volumes compared with the near past. Licensing for spectrum is a cumbersome process taking up to 3 years to complete. The challenge is further complicated when dealing with constellations operating intersatellite links, due to the licensing constraints related to spacecraft coordination, noninterference with geostationary assets, and shared spectrum utilization. Such limitations will drive CubeSat operators to push for the development of transceivers at higher frequency or rely on optical communication solutions for their cross-link and/or downlink communication needs. Many of those solutions are currently under development at the time of writing of this chapter [6–8]. They will in turn

entail challenges in terms of size, weight, and power (SWaP); pointing accuracy; and increased payload complexity.

Large numbers of CubeSats flying in orbit will also drive for the development of new solutions for space situational awareness, space debris, spacecraft autonomy, and on-orbit traffic management. Spacecraft coordination will in particular play an important role in the development of advanced CubeSat instrumentation, which impacts research and development in artificial intelligence (AI)-enabled decision-making, power-efficient flight avionics, advanced telecommunication protocols, and proximity flight operations, among other relevant technical areas.

### 2.1.2 *CubeSat clusters, series, swarms, and trains*

The literature on distributed satellite systems does not have yet a universally accepted nomenclature of all possible distributed mission concepts. Several classifications have been proposed to classify distributed satellite missions from different perspectives (such as from architectural, functional, operational, and other perspectives). The divergence in definitions is particularly wide in the discussion of swarms, series, clusters, and trains. In this chapter, we adopt the taxonomy of Selva et al. [4]. Their paper provides references to other classification systems. For these reasons, some of the concepts discussed in this chapter may be classified under different names rather than those defined by the original proponents.

*CubeSat clusters* are DCS made of a low number (typically 2–6) of identical flight units, flying at low along-track distance between each other while being mutually dependent from a functional and operational perspective to deliver on their mission goals. An example of a satellite cluster in the “traditional” domain is the TechSat 21 mission concept [9]. Satellites in a cluster can simulate the activity of larger monolithic satellites. In remote sensing, for example, a satellite cluster can be designed to reproduce large effective apertures by using sparse array interferometry and synthetic aperture techniques [10]. In the communication domain, torrent-like architectures have been proposed for increasing downlink and uplink capacity of CubeSat platforms, typically constrained by power, volume, and geometry [11]. In the CubeSat domain, no cluster mission has flown to date (to the best of this author’s knowledge). Several concepts have been proposed and are under development at the time of writing of this chapter. CubeSat-enabled cluster concepts are, for example, those proposed for bidirectional reflectance distribution function (BRDF) measurements [12]. Another cluster concept is that of the SunRISE mission currently under development at NASA JPL for improving the understanding of the acceleration of solar energetic particles (SEPs) in coronal mass ejection (CME) events using space-based interferometry [13].

*CubeSat series* are distributed concepts where identical (or quasi-identical) units are flown, usually for technology demonstration purposes such as demonstration of inter-satellite link or formation flight technology. For example, the AeroCube-4 series of three nanosatellites has among its objectives the demonstration of formation flight through differential drag strategies, using deployable solar arrays [14]. CubeSat series are quite common and flown, mostly as “*proof-of-concept*” technology demonstrators.

Closely tied to the concept of cluster is the DCS concept of swarm. *CubeSat swarms* differ from clusters in that they involve a large number of flight units that are functionally noninterdependent from each other. Swarms offer the advantage brought in by large numbers of spacecraft, wherein mission performance can be designed to degrade more gracefully in case of failure of an individual flight unit. CubeSat swarms have not flown to date; most notably, FemtoSats (100-g class) have been proposed in swarm implementations for synthetic aperture applications (1000 or more flight units) [10]. It is unlikely, but not impossible, that large swarms of CubeSats (1000+ units) will fly in the near future. The typical application of swarms is of scientific nature. As they entail large numbers, swarms bring significant technology challenges in terms of spacecraft in-orbit identification and discrimination after deployment, coordination, and relative navigation.

*CubeSat trains* are DCS of different spacecraft, flying in coordinated orbits while performing independent operations. Distributed concepts such as NASA's A-Train [15] use large monolithic spacecraft to take independent observations that are later fused in ground postprocessing activities. CubeSat trains have not yet appeared in orbit, but they are likely to emerge as a natural evolution of the small satellite industry. As CubeSat instrumentation is becoming of interest for operational purposes, CubeSat trains become ideal complements of large institutional programs such as the European Copernicus [16].

### 2.1.3 Fractionated CubeSat system concepts

Fractionated spacecraft allocates mission functionality to multiple flight units, which interact wirelessly with each other to deliver on mission goals [17]. Benefits brought in from fractionation come primarily from an uncertainty management perspective, with a real options approach. A fractionated architecture allows for flexible adjustment of satellite capacity through incremental addition of spacecraft modules over the lifetime of the mission. Fractionated spacecraft were originally proposed by DARPA with the F6 program, which was later canceled. The seminal paper by Brown and Eremenko proposed a technology demonstration of fractionated spacecraft on microsattelites. They envisioned technology challenges in cluster flying, data transmission, fractionated navigation, distributed computation and data resources, power transmission, and force and torque transmission [17]. Fractionated architectures for future CubeSat implementations may include hybrid systems where heterogeneous spacecraft of different sizes interact wirelessly in a functionally dependent configuration. A fractionated architecture could include a large "mothership" spacecraft with a set of "daughter" fractionated CubeSat appendices for distributed observations or advanced geostationary (GEO) communication systems. The latter are akin to GEO clusters that have been recently proposed in the scientific literature [18]. While some of these concepts may seem far away in the future, they offer the key advantage of flexibility for modular capacity expansion. Functional interdependence also allows developing fractionated systems with low cost units, each of which able to optimize platform performance to the specific needs of the payload. A fractionated approach also allows for diversifying service offering by allowing for flexible interchangeable

payload fractions. Despite the ambition of the technical idea and its high impact in the scientific literature, no fractionated spacecraft is being flown or developed to date, at least in the public domain.

### 2.1.4 Federated CubeSat system concepts

Federated spacecraft systems are a more recent concept of distributed satellite systems following the idea of shared economies [19] as seen on terrestrial applications for public transportation. Federated satellites are heterogeneous, independently operated systems that interact in orbit on a need basis. Interaction is enabled by intersatellite links, distributed computing approaches, and delay-tolerant network protocols [20]. Optical communications have been identified as a key enabling technology for federated systems. Free-space laser communications allow mitigating interference and spectrum saturation traditionally associated with radiofrequency (RF) cross-links among large numbers of orbiting spacecraft. Given the complex orbital geometries and cross-link configurations that are envisioned for federated systems, optical communications appear a key enabling technology for the concept.

The key advantage of satellite federations is the opportunity to provide operators the ability to “resell” part of their unused capacity or reconfigure their spacecraft to serve other mission needs in case of changing operational requirements or partial system failures. The advantages and limitations of federated spacecraft systems are very much akin to those of cloud computing infrastructure on Earth [21]. In-space cloud computing infrastructure has been proposed in the context of federated systems [22]. Potential applications of CubeSat federations include the ability of deploying “virtual satellite missions” [23] by coordinating the use of orbiting resources that are made available by satellite operators to a centralized coordinating infrastructure. The coordination infrastructure can also be decentralized through modern in-space blockchain approaches [24]. Auctioning systems have been proposed to regulate the operations of federated systems in orbit. Applications in the domain of Earth observation have been recently explored in a value chain analysis of the European Copernicus Earth observing infrastructure [25].

Federated systems represent a valuable opportunity for CubeSat systems. By operating in federations, CubeSats can tap in otherwise unaffordable computing and processing resources. These are typically out of reach of CubeSat systems due to the stringent SWaP requirements associated with CubeSat platforms. Previous research has explored the technical and commercial feasibility of customer spacecraft operating federated operations with the International Space Station (ISS) as a supplier node [19]. One could therefore conceive CubeSats as low cost, agile data gathering nodes, using the ISS or other large spacecraft for centralizing complex computations, data interpretation, and so on.

Federated CubeSat systems have not yet been demonstrated in orbit. A first technology demonstration is slated to fly in 2019 [6]. Federated CubeSat concepts and related enabled services are picking up traction in the space industry. A recent paper by ESA analyzed the concept of “\$99 satellite” or “SpaceBNB” of nanosatellites, which closely align to the concept of spacecraft federations [26].

### 3 Enabling technologies

Distributed CubeSat concepts are bringing new technology challenges related to coordination and interaction among flight systems. [Table 3](#) provides an outline of selected enabling technologies for the distributed CubeSat system concept survey in [Section 2.1](#). The technologies outlined in the table are being developed (or will be developed) for many platform sizes, including nanosatellites. CubeSats bring to those challenges additional constraints in terms of size, weight, and power (SWaP) typical of the CubeSat standard.

**Table 3** Overview of selected enabling technologies (in alphabetic order) for distributed CubeSat systems.

Technology	Enabled capability
Blockchain	Secure ledger to regulate data exchanges within a distributed CubeSat system. For example, to enable resource exchange marketplaces (for downlink, data storage, data processing, and other resources) in satellite federations
Capacity request forecasting and scheduling using deep neural networks	Regulation and interoperability coordination mechanism within DCSs with uncertain topology and uncertain demand (e.g., satellite federations)
Dynamic platform-distributed resource allocation and balancing	Operational coordination of satellite platform resources within DCSs
Explainable artificial intelligence (AI) for platform management and intelligent payload operations	Enabler for the use of AI in safety-critical (or reliability-critical) applications
High-accuracy CubeSat attitude control (<0.01 degrees) with high agility	Close-distance formation flight and high performance payload operations enabler (e.g., highly directional high-frequency antennas)
Higher efficiency/longer lifetime in miniaturized electric propulsion systems for CubeSats (e.g., next-generation ion electropray thrusters [27])	Orbital station-keeping and plane change corrections
In-orbit spacecraft identification	Space traffic management and reliable in-orbit commissioning in rideshare launch missions
In-space Internet connectivity	Ground stationless missions, relying on common multimission ground system infrastructure operating the Internet in space
Magnetic torque and force transmission [17]	Orbital reconfiguration of fractionated satellite systems

**Table 3** Continued

Technology	Enabled capability
Optical communications for CubeSats (intersatellite link and downlink)	Higher-performance communication capabilities with lower specific power consumption (in terms of W/kg) and with lower interference issues License-free communications
Out-of-plane reconfigurable intersatellite links	Enabling DCSs with complex orbital topologies (e.g., opportunistic networks between heterogeneous spacecraft nodes)
Power-efficient software-defined radio	Flexible and interoperable communication capabilities
Satellite quantum key distribution [28]	Secure in-space networking
Relative navigation	Formation flight
Satellite negotiator [29]	Interoperability with legacy spacecraft
Software-defined satellite	In-orbit reconfigurability of mission objectives
Space traffic monitoring and collision self-avoidance [30]	Secure deployment of large number of spacecraft
Virtual space missions [23]	Customer service offering of very lost cost mission capabilities

## 4 Conclusion

CubeSats have evolved from being systems designed for pure educational use to advanced satellite platforms for operational use in Earth observation, telecommunications, science, and other applications. CubeSats are of particular interest to the evolution of commercial space ventures due to the lower capital costs associated with their development and operations compared with traditional missions. The evolution of CubeSats has been largely facilitated by the exponential evolution of miniaturized technology and consequently the enabled advanced capabilities for those platforms. Distributed concepts and architectures are a similar evolution of CubeSat capabilities akin to the evolution observed in larger satellite platform systems in the past. Distribution in the form of constellations, formation flight, swarms, fractionation, and federations entails the capabilities of interaction and coordination among flight units. By means of distributed capabilities, CubeSat missions can effectively complement large institutional infrastructure or offer new instrument capabilities in space applications. Many (if not most) of the concepts described in this chapter—except for constellations—have not yet been demonstrated in flight. Distributed systems offer new opportunities for research and development and demonstration of new mission capabilities in orbit. The “distributed revolution” has started with the launch of operational CubeSat constellations. Given the opportunities they can provide at cost, it is likely to expect that other distributed CubeSat systems will appear in orbit in the future.

## References

- [1] M. Strauss, Planet earth to get a daily selfie, *Science* 355 (6327) (2017) 782–783, <https://doi.org/10.1126/science.355.6327.782>.
- [2] V. Nguyen, et al., Spire’s 3U CubeSat GNSS-RO constellation for meteorological and space weather applications, in: Presented at the AGU Fall Meeting Abstracts, December 1, 2017, 2017. Available from: <https://ui.adsabs.harvard.edu/abs/2017AGUFM.A33M..06N>.
- [3] E. Kulu, Nanosats Database, [www.nanosats.eu](http://www.nanosats.eu), 2019. (Accessed 4 September 2019).
- [4] D. Selva, A. Golkar, O. Korobova, I.L. i Cruz, P. Collopy, O.L. de Weck, Distributed earth satellite systems: what is needed to move forward? *J. Aerosp. Inform. Syst.* 14 (8) (2017) 412–438, <https://doi.org/10.2514/1.1010497>.
- [5] C. Henry, Cubesat voice-comms test paves way for sky and space global’s 200-satellite constellation, *SpaceNews* (2017),
- [6] A. Camps, et al., Fsscatt, the 2017 Copernicus Masters’ “Esa Sentinel Small Satellite Challenge” Winner: a federated polar and soil moisture tandem mission based on 6U Cubesats. in: *IGARSS 2018–2018 IEEE International Geoscience and Remote Sensing Symposium*, 22–27 July 2018, 2018, pp. 8285–8287, <https://doi.org/10.1109/IGARSS.2018.8518405>.
- [7] E. Clements, et al., Nanosatellite optical downlink experiment: design, simulation, and prototyping. *Opt. Eng.* 55 (11) (2016) 1–18, <https://doi.org/10.1117/1.OE.55.11.111610>.
- [8] R.P. Welle, C.M. Coffman, D.W. Pack, J.R. Santiago, CubeSat laser communication crosslink pointing demonstration, in: *Small Satellite Conference*, Utah State University, Logan, UT, 2019.
- [9] R. Burns, C.A. McLaughlin, J. Leitner, M. Martin, TechSat 21: formation design, control, and simulation, in: *2000 IEEE Aerospace Conference. Proceedings (Cat. No.00TH8484)*, 25–25 March 2000, vol. 7, 2000, pp. 19–25, <https://doi.org/10.1109/AERO.2000.879271>.
- [10] F.Y. Hadaegh, S. Chung, H.M. Manohara, On development of 100-gram-class spacecraft for swarm applications, *IEEE Syst. J.* 10 (2) (2016) 673–684, <https://doi.org/10.1109/JSYST.2014.2327972>.
- [11] O.N. Challa, J. McNair, CubeSat Torrent: Torrent like distributed communications for CubeSat satellite clusters, in: *MILCOM 2012–2012 IEEE Military Communications Conference*, 29 Oct.-1 Nov. 2012, 2012, pp. 1–6, <https://doi.org/10.1109/MILCOM.2012.6415828>.
- [12] S. Nag, Design of nano-satellite cluster formations for bi-directional reflectance distribution function (BRDF) estimations, in: *Small Satellite Conference*, Utah State University, Logan, UT, 2013.
- [13] F. Alibay, A.M. Hegedus, J.C. Kasper, T.J.W. Lazio, T. Neilsen, SunRISE status: concept development update, in: *2018 IEEE Aerospace Conference*, 3–10 March 2018, 2018, pp. 1–11, <https://doi.org/10.1109/AERO.2018.8396371>.
- [14] S. Bandyopadhyay, R. Foust, G.P. Subramanian, S.-J. Chung, F.Y. Hadaegh, Review of formation flying and constellation missions using nanosatellites, *J. Spacecr. Rocket.* 53 (3) (2016) 567–578, <https://doi.org/10.2514/1.A33291>.
- [15] T. L’Ecuyer, Touring the atmosphere aboard the A-train. *Phys. Today* 7 (2010) 36–41, <https://doi.org/10.1063/1.3463626>.
- [16] J. Aschbacher, Copernicus: a quantum leap in earth observation, in: *EGU General Assembly Conference Abstracts*, vol. 17, 2015, p. 15603.

- [17] O. Brown, P. Eremenko, The value proposition for fractionated space architectures, in: *Space 2006*, AIAA SPACE Forum: American Institute of Aeronautics and Astronautics, San Jose, CA, 2006.
- [18] P. Takats, A new paradigm: geostationary satellite clusters with inter-satellite links, in 21st International Communications Satellite Systems Conference and Exhibit, AIAA, 2003, Available from: <https://arc.aiaa.org/doi/abs/10.2514/6.2003-2322>.
- [19] A. Golkar, I.L. i Cruz, The federated satellite systems paradigm: concept and business case evaluation, *Acta Astronaut.* 111 (2015) 230–248, <https://doi.org/10.1016/j.actaastro.2015.02.009>.
- [20] I. Lluch, P.T. Grogan, U. Pica, A. Golkar, Simulating a proactive ad-hoc network protocol for Federated Satellite Systems. in: *2015 IEEE Aerospace Conference*, 7–14 March 2015, 2015, pp. 1–16, <https://doi.org/10.1109/AERO.2015.7118984>.
- [21] M. Armbrust, et al., A view of cloud computing, *Commun. ACM* 53 (4) (2010) 50–58, <https://doi.org/10.1145/1721654.1721672>.
- [22] S. Briatore, N. Garzaniti, A. Golkar, Towards the internet for space: bringing cloud computing to space systems, *IET Conference Proceedings*. (2018) p. 38, (5 pp.). <https://doi.org/10.1049/cp.2018.1719>. Available from: <https://digitallibrary.theiet.org/content/conferences/10.1049/cp.2018.1719>.
- [23] H. Matevosyan, C. Taylor, A. Golkar, Evaluating virtual satellite mission opportunities, in: *AIAA SPACE 2015 Conference and Exposition, 2015: American Institute of Aeronautics and Astronautics*, in *SPACE Conferences and Exposition, 2015*. <https://doi.org/10.2514/6.2015-4674>.
- [24] G. Zyskind, O. Nathan, A. Pentland, Decentralizing privacy: using blockchain to protect personal data, in: *2015 IEEE Security and Privacy Workshops*, 21–22 May 2015, 2015, pp. 180–184, <https://doi.org/10.1109/SPW.2015.27>.
- [25] H. Matevosyan, I. Lluch, A. Poghosyan, A. Golkar, A value-chain analysis for the Copernicus earth observation infrastructure evolution: a knowledgebase of users, needs, services, and products, *IEEE Geosci. Remote Sens. Mag.* 5 (3) (2017) 19–35, <https://doi.org/10.1109/MGRS.2017.2720263>.
- [26] L. Maresi, The \$99 satellite, in: *Small Satellite Conference*, Utah State University, Logan, UT, 2019.
- [27] K. Lemmer, Propulsion for CubeSats, *Acta Astronaut.* 134 (2017) 231–243, <https://doi.org/10.1016/j.actaastro.2017.01.048>.
- [28] C. Bonato, A. Tomaello, V. Da Deppo, G. Naletto, P. Villorresi, Feasibility of satellite quantum key distribution, *New J. Phys.* 11 (4) (2009) 045017, <https://doi.org/10.1088/1367-2630/11/4/045017>.
- [29] R. Akhtyamov, R. Vingerhoeds, A. Golkar, Identifying retrofitting opportunities for federated satellite systems, *J. Spacecr. Rocket.* 56 (3) (2019) 620–629, <https://doi.org/10.2514/1.A34196>.
- [30] G.L. Slater, S.M. Byram, T.W. Williams, Collision avoidance for satellites in formation flight, *J. Guid. Control. Dyn.* 29 (5) (2006) 1140–1146, <https://doi.org/10.2514/1.16812>.



# Constellations and formation flying

6

*Danil Ivanov and Mikhail Ovchinnikov*

Space Systems Dynamics Department, Keldysh Institute of Applied Mathematics of Russian Academy of Sciences, Moscow, Russia

## 1 Distributed space system definitions and features

The increasing complexity of approaches and methods of solving fundamental and applied problems of space exploration often leads to the need to create distributed space systems (DSS). In this case, several satellites united in one system and flying at a relatively short distance from each other or at similar orbits are simultaneously working on solving a common problem. The use of small satellites in such projects is the most natural and often the only possible way.

According to the most common definition, DSS is a system consisting of multiple space elements that can communicate, coordinate, and interact to achieve a common goal. Its main features are tolerance for failure of individual satellites, scalability and flexibility in design and deployment, and new capabilities compared with a single satellite. There are two main DSS types that can be distinguished depending on the degree of autonomy, communication between the satellites, number of satellites, and types of relative trajectories. These main DSS types are satellite constellations and satellite formations. Satellite constellations are characterized by similar orbits, the absence of intersatellite communication, and the lack of control of relative motion, and as a rule, the individual satellites are controlled from the ground. Satellite formations are associated with small relative intersatellite distances compared with the orbital size, onboard closed-loop control to preserve relative motion topology and often are characterized by supporting interspacecraft communication between the individual satellites. With the development of nano- and picosatellites (such as CubeSats and ChipSats) and the possibility of their standardized and mass production, a new class of formation flying began to develop—the so-called swarm of satellites. The swarm consists of a large number of near-flying satellites moving along arbitrary but limited relative trajectories.

Despite clearly defined features of types of distributed space systems, sometimes disputes arise as to whether a particular system belongs to a particular category. For example, satellites challenge the definitions in case they move along close relative trajectories but they are controlled from the ground or in case satellites have communication links but lack relative motion control. In such cases the degree of autonomy is the most crucial aspect. On-ground motion control and limited autonomy define these architectures as constellations. There are two main approaches to the autonomous

control of a group of satellites: centralized control and decentralized control. Centralized control implies the presence of a “head” or “mother” satellite in the formation; its motion is monitored by the remaining “deputy” or “daughter” satellites that are controlled to achieve the required relative trajectories. Centralized control is more suitable for small groups of satellites moving along predetermined relative trajectories. For a significant number of satellites like the swarm, this approach seems to be not reasonable since the head satellite may be beyond the communication range for some satellites. Additionally, intersatellite communication always has a limited number of channels. This makes it difficult to determine the motion of the “mother” satellites relative to the “daughters.” With the decentralized control approach, each satellite makes the decision to control its dynamic states, modes, and activities individually based on the information on motion of the nearest neighbors. This approach is more suitable for a swarm of satellites taking into account the communicational limitations.

## 2 CubeSats constellations: Control problems and solutions

Constellations of CubeSats firmly occupy a place among well-known constellations of satellites of greater mass. The low cost of CubeSat production and launch allows placing significant number of satellites on orbit. Though the reliability and obtained data quality still leave much to be desired for CubeSat constellations, the processing of the large amount of measurements outweighs all the disadvantages of the capabilities of this type of orbital system.

The main parameter of the constellation is coverage of the region of interest on the Earth surface or in near-Earth space, which depends on the mission goal. In the case that the coverage is not continuous, the period of repeatability is also of great importance. These constellation factors directly depend on the selected satellite orbits and number of satellites in each orbital plane. However, the orbits degrade over time due to perturbations, so to minimize natural relative changes, as a rule similar orbits for satellites are considered for constellations. For example, if the inclinations of the orbits are the same, then the drift in the right ascension of ascending node (RAAN) is similar due to  $J_2$  influence, and the relative orbit positions are maintained. A popular near-circular orbit geometry is the Walker Delta Pattern constellation, where a number of satellites are evenly distributed along the set of equally spaced orbital planes with the same inclination [1]. To construct this type of constellation, it is necessary to place each satellite in a specific location in orbit. There are two ways to do this: (1) to use launcher capabilities or (2) to perform maneuvers using onboard propulsion after the launch. In the case of the CubeSat constellation, often a cluster launch is applied when all the satellites are to be launched in a short time as a secondary payload in nearly one location in orbit. After such a cluster deployment, the satellites need to separate along the orbit. However, the challenge is that the propulsion systems onboard CubeSats are typically limited in capability or simply absent. The ability of CubeSats to maneuver from their insertion orbit into their required mission orbits

is therefore restricted. This is especially true if expensive out-of-plane maneuvers in RAAN or inclination are required.

To achieve mission-required orbits, a set of constellation deployment strategies have been developed and implemented, which allows the mission team to distribute satellites that are launched together into the working orbit positions [2]. For orbital plane separation, a differential rate of nodal precession is used. Due to the non-spherical geopotential of Earth orbits with different sizes, shapes, or orientation, the orbits precess at different rates, allowing plane separations to be achieved without out-of-plane maneuvering. The idea of this deployment method is to perform an in-orbit maneuver for one of the satellite to obtain an orbit with different nodal precession rate. After a time, a natural drift will lead a required orbital plane separation in RAAN, and then the second satellite performs a maneuver to achieve the orbit with the same nodal precession rate to fix the difference in RAAN. This procedure can be repeated to obtain all required orbital planes separation for a constellation. In the case of CubeSats without propulsion, the maneuvers for changing the relative nodal drift rate can be executed by carrier vehicle that launches the satellites into the orbits with required orbital plane separation [3]. This method of constellation deployment using differential nodal drift rates has been demonstrated by the FORMOSAT/COSMIC mission launched in 2006 [4].

Another problem of constellation deployment in the case of cluster launch is the phasing of the satellites along the orbit. It can be formulated as a problem of changing the satellite phase—an angle describing the position of satellites along its orbit. For constellations, the satellites in one orbital plane are usually required to be uniformly distributed in relative phase or just to be at the specified relative phases. The required maneuvers using onboard propulsion for solution of this problem are well studied [5–7] and have been implemented for massive satellite constellations. For CubeSats without propulsion, the problem can be solved using differential atmospheric drag in the case of LEO orbits. In this case the satellites are able to vary their individual cross-sectional areas with respect to the incoming airflow; it is possible to achieve the difference in the drag force acting on the satellites. This natural force is applied to control the relative orbital phase between the satellites in the constellation. This control scheme for solving phasing problem was first implemented in 2013 during the AeroCube-4 mission. AeroCube-4 consisted of three 1U CubeSats with deployable solar panels [8]. Later, this methodology was successfully used by Planet Inc. for dispersing their 3U CubeSats called Doves along a single orbital plane [9]. The record number of 88 Doves in one flock was launched in 2017 and was separated uniformly along the orbit in 8 months [10]. By mid-2019 the fleet of planet's constellation had 170 active CubeSats, making it the largest constellation to date [11].

CubeSat constellations that have been launched and that are planned are listed on the web page “Nanosat Database” [12], which lists the most up-to-date information on the number of CubeSats in constellations, their form factor, and also the field of their application. The second largest commercial constellation by number of satellites and the largest by number of sensors is Spire Global fleet, consisting of 70 3U CubeSats called Lemur [13]. Other CubeSats constellations are in the initial stages of deployment, and their number does not exceed seven satellites to date.

**Table 1** Summary of CubeSat constellation deployment problems in case of cluster launch.

Control problem	Solution	Onboard hardware required
Distribution of satellites along orbital planes with separation in RAAN	Perform the in-plane maneuvers and use natural drift to obtain required orbital plane separation in RAAN	Propulsion, three-axis attitude control system
Phasing satellites along a single orbital plane	Differential aerodynamic drag application in case of the launch in LEO	Active attitude control system, high area-to-mass ratio form factor or drag sail

A summary of the [Section 2](#) is presented in [Table 1](#).

### 3 Nanosatellites formation flight control

According to the equations of relative free motion in the common case of two satellites flying at close distances, the satellites will move along in an unbounded elliptical spiral relative trajectory. That is why the relative motion control is needed for keeping close formation flight. The control in formation flying can be used for various tasks: tracking or maintenance of the required relative motion, reconfiguration, proximity operations, and even docking to each other. This section describes the main features of CubeSat formation flying control, paying particular attention to their modest technical abilities.

#### 3.1 Relative navigation problems

Autonomous relative motion determination is one of the main problems of satellite formation flying. Formation flying control algorithms utilize the relative state estimation obtained using processing of measurements based on relative motion. In this section the main approaches to relative navigation are considered along with emphasis on the applicability to CubeSats.

The measurements that can be directly obtained include physical parameters such as relative distances determined through radio frequency or laser ranging. However, lasers require high attitude pointing accuracy, which is a challenge for low-cost CubeSat missions. Another approach is to use GPS receivers onboard the satellites. The absolute position of each satellite in Earth-fixed reference frame is transmitted to the other satellites via intersatellite communication links; thus the difference of absolute position vectors provides the relative position. In the CanX-4&5 missions launched in 2014, this strategy using relative navigation based on GPS receivers was implemented [14, 15]. The experimentally obtained relative position estimation errors were about 10m.

Image processing is often used for relative state determination in formation flying. An observing camera is required to be installed to take pictures of the other satellites in the group. Depending on the camera parameters and relative position, it is possible to estimate not only translational motion but also rotational motion. Satellite images with so-called feature points are recognized, defining known positions in the spacecraft-related reference frame. Using these measurements of feature point positions in the imagery and projective geometry equations, the relative position and orientation is estimated. A paper published by Opromolla et al. [16] provides an overview of the existing visual-based systems and the state of the art of the cooperative and uncooperative satellite pose determination techniques. A set of works are devoted to the developing and flight testing of the algorithms for relative position determination of the unknown target using angle-only visual navigation [17–19]. The relative navigation system based on image processing was implemented in a set of formation flying missions. Among them the PRISMA mission tested a wide variety of vision-based navigation approaches [20]. Though vision-based navigation is the most reliable, image processing in real time with available onboard CubeSat computers that typically have low computational power represents a challenge. Also by means of economy, the miniature star tracker can be used also as a navigation camera.

### ***3.2 Restricted propulsion and control approaches without propellant***

The conventional approach to formation flying is to use onboard propulsion for producing the required force to control relative position in the formation. To be able to implement a given thrust direction, a three-axis attitude control system must also be installed onboard. Such systems with full controllability are often used on satellites of a large size and mass, and a large number of different control algorithms have been developed for these large-scale missions [21–23]. As has been previously noted, the CubeSat ability to perform any maneuvers is restricted due to mass, cost, and volume constraints. There could be no propulsion system onboard at all. That is why in this subsection, we will focus on control approaches with restricted propulsion systems and fuelless control approaches.

In the case that the satellites are equipped with propulsion systems but there is no three-axis attitude stabilization onboard, the so-called single-input control approach has been developed. It is assumed that the thrust vector is fixed with respect to the body reference frame, and a number of simple and lightweight attitude control systems are available that can stabilize motion of that thrust axis. For example, if the satellite is equipped with a passive magnetic attitude control system that allows it to stabilize the longitudinal axis of the satellite with permanent magnet along the local geomagnetic field, a single-input control is able to achieve bounded relative trajectories of the two satellites in near-circular orbit [24]. Also the satellite can be stabilized by rotation along the rotational axis with a minimal inertia moment. In a 2012 paper [25], Guerman et al. show that it is possible to obtain the closed relative trajectories taking into account  $J_2$  perturbation in the cases of spin stabilization and passive magnetic

stabilization, though the shape of the closed relative trajectories depends on the orbital parameters and initial conditions.

Nowadays a number of nonconventional approaches for formation flying control have been proposed. The general idea that is the basis of these approaches is to develop an effective control method that does not require fuel consumption. Environmental forces, such as aerodynamic drag (AD) force and solar radiation pressure (SRP) force, can be used. Both approaches require a sail or form factor of satellites with high area-to-mass ratio. The CubeSats of 3U size are already appropriate for differential drag application. The principal idea here is to use a difference in environmental forces acting on each satellite in formation flying. This difference usually appears when the satellite changes its relative attitude but the effective size variation is also considered in the literature. Though in general the AD and SRP acceleration models are similar, there are a number of differences. One can apply AD control in low Earth orbits (LEO) only, and its value is varying due to the atmosphere density change caused by the day/night variations and the orbital altitude variations. So, it is usually difficult to predict the exact value of the control force. SRP can be used in different types of orbits, but the shaded parts of orbit should be taken into consideration.

Control based on the aerodynamic drag force was first proposed for the formation flying in 1986 by Leonard [26] under the assumption of a discrete change in the effective cross section of satellites flying in the group. He developed a control algorithm based on the proportional differential controller. A large number of papers applied a variety of the different control algorithms using differential drag including PID regulators [27], linear-quadratic regulators [28], Lyapunov-based control [29, 30], sliding mode control [31], and optimal control [32]. These papers only considered the aerodynamic differential drag and allow control of the relative motion in a single orbital plane only. Some recent papers take into account the differential lift and also consider the spatial relative motion control. The application of the differential lift along with the drag for the small satellite rendezvous problem was first proposed by Horsley et al. [33]. Control strategy developed in Ref. [33] is based on the bang-bang approach when only the maximum values of the lift and drag are used. Papers [28, 34] address the problem of the satellite formation keeping by the differential lift and drag under the  $J_2$  perturbation. The application AD for construction of tetrahedral formation flying using 3U CubeSats is considered in a paper by Ivanov et al. [35].

The idea of SRP application for CubeSat formation flying control is inspired by successful single satellite missions like LightSail 2 and NanoSail-D2 with sails onboard. The CubeSats are equipped with active attitude control systems to be able to orient the normal vector to the sail relative to the Sun direction to produce required SPR force. A set of papers are devoted to the control algorithm using conventional sail [36–41] and sails with variable reflectivity properties [42].

The classical control approach using propulsion and the use of SRP or AD do not affect the relative motion directly, but control the orbital motion of one or several satellites instead. This seems ineffective because the significant amount of acceleration is aimed to the whole formation flying momentum change. The electrostatic and the electromagnetic control approaches are free from these shortcomings. Since both forces appear when two or more satellites in a formation have either electrostatic

charge or dipole moment, the total momentum of the interacting satellites conserves. So, these approaches allow controlling relative motion directly.

A concept of electrostatic formation flying control was suggested by King et al. in 2002 [43]. This concept is based on the results of the SCATHA mission where the satellite electrostatic charge system was first tested. The miniature cold-cathode electron gun for the charging was used in Aalto-1 and in the ESTCube-1 3U CubeSat missions. The onboard gun charged deployed tether for the application of the Lorentz force in the geomagnetic field for faster deorbiting. Changing the value of this force can be used for formation flying control as well.

The concept of tethered satellite formation flying can also be implemented using CubeSats. The main idea is to link two or more satellites by some rope and to control the relative motion by changing its length [44–47]. The realization of this concept is complicated because of flexible rope motion [48]. So the relative motion of the two connected by tether satellites is usually designed to provide the tension of the tether.

A summary of the Section 3.2 is presented in Table 2.

### 3.3 Swarm of nanosatellites decentralized control

Swarm-type flight requires only bounded relative motion with no other restrictions in contrast to the formation type of constellation. Random relative trajectories in the swarm have several advantages: (1) economy of the control source of the satellites, (2) less dependence on the failure of the specific satellite, and (3) reduced demands for the onboard hardware and software. During the launch of the swarm, some error in the separation speed of nanosatellites from the launch vehicle is inevitable. This leads

**Table 2** Summary of CubeSat formation flying control approaches and its features.

Control approach	Motion features	Onboard hardware required
Single-input control	Able to achieve the closed relative trajectories, though its form and shape depends on orbital parameters and initial conditions	Propulsion, passive attitude control system
Differential AD	Allows to control the relative motion mainly in the orbital plane. Applicable for LEO	Active attitude control system, high area-to-mass ratio form factor or drag sail
Differential SRP	Applicable to orbits without Earth shading	Active attitude control system, solar sail
Lorentz force	Applicable for LEO and MEO	Electron gun system
Tether	The size of the relative orbit is limited by the tether length. Relative motion is chosen so as to achieve tether tension	Tether deployment system

to a slightly different orbital period of the satellites, the relative trajectories become unlimited, and the swarm degrades. Thus the problem of the relative drift reduction or elimination is of great importance.

For control of each satellite in the swarm, it is necessary that the information about the relative motion of all other satellites be made available. However, in the case of a significant number of satellites in the swarm, this is a difficult task due to the hardware limitations of the relative motion determination system and/or the intersatellite communication limitations. These restrictions that prevent the availability of information about the relative motion of all satellites in the swarm will henceforth be referred to as communicational constraints. In natural swarms, for example, for a swarm of insects, there is a limit to the number of communication links between each element of the swarm and its neighbors. In addition, there is a limit of the maximum distance between the elements of the swarm at which the relative motion can be known. Similar restrictions exist for a swarm of satellites. Each satellite can estimate the relative motion of other satellites using onboard motion determination systems. However, due to the limited capabilities of the sensors, each satellite can estimate the relative motion of those satellites that are located in a certain neighborhood only. Relative motion determination systems can be based on the processing of images, range finders, and other sensors, but the number of satellites whose relative motion can be determined simultaneously is generally small. Also, there is a limit on the range at which the system can operate with the necessary accuracy. These features of the autonomous motion determination system can be overcome by sharing information between satellites about the current orbital motion obtained, for example, using onboard GPS receivers installed on each satellite, and thus the relative motion can be computed [14]. However, intersatellite communication channels also cannot provide unlimited number of connections to one satellite owing to frequency restrictions of signals. Thus, during deployment of a swarm of satellites, it is necessary to take into account the features associated with communication constraints as described in a study by Ivanov et al. [49] in which they considered a set of control strategies for 20 3U CubeSats swarm deployment.

The so-called “agents” are considered in the literature about swarm motion to be independent and autonomous controllable units, in our case the satellites. In most papers on multiagent systems, a control plays according to four rules: attraction, alignment, collision avoidance, and achievement of the goal. In a study by Sabatini et al. [50], a linear-quadratic regulator using these rules to control the swarm of satellites is considered, and a comparison of characteristic velocity of centralized and decentralized strategies is performed for various parameters and tasks of the mission. A reduction in computational complexity for a large number of satellites is shown when a two-stage control (a combination of centralized and decentralized strategies) is used. A follow-on paper by the same authors [51] focuses on the study of the decentralized approach using an artificial potential function for control; however, the dynamics of the relative motion of satellites formation flying is not considered.

A propulsion system can be used for the swarm deployment, but the differential drag-based control is more suitable for nanosatellites in LEO. It does not require propellant; however, the active attitude control system is needed. However, almost all the studies on differential drag control consider only two satellites in formation flying with application of the centralized control approach [26–32]. A few papers are devoted to



differential drag control of the multiple satellites. The cyclic and optimal control strategies for a cluster flight with more than two satellites are proposed in a paper by Ben-Yaacov and Gurfil [52]. Stability and performance of cluster keeping while avoiding collisions were studied in 2015 by the same researchers [53]. The papers mentioned earlier do not address communication restrictions and decentralized control features.

The most critical issue in swarm control is collision avoidance between satellites moving along random relative trajectories. The collision avoidance algorithms are usually aimed at decreasing the probability of a dangerous rendezvous between the satellites. So the algorithm described in the work by Slater et al. [54] is intended to calculate the necessary maneuver for a predicted close distance and to minimize the collision probability and characteristic velocity. In work by Bombardelli and Hernando-Ayuso [55], an optimum algorithm is proposed to minimize the fuel consumption and maximize the relative distance between satellites in the same time. Another common approach for preventing collisions is the method of artificial potential fields considered [56]. The satellite forms a spherical potential field around itself. According to the control algorithm, if another satellite enters this sphere, a repulsive force directed along the radius from one satellite to the second acts on it. Schlanbusch et al. [57] describes an algorithm based on behavioral control for the reconfiguration of a group of satellites. If the satellites enter a spherical forbidden zone during reconfiguration, the satellite is affected by a predetermined repulsive pulse directed along the radius vector. Such an impulse is applied as long as the satellite is in the forbidden zone.

The 3U CubeSat KickSat-2 deployed 105 so-called ChipSats or Sprites in March 2019 representing the first launched swarm mission so far. The Sprites are 3.5-cm by 3.5-cm chips with all the satellite systems necessary for self-contained operations [58]. Sprite-like satellites could be distributed by the hundreds or thousands in orbit and could become a spatially distributed measurement system that even could form a planetary ring [59]. The ChipSats launched to date have no relative motion control, and they are flying apart passively, but small magnetic control system can be installed and differential drag applied in future missions. Another idea by the StartRocket company is to launch a swarm of CubeSats with sunlight reflectors for constructing the orbital display. Each satellite will represent a pixel in some image that can be seen from the Earth under appropriate illumination conditions [60]. The control of such a display is planned to be implemented using either onboard thrusters or using differential aerodynamic forces. This and the other recent developments in attitude control described earlier will likely facilitate the advancement of SmallSat constellations, formations, and swarms with an extremely wide variety of applications in Earth remote sensing, space weather monitoring, and other applications yet to be explored.

## References

- [1] J.G. Walker, *Satellite constellations*, *J. Br. Interplanet. Soc.* 37 (1984) 559–571.
- [2] N.H. Crisp, K. Smith, P. Hollingsworth, Launch and deployment of distributed small satellite systems, *Acta Astronaut.* 114 (2015) 65–78, <https://doi.org/10.1016/j.actastro.2015.04.015>.
- [3] Method and Apparatus for Deploying a Satellite Network, <https://patents.google.com/patent/US5199672A/en>, 1990. (Accessed 29 May 2019).

- [4] C.-J. Fong, W.-T. Shiau, C.-T. Lin, T.-C. Kuo, C.-H. Chu, S.-K. Yang, N.L. Yen, S.-S. Chen, Y.-H. Kuo, Y.-A. Liou, S. Chi, Constellation deployment for the FORMOSAT-3/COSMIC mission, *IEEE Trans. Geosci. Remote Sens.* 46 (2008) 3367–3379, <https://doi.org/10.1109/TGRS.2008.2005202>.
- [5] S.P. Trofimov, M.Y. Ovchinnikov, Optimal multiple-impulse circular orbit phasing, *J. Guid. Control. Dyn.* 39 (2016) 1678–1681, <https://doi.org/10.2514/1.G001513>.
- [6] C.D. Hall, V. Collazo-Perez, Minimum-time orbital phasing maneuvers, *J. Guid. Control. Dyn.* 26 (2003) 934–941, <https://doi.org/10.2514/2.6921>.
- [7] C. Cappelletti, S. Battistini, F. Graziani, Small launch platforms for micro-satellites, *Adv. Space Res.* 62 (2018) 3298–3304, <https://doi.org/10.1016/J.ASR.2018.05.004>.
- [8] J. Gangestad, B. Hardy, D. Hinkley, Operations, orbit determination, and formation control of the AeroCube-4 CubeSats, in: *27th Annu. AIAA/USU Conf. Small Satell. No. SSC13-X-4*, Logan, Utah, 2013.
- [9] C. Boshuizen, J. Mason, P. Klupar, S. Spanhake, Results from the Planet Labs Flock Constellation, in: *AIAA/USU Conf. Small Satellites*, 2014. <https://digitalcommons.usu.edu/smallsat/2014/PrivEnd/1>. (Accessed 29 May 2019).
- [10] C. Foster, J. Mason, V. Beukelaers, L. Stepan, R. Zimmerman, Differential drag control scheme for large constellation of planet satellites and on-orbit results, in: *Proceedings Int. Work. Satell. Constellations Form. Flying*, June 19–21, 2017, Boulder, CO, 2017, pp. 1–18.
- [11] Planet, Daily Satellite Imagery and Insights, n.d. <https://www.planet.com/> (Accessed 29 May 2019).
- [12] Nanosats Database, n.d. <https://www.nanosats.eu/tables#constellations> (Accessed 29 May 2019).
- [13] Spire, Space to Cloud Data & Analytics, n.d. <https://www.spire.com/en> (Accessed 29 May 2019).
- [14] N.H. Roth, B. Risi, R.E. Zee, Flight results from the Canx-4 and Canx-5 formation flying mission, in: *Proc. Int. Work. Satell. Constellations Form. Flying*, June 19–21, 2017, Boulder, CO, 2017, pp. 1–17.
- [15] G. Bonin, N. Roth, S. Armitage, J. Newman, B. Risi, R.E. Zee, CanX-4 and CanX-5 precision formation flight: mission accomplished! in: *29th Annu. AIAA/USU Conf. Small Satell. Uta, LoganSSC15-I-4*, 2015. <https://pdfs.semanticscholar.org/c5bd/33760a1b8c80781d299999c4ebe55ebc29da.pdf>. (Accessed 29 May 2019).
- [16] R. Opromolla, G. Fasano, G. Rufino, M. Grassi, A review of cooperative and uncooperative spacecraft pose determination techniques for close-proximity operations, *Prog. Aerosp. Sci.* 93 (2017) 53–72, <https://doi.org/10.1016/J.PAEROSCI.2017.07.001>.
- [17] F. Perez, D. Modenini, A. Vázquez, F. Aguado, R. Tubío, G. Dolgos, A. Gonzalez, R. Lasagni Manghi, M. Zannoni, A. Nazeeruddin, M. Melozzi, I. Carnelli, DustCube, a nanosatellite mission to binary asteroid 65803 Didymos as part of the ESA AIM mission, *Adv. Space Res.* 62 (2018) 3335–3356, <https://doi.org/10.1016/J.ASR.2018.06.019>.
- [18] S. D’Amico, J.-S. Ardaens, G. Gaias, H. Benninghoff, B. Schlepp, J.L. Jørgensen, Non-cooperative rendezvous using angles-only optical navigation: system design and flight results, *J. Guid. Control. Dyn.* 36 (2013) 1576–1595, <https://doi.org/10.2514/1.59236>.
- [19] D. Ivanov, M. Ovchinnikov, M. Sakovich, Relative pose and inertia determination of unknown satellite using monocular vision, *Int. J. Aerosp. Eng.* (2018) 1–16, <https://doi.org/10.1155/2018/9731512>.
- [20] R. Noteborn, Flight results from the PRISMA optical line of sight based autonomous rendezvous experiment, in: *Proc. 4th Int. Conf. Spacecr. Form. Fly. Mission. an Technol.* May 2011, Montr. Canada, 2011, p. 10.
- [21] K. Alfriend, S. Vadali, P. Gurfil, J. How, L. Breger, *Spacecraft Formation Flying: Dynamics, Control and Navigation*, Elsevier/Butterworth-Heinemann, Oxford, 2010.

- [22] D.P. Scharf, F.Y. Hadaegh, S.R. Ploen, A survey of spacecraft formation flying guidance and control (part 1): guidance, in: Proc. 2003 Am. Control Conf, IEEE, 2003, pp. 1733–1739, <https://doi.org/10.1109/ACC.2003.1239845>.
- [23] G. Di Mauro, M. Lawn, R. Bevilacqua, Survey on guidance navigation and control requirements for spacecraft formation-flying missions, *J. Guid. Control. Dyn.* 41 (2018) 581–602, <https://doi.org/10.2514/1.G002868>.
- [24] M.Y. Ovchinnikov, D. Bindel, D.S. Ivanov, G.V. Smirnov, S. Theil, I.E. Zaramenskikh, Development and laboratory verification of control algorithms for formation flying configuration with a single-input control, *Acta Astronaut.* 67 (2010) 1158–1163.
- [25] A.D. Guerman, M.Y. Ovchinnikov, G.V. Smirnov, S.P. Trofimov, Close relative trajectories for formation flying with single-input control, *Math. Probl. Eng.* 2012 (2012) 20, <https://doi.org/10.1155/2012/967248> Article ID 967248.
- [26] C.L. Leonard, *Formation Keeping of Spacecraft Via Differential Drag* (Master thesis). Massachusetts Inst. Technol, Cambridge, MA, 1986.
- [27] B.S. Kumar, A. Ng, A. Bang-Bang, Control approach to maneuver spacecraft in a formation with differential drag, in: Proc. AIAA Guid. Navig. Control Conf. Exhib. AIAA Pap. No. 2008–6469, Honolulu, Hawaii, August, 2008.
- [28] D. Ivanov, M. Kushniruk, M. Ovchinnikov, Study of satellite formation flying control using differential lift and drag, *Acta Astronaut.* 145 (2018) 88–100, <https://doi.org/10.1016/J.ACTAASTRO.2018.07.047>.
- [29] D. Pérez, R. Bevilacqua, Lyapunov-based adaptive feedback for spacecraft planar relative maneuvering via differential drag, *J. Guid. Control. Dyn.* 37 (2014) 1678–1684, <https://doi.org/10.2514/1.G000191>.
- [30] D. Pérez, R. Bevilacqua, Differential drag spacecraft rendezvous using an adaptive Lyapunov control strategy, *Acta Astronaut.* 83 (2013) 196–207, <https://doi.org/10.1016/j.actaastro.2012.09.005>.
- [31] K.D. Kumar, A.K. Misra, S. Varma, F. Bellefeuille, Maintenance of satellite formations using environmental forces, *Acta Astronaut.* 102 (2014) 341–354, <https://doi.org/10.1016/j.actaastro.2014.05.001>.
- [32] L. Dellelce, G. Kerschen, Optimal propellantless rendez-vous using differential drag, *Acta Astronaut.* 109 (2015) 112–123, <https://doi.org/10.1016/j.actaastro.2015.01.011>.
- [33] M. Horsley, S. Nikolaev, A. Pertica, Small satellite rendezvous using differential lift and drag, *J. Guid. Control. Dyn.* 36 (2013) 445–453, <https://doi.org/10.2514/1.57327>.
- [34] X. Shao, M. Song, J. Wang, D. Zhang, J. Chen, Satellite formation keeping using differential lift and drag under J2 perturbation, *Aircr. Eng. Aerosp. Technol.* 89 (2017) 11–19.
- [35] D. Ivanov, M. Mogilevsky, U. Monakhova, M. Ovchinnikov, A. Chernyshov, Deployment and maintenance of nanosatellite tetrahedral formation using aerodynamic forces, in: Proc. IAC-2018. Pap. IAC-18-B4.7.6, 2018, p. 11.
- [36] S. Gong, G. Yunfeng, J. Li, Solar sail formation flying on an inclined Earth orbit, *Acta Astronaut.* 68 (2011) 226–239, <https://doi.org/10.1016/j.actaastro.2010.08.022>.
- [37] K. Shahid, K.D. Kumar, Multiple spacecraft formation reconfiguration using solar radiation pressure, *Acta Astronaut.* 103 (2014) 269–281, <https://doi.org/10.1016/j.actaastro.2014.05.021>.
- [38] K. Shahid, K.D. Kumar, Formation control at the Sun-Earth L(2) libration point using solar radiation pressure, *J. Spacecr. Rocket.* 47 (2010) 614–626, <https://doi.org/10.2514/1.47342>.
- [39] S. Gong, H. Baoyin, J. Li, Solar sail formation flying around displaced solar orbits, *J. Guid. Control. Dyn.* 30 (2007) 1148–1152, <https://doi.org/10.2514/1.24315>.
- [40] T. Williams, Z.-S. Wang, Solar radiation pressure and formation-keeping in highly elliptical orbits, in: AIAA/AAS Astrodyn. Spec. Conf. Exhib, 2002, pp. 1–14.

- [41] K. Parsay, H. Schaub, Drift-free solar sail formations in elliptical Sun-synchronous orbits, *Acta Astronaut.* 139 (2017) 201–212, <https://doi.org/10.1016/J.ACTAASTR.2017.06.027>.
- [42] Y.V. Mashtakov, M.Y. Ovchinnikov, T.Y. Petrova, S.S. Tkachev, Attitude and relative motion control of satellites in formation flying via solar sail with variable reflectivity properties, in: *Proc. 69th International Astronaut. Congr.*, 2018, p. 8.
- [43] L.B. King, G.G. Parker, S. Deshmukh, J.-H. Chong, Spacecraft Formation-Flying using Inter-Vehicle Coulomb Forces, *Tech. Rep. NASA/NIAC (2002)* 103 p.
- [44] S.-J. Chung, D.W. Miller, Propellant-free control of tethered formation flight, part 1: linear control and experimentation, *J. Guid. Control. Dyn.* 31 (2008) 571–584, <https://doi.org/10.2514/1.32188>.
- [45] J. Zhang, K. Yang, R. Qi, Dynamics and offset control of tethered space-tug system, *Acta Astronaut.* 142 (2018) 232–252, <https://doi.org/10.1016/J.ACTAASTRO.2017.10.020>.
- [46] Y. Chen, R. Huang, X. Ren, L. He, Y. He, History of the tether concept and tether missions: a review, *ISRN Astron. Astrophys.* 2013 (2013) 1–7, <https://doi.org/10.1155/2013/502973>.
- [47] A.D. Guerman, G. Smirnov, P. Paglione, A.M. Vale Seabra, Stationary configurations of a tetrahedral tethered satellite formation, *J. Guid. Control. Dyn.* 31 (2008) 424–428, <https://doi.org/10.2514/1.31979>.
- [48] S.S. Gates, S.M. Koss, M.F. Zedd, Advanced tether experiment deployment failure, *J. Spacecr. Rocket.* 38 (2001) 60–68.
- [49] D. Ivanov, U. Monakhova, M. Ovchinnikov, Nanosatellites swarm deployment using decentralized differential drag-based control with communicational constraints, *Acta Astronaut.* 159 (2019) 646–657, <https://doi.org/10.1016/J.ACTAASTRO.2019.02.006>.
- [50] M. Sabatini, F. Reali, G.B. Palmerini, Autonomous behavioral strategy and optimal centralized guidance for on-orbit self assembly, in: *IEEE Aerosp. Conf. Proc.*, 12, 2009, <https://doi.org/10.1109/AERO.2009.4839582>.
- [51] M. Sabatini, G.B. Palmerini, P. Gasbarri, Control laws for defective swarming systems, *Adv. Astronaut. Sci.* 153 (2015) 749–768.
- [52] O. Ben-Yaacov, P. Gurfil, Long-term cluster flight of multiple satellites using differential drag, *J. Guid. Control. Dyn.* 36 (2013) 1731–1740, <https://doi.org/10.2514/1.61496>.
- [53] O. Ben-Yaacov, P. Gurfil, Orbital elements feedback for cluster keeping using differential drag, *Adv. Astronaut. Sci.* 153 (2015) 769–787, <https://doi.org/10.1007/s40295-014-0022-0>.
- [54] G.L. Slater, S.M. Byram, T.W. Williams, Collision avoidance for satellites in formation flight, *J. Guid. Control. Dyn.* 29 (2006) 1140–1146, <https://doi.org/10.2514/1.16812>.
- [55] C. Bombardelli, J. Hernando-Ayuso, Optimal impulsive collision avoidance in low Earth orbit, *J. Guid. Control. Dyn.* 38 (2015) 217–225, <https://doi.org/10.2514/1.G000742>.
- [56] D. Lee, A.K. Sanyal, E.A. Butcher, Asymptotic tracking control for spacecraft formation flying with decentralized collision avoidance, *J. Guid. Control. Dyn.* 38 (2015) 587–600, <https://doi.org/10.2514/1.G000101>.
- [57] R. Schlanbusch, R. Kristiansen, P.J. Nicklasson, Spacecraft formation reconfiguration with collision avoidance, *Automatica* 47 (2011) 1443–1449, <https://doi.org/10.1016/j.automatica.2011.02.014>.
- [58] KickSat, n.d. <https://kicksat.github.io/> (Accessed 3 September 2019).
- [59] C. Colombo, C. McInnes, Orbit design for future SpaceChip swarm missions in a planetary atmosphere, *Acta Astronaut.* 75 (2012) 25–41, <https://doi.org/10.1016/J.ACTAASTRO.2012.01.004>.
- [60] The Orbital Display by StartRocket, n.d. <https://startrocket.me/> (Accessed 3 September 2019).

# CubeSats for microbiology and astrobiology research

7

Luis Zea<sup>a</sup>, Sergio R. Santa Maria<sup>b</sup>, and Antonio J. Ricco<sup>b</sup>

<sup>a</sup>BioServe Space Technologies, University of Colorado, Boulder, CO, United States,

<sup>b</sup>NASA Ames Research Center, Moffett Field, CA, United States

## 1 Introduction

The study of microbiology in outer space falls within two broad categories linking biological science to space: astrobiology and fundamental space biology. Astrobiology seeks to satisfy human curiosity by expanding scientific understanding of life's origins, evolution, distribution, and future in the universe, including such topics as prebiotic chemistry, extraterrestrial adaptation and survival, and searching for habitable environments and nonterrestrial life. Fundamental space biology focuses pragmatically on the potential for terrestrial life to adapt and survive away from Earth. Critical studies are conducted by carrying organisms into space and studying every aspect of how that environment affects them. Space's primary perturbations to life are diminished gravitation and a complex, variable spectrum of ionizing radiation; studies of adaptation and basic survival are augmented by characterizing the degree to which organisms, communities, or ecologies can thrive and maintain functional performance relative to reference terrestrial conditions.

Both astrobiology and fundamental space biology are ripe for scientific advances achievable with small, microbial payload experiments that can be carried aboard CubeSats, albeit with limitations. For example, in astrobiology neither the study of prebiotic chemistry nor the search for extraterrestrial life requires carrying microbes into space, and while the study of microbes is central to fundamental space biology, complex multicellular organisms—up to and including humans—are also of great interest but not CubeSat appropriate.

Despite such limitations, emphasis by the world's large space agencies on the complex, costly task of supporting humans in space has led to a variety of basic biological studies utilizing so-called model organisms, many of which are microbes and thus generally CubeSat compatible. These microbiology experiments aim to anticipate and explain space environment effects on humans: the model organisms are well and widely characterized in terrestrial labs, and their similarities to, and overlaps with, cells and functional processes in the human body are understood and exploited.

Indeed, model organisms were the subjects of the first life science space studies conducted aboard early Soviet and American missions: In 1960 Korabl-Sputnik 2 carried *Escherichia coli*, and Discoverer 17 ferried *Clostridium sporogenes* into space [1–3]. Subsequently, the Soviet Vostok spacecraft, the Mir space station, and many

of the US Gemini, Apollo, and Space Shuttle missions supported space microbiology experiments. Basic biological studies were never, however, the core reason for these missions. This is now changing, thanks to CubeSats' enabling spaceflight missions designed explicitly to conduct microbiology experiments.

Given their academic origins, the first CubeSat developments and missions focused understandably on technology demonstration and student training—the earliest CubeSat science endeavors included physical characterization of the space environment and observations of Earth [4,5]. In 2006, this scientific scope expanded measurably when the *GeneSat-1* mission demonstrated that CubeSats can serve as Earth orbit science platforms for living microbes, thus providing the first opportunities for microbial biological studies to be the principal focus of entire spaceflight payloads [6].

From an engineering point of view, the establishment of a bus that permits interchangeable or even standardized payloads can streamline and hasten microbiological space research capability development, which in turn stands to reduce programmatic costs. This chapter presents the results and future potential of doing microbiology experiments on a CubeSat platform, including the benefits conferred to space biology research.

To date, NASA's Ames Research Center is the only institution to have operated nanosatellites with live biological payloads. The chronological listing in [Table 1](#) reveals NASA Ames' evolutionary approach to the development of the five space-life-sciences CubeSats flown to date by using the technologies of each satellite and its

**Table 1** Biological or astrobiological CubeSat missions.

Mission (format)	Description	Launch year	Outcome
<i>GeneSat-1</i> (3U)	<ul style="list-style-type: none"> <li>• 2U payload measured expression of green fluorescent protein in <i>Escherichia coli</i> and tracked microbe population via light scattering</li> <li>• First NASA nanosatellite mission; first biological payload to fly in space on a CubeSat platform</li> </ul>	2006	Full mission success
<i>PharmaSat</i> (3U)	<ul style="list-style-type: none"> <li>• 2U payload measured antifungal drug dose-response curves for <i>Saccharomyces cerevisiae</i> fungus using colorimetry to measure metabolic</li> </ul>	2009	Full mission success

Table 1 Continued

Mission (format)	Description	Launch year	Outcome
<i>O/OREOS</i> <sup>a</sup> (3U)	<p>activity and population versus time</p> <ul style="list-style-type: none"> <li>• First NASA principal investigator-led nanosatellite mission</li> <li>• Two independent 1U astrobiology payload modules measured               <ul style="list-style-type: none"> <li>(i) survival of <i>Bacillus subtilis</i> up to 6 months and</li> <li>(ii) long-term photodegradation of biomarkers and bio-building blocks for 1.5 years via UV-visible spectroscopy</li> </ul> </li> <li>• High-radiation, high-inclination orbit; deorbit mechanism</li> </ul>	2010	Full mission success, both payloads. Spacecraft remained operable ~5 years in orbit
<i>SporeSat-1</i> (3U)	<ul style="list-style-type: none"> <li>• 2U payload to measure gravitational response of <i>Ceratopteris richardii</i> fern spores via Ca<sup>2+</sup> ion channel response</li> <li>• Variable gravity in microgravity ambient using 50-mm microcentrifuges with 32 ion-specific [Ca<sup>2+</sup>] electrode pairs</li> </ul>	2014	Successful space demo of mini centrifuges with integral ion-sensitive electrodes
<i>EcAMSat</i> <sup>b</sup> (6U)	<ul style="list-style-type: none"> <li>• 2U payload measured antibiotic resistance in microgravity versus dose for uropathogenic <i>Escherichia coli</i></li> <li>• 6U format provided 50% more solar-panel power to keep payload experiment at 37°C for extended durations</li> </ul>	2017	Full mission success

<sup>a</sup> *O/OREOS* = Organism/Organic Exposure to Orbital Stress.<sup>b</sup> *EcAMSat* = *Escherichia coli* Antimicrobial Satellite.

payload as starting points and stepping stones for the next. This approach reduces risk and cost while increasing the probability of mission success.

*GeneSat-1* was designed, built, and flown to demonstrate that in situ biological research including integral microbial life support in a CubeSat was feasible without return of any biological samples [7]. *PharmaSat*, the first nanosatellite to host a competitively selected, peer-reviewed, science-driven mission, improved upon *GeneSat-1*'s 1U bus and took multiple lessons from its payload technologies [8]. The bus of the Organism/Organic Exposure to Orbital Stresses (*O/OREOS*) satellite was a modestly improved version of the 1U bus of *PharmaSat* [9–11]; this mission was the first dedicated to astrobiology and the first to support two completely independent 1U bio-science payloads. *EcAMSat* (*E. coli* Antimicrobial Satellite), selected by peer review from an open public opportunity, was the first 6U microbiology CubeSat; it not only utilized a copy of the 1U *PharmaSat* bus but also repurposed over 90% of *PharmaSat*'s payload system as well. *SporeSat*, selected for development during the same public competition as *EcAMSat*, utilized a new 1U bus design featuring a real-time operating system; its 2U payload implemented multiple new technologies, including variable-rate microcentrifuges with integral illumination and a pair of ion-sensitive electrodes for every specimen. The university-operated ground station and mission operations approach evolved from *GeneSat-1* to *PharmaSat*, remaining essentially the same for *O/OREOS* and the next missions to fly [8,12,13].

This chapter surveys and summarizes progress to date with “microbiology CubeSats” from the science, engineering, and programmatic points of view. In addition to their science payloads, key satellite “bus” subsystems, for example, power and communication, and their ground control systems are described. Operational parameters such as orbital information are also detailed. Special focus is given to the payload hardware design, development, and operation. Finally, the first biology experiment to be conducted in heliocentric orbit beyond Earth's magnetosphere since the final Apollo mission in 1972 is described and discussed: *BioSentinel* is a CubeSat scheduled for launch as soon as 2021.

## 2 CubeSats for microbiology research

This section will present all the CubeSats missions carrying microbiological experiments mentioned above. In all cases, the core of the payload was one or more microfluidic cards or disks, with multiple wells, placed inside a hermetic container filled with humidified air at 1 atm to allow for aerobic respiration [7,14–16].

### 2.1 GeneSat-1

*GeneSat-1*'s scientific objective was to characterize bacterial growth and metabolics using *E. coli* as the model organism. This implied growing bacteria in a suitable controlled environment and acquiring and transmitting data back to the scientists. These experiment objectives created the following mission requirements, constraints, and drivers [7]: (i) a microfluidic-based payload needed to be capable of operations in



microgravity, (ii) the payload temperature needed to be regulated to within  $\pm 0.5^\circ\text{C}$  of a defined set point, and (iii) high-quality optical sensors needed to be miniaturized for in situ data acquisition, preferably without moving parts. The core of *GeneSat-1*'s payload was a 12-well ( $110\ \mu\text{L}/\text{well}$ ) card, including two wells as solid-state controls. The card was an acrylic manifold that connected the 10 wells to an input and an output port; each well had a pair of  $0.22\text{-}\mu\text{m}$  nylon fiber membrane filters at its inlet and outlet to keep *E. coli* in the wells during fluid exchange. One of the faces of the card was covered with a  $0.5\text{-mm}$ -thick optical-quality acrylic plate and the other with a  $75\text{-}\mu\text{m}$ -thick gas-permeable membrane (polystyrene). The card was connected to a  $15\text{-mL}$  polyethylene vinyl acetate (PEVA) bag filled with growth medium through a solenoid valve (Parker). Similarly a second PEVA bag was connected to the card outlet. Each of the 12 wells had a 3-W blue LED to produce fluorescence excitation ( $470\text{ nm}$ ) and a  $2.3\text{-mW}$  green LED for illumination to acquire optical density. Data were acquired with an intensity-to-frequency detector and a  $525\text{-nm}$  emission filter to detect green fluorescence as a proxy of gene expression and to pass the green LED wavelength for light scattering to quantify cell counts [6]. The major payload components are shown during the integration process in Fig. 1.

As a secondary payload, a late load (or reload) was not possible for *GeneSat-1*. The reagents and biological samples had to survive a minimum of 6 weeks before launch, including a 4-week prelaunch period plus 2 weeks in case of launch delays—the time to operation in space ended up being just under 7 weeks due to launch slips [17]. Prior to payload integration, cells were loaded in the microfluidic card wells in a PBS-based stasis buffer to place them in metabolic dormancy. Two strains of K-12 *E. coli* were loaded into the fluidic cards for flight and for a parallel ground control experiment: DH5alpha (Arizona State University), with plasmid AcGFP to express green

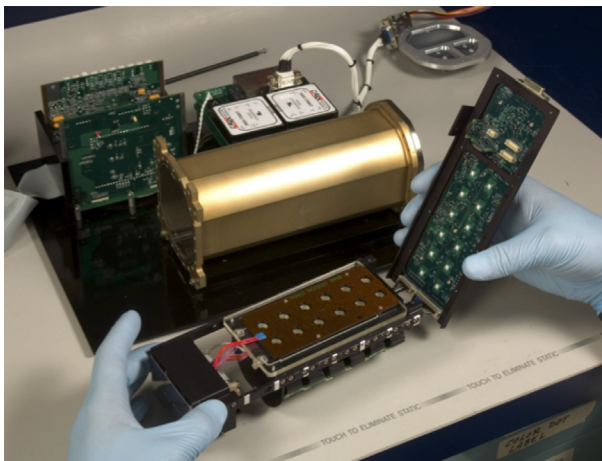


**Fig. 1** *GeneSat-1* payload components during integration. Fluidic card (sandwiched between heater plates), in left hand, with blue excitation and combined detection system beneath it; circuit board with green LEDs in right hand; hermetic container in the background. Credit: NASA.

fluorescent protein (GFP), and MM294 cells (Carolina Biological), with plasmid p-GREEN for GFP. Both engineered organisms express GFP constitutively (emission peak: 512 nm).

The mission launched into a 40-degree inclination, 413-km perigee, and 424-km apogee orbit, on December 16, 2006, aboard a Minotaur I rocket from the Wallops Flight Facility in Virginia, USA. Once the experiment was initiated, the card was warmed to 34°C, and growth medium was introduced into the wells, replacing the stasis buffer and initiating cell growth. Fluorescence and cell growth were monitored using the optical detection system described earlier. During flight, communication was limited to a few passes per day through prearranged ground stations, limiting the possibility of human control. Due to these limitations, *GeneSat-1* was designed for fully autonomous operations, including initiation of the experiment, temperature control, biological measurements, data recording, and telemetry.

*GeneSat-1* was a fully successful mission; fluorescence and cell growth were observed in all nine microfluidic wells containing one strain or the other of *E. coli*; one well carried no microbes and produced a flat baseline throughout the experiment, as did the solid-state controls. During the exponential phase of growth, the two strains of *E. coli* doubled with an average period of ~50 min per generation in space microgravity and ~35 min per generation on Earth. The slower growth rate in space was tentatively attributed to the absence of gravity-driven forces and flows in microgravity, namely, thermal convection, buoyancy, and sedimentation, which means that delivery of nutrients and removal of waste products to/from the cells occur only by diffusion. This altered extracellular mass transport phenomenon has been corroborated via a molecular genetic analysis [18]. The spaceflight results demonstrated a system capable of autonomous operations in low Earth orbit [17].

## 2.2 PharmaSat

*PharmaSat*'s scientific mission objective was to study the effects of microgravity on yeast (*Saccharomyces cerevisiae*) growth and metabolism and on antifungal drug efficacy via three-color optical absorbance. To achieve these goals, the satellite needed to accomplish four main functions: (i) provide life support for the microbes in the fluidic card in the payload, (ii) introduce antifungal agents into the wells at several concentrations, (iii) measure optical density in the wells to calculate population growth, and (iv) measure culture viability via a metabolic indicator dye [8,16,19]. The payload hardware was contained within a 1.2-L hermetically sealed vessel [16], which in turn was covered in multilayer insulation (MLI) blankets and gold plating for thermal optimization [19]. To reduce heat conduction, the payload was attached to the bus with titanium screws and Ultem washers. The payload components were warmed with a pair of flexible patterned nichrome-on-Kapton 2 W heaters (Minco), each bonded to an aluminum thermal spreader plate for spatial and temporal thermal uniformity [19]. The heaters were capable of providing a temperature stability of better than  $\pm 0.3^\circ\text{C}$ .

The  $6.4 \times 12.8$  cm fluidics card (the same length as standard 96-well plates but narrower due to payload size limitations), Fig. 2, was made of laser-cut poly (methylmethacrylate) layers and included 48, 100- $\mu\text{L}$  wells (4-mm diameter and 7.8 mm deep,

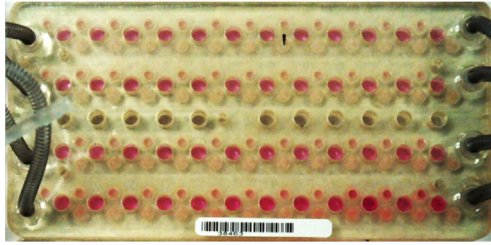


**Fig. 2** *PharmaSat* fluidic card with four banks of 12 fluidic wells designated, from top to bottom, for high, medium, low, and zero dosage of antifungal drug. The *pink color* (light gray in print version) is due to alamarBlue that has been converted by metabolites of growing yeast to its *pink* (reduced) form; *pink* is most intense in the control bank, and faintest in the high-dose bank, due to relative rates of metabolic activity. Center bank of dry wells was reserved for solid-state color standards.

Credit: NASA.

spaced 9 mm center to center) and 11 solid-state reference wells. Every fluidic well had 1.2- $\mu\text{m}$  nylon fiber membrane filters at its inlet and outlet to prevent removal of yeast from the wells during fluid exchanges. The card included four independent manifolds serving the four banks of wells to support three separate drug dose levels plus a zero-dose control. There was a 51- $\mu\text{m}$ -thick polystyrene gas-permeable membrane on each side of the fluidic card [16]. The payload hardware also included a miniaturized environmental control system, microfluidics system with pumps, valves, and an array of 59 optical sensors, one per well [8].

*PharmaSat* launched as a secondary payload aboard a Minotaur I rocket from Wallops Flight Facility on May 19, 2009. As with *GeneSat-1*, no late load was allowed, and no power was available for thermal control prior to deployment in space. During payload assembly, yeast cells were transferred into stasis buffer and loaded into the fluidic card microwells. After launch, *PharmaSat* was spring ejected into low Earth orbit (40-degree inclination, 432-km perigee, and 467-km apogee). The experiment was initiated by feeding the cells with growth medium containing a metabolic indicator dye, thus displacing the stasis buffer. Each microwell within the fluidic card was monitored using a three-LED optical source and detector system. This system measured yeast growth in two ways: (i) via optical density changes due to light scattering by the yeast cells, which is directly proportional to cell number, and (ii) via color change of the viability dye, alamarBlue. This dye changes from its oxidized blue form to its reduced pink form when the cells become metabolically active, at a rate dependent on the number of cells and their average metabolic output. After the cells were allowed to recover from stasis for 12 h (and before reaching high cell density), the fluidic system introduced three different doses of the antifungal agent voriconazole [16]. This antifungal acts by disrupting the fungal cellular membrane. Cell growth and viability after antifungal exposure were tracked with measurements every 15 min for 72 h. An identical satellite system housed in a thermal chamber was used as a delayed synchronous ground control unit to compare ground and flight results [16].

Comparison of zero-drug-dose results from spaceflight microgravity with results from the ground experiment showed that spaceflight yeast had a longer “lag time” than the corresponding ground specimens, whether measured by cell density (via turbidity) or metabolism (via alamarBlue depletion). Also, spaceflight samples exhibited a slower growth rate than those on the ground, again regardless of whether this was measured by metabolism or population doubling time during the exponential growth phase. At low and medium voriconazole concentrations, *once the difference in rates of the zero-dose controls was taken into account by normalization*, there was no significant difference between spaceflight and ground specimens in the rates of either cell growth or metabolic activity. *PharmaSat* was the first fully autonomous pharmaceutical dose-response system on a free-flying satellite.

### 2.3 SporeSat

*SporeSat* was developed to investigate the effect of gravity on the reproductive spores of the aquatic fern *Ceratopteris richardii*. Given its goal to improve understanding of biological gravity sensing, *SporeSat*'s objective was to measure calcium concentration that results from the opening and closing of calcium ion channels in these spores using lab-on-a-chip devices called biology compact discs (bioCDs), which allow for real-time measurement of calcium signaling using differential pairs of ion-sensitive electrodes, while the discs are rotated to create artificial gravity. To differentiate the role of the gravitational regime from other aspects of the spaceflight environment (e.g., radiation), *SporeSat* adapted the miniature centrifuge developed initially by the *GraviSat* project [20], integrating on-disk ion-selective microelectrodes, as well as LED illumination, to initiate and monitor the gravitational dependence of the germination of fern spores. Two such 50-mm bioCDs were to be rotated at defined rates to simulate variable gravity in a series of steps from 0.06 to 2g, while a third one remained stationary as a microgravity control [21]. This created new requirements, constraints, and drivers on the satellite design and implementation. The novel sensor discs flew in a 3U nanosatellite that utilized flight-proven technologies previously flown in *GeneSat-1*, *PharmaSat*, and *O/OREOS*.

Fern spores and media were loaded onto three bioCDs (32 spores each; each spore had its own 160- $\mu$ m-diameter well with integral ion-sensitive electrodes), then integrated into the CubeSat; see Fig. 3. *SporeSat-1* launched on April 18, 2014, on a SpaceX Falcon 9 rocket as a secondary payload on the International Space Station (ISS) resupply mission CRS-3. It was deployed en route to ISS at an altitude of 325 km and an inclination of 51.6 degrees; it reentered Earth's atmosphere after 47 days. The experiment was initiated by increasing temperature to 29°C and establishing artificial gravity (bioCD-1 and bioCD-2). While the experimental plan called for initiation of germination via red light spore activation for a duration of several hours, the large-area red organic light-emitting diode (OLED) failed to illuminate in the space experiment (with a similar failure for the ground control). Despite this, the rotating bioCDs were held at the desired temperature, the rotation occurred at the defined rates, and differential calcium ion signals were measured from each one of the 96 spores, albeit at nominal background levels expected in absence of biological

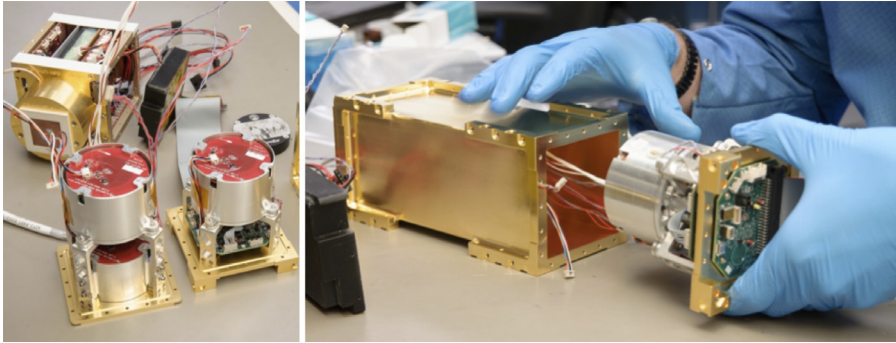


**Fig. 3** *SporeSat*'s two mini centrifuges with integral bioCDs (*left*, foreground) and bus (*background*); the left-hand centrifuge sits over an identical nonrotating bioCD (bioCD-3). *Right*: inserting one mini centrifuge into the payload hermetic container. Credit: NASA.

activity, with noise levels in the 10s of microvolts. Thus, *SporeSat-1* demonstrated several technologies relevant to measurement of spore gravitational sensing in a 3U CubeSat format, including the capability to generate artificial gravity while measuring ion channel response on a rotating bioCD [21].

*SporeSat-2* was developed to address software issues from *SporeSat-1* and to prepare a more robust means of illuminating fern spores to trigger their germination, namely, a set of 32 individual surface mount LEDs per bioCD, one directly opposite each spore-containing microwell. *SporeSat-2* was extensively ground tested [21] but is not currently scheduled to fly as a space mission.

## 2.4 EcAMSat

*EcAMSat*'s mission was to investigate the effects of microgravity on the dose-dependent antibiotic response and resistance in uropathogenic *E. coli* [22] and to do so by heavy reuse of *PharmaSat* designs and spare hardware. *EcAMSat* was the first 6U biological CubeSat and the first biological CubeSat to be deployed from ISS. Two strains of *E. coli*, a wild type and a mutant strain from which the stress-relevant *rpoS* gene had been deleted, were inoculated in 48 independent microwells in a fluidic card in stasis buffer. *E. coli* cells remained in stasis for approximately 8 weeks before cell growth was initiated. *EcAMSat* launched aboard the Orbital ATK OA-8 resupply mission to the ISS on November 12, 2017, and deployed from the Japanese Experiment Module (JEM) on November 20 (Fig. 4) (ISS' orbit is 51.6 degrees, 408-km perigee, and 410-km apogee). Once in space, growth medium was delivered into the wells, and the cells were allowed to grow to stationary phase; growth was monitored via optical density. After a starvation period, bacteria were exposed to three dose levels of the antibiotic gentamicin (12 wells per dosage and 6 for each strain) along with 12 wells of zero-dose controls. This antibiotic belongs to the aminoglycoside class of antibiotics, which inhibits bacterial ability to synthesize



**Fig. 4** Photograph of the 6U, 11-kg *EcAMSat* nanosatellite (*lower left-center*) above Earth seconds after deployment from the ISS (deployer is at *mid-upper center* of photo). It was the first 6U biology satellite and the first biological science satellite of any size to be deployed from ISS. Credit: NASA.

proteins by binding to the 30S subunit of the bacterial ribosome. The antibiotic was then replaced by a solution of the metabolic indicator alamarBlue, and bacterial metabolism was measured by the rate of reduction of the dye. Optical measurements were performed using the same three-color LED detection system (470, 525, and 615nm) used for *PharmaSat*, with measurements at 15-min intervals throughout the experiment. Heaters with embedded temperature sensors were attached to the fluidic card to allow for temperature control and ensure cell survival. Control experiments were performed in parallel several days later on the ground. The results of the development and ground testing of the *EcAMSat* payload are reported elsewhere [22], and the science results of the *EcAMSat* spaceflight experiment have been published [23].

### 3 CubeSats for astrobiology research

Thus far, only one CubeSat mission has had an astrobiology research focus: *O/OREOS*. This CubeSat carried two payloads, Space Environment Survivability of Life Organisms (SESLO) and Space Environment Viability of Organics (SEVO), each with its own astrobiology mission objectives [12]. SEVO characterized four organic compounds, an amino acid, a quinone, a polycyclic aromatic hydrocarbon (PAH), and a metalloporphyrin, as they were exposed to the space environment [9–11], particularly full-spectrum solar illumination extending deep into the ultraviolet (124nm). The objective of SESLO was to measure long-term survival, germination, and metabolic activity of *Bacillus subtilis* spores exposed to microgravity and ionizing radiation for up to 6 months [14]. The *O/OREOS* spacecraft bus and mechanical configuration, as well as many aspects of the SESLO payload, were derived from the *GeneSat-1* and *PharmaSat* 3U nanosatellites. Besides exploring the microgravitational regime, *O/OREOS* included radiation as another independent variable because of its highly

inclined orbit and altitude (72 degrees, 621-km perigee, and 646-km apogee), which made it travel through relatively weak regions of the magnetosphere twice per 98-min orbit: the estimated radiation dose rate was about 15 times that typical of an ISS-like orbit [12]. The SESLO payload, Fig. 5, was 1U in size and had three “bioblocks.” Each block has 12 75- $\mu$ L wells interconnected through microfluidic channels and a solenoid valve to a reservoir with germination medium colored with alamarBlue. Each block was used to independently assess growth at three different times: 14, 97, and 180 days after launch. Three different wavelengths were used to acquire data: 470, 525, and 615 nm. As alamarBlue reacted with metabolites in the cells in microwells, it changed from blue to pink and then from pink to colorless [14].

The *O/OREOS* nanosatellite was launched as a secondary payload on November 19, 2010, aboard a Minotaur IV rocket from Kodiak Launch Complex, Alaska. In SESLO, bacterium spores of two different strains of *B. subtilis* were first loaded and dried onto the walls of the bioblock microwells and maintained in desiccated state prior to growth. Fourteen days after launch the first SESLO bioblock was activated. After growth, target temperature stabilized at 37°C; then growth medium was delivered into the microwells, allowing rehydration of the spores. This was the first CubeSat experiment to fly its biological specimens in the dried state and rehydrate them in space. Germination, growth, and metabolism were monitored for 48 h. Optical readings were performed at 15-min intervals throughout the experiment. Delayed-synchronous ground control experiments were performed with identical hardware with biological samples loaded from the same flight cultures.

Very similar results were recorded at the 14- and 97-day timepoints from SESLO in space and its ground control. The main difference anticipated between the space microgravity and 1-g control environments was the previously explained altered mass transport phenomenon [18]. Thus it was not surprising that the blue-to-pink color transitions of alamarBlue for the ground controls occurred on average about 40 min sooner than they did for the spaceflight microwells. The other notable difference was between the 168 wild-type *B. subtilis* and the mutant strain, WN1087: the latter strain clearly metabolized alamarBlue more rapidly than the former, both on the ground and in space [14].

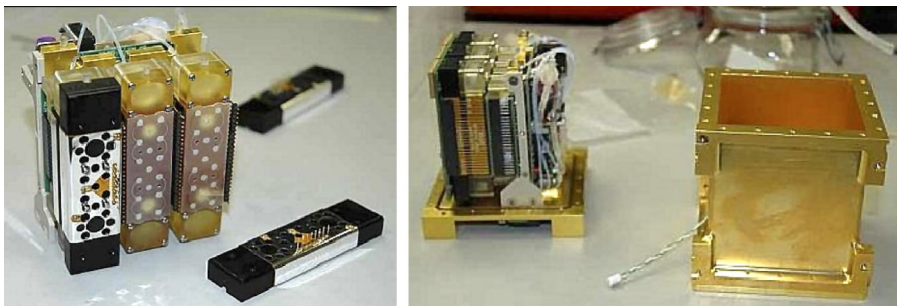


**Fig. 5** SESLO’s 3-bioblock payload shown partially assembled at *left* and next to its 1U hermetic container at *right*.

Credit: NASA.

## 4 Upcoming missions

*BioSentinel* is an upcoming nanosatellite mission and the first biological CubeSat that will fly into interplanetary space. *BioSentinel* is a 6U CubeSat that will fly as a secondary payload on the Space Launch System (SLS) Artemis 1 mission (formerly known as Exploration Mission-1 [EM-1]), currently scheduled to launch no earlier than 2021 [15,24–27]. A microgravity control experiment is also scheduled to fly to the ISS. The primary objective of *BioSentinel* is to investigate the DNA damage response to deep-space radiation in a eukaryotic organism, the budding yeast *S. cerevisiae*. Budding yeast was selected not only because of its known biology and flight heritage but also because of its ability to remain in desiccated state for long periods of time. Since *BioSentinel* is a secondary payload on Artemis 1, the payload has to be delivered up to 9 months prior to launch without power and/or thermal control, and the cells must also remain viable for its 6–12-month spaceflight mission, making it a requirement to keep them viable for a total of 15–21 months.

In the 6U *BioSentinel*, the biological samples and microfluidic delivery system are contained within a 4U hermetically sealed container. The 4U biosensor unit also has mounted on one of its outer surfaces a linear energy transfer (LET) spectrometer for radiation measurements and characterization. The remaining volume of the spacecraft contains all the bus components necessary for autonomous operations in deep space, including deployable, gimbaled triple-junction solar panels to generate up to 70W; a guidance, navigation, and control unit, including three orthogonal momentum wheels, star tracker, multiple sun sensors, and an inertial measurement unit; a cold-gas micro-propulsion system for detumbling upon deployment and desaturating momentum wheels; Li-ion batteries and an electric power management system; and an X-band radio/transponder (Iris, flown by the twin *MarCO* CubeSats) connected to multiple patch antennas to communicate with NASA's Deep Space Network (DSN).

Prior to payload integration, two different yeast strains will be loaded in fluidic card microwells using a trehalose stasis buffer and then allowed to air-dry to improve desiccation tolerance [26]. Growth medium and the metabolic indicator dye alamarBlue will be mixed during flight and delivered through a complex system of pumps and valves. To maintain a dry environment and thus cell viability prior to rehydration, the payload also carries silica gel-filled desiccation chambers integrated within the fluidic cards and manifold. In contrast to previous missions, the fluidic cards, Fig. 6, are made primarily of polycarbonate, so that they can be sterilized by autoclaving to prevent potential off-gassing of toxic volatiles from chemical sterilization. Each *BioSentinel* ground or flight unit will carry 18 microfluidic cards with 16 microwells each, for a total of 288 wells per unit (Fig. 6). In addition to a dedicated thermal control system for each card, each microwell is monitored using a three-color LED detection system (570, 630, and 850nm) to take optical measurements during cell growth. After CubeSat deployment and initial system checkout, two fluidic cards will be activated by temperature increase, followed by growth medium delivery. Optical measurements will be performed using a similar system to those developed for *PharmaSat* and also used by *EcAMSat* and *O/OREOS-SESLO* (see in the preceding text).



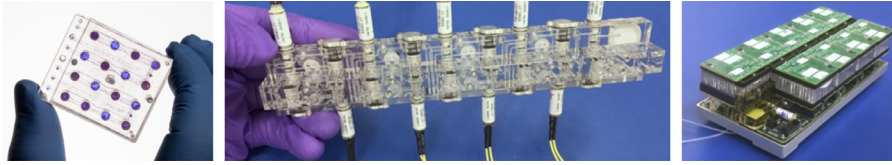


**Fig. 6** *BioSentinel*'s key fluidic components. *Left*: one of eighteen 16-microwell fluidic cards. *Center*: a 9-card manifold prior to integration with fluidic cards. *Right*: a 9-card manifold integrating fluidic cards, manifold, mechanical structure, thermal control, and optical measurement subsystems. Two such fully integrated manifolds along with a growth medium and indicator dye fluidic delivery system, as well as supporting electronics, comprise the *BioSentinel* biology payload.

Credit: NASA.

The alamarBlue dye and synthetic complete (SC) growth medium will be mixed at a 1:9 ratio during flight; both the concentrated  $10\times$  alamarBlue dye and the mixed dye-and-medium solution will be monitored using independent optical calibration cells. Cell growth and metabolic activity will be monitored using the optical detection system, and the data will be telemetered back to Earth using NASA's DSN. The biological data will be correlated to the onboard LET spectrometer data, which will provide a "space weather report" every few hours. A delayed-synchronous ground control unit carrying yeast cells from the same flight cultures will run in parallel to the Artemis 1 mission, as will another set aboard ISS.

Other future missions may be based on the preliminary work already performed on payloads such as the 2U *SporeSat-2*, designed to measure differences on *C. richardii* fern spore  $\text{Ca}^{2+}$  ion channel response and that includes 50-mm microcentrifuges with 32 ion-specific  $[\text{Ca}^{2+}]$  electrode pairs. Other ground-based work includes the GraviSat project, a 2U payload with a microcentrifuge to culture algae with pulse amplitude-modulated fluorescence and carbonate ion measurements (qualified to TRL 5) [20], and MisST, a 2U payload integrating a multistrain *Caenorhabditis elegans* fluidic habitat with a two-color fluorescence microscope (qualified to TRL 6). Now that CubeSats such as the Mars Cube One (*MarCO*) twins used during *InSight* mission to Mars have demonstrated the capability to support deep-space missions, future microbial and astrobiology CubeSats may venture farther into our solar system.

## 5 Discussion

To date, five microbiology or astrobiology missions have taken place in CubeSats, all developed by NASA. The success of these missions has verified the capability of this spacecraft platform to perform biological and astrobiological research. Furthermore, these free-flying satellites can provide less gravitational noise than inhabited spacecraft and stations, products of the operation of support machinery and human presence. NASA's evolutionary approach of basing a CubeSat's bus and payload on the previous mission has helped meet scientific success criteria while reducing risk and cost. Additionally, four of these missions achieved mission success thanks to

technological developments that have enabled, for example, temperature control of  $\pm 0.3^{\circ}\text{C}$ , autonomous experiment activation and termination, incorporation of centrifuges, and data acquisition and transmission to Earth. One of the key approaches contributing to the success of these missions has been the use of microfluidic cards and lab-on-a-chip devices, which in turn are becoming ever more sophisticated and powerful in terms of scientific output. The small size and mass of the CubeSat platform make it ideal for research beyond low Earth orbit, for example, to cislunar space for radiation investigations or data acquisition from geysers of Jupiter's and Saturn's moons via flybys.

## Acknowledgments

This material is based upon work supported by the National Aeronautics and Space Administration through the Office of Biological and Physical Research (OBPR), the Exploration Systems Mission Directorate (ESMD), the Space Life and Physical Sciences Research and Applications (SLPSRA) division within the Human Exploration and Operations Mission Directorate (HEOMD), the Science Mission Directorate's (SMD's) Astrobiology Small Payloads Program, and HEOMD's Advanced Exploration Systems Division. We gratefully acknowledge the contributions of the teams at NASA ARC and our many colleagues, collaborators, and students at other NASA centers, several commercial concerns, and multiple universities who made possible the spaceflight CubeSat missions described by this publication. LZ was supported by the National Aeronautics and Space Administration under Grant No. 80NSSC18K1468 and BioServe Space Technologies.

## References

- [1] E.J. Bulban, Anti-radiation shielding may be reduced, *Aviat. Res.* 74 (1961) 40–41.
- [2] K.J. Dickson, Summary of biological spaceflight experiments with cells, *Gravit. Space Res.* 4 (2) (2007) Retrieved from <http://gravitationalandspacebiology.org/index.php/journal/article/view/94>.
- [3] Zhukov-Verezhnikov, Maiskii, Yazdovskii, Pekhov, Gyurdzhan, Nefed'eva, Buiko, Results of first microbiological and cytological experiments on earth satellites in space, *Artif. Earth Satell.* 11 (1962) 47–71.
- [4] M. Martinez, D. Gonzalez, D. Rodriguez, J. Birnie, J.A. Bagur, R. Paz, et al., Guatemala's remote sensing CubeSat - tools and approaches to increase the probability of Mission Success, in: Proc. 32nd Annual AIAA/USU Conference on Small Satellites, The American Institute of Aeronautics and Astronautics, Reston, VA, 2018. SSC18-WKIX-06.
- [5] L. Zea, V. Ayerdi, S. Argueta, A. Muñoz, A methodology for CubeSat mission selection, *JoSS* 5 (3) (2016) 483–511.
- [6] A.J. Ricco, J.W. Hines, M. Piccini, M. Parra, L. Timucin, V. Barker, et al., Autonomous genetic analysis system to study space effects on microorganisms: results from orbit, in: Proc. 14th Int'l. Conf. on Solid-State Sensors, Actuators, & Microsystems (Transducers '07/Euroensors XXI), IEEE, New York, 2007, pp. 33–37, <https://doi.org/10.1109/SENSOR.2007.4300065>.
- [7] C. Kitts, K. Ronzano, R. Rasay, I. Mas, P. Williams, P. Mahacek, et al., Flight results from the *GeneSat-1* biological microsatellite mission, in: Proc. 21st Annual AIAA/USU Conference on Small Satellites, The American Institute of Aeronautics and Astronautics, Reston, VA, 2007. SSC07-XI-01.

- [8] C. Kitts, K. Ronzano, R. Rasay, I. Mas, J. Acain, M. Neumann, et al., Initial flight results from the *PharmaSat* biological microsatellite Mission, in: Proceedings of 23rd Annual AIAA/USU Conf on Small Satellites, The American Institute of Aeronautics and Astronautics, Reston, VA, 2009 SSC09-IV-10.
- [9] N.E. Bramall, R. Quinn, A. Mattioda, K. Bryson, J.D. Chittenden, A. Cook, et al., The development of the space environment viability of organics (SEVO) experiment aboard the organism/organic exposure to orbital stresses (*O/OREOS*) satellite, *Planet. Space Sci.* 60 (1) (2012) 121–130, <https://doi.org/10.1016/j.pss.2011.06.014>.
- [10] A.M. Cook, A.L. Mattioda, A.J. Ricco, R.C. Quinn, A. Elsaesser, P. Ehrenfreund, et al., The organism/organic exposure to orbital stresses (*O/OREOS*) satellite: radiation exposure in low-earth orbit and supporting laboratory studies of iron tetraphenylporphyrin chloride, *Astrobiology* 14 (2) (2014) 87–101, <https://doi.org/10.1089/ast.2013.0998>.
- [11] A. Mattioda, A. Cook, P. Ehrenfreund, R. Quinn, A.J. Ricco, D. Squires, et al., The *O/OREOS* mission: first science data from the space environment viability of organics (SEVO) payload, *Astrobiology* 12 (9) (2012) 841–853, <https://doi.org/10.1089/ast.2012.0861>.
- [12] P. Ehrenfreund, A.J. Ricco, D. Squires, C. Kitts, E. Agasid, N. Bramall, et al., The *O/OREOS* mission—astrobiology in low earth orbit, *Acta Astronaut.* 93 (2014) 501–508, <https://doi.org/10.1016/j.actaastro.2012.09.009>.
- [13] G. Minelli, C. Kitts, K. Ronzano, C. Beasley, R. Rasay, I. Mas, et al., Extended life flight results from the *GeneSat-I* biological microsatellite mission, in: Proc. 22nd Annual AIAA/USU Conf on Small Satellites, The American Institute of Aeronautics and Astronautics, Reston, VA, 2008 SSC08-II-4.
- [14] W.L. Nicholson, A.J. Ricco, E. Agasid, C. Beasley, M. Diaz-Aguado, P. Ehrenfreund, et al., The *O/OREOS* mission: first science data from the space environment survivability of living organisms (SESLO) payload, *Astrobiology* 11 (10) (2011) 951–958, <https://doi.org/10.1089/ast.2011.0714>.
- [15] A.J. Ricco, R. Hanel, S. Bhattacharya, T. Boone, M. Tan, A. Mousavi, et al., The *Biosentinel* bioanalytical microsystem: characterizing DNA radiation damage in living organisms beyond earth orbit, in: 2016 Solid-state Sensors, Actuators, and Microsystems Workshop Technical Digest, Transducer Research Foundation, San Diego, 2016, pp. 352–355, <https://doi.org/10.31438/trf.hh2016.95>.
- [16] A.J. Ricco, M. Parra, D. Niesel, M. Piccini, D. Ly, M. McGinnis, et al., *PharmaSat*: drug dose response in microgravity from a free-flying integrated biofluidic/optical culture-and-analysis satellite, in: Proc. SPIE 7929, Microfluidics, BioMEMS, and Medical Microsystems IX, SPIE, Bellingham, WA, 2011. <https://doi.org/10.1117/12.881082>. 79290T, 9 pp.
- [17] M. Parra, A.J. Ricco, B. Yost, M.R. McGinnis, J.W. Hines, Studying space effects on microorganisms autonomously: *GeneSat*, *PharmaSat* and the future of bio-nanosatellites, *Gravit. Space Biol.* 21 (2) (2008) 9–17.
- [18] L. Zea, N. Prasad, S.E. Levy, L. Stodieck, A. Jones, S. Shrestha, D. Klaus, A molecular genetic basis explaining altered bacterial behavior in space. *PLoS One* 11 (11) (2016), e0164359 <https://doi.org/10.1371/journal.pone.0164359>.
- [19] M.F. Diaz-Aguado, S. Ghassemieh, C. Van Outryve, C. Beasley, A. Schooley, Small Class-D spacecraft thermal design, test and analysis – *PharmaSat* biological experiment, in: 2009 IEEE Aerospace Conference, 2009. Retrieved from <https://ieeexplore.ieee.org/abstract/document/4839352>. Accessed 28 May 2019.
- [20] E.D. Fleming, B.M. Bebout, M.X. Tan, F. Selch, A.J. Ricco, Biological system development for *GraviSat*: a new platform for studying photosynthesis and microalgae in space. *Life Sci. Space Res.* 3 (2014) 63–75, <https://doi.org/10.1016/j.lssr.2014.09.004>.

- [21] J. Park, M.L. Salmi, W.W.A. Wan Salim, A. Rademacher, B. Wickizer, A. Schooley, et al., An autonomous lab on a chip for space flight calibration of gravity-induced transcellular calcium polarization in single-cell fern spores. *Lab Chip* 17 (6) (2017) 1095–1103, <https://doi.org/10.1039/C6LC01370H>.
- [22] A.C. Matin, J.-H. Wang, M. Keyhan, R. Singh, M. Benoit, M.P. Parra, et al., Payload hardware and experimental protocol development to enable future testing of the effect of space microgravity on the resistance to gentamicin of uropathogenic *Escherichia coli* and its  $\sigma^S$ -deficient mutant. *Life Sci. Space Res.* 15 (2017) 1–10, <https://doi.org/10.1016/j.lssr.2017.05.001>.
- [23] M.R. Padgen, M.P. Lera, M.P. Parra, A.J. Ricco, M. Chin, T.N. Chinn, et al., *EcAMSat* spaceflight measurements of the role of  $\sigma^S$  in antibiotic resistance of stationary phase *Escherichia coli* in microgravity, *Life Sci. Space Res.* 24 (2020) 18–24, <https://doi.org/10.1016/j.lssr.2019.10.007>.
- [24] B. Lewis, R. Hanel, S. Bhattacharya, A.J. Ricco, E. Agasid, D. Reiss-Bubbenheim, et al., *BioSentinel*: monitoring DNA damage repair beyond low earth orbit on a 6U Nanosatellite, in: *Proc. 28th Annual AIAA/USU Conference on Small Satellites*, The American Institute of Aeronautics and Astronautics, Reston, VA, 2014. SSC14-VI-3.
- [25] S. Massaro Tieze, L.C. Liddell, S.R. Santa Maria, S. Bhattacharya, *BioSentinel*: a biological CubeSat for deep space exploration. *Astrobiology* 20 (2020) <https://doi.org/10.1089/ast.2019.2068> [ahead of print].
- [26] S.R. Santa Maria, D.B. Marina, S. Massaro Tieze, L.C. Liddell, S. Bhattacharya, *BioSentinel*: long-term *Saccharomyces cerevisiae* preservation for a deep space biosensor mission. *Astrobiology* 20 (2020) <https://doi.org/10.1089/ast.2019.2073> [ahead of print].
- [27] A.J. Ricco, S.R. Santa Maria, R.P. Hanel, S. Bhattacharya, The Radworks group and the *BioSentinel* team, *BioSentinel*: a 6U nanosatellite for deep-space biological science, *IEEE Aerospace Electron. Syst. Mag.* 35 (3) (2020) 6–18, <https://doi.org/10.1109/MAES.2019.2953760>.

# Structure, new materials, and new manufacturing technologies

8

Chantal Cappelletti

Department of Mechanical, Materials and Manufacturing Engineering, University of Nottingham, University Park, Nottingham, United Kingdom

## 1 Introduction

The main objective of the structural system is to mechanically support and protect all spacecraft subsystems during the different mission phases and, in the case of CubeSats, to provide a mechanical interface to the deployer system. From the manufacturing phase to the end of the mission, the satellite faces different environments and different loads. The structure should guarantee the correct interface with the launch vehicle that, in the case of CubeSats, is partially determined by the deployer selected (see [Chapter 22](#)). The CubeSat standard specification document [1,2] gives a clear description of the constraints that the satellite should address, in order to be considered a CubeSat. Nevertheless, some of the constraints that dictate the structural design are derived from the mission and systems requirements. For this reason, it is important to give the CubeSat developer some useful tips and suggestions that can help them select the best structure for their mission.

To result in a successful structural product, the process can be divided into five steps: (1) requirements definition, (2) design or selection process, (3) analysis, (4) assembly, and (5) verification and testing. In the case of the CubeSat, some phases are standardized, resulting in a simplification of the work that is required of the satellite developer, but others are not. In addition, some additional aspects and restrictions with respect to traditional satellites need to be considered, such as the very small dimensions required, often dictate the use of deployable components.

Traditionally, the design of space systems makes a distinction between the *primary structure*, defined as the one that carries the major loads, and the *secondary structure*, defined as the one that supports components under 5 kg. When considering CubeSats, in particular 1U structures, this distinction does not make sense in terms of the weight to be considered but can still be meaningful in terms of the function of the structure. CubeSat primary structures are the ones designed to transmit loads through the spacecraft to the interface of the launch and deployment system and the ones that serve as the mechanical interface with the other bus systems, the payloads, and their associated components. The function of the secondary structures, on the other hand, is only to support themselves. Their failure does not necessarily result in a catastrophic event as in the case of a primary structure failure. A typical example of primary structure is the satellite chassis, while an example of a secondary structure is the antenna system.

In the process of designing and selecting the best structure that matches the mission and subsystem needs, structural engineers are strongly supported by the commercial availability of different solutions. An interesting report from NASA gives an overview of all the different primary structures and mechanisms available on the commercial market [3]. In some cases one of them may be the perfect match for the particular mission that will be performed, while in other cases a customized solution is needed.

This chapter gives insight into how the developers should orientate themselves to optimize the design, giving suggestions and indications coming from practical experiences. The chapter follows a step-by-step approach to help the CubeSat developer: from requirements definition to the design and analysis, manufacturing, and eventually testing for verification and validation.

## 2 Requirements and main characteristics

During the system design process, the first step that should be completed is the requirements definition. This step defines what the structure should perform and what its main goals are. A clear, accurate, and detailed requirements definition allows the designers to start an optimized process where time and costs are reduced to the minimum. If the developers know exactly what requirements the structure should satisfy, from the beginning of the project, they will be able to focus their attention clearly on the development of the best solutions for that specific mission.

Some conditions and constraints can change during the project development. As an example, the loads experienced at launch significantly affect the structural design. If, for some reasons (political, availability, price changes, etc.), the launch vehicle changes, the requirements can change dramatically, potentially causing the need of replacing the structure selected, affecting the overall costs and schedule.

A clear definition of the requirements is not always possible during the initial mission analysis phases, but adopting a conservative and iterative approach can help minimizing the effect of last minute changes. A conservative approach is adopted when considering the launch loads, for example.

Generally speaking, the structure should be:

- **rigid**, or able to support the dynamics loads during all the mission phases;
- **robust**, or able to support the quasi-static loads during the mission;
- **light**, to reduce the launch costs;
- **accessible**, in terms of easiness of access to the main subsystems if and when needed;
- **easy** to manufacture and to assemble.

When defining the structure requirements, developers need to concentrate their attention in two different areas:

- **internal requirements**: the ones that are dictated by the mission and the interface with the other subsystems;
- **external requirements**: the ones related to the launch vehicle, the mission phases, and the space environment.

Each of these is considered in the following text.

## **2.1 Internal requirements**

The structural internal requirements can be divided in two main categories:

- requirements dictated by the mission;
- requirements dictated by the bus.

These vary in function, being unique to the mission, but there are some general considerations that can be analyzed.

### **2.1.1 Requirements dictated by the mission**

The main goal of the structural system is to be able to accommodate and support the payload during all the mission phases. Requirements on the structure are not limited to dimensions compatibility with the payload, but will be dictated by the payload functions too. In an imaging satellite, for example, it is critical that the payload is accommodated in such a way that its aperture will have access to the exterior of the satellite. In other cases, this requirement might not be well defined. An example is the case of biomedical payloads, that usually require three levels of containment. Whether this is needed also in a small satellite mission depends on several other factors that should be analyzed during the preliminary mission design.

To support the payload during all the mission phases, the structure should support loads and operational conditions that depend on the mission nature and configuration. The resulting requirements are strictly related, sometimes overlapping, with some concerns regarding the bus and some related to the external requirements. This is due to the fact that to support the payload, developers need to guarantee that not only the payload but also the entire satellite bus will be able to work properly in an extreme environment and under specific stressful conditions such as those faced during the launch.

### **2.1.2 Requirements dictated by the bus**

The structural system design is subject to constraints and requirements dictated by several of the primary satellite bus system requirements. Bus elements that need to be considered in the structural design include the Electric Power System (EPS), the Telecommunications, Tracking and Command (TT&C) System, the Attitude Determination and Control System (ADCS), the Orbital Determination and Control System (ODCS), the electronics in general, and the thermal management system.

#### **Electric power system**

The power requirements indirectly drive the structural design in several ways. The power produced onboard by the solar panels, for example, is strictly related to the size of the solar panels, to the packing factor, and to the choice of body mounted or deployable solar panels. These three factors drive the selection of one structure instead of another.

Battery selection, on the other hand, influences the satellite total mass, and the design should take into account the way the different EPS subsystems are connected

and how power is distributed to the other systems with the proper voltages and currents and with the proper regulation. For CubeSats, this can be simplified owing to the use of standardized solutions and connectors. For example, the concept of having the boards stacked one on top of the other (such in the case of the use of PC104 standard) or inserted into one common board that act as an integrated backplane/connector (as in the case of the AESP-14 satellite [4]) reduces the use of wires inside the satellite and limiting the difficulties related to the cabling.

### Telecommunication, tracking and command

The TT&C system influences the structural design, due to the antenna requirements. The antenna dimensions are strictly correlated with the wavelength and, therefore, the frequency used for the transmission. Due to the satellite's small dimensions, when working with CubeSats operating at UHF or VHF frequencies, deployable antennas need to be considered. In the CubeSat mission design specifications [1], it is required that "all deployables such as booms, antennas, and solar panels shall wait to deploy a minimum of 30 minutes after the CubeSat's deployment switch(es) are activated from -POD ejection." From a structural point of view, this means that a deployable mechanism, for example an antenna, should be implemented as part of the secondary satellite structure. When using higher frequencies, patch antennas can be the best solution; the areas and the positions allocated for the antenna locations need to be considered.

Another aspect that should be taken in to account is the antenna radiation pattern that can be influenced by the satellite structure. The use of specific connectors also drives the structural configuration and should be taken into account during the design. For lower-frequency antennas, having the proper orientation and sufficient area for the ground plane should also be considered.

### Attitude determination and control system

During the structural design, designers need to take into account the mass distribution of the satellite and how it will influence the inertia matrix, since it strictly constraints the ADCS system. In some cases, the selected ADCS solution imposes a specific structural configuration. For example, the UniCubeSat-GG satellite, designed to study the librations due to the gravity-gradient stabilization, was characterized by the use of two booms, and two tip masses were used to stabilize the satellite (Fig. 1). The need to have a minimum inertia axis, achieved through the implementation of the two booms, completely constrained the satellite design and the system positioning inside the 1U CubeSat. The use of deployment mechanisms affecting the ADCS system should be considered during the design phase, since these systems can cause a torque during on-orbit operations.

ADCS and structures are also connected by the sensors' and actuators' volume allocations. A star sensor, for example, needs to be installed on a side facing the sky. However, this is not only a constraint for the ADCS sensor and actuators, but it also influences the position of the other systems' components. Another example is the design of a LEO satellite equipped with a GNSS receiver and a S-band transmitter,



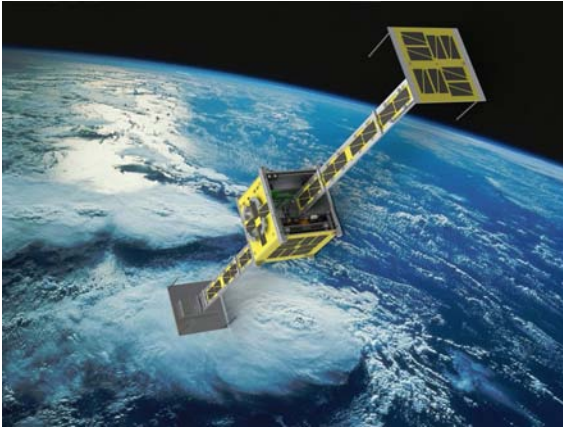


**Fig. 1** UniCubeSat-GG Structure with deployable booms.

for which it should be ensured that the GNSS antenna will face higher orbits, where the navigation satellites are located, and the S-band should point toward the Earth, where the ground stations are located. The position of both components can be determined only if the satellite's attitude position during the different orbit phases is clearly defined.

### Orbital determination and control system

As for the ADCS system, the ODCS is influenced by the mass distribution, in particular by the position of the Center of Gravity (CG). For example, if a thruster for orbital maneuvering is implemented in the system, it should be aligned with the position of the CG to avoid the generation of additional torques. Similar to the ADCS, sensors' and actuators' position is crucial for this system and should be carefully taken into account during the structure design.

### Electronics

When considering the structural design, one needs to remember that the system is working in the space environment and will be adversely affected by space radiation. One of the functions of the structure is to ensure the survival of satellite components during all the mission phases. This requires the structural engineer to also consider advanced solutions to protect the satellite's internal components, in particular the electronics from space radiation.

Another important point that constrains the structural design are the electronics interfaces used to assemble the different electronics boards. One of the most common standards for CubeSat electronics is the PC104 form factor. It allows developers to stack the boards one on top of the other, facilitating the connection between the different boards. The use of this standard constrains the satellite internal design, but at the same time, the use of standoffs between the boards helps to increase the structural performance of the satellite itself.

## Thermal system

The strict connection between the structural and the thermal systems often forces the developer to consider the thermal system as a subsystem of the structural system. In space, due to the environment and in particular due to the vacuum conditions, heat transfer mainly occurs through radiation and conduction, with convection only occurring in the artificial atmosphere of the manned systems. This means that the thermal system is limited by the position of the different systems and by the materials used to manufacture them. In this way, through material selection and component positioning, it is possible to constraint and modify the temperature exchange between internal components of the satellite and between the satellite and its environment.

## 2.2 External requirements

The external requirements can be divided into three main categories:

- requirements dictated by the launch vehicle;
- requirements dictated by the space environment;
- requirements dictated by the deployer.

### 2.2.1 Requirements dictated by the launch vehicle

The requirements related to the launch vehicle selection can be considered the most important for the structural design. Designing a structural system that is able to survive to the launch loads is one of the primary objectives for the structural engineer. The launch vehicle selection affects structural design mainly by requiring that the structure is rigid enough to sustain the loads during the launch. These conditions change as a function of the launch vehicle selected. It is possible to divide the loads that the structure is subject to during launch into two main categories: quasi-static and dynamical loads, as will be discussed in [Section 4.2.1](#). The approach that should be adopted is based on the following:

- the identification of the loads, as a function of the launch vehicle;
- the analysis of the load effects on the structure, using simulations;
- test and verification of the capabilities of the real structure to sustain the predicted loads.

CubeSat structures have an extreme advantage over traditional satellites: they are not constrained by the mechanical interfaces with the launch vehicle as is the case of conventional satellite systems. Their mechanical interfaces are with the deployer and do not change as a function of the launch vehicle. CubeSats are flexible and can be manifested on different launch platforms and the developers do not need to wait for a particular launch if the mission does not need a specific orbit. On the other hand, this peculiarity of CubeSats means that sometimes the structural designer is not aware of the launch vehicle selected and consequently cannot exactly identify the loads. To help during the process, some space agencies, as for example JAXA [5], provide specific suggestions to the loads that should be considered if the mission plans to launch from the International Space Station, considering different launch vehicles that could be used (HTV, ATV, Space X Dragon, and Orbital's Cygnus).

In addition to the traditional loads related to the launch vehicle, the loads generated during transportation to the launch site shall be considered as well. These loads are of a different nature and cannot be underestimated given that they can cause several damages to the satellite flight unit, particularly with reference to shock. To prevent damage during transportation, it is important to use protective shockproof, dustproof, and waterproof enclosures and to monitor the shock and humidity environment in these enclosures during transportation.

### 2.2.2 Requirements dictated by the space environment

In the process of designing a structural system, the developers need to consider where the system will operate and what its interfaces with the external environment are. In the case of low Earth Orbit (LEO) satellites, designers face an extreme environment with characteristics that deeply influence the design selections. **Vacuum conditions**, for example, impose a choice of materials that will have a reduced outgassing to reduce the total mass loss (TML) and/or the collected volatile condensable material (CVCM) under certain levels dictated by the launch vehicle or standards (see, e.g., [6]). In the case of launch from the International Space Station, for example, Rating “A” materials that are identified in [7] shall be used for a satellite. In other words, they should comply with the following low outgassing criterion per ASTM-E595-84:

- total mass loss (TML)  $\leq 1.0\%$
- collected volatile condensable material (CVCM)  $\leq 0.1\%$

Material selection is also constrained by UV degradation and degradation due to exposure to atomic oxygen, both typical of the space environment. **Atomic oxygen** oxidizes many metals, especially silver, copper, and osmium, and it reacts strongly with any material containing carbon, nitrogen, sulfur, and hydrogen bonds, meaning that many polymers react and erode. Even materials with atomic oxygen-protective coatings can degrade. **UV degradation** causes damage to polymers through either cross-linking (hardening) or chain scission (weakening). UV under high vacuum can also create oxygen vacancies in oxides, leading to significant color changes. Contrary to the atomic oxygen that may bleach materials, UV generally darkens them, particularly in the presence of contamination. Another space environment condition that should be taken into account is the presence of **plasma** that imposes grounding requirements on the spacecraft to avoid static charge buildup, sputtering, arcing, and parasitic currents. The effects of space radiation and the interface with the extreme thermal environment have previously been discussed.

### 2.2.3 Requirements dictated by the deployer

CubeSats do not have a direct interface to the launch vehicle but need to be installed into a deployer. An analysis of the different deployers is provided in [Chapter 22](#) of this book. In general, to comply with the constraints of the majority of commercially available CubeSat deployers, developers need to begin with the requirements defined in the CubeSat design specifications [1]. In addition to ensuring that the external satellite

envelope complies with the dimensions defined by [1], it is important to consider the position of the following:

- the access ports;
- the switches;
- the spring plungers (when needed);
- the CG.

Other CubeSats characteristics, including the use of deployment mechanisms and structures such as the antennas, and anodized rails should be designed in accordance with the standard [1]. Most of the commercially available deployers conform to the standards defined in the CubeSat design specifications document, but it is suggested that each deployer's interface control document (ICD) be referred to as a variety of deployer-related dimensions, volumes, masses, and mechanical and electrical interfaces exist nowadays.

### 3 Design and verification process

The design process is defined as the process used to generate the set of information describing the essential characteristics of a product [8]. Design means developing requirements, identifying options, doing analyses and trade studies, and defining a product in enough detail so that it can be built to specification [9].

On the other hand, the verification process is defined as confirmation by examination and provision of objective evidence that specified requirements have been fulfilled [10]. Verification means providing confidence through disciplined steps that a product will do what it is supposed to do [9].

The design and verification processes are usually described using a V-diagram as the one illustrated in Fig. 2, which represents the mission design and verification process for a specific 3U Mission (SERPENS). This is a common approach for all system design and verification processes. The following paragraphs describe in detail how designers can apply this approach to the structural design. Developers need also to remember that the verification process can be divided in two parts: the analyses that are conducted during the structural design and the tests that are conducted after the manufacturing phases. In this paragraph, only the analyses that should be conducted since they are integrated into the design process are presented.

#### 3.1 Structural design

The first step in the design phase is to have a clear idea of all the structural requirements, described in Section 1. From the analysis, it is possible to identify the structure constraints for the specific mission. How these constraints correlate with the CubeSat design specifications provides specific indications for the structure design and selection. Unlike other satellites, where a form factor is not specified, CubeSat developers have the opportunity to avoid the main frame structural design by selecting a commercially available structure. In fact, since the beginning of the CubeSat era, a number of

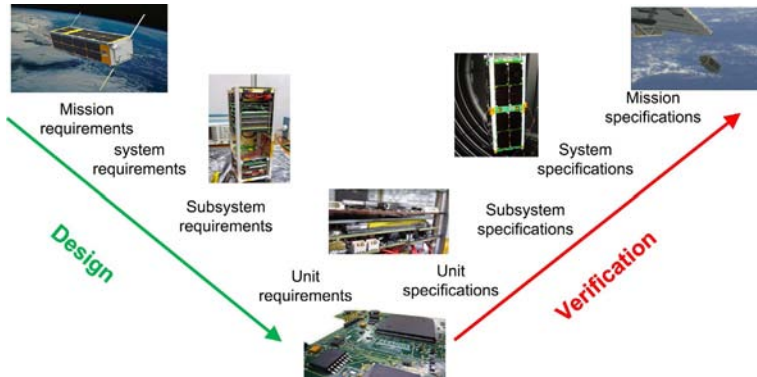


**Fig. 2** SERPENS mission V-diagram design and verification.

commercially available structures have been designed. The NASA report *State-of-the-art in Small Spacecraft Technology* [3] provides an interesting overview of the most commonly used structures that are available to date.

Effectively, CubeSat developers have three options for designing the structure:

1. selecting an existing commercially available structure, already qualified and tested;
2. developing their own structure;
3. customizing an existing structure.

The choice depends of course on the requirements and the constraints, and each one of these opportunities has advantages and disadvantages. If developers select the second opportunity, they should start a design process that depends on the experience and capabilities of the engineering team itself. The process can be resumed in the following steps:

1. requirements definition;
2. first design;
3. verification of the structure characteristics in terms of total mass, respecting the CubeSat design specifications;
4. design modifications;
5. final analysis.

The process is iterative, and the final result will be an optimized structure ready for manufacturing.

Several tools can be used during this phase, such as CAD software and FEM software. In particular, some CAD softwares offer the opportunity to perform virtual Fit-Checks not only between the satellite and the deployer but also between the different internal components. During the design process, it is extremely important to consider not only the structure itself but also how it should be assembled, what hardware works with the limited space available, and what sequence should be followed to integrate the different components. To know, for example, that during the assembly whether a specific fastener can be accessed and torqued or not, or if a connector can be reached

will be extremely important. All these aspects can be simulated in advance using CAD tools. This approach will avoid wasting time and money and will ensure that the product not only satisfies the requirements but it is also easy to assemble.

Other important issues that should be looked at are related to manufacturing capabilities. Not all complex structures can be manufactured, and it is important to consider also how much material will be wasted during the manufacturing process to constrain the costs. The use of rapid prototyping technologies such as 3-D printing can help solving several issues related to the interface between design and manufacturing capabilities, but the engineer should always keep the design simple.

## 3.2 Structural analysis

Structural analysis can be considered a part of the iterative design process. Based on its results the engineer can decide which changes in the design will yield better performance and an optimization of the structure. Structural analysis can usually be performed using commercially available FEM software that allows designers to perform static and dynamical analyses on the structural model. The CAD file can be directly imported into the FEM software, but, in some cases, due to the complexity of the structure, it is easier to design a simplified model for use with the FEM tools. Some CAD software systems have tools and features that can be used to also perform dynamical and static analyses.

The main steps in conducting the FEM analysis are as follows:

- importing the CAD model, remembering to apply the correct materials;
- defining the FEM model using nodes and elements;
- applying the loads that depend on the analysis that should be conducted;
- defining the constraints;
- running the analysis;
- analyzing the results.

A detailed explanation of how to perform the analysis is beyond the scope of this chapter, but it is important to remember to define the main loads that should be considered for the analysis.

### 3.2.1 Loads

During a space mission, several loads will be applied to the satellite structure. Mainly, they are due to the launch conditions and are well defined in the interface control manual (ICD) between the rocket and the spacecraft or in the launch vehicle manual. Other loads can be caused by opening mechanisms, transportation or by thermal loads, such as the stresses caused when two materials, with different coefficient of thermal expansions, are coupled together. In general the loads are caused by forces and accelerations and can be divided in three categories:

- **static loads**, which are time independent;
- **dynamic loads**, which are time dependent and for which inertial effects cannot be ignored;

- **quasi-static loads**, which are time dependent but are “slow” enough so that inertial effects can be ignored [11].

Note that a quasi-static load for a given structure may not be quasi-static for another structure (made of a different material). Spacecraft structures are not normally affected by static loads, but quasi-static loads caused by steady state accelerations are typical of launches. Dynamic loads can be divided into low-frequency vibrations, broadband vibrations (such as random vibrations and acoustic loads) and shocks. While the various loads have different origins and time constants, all must be considered during the design of the spacecraft structure.

## 4 Materials and manufacturing

Material selection and manufacturing technologies are key considerations in producing an optimized structure. CubeSat design specifications impose the use of aluminum alloys 6061, 7075, 5051, or 5005 for the main CubeSat structure and the rails, making material selection a comparatively easy choice. The designer should select the best alloy that matches his design as it relates to the function of the mechanical systems, the costs, and possible procurement restrictions. Nevertheless, in some cases, aluminum alloys do not guarantee an optimized structure. In particular, when an extremely light frame is needed or the design complexity of a specific structure impedes the use of traditional manufacturing technologies, traditional aluminum alloys may not be optimal. For this reason, in some specific cases, it is possible to request a waiver and adopt different materials for the main structure.

The next section will focus on new materials and new manufacturing technologies that can be used to manufacture CubeSat frames and secondary structures.

### 4.1 *New manufacturing technologies*

Different developers are focusing their attention to the use of new manufacturing technologies that guarantee more flexibility during the design process and to get an optimized solution in a reduced time. New technologies are mainly based on additive manufacturing solutions and in particular on 3-D printing. Compared to manufacturing through traditional machining, 3-D printing technology has several advantages including short periods of manufacturing, relatively high accuracy in manufacturing small parts, and low cost [12].

In general, it is possible to use additive manufacturing as a solution to manufacture not only single parts or secondary structures but also complete satellite chassis. This solution allows developers to enable new applications for CubeSats. For example, a design has been recently developed for a 3-D-printed aluminum CubeSat structure that incorporates a cold-gas propulsion system [13]. Since many CubeSat missions are more limited by volume allocation than by mass allocation, volumetric efficiency of a propulsion system is crucial. In addition, the flexibility of additive manufacturing allows the exact location and angles of the nozzles to be tailored to a specific trajectory

or set of trajectories. The use of the additive manufacturing induces a complete revolution of the design process. An overview of additive manufacturing technologies and how to identify optimal design strategies for additive manufacturing has been considered in various studies, for example, by Gaudenzi et al. in [14]. Additive manufacturing is not a complete or effective solution for all structures given that it has limitations too, but new possibilities for CubeSat structures are certainly facilitated by 3-D printing.

## 4.2 New materials

Additive manufacturing does not always mean the use of new advanced materials. The general approach is to use the capability to 3-D print traditional materials such as aluminum and/or to generate new structural solutions. Nevertheless, the new trend is to space qualify new materials typically used in additive manufacturing. Of course, not all of these materials are suitable for space applications and the restrictions in terms of outgassing and other proprieties have always to be considered. In the following, two examples of materials qualified for space applications that have been effectively used will be described.

### 4.2.1 Windform XT 2.0

In 2016 the TuPOD, the first completely 3-D-printed satellite, was launched into space. TuPOD is the acronym for TubeSat PicoSatellite Orbital Deployer, result of a cooperation between GAUSS Srl and TetonSys. Similar to the UniSat platform from GAUSS, the TUPOD was designed to be a completely autonomous satellite with the main goal of releasing two smaller satellites once on orbit. Considering its shape, it is directly analogous to a 3U CubeSat; see Fig. 3 [15].

The satellite was completely made of Windform XT 2.0, a carbon microfiber-reinforced polymer material produced by CRP Technology. The material mechanical proprieties are shown in Table 1. The technology adopted to manufacture the satellite was the selective laser sintering (SLS) method. The satellite mission was a success, and the structure performed properly during the in orbit phase, releasing the daughter satellites in the proper orbits.



Fig. 3 TUPOD structure: X+ face to the right, Z+ face to the left.



**Table 1** Windform XT 2.0 mechanical properties.

Mechanical properties	WINDFORM XT 2.0
$\rho$ (kg/m <sup>3</sup> )	1097
$\sigma_y$ (MPa)	48
E (GPa)	8

The use of rapid prototyping allows developers to have great design flexibility. For example, the main internal section of TU-POD was a unique block divided in two completely separated areas (payload and bus) avoiding the use of any secondary surfaces or components, reducing weight and optimizing the available room. While the TU-POD was the first satellite to have a structure completely 3-D printed in Windform XT 2.0, it was not the first satellite to use the Windform XT 2.0 material, as other satellites such as KySat-2 and SERPENS had already adopted it to design components or secondary structures such as camera annulus, lens cover, deployable extensions, antenna clips, and battery holders.

#### 4.2.2 Polyether Ether Ketone (PEEK)

PEEK is a polyether ketone material under study at the European Space Agency in cooperation with the Portuguese company PIEP. It is an advanced thermoplastic with very good intrinsic properties in terms of strength, stability, and temperature resistance, with a melting point of 370°C [16]. The 3-D-printed PEEK CubeSat developed by ESA and PIEP is light, and, compared with other satellite fabrication methods, is cheap to produce. This material in addition to having all the benefits of new advanced materials such as being lightweight, cheaper, and faster to produce has the additional advantage of allowing developers to incorporate electrically conductive lines in place of the wire harness that normally connect the different CubeSat subsystems, reducing problems related to cabling and harnessing. As a next step in the use of this material, ESA is researching a space-optimized PEEK printer for initial testing on “zero-g” aircraft flights that will eventually be used by astronauts on the International Space Station.

## 5 Tests

The final phase before the launch is the testing phase. A section of this book (Part IV: CubeSat AITV activities) is dedicated to the description of the environmental tests that are required or suggested to be performed before launch. This section deals with the tests relevant to CubeSat structures, which should be performed at several levels: from the subsystems to the entire satellite.

In this phase, it should be emphasized that the load levels to be applied during the tests depend on the launch vehicle. Nevertheless, the developer can perform a wider variety of tests, even at higher levels than those required by the launch vehicle. These

tests and test levels can include data coming from different launch vehicles. This will allow developers to maintain an important level of flexibility during the launcher selection and to be able to move from one launch opportunity to another. This is an approach adopted by JAXA [5] that allows launches from International Space Station.

During the mission planning phase, it is important to consider the possibility of developing two nearly identical satellites: one engineering model (EM) and one flight unit (FU). Of course, budget and time might limit this approach, but this solution will allow designers to perform more invasive tests such as the qualification tests, normally performed at higher level than acceptance tests, on the EM, while testing the FU at lower levels during the acceptance tests.

## 6 CubeSat-derived form factors

Following the invention of the CubeSat standard, new small satellite form factors have been introduced. An overview of the most commonly adopted ones, along with their respective deployers and the main mission performed up to date, is provided.

### 6.1 *PocketQubeSat*

PocketQubeSats (initially called PocketQubs) are pico-class satellites (mass between 0.1 and 1 kg) that are envisioned to fly in constellations and perform a variety of functions from communications to Earth remote sensing and space research. The PocketQubeSat standard was first proposed by Prof. Bob Twiggs (Morehead State University) in 2009, with the idea of having a smaller and cheaper satellite than a CubeSat, and which could fit in a pocket, hence the name PocketQube. With the PocketQubeSat idea the concept of a “personal satellite” was introduced, a satellite that can be developed by a single developer interested in having its own satellite in space and able to afford the mission costs. The original concept envisioned the entire mission cost to be lower than the cost of an automobile.

The PocketQube dimensions are 1/8th of CubeSat since this miniaturized satellite has a size of 5 cm cubed. It is possible to design different units of PocketQubeSat remembering that the letter “p” indicates a unit of 5x5x5 cm. Regarding the mass, 1p weights no more than 180g. The electronic bus typically uses commercial off-the-shelf components [17]. Several PocketQubeSat dimensions have been considered in the last decade. In 2018 GAUSS Srl, TU Delft and Alba Orbital standardized the external dimensions publishing the PocketQube Standard available at [18].

#### 6.1.1 *Deployer*

PocketQubeSats can be placed in orbit using a deployer mechanism called MRFOD (Morehead Rome Femtosatellite Orbital Deployer). The MRFOD system is the result of a joint project between the Space Science Center at Morehead State University and GAUSS (Group of Astrodynamics of University of Roma Sapienza) at University of

Rome Sapienza. The MRFOD is directly analogous to the P-POD with the main difference being that, instead of having four rails, the FOD features slotted rail systems toward the bottom of the unit. PocketQubes have extended bottom faces (tabs), which allow them to slide along the guide rails. The ejecting force is created using an extension spring and a pusher plate located toward the rear of the guide rails.

MRFOD was first tested on board the EduSat.it satellite developed by GAUSS at the School of Aerospace Engineering in Rome and funded by the Italian Space Agency. The purpose of this first mission was to test the opening mechanism without the release of satellites. The first launch of PocketQubeSats was performed using MRFOD during the UniSat-5 mission. UniSat-5 was the first satellite designed, built, and launched in 2013 by GAUSS Srl (Group of Astrodynamics for the Use of Space Systems), the company that spun out of the experience of the UniSat program at the School of Aerospace Engineering of the University of Rome Sapienza. A CAD representation of EduSat.it with the MRFODs installed is shown in Fig. 4.

### 6.1.2 Maiden mission

During the UniSat-5 flight, four PocketQubeSats were launched. The smallest one, called WREN, was produced by the German startup STADOKO UG. Even though it was a 1p PocketQubeSat, it was able to carry onboard four pulsed plasma thrusters, a three axis reaction wheel, and a color camera. Two of the other PocketQubeSats were designed at Morehead State University with the support of various partners. Both of them were designed to provide a component test bed for various spacecraft technologies, primarily among them being a deorbit system that also increased the spacecraft radar cross section. In particular Eagle-1 (aka T-LogoQube) was a 1.5p PocketQube, and Eagle-2 (aka \$50SAT) was a 2.5p PocketQube. T-LogoQube/Eagle-1 was developed by Morehead State University and Sonoma State, and \$50Sat/Eagle-2 was developed by an Amateur Radio group and Morehead State University. T-LogoQube/Eagle-1 and \$50Sat were successful. The \$50 sat worked over 2 years, and T-LogoQube worked for about 6 months. In the same mission another 2.5p

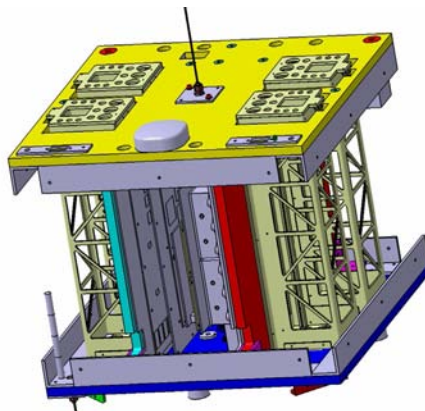


Fig. 4 EduSat.it with the MRFODs installed.

PocketQubeSat was boarded, called QBScout. Developed by University of Maryland BC, LACO Lab, it boarded a fine sun sensor. One of its main goals was the dynamic measurement of altitude.

## 6.2 TubeSat

The TubeSat is a satellite standard proposed by the US company Interorbital System (IOS). The purpose of IOS is to provide a low-cost alternative to CubeSats, since TubeSat has three-quarters of the mass (0.75 kg or 1.65 lb) and volume of a CubeSat [13] and can be launched using the ultra-low-cost NEPTUNE orbital launch vehicle developed and built by Interorbital Systems. Nevertheless, up to now, no TubeSats have flown in orbit using this system. The only two TubeSats launched to date (Tancredo I, OSNsat) have used the TuPOD previously described in Section 3.2.1.

Since its weight is less than 0.75 kg, it can be classified as a picosatellite. The TubeSat envelope is almost a cylinder of 8.94 cm of external diameter and 12.57-cm height. The TubeSat Kit sold by IOS has a hexadecagon shape, and it is assembled from a set of printed circuit boards. Nevertheless, some developers (i.e., Open Space Network) have decided to build their own structure and subsystems, maintaining the external dimensions and the weight defined by IOS.

### 6.2.1 First TubeSat mission

The first TubeSat missions were performed using the TuPOD system. In particular the TuPOD was carried on the JAXA spacecraft “KOUNOTORI-6” launched on December 9, 2016, on a mission to resupply the International Space Station. The TuPOD was deployed from the Japanese Experiment Module “Kibo” on January 16, 2016. In accordance with ISS safety regulations, on January 19, 2017, at 23:30 UTC, the TuPOD successfully dispensed the two TubeSats Tancredo I and OSNSAT. One hour later, at around 00:30 UTC, the satellite contacted the GAUSS ground station in Rome indicating the successful deployment of the TubeSats [19].

The Tancredo 1 TubeSat is the first satellite of the Ubatuba Sat Project, designed by the primary school Presidente Tancredo de Almeida Neves, located in Ubatuba, Brazil. The satellite was developed using the IOS commercial kit that was significantly modified and improved by the project team. Tancredo 1 had an onboard voice recorder IC as payload that transmitted a message chosen by a contest among the students.

OSNsat was the first satellite developed by the US company Open Space Network (OSN). In this case the developer decided not to adopt the IOS kit but to design its own platform using additive manufacturing technologies and to use part of the electronics already tested on 50\$Sat. Because of its short life, the satellite was equipped only with primary batteries and did not use solar cells. The objective of OSNSat mission was to test new technologies for satellite communications.

### **6.3 ThinSat**

ThinSat is a relatively new standard, invented in 2016 by Twiggs Space Lab, LLC (TSL), and Morehead State University. ThinSat has a mass of 250 g and is sold by TSL in kits equipped with flexible solar cells on both sides and a GlobalStar Antenna. The idea is very similar to the PocketQubeSats, but the use of a form factor of  $4.5'' \times 4.5'' \times 5/8''$  allows better accommodation of batteries and other internal components. What is completely new on ThinSats is that seven satellites are tethered one to the other. This concept allows a simplification of the documentation needed for the launch and in orbit operation; for example, one satellite needs to be licensed as opposed to seven individual ThinSats. In addition, the form factor allows developers to easily accommodate 21 ThinSat (three string of seven satellites) in a 3U CubeSat System Deployer (CSD).

#### **6.3.1 Maiden mission and launch opportunities**

Virginia Space and program participants launched 60 ThinSats on April 17, 2019, as a secondary payload on Northrop Grumman's Antares rocket from Pad 0A of the Mid-Atlantic Regional Spaceport located at NASA Wallops Flight Facility. Forty-nine of the ThinSats carrying standard and custom payloads successfully transmitted data via the orbiting Globalstar constellation system. Virginia Commercial Space Flight Authority (VCSFA) and TSL have the opportunity to launch up to 96 PocketQubeSat, 84 ThinSat, or other picosatellite equivalents on four (4) 3U containerized satellite dispensers on each of the Antares resupply missions through June 30, 2021. Additional capacity may be added to meet future demand.

### **6.4 ChipSat**

Developed at Cornell University in Ithaca, NY, USA, SpriteSats or "ChipSats" are femtosatellites of  $3.2 \times 3.2$  cm with a thickness of a few millimeter. In the size of a couple of postage stamps, they are able to board solar cells, a radio transceiver, and a microcontroller. The idea is to deploy the ChipSats using a 3U CubeSat. In particular, Cornell University developed in 2011 the KickSat satellite with the aim to deploy in orbit 104 SpriteSats. KickSat was launched with the Dragon cargo capsule on April 18, 2014 (19:25:22 UTC) from Cape Canaveral, FL, but unfortunately, the system was not able to command the Sprite deployment in time. The 104 Sprite satellites were supposed to be released on May 4, 2014, but a reset of the timer by the onboard "watchdog" microcontroller on April 30, 2014, did not allow the release of the satellites before the mothership KickSat reentered and burned up in the atmosphere (May 14, 2014).

Subsequently the team attempted a second launch of KickSat-2. In March 2019 105 ChipSat miniprobes were successfully contacted, 1 day after deploying from their KickSat-2 carrier spacecraft. The success of the ChipSats has implications for an accelerated "democratization of space."

## 7 Conclusions

In this chapter an overview of best practices during the structural system design and manufacturing has been presented. In particular, attention has been focused on the definition of the requirements and how they affect the overall satellite design. Some aspects are strictly related to the mission itself and cannot be analyzed in detail, but the developer can use this chapter to analyze their particular case and find the best solution to be adopted.

## References

- [1] CubeSat, CubeSat Design Specification (Revision 13 – Updated 6 April 2015). The CubeSat Program, Cal Poly SLO, 2015.
- [2] CubeSat, 6U CubeSat Design Specification (Revision 1.0 – Updated 7 June 2018). The CubeSat Program, Cal Poly SLO, 2018.
- [3] State of the Art-Small Spacecraft Technology, Small Spacecraft Systems Virtual Institute, Ames Research Center, Moffett Field, California, 2018. NASA/TP—2018–220027.
- [4] E.E. Bürger, G. Loureiro, R.Z.G. Bohrer, L.L. Costa, C.T. Hoffmann, D.H. Zambrano, G. P. Jaenisch, Development and analysis of a Brazilian CubeSat structure, in: Proceedings of the 22nd International Congress of Mechanical Engineering—COBEM, 2013.
- [5] Japan Aerospace Exploration Agency (JAXA), JEM Payload Accommodation Handbook – Vol. 8, Small Satellite Deployment Interface Control Document, 2015. Initial Release: March, 2013; Revision A: May, 2013; Revision B: January, 2015. JX-ESPC-101133-B.
- [6] ECSS-Q-ST-70-02C, Space product assurance: Thermal vacuum outgassing test for the screening of space materials, ECSS Secretariat ESA-ESTEC Requirements & Standards Division, Noordwijk, The Netherlands, 2008.
- [7] MSFC-HDBK-527F, Material Selection List for Space Hardware, NASA/Marshall Space Flight Center, AL, 1988. September 30.
- [8] A. Calvi, Spacecraft Loads Analysis. An Overview, ESA/ESTEC, 2011.
- [9] T.P. Sarafin, W.J. Larson, Spacecraft Structures and Mechanisms – From Concept to Launch, 1995.
- [10] International Organization for Standardization, ISO 8402: 1994: Quality Management and Quality Assurance-Vocabulary, International Organization for Standardization, 1994.
- [11] ECSS-E-ST-32 C-Rev. 1, Space Engineering—Structural General Requirements, 2008.
- [12] Z. Chen, N. Zosimovych, Mission capability assessment of 3D printing Cubesats, in: IOP Conference Series: Materials Science and Engineering, August, Vol. 608, IOP PUBLISHING, 2019, p. 012025.
- [13] T.H. Stevenson, E.G. Lightsey, Design and optimization of a multifunctional 3D-printed structure for an inspector Cubesat, *Acta Astronaut.* 170 2020 331–341.
- [14] P. Gaudenzi, S. Atek, V. Cardini, M. Eugeni, G.G. Nisi, L. Lampani, et al., Revisiting the configuration of small satellites structures in the framework of 3D additive manufacturing, *Acta Astronaut.* 146 2018 249–258.
- [15] A. Djamshidpour, C. Cappelletti, B. Twiggs, K. Biba, TuPOD, a Cube Satellite (CubeSat) and Tube Satellite Dispenser Produced via 3D Printing, Successful Launch, Orbit and Dispensing of Two Tube Satellites, 2017.
- [16] [https://www.esa.int/Enabling\\_Support/Space\\_Engineering\\_Technology/3D\\_printing\\_CubeSat\\_bodies\\_for\\_cheaper\\_faster\\_missions](https://www.esa.int/Enabling_Support/Space_Engineering_Technology/3D_printing_CubeSat_bodies_for_cheaper_faster_missions).

- 
- [17] C. Cappeletti, Femto, pico, nano: overview of new satellite standards and applications, in: *Advances in Astronautical Sciences, Proceedings of the 4th IAA Conference on University Satellite Missions and CubeSat Workshop*, Vol. 163, 2018, pp. 503–510.
  - [18] <https://dataverse.nl/api/access/datafile/11680>.
  - [19] C. Cappelletti, S. Battistini, F. Graziani, Small launch platforms for micro-satellites, *Adv. Space Res.* 62 (12) 2018 3298–3304.

# Electric power systems

# 9

*Jose L. Garcia*

Morehead State University, Space Science Center, Morehead, KY, United States

## 1 Introduction

Because of the CubeSats' small size, one of the main challenges during the mission design process is to design (or select from a provider) an electric power system (EPS) that assures enough electrical power for the satellite bus and payload during the entire mission duration. The EPS functions are to generate, store, regulate, and distribute the electrical power that a satellite requires to fulfill the mission requirements. Fig. 1 shows the basic EPS block components. The mission team needs to understand the behavior behind electric power generation in orbit, to size and select the proper components on the electric power generation block. Although there are several technologies that can be used for generating electrical power on a satellite, only solar cell generation will be addressed in this chapter (Section 2), because approximately 85% of nanosatellites (as of 2010) are using solar cells for power generation according to a NASA report on state of the art of small spacecraft technology [1].

Section 3 discusses some of the most used electric power storage devices and the main parameters required for the design. In addition the power supply control that is part of the electric power storage block will be discussed on this section, and methods like peak power tracking (PPT) to optimize the power capture from solar panels will be showed. The power distribution architectures for small satellites will be reviewed in Section 4 and the types of voltage regulators, to allow mission team to have decision elements essential to select the proper devices based on the sub-system requirements.

The creation of an electric power budget will help the mission teams in the design of the EPS. The electric power budget shows a relationship between in-orbit satellite subsystem electric power consumption, in-orbit satellite electric power generation, and in-orbit satellite electric power storage. This tool will help the mission teams to determine the size and performance of several components required by the EPS design, and also, it can help the teams to make the final decision about what kind of EPS will be used on the mission (i.e., their own development or one obtained from a commercial provider). Section 5 will explain how to create an electrical power budget for a particular mission.



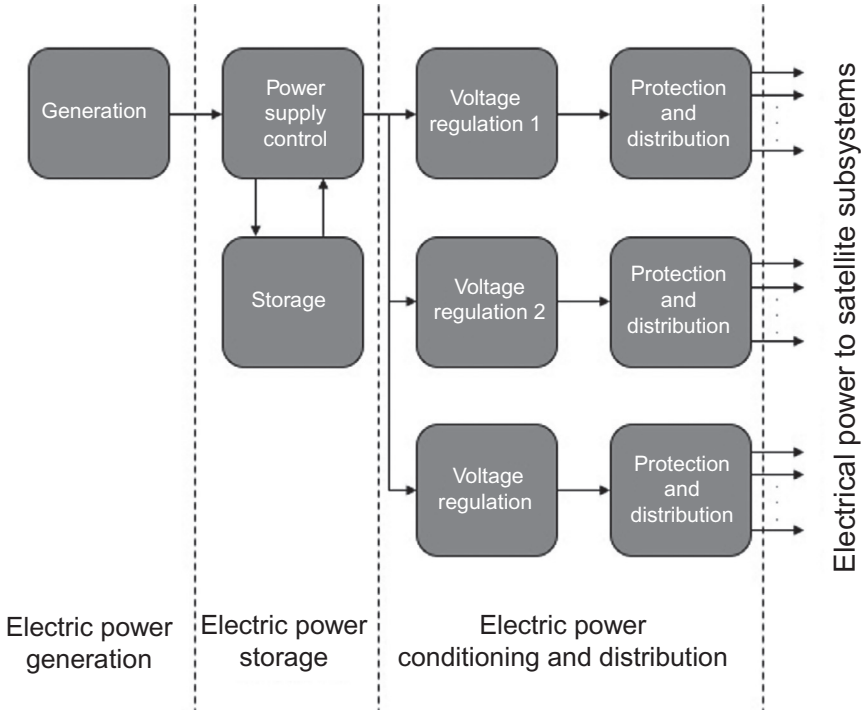


Fig. 1 Electric power system block components.

## 2 Electric power generation

A CubeSat requires electrical energy to operate. There are several sources of energy that can be transformed to electricity. The different electric power sources that can be used on a satellite can be classified, based on the type of energy, as chemical energy, solar energy, and nuclear energy.

Chemical energy sources for satellites refer mainly to various types of chemical batteries. Nuclear energy sources are primarily radioisotope thermoelectric generators (RTGs) that generate electrical power when the thermocouples are heated by the nuclear reaction. These kinds of energy sources are mentioned as a reference of energy sources on satellites, but as previously indicated, the most common used source of power for CubeSats is solar power by using the photovoltaic effect.

The photovoltaic effect is the direct transformation from light to electricity. The photovoltaic effect was discovered in 1839 by the French physicist Becquerel while he experimented with metal electrodes and electrolytes. Since then, solar cells (devices created to use the photovoltaic effect) have been created using different types of semiconductor materials and techniques to improve the energy transformation efficiency.

The most common materials used in commercial solar cells are silicon (Si) (medium efficiency) and gallium arsenide (GaAs) (high efficiency). Based on the

**Table 1** Important solar cell parameters.

Parameter	Commonly referred as	Units
Open circuit voltage	$V_{cc}$	mV
Open circuit current	$I_{cc}$	mA
Voltage at max. power	$V_{mp}$	mV
Current at max. power	$I_{mp}$	mA
Average efficiency	$\eta$	%
Dimensions	Length $\times$ width	mm
Cell area	$A$	cm <sup>2</sup>

manufacturing process, solar cells can be monocrystalline (higher efficiency and high cost), polycrystalline (less efficient than monocrystalline cells and less expensive), or amorphous (thin film, flexible solar cells with low efficiency). The most common solar cells for CubeSats are based on monocrystalline GaAs technology and can reach up to 30% efficiency or slightly above. The most important solar cell parameters that the mission team requires for the design are shown in [Table 1](#).

To obtain a proper voltage and current for the satellite power bus, arrays of solar cells are commonly used. If high voltage is needed by the power supply control, then parallel solar cells connections are required; if high current is needed, then serial solar cell connections are required. When solar arrays are used, it is important to consider a solar cell bypass diode for reverse bias protection. Some commercially available solar cell providers include a protection diode on the solar cell.

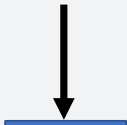



A solar cell or solar array will produce the maximum electrical power when the light source is perpendicular to its surface, that is, with an incidence angle equal to 0 degrees. If the Sun is considered as the light source, the energy received close to the Earth (specifically the solar flux) can be considered as 1358 W/m<sup>2</sup>, and the solar cell or solar array generated power can be calculated by the equation shown below in [Table 2](#).

[Table 3](#) shows the power generated based on different incidence angles, the arrow representing the light source and the bar representing the surface of the solar array or solar cell.

**Table 2** Solar power generated calculation.

Parameter	Units	Equation	Comments
Solar cell or solar array power generated	W	$P_{SA} = P_{in} \eta A_{eff} \cos \theta$	$P_{in}$ : solar input density = 1358 (W/m <sup>2</sup> ) $A_{eff}$ : solar cell or solar array's effective area (m <sup>2</sup> ) $\eta$ : solar cell efficiency (%) $\theta$ : incidence angle (degree)

**Table 3** Solar power generated by different incidence angles.

			
$\theta = 0$ degree $P_{SAmax}$	$\theta = 45$ degrees $0.707 \times P_{SAmax}$	$\theta = 70$ degrees $0.342 \times P_{SAmax}$	$\theta = 90$ degrees $0$ (W)

As previously mentioned, the maximum power generated for the solar cell (or solar array) is when the incidence angle is equal to zero degrees. For that reason, some satellites require the use of Sun-tracking arrays or particular attitude control systems, to guarantee maximum power generation. Other factors that need to be considered in a solar cell's on-orbit performance evaluation are temperature, chemical degradation, and eclipses. Solar cells' performance can be affected by high temperatures (above 28°C) [2], solar cell degradation, and eclipses. Typically, solar cells' efficiency is reduced between 0.025% and 0.075% per degree Celsius when the temperature increases above 28°C. Also, solar cells are degraded around 3% by year because of radiation and charged particles. In addition, solar cells cannot generate electrical power during eclipses. In [Section 4](#) a method to calculate the eclipse time is presented within the power budget.

### 3 Power storage

The previous section mentioned that during eclipses there is no electric power generation; for that reason a device that stores power during sunlight is need. Batteries are devices than can be used to store energy and then release it as electricity.

Batteries can be classified in two main groups: primary batteries that are not rechargeable and secondary batteries that can be recharged. Considering that a CubeSat in Low Earth Orbit (LEO) can undergo an eclipse 15 times a day, a 2-year mission might face an eclipse more than 1000 times. For this reason the use of rechargeable batteries is required.

There are several types of secondary batteries used for CubeSats, but the most commonly used for short mission durations are lithium ion (Li-ion) and lithium polymer (LiPo). The selection of the type of battery mainly depends on the parameters of energy capacity (Wh), specific energy (Wh/kg), and voltage (V). [Table 4](#) shows the most import battery parameters to consider in the EPS design. In [Section 4](#) a method to calculate the battery capacity is presented within the power budget.

Typically, Li-ion batteries have a 0–45°C charge temperature range and –20°C to 60°C discharge temperature range. Batteries can be discharged over a large temperature range, but the charge temperature is limited. Extreme cold and high heat reduce

**Table 4** Important batteries parameters.

Parameter	Units
Nominal capacity	mAh
Nominal voltage	V
Constant current charge ( <i>CC</i> )	A to V
Constant voltage charge ( <i>CV</i> )	V to mA
Max. discharge current	A
Charge operating temperature	°C range
Discharge operating temperature	°C range
Cycle life at $\times\%$ <i>DOD</i>	Cycles
Gravimetric energy density	Wh/kg
Volumetric energy density	Wh/L
Nominal weight	g
Dimensions (length $\times$ width $\times$ height)	mm $\times$ mm $\times$ mm

charge acceptance, so the battery must be brought to a moderate temperature before charging. Due to this limitation, electrical heaters are installed close to the batteries to avoid low temperatures, and batteries are usually mounted on heat dissipaters to keep batteries on the proper temperature range to avoid battery life reduction.

The depth of discharge (*DOD*) parameter indicates the percentage of the battery that has been discharged relative to the overall capacity of the battery. The higher the *DOD*, the lower the cycle life. Cycle life is defined as the number of cycles (with a 100% *DOD*) a cell can perform before its capacity drops to 80% of its initial specified capacity and then starts to reduce visibly its performance. It is an important parameter to consider based on the number of eclipses expected for the mission as was discussed on the previous section. Commonly, Li-ion has 500–1000 cycles and LiPo 300–500 cycles. How can it be possible to support a LEO mission of 2 years with more than 1000 eclipses with those numbers then? The answer is to change the percentage of *DOD*. There is a logarithmic relation between cycle life and *DOD*: the number of life cycles for a battery goes up exponentially when the *DOD* is reduced. This means that if a battery has 500 cycles at 100% *DOD*, it will have 2050 cycles at 30% *DOD* and 15,000 cycles at 5% *DOD*, approximately. For that reason, *DOD* lower than 30% is considered during the initial design.

According to Fig. 1, the stage of the EPS indicated as “electric power storage” consists of the storage device and the power supply control. The power supply control is in charge of receiving the generated electricity, sending part of it to the storage device, and sending other parts to the power bus for regulation and distribution to the next stage. There are many techniques to control the electrical power, but the two primary strategies used in CubeSat power supply controls are direct energy transfer (DET) and peak power tracker (PPT) [3].

All solar cells have a unique current versus voltage curve ( $i/V$ ) that describes the power output based on voltage and current variations. There is a point on the curve that represents the maximum power output point (MPP). The DET technique is the

easiest way to control the generated electricity. Given that the output voltage from the solar cells is constant and the total current varies depending on the operating location on the  $i/V$  curve, this technique can waste power. The PPT technique constantly adjusts the current and voltage from the solar cells to stay on the MPP; this maximizes the generated power. Both strategies are viable, and the one to be used depends on the mission profile.

## 4 Power conditioning and distribution

The last EPS stage is the electric power conditioning and distribution stage (see Fig. 1). At the end of the stage previously considered (electric power storage), a power bus is provided with a specific voltage and a maximum current capability. Because the CubeSat subsystems may need different voltages, voltage regulators may be required to increase or reduce the voltage bus to proper levels. In addition, some kind of protection is needed to avoid a collapse of the EPS because of a circuit shortcut or due to an overload.

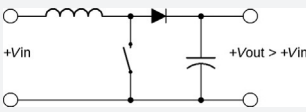
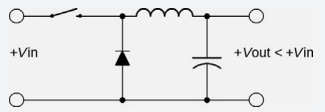
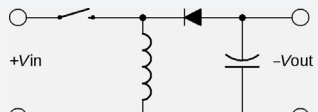
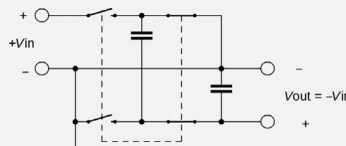
Conditioning the electric power can be accomplished by using two different EPS architectures, a centralized EPS or a decentralized EPS. The difference between these is that a centralized system conditions the electric power within the EPS and a decentralized system conditions the electric power at each satellite subsystem. Considering the integration of the CubeSat subsystems from different providers, the centralized EPS is often the best option.

The device in charge of conditioning the voltage bus to match the required subsystem voltage level is the voltage regulator. A voltage regulator is used to regulate (maintain) a voltage level. It generates a fixed output voltage that remains constant even in the event of changes in an input voltage or load conditions. In general, there are two types of voltage regulators, linear voltage regulators (LVR) and switching voltage regulators (SVR).

LVRs are compact and easy to use; they act like a voltage divider; for that reason, they have low efficiency. Other advantages are their low output ripple voltage, fast response time for load or voltage input changes, low electromagnetic interference, and low electronic noise. The main disadvantages are low efficiency and the fact that the output voltage cannot be increased above the input voltage. LVRs are commonly used as voltage reference only.

SVRs use elements to rapidly switch devices like capacitors and inductors to provide the proper current and voltage level at the SVR output. Switching is controlled by a feedback mechanism. SVRs are high efficiency because they dissipate almost no power. SVRs are able to generate output voltages that are higher than the input voltage or output voltages with opposite polarity than the input voltage. The main disadvantages are higher output ripple voltage, slower transient recovery time, and very noisy output because of the generation of electromagnetic interference (EMI). Different SVR configurations are summarized in Table 5.

**Table 5** Switching voltage regulator configurations.

 <p>Step-up Boost Raises input voltage</p>	 <p>Step-down Buck Lowers input voltage</p>	 <p>Step-up/step-down Boost/buck Raises or lowers or inverts input voltage</p>	 <p>Charge pump DC-DC converter without inductors Raises or lowers or inverts input voltage (low power applications)</p>
---	--	--	---

## 5 Power budget

The most common method of generating power on a CubeSat is using solar arrays, as previously mentioned. Solar arrays are made up of solar cells that, owing to several factors, will reduce the power generated over time, which has to be considered in a power budget (PB). There are several ways to create a power budget; some of them are very complex and require the use of additional software tools [like Systems Tool Kit (STK) by Analytical Graphics, Inc.] to simulate several conditions. In this section, a method to estimate a power budget with a sufficient precision for typical CubeSats missions in LEO is shown. By using the requirements in Table 6, a power budget will be created with the goal to determine the solar array power generation margin ( $P_{SAM}$ ) and the battery capacity ( $Batt$ ) required by the specific mission.

Table 7 shows the equations that will be used to calculate the primary parameters for a specific orbit. The time of eclipse ( $TE$ ) and the time in sunlight ( $TS$ ) are required to calculate the power budget; it is important to determine how much power can be generated during  $TS$  and how much power the batteries must provide during the  $TE$ .

**Table 6** EPS requirements.

Requirements	Comments
1U CubeSat using body-mounted solar cells	Solar cells covering the complete surface of each side
Mission duration 3 years	
Orbit height 500 km	Circular orbit
Solar cells 30% efficiency	Gallium arsenide (GaAs)
Solar cells efficiency degradation 3% per year	
Solar array packing factor ( $PF$ ) 0.75	
Batteries depth of discharge ( $DOD$ ) 30%	Lithium ion (Li-ion)
Onboard data handling (OBDH) system	Duty cycle 100%
$V = 3.3\text{ V}$	
$P = 0.5\text{ W}$	
Telemetry, tracking, and command system (TT&C)	RX mode: duty cycle 100%
$V = 12\text{ V}$	TX mode: duty cycle 15%
RX mode: $P = 0.2\text{ W}$	
TX mode: $P = 2.5\text{ W}$	
Electric power system (EPS)	Duty cycle 100%
$P = 0.1\text{ W}$	
Attitude determination and control system (ADCS)	Duty cycle 100%
$V = 3.3\text{ V}$	
$P = 0.3\text{ W}$	
Payload (PLD)	During sunlit: duty cycle 30%
$V = 5\text{ V}$	During eclipse: duty cycle 0% (off)
$P = 0.8\text{ W}$	

**Table 7** Equations for calculating orbital parameters required by the power budget.

Parameter	Units	Equation	Comments
Orbital period ( $T$ )	s	$T = \sqrt{\frac{4\pi^2 R^3}{\mu_{\text{Earth}}}} = 2\pi \sqrt{\frac{R^3}{\mu_{\text{Earth}}}}$	LEO and circular orbit $\mu_{\text{Earth}}$ : $3.986 \times 10^5$ (km <sup>3</sup> /s <sup>2</sup> ) $R$ : Earth's radius 6378 (km)
Earth's angular radius ( $\rho$ )	degrees	$\rho = \sin^{-1}\left(\frac{R}{h+R}\right)$	$h$ : orbital altitude (km) $R$ : Earth's radius 6378 (km)
Time of eclipse ( $TE$ )	s	$TE = \frac{2\rho}{360^\circ} T$	$\rho$ : Earth's angular radius (degrees) $T$ : orbital period (s)
Time in sunlight ( $TS$ )	s	$TS = T - TE$	$T$ : orbital period (s) $TE$ : time of eclipse (s)

**Table 8** Orbital parameters obtained based on the EPS requirements.

Parameter	Units	Value
Orbital period ( $T$ )	s	5676.81
	min	94.61
	h	1.58
Earth's angular radius ( $\rho$ )	degrees	68.02
Time of eclipse ( $TE$ )	s	2145.15
	min	35.75
	h	0.60
Time in sunlight ( $TS$ )	s	3531.66
	min	58.86
	h	0.98

To calculate  $TE$  and  $TS$ , the orbital period ( $T$ ) and the Earth's angular radius ( $\rho$ ) need to be known or calculated. Using the equations in [Table 7](#), the results of [Table 8](#) are obtained.

The next step is to calculate the power generated and the power required by the CubeSat to determine the power generation margin. [Table 9](#) shows the equations that will be required to calculate the power generated considering the requirement parameters for this particular mission.

The first calculation is to determine the solar array power generated at the beginning of operational life ( $BOL$ ). To do this, several factors need to be considered. As was shown in [Section 2](#), the solar array area, solar cell efficiency, and the incidence angle are required to determine the generated power. The solar cell efficiency will be affected by degradation and high temperatures. Degradation will change solar cell efficiency over the years until the end of life time ( $EOL$ ), and high temperatures will change it during sunlight periods on every orbit. On the other hand, if the CubeSat is



**Table 9** Equations for calculating primary power parameters required by the PB.

Parameter	Units	Equation	Comments
Solar array power generated at BOL ( $P_{SA BOL}$ )	W	$P_{SA BOL} = P_{in} \eta A_{eff} \cos \theta$	$P_{in}$ : solar input density = 1358 (W/m <sup>2</sup> ) $A_{eff}$ : solar array's effective area = long × wide × PF = 10 cm × 10 cm × 0.75 = 0.0075 (m <sup>2</sup> ) $\eta$ : solar cell efficiency = 30% $\theta$ : incidence angle = 0 (degrees)
Solar cell efficiency at EOL ( $\eta EOL$ )	%	$\eta EOL = \eta(1 - YD)^{YM}$	$\eta$ : solar cell efficiency = 30% $YD$ : solar cell eff. Degradation per year = 3 (%) $YM$ : years of mission duration = 3
Solar array power generated at EOL ( $P_{SA EOL}$ )	W	$P_{SA EOL} = \eta EOL(P_{SA BOL})$	$\eta EOL$ : solar cell efficiency at EOL (%) $P_{SA BOL}$ : solar array power generated at BOL (W)

using body-mounted solar cells, it is expected that the CubeSat will have some rotation or tumbling (depending on the attitude motion), and because of this, the incidence angle will be constantly changing; therefore the power generated will also change. As can be expected to calculate the power generated, a simulation including the satellite dynamics in orbit and the solar array temperature variations in orbit is required. To create a realistic model is nontrivial and requires simulation tools. Based on previous experience with body-mounted solar cells on CubeSats, a practical estimation for keeping the incidence angle constant and equal to zero is to consider that one side of the 1U CubeSat will be generating energy during sunlight. Table 10 shows the practical values for different types of CubeSats.

Note that for this power budget and based on the EPS requirements shown in Table 10, the effective area is the area of one of the CubeSat sides times the packing factor  $PF$  ( $0.1 \text{ m} \times 0.1 \text{ m} \times 0.75 = 0.0075 \text{ m}^2$ ). The packing factor indicates the portion of a CubeSat face covered by solar cells. A  $PF = 1$  means that the whole face is

**Table 10** Practical solar array effective area consideration.

CubeSat	No. of CubeSat sides with solar cells	Solar array's effective area practical consideration (m <sup>2</sup> )
1U	6	$1 \times A_{eff}$ from 1 side ( $0.1 \text{ m} \times 0.1 \text{ m} \times PF$ )
2U	4 (X/Y facets)	$0.80 \times A_{eff}$ from 1 side ( $0.1 \text{ m} \times 0.2 \text{ m} \times PF$ )
3U	4 (X/Y facets)	$0.86 \times A_{eff}$ from 1 side ( $0.1 \text{ m} \times 0.3 \text{ m} \times PF$ )

**Table 11** Power parameters obtained based on the EPS requirements.

Parameter	Units	Value
Solar array power generated at <i>BOL</i> ( $P_{SA BOL}$ )	W	3.06
Solar cell efficiency at <i>EOL</i> ( $\eta_{EOL}$ )	%	27.38
Solar array power generated at <i>EOL</i> ( $P_{SA EOL}$ )	W	2.79

covered by solar cells. A  $PF = 0.75$  has been considered in this example, meaning that the cells cover 75% of the face. Considering another mission in which the solar cells will have a different size, the effective area will be adjusted to the proper packing factor ( $PF$ ).

Table 11 shows the results for the power parameters calculated considering the power generated at the beginning of operational life, the solar cell efficiency after 3 years, and the power generated 3 years after operating in orbit.

Once the generated power is calculated, it is time to calculate the power required by the CubeSat and the average orbital power required ( $AOPR$ ) for each subsystem and for eclipse and sunlight events. This can be calculated by multiplying the power requirements by the duty cycle. Considering the requirements of Table 11, Table 12 is obtained.

The results in Table 12 show the  $AOPR$  during sunlit and during eclipse; the next step is to calculate the energy required per orbit to calculate the power required by the solar array during one orbit. Table 13 shows how to calculate these parameters for one orbit.

After calculating the required energy during sunlit and eclipse, the power required by the solar array can be calculated. Table 14 shows these results.

Finally, after knowing the amount of power generated and the amount of power required per orbit, a power margin can be obtained. If the power margin is high, the power system is likely to work properly and can handle possible power anomalies.

**Table 12** Average orbit power required.

Subsystem	Power requirement (W)	Sunlit duty cycle (%)	Average orbit power required during sunlit $AOPR_S$ (W)	Eclipse duty cycle (%)	Average orbit power required during eclipse $AOPR_E$ (W)
OBDH	0.5	100	<b>0.5</b>	100	<b>0.5</b>
TT&C (RX)	0.2	100	<b>0.2</b>	100	<b>0.2</b>
TT&C (TX)	2.5	15	<b>0.375</b>	15	<b>0.375</b>
ADCS	0.3	100	<b>0.3</b>	100	<b>0.3</b>
EPS	0.1	100	<b>0.1</b>	100	<b>0.1</b>
PLD	0.8	30	<b>0.24</b>	0	<b>0</b>
Total power (W)			<b>1.715</b>		<b>1.475</b>

**Table 13** Equations to calculate the energy and solar array power required per orbit.

Parameter	Units	Equation	Comments
Energy required during eclipse ( $E_E$ )	Wh	$E_E = AOPR_E TE$	$AOPR_E$ : average orbit power required during eclipse = 1.475 W $TE$ : time of eclipse = 0.60 (h)
Energy required during sunlit ( $E_S$ )	Wh	$E_S = AOPR_S TS$	$AOPR_S$ : average orbit power required during sunlit = 1.715 W $TS$ : time in sunlight = 0.98 (h)
Energy required to produce ( $EP$ )	Wh	$EP = E_E + E_S$	$E_E$ : energy required during eclipse (Wh) $E_S$ : energy required during sunlit (Wh)
Solar array power required ( $P_{SAR}$ )	W	$P_{SAR} = \frac{EP}{TS}$	$EP$ : required to produce (Wh) $TS$ : time in sunlight = 0.98 (h)

**Table 14** Energy and solar array power required per orbit obtained based on the EPS requirements.

Parameter	Units	Value
Energy required during eclipse ( $E_E$ )	Wh	0.88
Energy required during sunlit ( $E_S$ )	Wh	1.68
Energy required to produce ( $EP$ )	Wh	2.56
Solar array power required ( $P_{SAR}$ )	W	2.61

If the margin is negative, it means that the satellite requires more power than the generated and needs to be modified in some way, reducing the power consumption of its subsystems, modifying satellite system's duty cycle, increasing the power generation, or by other methods.

In addition, the required battery capacity can be calculated based on the requirements. Tables 15 and 16 show how to calculate the solar array power margin and battery capacity as well as the results based on the EPS requirements.

**Table 15** Equations to calculate the solar array power margin and battery capacity.

Parameter	Units	Equation	Comments
Solar array power margin ( $P_{SAM}$ )	W	$P_{SAM} = P_{SAEOL} - P_{SAR}$	$P_{SAEOL}$ : solar array power generated at EOL (W) $P_{SAR}$ : solar array power required (W)
Battery capacity ( $Batt$ )	Wh	$Batt = \frac{E_E}{DOD}$	$E_E$ : energy required during eclipse (Wh) $DOD$ : battery's depth of discharge (%)

**Table 16** Solar array power margin and battery capacity obtained based on the EPS requirements.

Parameter	Units	Value
Solar array power margin ( $P_{SAM}$ )	W	0.18
	%	6.81
Battery capacity ( $Batt$ )	Wh	2.93

Results for this specific example show that there is a low positive power margin at the end of the operational life equal to 6.81%. The battery capacity is 2.93 Wh; therefore the mission team can create battery arrays (in series and/or in parallel) to meet the required battery capacity. Using the generated power budget, the mission team can modify some of the parameters to adjust the final results.

## 6 Conclusions

In summary, it is important to understand the technology behind the generation, storage, regulation, and electrical distribution in the CubeSat design to select the appropriate components to meet the requirements of the specifications for the power system. In addition, the creation of a power budget can be as complex as required by the mission. In [Section 5](#) a method to create a relatively simple power budget was shown, which proved to be a good approximation. These elements and factors can be very useful for modeling the first numbers during the CubeSat mission design process.

## References

- [1] S. Weston, *State of the Art of Small Spacecraft Technology*, Small Spacecraft Systems Virtual Institute, Ames Research Center, Moffett Field, CA, 2018. NASA/TP-2018-220027.
- [2] J. Sellers, D. Kirkpatrick (Ed.), *Understanding Space: An Introduction to Astronautics*, third ed., Space Technology Series 2005.
- [3] J. Wertz, D. Everett, J. Puschell (Eds.), *Space Mission Engineering: The New SMAD*, In: Space Technology Library Space Technology Series, Microcosm Press, Hawthorne, CA, 2015.

# On-board data handling systems

# 10

James W. Cutler<sup>a</sup> and Jacob Beningo<sup>b</sup>

<sup>a</sup>University of Michigan, Ann Arbor, MI, United States, <sup>b</sup>Beningo Embedded Group, LLC, Linden, MI, United States

## 1 Introduction

The primary purpose for nearly all space missions is to generate data. Data are the key driver and motivation for a space mission. In most instances, a space mission is designed around a primary payload that generates specific data which could include applications from Earth imaging, space environment research, astrophysics, heliophysics, or new technology demonstrations. Space mission data are by no means limited to the payload, even though they tend to be the largest dataset. Missions generate a wealth of additional data such as the telemetry, which catalogs the health and status of the spacecraft, its attitude, system and subsystem states, log files, and configuration settings. These data are managed by the on-board data handling system (OBDH).

There are at least four main functions on-board a spacecraft for handling data. These functions can be broken down into sources, sinks, processors, and transfers. *Sources* are subsystems that generate data. These could be individual sensors within a subsystem such as a magnetometer, or they can be an entire subsystem such as an attitude determination and control system (ADCS). When data are generated, those data often need to be stored. The destination for the data is known as a *sink* because it receives the data. Data find its way from a source to a sink through a data *transfer*. Again the transfer could be within a single subsystem from a sensor to local memory or it could be from a subsystem to another subsystem or from a subsystem into non-volatile memory storage. Finally, data are often *processed* on-board. The spacecraft must decide whether it will act immediately with the data or transfer it for processing in the future. A component or subsystem can carry out one or more of the four main functions of data handling.

Space systems are inherently distributed computing systems, and data handling is a critical issue to consider during the design stage. Failure to adequately consider data handling can result in lost mission data, overly intensive computing operations, power budget issues, and many other problems that will threaten mission viability. This chapter addresses these common data handling functions and CubeSat mission design. The four main functions of generation, storage, transfer, and processing are described. A fifth element, time, is discussed, which is crucial for understanding data. Various design considerations for OBDH systems are summarized, and an example reference design is provided. A summary of emerging trends concludes the chapter.

## 2 Component overview

Spacecraft OBDH systems are not one-dimensional data systems and, as such, cannot be considered at a single, architectural level. Instead, they should be visualized as multitiered systems, where data flow upward from lower level components to subsystems of increasing complexity until it arrives at the user’s fingertips. Data are generated at the lowest levels of the system by individual components, also known as sources. Data generated by a source are then transferred to a subsystem that aggregates the data and acts as a source for a higher-level subsystem that will eventually consume the data. For example, Fig. 1 shows a simplified ADCS that acts as a data sink for several magnetometers. The magnetometers act as data sources whose data are stored locally within the sensor memory. It is then transferred over a data bus to the ADCS which acts as a data sink. The ADCS subsystem stores the data it receives until they are needed. The ADCS acts as a data aggregator that collects data from a wide range of sources such as magnetometers, temperature, current, and voltage sensors. A subsystem may act on the data that are transferred to it by storing them, processing them locally, or transferring them to another subsystem that could do the same.

This same scheme also applies at a higher-level within the spacecraft. The spacecraft may contain several subsystems, all of which aggregate sensor data while acting as a data generator for other on-board, higher-level systems such as the flight computer. An example data flow diagram can be seen in Fig. 2. Notice that the flight computer is acting as a data sink to several subsystems such as the ADCS, payload,

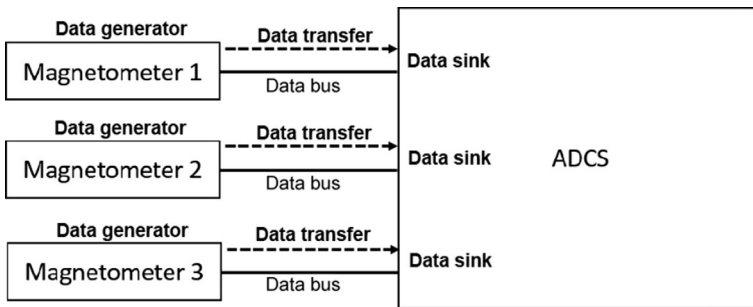


Fig. 1 Data flowing from sensors to a subsystem.

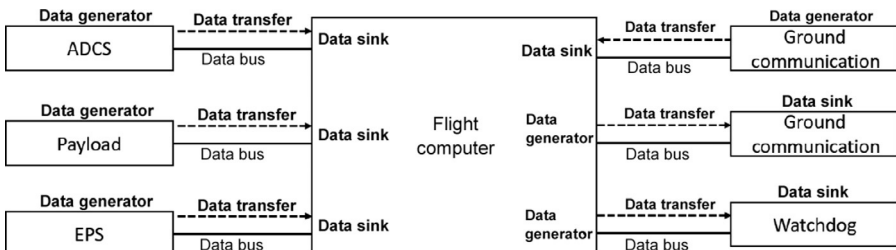


Fig. 2 Data flowing through the spacecraft.

and electronic power supply (EPS) while acting as a data generator for a watchdog subsystem. There is also a unique case with the ground communication system where the flight computer and the communication system act as data generators and sinks for each other.

Understanding how data flows through a component, a subsystem, and eventually through the spacecraft is critical for developing an appropriate hardware and software architecture for each of those components. As an introduction to the design process for on-board data handling, it is first discussed how data are generated, stored, and transferred.

## 2.1 Generation

Data on-board a spacecraft may be generated by several different sources depending on the overall system architecture. These include the flight computer, the attitude determination and control system, electronic power supplies, the fault management, and the telecommunication systems, but the primary data generator for a space mission is the payload. The payload on any given mission will typically generate data magnitudes larger than all other subsystems combined. Data generation can be characterized with four temporal qualities: deterministic versus event based and continuous versus variable rate. Each of these is briefly described in the following text.

*Deterministic* data collection occurs at regular or known time intervals with bounds on timing errors. A periodic telemetry beacon is an example. *Event-based* generation is opportunistic in nature and occurs when a stochastic event is detected. Data are generated in response to that event. Thresholding on telemetry points is an example event, where a particular value is reached for a data point, such as battery voltage. Additional sampling can occur to monitor the potential fault or take corrective action.

The data generation rates can approximately be divided into two categories: continuous or variable rate. Data generation over time can be at a *continuous rate* with sampling at fixed intervals. Low rate telemetry data are often generated in this manner as is payload data collected over the entire flight path of the mission. Variable rate sampling is useful for specialized data collection. Lower rates can be used to conserve resources such as storage space or power. Higher rates (sometimes called burst data collection) can provide higher fidelity measurements when needed.

Designers should consider at least four key attributes of data generation systems:

*Sample rate*—The number of times per time interval that data are generated or collected. Typically, this is given in terms of samples per second. Rates are determined based on expected features where sampling is done at least two times the expected signal frequency (the Nyquist rate [1]). Higher sampling rates provide greater resolution in time of signals.

*Sample size*—The number of bits per sample. A larger number of bits per sample provides greater resolution in signal levels.

*Sampling time period*—The time over which data are sampled. There are two aspects to this. First, there is a low-level sample and hold time for when analog to digital converters make their measurements. The second, which is the main concern here, is the length of time that samples are taken at a particular sample rate. This is governed by the deterministic or event-base sampling described earlier.

**Table 1** Example telemetry points from subsystems.

Subsystem	Telemetry points
Power system	Battery voltages/currents/temperatures, on/off switch states, solar panel voltages/current/temperatures, battery heater status, output regulator temperatures/voltages/current
Attitude determination	Magnetic fields, rotation rates, sun sensor outputs (solar flux magnitude or sun vectors), star tracker outputs
Attitude control	Controller mode, magnetic torque rod settings, reaction wheel speeds and directions, thruster power outputs
Communications	Bytes received, bytes transmitted, error rates
Flight computer	Time, command queue status, commanded on/off state, free memory, free storage, number of processes
General purpose	Voltage, current, temperature

*Latency*—The time before data are made available for usage. Delays exist at all levels of system interaction. Designers should understand where the latencies are in their system which exists throughout the spacecraft between sensors and subsystems and for transferring data between generators and sinks. Low-latency requirements for systems like feedback control require real-time operating considerations.

In addition to payload data, data are also generated by spacecraft subsystems that are used to determine the spacecraft's health, wellness, and status. Common measurements across these systems include power supply voltages, current draw, and temperatures. A nonexhaustive list of specialized telemetry is found in [Table 1](#).

One key common denominator among all generators is that they need somewhere to store their data. The different ways that data can be stored on the spacecraft will now be described.

## 2.2 Storage

Data storage is a fundamental element of computing [2] that provides a system with the ability to retain generated data and code. Requirements for storage vary greatly across a spacecraft's subsystems and can be summarized with the following attributes:

*Size*—The number of bytes that can be stored.

*Volatility*—Storage persistence over a power cycle. Volatile storage loses the data when power cycled. Nonvolatile storage maintains the data through power cycles.

*Durability*—Data have a limited lifetime when stored. Volatility is a form of durability to power cycles. Electronic leakage current and radiation are additional degraders of storage. Durability describes the expected lifetime of the storage media.

*Write/read speed*—Storage has limits to the speed with which you can read and write to it. Typically, larger storage systems are slower to access.

*Latency*—There is a delay between when a read/write action is requested and when it is performed. When reading, this is a delay in the response of the data returning to the requester. When writing, it is a delay to when the data are physically written to the storage media.



Note: memory and storage are often used interchangeably by users. However, typically memory is used for short-term storage and storage is reserved for long-term storage. Short and long are not specifically defined, but memory is typically volatile RAM, and storage refers to nonvolatile, durable storage.

Location of the storage often constrains the design of storage systems. Storage that is close to sources and sinks of data is generally faster and has lower latency. Most subsystems have some small storage capability. If there is a processor, there will be volatile RAM and sometimes nonvolatile storage such as flash or MRAM. There are many different types of electronics chips that provide most forms of memory and storage to embedded systems; embedded multimedia cards (eMMC) are an example [3]. Larger storage systems may be an independent subsystem or part of a flight computer system. These storage systems provide retention of data for long-term archival on the satellite or as a buffer until they are downlinked to operations centers.

RAM is often used to store temporary data that will be used immediately or quickly transferred to another subsystem for use. Data stored in RAM are typically health and wellness information, subsystem state variables, and other subsystem specific information. When storing data in RAM, it is important to consider the radiation environment that the spacecraft will be operating in. Designers may need to protect the data's integrity by adding a cyclical redundancy check (CRC) to the data. If the data are considered critical, designers can also create duplicate copies of the data and store them in separate memory banks to improve the chances that the data remain intact.

Managing nonvolatile memory is complex. Many modern nonvolatile memory devices will automatically manage load wearing (equally distributing access to memory across the entire device) for a designer to improve the memory's durability, but a software driver is often required to interact with these devices. Designers need to carefully select their drivers. Open source software stacks such as FatFS may not be mission appropriate and are typically not fault tolerant. There are open source software stacks such as Yaffs, which have been used in NASA's Transiting Exoplanet Survey Satellite (TESS) if a commercial solution is not viable. An additional key design feature has been identified here; data need to be transferred from one system to another. This leads to the next section, data transfer between subsystems.

## 2.3 *Transferring*

In every spacecraft, data are transferred from one subsystem to another. That data may be health and wellness information, payload data, fault information or other data. Data are transferred through the spacecraft using a variety of mechanisms which can be categorized as hardware and software.

The hardware mechanisms used directly relate to the spacecraft bus architecture and the communication interfaces that are established between the various subsystems. The subsystems may be connected in a bus architecture that uses point-to-point communication such as a USART, Ethernet, or USB. Alternatively, a subsystem might use a multidrop or multipoint architecture such as RS-485 or CAN bus. The difference is that in a point-to-point topology the sender communicates directly with a single receiver while a multidrop topology allows for a sender to communicate with

multiple receivers, sometimes even simultaneously. These topologies are shown in Fig. 3.

There are two main characteristics that determine how effectively a communication bus can transfer data: bus type and data rate. There are two types of data buses, serial and parallel. Serial data present the data one bit at a time for transmission unlike parallel data that present an entire byte or more across multiple transmission lines at the same time. Serial is most often used today because it minimizes the number of transmission lines, which can reduce noise, transmission errors, cable size, and weight.

Serial communication protocols can also be either synchronous or asynchronous. Data that are sent synchronously are always with a clock to synchronize the communication between the devices. For example, the serial peripheral interface (SPI) uses two unidirectional transmission lines for master out/slave in (MOSI) and master in/slave out (MISO), which are paired with a clock (CLK) line to synchronize when to clock-in and clock-out a data bit. Asynchronous communication protocols do not use a clock to synchronize data transmission, which allows them to use fewer I/O pins. However, the lack of synchronization requires additional complexity such as adding start or stop bits to the transmission, which can decrease throughput. A USART is a classic example of asynchronous communication.

The interface that is selected to transfer a given set of data is greatly dependent on the amount of data to transfer and the data rate, which was discussed in the section on storage. The data rate is the rate at which the system can transfer data from one location to another and is highly dependent upon the communication interface that was chosen. Most modern interfaces today support at least 1 Mbps, as can be seen in Table 2, but the transfer rates can vary dramatically. For example, a standard USART found on nearly every microcontroller is capable of transfer speeds up to 4 Mbps. USARTs are often optimized for low-power operation, which can have advantages over more energy consuming interfaces such as USB or Ethernet. Designers need to carefully consider their communication interfaces data rate. While a USART can transfer at speeds up to 4 Mbps, the transmission line length can affect noise and error rates. It is not uncommon to see these very capable interfaces running at 115,200 bits per second (bps) or even 9600 bps! This is less a problem with noise than it is a problem with legacy thinking and supporting legacy communication stacks.

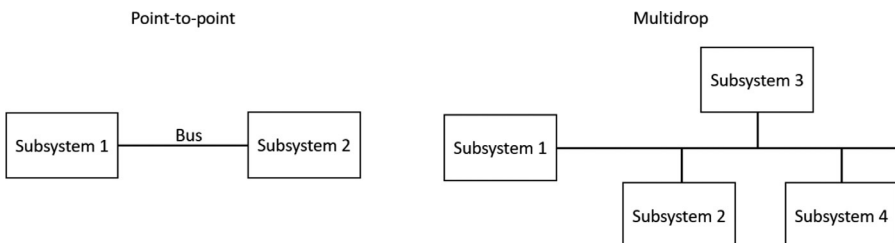


Fig. 3 Communication bus topologies.

**Table 2** Common communication interface topology and transfer rates.

Bus interface	Data bus type	Topology	Data rate (Mbps)
USART	Serial	Point-to-point	4
RS-485	Serial	Multidrop	10
SPI	Serial	Multidrop	1–20
QSPI	Serial	Multidrop	54–108
I2C	Serial	Multidrop	0.1, 0.4, 1.0, 3.2
CAN bus	Serial	Multidrop	Up to 1
USB	Serial	Point-to-point	1.5–480
Ethernet	Serial	Point-to-point	10–1000

No matter how fast an interface may be, a major factor determining the actual transfer rates will be the software stacks that run the communication interface. A commonly used, layered architecture for communication stacks is the open systems interconnection (OSI) model. The model contains seven layers (Table 3) that standardize communication functions without regard to the underlying hardware. It is easy for designers to think only about the physical layer (layer 1), which is typically the processors low-level hardware peripheral such as SPI, I2C, USB, CAN, or Ethernet. There can be quite a few layers within the software stack that make transferring the data successful.

For example, Ethernet is a popular communication interface because of its high data transfer rates and its flexibility. A typical Ethernet transfer might involve the following software layers and protocols:

- Physical layer—10BASE-T Ethernet Peripheral
- Data Link—Ethernet
- Network—Internet Protocol (IP)
- Transport—Transmission Control Protocol (TCP)
- Session—Sockets Direct Protocol (SDP)
- Presentation—Secure Socket Layer (SSL)
- Application—File Transfer Protocol (FTP)

**Table 3** OSI model layer summary.

Layer			Function
Host layers	7	Application	High-level API's
	6	Presentation	Data translation between application and network service
Media layers	5	Session	Communication session management
	4	Transport	Data segment transmission between network points
	3	Network	Multinode network management
	2	Data link	Data frame transmission between nodes on the physical layer
	1	Physical	Raw bit stream transmission and reception in hardware

The OSI model provides developers with a flexible layered architecture that can use a single model to communicate across several communication interface types and protocols (see Ref. [2] for a list of protocols by layer.) In many cases, developers can leverage existing software stacks to configure their software to use the desired transfer protocol(s).

## 2.4 Time

Space systems are inherently distributed, and time is typically used for coordination. Coordination includes such things as execution of commands at the proper time and time tagging of data to enable comparison with specifics. The scale of time distribution varies from subsystems on a satellite to interplanetary infrastructure.

A reference clock is chosen for the system, and distributed clocks synchronize to it. Usually there is a global reference standard as well that enables synchronization across multiple systems. Key attributes of a timing system include the following (Fig. 4):

*Skew*—Error between local clock and the reference clock measured in units of time.

*Jitter*—A measure of error in the periodic signal that clocks output (often a sine or square wave).

*Drift*—The change in skew over time is called drift. External factors can cause deterministic drift such as radiation and temperature.

A variety of clocks are used on CubeSat systems. Simple clocks are crystal oscillators or 555 timers that provide a periodic signal. Counters or a processor can count these periodic signals and produce a time stamp that includes years, months, days, minutes, and seconds. GPS receivers provide a clock signal and time stamp referenced to the GPS satellite network. Advanced oscillators are temperature controlled to minimize drift. Recent advances in chip-scale atomic clocks enable highly accurate time stamps over large time horizons [4].

Some designs have external triggers that provide a reference event for timing. This event can be seen by portions of the system and aligned with local clock sources. The RAX mission described in Section 4 was able to use radar pulses from the ground with known time of flight for accurate time stamps. Other impulse events like lightning strikes can provide events as well. Some mission architectures use time

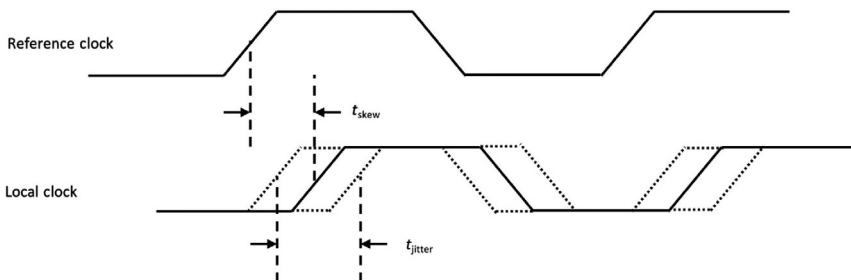


Fig. 4 Example of clock skew and jitter of a local clock with respect to a reference clock.

synchronization during ground contacts—that is, synchronize mission elapsed time with universal time (UTC) or similar to compensate for drift and other effects.

There are multiple methods for *time tagging* or *time stamping*. Data sampling systems tag their output with references to clock signals. If the skew and jitter associated with the time tagging is low enough between samples, an initial absolute clock reference can tag the start of the data and offsets from this based on the clock used for following samples. If the time uncertainty is too great when sampling, the time can be written per sample to provide greater accuracy.

## 2.5 Processing

Once data have been generated, it is often processed in one form or another before it is stored in nonvolatile memory or transferred to another subsystem. How the data are processed will depend on what the data are used for, the real-time performance requirements, along with the available software and hardware. For example, data that are generated and immediately transferred to the flight computer for immediate control must be as close to real-time as possible and may be processed very little. On the other hand, payload data that are generated and not immediately used might be compressed to minimize memory storage use. Several operations that may be performed on the data can now be examined to understand where these operations are normally applied to for data in flight and at rest.

First, data that are transferred between subsystems will generally be encoded in a common packet format that allows commands and data to be propagated throughout the spacecraft. For example, a subsystem may generate health and wellness data and then encode them into a packet that is then transmitted to the flight computer for analysis. When the flight computer receives the packet, it needs to verify the packets integrity, decode it, and then it can act on the data that were received.

Data and commands can be encoded into many different types of formats, but many represent some type of framed, or packetized scheme. For example, one encoding scheme that uses point-to-point communication might provide a frame sync, an operational code (OP code), data length specifier, the data to be transferred and then a packet checksum to verify the packet's integrity, similar to the encoding scheme shown in Fig. 5. An alternative encoding scheme that could handle multidrop communication might instead leverage a starting frame sync, an address scheme, an OP code, data, checksum, and then a closing frame sync, similar to the encoding scheme shown in Fig. 6.

The encoding schemes used to command and transfer data are nearly limitless, but designers should consider the hardware interface, bus speed, data size to transfer, and real-time requirements to encode the data and generate checksums or cycle

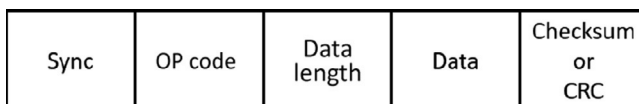


**Fig. 5** An example encoding scheme to command or transfer data for point-to-point communication.

Sync	Address scheme	OP code	Data	Checksum Or CRC	Sync
------	----------------	---------	------	-----------------------	------

**Fig. 6** An example encoding scheme to command or transfer data for a multidrop communication network.

redundancy checks (CRCs). These all need to be carefully balanced to meet system requirements. Note, many modern processors have fast, hardware support for CRC calculations, which can reduce needed resources.

Next, considerations can be made for encrypting the data. *Encryption* is typically only used on the communication link between the spacecraft and the ground station. Encryption provides a method for designers to protect their data by using an encryption key to convert their data or even their data packet into ciphertext. The only way that an entity would be able to decode the data is if they have a corresponding key. Encryption is not a guarantee that someone will not be able to decode data transmitted over RF. Designers need to ensure that they follow best practices for encryption such as a sufficiently long key and seed data that are changing in every packet, even if the packet data have not changed.

Encryption schemes can also be processing intensive. Implementing encryption should employ cryptographic hardware accelerators that are built into many modern microcontrollers and application processors. These hardware accelerators can often decrease the computing cycles required by 10–100 times. Hardware-based encryption can also simplify the software and decrease the power used during the operation.

Another process that can be performed on data is *compression*. Compression algorithms can be used to decrease the amount of storage space that a dataset will occupy. Compression is most often employed for payload data since it is typically the largest dataset generated on-board the spacecraft. When examining compression algorithms, there are two primary considerations that a designer should consider: first the compression/decompression speed, which is the number of megabytes per second (MB/s) that the algorithm can compress or decompress, and second the compression ratio, which is the ratio between the original file and the compressed file. The compression/decompression speed and the compression ratio are not necessarily in opposition, that is, just because the compression ratio is high it does not mean that the algorithm can process it quickly. Care needs to be taken to understand the trade-offs for various algorithms to balance their throughput, resultant data size, and the energy used for the process.

Finally, data that are retained may need to be cleaned or scrubbed. *Data cleaning* is the process of detecting and correcting or removing corrupt or inaccurate records from a dataset. For a spacecraft, this often pertains to the need to monitor memory locations and detect whether the data have become corrupted. Corruption could occur due to bit flips from radiation. It is particularly useful to include a CRC with data that are in memory in order to detect if the data have become corrupt in some way.

Once the data corruption have been detected, the data can be scrubbed. *Data scrubbing* is the act of detecting where the corruption is and correcting it. One technique that is often employed in spacecraft is to maintain multiple copies of critical data that is

resident in volatile memory. The data are stored in different memory locations that are not within the same memory segment. Periodically a background task will review the memory state to detect if the memory has become corrupted. If the data have corrupted, the back-up memory is tested and if its integrity is intact, then an update is performed to repair the corrupted memory.

### 3 Design considerations

An important part of the design process is developing the *architecture*, which is the distribution of data handling functions in the spacecraft. Generation is distributed by nature as data are generated throughout all subsystems. Processing and storage can be centralized or distributed depending on a variety of constraints related to the amount of data and transfer rates, as described in the preceding text. When designing any system, mapping out how data flow through and are processed in the system is absolutely critical to developing a system and software architecture that not only meets mission requirements but also provides flexibility and scalability to the design. In this section, additional tools are provided to help develop the architecture and other important design considerations.

There are four budgets to develop and analyze carefully when architecting the OBDH systems: data, processing, storage, and transfer. Each of these budgets map to the design elements described earlier. These budgets are not mutually exclusive but instead must be carefully balanced against each other to design an efficient and fully functional data handling system.

A *data budget* identifies and describes the data that are generated by each subsystem. The data budget helps designers understand what data are generated by their subsystems, how often it is generated, how much of it there will be, and determine the frequency and usefulness of that data. An example summary table is shown in [Table 4](#). The data budget provides an estimate of the amount of raw data that will be generated. These values can be tuned by adjusting sample rates and resolution at the expense of accuracy in values.

**Table 4** An example data budget for an active magnetic attitude determination and control system.

Data	Data type (bytes)	Data size (bytes)	Sample rate (Hz)	kB/s	Data per orbit (kB)
Magnetometer	2	6	2	0.012	63.3
Temperature	2	6	1	0.006	31.7
Torque current	2	6	5	0.029	158.2
Torque voltage	2	6	5	0.029	158.2
Status packet		64	0.1	0.00625	33.75

Raw, unprocessed data do not exist in this form for very long within most systems. The data are processed by the subsystems almost immediately whether it is to encode the data in a structure or compress it for storage. The data may even be generated, checked for faults, and then simply discarded. Designers can examine the data that they are generating and then list out how that data will be processed using a *processing budget*, as shown in [Table 5](#).

Notice that for the processing budget, the processing time is estimated in relation to the CPU utilization. *CPU utilization* is the percentage of time that the process is expected to take from the CPU between 0% and 100%. The CPU utilization for each data item is normalized to account for the various sample rates, data sizes and the algorithms that will be executed on the data. Designers should also keep in mind that in order for a CPU to be responsive and not overwhelmed, the target CPU utilization for all system tasks, processes, and algorithms should be approximately 70% or less. CPU utilization estimates are often highly prone to error due to coding complexity and variation and can change based on the processor architecture, execution mode, and clock speed. Estimations should be backed up with measurements during development.

Once the designer has established how much data will be generated and how it will be processed and handled, the storage budget will need to be examined. As seen earlier, there are two main storage mediums, volatile, and nonvolatile memory. If data will be stored locally in volatile memory, that data may require additional processing such as cleaning and scrubbing to ensure that its integrity remains intact (note, this was

**Table 5** An example processing budget from the active magnetic control system.

Data	Sample rate (Hz)	kB/s	Data per orbit (kB)	Process	Estimated CPU utilization (%)
Magnetometer	2	0.012	63.3	<ul style="list-style-type: none"> <li>Running average (5 samples)</li> <li>Encoded for health and status</li> <li>Logged in storage</li> </ul>	2.0
Temperature	1	0.006	31.7	<ul style="list-style-type: none"> <li>Encoded for health and status</li> </ul>	0.1
Torque current	5	0.029	158.2	<ul style="list-style-type: none"> <li>Encoded for health and status</li> </ul>	0.1
Torque voltage	5	0.029	158.2	<ul style="list-style-type: none"> <li>Encoded for health and status</li> </ul>	0.1
Status packet	0.1	0.00625	33.75	<ul style="list-style-type: none"> <li>Transferred to flight computer, stored in nonvolatile memory log</li> </ul>	5.0



not included in Table 5). If data will be stored in nonvolatile memory, the data may need to be compressed before storing.

The *storage budget* enables development of storage requirements for a system. It captures what data will be stored and the length of time for storage, which allows the required storage capacity for the subsystem or spacecraft to be determined for the entire mission. The storage budget also specifies the lifetime for the data stored, which is the amount of time the data will reside in storage before it is deleted. Missions that downlink data often, or at a high rate will be able to free storage capacity, which will decrease the total storage required for the mission.

The storage degradation rate should also be considered. Nonvolatile memory, such as flash memory systems, typically degrades out after a specified number of read/write/erase cycles. Some flash media will automatically perform wear leveling to try and maximize the storage media useful life and minimize degradation. The degradation or failure rate for a generic storage device can be calculated using the following procedure:

1. Based on the processing and generation rates, calculate the amount of read writes associated with the data.
2. For a given storage medium, determine the limits on reading/writing. (Note also that storage has a read/write speed which limits access rates as well.)
3. Develop a concept of operation that allots the budget to various storage elements.
4. Review the storage medium specifications for maximum read, write, and erase cycles.
5. Ensure that not only the expected read/write/erase cycles are less than the specifications but also there is at least a 20% buffer.

Storage degradation is not the only issue to consider. The storage media may fail as well and backup strategies are necessary to continue the mission during the presence of failures.

The *transfer budget* examines several different transfer mechanisms to ensure there is enough bandwidth to move data around subsystems and the spacecraft effectively. First, there is a transfer budget within a subsystem to transfer data from sensors into volatile memory and then into any nonvolatile storage. Next, there is a transfer budget for transferring data between subsystems. Finally, there is a transfer budget for the data to go from the spacecraft to the ground. The mission concept of operation governs how and when these transfers occur. Thus a full systems perspective is needed to budget data transfer appropriately to meet mission requirements.

These budgets are not mutually exclusive. They are interdependent and must be optimized together in order to maximize the amount of data that can be downloaded to the ground. Increasing the amount of data generated will affect the processing budget. It may also affect the storage and transfer budget as well.

A useful set of properties to consider when designing a data handling system are atomicity, consistency, isolation, and durability. Collectively, these are known as ACID [5], and they were derived during the development of databases. *Atomicity* means that the transaction completely succeeds or completely fails. *Consistency* ensures that the data will be valid. *Isolation* ensures that all transactions are isolated and will not affect others. *Durability* means that even if a failure occurs, the

transaction will still remain. Implementations of these transactions in a data handling system will promote robust operation.

At first, this might all seem overwhelming, but designers do not need to start from scratch; there are a variety of standards to review and consider for data handling. For example, the Consultative Committee for Space Data Systems (CCSDS) publishes a wide range of standards including spacecraft on-board interface services. Standards such as IP-based protocols from the Internet can also be used. These can provide design architectures with example code and existing solutions that ensure a shorter development time and a more robust solution.

There are other system-level considerations that are not covered in detail, for example, power usage. There are trade-offs between the processing technology used on a subsystem with the available energy for a mission. The more data that are available to be transferred or processed, the higher the power usage will be for the system. The power budget should be used to guide the design of the data handling system as well.

In summary, design can be guided by seeing this as an optimization process; the goal is to optimize data downloaded. To achieve this optimization, designers trade-off between the amount of data they generate, store, process, and transfer based on the overall mission objectives and available power budget.

## 4 Design example—RAX

As an example, consider the Radio Aurora Explorer (RAX) mission, a partnership by SRI International and the University of Michigan [6]. The primary mission of RAX was to study the polar ionosphere and the plasma irregularities that develop along the magnetic field lines. Measurements were made with a bistatic radar system; see Fig. 7. A ground radar illuminated the ionosphere and RAX received the signal scatter from the irregularities. Two satellites were launched: RAX-1 on November 19, 2010 on-board a Minotaur-IV rocket from Kodiak, Alaska, and RAX-2 on October 28, 2011 on-board a Delta-II rocket from Vandenberg US Air Force Base, California. RAX-2 detected and measured irregularities during multiple experiments over Alaska and Canada (Fig. 8).

RAX captured the “spirit” of many early CubeSat missions; a novel science mission with limited funding and an aggressive schedule centered in a university research environment. It was the first nanosatellite mission funded by the US National Science Foundation to study space weather [7]. Beyond the science the mission itself was an experiment to see if the constrained CubeSat platform could be used for novel, science measurements. The schedule was aggressive, with only 12 months from start to delivery for launch of RAX-1. Funding was constrained to US\$ 900K for payload and satellite development. These constraints encouraged creative, higher-risk solutions to perform the radar science mission.

The data handling requirements for RAX were driven by the payload radar receiver. It generated 32Mbps of data; its output was 16 bits wide, clocked at 1 MHz with data on each clock edge. Each radar experiment lasted approximately 5 minutes with a science goal of one experiment per day. Thus 1.2GB were generated

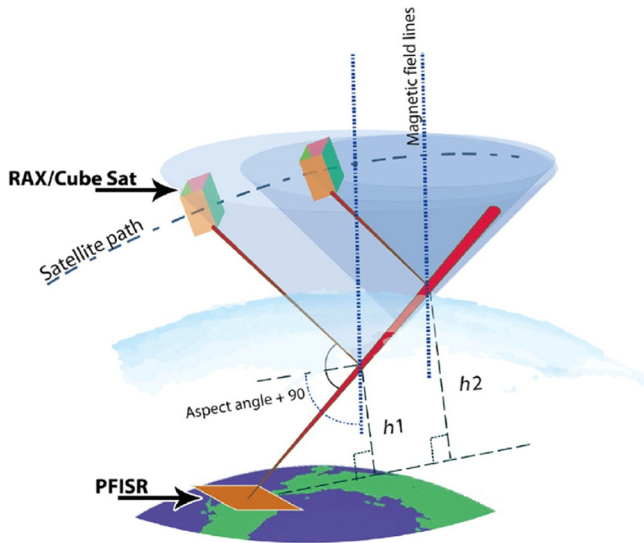


**Fig. 7** The radar experiment performed by the RAX mission.

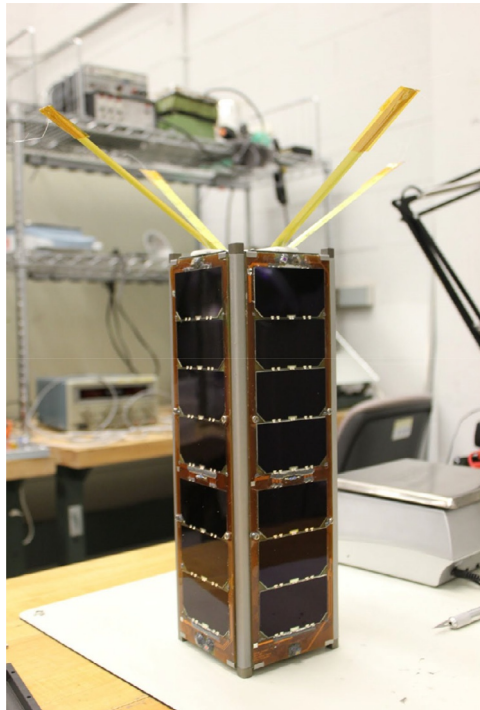


**Fig. 8** The RAX-2 CubeSat.

per day. The set of driving requirements and constraints for RAX are summarized in the following text:

- (1) Collect data at 32Mbps, store it, and process 1.2GB per day.
- (2) Time tag data to better than 20  $\mu$ s.
- (3) Limit system size to a 3U CubeSat.
- (4) Meet the aggressive schedule and funding constraints.

At RAX design time, there were no off-the-shelf CubeSat processor systems that could handle the payload data requirements. Thus the team developed a distributed architecture to leverage existing capabilities when possible and use custom developed systems when needed, which is shown in Fig. 9. The system consisted of a specialized payload interface that collected and stored high speed payload data and provided an interface to embedded processor-based flight computer.

The RAX OBDH architecture is shown in Fig. 10. Processing and data storage were distributed through the satellite to provide a flexibility and redundancy. Each of the subsystems is described in detail in the succeeding text.

A custom *payload interface module* (PIM) was developed to collect and store data from the receiver and provide access to the data to other computing elements of the

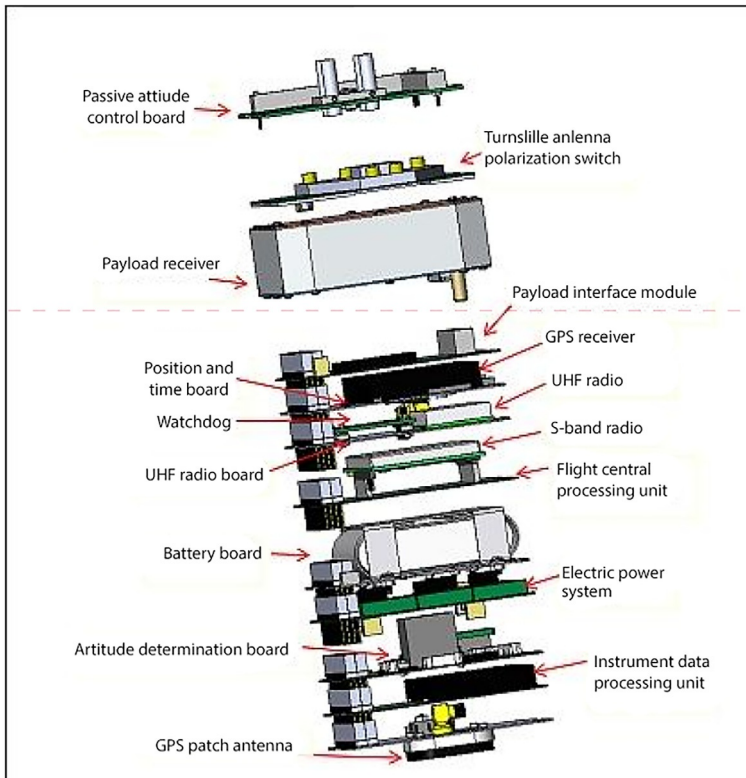
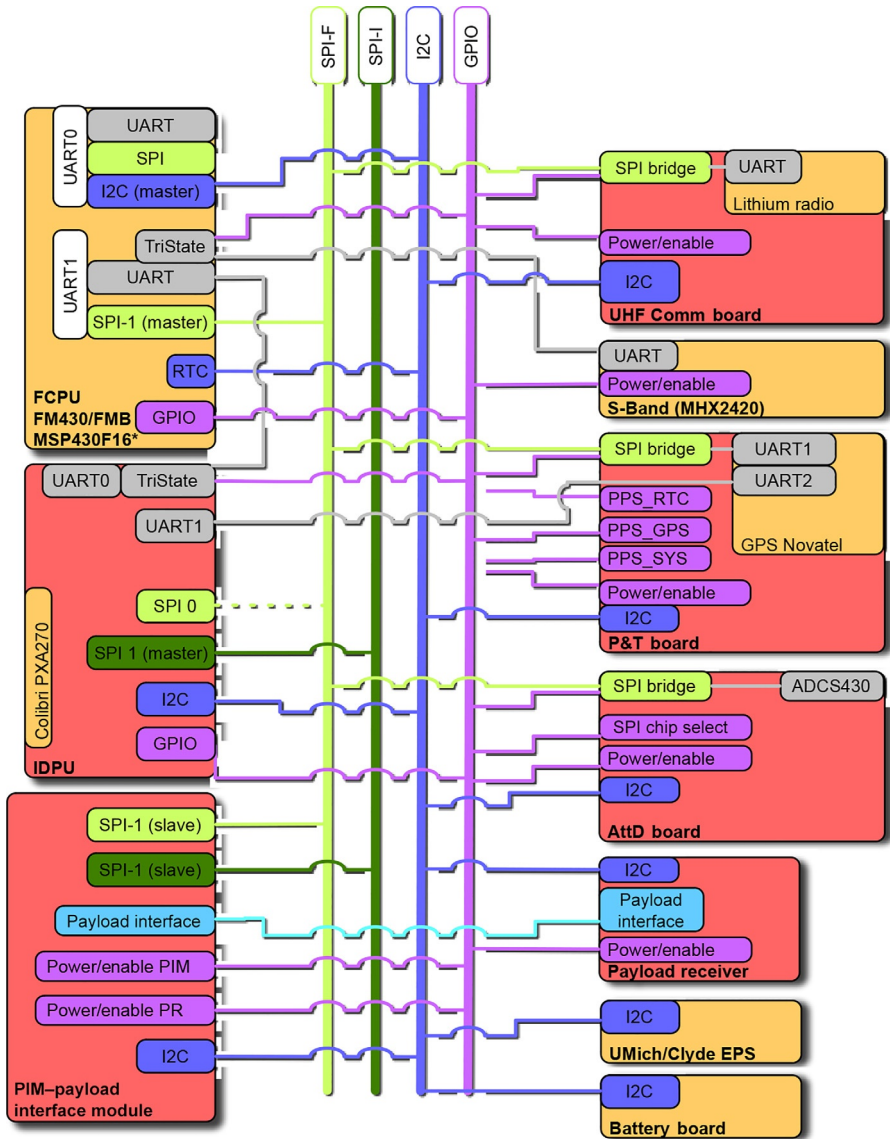


Fig. 9 The RAX board stack.



**Fig. 10** The RAX OBDH architecture.

system. The PIM contains a gate array clocked at approximately 50 MHz. The frequency is slightly lower than 50 MHz to prevent electromagnetic interference from 50 MHz harmonics appearing in the science data. Data were stored to 4 GB of mirrored flash memory bank and packetized with checksums and time tags inserted based on timing and pulse-per-second output from the position and time system. The interface module is accessible by both the flight computer and the instrument data processing

unit through dual SPI busses. It provides a shared storage system to enable large file transfer between the flight computer and the processing unit. The processing unit retrieves payload data from the interface module and copies processed data back to it. The flight computer retrieves these files and stores them on flight-computer-based storage for later downlink. In a similar manner, files are transferable from the flight computer to the processing unit to enable code updates on the processing unit.

The *instrument data processing unit* (IDPU) processes radar data to reduce downlink requirements. On-board processing sorts through time series receiver data stored on the payload interface module and extracts data with radar pulses of interest. The segmented data are then processed with radar analysis code to calculate signal-to-noise ratios and range delays. The processing unit then stores the data on the payload interface module for downlink by the flight computer to the science operations center. It also has direct interface to the GPS unit for enhanced configuration and monitoring of GPS performance.

The *flight computer* (FCPU) was a low-power embedded processor system based on the Texas Instruments MSP430 microprocessor and was developed internally by the RAX team. It performs typical flight computer functions such as telemetry collection, ground command processing, experiment sequencing, scheduled command execution, data storage, and communication through the radio systems. An integrated secure digital (SD) card provides 2 GB of data storage. Custom SD-card drivers were written because off-the-shelf libraries were too large in terms of code space; the libraries would not fit on the MSP430 with the other flight-specific code. An external watchdog timer system provided fault detection and recovery of flight computer transient failures [8]. The watchdog monitors a heartbeat signal from the computer and reboots it if a failure is detected. It can also be commanded from the ground through the UHF radio to force power resets of the flight computer. The watchdog itself is periodically power cycled by a 555-timer circuit to clear any internal transient errors. Flight software was custom written for RAX in C and ran on the Salvo operating system [9]. All available code space was used.

The *position and time system* (PTS) provided spatial and temporal information for the satellite to improve resolution of the irregularities and their fine scale features. The primary position and time source was an on-board GPS receiver. Detailed simulations of proper antenna placement in the context of the attitude control scheme were performed to estimate expected on-orbit performance [10]. A secondary timing system, based on a real time clock, provides time synchronization when GPS is not available, such as during planned GPS power off for energy conservation. The clock provides millisecond accuracy and maintains time during satellite reboots and resets. A pulse-per-second signal, sourced by either the GPS or the clock, is distributed throughout the satellite to synchronize data collections. The payload interface module and attitude determination system then use the signal to time tag data collections. A secondary ground-based position determination system uses publicly available two-line element sets published by the US government. Two-line element-based position error is expected to be less than 1 km within several days after the element set epoch [11].

The FCPU coordinated serial connections to all subsystems. It has minimal processing capability and data storage. Telemetry measurements are made throughout

the satellite with I2C enabled ADCs. It is collected by the FCPU and stored on SD-cards. SPI, I2C, and UARTs are used for communication. Point-to-point links were made with UARTs. The I2C bus was used for distributed telemetry collection. The SPI bus was used for high speed, point to point links. The FCPU configures the system for payload data collecting. It enables the payload to take data and commands the PIM to collect data. When the data collection is over, the FCPU commands the IDPU to copy data from the PIM, which is stored on the IDPU flash storage. The IDPU then processes the data. The FCPU transfers the processed data for storage until downlink to ground occurs.

The FCPU system on the RAX CubeSat's completed its mission to record, process, and download the payload data. The specialized PIM and IDPU provided the proper transfer rate and computational abilities. Redundancy in the storage capabilities allowed for multiple data storage configurations that prolonged mission flight in the presence of component failures.

## 5 Emerging trends

The emergence of CubeSats as a viable tool for scientific measurements is leading to increased innovation for on board data handling systems. Despite the inherent constraints imposed by the CubeSat form factor, many CubeSat missions have advanced OBDH systems due to their risk posterior; given cost and schedule pressure, the missions accept higher risk, more capable processing systems. There are several emerging trends that are increasing CubeSat OBDH capabilities:

*Parallel processing*—As processing systems decrease in physical size, missions are leveraging multiple processors for a variety of parallel processing applications. Computer on modules (COMS) provide off-the-shelf computers that can be parallelized into complex computing platforms [12]. Multicore processors provide on-chip parallel processing opportunities. For example, a low-power, real-time core can be used for continuous monitoring and low-level details. When an event of interest occurs, the second core can be woken up to increase processing capabilities and later return to a low power mode.

*Advanced coprocessors*—As processor technology advances, customized processing is available for specific computation needs. Graphical processing units (GPUs) are used terrestrially to provide high speed imaging processing capabilities. These capabilities are being deployed in mobile technology to provide advanced facial recognition and image enhancements. Field programmable gate arrays (FPGAs) provide software configured hardware, which runs faster than general purpose architectures but not necessarily as fast as custom processing [13]. Many FPGAs are capable of in-flight reprogramming to enable algorithmic upgrades.

*Edge computing*—The location of processing is a design variable. Recently, *orbital edge computing* has addressed the location of computational capabilities within low-Earth orbiting networks [14]. As intersatellite links improve, CubeSats will be able to share and distribute processing to other nodes in the network.

*Hypervisors*—Operating systems (OS) can be decoupled from hardware through virtualization. Hypervisors virtualize the hardware and provide a common, abstract hardware interface to the OS. This allows *virtual machines* to be run on distributed, heterogeneous hardware [15]. They can be used for fault tolerance and recovery as well [16].

*Advanced algorithms*—Machine learning (ML) techniques are being used to improve data management and processing. ML has been used to automatically detect events of interest and enable advanced data collection [17]. Future algorithms can be used to identify additional interesting or unexpected features in data. These capabilities should reduce required data download and latency of event detection.

These advancements are leading to novel OBDH systems for CubeSats that are providing enhanced capabilities and greater fault tolerance.

## References

- [1] A. Grami, *Introduction to Digital Communications*, Academic Press, 2016, .pp. 217–264. <https://www.elsevier.com/books/introduction-to-digital-communications/grami/978-0-12-407682-2>.
- [2] J.L. Hennessy, D.A. Patterson, *Computer Architecture: A Quantitative Approach*, Elsevier Science, Netherlands, 2017.
- [3] JEDEC, eMMC 5.0 Specification (JESD84-B50), Available from: [www.jedec.org](http://www.jedec.org), September 2013.
- [4] S. Nydam, J. Anderson, N.S. Barnwell, J. Peace, F. Pistella, T. Ritz, S. Roberts, et al., A compact optical time transfer instrument for ground-to-space synchronization of clocks, in: *AIAA SPACE and Astronautics Forum and Exposition*, 2017, p. 5381.
- [5] J. Gray, Why do computers stop and what can be done about it? in: *Symposium on Reliability in Distributed Software and Database Systems*, 1986, pp. 3–12.
- [6] H. Bahcivan, J.W. Cutler, Radio aurora explorer: mission science and radar system. *Radio Sci.* 47 (2) (2012) RS2012, <https://doi.org/10.1029/2011RS004817>.
- [7] T. Moretto, CubeSat mission to investigate ionospheric irregularities. *Space Weather* 6 (11) (2008)<https://doi.org/10.1029/2008SW000441>.
- [8] J. Beningo, *A review of watchdog architectures and their application to Cubesats*, Beningo Embedded Group, Linden, MI, 2010.
- [9] A.E. Kalman, Overview of the CubeSat Kit™, in: *Proceedings of the 18th Annual AIAA/USU Conference on Small Satellites*, Logan, USA, 2004.
- [10] S. Spangelo, A. Klesh, J. Cutler, Position and time system for the RAX small satellite mission, in: *AIAA/AAS Astrodynamics Specialist Conference*, 2010, p. 7980.
- [11] D. Oltrogge, A.G.I. Ramrath, A.G.I. Jens, Parametric characterization of SGP4 theory and TLE positional accuracy, in: S. Ryan (Ed.), *Proceedings of the Advanced Maui Optical and Space Surveillance Technologies Conference*, Wailea, Maui, Hawaii, September 9–12, The Maui Economic Development Board, 2014 id.E872014. <https://ui.adsabs.harvard.edu/abs/2014amos.confE..87O/abstract>.
- [12] J.R. Samson, Update on dependable multiprocessor CubeSat technology development, in: *2012 IEEE Aerospace Conference*, IEEE, Big Sky, MT, USA, 2012, pp. 1–12. <https://ieeexplore.ieee.org/abstract/document/6187238>.
- [13] D.L. Bekker, T.A. Werne, T.O. Wilson, P.J. Pingree, K. Dontchev, M. Heywood, R. Ramos, et al., A CubeSat design to validate the Virtex-5 FPGA for spaceborne image processing, in: *IEEE Aerospace Conference*, IEEE, Big Sky, MT, USA, 2010, pp. 1–9.
- [14] B. Denby, B. Lucia, Orbital edge computing: machine inference in space, *IEEE Comput. Archit. Lett.* 18 (1) (2019) 59–62.
- [15] P. Barham, B. Dragovic, K. Fraser, S. Hand, T. Harris, A. Ho, R. Neugebauer, I. Pratt, A. Warfield, Xen and the art of virtualization, *ACM SIGOPS Oper. Syst. Rev.* 37 (5) (2003) 164–177.



- 
- [16] D. Lucchetti, S.K. Reinhardt, P.M. Chen, ExtraVirt: detecting and recovering from transient processor faults, in: Proceedings of the Twentieth ACM Symposium on Operating Systems Principles, 2005, pp. 1–8.
  - [17] S. Chien, R. Sherwood, D. Tran, B. Cichy, G. Rabideau, R. Castano, A. Davis, et al., Using autonomy flight software to improve science return on Earth Observing One, *J. Aerosp. Comput. Inf. Commun.* 2 (4) (2005) 196–216.

# Telemetry, tracking, and command (TT&C)

11

Alessandra Babuscia and Krisjani Angkasa

Jet Propulsion Laboratory, California Institute of Technology, Pasadena, CA, United States

## 1 Introduction: Key factors to consider when designing TT&C for CubeSats

SmallSats and CubeSats are subject to very stringent constraints in mass, power, and cost. Hence, in designing the telecommunication system, it is especially important to be aware of the key factors that can affect the design. Specifically, these are the following:

- *Spacecraft data generation, buffering, and computational power of the avionics:* it is important to quantify as early as possible in the design the amount of data to transmit, since this can significantly affect the design. Sometimes the amount of data will be given to the communication system designer, while in some cases it will be necessary to compute it using the information available such as number of sensors, type of sensors, amount of information (bits) acquired over time, and number of pictures. When the amount of data is computed, it is important to analyze the computational capabilities of the onboard avionic and whether or not it can implement some form of compression. Processors for SmallSats and CubeSats [1] are currently capable of significant data processing on board with limited power consumption. Hence the designer should explore all these possibilities whenever the initial estimate of the amount of data to transmit appears to be high. Finally, it is important to quantify the buffering capacity of the avionics to compute the optimal data rate that should be as low as possible to minimize power consumption but sufficient to relay all the data.
- *Electrical power system:* many of the CubeSat radios can consume a significant amount of power, even if just powered in receiving mode. Hence the designer of the communication system will evaluate the required power for the radio and the transmission time required to download the data.
- *Ground stations availabilities and characteristics:* different types of ground stations are used to support CubeSat missions: university stations, commercial networks, and stations managed by space agencies. University stations are mostly operating in UHF/VHF and S band [1]. They are generally low cost, with very minor scheduling constraints, but they suffer from limited geographic diversities (they are generally in very few locations), covering only a small portion of the satellite orbit with very limited passes. The commercial alternatives and the stations supported by space agencies present different characteristics. They offer multiple frequency bands (UHF, L, S, X, Ku, and in certain cases, Ka) allowing the designer to trade across the different alternatives. They are generally more reliable, and they can offer higher gains and lower noise temperature, thanks to powerful cooling equipment that can result in a considerable improvement of the link performance. Disadvantages of

these kinds of stations are mainly cost and availability as they generally support multiple missions at the same time.

- *Range and pointing capabilities*: free-space loss scales quadratically with the distance. Hence, closing the link with adequate margin is challenging for CubeSats, especially on interplanetary trajectories and considering the limitations in volume, mass, and power that inevitably constrain the type of antennas or amplifiers that can be used. Another important issue for CubeSats is pointing capabilities especially for higher gain antennas.
- *Spectrum and licensing*: especially for low Earth orbit missions in which the link can be closed at higher data rates (in the order of Mbps), it is important to remember that the final bottleneck in the effective data rate will be determined by how much bandwidth the CubeSat is legally allowed to use. For example, NTIA restricts the bandwidth to be 5 MHz or less for S-band telecommunication systems and 10 MHz or less for X-band telecommunication systems.

## 2 Telecommunication system design

This section describes a typical process of modeling and designing a communication system for a SmallSat mission. The key aspect of the process is the fact that it is iterative: this is due to the peculiar constraints that distinguish SmallSats and CubeSats from other kind of missions. In fact, as mentioned previously, small satellites differ from other missions in the computational capabilities, power availability, ground station characteristics, and limited range and pointing capabilities. Hence, to optimize the design, it is necessary to consider all these factors while trying to maximize the data return. An overview of the approach is presented in the following block diagram. The following subsections are dedicated to the different aspects of the approach (Fig. 1).

### 2.1 Requirements

The first step in the communication system design approach is the analysis of the requirements to identify all the constraints that cannot be changed or that can be changed with corresponding cost increases or reduction of mission objectives. The requirements considered in this section are the most commonly experienced [2] in the design of the communication system for small satellites:

- *Data volume*: it is important to estimate early on in the design process the amount of data to be transmitted. The requirement impacts small satellite missions heavily especially when a lot of images are transmitted: in these cases, techniques of compression are considered. It is also important not to forget that engineering data need to be transmitted as well. Fig. 2 shows an overview of the spacecraft downlink data flow.
- *Ground station*: in some cases, the ground station is selected independently from the design of the communication system. In other cases a trade-off can be performed considering metrics such as station locations, availabilities, frequency compatibility with the spacecraft, geometry, and passes duration.
- *Orbit*: in many cases, small satellites are launched as secondary payloads, and the orbit is determined by the primary mission. In these cases the orbit cannot be changed, and as an additional challenge, the orbit is generally unknown for a long time during the design phase.

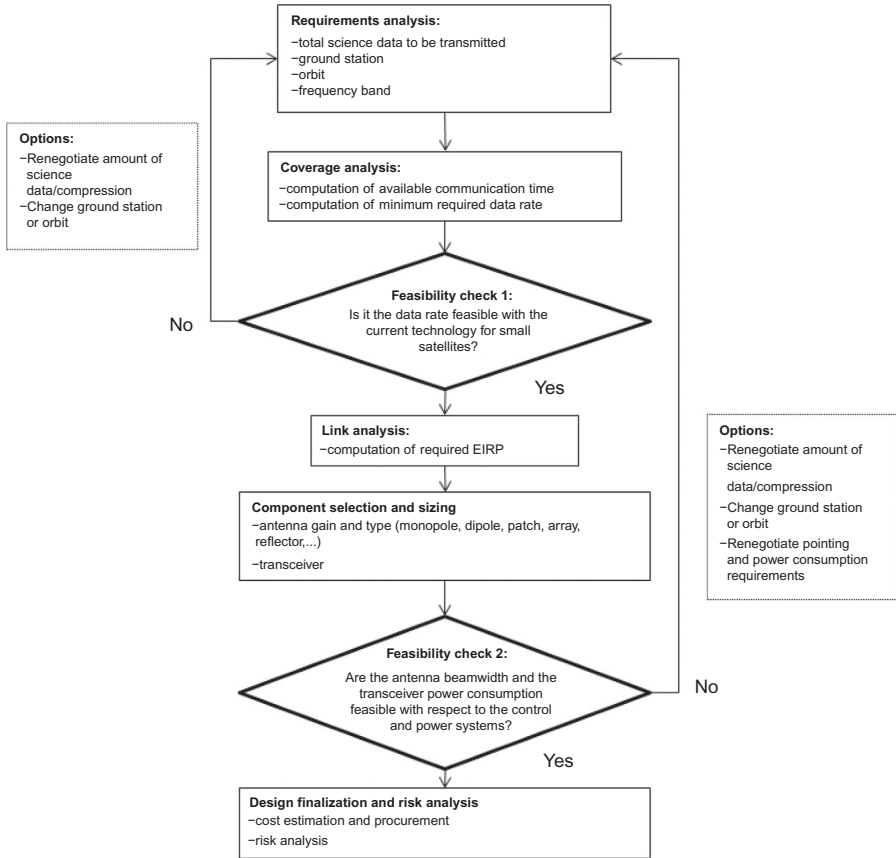


**Fig. 1** Summary of the iterative process for designing a communication system for small satellites.

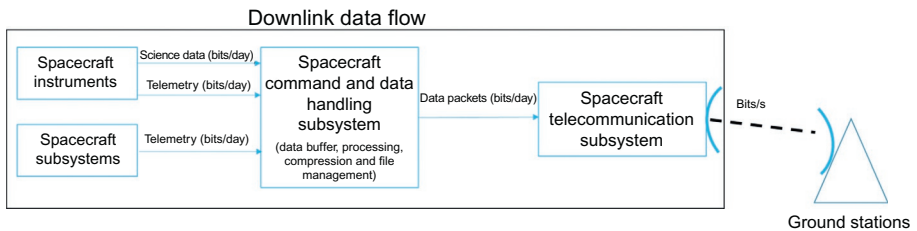


**Fig. 2** Downlink data flow.

In some cases, altitude and inclination may be known; in some case, not even these data are available. The uncertainty of the orbit represents one of the biggest challenges for the designers of the communication system.

- *Frequency*: especially in the cases in which the ground station has already been selected, it is very common to face restrictions on which frequencies can be used. Additionally, constraints

on licensing can limit the choices in terms of band. Specifically, bands allocated for near-Earth spacecraft (any spacecraft at a distance of less than 2 million of kilometers from Earth) are different from those allocated for deep space spacecraft that can affect hardware selections.

When requirements are identified, a coverage and a link analyses for the mission can be performed.

## 2.2 Analysis

Two main analyses are performed when designing the telecommunication system: coverage and link. Coverage analysis is the first computational step in the design of the communication system, and it can be performed early on, as it depends mostly on ground station selection and orbit. Other factors can impact the coverage time, such as antenna directionality, pointing, ground station scheduling, and synchronization. However, for a first cut analysis of the communication system for small satellites, coverage can be considered a geometric problem assuming that ground station availability is not an issue; this is the case when a university ground station is used, especially when it is operating only one mission at the time. In that case, no conflicts with other missions or scheduling problems will arise, and the ground station will be able to communicate with the satellite whenever it is in visibility. If coverage is treated as a geometric problem, then simple orbital calculations can allow the designer to compute the coverage time and to compute the minimum required data rate. The steps are described in the succeeding text.

- Set up an orbital simulation: this step can be accomplished by using a commercial software [3] or by writing a simple code that uses basic astrodynamics equations [1]. The simulation should include the orbit of the satellite and the location of the ground stations. It should be noted that different orbits can provide different telecommunication characteristics. For example, a geostationary satellite positioned directly over the country of Ecuador will give users in that country 100% temporal coverage. Differently a polar-orbiting spacecraft will allow for good coverage around the polar regions, while worst coverage will be around the equator. Hence, if a particular orbit is not already selected, the optimal orbital characteristics for a particular satellite should be studied prior to designing the telecommunication system for the mission.
- Compute the coverage profile: the coverage profile is binary graph that indicates for any instant of time whether the satellite is in coverage or not. The mathematical formulation is

$$c(t) = \begin{cases} 1 & \text{if sat is covered} \\ 0 & \text{if sat is not covered} \end{cases} \quad (1)$$

- Create a data cumulating function: in prime approximation, it can be a linear function. If we define  $D$  as the total amount of data to be transmitted per day, the amount of data cumulated in function of time (bit/s) can be approximated by

$$f(t) = \frac{D}{86,400} \cdot t \quad (2)$$

- Compute the amount of data download over time to determine the minimum required data rate: in this last step the coverage profile and the data cumulating function are used to identify how much data rate is required to transmit the required amount of data. The approach is iterative. The algorithm starts with an initial data rate  $r(t)$ , which is increased or decreased depending on the result of the computation. The algorithm works as follows: for any instant of time, if the coverage function is zero, data are cumulated in the buffer ( $b(t) = b(t-1) + f(t)$ ). If coverage is one, data are cumulated, but they are also transmitted at a speed given by the data rate ( $b(t) = b(t-1) + f(t) - r(t)$ ).

The algorithm produces a triangular shaped plot where the data are cumulated for every instant of time in which there is no coverage (increasing ramp), while data are downloaded for every instant in which there is coverage. This plot provides the following information:

- (a) The peak of the triangles indicates how much data will be cumulated over time before a download, which helps to size the buffer memory required for the avionics.
- (b) Every time the amount of data stored reaches zero, it means that every data collected have been successfully downloaded. It is important to ensure that the data storage plot goes periodically to zero, otherwise the data rate  $r(t)$  needs to be increased, and/or the data cumulation  $f(t)$  needs to be decreased to ensure a complete download of mission data.

Link analysis follows coverage analysis in the design. It uses the data on ground station, orbit, and data rate to determine the minimum EIRP for the SmallSat. Link analysis needs to be computed for both downlink and uplink. However, it is generally recommended to start from the downlink that is key to estimate the kind of communication equipment that will need to be carried by the satellite. The steps are as follows:

- Computation of the quality requirement  $\left( \left( \frac{E_b}{N_0} \right)_{\text{required}} \right)$ : depending on which type of modulation is selected and on the bit error rate (BER) probability desired, a minimum  $E_b/N_0$  can be computed [1].
- Computation of the ground station gain: the gain can be obtained directly by contacting the agency/company/team responsible for the stations, or it can be computed for a parabolic dish as ( $D$  is the diameter,  $\eta$  is the efficiency, and  $\lambda$  is the wavelength):

$$G_r = \eta \left( \frac{\pi \cdot D}{\lambda} \right)^2 \quad (3)$$

- Computation of the noise temperature: it is the sum of two components, the antenna noise and the internal (receiver) noise. The antenna's noise temperature is the thermal noise that originates from objects within the field of view of the antenna. The formula ( see Ref. [1]) is the following:

$$T_A = \frac{1}{4 \cdot \pi} \iint T(\theta, \varphi) \cdot D(\theta, \varphi) \cdot \sin(\theta) \cdot d\theta \cdot d\varphi \quad (4)$$

However, since it can be difficult to identify the distribution of the noise temperature across the space ( $T(\theta, \varphi)$ ), the antenna noise temperature is often measured

experimentally. Data on the noise temperature for the Deep Space Network (DSN) ground stations can be found in Ref. [4]. The internal (receiver) temperature depends mostly on the technology of the receiver. Generally, receivers are characterized by the noise figure  $NF$ :

$$T_r = 290 \cdot \left( 10^{\frac{NF}{10}} - 1 \right) \quad (5)$$

- Computation of free-space loss at maximum distance ( $d$  measured in the same units as  $\lambda$ ) as:

$$L_{d_{\max}} = - \left( \frac{4 \cdot \pi \cdot d}{\lambda} \right)^2 \quad (6)$$

- Computation of additional losses: a nonexhaustive list of these losses is as follows:
  - (a) Pointing losses experienced as a result of not precise pointing: Pointing errors can be static due to misalignments or variables. They can be approximately computed as:

$$L_p = -12 \cdot \left( \frac{e}{\theta} \right)^2 \quad (7)$$

where  $e$  is the pointing offset in degree and  $\theta$  is the antenna beam width in degree.

- (b) Atmospheric losses ( $L_a$ ): ionospheric losses (generally insignificant above 1GHz and very little impact in the UHF Band [1]) and tropospheric losses due to rain, oxygen, and water vapor (they are negligible for UHF frequency, and they cause fractions of dB of attenuations in the S band. Tropospheric losses start causing significant attenuation for frequencies above 10GHz). A summary of tropospheric losses can be found in Fig. 3. The reader can also find additional information in Ref. [5].
- (c) Line loss: caused by cables. If the length of all the cables is known ( $l$ ) and also the coefficient of attenuation, then line loss results:

$$L_l = -\alpha \cdot l \quad (8)$$

- (d) Modem implementation losses (spectral efficiency): these depend on modulation, coding, and roll-off. The most basic modulation scheme is binary phase-shift keying (BPSK): information is coded using two phase states per symbol that corresponds to 1 bit of information per symbol. Higher-order modulations are quadrature phase-shift keying (QPSK), 8 phase-shift keying (8-PSK), 16-PSK, and more. The advantage of higher-order modulation schemes lies in their spectral efficiency, since they can encode more bits per symbol (QPSK encodes 2 bits per symbol, 8-PSK 3 bits per symbol, and 16-PSK 4 bits per symbol). However, as the modulation order increases, the sensitivity to phase-induced errors also increases. A key parameter in the modulation is the number of bits per symbol for the specific encoding scheme used ( $m$ ). In addition to modulation, the use of forward error correction (FEC) coding is the idea of adding redundant bits that can be used to improve the ability of the receiver to correct bit errors. The redundant bits not only improve reception and correction but also can affect spectral efficiency. The coding efficiency can be computed as [1]:

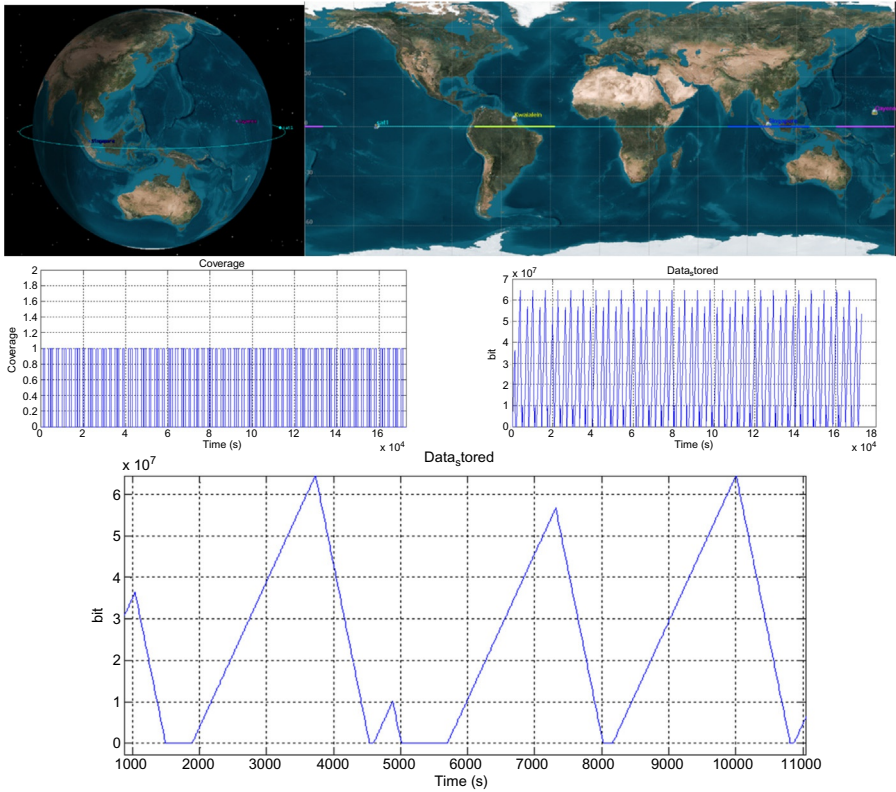


**Fig. 3** Tropospheric attenuation [5].

$$k = \frac{n}{n + r} \tag{9}$$

where  $n$  is the number of information bits and  $r$  is the number of redundant bits added as a result of the specific coding scheme adopted. Roll-off factor ( $\rho$ ) is the amplitude of the filters used to minimize interference across adjacent frequency bands. Spectral efficiency is [1]:

$$L_e = -10 \cdot \log_{10} \left( \frac{m}{k \cdot (1 + \rho)} \right) \tag{10}$$

- Computation of the minimum required EIRP: when all the previous elements have been computed, it is possible to calculate the minimum required EIRP, using the following formula:

$$EIRP_{\min} = \frac{E_b}{N_{0\text{Required}}} + M - L_{d_{\max}} - L_p - L_a - L_l - L_e - G_r - 228.6 + 10 \cdot \log(T_s) + 10 \log(R_{\min}) \tag{11}$$



The formula provides the EIRP in dBW as described in Ref. [1].  $R_{\min}$  indicates the minimum data rate, and  $M$  is the margin on the communication system, which is generally (rule of thumb) at least 3 dB.

### 2.3 Components selection and design finalization

Component selection is the process in which the designer selects COTS or custom-made components to reach the EIRP estimated through link analysis. Specifically the designer needs to pick at least an antenna and a transceiver (amplifiers are sometimes incorporated in the radio assembly). Additional antennas and transceivers for redundancy are generally not used for SmallSats and CubeSats, due to the volume and mass constraints. More information on components are included in the next section.

The last step in the design of the communication system is to finalize the design by performing cost estimation and risk analysis. The cost estimation can be basically broken into two main categories: components and labor. The estimation of the hardware cost can be easily performed when products are available on the market. More complex is the case in which the component needs to be fabricated. Labor cost is challenging to estimate, and it varies widely depending on the organization performing the work. Data on previous missions should be used if possible, to refine the estimates. A detailed analysis of cost modeling is beyond the scope of this chapter. The reader can find more in numerous reference documents; a good reference to start with is the new Space Mission Analysis and Design [1].

Regarding risk analysis, it is the process of estimating the risk that a given design will exceed mass and power consumption constraints over the temporal evolution of the design. Risk analysis [6] can be performed using two types of statistics: data and expert. To develop data statistics, it is necessary to create a database of already developed components. Until a few years ago, this was a great challenge in the field of small satellites, because very few components existed. However, in recent years, the development of SmallSats and CubeSats caused a great development of new products and components. Regarding expert statistics, it is important to take into account that SmallSats and CubeSats are still new in the engineering community. Hence, it is necessary to pay attention in selecting the expert statistics to reference to avoid over-estimation issues caused by engineers that are accustomed to work on larger spacecraft.

## 3 Telecommunication components for CubeSats

This section provides an overview of the main telecommunication components for CubeSats. The components presented are not meant to be an exhaustive list as this is an active field of research and new components are continuously being developed.

### 3.1 Antennas

The most common CubeSat antennas are low gain: monopole, dipoles, and patches [7]. The main characteristics of the antennas are summarized in Table 1.

For interplanetary missions, medium-gain antennas (MGA) and high-gain antennas (HGA) are in most cases necessary, due to the longer distances and higher free-space losses. MGA and HGA tend to be selected on CubeSats, which are at least six CubeSat units as the volume and side surfaces allow for their accommodations. MGAs for CubeSats are typically at X band, and they are generally designed as arrays of patches, which can fit on one of the  $20 \times 30$  cm sides [8]. Typical MGAs are  $4 \times 4$  and  $8 \times 8$  elements. CubeSats HGA are generally at X band or Ka band, and they are mostly reflectarrays, mesh reflectors, or inflatables [8]. Characteristics are summarized in Tables 2 and 3 for MGA and HGA, respectively.

### 3.2 Radios

Commercial transceivers are currently available for SmallSats and CubeSats from a variety of vendors. These products mostly operate at UHF and S band, and they support data rates that range from a few kilobits per second to a few megabits per second. The main characteristics of some of these transceivers are summarized in Table 4 (NA indicates that data are unavailable). It is important to notice that depending on the type of mission (deep space vs near Earth), the frequency regulations limit the frequency

**Table 1** Typical low-gain antennas for SmallSats and CubeSats.

Antenna	Typical band of operation	Typical gain (dBi)	Typical half power beamwidth	Polarization	Typical volume	Typical mass (g)
Monopole	Mostly UHF/VHF It can be used also in S band	0–3	Omni	Linear or circular	$10\text{mm (diam)} \times \lambda/4$	<20
Dipole	Mostly UHF/VHF It can be used also in S band	0–3	Omni	Linear or circular	$10\text{mm (diam)} \times \lambda/2$	<30
Patch	S band and X band	5–8	60 degrees	Linear or circular	$10 \times 10 \times 0.1$ cm (S band) $5 \times 5 \times 0.1$ cm (X band)	<50

**Table 2** Typical medium-gain antennas for CubeSats.

MGA	Typical band of operation	Typical gain (dBi)	Typical half power beamwidth (degrees)	Typical volume	Typical mass (g)
4 × 4	X band	11	~26	10 × 10 × 0.1 cm	<50
8 × 8	X band	23	~7	20 × 20 × 0.1 cm	<200

**Table 3** Typical high-gain antennas for CubeSats.

HGA	Typical band of operation	Typical gain	Typical half power beamwidth	Typical volume	Typical mass (kg)
Reflectarray	X band and Ka band	29.2 dBi for 60 × 30 cm array at X band [8] 26 dBi for 30 × 30 cm array at Ka band [8]	~3 degrees (X band) ~0.5 degrees (Ka band)	60 × 30 × 0.5 cm at X band (once deployed) 30 × 30 × 0.5 cm at Ka band (deployed)	<1
Inflatable	X band and Ka band	29 dBi for 0.7 m reflector at X band [9]	~3 degrees (X band)	10 × 10 × 5 cm (stowed)	<1
Mesh reflectors	X band and Ka band	42 dBi for a 0.5 m deployable at Ka band [8]	~0.7 degrees (Ka band)	1.5 U (stowed)	<2

bands that can be used. As a result, not all the transceivers shown in [Table 4](#) can be used for every mission. The reader should always verify that a given transceiver can be compliant with the particular frequency regulations required for any given mission.

For deep space applications where a transponder is needed, the main radio currently used is the Iris radio developed at the Jet Propulsion Laboratory. Designed for both near-Earth and Deep Space X-band frequency allocations, the Iris radio provides telecommunication and navigation services for CubeSat missions. Originally developed for the Interplanetary NanoSpacecraft Pathfinder in Relevant Environment (INSPIRE) program [20], the Iris design was subsequently improved for use on the Mars Cube One (MarCO) mission. MarCO-A and MarCO-B carried the Iris radio, and they were successful in relaying back to Earth the data for the InSight Mars entry, descent, and landing (EDL) [21]. The new version of the Iris radio, developed after

**Table 4** Transceivers for SmallSats and CubeSats [10–19].

Component	Manufacturer	Transmitting power	Supported data rate	Frequency band	Modulations and coding	Dimensions	Mass (g)
Beryllium S-band transceiver	AstroDev	2 mW	NA	2400–2485 MHz (up and down)	GFSK	46 × 46 × 10.5 mm	32
Lithium I radio	AstroDev	250 mW–4 W	9.6, 38.4, 76.8 kbps	130 (up)–450 MHz (down)	FSK-GMSK	10 × 33 × 65 mm	52
S-band transmitter	Clyde Space	6 W max	2 Mbps (max)	2200–2300 MHz	QPSK-OQPSK	96 × 90 × 16 mm	80
UHF-VHF transmitter	Clyde Space	4–10 W	9.6 kbps	2400–2483 MHz	GMSK-AFSK	96 × 90 × 16 mm	90
NanoCom U482C	GomSpace	1 W	1.2, 4.8, 9.6 kbps	130–150 MHz	MSK	95.4 × 90.15 × 18 mm	80
VHF-UHF transceiver	ISIS	1.7 W	1.2, 2.4, 4.8, 9.6 kbps	435–438 MHz (up and down) 400–450 MHz (down) 130–160 MHz (up)	BPSK, AFSK	96 × 90 × 15 mm	85
S-band transceiver	ISIS	3.5 W	100 kbps	2100–2500 MHz (up and down)	BPSK, GSMK	90 × 96 × 15 mm	62
Nano 2420	Microhard	1 W	115–230 kbps	2400–2483 MHz (up and down)	BPSK	32 × 51 × 6.35 mm	19
Nano 920	Microhard	1 W	1.2 Mbps	920–928 MHz (up and down)	BPSK	32 × 51 × 6.35 mm	19
SWIFT-XTS	Tethers Unlimited	1–7 W	Up to 100 Mbs	8400–8450 MHz (down) 2100–2400 MHz (up)	BPSK, OQPSK	86 × 86 × 50 mm	NA

*Continued*

Table 4 Continued

Component	Manufacturer	Transmitting power	Supported data rate	Frequency band	Modulations and coding	Dimensions	Mass (g)
CSR-SDR-S/S	Vulcan Wireless	1–2 W	1 Mbps	2200–2400 MHz (down) 2025–2110 MHz (up)	OQPSK	85 × 85 × 40 mm	380
SCR-100	Innoflight	3 W	Up to 4.5 Mbps	2200–2400 MHz (down) 2025–2110 MHz (up)	BPSK, QPSK, GMSK	82 × 82 × 45 mm	330
EWC27 +OPT27-SRX	Syrlinks	2 W	Up to 100 Mbps	8400–8500 MHz (down) 2025–2110 MHz (up)	BPSK, OQPSK	85 × 85 × 50 mm	700
μSDR-C	Space Micro	5 W	Up to 42 Mbps	70 MHz–3 GHz	BPSK, QPSK, 8-PSK	102 × 117 × 100 mm	750

MarCO, is targeted to serve 6 of the 13 secondary CubeSat missions that will act as secondary payloads onboard the NASA Space Launch System (SLS) Exploration Mission 1 (Artemis 1): BioSentinel, Lunar IceCube, Lunar Flashlight, LunaH-Map, Near-Earth Asteroid Scout (NEA Scout), and CubeSat for Solar Particles (CuSP). The Iris radio is designed to operate at X band, in coherent and noncoherent mode with 880/749 turn around ratio and less than 5-dB noise figure. The uplink modulation is PCM/PSK/PM with BCH encoding and a variety of data rates that are compatible with the NASA Deep Space Network. The downlink modulation is BPSK with several encoding options (Manchester, suppressed carrier, and subcarrier) and coding schemes (Reed-Solomon, convolutional, and turbo). Downlink data rates range from 62.5 bps to 256 kbps. For navigation functions the Iris radio provides turnaround ranging and Delta-Differential One-Way Ranging (Delta-DOR) tones. Different from other CubeSat radios where generally the low-noise amplifier (LNA) and solid-state power amplifier (SSPA) are included in the radio chassis, the Iris radio requires an external LNA and SSPA. The Iris LNA provides two ports for up to two receiving antennas. The SSPA provides three input ports for the connection of up to three transmitting antennas. The RF output power of the SSPA comes in two options: 2 or 4 W. The Iris transponder is an enabling technology that made the MarCO mission successful and makes the Artemis 1 missions possible.

## 4 Optical telecommunications for CubeSat

Optical communication systems for CubeSats are currently under study. They have the potential of enabling compact and low power uplink/downlink for SmallSat interplanetary missions. A paper from Staehle [22] describes a possible optical communication package for CubeSat to occupy 1U in a 6U mission concept, designed for interplanetary CubeSat exploration. The proposed package is based on JPL laser telecommunication developments, and it is supposed to achieve a link capacity of 1–4 kbps at 2AU of distance from Earth. The future use of optical communication for CubeSats and small spacecraft is a very promising option. However, some challenges need to be addressed before being able to actually develop an optical communication system for small platforms:

- Packaging: more work needs to be done to incorporate a flight laser communication payload into a 1U CubeSat. Specifically the terminal optical assembly needs to be reduced up to a point where it can really fit the CubeSat standard dimensions. In Ref. [22], different assembly options are mentioned.
- Transmitting power (laser): in Ref. [22] a 10% efficiency, highly compact, master oscillator laser is proposed. However, improvements of the laser efficiency are required to increase its transmitting power up to 5 W, which is what is necessary in Ref. [22] to close the interplanetary link at 2AU.
- Control and pointing: microradian-level fine pointing is required to successfully communicate using lasers. Multiple efforts are currently being conducted worldwide to develop fine control and pointing for miniaturized platforms. However, it is a very challenging problem,

and microradian-level fine pointing for small spacecraft has not been yet successfully demonstrated in space.

If these challenges are successfully addressed, optical communication will greatly improve the interplanetary capabilities of small spacecraft.

## References

- [1] J. Wertz, D. Everett, J. Puschell, *Space Mission Engineering: The New SMAD*, Space Technology Library, Microcosm, 2011.
- [2] A. Babuscia, M. McCormack, M. Munoz, S. Parra, D. Miller, MIT castor satellite: design, implementation and testing of the communication system, *Acta Astronaut.* 81 (2012) 111–121.
- [3] STK-AGI, Satellite Toolkit, Available from: <http://www.agi.com/products/stk>. Accessed 28 January 2014.
- [4] JPL, DSN Telecommunications Link Design Handbook, Pasadena, CA, JPL, 2000.
- [5] L.J. Ippolito, *Propagation Effects Handbook for Satellite Systems Design*, NASA Reference Publication 1082, NASA Public Document 1989.
- [6] A. Babuscia, K. Cheung, Statistical risk estimation for communication systems design, *IEEE Syst. J.* 7 (1) (2013) 1–12.
- [7] B. Klofas, A survey of CubeSat communication systems: 2009-2012, in: *Proceedings of CubeSat Developers' Workshop*, San Luis Obispo, California, 2013.
- [8] N. Chahat, E. Decrossas, D. Gonzalez, O. Yurduseven, M. Radway, R. Hodges, P. Estabrook, J. Baker, T. Cwik, G. Chattopadhyay, A review of CubeSat antennas: from low Earth orbit to deep space, *IEEE Antennas Propag. Mag.* 61 (5) (2019) 37–46.
- [9] A. Babuscia, J. Sauder, A. Chandra, J. Thangavelautham, L. Feruglio, N. Bienert, Inflatable antenna for CubeSat: a new spherical design for increased X-band gain, in: *Proceedings of IEEE Aerospace Conference*, Big Sky, MT, 2017.
- [10] Astrodev, Astronautical Development, LLC, Available from: [http://www.astrodev.com/public\\_html2/](http://www.astrodev.com/public_html2/). Accessed 28 January 2014.
- [11] S. Clyde, Clyde Space, Available from: <http://www.clyde-space.com/>. Accessed 28 January 2014.
- [12] GomSpace, GomSpace, Available from: <http://gomspace.com/>. Accessed 28 January 2014.
- [13] ISIS, ISIS: Innovative Solutions in Space, Available from: <http://www.isispace.nl/cms/>. Accessed 28 January 2014.
- [14] Microhard, Microhard Systems Inc: Spread Spectrum, Available from: <http://www.microhardcorp.com/IPn2420.php>. Accessed 28 January 2014.
- [15] U. Tethers, Tethers Unlimited Home Page, Available from: <http://www.tethers.com/>. Accessed 28 January 2014.
- [16] Vulcan Wireless Inc., Vulcan Wireless, Available from: <http://www.vulcanwireless.com/>. Accessed 13 May 2019.
- [17] I. Inc., Innoflight, Available from: <https://www.innoflight.com/>. Accessed 13 May 2019.
- [18] Syrlinks, Syrlinks, Available from: <https://www.syrlinks.com/>. Accessed 13 May 2019.
- [19] Spacemicro, Spacemicro, Available from: <https://www.spacemicro.com/>. Accessed 13 May 2019.
- [20] C. Duncan, Iris for INSPIRE CubeSat compatible DSN compatible transponder, in: *27th Annual AIAA/USU Small Satellite Conference*, Logan, Utah, 2013.

- 
- [21] S. Holmes, M. Kobayashi, M. Shihabi, Iris at Mars: first use of Iris Deep Space Transponder to support MarCO Relay Mission, in: Interplanetary Small Satellite Conference, San Luis Obispo, CA, 2019.
  - [22] R. Stahele, B. Anderson, B. Betts, D. Blaney, C. Chow, L. Friedman, H. Hemmati, D. Jones, A. Klesh, P. Liewer, J. Lazio, M.W. Lo, P. Mouroulis, N. Murphy, P. Pingree, J. Puig-Suari, T. Svitek, A. Williams, T. Wilson, Interplanetary CubeSats: opening the solar system to a broader community at lower cost, in: NIAC Report to NASA Office of Chief Technologist, 2012.



# Onboard software

12

*Santiago Iglesias Cofán and Arno Formella*

Computer Science Department, University of Vigo, Ourense, Spain

## 1 Introduction

Thanks to hardware evolution over the last 50 years, software has been increasingly introduced into the onboard computers (OBCs) of satellites. The capabilities of flight software are constantly increasing due to this continuous evolution of technology [1]. As a result, software has acquired fundamental responsibilities and plays a crucial role in almost all space missions [2, 3].

Nowadays, the onboard software (OSW) also referred to as flight software (FSW) has become integral to the functionality that a satellite provides. Proof of this is the close relationship between the concept of operations (CONOPS) and the software requirement specifications as seen in the degree of functional suitability, reliability, performance efficiency, maintainability, and portability being achieved by the software development.

However, software is subject to faults which may lead to failures, and a mission can fail due to an implementation error. For this reason, it is very important to follow a well-defined development process and good engineering practices to try to minimize risks.

One of the principal challenges that a software engineer has to face is to achieve a reasonable balance between the characteristics listed earlier and the constraints imposed onto the project, such as available hardware, time schedules, human resources, test environment, etc.

This chapter focuses on the software operating on the onboard computer (OBC), also referred to as the onboard data handling system (OBDS) of a satellite which usually controls and manages all other subsystems. The following sections describe the most important aspects to be taken into account when developing OSW and are organized as follows. [Section 2](#) introduces the main responsibilities of the OSW of a CubeSat, [Section 3](#) shows different architecture aspects to be considered in the software design phases, [Section 4](#) explains the importance of performing a complete and reliable development process in CubeSat software projects, [Section 5](#) shows some specific details of real-life missions, and finally, [Section 6](#) concludes the chapter with an overview of software development in CubeSat projects.

## 2 Responsibilities of the onboard software

The OBC is the central subsystem in the satellite [4]. The OBC, from a hardware perspective, is described in Chapter 10, while this chapter focuses on OBSW running on the OBC. In general, the OBC stores, loads, and executes the OBSW to perform mainly the following actions:

- control of subsystems,
- control of payloads,
- management of communication channels,
- telemetry generation and telecommand handling (TMTC), and
- failure detection, isolation, and recovery (FDIR).

The control of subsystems consists of commanding different components integrated into the overall system, such as real-time clocks (RTC), electronic power system (EPS), altitude and orbital control system (AOCS), platform sensors, etc., and collecting their data to be stored onboard, to be transmitted to the ground segment, or to be monitored for failure detection.

The control of payloads is similar to the control of subsystems, being considered less critical. Depending on the type of payload and the software that the payload itself executes, the generated scientific data can be managed and transmitted by the payload itself. However, general control, especially operation scheduling, is usually coordinated by the OBC.

The management of communication channels means the selection and the usage of different physical or virtual channels to perform the contact with a ground station. Depending on the type of information and the requirements of the mission, the OBSW could transmit or receive data through different frequency bands (UHF, S-band, X-band, etc.) and use different transport protocols and data encoding.

The TMTC refers to services that the OBSW provides for satellite operation. Reporting of housekeeping data, task scheduling, event logging, and storage of telemetry are some examples of services that an OBSW could offer to satellite operators (at the ground station) for commanding the space segment and obtaining information from each of its components.

FDIR is a very important responsibility to be assumed by the OBSW and consists in monitoring sensors, registers, memory values, or any other condition that allows to detect certain software or hardware failures. The OBSW can notify the problem to the ground segment, handle or fix the problem to a certain degree onboard, or, at least, try to prevent an error propagation. An important issue in FDIR is the analysis of possible failure chains and the possibility to override onboard actions by ground commands.

## 3 Software architecture

A software architecture is a description of how a software system is organized [5]. It further defines and models the interactions between components and system elements.

The software architecture is a major topic in the software development process, because it drives the implementation and testing phases as it is the backbone that supports and guides these stages. The design of the software architecture has a direct impact on costs, time, efficiency, and complexity of the project. Requirements, risks, hazards, mission constraints, and available hardware are crucial factors that must be taken into account in the design of an adequate software architecture. Usually, the software architecture allows developers to maintain, scale, and add new features to the existing software. In addition, understanding the underlying design principles is vital to encounter bugs or to detect unexpected behaviors.

The decomposition of the software into components is a common element of the software architecture, because it allows developers to break down the overall task into simpler subproblems and to assign responsibilities, both in functionality and in development, in a coherent way. The selection of adequate programming languages and other software technologies plays a fundamental role, because they can notably affect the design of solutions, the reuse of existing libraries, and the testability of the software. The usage of object oriented or procedural languages, the utilization of single-tasking or multitasking operating systems, the employment of file systems or the direct access of memory, etc., are decisions to be made at this stage.

As the design of a software architecture is a frequent activity in any software development process, it is common to reuse solutions and decisions already known. These solutions are often called patterns and they can be tailored for a specific use case in an overall design process. Common software architecture patterns are described below:

**Pipe-and-Filter** is an architectural pattern in which the data are passed through a set of software components that transform or filter it. The result or output of each component becomes the input of the next component forming a processing pipeline. Components are independent to each other, they only share the data to be processed.

**Layered Architecture** is a pattern that consists of several horizontal layers stacked on top of each other. Each layer has a responsibility to perform a set of actions. Normally, lower layers provide services to the upper layers through a well-defined programming interface. In this way, the implementation details and underlying technologies in lower levels remain hidden to the higher level components.

**Service-Oriented Architecture** is a pattern where components are entities that provide services to other components through a communication protocol. This protocol is the interface among the services. The pattern allows to use components to be distributed with a somewhat loose coupling.

Note that all of these patterns can be present simultaneously in an OBSW architecture at different levels of the design hierarchy. For example, the main architecture of the system can be seen as a stack of layers that provide more and more abstraction in the bottom-up direction. This allows designers to update or replace the implementation without affecting upper layers. Note that it is very important to define and use sufficiently generic interfaces between the layers. As an example, [Fig. 1](#) shows the following layers:

- BIOS (basic input/output system)
- RTOS (real-time operating system)

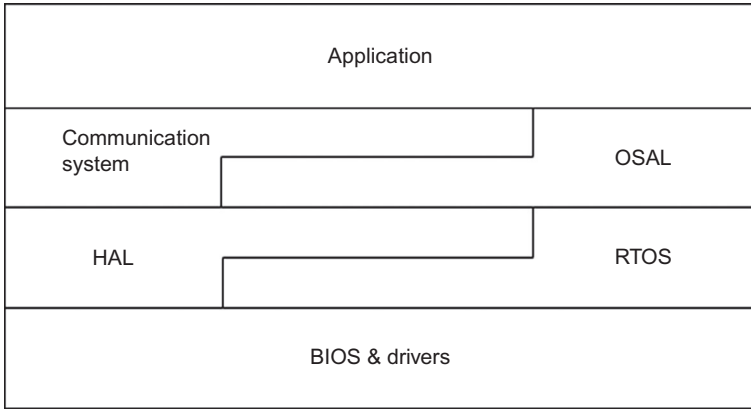


**Fig. 1** OBSW layers. Example of a layered structure for an architecture of an onboard software.

- HAL (hardware abstraction layer)
- OSAL (operating system abstraction layer)
- CSL (communication system layer)
- APP (application layer)

The BIOS is a software layer, typically located in a nonvolatile memory, that is used to initialize all hardware components that need such an initialization or configuration step. In most cases, the BIOS contains a bootloader that loads certain other components of the OBSW to memory. This process is called booting and it finalizes once the operating system is started.

The RTOS is a software system that manages the computer hardware taking into account specific time requirements. Often, it provides multitasking and interrupt management through particularly suited scheduling algorithms. FreeRTOS [6], VxWorks [7], and RTEMS [8], are examples of such real-time operating systems. As for all software reuse, one must take into account possible risks and vulnerabilities that might be present.

The HAL allows the operating system, the communication system, and the application layer to use features of the platform in a more homogeneous way regardless of the employed hardware. The management of memories and communication buses and other instruments should be handled in this component as well.

The OSAL allows the communication system and the application layer to use common features of the operating system in a homogeneous way regardless of the underlying operating system. The management of tasks and files (or more general, permanent storage) should be located in this component.

The CSL is the software layer that allows interactions with external systems. In general, the communication system is inspired in the OSI model [9], which organizes the communication process in a certain number of sublayers.

The application layer (Fig. 2) represents all services that the OBSW should provide to the rest of the satellite. This last layer, in turn, can be based on a service-oriented

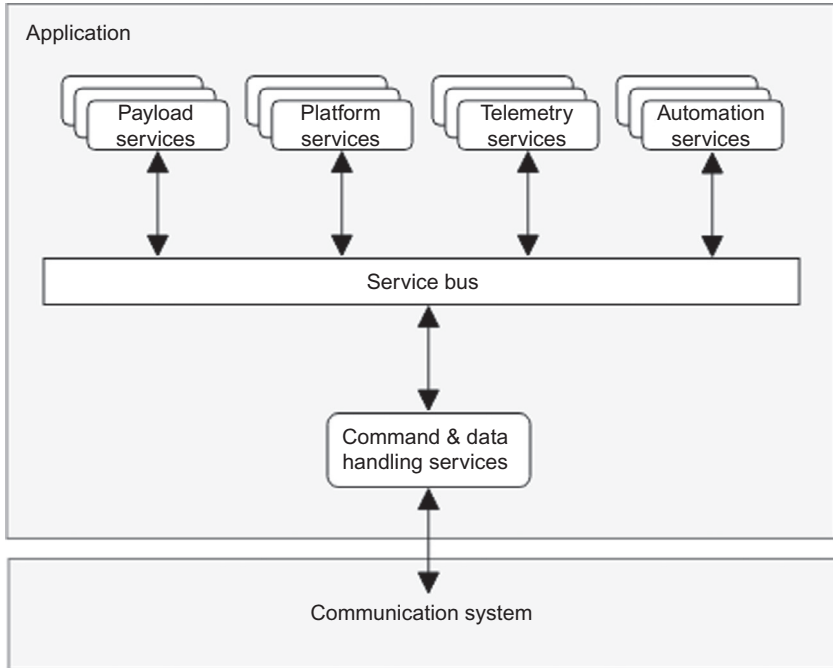


**Fig. 2** Application layer components. A typical overview of a service-based software architecture where a service bus is connected to the communication system.

architecture, the logic of each service can be organized in further sublayers, and the processing of input and output data on the other hand as a pipe-filter pattern.

A good architecture design is one that allows mission designers to respond to current and future software needs. Therefore, sometimes a mixed approach might be necessary.

In the following, certain application components are described in detail.

Some of the following components are inspired by the ECSS-E-ST-70-41C standard [10], which defines a set of services that satisfy all fundamental operational requirements for spacecraft monitoring and control. In this standard, a service is defined as a functional element of the space system that provides a number of closely related functions that can be remotely operated. All these services use features that are provided by CSL, OSAL, and HAL components.

### **3.1 Command and data handling services**

The command and data handling services have the responsibility of managing the communication channels and acting as a gateway between the ground segment and the OBSW. This involves routing of received telecommands to the corresponding service component through the service bus and deciding whether a specific telemetry is forwarded to the ground segment or stored onboard in nonvolatile memory.

### **3.2 Telemetry services**

The telemetry services are a set of components whose objective is to provide information about the system. They include housekeeping reporting, event logging, parameter statistics, and onboard monitoring.

### **3.3 Automation services**

The automation services are a set of providers that allows to operate the satellite using preloaded commands or preprogrammed actions that can be executed autonomously. Time-based scheduling, request sequencing, position-based scheduling, event-action, FDIR, and operational modes are some examples of automation components.

### **3.4 Payload services**

The payload services are a set of components that provide operational control over mission payloads. These type of components are tightly coupled with the mission and the payloads to be managed. It is very important for the design of these services to dispose of detailed specifications of all interfaces, their capabilities, and restrictions respective to all payloads.

### **3.5 Platform services**

The platform services are services that allow the system to manage different instruments of the platform such as RTC, global positioning system, AOCS, or special memories. These services are highly dependent on the available hardware components and their capabilities.

### **3.6 Service bus**

The service bus is a component that connects the other software services. It is responsible for the communication among the services. All internal messages that are produced in the application are routed to the corresponding component via the service bus.

## **4 Software development process**

The main goal of a satellite software development program is to produce a high-quality product considering all project constraints, such as time, cost, resources, and scope. The definition of software quality, according to ISO/IEC 25010 [11], is the degree to which the system satisfies the explicitly stated or further implied needs of its stakeholders, and thus provides value. These needs are as follows:

**Functional suitability** represents the degree to which a software provides functions that meet specifications.

**Performance efficiency** represents the performance of the product relative to the amount of resources it uses.

**Compatibility** represents the degree to which a software can coexist and exchange information with other systems.

**Usability** represents the degree to which a software can be used by users to achieve specified goals with effectiveness, efficiency, and satisfaction.

**Reliability** represents the degree to which a software performs specified functions under specified conditions, especially actions executed on hardware or software faults, interruptions, etc.

**Security** represents the degree to which a software protects information.

**Maintainability** represents the degree of effectiveness and efficiency with which a software can be modified in order to improve it, to correct it, or to adapt it to other requirements.

**Portability** represents the degree of effectiveness and efficiency with which a software can be transferred from one hardware or software environment to another.

The main way to achieve a high degree of compliance of these needs consists in a well-organized and implemented software development process. There are two important issues to be considered when defining the process: first, the software engineers should be present early in technical meetings of the development team, so they can provide a promptly feedback on software-related risks; second, one should avoid a shift of responsibilities to the application software, because such a decision might increase the complexity of the software to be developed to an undesired level.

Depending on the nature of the CubeSat project, two different approaches can be applied during the software development process [1,12]:

**Predictive methodologies** focus on analyzing and planning the future.

**Adaptive methodologies** focus on adapting quickly to changing requirements or needs.

The predictive methodologies, usually based on waterfall models, are driven by a plan. The plan predicts what will happen in the following phases. These methodologies are useful when requirements are well known beforehand and risks caused by changes can be controlled sufficiently. An application of these methodologies is recommended for large projects, because the generated documentation allows to manage the project and its coordination within different teams of developers.

The V-model is an example of a predictive methodology. It usually consists of seven phases: requirement analysis, architecture design, component design, coding, unit testing, integration testing, and acceptance testing. The first three phases are merely design stages where the system is increasingly refined. The last three phases are testing stages that validate the results of the design stage. The coding phase is the connection between these two groups. This methodology focuses on the software verification and validation.

The adaptive methodologies based on prototyping models are driven by the value of the product. This means that the main objective is to satisfy needs of stakeholders quickly with the goal of minimizing risks as soon as possible. These methodologies are useful when requirements are not completely known in advance. The process of developing functional prototypes in an iterative and incremental way allows developers to discover contingencies and solve problems in early stages. The application

of these methodologies is recommended for small/medium projects, because the creation of prototypes requires a high interaction of all members of a collocated team.

Agile methodologies are an example of adaptive methodologies [13]. In particular, Scrum, a popular agile software development framework, defines an iterative and incremental framework for the management of an agile development. Scrum establishes responsibilities for each team member, a collection of artifacts to be employed, and a set of meetings with all involved team members including the final customer, if needed, to guide the overall development process. Such a process is organized into short iterations whose final results are a valuable product. Scrum is inspired by the agile manifesto, hence, it is a flexible, lightweight, and highly disciplined process.

In space projects, predictive methodologies are the most common approach, mainly due to the size and the critical degree of such projects. Besides, the cost of a requirement change might force an abort of the mission.

In the case of CubeSat projects, however, the agile adaptive methodologies are acquiring a more and more relevant role, because they allow to reduce the development time and costs due to the removal of certain overhead that is produced by formal communications and rigid structures of the documentation to be generated. The agile philosophy normally fits targets of CubeSat projects in a better way than a more heavyweight predictive methodology.

Independently of the selected methodology, software verification and validation must be taken seriously. Here, verification means the process of evaluating work-products (not the actual final product) as the outcome of a development phase to determine whether they meet the specified requirements for that phase, i.e., whether the product is built right; and validation means the process of evaluating software during or at the end of the development process to determine whether it satisfies specified requirements, i.e., whether it is the right product built. It is possible that, according to the specific size of the overall project, part of the verification and/or validation could be performed externally to the development team [14].

In the following sections, the main activities of the software development process are described [5].

## **4.1 Planning**

Planning is the process of identifying the required actions to achieve a specific objective. Some of these actions to be identified could be

- setting goals,
- definition of responsibilities,
- viability studies,
- evaluation of risks,
- selection of development tools and technologies,
- scheduling of development tasks,
- adaptations and reuses from other projects,
- definition of the documentation to be generated.



It is important that the scheduling of actions that result from these activities is consistent with the due date of the tasks from the hardware and system teams in order to avoid dependencies that might block the ongoing software development or testing. As shown in the responsibilities of the following section, the OBSW is strongly coupled to the hardware. Therefore, it is critical to agree, at least, on the delivery of adequate system models on-time.

## **4.2 Analysis**

Analysis is the process of understanding and defining services that are required from the system. All imposed constraints must be identified. This activity is vital to guarantee the correctness of the design and the implementation activities.

In space missions, software requirement analysis is usually derived from the mission and system analysis. The main result of the analysis is the definition, specification, and prioritization of functional and nonfunctional requirements. Each requirement should be unambiguous, testable, and traceable.

The concept of operations, use cases, system interfaces, and hazard analysis are useful for detailing the requirements.

## **4.3 Design**

The software design is a description of the structure of the software to be implemented. Besides, it defines all interfaces between the components, the data models and, sometimes, the specific algorithms to be used. The requirements specification, the spacecraft system design, and the data description are required inputs for performing the software design in its architectural, interface, and component parts.

There are two typical iterations in the design process: preliminary design review (PDR) and critical design review (CDR). In the PDR, the design of the architecture and the communication flow should be presented. Moreover, the telemetry and telecommand format should be defined, at least at a high level. The CDR should include all elements of the PDR and the originated changes since its last review. Further, the individual design of the components, the detailed interface description, and a test plan should be presented.

To express the design concepts UML (unified model language) [15] is usually employed. UML is a mostly graphical language whose objective is to standardize the notation of a software design whenever possible.

## **4.4 Implementation**

The implementation is the art of converting a design with its specifications into an executable application [5]. A large set of programming languages exist, which can be used for the final coding. The selection of a programming language should be motivated by one of the following reasons:

- portability,
- abstraction,

- determinism,
- efficiency,
- simplicity.

Assembly, C, C++, Ada, and Rust are typical examples of languages that are used in space projects. It is not unusual for different parts of the system to be coded in different languages.

On the other hand, automatic code generation is a technique that allows developers to produce executable code from a processable specification. Automatic code generation permits to perform high-level changes (in the specification) quite quickly. The advantage is that changes and modification can be adapted fast and with less probability of error. The disadvantage is that the code generator can be very complex and hard to be tested.

In this stage of the project, it should be noted that traceability is a relevant aspect to be considered, because tracing the fulfillment of requirements provides quality to the overall process. Further it is important to manage configurations and to control different versions of the software properly and efficiently in order to be able to locate possible defects—for instance, via binary search strategy over a fine-grained revision history—and perform the improvements consistently.

Last but not least, satellite flight systems software should be developed taking into account available techniques, good practices to guarantee reliability and portability. The use of adequate coding standards, programming philosophies, and interface descriptions allow to reach high-quality code. Moreover, there are tools that can be employed for a static and dynamic analysis of the developed software that help to detect defects, visualize memory usage, analyze deadline matching, profile the code coverage, and estimate power consumption.

## 4.5 Testing

The objective of testing is to show that a software system does what it is intended to do. It allows to discover program defects and inefficiencies. The main goals are as follows:

- Demonstrate to the developer and the customer that the software meets its requirements.
- Discover situations in which the behavior of the software is incorrect or does not meet some specification.

Such testing is a vital task for space projects, because, due to the existing dependencies within the overall space project, the possibility of fixing problems in production is very limited and the costs produced by a software failure could jeopardize the entire mission. To verify and validate software it is common to perform different levels of testing.

**Unit test** : This type of test aims at checking a specific case of a specific functionality.

**Integration test** : This type of test aims at checking the communication and joint functionality between different components.

**Acceptance test** : This type of test aims at checking high-level requirements.

Note that the ease with which software can be tested depends mainly on the design primarily made. Hence, test plans should be made part of the requirements specification for the software design. Automating the test procedures and repeating the tests when changes have been applied to the software help increase reliability.

Last but not least, simulations play an important role in the test stage of a space mission. They allow mission developers to discover risks, exploit alternatives, reduce uncertainty in early phases, and provide additional validation input and output. Further, simulation of components in software are useful to test failure cases that are very complicated or just impossible to produce with real elements. For example, electronic components happen to work well and cannot be asked to produce a certain fault repeatedly for the purpose of testing.

There are two different main levels of simulation:

- Simulation of hardware systems consists in replicating the behavior of a device or part of it. To do so, driver interfaces or HALs are used to mimic the functionality that is provided by the hardware.
- Simulation of software systems consists in replicating the behavior of a software component or an entire subsystem. The use of mocks, dummy components, and stubs are common techniques that are employed in this type of simulations.

To develop and perform simulations the interface definition is crucial. The closer the simulations models the real behavior, especially regarding time requirements, the better the testing can be performed. All thinkable scenarios should be dealt with, especially when human interactions are part of the overall system. However, simulations can never replace test-like-you-fly validation.

## 5 Mission experiences

In this section four CubeSat missions, namely Xatcobeo, HumSAT, Serpens [16–18], and Lume-1 missions, are briefly commented on from the point of view of the software engineering.

Xatcobeo (2012) was a technology demonstration mission in which a software-defined reconfigurable radio, a panel deployment mechanism, and a system for measuring the amount of ionizing radiation were verified in space. HumSAT (2013) and Serpens (2015) were space missions whose objective was to provide a messaging service to areas without infrastructure through low-cost terminals on the basis of the store-and-forward concept.

Lume-1 (2018) was a space mission whose objective was to receive wildfire alerts from terrestrial sensors and to provide information to unmanned air vehicles (UAVs) and ground segment elements as an additional support to the fire extinguishing procedure.

In the case of the Xatcobeo, HumSAT, and Serpens satellites, the challenge of the OBSW was to meet the mission requirements employing a very limited hardware. The main software requirements were as follows:

- Antenna deployment.
- Managing payloads via IIC-bus.

- Managing subsystems (TTC, EPS, and RTC) via IIC-bus.
- Managing telemetry of subsystems and payloads.
- Executing time-scheduled tasks.

The principal hardware characteristics of the OBC were as follows:

- An FPGA implementing a soft 32-bit microblaze microprocessor.
- 1 MByte of static RAM for code and data (volatile).
- 512 MByte of NAND-based flash memory (nonvolatile).

For these reasons, the employed software architecture was a simple layered architecture on a tailored operating system based on a finite-state machine. The operating system was developed without employing explicit concurrency and without dynamic memory management (besides the program stack). A file system was not used, so a custom NAND flash memory manager had to be developed. These decisions had been taken due to the lack of nonvolatile RAM; 1 MByte RAM was not enough to store the program and data, the file system footprint, and possible thread contexts.

In the case of Lume-1, the main purpose of the software development was to build a generic software platform where specific mission services can be integrated with a set of common services for any mission. Thus, the main challenge was to develop a generic software infrastructure that could be employed by other platforms in other missions with different payloads and subsystems. In this mission, the following hardware features were available:

- AVR-32 processor with 32 MHz clock frequency,
- 512 KBytes of build-in flash for code and data (nonvolatile),
- 32 MBytes of RAM (volatile),
- 32 KBytes of FRAM (nonvolatile), and
- 128 MBytes of NOR-based flash memory (nonvolatile).

With these capabilities and requirements, a distributed architecture was developed using an existing real-time operating system. The operating system provides a uniform interface to interact with several microcontrollers. In addition, it allows designers to use and manage concurrency. Additionally, an existing file system was adapted to handle persistent data. These two software components allowed the software development team to build a generic and extensible architecture where a great part of command and data handling services, as described earlier, were implemented.

According to our experience, two different approaches were described earlier. Both have their pros and cons. In the first three cases, every piece of software was developed, managed, tested, and debugged by the software team, so the software was well known and could be ported quite easily to similar low-performance platforms. The software was simulated completely in a linux development environment. In the case of Lume-1, there were pieces of code that had to be trusted and the minimum hardware requirements should be considered in future missions. On the other hand, Lume-1 uses high-level software concepts, so its scalability is much better and the degree of functionality is improved considerably.

However, in both cases, there was a set of requirements that was covered considering the specific project constraints. Thus, it is very important to know and analyze

the scope, the available resources, and the available time, because these three elements will condition the design, the implementation, and the test stages.

Finally, this section concludes with the main lessons learned by the software team in these CubeSat projects:

- The usage of standards makes the integration easier and reduces problems.
- Errors are found faster thanks to a rigorous development process.
- The usage of third-party software implies more hours of integration, testing, and debugging.
- There are never enough tests.
- Simple solutions are the best.
- Automatic code generation improves productivity and reduces human errors as long as it is combined with automatic testing.
- Continuous integration is a development practice that prevents many problems.

## 6 Conclusion

In this chapter, the most important aspects of onboard satellite software development have been treated. One thing that the reader may have noted is the similarity between the OBSW development for a CubeSat and the development of any other software system. The reason for this similarity is quite simple: the main goal of any software development is to meet all requirements in the best possible way.

The compliance with requirements in aerospace is not more important than that in other sectors but, most of the time, the cost of errors or the nonfulfillment of requirements is much greater in space projects than in any other field of engineering. For that reason flight software is normally developed with a very high degree of perfectionism. The perfectionism is achieved by implementing a reliable development process in which each stage is performed employing standards, good practices and techniques, quality management tools, etc.

With the arrival of CubeSats, mission costs are going down. The miniaturization of technology allows developers to reduce costs and improve the performance of missions. However, this sometimes produces a decrease in quality and especially in software quality. Nowadays, a CubeSat has the same capabilities and performance as bigger satellites from 30 years ago. This means that a CubeSat might have the same software requirements as a traditional conventional satellite. Thus, a CubeSat should satisfy the same exigency and quality levels as other satellites from the point of view of software engineering. The fact that the software flies onboard a less costly platform does not mean that the software and its development become less costly as well. Of course, at present there are many more technologies and possibilities than in the past and the usage of general purpose hardware allows mission developers to reduce software costs to some extent, but it should never be at the expense of quality.

## References

- [1] M. Macdonald, V. Badescu, *The International Handbook of Space Technology*, Springer Verlag, 2014. ISBN 978-3-642-41100-7.

- [2] Space engineering: software, ESA-ESTEC, Requirements & Standards Division, 2009. Tech. Rep. ECSS-E-ST-40C.
- [3] Space engineering: software engineering handbook, ESA-ESTEC, Requirements & Standards Division, 2013. Tech. Rep. ECSS-E-HB-40A.
- [4] J. Eickhoff, *Onboard Computers, Onboard Software and Satellite Operations*. Springer Verlag, 2012, <https://doi.org/10.1007/978-3-642-25170-2>.
- [5] I. Sommerville, *Software Engineering*, Pearson Education, 2011. ISBN 978-0-13-703515-1.
- [6] The FreeRTOS kernel, (2019), <http://www.freertos.org>.
- [7] VxWorks, (2019), <https://www.windriver.com/products/vxworks/>.
- [8] RTEMS Real Time Operating System (RTOS), (2019), <https://www.rtems.org/>.
- [9] Information technology—open systems interconnection—basic reference model: the basic model, International Organization for Standardization, 2011. Tech. Rep. ISO/IEC 15504.
- [10] Space engineering: ground systems and operations, ESA-ESTEC, Requirements & Standards Division, 2008. Tech. Rep. ECSS-E-ST-70C.
- [11] Systems and software engineering—systems and software quality requirements and evaluation (SQuaRE)—system and software quality models, International Organization for Standardization, 2011. Tech. Rep. ISO/IEC 25010:2011.
- [12] NASA software safety guidebook, National Aeronautics and Space Administration, 2004. Tech. Rep. NASA-GB-8719.13.
- [13] Space engineering: agile software development handbook, ESA-ESTEC, Requirements & Standards Division, Tech. Rep. ECSS-E-HB-40-01A, 2020.
- [14] ESA guide for independent software verification and validation, ESA-ESTEC, 2005. Tech. Rep. ESA ISVV Guide.
- [15] S. Cook, C. Bock, P. Rivett, T. Rutt, E. Seidewitz, B. Selic, D. Tolbert, *Unified Modeling Language (UML) Version 2.5.1*, Tech. Rep., Object Management Group (OMG), 2017. <https://www.omg.org/spec/UML/2.5.1>.
- [16] A. Castro, R. Walker, F. Emma, F. Aguado, R. Tubio, W. Balogh, *Hands-on experience—the HumSAT system and the ESA GEOID initiative*, *ESA Bull.* 149 (2012) 45–50.
- [17] R. Tubío-Pardavila, S.A. Vigil, J. Puig-Suari, F. Aguado Agelet, *The HUMSAT system: a CubeSat-based constellation for in-situ and inexpensive environmental measurements*, in: *AGU Fall Meeting Abstracts2014*, p. A23I-3365.
- [18] J.A.V. Vilán, F.A. Agelet, M.L. Estévez, A.G. Muino, *Flight results: reliability and lifetime of the polymeric 3D-printed antenna deployment mechanism installed on Xatcobeo & Humsat-D*, *Acta Astronaut.* 107 (2015) 290–300.

# Orbit determination and control system

13

Filippo Graziani<sup>a</sup> and Simone Battistini<sup>b</sup>

<sup>a</sup>GAUSS Srl, Rome, Italy, <sup>b</sup>Department of Engineering and Mathematics, Sheffield Hallam University, Sheffield, United Kingdom

## 1 Introduction

Orbit determination and control are well-established concepts in traditional space missions [1–4]. These techniques cover a wide range of applications, from ground based to onboard orbit determination, and from single spacecraft to formation flying control. Early CubeSat missions did not include these capabilities onboard, because of the scarce resources and the simplicity of the missions. Orbit determination was provided by propagating ephemerides with commercial software.

The growth of CubeSat missions in terms of complexity and capabilities has required the development of dedicated orbit determination and control systems (ODCS). Nowadays, in fact, many missions are using or planning to use these devices in order to reach their mission's goals or simply to test new products and equipment on orbit. For example, orbit determination and control might be required for performing certain tasks at specific points on the orbit or to make changes to the trajectory. These are key factors in the development of CubeSat constellations, which have been proposed and launched for several purposes, such as Earth observation, atmospheric measurements, surveillance, and disaster management [5–7]. Achieving and maintaining specific orbits requires the capability of performing orbital maneuvers and navigating autonomously, even without GPS or Earth's magnetic field, as in the case of deep space missions. CubeSat missions outside of Earth orbit allow mission operators to undertake science measurements in several areas at an affordable cost and, at the same time offer more redundancy and increased launch opportunities compared to traditional satellites. At the end of the 2010s, CubeSat interplanetary missions have been successfully launched or are in preparation for the first time in history. In 2018, the MarCO mission was the first CubeSat interplanetary mission to be launched. It consisted of two CubeSats that completed a Mars fly-by, serving as a radio link provider for the InSight Mars lander. The radio link was also used to determine the spacecraft positioning. Another relevant initiative is the maiden launch of the Artemis 1 mission, currently planned for 2021, that will carry 13 6U CubeSats to lunar orbit, to an asteroid encounter and other destinations, with different solutions for orbit control and determination. For further details on interplanetary missions, the reader is referred to the chapter of this book dedicated to this topic.

This chapter is organized as follows: [Section 2](#) describes the main orbit determination techniques, along with the main algorithms; [Section 3](#) describes the main orbit control technologies, the maneuvers, and the implementation of control commands.

## 2 Orbit determination

Determining the orbit of a spacecraft involves reconstructing its trajectory from a set of measurements. A distinction can be made between what is usually called *preliminary orbit determination* and *orbit estimation* [2]. The former consists of processes associated with defining the full set of orbital parameters from six observations. The latter is the reconstruction of the orbit from a large set of measurements, and from the use of numerical techniques. For CubeSats, preliminary orbit determination is useful when TLEs (two-line elements) are not yet available (e.g., at the release from the launcher). Orbit estimation is instead crucial for all the rest of the mission phases, particularly for cases in which orbital knowledge is of interest to the mission itself.

The methods of orbit determination can be divided between ground-based and onboard technologies. In general, the spacecraft is tracked from a network of ground stations that provide an estimate of its orbit. However, some missions may require an onboard orbit determination system for several reasons (e.g., visibility of the spacecraft from the Earth, requested accuracy, short-time scale of the orbital motion, etc.). Orbit determination can be performed in several ways, depending on what measurements are available.

### 2.1 Ground-based technologies

The simplest and most employed method of orbit determination for CubeSat missions has been to propagate ephemeris with numerical orbital models. The most widely used common set of ephemeris are the TLEs, which are issued by the North American Aerospace Defense Command (NORAD) for a large number of satellites and objects orbiting the Earth [8]. TLEs are compatible with many orbital propagation models, such as SGP-4 and SDP-4, and include terms that account for the atmospheric drag effects. The position of a 3U CubeSat reconstructed with NORAD TLEs is reported to be accurate to 1 km and grows approximately 1–2 km per day [9]. More accurate TLEs can be generated by radio-frequency ranging as in the case of the Planet CubeSats [10].

The propagation of the TLEs can happen on board or on the ground. Ground-based propagation is used either when orbit information is not needed on board or when it is sufficient to transmit the propagated orbit once the spacecraft is passing over an available ground station. Onboard propagation requires a computer capable of running an orbital model and a radio to receive updated ephemeris.

Ground tracking methods, including optical tracking through LED [11] and laser illuminated retroreflectors [12], have also been recently proposed for CubeSats.



## 2.2 Onboard technologies

Onboard orbit determination using Global Navigation Satellite Systems (GNSS) has recently found application in CubeSat missions [13, 14]. Commercial Off-The-Shelf (COTS) receivers for CubeSats are currently available on the market, including dual-frequency and multiconstellation receivers. In some cases, they need to be modified in order to remove the speed and altitude limitations imposed by the manufacturers that prevent the use in space missions. If available from the onboard receiver, GNSS raw measurements can be numerically processed on board to reconstruct the orbit with a high accuracy. The major sources of error in the GNSS signals are clock bias, ionospheric, tropospheric, and multipath errors. Some of these errors can be canceled by processing the measurements with proper algorithms or by using differential GNSS [15].

Another onboard orbit determination technology is optical navigation. It employs cameras to position the spacecraft with respect to some known objects. In case the position is calculated in a local reference frame, a second instrument (e.g., a star tracker) is needed to position the spacecraft in an inertial frame. The advantage of this technology is that it allows autonomous navigation in deep space missions with a sufficient level of accuracy. Furthermore, it can be used in rendezvous or flybys in proximity of the targets, as in the case of the DustCube mission. DustCube uses two infrared cameras to calculate the line of sight from the spacecraft to the two asteroids that are targeted for study; the position of the spacecraft is then calculated at the geometrical interception of the two beacons [16]. The Cislunar explorers are two other CubeSats that plan to use optical navigation. They are equipped with commercial cameras to reconstruct their position from images of the Earth, the Moon, and the Sun. The sizes of these objects and their relative displacements are used to calculate the distance of the spacecraft from these known objects [17].

Sometimes calculation of the orbital position in an absolute reference frame is not needed, but calculation of the relative motion with respect to some other body (another spacecraft or a celestial body) is required. This is the case, for example, of two satellites in a leader-follower configuration, where one is tracked with high precision (from ground or with a GNSS receiver) and the orbit of the latter is reconstructed with relative measurements from the former. Some recent CubeSat missions have proposed the use of intersatellite links: the RANGE mission will use a compact on board laser ranging system to implement formation flying [18]; the AAReST mission will use an active lidar sensor for relative navigation between CubeSats that compose a reconfigurable space telescope [19].

## 2.3 Algorithms of orbit determination

The first algorithms of orbit determination date back to the early years of the 19th century with the method described by Gauss for preliminary orbit determination. To obtain the six orbital parameters, six independent observations are needed, for example, two position vectors or three direction vectors [2]. These algorithms are based on geometrical rules and are quite sensitive to measurement noise and modeling

uncertainties that are likely to affect the observations. Nevertheless, they can be used for preliminary orbit determination.

Orbit estimation usually relies on a large amount of data. In this case numerical algorithms are employed to cancel the effects of noise and uncertainties. A number of batch and recursive algorithms are used toward this end [2]. Batch algorithms are based on least-squares estimation and are usually employed at ground for solving the preliminary orbit determination problem. Recursive algorithms are more likely to be employed on board, due to the limited computational burden and the production of an online solution. Kalman filtering is the common framework for recursive orbit determination.

For both batch and recursive algorithms, the problem of orbit estimation consists in determining the best estimation for the state vector  $x$

$$\vec{x}(\vec{x}) = (\vec{r}(t) \ \vec{v}(t) \ \vec{p})^T \quad (1)$$

where  $\vec{r}(t)$  and  $\vec{v}(t)$  are the satellite's position and velocity, respectively, and  $\vec{p}$  is a vector of parameters that possibly affect the model (e.g., the ballistic coefficient or the GNSS receiver bias). The time evolution of  $\vec{x}$  follows a generic nonlinear model

$$\dot{x}(t) = f(t, x) \quad (2)$$

The available observations  $\vec{z}$  are described by another nonlinear model corrupted by the noise  $\vec{v}$  due to measurement errors

$$z(t) = h(t, x) + \nu(t) \quad (3)$$

### 2.3.1 Batch estimation

The most widely used common batch estimation method is the weighted least-squares algorithm. It consists in finding the value of the state at the reference epoch  $t_0$ ,  $x_0 = \vec{x}(t_0)$ , which minimizes the quadratic cost function

$$J(x_0) = (z(t_0) - h(t_0, x))^T (z(t_0) - h(t_0, x)) \quad (4)$$

over a set of given measurements  $\vec{z}$ . Defining  $H$  as the Jacobian matrix of  $\vec{h}$  on a reference trajectory

$$H = \left. \frac{\partial h(t_0, \vec{x})}{\partial x_0} \right|_{x_0 = x_0^{ref}} \quad (5)$$

the cost function can be rewritten in terms of the differences  $\Delta x_0 = x_0 - x_0^{ref}$  and  $\Delta z_0 = z(t_0) - h(x_0^{ref})$  as

$$J(\Delta x_0) = (\Delta z_0 - H\Delta x_0)^T (\Delta z_0 - H\Delta x_0) \quad (6)$$

The minimum is found by the condition that  $\frac{\partial J(\Delta x_0)}{\partial \Delta x_0} = 0$  and the least-squares solution is

$$\Delta x_0^{lsq} = (H^T H)^{-1} (H^T \Delta z_0) \quad (7)$$

Since not all measurements have the same accuracy, they can be weighted by normalizing the residuals in accordance with the respective noise variances  $\sigma_1, \dots, \sigma_n$ . Defining the matrix  $S = \text{diag}(\sigma_1^{-2}, \dots, \sigma_n^{-2})$ , the weighted least-squares solution can be defined once again as

$$\Delta x_0^{wlsq} = (H^T S H)^{-1} (H^T S \Delta z_0) \quad (8)$$

### 2.3.2 Filtering

Real-time measurement processing requires the use of a sequential algorithm. Among the available solutions, the Kalman filter (KF) family of algorithms provides consolidated real-time, recursive state estimation from noisy measurements [2, 20]. The KF algorithm is composed of two phases, prediction and correction. Within the prediction phase, the current estimate  $\hat{x}$  and the estimation error covariance  $P$  are propagated forward in time using the dynamic model of the system in Eq. (2). Within the correction phase, the propagated estimate and covariance are corrected with a term that weighs the difference between the noisy measurements from the sensors and the measurements that the estimated state would produce.

The original formulation of the KF is suitable for linear systems. When it comes to nonlinear applications, such as orbit estimation, more advanced algorithms are required. The extended Kalman filter (EKF) was developed during the Apollo program exactly for this purpose. Its main feature is the linearization of the dynamical model around the actual conditions at each time step. This allows the mission designers to approximate and propagate the mean and the covariance of the state variables as in the KF equations. Other nonlinear algorithms have been proposed that improve EKF's performance in terms of robustness and accuracy. The unscented Kalman filter (UKF) uses a finite number of state-space points to propagate the nonlinear model, avoiding the EKF linearization. The particle filter (PF) is a probability-based estimator that recursively implements Monte-Carlo-based statistical signal processing. One of the drawbacks of these two algorithms is that they generally require more computational power than the EKF. The improvements in CubeSat computers capacities in this sense has made possible their use onboard.

The equations associated with the above-mentioned algorithms will not be reported here for the sake of conciseness as they can be found in Refs. [2, 20]. The rest of this section is dedicated to showing some of the issues related to orbit reconstruction with filters. A first important point is related to the kind of model provided to the filter: the main types are pure kinematic, pure dynamic, and reduced dynamic. The first does

not require a representation of forces, but is very sensitive to measurements; the second is difficult to implement, especially in low orbits, because disturbances are hard to model (e.g., atmospheric drag); the third is perhaps the most practical, because disturbances can be modeled as empirical accelerations through the process noise covariance matrix  $Q$  of the filter [21].

The  $Q$  matrix is one of the most important tuning parameters of a KF. It represents the level of uncertainty in the model. Even though CubeSats have standard dimensions and shape, modeling the effects of perturbations such as atmospheric drag, third bodies, solar radiation pressure, and so on is particularly difficult and not so cost-effective in terms of computational burden. It is easier to consider a model of motion represented by the state  $x(t) = \begin{pmatrix} r(t) & v(t) \end{pmatrix}^T$  and to inject noise in the model through the  $Q$  matrix to account for these effects.  $Q$  is defined as

$$Q = \int_0^{T_s} \Phi(\eta) \Omega \Phi(\eta)^T d\eta \quad (9)$$

where  $\Phi$  is the state transition matrix of the model,  $T_s$  is the sampling time of the measurements, and  $\Omega$  is the matrix whose structure reflects how the noise enters in the dynamics. In the case of a simple position-velocity state vector, where the noise enters the model as a disturbance acceleration,  $\Omega$  is defined as

$$\Omega = q_0 \begin{pmatrix} 0 & 0 \\ 0 & 1 \end{pmatrix} \quad (10)$$

where  $q_0$  is a numerical value representing the level of noise. Finally, the structure of  $Q$  in this case is

$$Q = q_0 \begin{pmatrix} T_s^3/3 & T_s^2/2 \\ T_s^2/2 & T_s \end{pmatrix} \quad (11)$$

By adjusting the value of  $q_0$  the effects of unmodeled disturbances can be accounted for in the algorithm.

An example of parameter estimation with the KF is the evaluation of the GNSS constant clock bias  $b$ . To do that it suffices to add to the filter model in Eq. (2) a null differential equation:

$$\dot{b} = 0 \quad (12)$$

and to adjust the  $Q$  matrix structure in accordance.

### 3 Orbit control

Orbit control generally involves maneuvers that alter a spacecraft's trajectory and involve some sort of propulsion: orbit parameters changes (e.g., inclination), altitude raising, deorbiting, formation control, station keeping, etc. Depending on the goals of the mission, different technologies might be more or less adequate.

### 3.1 Orbit control technologies

Orbit control has not been employed in many CubeSat missions so far, due to the limitation of resources and the absence of specific mission requirements. Nevertheless, several different technologies have been proposed for use [22]. Orbit control technologies can be divided into active and semiactive: the former directly spend energy in order to produce a momentum change in the spacecraft; the latter employs some sort of energy to indirectly change the orbit.

In most spacecraft, orbit control is provided by some sort of propulsion (e.g., chemical, electrical, etc.). However, propulsion solutions for CubeSats must comply with several limitations and restrictions at the same time, as, for example, the prohibition of pyrotechnics on board, the limitation on the amount of chemical propellant, and the safety procedures relating to pressurized tanks. For these reasons, only cold-gas thrusters and electric propulsion have been employed in CubeSat missions to date.

Alternative, propellantless methods to traditional propulsion systems have been proposed and launched, such as solar sails [23] and differential drag [10]. Solar sails collect photons emitted by the Sun in order to produce a propulsive force. The sail should be large enough to guarantee a sufficient momentum change. Differential drag is a method of controlling a spacecraft ballistic coefficient in order to produce a suitable amount of drag force. The ballistic coefficient can be changed with an attitude maneuver of the spacecraft so that the aerodynamic cross-section of the spacecraft changes. This can be used to space two CubeSats along the same orbit. Another way of obtaining this effect is to release the CubeSats at different points of the same orbit, if the dispenser has the possibility to do so [24].

### 3.2 Maneuvers

Orbital maneuvers can be divided into in-plane and out-of-plane maneuvers. In-plane maneuvers are produced by a combination of forces tangential and normal to the trajectory. They result in a change of the semimajor axis  $a$ , the eccentricity  $e$ , and the argument of perigee  $\omega$  of the orbit. In the case of CubeSats, the most common in-plane maneuvers are, for example, the altitude raising and reentry. These maneuvers are directly related to variations of the semimajor axis  $a$  and therefore to tasks such as deorbiting and mission life extension.

Changes in  $a$  are produced by altering the speed of the spacecraft. From the *vis viva* equation, it is known that the orbital speed  $v$  in an elliptical orbit is

$$v = \sqrt{\mu \left( \frac{2}{r} - \frac{1}{a} \right)} \quad (13)$$

Differentiating the two sides, a change in velocity  $\Delta v$  is related to a variation  $\Delta a$ :

$$\Delta v = \frac{\mu}{2va^2} \Delta a \quad (14)$$

Since in general orbits do not have constant speed, the minimum required  $\Delta v$  to obtain a certain  $\Delta a$  is when  $v$  is maximum, that is, at the perigee.

When the  $\Delta v$  is impulsively applied to the spacecraft in the direction of the speed, that is, after the activation of a thruster, the semimajor axis changes instantaneously and the spacecraft is transferred to another orbit. The simplest example of orbital transfer is that between two circular orbits (a higher and a lower one), called the Hohmann transfer. In its minimal configuration, shown in Fig. 1, it is composed of two impulsive maneuvers  $\Delta v_1$  and  $\Delta v_2$ : the first takes the spacecraft on an elliptical orbit with perigee at point 1; the second circularizes the orbit at the altitude of the apogee of the transfer orbit. Other similar methods are the bi-parabolic, bi-elliptical, and multiple impulse Hohmann transfers. The performance of these methods in terms of required  $\Delta v$  depend on the ratio between the final radius and starting radius of the orbits, with the Hohmann transfer being the best solution for  $r_2/r_1 \leq 11$ .

Out-of-plane maneuvers are produced by forces perpendicular to the orbital plane. The effect is a variation of the inclination  $i$  of the orbital plane. Changing only the orbital plane requires that the orbital velocity vector is rotated by an angle  $\Delta i$  maintaining its absolute value. Observing Fig. 2, the  $\Delta v$  required to perform the maneuver is calculated with simple trigonometric rules as

$$\Delta v = 2v \sin \frac{\Delta i}{2} \quad (15)$$

### 3.3 Commands implementation

The velocity variations calculated in the previous sections can be seen as *commands* to the propulsion system. A few considerations have to be taken into account in order to implement these commands. From the mission planning point of view, for all those

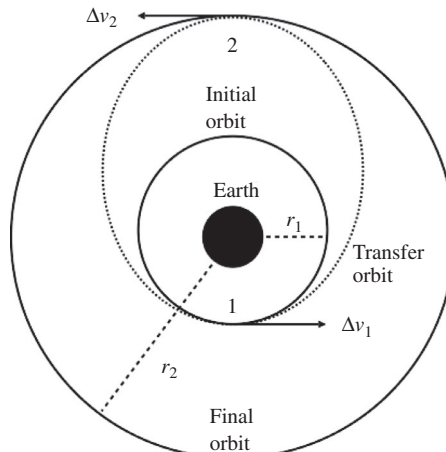


**Fig. 1** The Hohmann transfer.

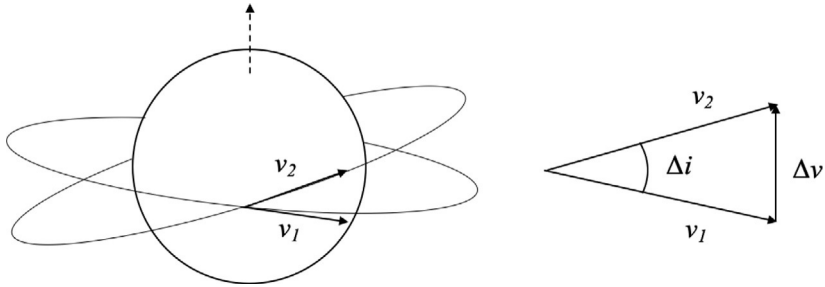


**Fig. 2** Orbital plane change maneuver.

spacecraft using some sort of propellant, it must be considered that its onboard availability is limited. Therefore, it is fundamental to establish in advance the total amount of the propellant required for the entire mission. This quantity is defined as the  $\Delta v$  budget. First of all,  $\Delta v$  is calculated from the knowledge of the actual orbital state of the spacecraft, which is precise only up to a certain level of accuracy. Another important fact is that impulsive  $\Delta v$ s cannot be implemented by any real propulsive system, which is characterized by finite time responses and delays. Furthermore, each propulsive system might present errors relating to operating conditions, degradation, unmodeled behaviors, and precision.

A  $\Delta v$  command is implemented in a series of firings or as a continue force in the case of solar sails. Neglecting mass variation, the second law of dynamics can be written as

$$f \Delta t = m \Delta v \quad (16)$$

where  $f$  is the total force from the propulsion system,  $\Delta t$  is the total thrusting time, and  $m$  is the mass of the spacecraft. Splitting the force in multiple impulses, as in the case of the multi-impulse Hohmann transfer, one obtains

$$\sum_i f_i \Delta t_i = m \sum_i \Delta v_i \quad (17)$$

The duration of the thrust varies with the propulsion system: electric propulsion has very short firings repeated for very long time, while other kinds of propulsion may have less firings. After a single firing, the spacecraft status might be checked to correct the errors in the successive maneuver. This is usually performed on the ground by the mission operations team. Of course, this open-loop strategy might not be adequate in the case of very strict requirements related to the precision and timing.

A different, onboard-based approach is to build a control loop around the actuator, which can be also characterized by a transfer function between the command and the implemented force. Here, onboard accelerometers would be employed as a feedback measurement to calculate the error between the command and the actual values provided by the actuator [4]. Decisions regarding which of these orbit determination and control methods to use should be carefully considered and driven by the mission requirements.

## References

- [1] J.R. Wertz, D.F. Everett, J.J. Puschell, *Space Mission Engineering: The New SMAD*, Microcosm Press, Hawthorne, CA, USA, 2011.
- [2] O. Montenbruck, E. Gill, *Satellite Orbits: Models, Methods, and Applications*, Springer Science & Business Media, Berlin, Germany, 2012.
- [3] M.H. Kaplan, *Modern Spacecraft Dynamics and Control*, John Wiley & Sons, Inc., New York, 1976. 427 pp.
- [4] K. Alfriend, S.R. Vadali, P. Gurfil, J. How, L. Breger, *Spacecraft Formation Flying: Dynamics, Control, and Navigation*, vol. 2, Elsevier, Oxford, UK, 2009.
- [5] S. Bandyopadhyay, R. Foust, G.P. Subramanian, S.-J. Chung, F.Y. Hadaegh, Review of formation flying and constellation missions using nanosatellites, *J. Spacecr. Rocket.* 53 (3) (2016) 567–578.
- [6] N. Lazreg, O.B. Bahri, K. Besbes, Analysis and design of Cubesat constellation for the Mediterranean south coastal monitoring against illegal immigration, *Adv. Space Res.* 61 (4) (2018) 1017–1024.
- [7] G. Santilli, C. Vendittozzi, C. Cappelletti, S. Battistini, P. Gessini, CubeSat constellations for disaster management in remote areas, *Acta Astronaut.* 145 (2018) 11–17.
- [8] D. Vallado, P. Crawford, R. Hujsak, T.S. Kelso, Revisiting spacetrack report# 3, in: *AIAA/AAS Astrodynamics Specialist Conference and Exhibit 2006*, p. 6753.
- [9] E. Kahr, O. Montenbruck, K.P. O’Keefe, Estimation and analysis of two-line elements for small satellites, *J. Spacecr. Rockets* 50 (2) (2013) 433–439.
- [10] C. Foster, H. Hallam, J. Mason, Orbit determination and differential-drag control of planet labs Cubesat constellations, in: *26th AAS/AIAA Spaceflight Mechanics Meeting* vol. 156, 2016, pp. 645–657.
- [11] F. Santoni, P. Seitzer, T. Cardona, G. Locatelli, N. Marmo, S. Masillo, D. Morfei, F. Piergentili, Optical tracking and orbit determination performance of self-illuminated small spacecraft: LEDSAT (LED-based SATellite), *Adv. Space Res.* 62 (12) (2018) 3318–3334.
- [12] M. Rothacher, M. Meindl, M. Joss, E. Styger, Requirements for CubeSats: the astrocast CubeSat mission, in: *ILRS Technical Workshop*, 2017.
- [13] O. Montenbruck, M. Markgraf, M. Garcia-Fernandez, A. Helm, GPS for microsatellites-status and perspectives, in: *Small Satellites for Earth Observation* Springer, 2008, pp. 165–174.
- [14] S.C. Spangelo, M.W. Bennett, D.C. Meinzer, A.T. Klesh, J.A. Arlas, J.W. Cutler, Design and implementation of the GPS subsystem for the radio aurora eXplorer, *Acta Astronaut.* 87 (2013) 127–138.
- [15] M.S. Grewal, L.R. Weill, A.P. Andrews, *Global Positioning Systems, Inertial Navigation, and Integration*, John Wiley & Sons, New York, NY, USA, 2007.
- [16] F. Perez, D. Modenini, A. Vázquez, F. Aguado, R. Tubío, G. Dolgos, P. Tortora, A. Gonzalez, R.L. Manghi, M. Zannoni, DustCube, a nanosatellite mission to 65803 Didymos binary asteroid as part of the ESA AIM mission, *Adv. Space Res.* 62 (12) (2017) 3335–3356.
- [17] H. Van Adams, M.A. Peck, Interplanetary optical navigation, in: *AIAA Guidance, Navigation, and Control Conference 2016*, p. 2093.
- [18] B.T. Davis, B.C. Gunter, Improving the collective precision orbit determination of constellation satellites using ancillary intersatellite ranging data, in: *AIAA/AAS Astrodynamics Specialist Conference 2016*, p. 5368.



- 
- [19] C. Underwood, S. Pellegrino, V.J. Lappas, C.P. Bridges, J. Baker, Using CubeSat/micro-satellite technology to demonstrate the autonomous assembly of a reconfigurable space telescope (AAReST), *Acta Astronaut.* 114 (2015) 112–122.
  - [20] D. Simon, *Optimal State Estimation: Kalman,  $H$  Infinity, and Nonlinear Approaches*, John Wiley & Sons, New York, NY, USA, New York, NY, USA, 2006.
  - [21] Y. Yang, X. Yue, A.G. Dempster, GPS-based onboard real-time orbit determination for LEO satellites using consider Kalman filter, *IEEE Trans. Aerosp. Electron. Syst.* 52 (2) (2016) 769–777.
  - [22] K. Lemmer, Propulsion for CubeSats, *Acta Astronaut.* 134 (2017) 231–243.
  - [23] V. Lappas, N. Adeli, L. Visagie, J. Fernandez, T. Theodorou, W. Steyn, M. Perren, CubeSail: a low cost CubeSat based solar sail demonstration mission, *Adv. Space Res.* 48 (11) (2011) 1890–1901.
  - [24] C. Cappelletti, S. Battistini, F. Graziani, Small launch platforms for micro-satellites, *Adv. Space Res.* 62 (12) (2018) 3298–3304.

# Attitude determination and control systems

14

*Mikhail Ovchinnikov<sup>a</sup> and James Barrington-Brown<sup>b</sup>*

<sup>a</sup>Space Systems Dynamics Department, Keldysh Institute of Applied Mathematics of Russian Academy of Sciences, Moscow, Russia, <sup>b</sup>NewSpace Systems, Somerset West, South Africa

## 1 Introduction

The cubeSat evolution has followed a historical progress similar to that of conventional spacecraft, that is, from elementary to complex. The latter has tended to become bigger and heavier. Since the late 1990s, CubeSats have increased in size from 1U to 12U and beyond to enable more complex tasks to be undertaken that require more accurate attitude control and more complex attitude determination and control systems (ADCS). However, while conventional big satellites are adapted to bigger launchers, CubeSats generally do not follow this approach, because the advantage of small satellites is the low cost of launch using light launchers and the piggy-back (ride share) launch strategy. CubeSats are subject to significant launch constraints relative to their size and mass. Consequently the auxiliary equipment including ADCS has to follow this constraint. The size and mass of ADCS are mostly defined by sensors and actuators. At the stage of feasibility study and preliminary design, the compromise between attitude requirements (accuracy and time response) and sensors and actuators has to satisfy these constraints while simultaneously achieving mission requirements. To maintain a reasonable cost for a CubeSat, the ADCS hardware that is already available in the commercial market should be considered first. This is why the chapter begins by presenting sensors and actuators. Next, the principles of attitude control are presented, and finally the mathematical techniques available to interface with the hardware chosen for the mission are reviewed, which together provide the required accuracy within the mass and size limitations. Sensors, actuators, physical principals, and algorithms suitable for CubeSats are described from a general point of view, because there are so many realizations of ADCS. It is currently impossible to fix the state of the art as the adaptation to specific missions is rapid and ongoing.

The attitude control system has to provide initial damping of the satellite angular motion after its deployment from the launcher, acquisition and maintenance of the required attitude position or attitude motion, and attitude maneuvering if the latter is required. To realize the required angular motion, the current attitude state of the satellite has to be known. The mismatch measured between the required and actual motion of the satellite is corrected by a control torque calculated via attitude control

algorithms. To undertake these two tasks, that is, determination of the current attitude state and the development of angular motion control torque, the satellite has to be equipped with sensors, actuators, an on-board computer, and a power source. The approach to the design of the attitude control system is dictated by the satellite dynamics requirements, irrespective of its size and form factor. The form factor of a satellite, particularly of a CubeSat, due to constraints and limitations of mass, size, energy capability, component redundancy, etc., forces the selection of an appropriate attitude control system design as a compromise between requirements and constraints.

The measurements of the environmental characteristics depend on the angular position and/or angular velocity of the satellite. Usually, sensors are defined as either *positioning* or *inertial*. The positioning sensor measurement samples depend on their orientation with respect to external field gradient (gravity and magnetic), aerodynamical resistance and solar radiation pressure force directions, infrared radiation of the Earth, optical measurements of stars, visible planets, limb of the atmosphere in the vicinity of the horizon, etc. This means that for the sensor's operation, an environment is compulsory, namely, no environment means no measurements. The inertial sensors do not require environmental knowledge. Their operation is based on centrifugal acceleration measurement due to the satellite's rotation. Inertial sensors directly measure the angular velocity of the satellite. Positioning sensors do not. They provide indirect measurements.

Positioning sensors become sensors, while their measurements depend on the orientation of the satellite with respect to a gradient of fields and other known directions in space, and these measurements vary as the angular position of the satellite varies. The positioning sensors are incapable of measuring the angular position of the satellite with regard to a reference frame or any direction. This means that to transform the sensor measurements to attitude knowledge, attitude determination algorithms have to be developed and incorporated. If attitude information is required to provide a real-time attitude motion control, then an onboard computer has to be used to process the attitude determination algorithms.

When the current attitude is *known*, the difference between the actual attitude and the required attitude generates control actuation commands via attitude control algorithms. These commands, via controllers, initiate actuators to develop the required control torque to reduce the difference. Control algorithms, therefore, must be implemented onboard. Within a specific attitude control system, a few or even all components listed above can be absent. The complexity of the attitude control system depends on requirements for the attitude motion and capabilities of available onboard components. For instance, passive attitude control systems do not need sensors, algorithms, a computer, or power at all.

This chapter is organized as follows: Section 2 describes the most common attitude sensors; Section 3 deals with the attitude actuators; the main types of attitude control systems are described in Section 4; attitude determination and control methods are presented, respectively, in Sections 5 and 6; concluding comments are given in Section 7.

## 2 Sensors

### 2.1 Sun sensors

There are a wide range of technologies used to measure Sun angles for a spacecraft. The Sun angle is a convenient absolute attitude measurement for a CubeSat in the inner Solar system as the Sun is easily the brightest object and very easy to detect. However, it is a point source, so it can only generate a vector (i.e., two dimensions). The actual attitude can be any rotation about that vector, so a second vector is required to generate full attitude knowledge. The second vector would typically be measured using the Earth for a LEO spacecraft, and this can be achieved either directly by observing the Earth disc or through the measurement of the Earth's magnetic field using magnetometry.

There are two basic divisions of sensing the Sun angle, usually referred to as analogue sensors and digital sensors. Analogue sensors will directly use the Sun's energy to generate current in a photodiode to be used in the attitude control computations. The maximum number of sensing elements in an analogue detector is four. Other sensors, referred to as digital Sun sensors, use multidetector arrays either dependent on linear or two-dimensional photodiode arrays. They are referred to as digital as they use some type of digital calculations or image processing to obtain the Sun angle. An analogue detection system with a local analogue to digital (AtoD) converter is still considered to be an analogue Sun sensor even if the output from the sensor head is in the digital domain.

A second classification of Sun sensors type is referred to as either *course* or *fine* Sun sensors. This is a simplistic way of describing the accuracy of the measurement of the Sun angle from different types of sensor. There is no standard definition of these terms, but sometimes the term course Sun sensor is incorrectly used to describe all analogue Sun sensors.

For detumbling and safe modes, it is appropriate to use course Sun sensors when low accuracy is acceptable and robustness when high rotation rates are more important. Once the spacecraft is in its nominal orientation and the body rates are low, a digital Sun sensor will typically give much higher performance.

Although Sun sensors will not have the absolute accuracy required for an Earth imaging mission, they are sufficient for most other aspects of a mission, such as pointing requirements for communications (even laser communications that uses internal steering mirrors). They should therefore be considered as a low-cost backup for star mapper-based ADCS solutions if the mass/volume budgets allow.

### 2.2 Magnetic sensors

The attitude of a spacecraft can be ascertained by measuring the vector of the Earth's magnetic field. However, the measurement needs to be processed according to two further factors. Firstly, as the field varies around the Earth's orbit, the position in orbit has to be known. Secondly, the field vector at that location in orbit has to be compared

with that measured to calculate the relative offset between the two that provides the attitude vector. The known vector at any location is created by using a mathematical model of the field, for example, using the IGRF model (the International Geomagnetic Reference Field model [1]). This predicts the field at any point and any altitude in space but is only an approximation, resulting in an inherent error.

Like Sun sensors, magnetometers are available with both analogue and digital outputs. There are a variety of ways of measuring magnetic fields with various degrees of accuracy and complexity of supporting electronics. The two most common measurement methods are fluxgate and magnetoresistive. A magnetometer produces three measurements of the perpendicular fields that are usually measured in nano-Tesla (nT) or occasionally Gauss. One Gauss is equal to 100,000 nT. The decision regarding the type and sensitivity of the magnetometers used for a CubeSat mission should be driven by the attitude knowledge requirements.

### **2.3 Star mappers/trackers**

Like the ancient naval explorers, it is possible to navigate using the stars. A camera takes an image of the star field and compares it to a catalogue of star positions so that it can unambiguously recognize in which direction the camera is pointing in inertial space. Unlike the Sun, which is a point source, the star field is a two-dimensional image allowing an absolute attitude orientation to be gained from a single image.

With the use of digital cameras and the ability to measure star positions at subpixel accuracy, the star mapper provides the highest accuracy pointing knowledge, typically 0.01 degrees and better, and is therefore the main sensor used for applications needing excellent pointing such as high-resolution Earth imagery.

As the star brightness is low compared with that of the Sun, Moon, and Earth, a high accuracy star mapper will typically need a large baffle to avoid stray light entering the camera and causing noise or errors in the image. Typically, the higher the accuracy of the star mapper, the larger the baffle requirement and, for a small satellite, this can be volume prohibitive. For the CubeSat form factor, this baffle requirement limits the performance of star cameras that have to fit within the 10-cm square envelope.

### **2.4 Earth sensors**

For the vast majority of communication missions, the important attitude vector to know and control is to point the antennas toward the Earth. Depending on the solar panel configuration, it may be possible to rotate around that vector without needing to have a fixed pointing orientation other than Nadir.

The best way to get an accurate knowledge of Earth's center is to look at the Earth via infrared. The Earth is a warm body in a sea of cold space. If looked at in the absorption bands of water molecules, the Earth is almost a uniform "color," which makes it very easy to identify and calculate the central point. However, working in the infrared

usually requires expensive detectors and mechanisms, which make them expensive, heavy, and power hungry, so they are not well suited to CubeSats. They are also located on the nadir face, which is often competing for real estate with the payload. As a consequence, Earth sensors are rarely found on CubeSat missions nowadays, with star mappers and gyros are used in their place.

## **2.5 GNSS-based attitude knowledge**

Differential Global Navigation Satellite System (GNSS) measurements can be very accurate, with resolution in the range of centimeters, whereas a single GNSS measurement might be accurate to 1 m or perhaps submeter. GNSS techniques have been used on spacecraft to measure attitude by using multiple antennas on a long baseline, where the difference of a centimeter can translate into a fairly accurate attitude knowledge. Three or more antennas are needed to get an attitude fix in three dimensions.

## **2.6 Measuring attitude change—Gyros**

All the sensors previously discussed measure an absolute attitude, so the errors in the measurement are one time and simply suffer from accuracy and noise error sources. An alternative measurement system is to use the rate of change of the satellite motion to estimate where the satellite is at the current time compared with an absolute reading of attitude sometime in the past. This technique is often used on simple CubeSats that use a Sun/magnetometer pair to give absolute attitude knowledge during the sunlight phase. When the CubeSat moves into eclipse, the primary attitude reference of the Sun is lost, so a rate sensor (gyro) is used to estimate the change in attitude since the last known absolute attitude.

There are a wide range of gyros on the market, and as would be expected, there is a trade-off between accuracy, cost, and volume. Originally, gyros were based on spinning masses, and the force created when these masses were moved off their axes was used as a measurement of rate of change. Mechanical gyros are very rarely used in space nowadays due to their inherent reliability problems.

The most accurate units are ring laser gyros (RLGs). These can measure delays in time of travel of a laser to subwavelength accuracies resulting in very high performance but at the expense of size and power. In the middle range of cost/performance are fiber-optic gyros (FOGs) followed by a wide range of microelectromechanical system (MEMS) gyros, which are the smallest and lowest cost, but do not have very good performance.

For a gyro to perform well, it must have a minimum amount of drift and noise. Drift is how accurately the rate reading reports the real measurement, and the noise is the random variation on that signal. MEMS gyros have the worst drift performance. As there is no absolute measurement, the buildup of drift on the gyro reading is critical. At each reading of the rate, the error is summed, so the error gets worse and worse over time. If the drift rate is poor, then the satellite can be pointing many

degrees off from the pointing angle that is anticipated when the satellite comes out of eclipse.

### **2.6.1 Stellar gyro**

A stellar gyro has a built-in star camera, similar to a star mapper, but works as a rate sensor rather than an absolute measurement of attitude. It does this by correlating two sequential images of the star field to determine the rotation and translation of the image, which reflects the motion of the satellite that the camera is mounted to. The benefits are that the image does not have to be that accurate as the correlation algorithm will remove issues such as hot pixels, dead pixels, and noise.

It is understood that the stars have not moved between the two images, so this information can be used to reset the drift on the internal MEMS gyros resulting in a near drift-free rate sensor. Even if this process is implemented, the accuracy of a MEMS gyro is still dependent on the absolute measurement of attitude in sunlight by the Sun sensor and magnetometer, so it is only suitable for communication missions, not highly precise Earth observation, which requires a star mapper.

## **3 Actuators**

### **3.1 Reaction wheels (flywheels)**

Following Newton's third law, accelerating a mass in one direction will create an equal and opposite reaction in the other direction. A reaction wheel accelerates a relatively massive disc through the use of a high torque motor to achieve a reaction of the spacecraft in the opposite direction. Using three such wheels, in orthogonal axes, allows the spacecraft attitude to be moved in any direction required.

A reaction wheel is usually defined by two attributes. The torque, measured in newton-meters (Nm), represents the amount of force that the wheel can apply to the satellite, so the higher the torque, the more agile the spacecraft can be. The other attribute is the momentum measured in newton-meter-seconds (NmS), which defines the maximum energy that can be stored up in the inertia of the wheel.

A momentum wheel is a reaction wheel that is run at a constant high speed. It therefore generates no torque directly on the spacecraft but will produce a gyro stiffness in the axis perpendicular to the mass rotation direction. A high momentum wheel is beneficial when pointing stability is needed, as it requires significant energy (disturbance torques) to move it off its axis.

### **3.2 Control momentum gyro (CMG)**

If a momentum wheel is mounted on a pivot, then when the pivot is driven to change the axis of the spinning wheel, a very high torque is generated on the spacecraft to resist the gyro stiffness of the wheel. This is the basic operating method of a CMG. Either two wheels with single pivots can be used to control a satellite in three axes, or a single wheel with two degrees of freedom, mounted on a dual rotating pivot,

can be used. A CMG can have a significant mass advantage over a reaction wheel with equivalent torque, but they do not scale to small sizes well, so they are less applicable to CubeSat applications. The control algorithms are complicated as there are certain positions of the CMGs where they cannot generate torque in the right direction—these are called singularities.

### **3.3 Fluid dynamic actuator**

A relatively new technology involves the use of a heavy fluid, pumped through a tube, to achieve the same effect as a reaction wheel. The acceleration of the reaction mass will create a reactive force on the spacecraft in the opposite direction. The use of a pump relieves the bearings from carrying the full load of the mass at launch. When a conductive liquid is used, such as a liquid metal, then magnetic fields can be used to drive the fluid using the Lorentz force. This removes the need for bearings in the system, which is one of the lowest reliability components of reaction wheels; this potentially gives fluid dynamic actuator (FDA)-based systems very long lifetime.

Another major advantage of an FDA is that the fluid does not have to run around a circle; it can be any shape that encloses an area, allowing the design to be square, for example, which maximizes the inertia of the fluid by following the outline of the CubeSat frame. Much of this technology is proprietary, and its use is restricted by patents.

### **3.4 Magnetorquers**

Magnetorquers are electromagnets. They generate a large magnetic field when energized. This interacts with the local magnetic field and generates a torque on the spacecraft when their field is offset from the local Earth's magnetic field vector, much like a compass needle will turn toward North. The unit of measure for a torque rod is magnetic moment, measured in ampere-square-meter ( $\text{Am}^2$ ).

The simplest method of generating a field is a coil of copper wire. This is typically square and follows the outline of the spacecraft to maximize the surface area enclosed by the coil. However, air-cored magnetorquers require high power to generate a reasonable magnetic field and are relatively heavy as copper is a dense material. The alternative is to use a magnetorquer rod. The rod constrains and amplifies the field generated by the coil wrapped around it. The potential disadvantage of a rod is that when the coil is not energized, there will still be a small residual magnetic field, called the remnant. If the remnant is significant, it will cause a disturbance on the spacecraft attitude that has to be compensated for. The material chosen for the rod therefore has to result from a trade-off between having high amplification of the field, combined with low remnance.

The rods fabricated from the soft magnetic material can be used on their own within passive attitude control systems as a passive damper and are called hysteresis rods. Due to the magnetization reversal under angular motion of the CubeSat, the hysteresis



effect within the rods causes a transformation of the angular kinetic energy to a heat and, consequently, decreases the angular velocity.

### 3.5 Other methods

Spacecraft attitude can be adjusted by using a propulsion system and multiple thrusters that are switched depending on which axis needs to be corrected. Various thruster types are available and are described in Chapter 15. They are not typically used in CubeSat applications.

In low orbits the small atmospheric drag can be used to control a satellite using aerodynamics. The attitude can either be passively stabilized or actively controlled by moving the aerodynamic surfaces.

Similar to moving aerodynamic surfaces, the center of mass of a satellite can be moved through sequential movement of appendages resulting in an overall rotation of a satellite body. The appendages that are moved are typically deployed solar panels. These unconventional methods of attitude control are not typically implemented on CubeSat missions, but have been flown and are planned on upcoming missions planned, to meet specific mission requirements.

## 4 Attitude control classification

When trying to describe or differentiate between attitude control systems, we usually describe the physical principles under which a specific attitude control system operates. We classify the systems with regard to their attitude motion modes, passive or active types, which sensors and actuators can be implemented, what features the systems for CubeSats have, and what mathematical models are to be implemented to describe and simulate attitude motion. We need to consider the environment that can be used for attitude determination and control. This can apply to both passive and active control schemes. To generate a passive control system, no active actuators, power, computing, mathematical algorithms, or knowledge of attitude can be utilized. Active control demands all of these systems.

### 4.1 Gravity field and gravity-gradient ACS

Different parts of the satellite have varying distances to an external large attracting gravitational force, such as the Earth; hence the attracting forces are different too, and the sum of forces develops a *gravity-gradient torque* acting on the satellite. If the orbit of the satellite is assumed to be circular and Keplerian, then the satellite with different principal moments of inertia has 24 equilibria where principal axes coincide with the axes of the orbital reference frame (local-vertical-local-horizon frame). Four of those are stable. To increase the magnitude of the gravity-gradient torque, the satellite has to be elongated, which can be realized by booms with tip mass. To make the equilibria asymptotically stable, a *damper* has to be installed. One can use relative motion of the satellite structures with friction and elasticity in the hinge to connect

the elements, magnetic elements like hysteresis rods fabricated from soft magnetic material. Accuracy of the gravity-gradient attitude control system is on the order of a few degrees. Eccentricity of the orbit increases the amplitude of the satellite libration with regard to the local vertical. The installation of a gravity-gradient boom on a CubeSat requires a deployment mechanism. For 1U–3U CubeSats, it would occupy a dominating part of the available volume. However, a reconfiguration of the CubeSat’s masses can provide a proper tensor of inertia for such type of stabilization. Bigger CubeSats usually demand higher pointing accuracy that cannot be achieved by the gravity-gradient attitude control system (GGACS). However, GGACS can be applied for a mission without high accuracy requirement (REFLECTOR with hysteresis rods, 2001; NCube-2 with magnetorquers, 2005)<sup>a</sup>. The gravity-gradient boom provides a single-axis orientation of a satellite along the local vertical; however, a rotor spinning with a constant velocity around the pitch axis can provide a three-axis orientation.

When an axisymmetrical satellite is spun around the axis of symmetry, the axis can achieve a relative equilibrium with respect to the orbital reference frame due to compensation of the gravity-gradient torque and torque developed by the centrifugal forces due to satellite rotation together with the frame. The axis can lie in the plane perpendicular to the local horizon or in the plane perpendicular to the local vertical or coincide with the normal to the orbital plane. It depends on satellite moments of inertia and its spin velocity. These effects can be leveraged to design effective gravity gradient attitude control systems that can satisfy a range of mission requirements.

## 4.2 *Magnetic field and magnetic ACS*

Onboard measurements of the geomagnetic field are used for attitude determination using a magnetometer. It is not possible to estimate the angle of the satellite rotation about the local vector of the magnetic field and implementation of statistical methods like the least mean square (LMS) or Kalman Filter (KF) to determine three-axis orientation is required. Local methods cannot determine three-axis orientation using measurements of the geomagnetic field only. However, using another positioning sensor measuring any vector noncollinear to the local magnetic vector allows determination in three axes.

A permanent magnet, hysteresis rods, or magnetorquers interacting with the geomagnetic field develop a control torque. This torque does not have a projection onto the direction of the local vector of the geomagnetic field, and consequently, there is no control about this direction. Such a mechanical system is called “underactuated.” However, there are algorithms that enable single- and three-axis orientation of the satellite with respect to the orbital [2] or inertial reference frames. For damping the angular velocity, there exist algorithms such as the popular B-dot algorithm and the less common S-dot algorithm. The latter orients the satellite to the Sun

<sup>a</sup>Detailed description of satellites given in parentheses a reader can find, for instance, at websites <http://www.nanosat.eu/>, Gunter’s page <https://space.skyrocket.de/> and others.

using an approach similar to B-dot. For CubeSat attitude control magnetometers, Sun sensors, and magnetorquers are the most common used components (Compass-1, 2008).

A combination of a strong permanent magnet and a set of hysteresis rods can create a passive magnetic attitude control system (CubeSat XI-IV, 2003; TNS-0 #2, 2017). The system provides 10–15-degree accuracy of orientation of the permanent magnet with respect to the local geomagnetic vector. The time response of the system is strongly dependent on the initial conditions and can take a few days or even weeks to stabilize. However, the system is of low cost and high reliability if the design and fabrication stages are skillfully conducted. Roughly, the motion achieved by this type of system is a rotation of the axis with the magnet along the surface of a cone with the vertex lying in the satellite center of mass, and its half angle depends on the inclination of the satellite orbit with almost noncontrolled motion about the axis with the magnet. In polar and near-polar orbits, the axis lies almost in the orbital plane and rotates at double the orbital angular velocity of the satellite. Hysteresis rods should form a grid located at a specified distance from the magnet or lying in the plane perpendicular to the magnet and crossing the magnet in the middle. These strategies represent ways to minimize magnetization of the rods by the magnet's field and even prevent their saturation, which would cause a malfunction of the damper.

### **4.3 Atmospheric resistance and aerodynamical ACS**

For low Earth orbit satellites with altitudes between 200 and 400 km, the resistance of the atmosphere is noticeable and, consequently, can be used to develop a restoring passive torque, while the center of pressure is shifted from the center of mass of the satellite. To shift the center of pressure, a special aerostabilizer like a sphere fixed by a rod that is connected to the satellite or “an aeroskirt” again moved from the center of mass should be installed. The problem of damping can be solved using a grid of hysteresis rods (MAK-A, 1993; PAMS, 1996; SamSat QB50, 2019) or magnetorquers. However, the lifetime of a CubeSat with an aerodynamical attitude control system can be relatively short depending on the strength (time response) of the hysteresis rods and the eventual deorbiting due to atmospheric drag.

### **4.4 Spinning and spin stabilization**

Spinning a body with a high enough spin velocity can maintain the position of the spin axis with respect to the inertial space through gyroscopic stiffness. To decrease the angle of the spin-axis nutation after deployment of the satellite from the launcher, two types of devices can be implemented. The first one is the *passive nutation damper*. There are various designs, but they all work on a similar principle. Usually, the damper is a hollow tube filled with a viscous liquid and a moving mass, like a ball, held in the middle of the tube by two springs attached to the

opposite ends of the tube. The nutational motion of the satellite generates a centrifugal force that effects the ball. The translational motion of the ball along the tube generates a friction force in the liquid and, consequently, dissipates the energy of the nutational motion. The damper parameters to be tuned for a given spin velocity are the orientation of the tube relative to the spin axis, the mass of the ball, the viscosity of the fluid, and the spring force. Effectiveness of the damper is dramatically increased by spinning. The higher the angle of nutation, the higher the force and the higher the friction that decreases the energy of the nutational motion. The main advantage of this damper approach is that it is passive and it generates no disturbing torques. The resonant tuning of its parameters is required during development as it cannot be adjusted in space. The main disadvantage is that the damper will resist any change in the orientation of the spinning axis in space if it is required. The temperature of the liquid is a very critical parameter. Instead of a viscous liquid, eddy currents can be used. A damper based on magnetorquers offers more flexibility. They can be used as an *active nutational damper* and allow changing the spin-axis orientation and spin up the satellite. Of course the active unit requires the whole set of components of an active attitude control system (sensors, calculator, algorithm of control, and power). Both types of damper have been used on CubeSats. Spin stabilization is a popular ACS strategy for CubeSats (DICE CubeSat, 2011).

#### **4.5 Solar radiation pressure**

The use of solar radiation pressure has similarities to aerodynamical ACS because both require a shift of the center of pressure with respect to the center of mass of the satellite. The line connecting these centers has equilibrium along with the direction to the Sun. The torque generated by the solar radiation pressure plays the role of a restoring one. An active damper is required. The torque is very weak, and for it to dominate over other torques, the orbit should have a high altitude. In some missions (Nanosail-D, Cubesail, Lightsail-1, and Deorbitalsail) the use of the sail was intended to deorbit the satellite rather than for attitude control.

#### **4.6 Flywheels**

A flywheel (or reaction wheel) is an electrical engine with a large axisymmetrical disk fixed on its axis of rotation. Installation of three flywheels along the principal axes of inertia of the satellite allows operators to turn the satellite about these axes by varying the angular velocity of the motors due to the angular momentum conservation law, if accelerating and decelerating of the motors are fast in comparison with orbital motion of the satellite. While the satellite is affected by the disturbance torque with a nonzero average value, the corresponding flywheel speeds up permanently and within a certain time becomes saturated, that is, reaches a maximum speed for the system. For desaturation the satellite has to be retained in an angular

position, and the corresponding flywheel can be decelerated. An external torque should be applied. Magnetorquers or a thruster can be used. Of course, this approach increases the total mass and volume of the attitude control system or can decrease the lifetime of the satellite if fuel-dependent thrusters are used. Flywheel attitude control systems provide high accuracy, and with relatively small electrical power draw, the solar panels should produce enough power to maintain a long lifetime of the satellite. The system may be compact and require minimal electrical energy. CubeSats use the system widely if attitude accuracy of a fraction of degree is demanded (BeeSat-1, 2009).

A single flywheel spinning with the constant angular velocity may be fixed along a certain axis of the satellite to resist changing its attitude. This architecture is referred to as a momentum biased system. The most common architecture employs a pitch flywheel to maintain the orientation of the pitch axis of the satellite along the perpendicular to the orbital plane.

## 5 Attitude determination mathematical techniques

1U–3U CubeSats are usually equipped with an elementary set of sensors for attitude determination. Advanced 6U–12U CubeSats typically use a more complex set of sensors. Although such CubeSats could be classified as nanosatellites or microsatellites, we describe techniques to be used for their attitude determination also.

### 5.1 Local methods

The simplest approach for attitude determination is realized by a *local method* [3]. It requires the operator to measure two noncollinear vectors in the satellite reference frame and to calculate the same vectors in the reference frame one needs to determine the satellite orientation relative to. For a calculation, one should be able to simulate these vectors via mathematical models. The problem of attitude determination lies in ascertaining the orthogonal matrix  $\mathbf{A}$  called *matrix of directional cosines* or *matrix of orientation* that provides a relationship  $\mathbf{A}\mathbf{V}_i = \mathbf{W}_i$ . Here,  $\mathbf{V}_1, \dots, \mathbf{V}_n$  is a set of the unit vectors directed to  $n$  targets, for instance, to the Earth, the Sun, or a star, along with vector of the geomagnetic field induction;  $\mathbf{W}_1, \dots, \mathbf{W}_n$  are the vectors directed to the same targets but measured in the satellite-fixed frame. If measurements are subject to errors, the described task does not have a solution, generally speaking. However, there are a few ways to solve the problem like the *determined method* and the *optimum method* in the sense of a functional minimization.

The determined method called *TRIAD algorithm* allows the satellite operator to ascertain an orientation using first measurements [4]. The algorithm is rather simple, and due to this, it has been widely used since the 1970s. Let the vectors  $\mathbf{S}$  and  $\mathbf{H}$  be directed to the Sun and along the induction vector of the local geomagnetic field. They are calculated using the corresponding models. Let  $\mathbf{s}$  and  $\mathbf{h}$  be the same vectors but measured by onboard sensors. To determine the transient matrix  $\mathbf{A}$ , one has to

compose two right-hand orthonormal triads of vectors  $\mathbf{G} = \begin{pmatrix} \frac{\mathbf{H}}{|\mathbf{H}|} & \frac{\mathbf{H} \times \mathbf{S}}{|\mathbf{H} \times \mathbf{S}|} & \frac{\mathbf{H} \times (\mathbf{H} \times \mathbf{S})}{|\mathbf{H} \times (\mathbf{H} \times \mathbf{S})|} \end{pmatrix}$  and  $\mathbf{g} = \begin{pmatrix} \frac{\mathbf{h}}{|\mathbf{h}|} & \frac{\mathbf{h} \times \mathbf{s}}{|\mathbf{h} \times \mathbf{s}|} & \frac{\mathbf{h} \times (\mathbf{h} \times \mathbf{s})}{|\mathbf{h} \times (\mathbf{h} \times \mathbf{s})|} \end{pmatrix}$ . The relationship between these matrices is defined via the matrix  $\mathbf{A}$  as  $\mathbf{G} = \mathbf{A}\mathbf{g}$ . Since the matrix  $\mathbf{G}$  is orthogonal, then  $\mathbf{A} = \mathbf{g}\mathbf{G}^T$ . The presented technique is simple for onboard implementation, but it does not work when the satellite moves into the eclipse part of the orbit or when the Sun and the induction vectors are collinear. The technique requires the position of the satellite in space to use models of the Sun and induction vectors. An important factor to be taken into account is the *albedo*, that is, the Sun radiation reflected by the Earth surface. In an analogue Sun sensor, the incoming radiation from the Sun and reflected by the Earth combines together with the vector  $\mathbf{S}$  to be simulated and the vector  $\mathbf{s}$  to be measured.

The TRIAD algorithm has low accuracy because only two observations are used and no measurement errors are taken into account. The *optimum algorithm* QUEST, based on the *loss function* implementation on the whole set of measurement [5], provides a better result. The loss function is  $L(\mathbf{A}) = \frac{1}{2} \sum_{i=1}^n a_i |\mathbf{W}_i - \mathbf{A}\mathbf{V}_i|^2$ , where  $n$  is the number of measurements and  $a_i$  is the weight of the  $i$ th measurement. The matrix  $\mathbf{A}$  is obtained by minimizing  $L(\mathbf{A})$ . The introduction of the cost function allows transformation of the task to quaternion statement. The quaternion corresponding to the optimum solution for any required accuracy can be determined without calculating the eigenvalues of the matrix.

## 5.2 Least mean squares algorithm (LMS)

Local methods do not use information about the dynamics of the satellite. Let  $m$  parameters of the satellites motion  $x_i$ , ( $i = \overline{1, m}$ ) be measured. They can be presented as known functions of the initial conditions of motion  $a_1, \dots, a_6$  as  $\Phi_1(a_1, a_2, \dots, a_6) = b_1, \dots, \Phi_m(a_1, a_2, \dots, a_6) = b_m$  where  $\Phi_i$  are known functions and  $b_i$  are measured values containing errors. The number of equations above is more than the number of variables  $a_1, \dots, a_6$  contained there. Thus we cannot solve these equations with regular mathematical methods. Introducing the *loss function*  $T = \sum_{k=1}^m (\Phi_k(a_1, a_2, \dots, a_6) - b_k)^2$  that composes the differences between the *measured* and *calculated* quantities, one can require that the loss function is minimized. To do this, one has to obtain the variables  $a_1, \dots, a_6$  that provide minimum error in the determination of the variables  $b_k$ . The necessary conditions for minimizing  $T$  are  $\frac{\partial T}{\partial a_k} = 0$ , ( $k = \overline{1, 6}$ ). The number of these equations is equal to the number of unknown variables  $a_1, \dots, a_6$ , and they can be solved by an iterative method. This technique has the advantage that the dynamical model is used. It allows us to extrapolate the solution at a time instant. The disadvantage is that the method requires long enough intervals of measurements. This is why the method is widely used for postprocessing of CubeSat flight data.

### 5.3 Kalman filtering (KF)

The Kalman filter is a recursive algorithm that uses a model of dynamics and onboard sensor measurements to obtain an estimation of the state vector [6]. Sometimes the whole state vector is required to control the system. In this case the KF allows reconstruction of missing information in the presence of noise and through, generally speaking, indirect measurements. Various sensors can be used with the KF, for example, Sun sensors, magnetometers, star trackers, and positioning sensors together with an angular velocity sensor. There are algorithms that estimate orientation via Euler angles and based on vector measurements and also via quaternions. The survey in [7] gives various representations of satellite attitude. However, the most popular is the quaternion representation, due to its nonsingularity, minimum dimension, and linearity of the kinematic equations.

Nonlinear formulations of the KF exist, like the extended KF, where the nonlinearity is approximated along a nominal trajectory. Another nonlinear filter is the unscented Kalman filter (UKF), which uses a limited number of points from the state space to approximate the nonlinear dynamics. A very popular version of the UKF that uses a quaternion formulation is the USQUE [8].

Despite the wide popularity of the recursive filtering scheme of the KF, there are several problems to be solved for its implementation in real-time applications. The main problem is the tuning, that is, the choice of the matrices of measurement and motion model errors. These matrices determine the KF quality in terms of the accuracy of the state vector estimation and the convergence time of estimation. In practice the filter tuning is a heuristic process via a trial-and-error procedure. However, there are a set of automatic tunings such as the method of numerical optimization and the simplex method. Another technique uses the Monte Carlo method based on multiple runs of the KF under random settings of the simulation. A generic algorithm for KF tuning consists of randomly changing the state vector in accordance to the improvement of the estimation accuracy. The best one is chosen for the next iteration. All of the aforementioned techniques based on multiple runs of the KF simulation require big computing power and are therefore not always suitable for CubeSats. Another technique to study the accuracy of motion estimation can be used for a stationary motion. It does not require to simulate KF work and is analytical. The error matrix for a stationary motion can be obtained after convergence from the quadratic matrix equation. For single-axis motion, this equation is solved in an explicit form. In a general case, this equation can only be solved numerically. Analytical methods to tune the KF that can be used for quasi-stationary motion are developed in [9] and are based on calculation of the covariance matrix after convergence. An advantage of this technique is that it does not require the operator to simulate KF work and may be easily implemented on a CubeSat.

In one effective use case of Kalman filtering, the current output of the solar panels can be interpreted as Sun sensor's measurements, but they have to be calibrated, and the albedo is to be taken into account. It was successfully used for postattitude determination in the Munin mission (2001). However, many power systems now

use peak-power trackers, where the direct relationship between panel current and Sun orientation is no longer applicable.

## 6 Active attitude control approaches, techniques and algorithms

Among a wide variety of attitude control algorithms, two of them are the most relevant for CubeSat missions, namely, those based on the geomagnetic field use and the implementation of the angular momentum conservation law. Transferring this to the engineering field means the use of passive or active magnetic actuators to develop a control torque under interaction with the geomagnetic field and use of the reaction wheels, which are usually composed as a triad of flywheels. Magnetic actuators (magnetorquers) in active configuration compose a triad of mutually orthogonal rods to develop a magnetic moment in any direction. Both systems require electrical power, controller, actuators, sensors, and algorithms for attitude determination and control.

Other types of active attitude control systems are not widely used for CubeSats because they either require consumable propulsion fuel or are heavy and bulky. This chapter will therefore focus on control algorithms for magnetorquers and reaction wheels. Momentum wheel (i.e., flywheel spinning with constant velocity) sometimes is used in combination with other actuators like magnetorquers or gravity-gradient boom. It is called a *pitch flywheel* and does not require a control algorithm.

### 6.1 B-dot

The B-dot algorithm implemented through magnetorquers is used for initial detumbling [10]. Generally, it imitates the viscous friction of the rotated satellite with regard to the vector of the geomagnetic field induction  $\mathbf{B}$ . The magnetic dipole  $\mathbf{m}$  is calculated as  $\mathbf{m} = k d\mathbf{B}/dt$  where  $k$  is a positive gain factor either scalar or matrix. The time derivative is calculated as a ratio of increments of the sequential measurements  $\mathbf{B}_{j-1}$  and  $\mathbf{B}_j$  of the vector  $\mathbf{B}$  and their corresponding moments of time. If the satellite is equipped with a pulse width converter, then the gain coefficient  $k$  should be chosen to adjust a time response of such a damping algorithm. Also the duty cycle of measurements should be chosen with respect to the expected angular velocity of the satellite and duration of magnetorquers' switched-on time; otherwise the magnetometer can be saturated, or, at least, measurements are disturbed, while the magnetorquers are active. This algorithm does not require measurement processing. The procedure of measurement smoothing is applied only to minimize the effect of measurement errors. In practice, magnetorquers' magnetic moments are considered either positive ( $+m_0$ ), negative ( $-m_0$ ), or null. Then, the instant when the control action is implemented needs to be evaluated in order to optimize the time response of the system. If a KF is already used for attitude determination, it can also be utilized to determine  $d\mathbf{B}/dt$ . Many studies of the satellite dynamics with B-dot algorithm have been carried out with respect to the manner of magnetic moment realization (either continuous or bang-bang style, etc.) and off-duty ratio of measurements. This algorithm can also



be used for attitude stabilization when a satellite has to rotate in inertial space with a double orbital velocity. If the magnetic torque dominates over other torques acting on the satellite, then the rotation about the satellite axis of the maximum moment of inertia is asymptotically stable. For those who begin to develop an active ACS, B-dot can be a first step.

## 6.2 Spin stabilization

Magnetic attitude control is also widely used to provide single-axis orientation of a satellite with respect to inertial space. It could be spin stabilization when magnetorquers maintain required spin velocity and point the spin axis to the needed direction by damping the nutation motion and turning in space. The effective way for realization of this strategy consists of three stages. At first the satellite has to be detumbled and damped, for instance, by B-dot algorithm, or to avoid damping spin velocity, the dipole moment  $\mathbf{m} = k(0, 0, \mathbf{e}_3(\boldsymbol{\omega} \times \mathbf{B}))_x$  can be utilized. Here, three components in the body-fixed reference frame (indicated by the subindex  $x$ ) are shown, while  $\mathbf{e}_3$  in the scalar multiplication is the unit vector of the third axis of the reference system defining the third component of  $\mathbf{m}$ . Next, the satellite is spun up about the axis of symmetry up to the required velocity by the moment  $\mathbf{m} = k(B_{2x}, -B_{1x}, 0)_x$  where  $B_{1x}, B_{2x}$  are the projections of the vector  $\mathbf{B}$  onto the first two axes of the body-fixed reference frame. In the third stage the satellite is turned to the required angular position as a gyroscope by the external control torque (in this case by the magnetic torque) with  $\mathbf{m} = k(0, 0, \mathbf{e}_3(\mathbf{B} \times \Delta\mathbf{L}))_x$  where  $\Delta\mathbf{L}$  is a mismatch between demanded and current angular momentum of the satellite. While the spin axis approaches the required position, the acting torque ends. The advantage of this is that there is no need to damp the axis motion at the end since as soon as the control torque ends, the angular motion of the axis stops too.

Another approach for spin stabilization is to turn the axis of symmetry to the required position and, next, to spin up the satellite. This requires an accurate turn of the axis via solving the boundary value problem.

## 6.3 Three-axis stabilization

Three-axis orientation of the satellite using magnetic control torque only is slightly exotic but nevertheless attractive. Exotic because the magnetic control is locally underactuated, that is, the satellite cannot be commanded to follow arbitrary trajectories in the configuration space due to the impossibility to develop a control torque along the geomagnetic induction vector. However, there are approaches to provide orientation with regard to the orbital and inertial reference frames. There are two popular techniques based on the Lyapunov control and sliding control. The first one minimizes the Lyapunov function and is close to a PD regulator (but not the same). It dictates the expression for magnetic dipole  $\mathbf{m} = -k_\omega(\mathbf{B} \times \boldsymbol{\omega}) - k_a(\mathbf{B} \times \mathbf{S})$ , where  $k_\omega, k_a$  are positive constants to be chosen,  $\mathbf{S} = (a_{23} - a_{32}, a_{31} - a_{13}, a_{12} - a_{21})$ , with non-diagonal elements of matrix  $\mathbf{A}$  transforming a vector from the body fixed to the inertial reference frame, and vector  $\boldsymbol{\omega}$  is the angular velocity of the satellite. The same

expression for  $\mathbf{m}$  can be utilized for the satellite stabilization with regard to the orbital reference frame relating  $\boldsymbol{\omega}$  and components of the matrix  $\mathbf{A}$  to this frame. The most critical issue to the implementation of such a control is the choice of the factors  $k_\omega, k_a$ , which requires skill.

The problem of the local underactuation of the magnetic control has a peculiarity by the rotation of the local vector  $\mathbf{B}$  in space due to the orbital motion of the satellite. This allows that a trajectory that leads the satellite to a needed point in the phase space can be built, as at any time the control torque has to be perpendicular to  $\mathbf{B}$ . Sliding mode control might be used for this purpose. To develop the control algorithm, a two-stage approach is used. First the surface in the phase space  $x(\boldsymbol{\omega}, \mathbf{A}, t) = 0$  is to be built so that it is reachable. Second the phase point corresponding to the satellite has to move along this surface. Also the surface should allow the changing of its orientation relative to the control torque to be perpendicular to  $\mathbf{B}$ . The global controllability of three-axis magnetic control is proven in [11]. A survey of the most widely used magnetic attitude control algorithms for CubeSats was published by Ovchinnikov et al. in 2019 [12].

For the flywheel control, the Lyapunov approach can be implemented. The control torque  $-k_\omega \boldsymbol{\omega}_{rel} - k_a \mathbf{S}$  is to be developed by the flywheels with angular momentum  $\mathbf{H}$  as  $-\dot{\mathbf{H}} - \boldsymbol{\omega} \times \mathbf{H}$  where  $\boldsymbol{\omega}_{rel}, \boldsymbol{\omega}$  are the angular velocities with regard to the reference (for instance, the orbital) and inertial frames, respectively. Equating these two expressions, one obtains the differential equation with respect to  $\mathbf{H}$ . Its solution is a way for control synthesis. Usually, instead of solving the differential equation, the finite difference method generated iteration formula is applied.

To use magnetorquers only to provide three-axis attitude is very attractive due to seeming simplicity. However, because of the disturbing torques affecting a required attitude of a very small CubeSat like 1U, such systems are not always feasible [13].

## 7 Concluding comments

Since CubeSats occupy the whole range of applications bounded on one side by missions for beginners and advanced missions on the other, their attitude requirements can range from nonstabilized to very precisely oriented. Based on the two main CubeSat developers, that is, educational or commercial one, the configuration of the attitude control system depends on the requirements of attitude motion and the ability of the designers, that is, their skills, time, and available budget. A set of attitude motion regimes is shown in Table 1. The possible combinations of sensors and actuators versus attitude required to design attitude control system starting from noncontrolled motion and up to advanced three-axis attitude motion are given. A regime purposed for the same attitude can be implemented by different configurations. For example, to avoid a chaotic angular motion without requirements of accuracy and time response can be done via implementation of B-dot algorithm with magnetometer and magnetorquers or a permanent magnet with hysteresis rods. So, Table 1 shows what sensors and actuators can be used for a given attitude motion regime realization. The subset of sensors and actuators required depends on the accuracy demanded,



algorithms implemented, and budget of the designer. The latter being a key parameter for a choice of CubeSat attitude control system configuration.

## References

- [1] IGRF model description, <https://www.ngdc.noaa.gov/IAGA/vmod/igrf.html>.
- [2] M.Y. Ovchinnikov, D.S. Roldugin, D.S. Ivanov, V.I. Penkov, Choosing control parameters for three axis magnetic stabilization in orbital frame, *Acta Astronaut.* 116 (2015) 74–77.
- [3] H.D. Black, A passive system for determining the attitude of a satellite, *AIAA J.* 2 (1964) 1350–1351.
- [4] I.Y. Bar-Itzhack, R.R. Harman, Optimized TRIAD algorithm for attitude determination, *J. Guid. Control. Dyn.* 20 (1) (1997) 208–211.
- [5] S.-H. Lee, H.-S. Ahn, K.-L. Yong, Three-axis attitude determination using incomplete vector observations, *Acta Astronaut.* 65 (7–8) (2009) 1089–1093.
- [6] R.E. Kalman, A new approach to linear filtering and prediction problems, *J. Basic Eng.* 82 (1) (1960) 3545.
- [7] M.D. Shuster, A survey of attitude representations, *J. Astronaut. Sci.* 41 (4) (1993) 439–517.
- [8] J.L. Crassidis, F.L. Markley, Unscented filtering for spacecraft attitude estimation, *J. Guid. Control. Dyn.* 26 (4) (2003) 536–542.
- [9] M.Y. Ovchinnikov, D.S. Ivanov, Approach to study satellite attitude determination algorithms, *Acta Astronaut.* 98 (2014) 133–137.
- [10] A.C. Stickler, K.T. Alfriend, Elementary magnetic attitude control system, *J. Spacecraft Rockets* 13 (5) (1976) 282–287.
- [11] S.P. Bhat, Controllability of nonlinear time-varying systems: Applications to spacecraft attitude control using magnetic actuation, *IEEE Trans. Autom. Control* 50 (11) (2005) 1725–1735.
- [12] M.Y. Ovchinnikov, D.S. Roldugin, A survey on active magnetic attitude control algorithms for small satellites, *Progr. Aerospace Sci.* 109 (2019) 100546.
- [13] D.S. Roldugin, A. Guerman, D.S. Ivanov, M.Y. Ovchinnikov, Three-axis magnetic control for a nanosatellite: practical limitations due to a residual dipole moment, in: *The 5th IAA Conference on University Satellite Missions, Rome, 28–31 January, 2020, Paper IAA-AAS-CU-20-06-02, 2020.*

# Propulsion system

# 15

Khary I. Parker<sup>a</sup> and David C. Folta<sup>b</sup>

<sup>a</sup>NASA/Goddard Space Flight Center, Propulsion Branch, Greenbelt, MD, United States,

<sup>b</sup>NASA/Goddard Space Flight Center, Navigation and Mission Design Branch, Greenbelt, MD, United States

## Nomenclature

$e$	ion charge (A)
$F$	thrust (N)
$g_0$	earth gravity acceleration ( $m/s^2$ )
$I_b$	ion beam current (A)
$I_d$	density specific impulse ( $(kg\ s)/m^3$ )
$I_{sp}$	specific impulse (s)
$I_t$	total impulse (Ns)
$m_f$	final (dry) spacecraft mass (kg)
$m_i$	initial (wet) spacecraft mass (kg)
$m_p$	propellant mass (kg)
$\dot{m}_p$	propellant mass flow rate (kg/s)
$t_b$	thruster burn time (s)
$V_b$	effective beam voltage (Vdc)
$v_e$	combustion exit velocity at the nozzle (m/s)
$V_{S/C}$	CubeSat spacecraft volume (U or L)
$\Delta v$	change in velocity (m/s)
$\eta_m$	thruster mass utilization efficiency
$M$	mass of planet (kg)
$\gamma$	total thrust correction factor
$\rho$	density ( $kg/m^3$ )

## 1 Overview

The need for highly reliable and capable CubeSat propulsion systems becomes more important as the variety of mission applications increases. There is an expectation that these systems are commercial off the shelf (COTS) and ready to fly. As of 2020 the majority of these propulsion systems are very early in their development. The purpose of this chapter is to assist developers in understanding how to evaluate and apply these propulsion systems for a mission. The types of propulsion systems range from chemical, electric, solid, to propellantless (e.g., solar sails and tethers). To meet the goals of this chapter, only chemical and electric propulsion systems will be considered.

To select the appropriate solution, the mission goals and objectives need to be clear. Additionally, the solution should accommodate all applicable types of maneuvers: midcourse corrections, orbit insertions, station keeping and pointing once the mission orbit is achieved, and, if necessary, disposal. For example, a mission that has tight pointing requirements may elect to employ a cold gas or electrospray propulsion system to meet that requirement. However, it may also need a monopropellant or gridded ion system for orbit insertion. On the other hand a three-axis stabilized planetary observation mission may be able to meet the trajectory, orbit insertion, and attitude control requirements with a single type of propulsion system.

The decision of which type of system to use depends on a number of factors: available mass, volume, power, desired transit time (i.e., how long it takes to get to mission orbit), propulsion system performance requirements, and cost. A chemical propulsion system generates a gas to propel a spacecraft [1–4]. This gas comes from either a compressed gas or saturated liquid (e.g., cold gas systems), or via a chemical reaction (e.g., monopropellant, bipropellant, and solid propulsion systems). The compressed gas and chemical reaction systems typically require high propellant feed pressures, which can be a safety concern for CubeSats. A chemical propulsion system is typically less expensive, less complex, and requires less power than an equally sized electric propulsion (EP) system. Chemical systems can also produce more thrust, allowing a spacecraft to achieve its final orbit in less time than an electric system.

EP systems accelerate plasma by generating either an electromagnetic (e.g., Hall effect and vacuum discharge) or electrostatic (electrospray, gridded ion, etc.) field [1, 2, 5]. There are also electrothermal EP systems that preheat either hydrazine (arcjets and resistojets) or saturated liquids (microcavity discharge) to increase their respective performance. The advantages of an EP system over chemical are lower propellant mass, less volume, and higher performance in terms of specific impulse. The higher specific impulse is the primary reason that EP is the system of choice for long duration station keeping or interplanetary missions.

Even with the differences stated previously, power availability is a limiting factor for both types of systems. Propulsion systems must draw as little power as possible given limited solar array size and battery capacity. EP systems require more energy than chemical systems to power their power processing unit (PPU) and the thruster. Because of this, spacecraft using EP systems will have larger solar arrays and batteries. There are design modifications that can be made to accommodate higher power propulsion systems, but the changes could affect other subsystems in the spacecraft. During the planning stage, if the higher power propulsion system is found to adversely affect the mission, then a lower power system should be considered. These are but a few of the considerations a mission designer needs to keep in mind.

[Section 2](#) discusses the key figures of merit and other evaluation criteria that are used to assess the chemical and electric propulsion systems on the market and in development today. [Section 3](#) discusses how to size both chemical and electric propulsion systems by means of an example. Finally, [Section 4](#) discusses trajectory designs using chemical and electric propulsion systems for different mission architectures.

## 2 Propulsion system assessment

There are fundamental performance metrics, or figures of merit (shown in [Table 1](#)), that are used to assess the capabilities of any propulsion system. Any single metric is not sufficient to understand a system completely. One must use a combination of these metrics to characterize system performance and system mass and volume. For EP systems, thrust and specific impulse ( $I_{sp}$ ) are further derived from first principles, to consider the propellant's ionic mass and charge, as well as the voltage and current needed to accelerate the propellant ions.

A key parameter mission planners base their missions on is  $\Delta v$  for both chemical and electric systems. This works well for characterizing discrete impulse maneuvers using chemical systems. However, electric systems operate continuously, and their maneuver accelerations are integrated over the total burn duration. This can result in a  $\Delta v$  for an EP system that could be misleading. The parameters that should be considered, especially when comparing EP and chemical systems, are propellant mass, propellant mass fraction, and other propellant mass-based figures of merit from [Table 1](#).

Other metrics to consider for chemical and electric propulsion systems are the launch and thermal environmental tests that have been conducted, throughput (amount of propellant that can flow through a thruster before performance degrades), total steady state on time (the length of time a thruster operates before performance degrades), and pulse mode operation capability. For electric systems a vendor should provide thrust and  $I_{sp}$  ranges over a predefined input power range, or at a set of as-tested design points. For chemical systems a vendor should provide thrust and  $I_{sp}$  range over predefined propellant feed pressures, or at a set of as-tested design points.

A propulsion system can also be assessed by understanding the maturity of its development, which can be described by technology readiness levels (TRLs). The TRLs are a set of voluntary guidelines followed by the U.S. government to rate the development status of a technology. NASA has developed TRLs that can be applied to any system within a spacecraft or launch vehicle [7]. The Spacecraft Propulsion Subcommittee, of the Joint Army, Navy, NASA, Air Force (JANNAF) Interagency Propulsion Committee, has also developed a set of TRL guidelines that specifically address CubeSat propulsion system maturity [8]. These JANNAF guidelines are based on TRLs defined by NASA and Department of Defense. A system has to demonstrate predefined exit criteria before being assigned a TRL ranking. A system prototype that demonstrates required performance in its flight environment, as defined by the TRL 6 exit criteria, is considered qualified for flight. These qualification criteria are typically governed by applicable flight design and safety requirements such as those defined in AIAA S-080 [9], GSFC-STD-7000A (GEVS) [10], NASA-STD-8719.24 [11], and AFSPCMAN 91-710 [12].

The NASA Ames Research Center (ARC) publishes the State of the Art of Small Spacecraft Technology [13] (SoA) document that covers recent developments and status of technologies for various CubeSat subsystems. Their section on propulsion systems provides an overview of the various types of systems and technologies currently

**Table 1** CubeSat propulsion figures of merit<sup>a</sup> [6].

Figures of merit	Units (SI)	Newtonian physics	EP application [5]	Definition
Thrust (F)	N	$F = \dot{m}_p v_e$		Total amount of force produced by a system or thruster
Specific impulse ( $I_{sp}$ )	s	$I_{sp} = \frac{F}{g_0 \dot{m}}$	$F = \gamma \sqrt{\frac{2M}{e}} I_b \sqrt{V_b}$ $I_{sp} = \frac{\gamma m_b}{g_0} \sqrt{\frac{2eV_b}{M}}$	Measures propellant performance by quantifying the total impulse per unit mass of propellant
System change in velocity ( $\Delta v$ )	m/s	$\Delta v = g_0 I_{sp} \ln \left( \frac{m_i}{m_f} \right)$		Quantifies system ability to change its velocity based on propellant performance and spacecraft mass
Density specific impulse ( $I_d$ )	kg s L	$I_d = \rho I_{sp}$		Used to compare propellant performance for given $I_{sp}$ and density. This is generally how well the propellant packages
Total impulse ( $I_t$ )	Ns	$I_t = \int_0^{t_b} F dt = F t_b$		Change in momentum given by integrating thrust over a given burn time. Quantifies total amount of force produced by the propellant
Volumetric impulse	$\frac{Ns}{L}$ or $\frac{Ns}{U}$	$\frac{I_t}{V_{S/C}}$		This efficiency parameter used for SmallSat propulsion systems describes the amount of total impulse (Ns) a system imparts to a body per unit volume (U or L)
Propellant mass fraction <sup>b</sup>	None	$\zeta = \frac{m_p}{m_f}$		Quantifies the efficiency of a propulsion system to move a given mass ( $m_f$ )

<sup>a</sup> This parameter is not found in Ref. [6]. However, it is a commonly used Figure of Merit for evaluating system performance.

<sup>b</sup> See Section 1 for variable definitions.



**Table 2** Propellant system types for small spacecraft [13].

System type	Product	Thrust	Specific impulse (s)	TRL status
Chemical	Hydrazine	0.5–30.7 N	200–235	9
	Cold gas	10 mN–10 N	40–70	GN2/ Butane/ R236fa 9
Electric	Alternative (green) propulsion	0.1–27 N	190–250	HAN 6, ADN 9
	Pulsed plasma and vacuum arc thrusters	1–1300 $\mu$ N	500–3000	Teflon 7, titanium 7
	Electrospray propulsion	10–120 $\mu$ N	500–5000	7
	Hall effect thrusters	10–50 mN	1000–2000	Xenon 7, iodine 3
Propellantless	Ion engines	1–10 mN	1000–3500	Xenon7, iodine 4
	Solar sails	0.25–0.6 mN	N/A	6 (85 m <sup>2</sup> ), 7 (35 m <sup>2</sup> )

on the market. [Table 2](#) lists the various types of propulsion systems the NASA-ARC SoA addresses.

A review of the NASA-ARC SoA shows that there are many types of CubeSat propulsion systems on the market. Propulsion system technology developers use the aforementioned assessment tools to communicate the capability and development status of their systems. An understanding of these tools will help mission designers select the best propulsion system for their missions.

### 3 Propulsion system sizing

The sizing methods discussed here can be applied to many mission types. Note that the sizing examples discussed here are purposely not optimized to highlight the iterative nature of the process. By pointing out how the design “does not close,” or is incomplete, illustrates how other considerations need to be made to reach an optimal design. These examples will also highlight the information passed between systems engineers, mechanical designers, orbit analysts, and attitude control system (ACS) developers during trade studies, to understand the mission needs and requirements levied on the propulsion system.

The example mission considered first is to fly a lunar communications CubeSat, called CommCubeSat1, in cislunar space. It is a three-axis controlled, 12U CubeSat that will provide communications between Earth and the Moon for a baseline mission

duration of 1 year. It will be deployed from a launch vehicle upper stage in cislunar space and then achieve a transfer trajectory to reach a critically inclined lunar elliptical orbit, at  $250\text{ km} \times 6365\text{ km}$ , with an inclination of  $57.4$  degrees. The maximum spacecraft wet mass (dry mass + propellant mass) allocation is  $24.0\text{ kg}$ .

For this example a proposed chemical and an electric propulsion system were selected from the NASA-ARC SoA for comparison. **Note that the selection of these specific systems is not an endorsement and should not be interpreted as rating them better as or worse than any other.** However, they will be used to discuss the considerations made when sizing different types systems in a realistic example. For this example the VACCO green propellant integrated propulsion system (IPS) will represent the proposed chemical propulsion system, and the Busek BIT-3 RF Ion propulsion system will represent the potential electric propulsion system. Their figures of merit are shown in [Table 3](#).

### 3.1 Chemical propulsion system sizing

A ballistic orbit trajectory has been designed with an insertion  $\Delta v$  ( $\Delta v$ ) of  $269.4\text{ m/s}$  (methodologies of determining this will be discussed in the next section). An initial guess of the spacecraft dry mass (instruments, avionics, propulsion system, structure, power system, etc.) is assumed to be  $15.0\text{ kg}$  based on available component data. Component masses widely vary according to how well developed they are. To account for

**Table 3** Sample CubeSat propulsion systems [13].

	Integrated propulsion system (IPS)	BIT-3
Propellant	LMP-103S (ADN based)	Iodine (solid)
Manufacturer	VACCO	Busek
Propellant mass capacity (kg)	5.7	1.5
Total propellant volume (L)	4.6	0.3
Propulsion system dry mass (kg)	9.0	1.5
Peak power (W)	15.0 <sup>a</sup>	80.0
# of Thr./avg. unit steady-state thrust (N)	4/1.0	1/0.0012
Steady-state thrust (N)	4.0	0.0012
Steady-state specific impulse (s)	220.0	2160.0
$\Delta v$ (m/s)	585.0	1367.1
Propellant mass fraction (%)	31.1	6.7
Density specific impulse (kg s/L)	272.8	9288.0
Total impulse (Ns)	12,297.5	31,773.5
Volumetric impulse (Ns/L)	2673.4	105,911.8
TRL status	6	5

<sup>a</sup> Includes catbed heater power on time for  $\sim 30\text{ min}$ .

these variations, a percentage margin [14] is added to these masses to obtain a more conservative estimate. For this example the conservative dry mass estimate ( $m_p$ ) is determined to be 20.0kg. This mass estimate includes the conservative dry mass estimate of the baselined VACCO integrated propulsion system (IPS), which is 9.0kg.

Orbital analysis determines the minimum spacecraft acceleration needed to reach the mission orbit to calculate the required total steady-state thrust force. This acceleration is constrained by the spacecraft body dynamic modes and the dynamic modes of any deployables (e.g., solar arrays, magnetometer, and booms). Fig. 1 shows the relationship between acceleration and spacecraft wet mass for given total thrust. The labels on the right of the plot indicate the standard small satellite sizes for the corresponding spacecraft wet masses [15].

Using the allocated spacecraft wet mass of 24.0kg in this example, the calculated acceleration is  $0.16 \text{ m/s}^2$ , and resulting in a total steady-state thrust of 4.0 Newtons (N) needed to perform the mission. The total thrust will be produced using four 1.0N force thrusters that will be mounted to the spacecraft aft face, as shown in Fig. 2.

The 1.0N chemical thruster baselined for this example mission—the VACCO IPS utilizes four Bradford-ECAPS 1.0N High Performance Green Propellant (1N HPGP) thrusters. These thrusters operate with the LMP-103S green propellant and has a reported steady-state  $I_{sp}$  of 220.0s [13]. Variability in thruster manufacturing and in on-orbit conditions (thermal, power, etc.) during thruster operation can cause sub-optimal performance, though. To account for these variations and provide propellant margin, the thruster performance is adjusted by  $-3\sigma$ . In this case the worst-case steady-state  $I_{sp}$  and total thrust are assumed to be 209.0s and 3.7N, respectively.

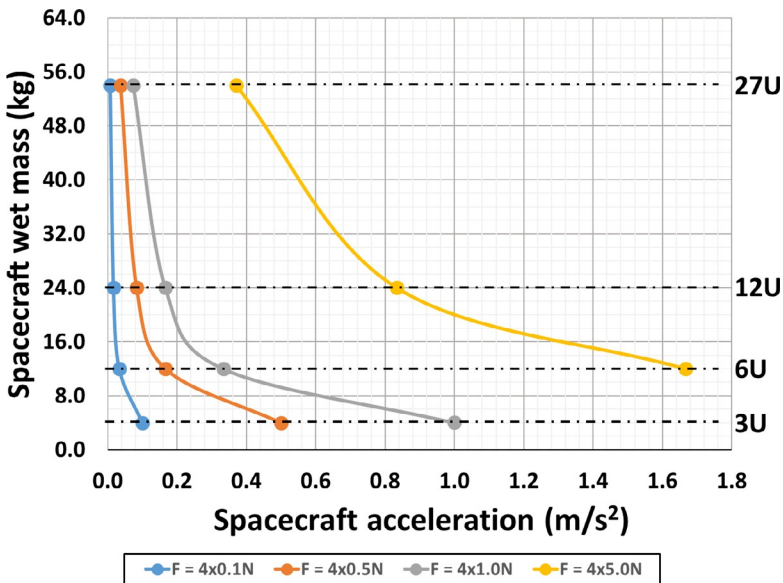
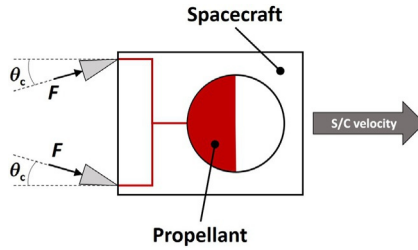


Fig. 1 Spacecraft acceleration plot for various thrust classes.



**Fig. 2** Spacecraft thruster orientation.

A spacecraft can take advantage of full thruster performance when its thrust vector ( $F$ ) is parallel to the spacecraft velocity vector (see Fig. 2). The thrust vector could be angled, or canted, off of the velocity vector by a cant angle ( $\theta_c$ ), typically determined by the ACS engineer, to provide three-axis control authority. Known as cosine loss, this effectively reduces thruster performance on the spacecraft in return for pointing control by a factor equal to the cosine of the cant angle. For this example the ACS engineer defined  $\theta_c$  to be 15.0 degrees. Hence the cosine of  $\theta_c$  is multiplied by the worst-case steady-state thrust force and  $I_{sp}$  to reflect the reduced performance. Therefore the effective thrust force ( $F_{\text{eff}}$ ) imparted to the spacecraft from our set of thrusters at steady state is calculated to be about 3.6 N, and the effective  $I_{sp}$  ( $(I_{sp})_{\text{eff}}$ ) is 201.9 s.

Another design requirement that must be accounted for when sizing a propulsion system is momentum unloading. Many different external forces (such as solar pressure, gravity gradients, magnetic fields, and atmospheric pressure) act on the spacecraft. These forces create disturbance torques when they are not coincident with the spacecraft center of mass. The reaction wheels (part of the ACS) typically absorb the momentum imparted by these torques to maintain spacecraft attitude. To do this, they produce momentum that is equal to and opposite of the direction of the disturbance torque. However, they do have a maximum speed, limiting the amount of momentum they can absorb. Rotating at their maximum speed for long durations can lead to the wheels becoming oversaturated or excessive wear on the wheel bearings. To extend wheel life and spin the wheels back down, specific thrusters are fired to generate an opposing angular momentum to that of the spinning wheel, thereby “dumping”, or unloading the momentum. This is known as a  $\Delta H$  maneuver. When performing this maneuver the thrusters cycle, or pulse, on/off for a short period of time. The pulsing, or pulse mode, thruster performance is characterized by a thruster’s impulse bit, given in terms of Newton-seconds (Ns). Thruster minimum impulse bit is driven by the minimum amount of time a thruster valve that can cycle open/close while flowing enough propellant to produce measurable thrust. The corresponding pulse mode  $I_{sp}$ , which is lower than steady-state  $I_{sp}$ , is calculated based on the thruster impulse bit and consumed propellant.

The total amount of propellant needed for the  $\Delta H$  maneuvers is calculated using Eq. (1). It is based on the total angular momentum the spacecraft will need to unload

during the life of the mission, the thrusters' pulse mode performance, and the effective length of the thrusters' moment arm [16]:

$$m_{p,\Delta H} = \frac{\Delta H}{I_{sp,pl} g_0 L_{CA}} \quad (1)$$

For this example, assume that the total life time accumulated angular momentum ( $\Delta H$ ) is 76.8 Newton-meter-second (Nms), pulsed specific impulse ( $I_{sp,pl}$ ) is 178.0 s [17], and the thruster moment arm ( $L_{CA}$ ) is 0.25 m. Therefore, given that the acceleration of gravity on Earth ( $g_0$ ) is 9.81 m/s<sup>2</sup>, the propellant mass needed over the course of the mission for momentum unloading ( $m_{p,\Delta H}$ ) is 0.18 kg.

Using Eq. (2) the  $\Delta v$  propellant mass ( $m_{p,\Delta v}$ ) is calculated using the spacecraft dry mass,  $\Delta H$  propellant mass, and worst-case steady-state  $I_{sp}$ . This equation shows a conservative approach to calculating  $\Delta v$  propellant mass by considering the  $\Delta H$  propellant mass as part of the spacecraft dry mass:

$$\begin{aligned} m_{p,\Delta v} &= m_i - m_f \\ &= (m_f + m_{p,\Delta H}) e^{\frac{\Delta v}{g_0 I_{sp}}} - (m_f + m_{p,\Delta H}) \\ &= (m_f + m_{p,\Delta H}) \left( e^{\frac{\Delta v}{g_0 I_{sp}}} - 1 \right) \end{aligned} \quad (2)$$

From Eq. (2) the  $\Delta v$  propellant mass is 2.9 kg. Using this result along with the  $\Delta H$  propellant mass calculated in Eq. (1), the total propellant mass is 3.1 kg.

Once the total propellant mass is known, the maximum propellant volume, a key consideration for mechanical packaging, can be determined using the propellant density at the maximum expected temperature. Based on a propellant density of 1240.0 kg/m<sup>3</sup> [13] for the selected LMP-103S, the propellant volume is 2.5 L. With the total propellant mass being 3.1 kg, the total spacecraft wet mass is 23.1 kg, including margins. Therefore the VACCO IPS, using four Bradford-ECAPS 1 N HPGP thrusters, appears to meet mission requirements. As the spacecraft design matures (i.e., changes in component masses, refining orbit parameters, and cost), this process will be iterated until a satisfactory solution is found. A summary of this first iteration with a chemical propulsion system is detailed in Table 4.

### 3.2 Electric propulsion system sizing

If CommCubeSat1 uses an EP system, it will have to burn continuously given the low amount of thrust it produces. Analytically, the maneuver accelerations are integrated over the total burn duration required for the spacecraft to reach its mission orbit. The result of that analysis is the amount of propellant consumed. Inputs into this analysis are the performance curves of the candidate EP systems, the performance curves for the candidate solar arrays, and the potential mission launch and departure dates. Given

**Table 4** CommCubeSat1 chemical propulsion system sizing.

Insertion $\Delta v$ (m/s)	269.5
S/C dry mass (kg)	20.0
Prop system dry mass (kg)	9.0
Thruster cant angle (degrees)	15.0
Worst-Case thrust force (N)	3.6
$-3\sigma$ Specific impulse (s)	201.9
$\Delta H$ Propellant mass (kg)	0.2
$\Delta v$ Propellant mass used (kg)	2.9
Propellant vol. used (L)	2.5
S/C wet mass (kg)	23.1

that CommCubeSat1 will deploy as a secondary payload near cislunar space, the deployment energy of the spacecraft can be assumed. In addition, gravity models, planetary eclipse, and near body perturbations are also used as inputs. These results are evaluated to determine the optimal trajectory scenarios, EP system, solar array, and battery size.

Section 4.1 discusses the orbital analysis that was performed assuming the use of two Busek BIT-3 systems as the baseline. The thrust and  $I_{sp}$  versus input power curves [18] (Fig. 3) are used as input into the orbital analysis for this mission. The results in Section 4.1 show that their combined performance appears to reach the mission orbit using a small amount of propellant, if there is an appropriately sized solar array and battery. Each BIT-3 contains 1.5 kg of solid iodine propellant. With an 83% efficient power-processing unit (PPU) [18], the BIT-3 draws up to 80.0 W to produce a maximum thrust of 1.2 mN with an  $I_{sp}$  of 2160.0 s. Since two systems are needed, the total required power is 160.0 W and the maximum thrust produced is 2.4 mN.

A spacecraft consideration to be accounted for is that the BIT-3 PPU will dissipate about half of its input power in as waste heat, which is up to 40.0 W per system. For a CubeSat, this is not a trivial amount of heat to manage. Therefore the thermal engineer will have to develop a way to remove this heat from the EP system and the spacecraft into their thermal control system.

Table 5 shows the results for the CommCubeSat1 EP system design. The results show that the use of two BIT-3 systems is oversized, given the small amount of propellant used. At this point the project leads can elect to keep both BIT-3 systems and use the extra propellant for extended mission, or downsize to a single BIT-3 and save mass, power, and cost. As the design matures, this process will be iterated until a satisfactory solution is found.

Although these examples are simplified, they show mission developers what is involved in sizing different propulsion system types. There are key differences in sizing for chemical and EP systems, and each has their respective advantages and disadvantages. The next section will take these concepts a step further and compare these same propulsion systems for different mission applications.

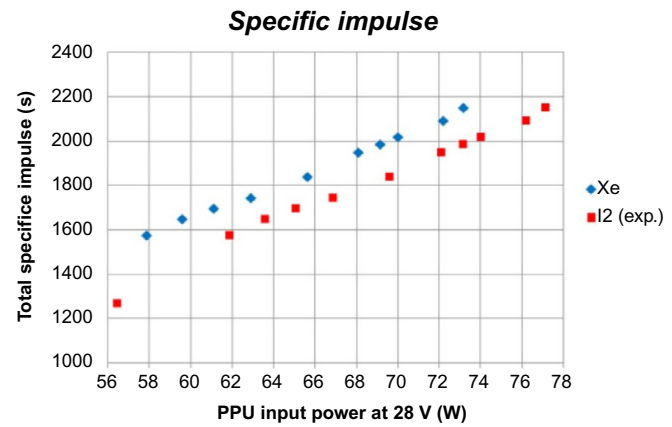
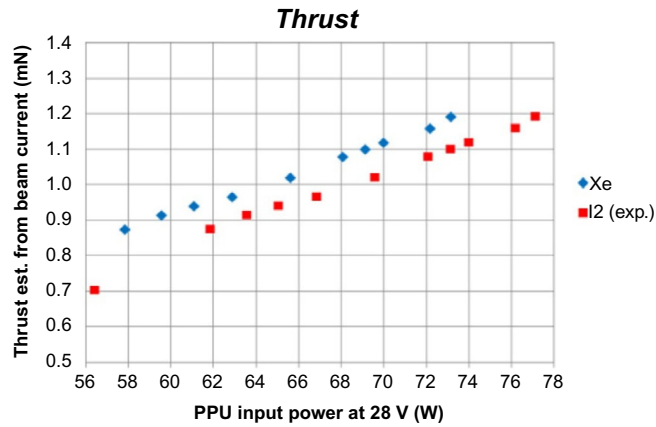


Fig. 3 Busek BIT-3 performance curves [18].

**Table 5** CommCubeSat1 electric propulsion system sizing.

<i>S/C</i> dry mass (kg)	18.0
Max. input power (W)	160.0
Max. thrust force (N)	0.0024
Specific impulse (s)	2160.0
Propellant mass used (kg)	0.4
Prop system dry mass (kg)	3.0
<i>S/C</i> wet mass (kg)	21.4

## 4 Propulsion technology mission applications

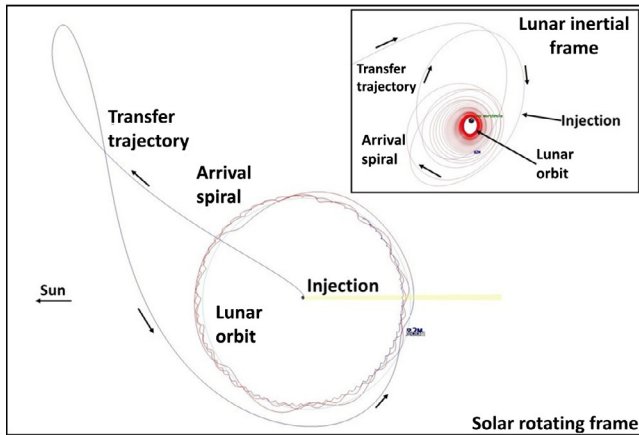
The trajectory is another key aspect of designing a mission. This section explores the trajectory designs for three missions: lunar, libration, and planetary. Each mission will use the CommCubeSat1 spacecraft bus and the previously selected chemical and electric propulsion systems. The propulsion system sizing methods for the lunar mission that was discussed in [Section 3](#) will be used to calculate sizing results for the libration and planetary trajectories. This section will also discuss the orbital mechanics parameters used to determine the inputs needed to size the propulsion systems. Disturbance torques are not considered in this example, which incorporates third body perturbations, solar radiation pressure acceleration, and lunar gravity modeling. The propulsion system sizing comparisons for these missions are summarized in [Section 4.4](#). As with the previous example, these nonoptimal designs provide a feasible assessment of their implementation including trajectory constraints required for their use and a representative result.

### 4.1 Lunar mission example

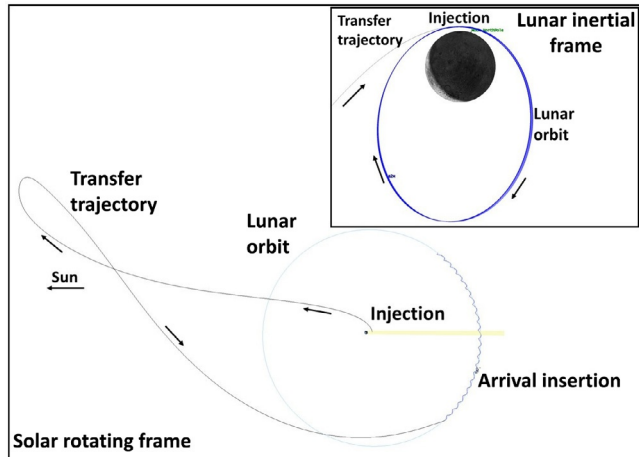
The trajectories designed for the Lunar Mission incorporate multibody dynamics to minimize the lunar orbit insertion  $\Delta v$  and propellant mass. The final orbit is the critically inclined lunar elliptical orbit of 57.4 degrees with a semimajor axis of 5049 km and an eccentricity of 0.605 [19]. [Fig. 4A](#) shows the EP system transfer and capture, while [Fig. 4B](#) presents the chemical system. Both figures use a solar rotating coordinate frame for the transfer followed by a lunar-centered inertial frame for the near lunar arrival and capture. The chemical design incorporates the same force models used for the EP design. To capture into the mission orbit with a EP system, consideration needs to be given to the Earth, Moon, and Sun dynamic system about the Moon at the arrival distance of  $\sim 60,000$  km. The chemical propulsion system design permits a direct capture into the mission orbit with a maneuver performed at a radius of 1937 km.

Based on these trajectory parameters, the chemical system has an insertion  $\Delta v$  of 269.5 m/s, a total transfer time of 102 days, with a maximum maneuver duration of 29 min. The EP system results in a total transfer time of 184 days and a maneuver duration of 82.5 days, in an antivelocity vector direction throughout the maneuver.





(A)



(B)

**Fig. 4** Lunar mission trajectory design: (A) EP trajectory design and (B) chemical trajectory design.

Looking at Fig. 4A, the wavy lines around the lunar orbit represent the spacecraft spiraling down to its final orbit. The spiraling maneuver is further highlighted in this figure’s inset. The resulting insertion  $\Delta v$  is 730.0m/s. (This  $\Delta v$  is not used to size an EP system and is only provided for the purpose of comparison.)

### 4.2 Libration orbit example

A libration orbit design was generated for CommCubeSat1 based on the lunar mission system parameters discussed in the previous section. This orbit is a direct transfer from a low Earth parking orbit of 200km to a Sun-Earth Libration-1 (SE-L1) Lissajous orbit

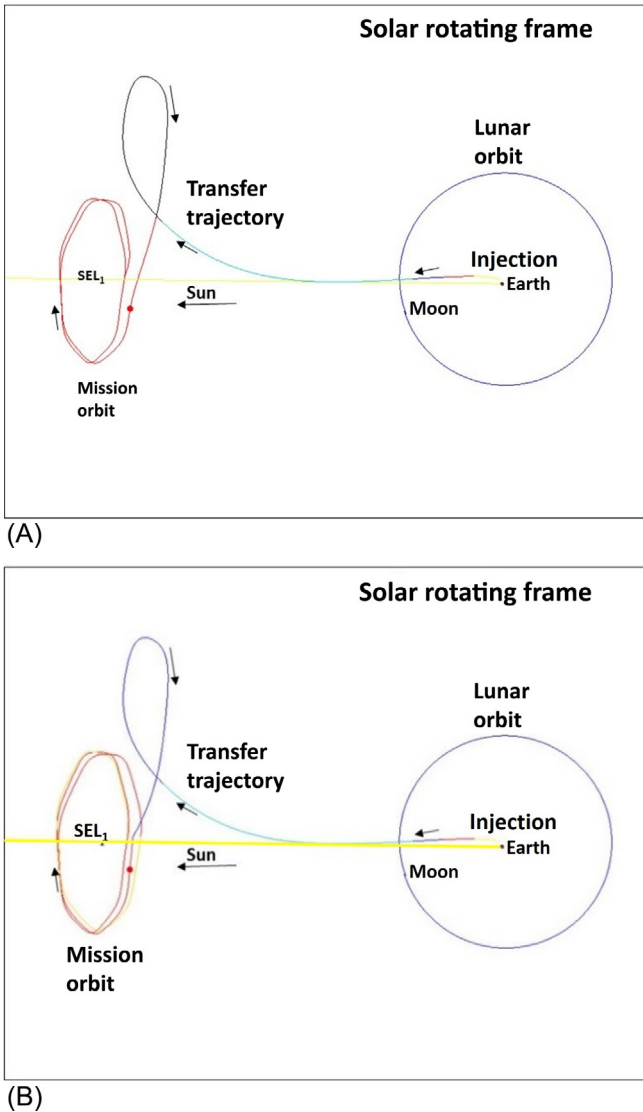


**Fig. 5** SE-L1 Lissajous orbit design: (A) EP trajectory design and (B) chemical trajectory design.

that has a Y-amplitude of 1,370,457 km (a  $4.0 \times 14.0$  degrees angle off the Sun-Earth line). The designs shown in Fig. 5A and B are illustrated in a solar rotating coordinate frame. Insertion into the Lissajous orbit is a single maneuver targeting a required energy level that permits the transition onto the libration orbit.

The chemical system insertion  $\Delta v$  of 174.0 m/s has a maximum burn duration of 19 min. The EP system has a maximum burn duration of 19.4 days, consuming

0.2 kg of propellant, where half of the burn is performed before the Sun-Earth  $X$ - $Z$  plane crossing. Looking at [Table 6](#), the libration orbit insertion  $\Delta v$  for the chemical and EP systems are similar, but this is attributed to the maneuver being performed in open space, with similar changes in inertial velocity, and not influenced by a maneuver location within the gravitational effects of Earth. This illustrates the misleading nature of using  $\Delta v$  to size an EP system.

### 4.3 Planetary mission (Mars) example

A planetary mission design was generated for CommCubeSat1 using a Mars capture trajectory into the Phobos orbit (assuming a 9216 km circular orbit). This design is based on a Type-I heliocentric transfer from Earth to Mars. Several other transfer types could be used, but this feasible case was designed to demonstrate only the differences in the capture dynamics and the capture maneuver.

The designs shown in [Fig. 6A](#) and [B](#) are presented in a Mars Inertial Coordinate Frame. The initial location is based on the heliocentric position with respect to Mars so that the planetary excess energy is zero. This excess velocity is required as the initial condition for the EP system as it targets a zero excess planetary velocity upon arrival. The differences in this example are more prominent than in the previous examples. Two chemical maneuvers (approximately 729.7 m/s each) are required to capture the Phobos orbit. An additional chemical maneuver (approximately 511.1 m/s), based on Oberth's rule [\[20\]](#), is performed to increase the maneuver's efficiency and to circularize. The total  $\Delta v$  magnitude with the chemical system is 1970.5 m/s and has a total burn duration of 5.3 h. The EP maneuver begins at the zero excess velocity location and a burn duration of approximately 215 days, and 2.1 kg of propellant is required to reach the Phobos mission orbit. The spacecraft wet mass for the EP cases is 24.0 kg.

### 4.4 Summary of examples

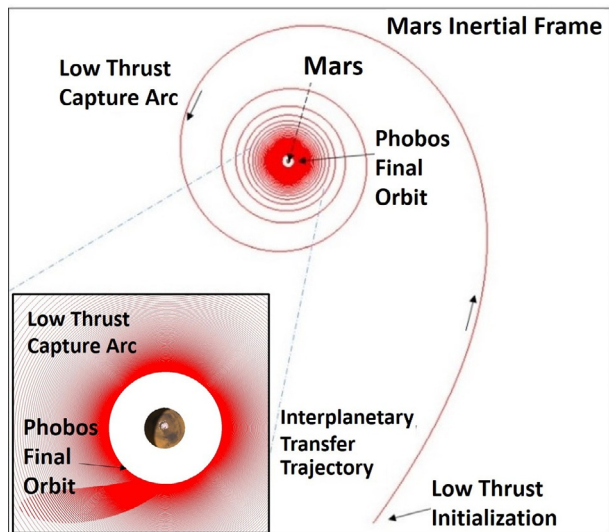
The previous nonoptimal examples present feasible designs using the selected chemical and EP systems. [Table 6](#) shows the results from each of these designs. The figures of merit that are prefixed with "Mission" are calculated based on the sizing results. The figures of merit that are prefixed with "Spacecraft" or "Propulsion System" are based on the capability of the selected propulsion system within the spacecraft bus, as defined in [Table 3](#).

[Table 6](#) shows that missions using the EP system are more efficient with respect to propellant use but requires longer maneuver durations. Longer maneuvers lead to longer mission operational support (including navigation tracking during the maneuver) and hence greater mission cost. The selected chemical system provides lower transfer times for the lunar and libration trajectories. However, the selected chemical propulsion system is not feasible for the planetary mission.

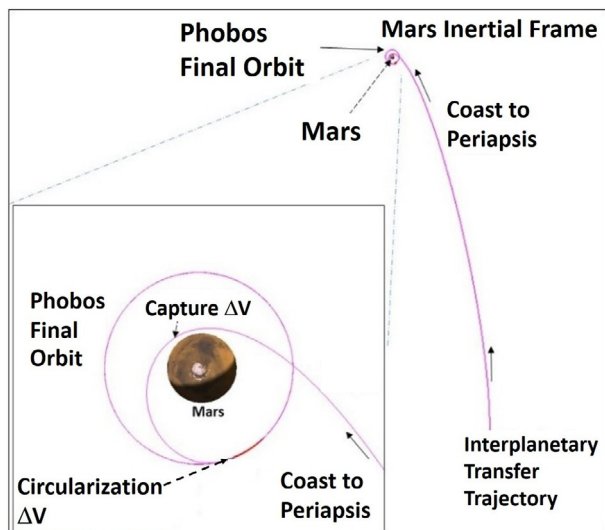
**Table 6** Comparison parameters for chemical and electric propulsion systems.

	<b>Lunar chemical</b>	<b>Lunar EP</b>	<b>Libration chemical</b>	<b>Libration EP</b>	<b>Planetary chemical</b>	<b>Planetary EP</b>
Spacecraft wet mass (kg)	23.1	24.0	22.0	24.0	54.6	24.0
Insertion $\Delta v$ (m/s)	269.5	730.0	174.0	172.0	1970.5	1935.0
Effective $I_{sp}$ (s)	201.9	2160.0	201.9	2160.0	201.9	2160.0
$\Delta v$ Propellant mass (kg)	2.9	0.4	1.9	0.2	34.4	2.1
Mission propellant mass (kg)	3.1	0.4	2.0	0.2	34.6	2.1
Mission propellant volume (L)	2.5	0.1	1.6	0.04	27.9	0.5
Mission total impulse (Ns)	6173.3	8472.9	4017.9	4024.6	68,472.1	44,483.0
Mission propellant mass fraction (%) <sup>a</sup>	15.6	1.5	10.1	0.7	172.9	8.4
Propulsion system total impulse (Ns) <sup>a</sup>	11,285.8	63,547.1	11,285.8	63,547.1	11,285.8	63,547.1
Spacecraft propellant mass fraction (%) <sup>a</sup>	28.5	11.3	28.5	11.2	28.5	12.0
Propulsion system propellant mass (kg)	5.7	3.0	5.7	3.0	5.7	3.0
Propulsion system dry mass (kg)	9.0	3.0	9.0	3.0	9.0	3.0
Spacecraft bus dry mass w/o prop. sys. (kg)	11.0	23.6	11.0	23.8	11.0	21.9
Burn duration (h)	0.5	1980.0	0.3	465.8	5.3	5148.5
Total transfer time (days)	102.0	184.0	111.0	121.0	203.0	418.0

<sup>a</sup> Based on propellant capacity listed in [Table 3](#).



(A)



(B)

**Fig. 6** Mars capture to phobos orbit: (A) EP trajectory design and (B) chemical trajectory design.

## 5 Conclusion

This chapter discussed the methods used to assess and size a CubeSat propulsion system. The figures of merit and TRLs help mission designers evaluate the systems on the market. The examples presented illustrate how to size a system for different types of missions. Each of these designs highlight various considerations and trades that could be made to reach an optimal system, such as a lighter weight chemical system with similar performance compared with what is being assessed, or a lower power EP system with higher thrust. Other trades that could be made include using a lighter mission payload (e.g., communications system and instrument), other trajectory options, or making a lighter structure. Frequently these design iterations take many weeks, or months, to close, but understanding and proper application of these tools will lead to successful missions.

## References

- [1] R. Humble, G. Henry, W. Larson (Eds.), *Space Propulsion Analysis and Design* (Rev.), McGraw-Hill, New York, NY, 1995.
- [2] J. Wertz, D. Everett, J. Puschell (Eds.), *Space Mission Analysis and Design*, In: *Space Technology Library Space Technology Series* Microcosm Press/Kluwer Academic Publishers, El Segundo, CA/Dordrecht, Netherlands, 2011.
- [3] G. Sutton, O. Biblarz (Eds.), *Rocket Propulsion Elements*, seventh ed., John Wiley & Sons, New York, NY, 2000.
- [4] C. Brown, *Spacecraft Propulsion*, AIAA Education Series American Institute of Aeronautics and Astronautics, Washington, DC, 1996.
- [5] D. Goebel, I. Katz, *Fundamentals of Electric Propulsion: Ion and Hall Thrusters*, JPL Space Science and Technology Series Jet Propulsion Laboratory, California Institute of Technology, NASA, Pasadena, CA, March 2008.
- [6] W.A. Hargus, J.T. Singleton, Annual assessment of cubesat propulsion technology and maturity, in: *Proceedings of the 6th Government CubeSat Technical Interchange Meeting*, Pasadena, CA, April, 2014.
- [7] *NASA Systems Engineering Processes and Requirements*, NPR 7123.1, National Aeronautics and Space Administration, February 14, 2020.
- [8] W. Hargus, JANNAF guidelines for the application of technology readiness levels (TRLs) to micro-propulsion systems, in: *JDOC 2019-0004FO, JANNAF 10th Spacecraft Propulsion Meeting*, December, 2019.
- [9] *Space Systems—Metallic Pressure Vessels, Pressurized Structures, and Pressure Components*, ANSI/AIAA S-080A-2018, American Institute for Aeronautics and Astronautics, March 20, 2018.
- [10] *General Environmental Verification Standard (GEVS)*, GSFC-STD-7000, National Aeronautics and Space Administration, April 22, 2013.
- [11] *NASA Expendable Launch Vehicle Payload Safety Requirements*, NASA-STD-8719.24, National Aeronautics and Space Administration, September 30, 2015.
- [12] *Range Safety User Requirements Manual*, AFSPCMAN 91-710, United States Air Force Space Command, November 3, 2016.

- 
- [13] S. Weston, *State of the Art of Small Spacecraft Technology*, Small Spacecraft Systems Virtual Institute, Ames Research Center, Moffett Field, CA, 2018 NASA/TP-2018-220027.
  - [14] *Mass Properties Control for Space Systems*, ANSI/AIAA S-120A, American Institute for Aeronautics and Astronautics, November 23, 2015.
  - [15] R. Hevner, et al., *An Advanced Standard for CubeSats*, SSC11-II-3, 2011 Small Satellite Conference, Logan, UT, August 2011.
  - [16] W. Willis, *Propulsion System Design for MDL Studies*, NASA Goddard Space Flight Center, Greenbelt, MD, July 2018 (unpublished).
  - [17] K. Anflo, et al., *Flight Demonstration of New Thruster and Green Propellant Technology on The PRISMA Satellite*, SSC07-X2, 2007 Small Satellite Conference, Logan, UT, August 2007.
  - [18] D. Courtney, M. Tsay, N. Demmons, *Busek SmallSat technologies*, in: Planetary CubeSat Symposium, NASA Goddard Space Flight Center, August, 2018.
  - [19] D. Folta, et al., *Applications of multi-body dynamical environments: the ARTEMIS transfer trajectory design*, in: 61st International Astronautical Congress 2010, Prague, Czech Republic, Paper ID: 7461, September 2010, 2012.
  - [20] P. Blanco, C. Mungan, *Rocket propulsion, classical relativity, and the Oberth effect*. *Phys. Teach.* 57 (439) (2019). <https://doi.org/10.1119/1.5126818>.

# Thermal control system

16

Boris Yendler

YSPM LLC, Saratoga, CA, United States

## 1 Introduction

The role of the thermal control system is to keep the temperature of the spacecraft components within required temperature limits for given orbits, power demand, operations, and other considerations. The thermal control system should also reduce temperature gradients across the spacecraft and some components like lenses. Two temperature limits are typically defined when considering temperature control of thermal systems: an *operational limit* and a *survival limit*. An effective thermal control system will keep the component temperatures within their operational limits. A component should not lose operability within the survival limit even at extreme temperatures. The survival limit typically  $\pm 10^{\circ}\text{C}$  is wider than the operational limit. The following sections describe the workflow required to design a thermal control system. It discusses the design process and hardware systems that are currently available to CubeSat developers. An application of the process to design a CubeSat thermal control system is also demonstrated.

A spacecraft's heat rejection capability is directly related to its size due to the fact that heat is rejected into space only by radiation. Powerful spacecraft should have large radiators to have a significant cooling capability. The same dependency of cooling capability upon unit dimensions is demonstrated by a computer workstation. Computer workstation enclosure size is determined mostly by fan diameter, which is required to remove generated heat. The similarity of two different examples from different industries confirms the fact that cooling capabilities play a significant role in design (Fig. 1).

As we see later, in Section 5, radiator sizing should be included into the spacecraft design process. If radiator size does not match the required waste energy rejection, the spacecraft temperature will increase (or decrease if a radiator is too big) and can exceed an upper limit (or a lower limit if a radiator is too big) of survivable level. This condition could lead to mission failure.

Thermal control technology for CubeSats is primarily based on passive methods, that is, surface finishes, radiators, and, sometimes, heat pipes. The active methods like liquid pumps are not typically used in CubeSats at this moment.

It is not widely recognized that thermal management for CubeSats is more complicated than for large spacecraft like GEO communication satellites. As an example, Table 1 compares a thermal situation in two satellites, GEO communication and 3U CubeSat under following assumptions:

- Only two sides (North and South) are used for heat rejection.
- Power generations are 5000 W for GEO and 50 W 3U CubeSat correspondingly.
- Electronics efficiency is 60% on both satellites, that is, 40% of generated energy is converted into waste heat.



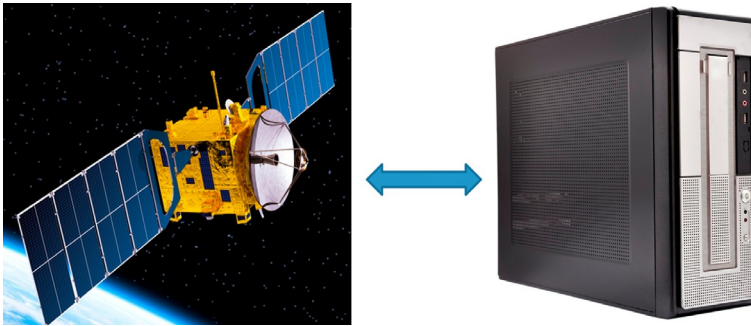


**Fig. 1** Satellite versus computer—similar problem and solutions [1].  
Reproduced with permission from iStock.

**Table 1** Comparison of GEO com and 3U CubeSat satellites.

	GEO com	3U cube sat	Ratio GEO/cube
Satellite dimension [m]	$3.0 \times 3.0 \times 6.0$	$0.1 \times 0.1 \times 0.3$	
Satellite volume [m <sup>3</sup> ]	54.0	0.003	18,000
Radiator surface [m <sup>2</sup> ] <sup>a</sup>	42.88	0.06	715
Power [W]	5000	50	100
Power density [W/m <sup>3</sup> ]	92.6	16,666.7	0.6%
Efficiency	60%	60%	
Waste heat	2000	20	100
Rejected heat flux [W/m <sup>2</sup> ]	46.6	333.3	0.14

<sup>a</sup> Only two largest surfaces are used as radiators.

The data presented in [Table 1](#) clearly shows that thermal management in CubeSat is much more complicated than for large satellites where power density is much lower and the required flux for waste heat rejection is less. This means that thermal control is less complicated in large satellites than for CubeSat due to the large volume and surfaces of GEO satellites available to radiate waste heat.

## 2 Workflow to design thermal control system for SmallSat spacecraft/CubeSats

Historically, designs of CubeSat thermal systems either never performed methodically or performed in a sporadic manner due to the incorrect opinion that a thermal control system is not important. Descriptions of often limited approaches to CubeSat thermal management systems and related hardware can be found in the existing literature [2].

Previously, CubeSats had been built mostly by universities with very low power levels, around 1–5 W. As we will see in the following sections, the current demand for CubeSats with 50 W or more changes completely the thermal requirements and, therefore, the approach to the spacecraft design. An effective thermal control system must be included in the design of the CubeSat to prevent failure of the mission.

The primary goals of thermal management are to:

- Keep spacecraft components like bus/payload/battery within temperature limits. This requires identification of factors, which affect the component temperatures and manage these factors.
- Support the structural integrity of the spacecraft considering all external conditions, that is, external panels facing the Sun, and facing deep space.
- Determine the effects of a short-term temperature excursion, which go beyond of design limits on component integrity and performance.
- Provide redundancy in thermal management.

The spacecraft industry has developed a systematic approach to the design of thermal subsystems for large spacecraft. Following best practices of the spacecraft industry, the thermal design process for CubeSats should consist of several steps (Fig. 2). If a CubeSat designer will follow the proposed approach, many mistakes in the design and potential mission failure could be prevented.

## 2.1 Requirements

A first step in good engineering design should be the establishment of requirements. Before starting a CubeSat design, the following information should be available upon which the design requirements will be based:

- Mission parameters: design life, orbit, vehicle operations, safe mode, mass limits, and deorbiting;
- Thermal parameters: amount of waste heat, temperature limits, and material criteria.

The worst-case scenario in waste heat generation and dissipation, environments (e.g., sun loading), operating modes and contamination/degradation of radiator surfaces, etc. from launch to deorbiting should be considered.

## 2.2 Conceptual design

The conceptual design process consists of two steps. First a designer should consider *conceptual design options* like aspects of the CubeSat form factor (e.g., 1U and 2U, etc.), solar array location (e.g., body mounted or deployable), radiator design (e.g., location of body mounted, material, and surface finish), multilayer insulation (MLI) (e.g., type and size), phase change material (PCM) (e.g., type and melting

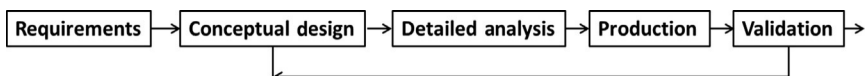


Fig. 2 Workflow of design of thermal system.

temperature), and louvers [3]. Secondly a *preliminary analysis* should be undertaken. It should include steady-state heat balance estimation at “a back-of-the-envelope” level. Hot and cold cases should be considered based on the mission requirements, orbit conditions (Section 2.1), and options selected from the aforementioned. The analysis conducted should answer a basic question: for given requirements and chosen options, will all thermal requirements met? If the answer is NO, the designer should reconsider options and find the ones (e.g., do we need heat pipes, PCM, and deployable radiator?) that meet all of the thermal requirements.

### 2.3 Detailed analysis

After completion of the conceptual design, a detailed analysis should be conducted to determine if the CubeSat design meets all requirements. It includes building a spacecraft thermal model that should take into account all important components, thermal links, orbits, etc. This thermal model predicts temperatures at the interface between components and the bus frame under worst-case hot and cold conditions. Sometimes a detailed thermal model at the component level is needed, in particular, for components with significant heat discharge.

### 2.4 Design validation

The thermal control system design is validated during thermal vacuum testing (TVAC testing). Test procedures for TVAC tests are prepared using the thermal model previously developed (Section 2.3). The TVAC test validates the thermal model and the thermal control system design, if successful. The model is also used to determine ideal positions of test thermocouples during TVAC testing. The accuracy of the thermal model is determined by comparison of the simulation results with the thermal vacuum test.

## 3 Thermal management challenges

The simplest way to remove waste heat from components is to mount heat dissipating components on a radiator inner surface. The waste heat will spread over the panel by conduction or with help of heat pipes and dissipate into space via radiation. However, CubeSat architecture often forces designers to mount boxes internally on a spacecraft frame, away from the radiators.

Previously, radiators have not been used widely on CubeSats. Waste heat has been traditionally rejected from components into the space from component surfaces. This strategy has been relatively effective because not much waste heat has been generated and the components were distributed sparsely so each component had a direct view to space. However, most component surfaces have not been treated to serve as a radiator so the efficiency of heat rejection is not high utilizing this strategy.

With the increasing complexity of CubeSat missions and corresponding CubeSat designs, the packing factor of components in the new generation of CubeSats is dense.

Components block each other so their view factor to space is minimal. Under such circumstances, radiators must be used for waste heat rejection into the space. This creates a need to transfer waste heat from the components to the radiators. Both mechanisms of heat transfer, conduction and radiation, transfer waste heat from components to radiators. The radiation portion can be enhanced by increasing emissivity of both, the internal and external surfaces and increasing radiator temperature. This can significantly contribute of total heat transfer, for example, up to 20%–30% [4]. For high fluxes of waste heat, heat pipes could be needed also to enhance waste heat transfer from components to the radiators and spreading heat over radiator surface.

Typical CubeSat systems that present thermal management challenges include the following:

- Batteries—usually operate in smaller temperature range than other electronics and lower operating temperatures. The best way to achieve effective thermal control of batteries is to have a separate thermal control system with dedicated radiator and heater.
- Optical elements—do not tolerate large temperature changes. Large temperature gradients across the optics should be also avoided to prevent thermal distortion.
- IR detectors—operate at very cold temperatures and typically require cryogenic systems. Complications might come from very close proximity of components operating at high temperatures (e.g., electrical propulsion) to IR detectors.
- Radiators—as the data in [Table 1](#) indicates, rejection of waste heat from CubeSats require much higher density than from GEO communication satellites. Essentially, the required heat flux is above a typical range of heat rejection like 150–300 W/m<sup>2</sup>. There are two possible solutions to this problem:
  - Increase radiator temperature. This can be done only if different radiators will be assigned to different heat generating components. This allows increasing radiator temperature for some components and reducing the radiator size. For example, some electronics can work at 70°C, while battery temperatures cannot exceed 40°C. If both, electronics and batteries, are connected to the same radiator, the radiator size is determined by sum of fluxes of waste heat from both sources and the maximum allowable temperature for the battery. However, if electronics and the batteries are connected to different radiators, a total radiator area would be less than in the first case.
  - Use a deployable radiator that increases radiator area while keeping the spacecraft size constant. However, use of the deployable radiator necessitates a solution of a very complicated technical problem: transferring waste heat from the spacecraft body into the deployable radiator across the hinge with a minimal temperature drop across the hinge. The loop heat pipe (LHP) represents one of the possible solutions. However, the LHP brings its own set of problems.

## 4 Heat balance estimation

At the conceptual design step ([Section 2.2](#)), it is paramount to conduct a preliminary analysis based on steady-state heat balance estimation for extreme thermal environments (hot and cold cases) that will drive the spacecraft design. The thermal environments depend on orbit and spacecraft parameters including spacecraft dimensions and power dissipation. The operating environments are described in the succeeding text:

- I. Low Earth orbit (LEO) missions are between 400 and 800 km altitude. Albedo and Earth infrared loads significantly contribute into the thermal environment and must be taken into account. Typically a period of a circular orbit is around 90–95 min.
- II. Geostationary (GEO) missions generally maintain a constant altitude. Albedo and Earth infrared contribution into thermal environment is small.
- III. High Earth orbits can be highly eccentric with a very low perigee (several hundreds of kilometers) and with an apogee of many thousands of kilometers. The thermal environment changes from significant influence of Albedo and Earth IR at the perigee to only direct solar contribution at the apogee.
- IV. Interplanetary missions can have a significant variation in solar flux depending on the distance to the Sun.

The major task of a preliminary analysis is to determine thermal balance of the radiators. This will affect the spacecraft design in a significant way. A rough estimation of required radiator size and optical treatments will be determined based on the thermal balance equation. Fig. 3 shows a hot case thermal environment for a CubeSat: the spacecraft is exposed to solar, Albedo and Earth IR fluxes. The absorbed heat is radiated to space through radiators. Under these assumptions, the energy balance for a radiator can be written as follows:

$$Q_{ext} + Q_{int} + Q_{backload} = Q_{rad} \quad (1)$$

where  $Q_{ext}$  is the external heat (e.g., from the Sun) absorbed by the radiator,  $Q_{int}$  is the internal heat generated by the satellite,  $Q_{backload}$  is the external heat load on other surfaces, and  $Q_{rad}$  is the heat radiated by radiator.

Substituting Eq. (1) for

$$Q_{ext} = q_{ext}A \text{ and } Q_{rad} = \epsilon\sigma AT^4$$

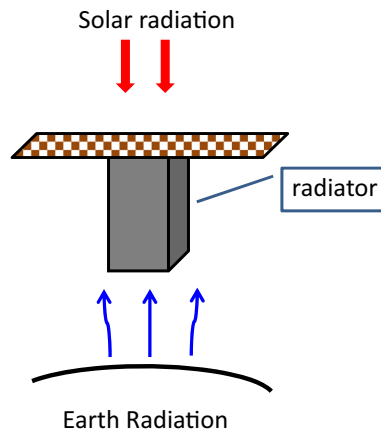


Fig. 3 Thermal environment.

The radiator heat balance becomes

$$q_{ext}A + Q_{int} + Q_{backload} = \epsilon\sigma AT^4 \quad (2)$$

where  $q_{ext}$  is the external heat load on the radiator per unit area,  $A$  is the radiator area,  $\epsilon$  is the radiator emissivity,  $\sigma$  is the Stefan-Boltzmann constant ( $5.67 \times 10^{-8} \text{ W/m}^2 \text{ K}$ ) and  $T$  is the radiator temperature.

The external heat load on the radiator can be split on four components:

$$q_{ext} = q_{solar} + q_{albedo} + q_{EarthIR} \quad (3)$$

where  $q_{solar}$  is the solar load per unit area,  $q_{albedo}$  is the albedo load per unit area, and  $q_{EarthIR}$  is the Earth IR load per unit area. Typically,  $q_{albedo} = 0.3 * q_{solar}$ , and  $q_{EarthIR}$  is calculated as the blackbody radiation at temperature of 250 K.

Heat balance Eqs. (2), (3) are used for consideration of two extreme, hot and cold, cases to design a spacecraft that meets the temperature requirements on both upper and lower limits. The power profile for the hot case corresponds to the case in which all components are at the highest level of heat dissipation, while the orbit is such that the spacecraft is exposed to maximum solar, albedo and Earth IR loads. All margins should be included into the input data to produce the maximum possible temperature. Similarly the input data for the cold case should be selected to result in the lowest possible temperature. However, the assumptions made for both cases should be realistic and correspond to the considered mission. For example, solar flux cannot be perpendicular to both, radiator and solar array, if they are perpendicular to each other.

A preliminary analysis always begins with consideration of the hot case. In the hot case a radiator area is estimated for a given external heat load, a given internal heat generation level, and a given radiator temperature. The estimated radiator area should be compared with an available external surface of the spacecraft for heat rejection into space. In the cold case, radiator temperature is determined for a given radiator area (determined earlier in the hot case study) and the lowest possible heat load including external and internal heat loads.

Both cases are very important for a preliminary analysis. The hot case determines the minimum required size of the radiator area. If the analysis shows that the required radiator area is larger than the available CubeSat external surface, something must be done to resolve the problem. Possible solutions include the following:

- (a) Increase radiator temperature.
- (b) Use a deployable radiator.
- (c) Accumulate waste heat at the peak demand and reject heat later.
- (d) Increase spacecraft size, that is, add section(s) to satisfy requirement for radiator area.

The solutions (a) and (b) have been discussed in [Section 3](#). The solution (c) is possible when generation of waste heat varies with time. The heat is stored at the time of peak generation and rejected into space at the time of low demand. The heat accumulator could be a component with high heat capacity or phase change material (PCM). The later uses a latent heat of melting/solidifying to store and release heat at the constant temperature.

The cold case defines the coldest spacecraft temperature under given thermal conditions when a spacecraft radiator is defined per the hot case. If the lowest temperature is below allowable temperature, heaters must be used to raise component temperature above the lowest limit. If a PCM-based accumulator is used for temperature fluctuation moderation, latent heat of solidification must be included in the heat source contributions.

## 4.1 Example

*Problem:* Determine the required radiator area and heater size (if mandatory) for the 6U CubeSat depicted in Fig. 4. The component heat dissipation is 50 W. The spacecraft has deployable solar arrays. Assuming an isothermal radiator and energy balance governed by Eqs. (2), (3), the radiator area that will keep temperature of the radiator below or equal to  $T_{max}$ , is determined to be

$$A = \frac{Q_{int} + Q_{backload}}{\epsilon \sigma T_{max}^4 - (q_{solar} + q_{albedo} + q_{EarthIR})} \quad (4)$$

Assume heat generation:  $Q_{int} = 50$  W (hot case);  $T_{min} = 273$  K;  $T_{max} = 313$  K;  $q_{solar} = 1420$  W/m<sup>2</sup>;  $q_{albedo} = 0.3 * q_{solar} = 426$  W/m<sup>2</sup>; and  $q_{EarthIR} = 240$  W/m<sup>2</sup>. Optical properties of external surfaces are as follows: emissivity ( $\epsilon$ )—0.8, solar absorptivity ( $\alpha$ )—0.2; orbit parameters, inclination 0 degrees, altitude—500 km; view factors for  $\pm Y$  and  $\pm X$  panels to Earth is 0; and view factors  $\pm Y$  and  $\pm X$  panes to Space is 1.0.

### 4.1.1 Hot case

We will explore which of the two positions, (a) and (b), depicted in Fig. 4 constitutes the worst case.

As one can see from Table 2, position (b) is the most challenging, because the required radiator area is large than the available external surfaces available for radiation, that is, there is not enough surface to keep the radiator temperature below 313 K. Calculations show that an available radiator area of 0.14 m<sup>2</sup> can keep the radiator

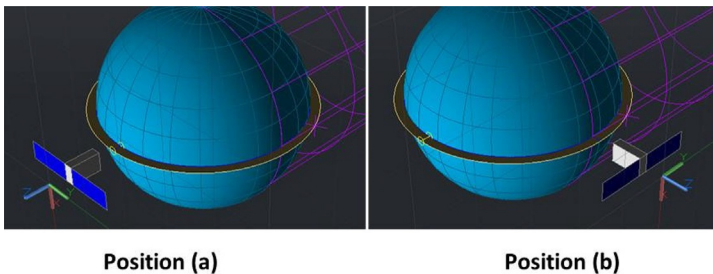


Fig. 4 Example.

**Table 2** Hot case study.

	Position (a)		Position (b)	
+Z Panel 0.02 m <sup>2</sup>	Receives solar heat load	$Q_{+Z} = 0.02 * 0.2 * 1420 = 5.68 \text{ W}$	Radiates heat into space	
−Z Panel 0.02 m <sup>2</sup>	Receives albedo and Earth IR heat loads	$Q_{albedo} = 0.3 * 5.68 = 1.74 \text{ W}$ $Q_{Earth IR} = 0.02 * 240 = 4.8 \text{ W}$	Receives albedo and Earth IR heat loads	$Q_{albedo} = 0.3 * 5.68 = 1.74 \text{ W}$ $Q_{Earth IR} = 0.02 * 240 = 4.8 \text{ W}$
+Y Panels 0.06 m <sup>2</sup>	Radiates heat into space		Radiates heat into space	
−Y Panels 0.06 m <sup>2</sup>	Radiates heat into space		Receives solar heat load	$Q_{-Y} = 0.06 * 0.2 * 1420 = 17.04 \text{ W}$
±X Panels 0.03 m <sup>2</sup>	Radiates heat into space		Radiates heat into space	
Backload	$Q_{backload} = 5.68 + 1.74 + 4.8 = 12.22 \text{ W}$		$Q_{backload} = 17.04 + 1.74 + 4.8 = 23.58 \text{ W}$	
Available radiator [m <sup>2</sup> ]	$2 * 0.06 + 2 * 0.03 = 0.18$		$0.02 + 0.06 + 2 * 0.03 = 0.14$	
Required radiator [m <sup>2</sup> ]	$A = \frac{55 + 12.22}{0.8 * 5.68 * 10^{-8} (313)^4} = 0.14$		$A = \frac{55 + 23.58}{0.8 * 5.68 * 10^{-8} (313)^4} = 0.17$	

temperature equal or below 328 K, that is, 15 K higher than  $T_{max}$ . Another option would be to use 12U satellite to increase area of  $\pm X$  panels.

#### 4.1.2 Cold case

The spacecraft is in an eclipse; maximum internal heat generation is assumed to be 10 W; the minimum radiator temperature  $T_{min}$  should be equal to or higher than 273 K (0°C); all panels with exception of the −Z panel radiate heat into space. The spacecraft temperature is determined from heat balance Eqs. (2), (3):

$$T = \sqrt[4]{\frac{Q_{int} + Q_{backload}}{\varepsilon \sigma A}}$$

Table 3 shows that the radiator temperature would be around 200 K (−73°C) in the cold case, much lower than  $T_{min}$ . Additional heater(s) are required to bring the spacecraft radiator temperature to a reasonable level. For example, an additional 35.5 W heater is required to bring the radiator temperature to 0°C. To meet such a requirement



**Table 3** Cold case.

	<b>Eclipse</b>	
+Z Panel 0.02 m <sup>2</sup>	Radiates heat into space	$Q_{Earth\ IR} = 0.02 * 240 = 4.8\ W$
−Z Panel 0.02 m <sup>2</sup>	Receives Earth IR heat loads	
±Y Panels 0.06 m <sup>2</sup>	Radiates heat into space	
±X Panels 0.03 m <sup>2</sup>	Radiates heat into space	
Available radiator [m <sup>2</sup> ]	$2 * 0.06 + 2 * 0.03 + 0.02 = 0.2$	
Radiator temperature [K]	$T = \sqrt[4]{\frac{10 + 4.8}{0.8 * 0.2 * 5.68 * 10^{-8}}} = 200$	

could be a challenge because it will require the use of a battery during eclipse when battery charging is not possible. This means that the results of cold case analysis affect battery sizing.

## 5 Power

A CubeSat designer should be aware that the capacity of waste heat rejection for a given radiator can limit energy generation by the spacecraft energy sources (solar arrays), specifically the ability for the spacecraft thermal control system to dissipate the residual heat associated with the power source. As an illustration, consider a problem from [Section 4.1](#) assuming 60% efficiency of power utilization. This means that the total power generated by the solar arrays is 125 W. If the power level generation surpasses 125 W, the waste heat generation will exceed 50 W, which will lead to an increase in the radiator temperature. Such an increase will affect component temperatures.

Maximum energy production for different CubeSats was investigated in previous studies by Yender [1] (see [Fig. 5](#)). The study assumes that spacecraft has solar deployable arrays and energy efficiency of 60%. The study has shown also a strong effect of optical properties of external surfaces on upper limit of energy production. Higher solar absorptivity leads to low energy production limit. On the other hand, higher emissivity facilitates higher energy generation limits.

## 6 Hardware for satellite temperature control (STC)

The goal of the STC system is to keep the temperature of all satellite components within limits. The STC employs many different types of hardware to achieve this goal. Heaters, multilayer insulation (MLI), heat pipes, finishes of surfaces, phase change materials, etc. are employed by the STC. A detailed description of the hardware that is used in large satellites can be found elsewhere [5]. We will concentrate on use of the hardware in CubeSats.

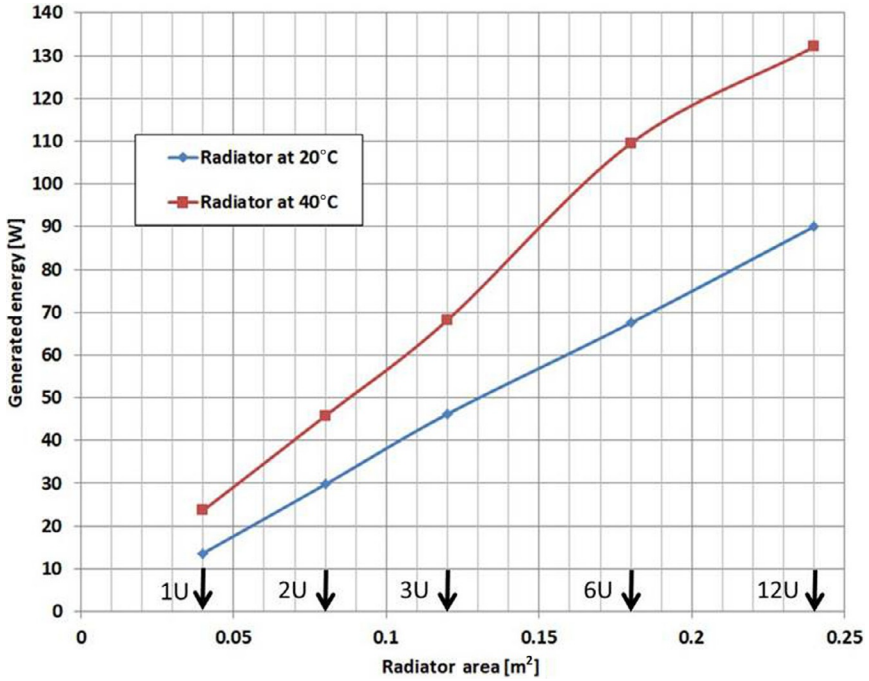


**Fig. 5** Useful energy generation for CubeSats [1].  
Reproduced with permission from author, B. Yendler.

## 6.1 Multilayer insulation (MLI)

MLI is typically made of multiple layers of metallized plastic film conductively isolated from each other by spacers and assembled as blankets. Externally, MLI reduces thermal radiation to space and protects against excessive heat fluxes such as Sun and thruster plume heating. Internally, MLI blankets are used to create areas of separate thermal control, to reduce temperature gradients across the spacecraft, and to reduce heater power consumption. Blankets have to be grounded to the spacecraft structure to prevent electrostatic charge buildup and arcing. MLI blankets have to have vents to reduce outgas pressure to minimize gaseous conduction effects. Due to fact that both radiative and conductive heat transfer occur simultaneously, the best way to describe heat transfer through MLI is to use coefficient of effective emissivity ( $\epsilon^*$  or ESTAR) which is defined as

$$Q_{net} = A_{MLI} \epsilon^* \sigma^* (T_{in}^4 - T_{ex}^4)$$

where  $A_{MLI}$  is MLI area,  $\epsilon^*$  is effective emissivity (Estar), and  $T_{in}$  and  $T_{ex}$  are temperatures of the inner and out layers.

CubeSat designers should be aware that small patches of MLI show a significant variation of properties across their surface. For example, Estar for 20 layers MLI blanket (12 in  $\times$  12 in) changes from 0.006 in the middle to 0.15 close to seam, which

indicates a change of heat loss from  $3 \text{ w/m}^2$  to  $30 \text{ w/m}^2$  [5]. The situation will be even worse for smaller MLI blankets.

## 6.2 Highly conductive strips

Typically, components inside a CubeSat are mounted on shelves that are attached to the space frame. Heat that is generated by a component has to flow from the component through fastener to the shelf, along the shelf, through fastener of the shelf to the CubeSat frame and from the frame to the radiator. Rough estimations indicate that the thermal conductivity of such a pass is about  $0.5 \text{ W/K}$ . If the amount of the transferred heat is a couple of  $\text{W}$ , a temperature drop across the pass is not significant. However, transfer of  $20 \text{ W}$  would require a temperature difference of  $40^\circ\text{C}$ . Assuming the maximum component temperature of  $60^\circ\text{C}$ , the radiator temperature has to be at  $20^\circ\text{C}$ . This requirement will lead to a significant increase in the radiator size. Creation of a thermal path with minimum resistance is very important for CubeSats with power above  $20\text{--}30 \text{ W}$ . Thermal resistance of fasteners like screws and bolts can be very significant [5] and must be taken into account during design of the thermal control system.

Using a copper strip could help but only for a small heat flux. For example, transferring  $10 \text{ W}$  from the middle of the CubeSat to the surface at a  $3^\circ\text{C}$  temperature difference would require the cross section of the strip be about  $4 \text{ cm}^2$ , which is quite significant. A heat pipe is the best solution for transferring more than  $10 \text{ W}$  of heat across these types of junctures.

## 6.3 Heat pipes

Heat pipes could be useful for several applications. Among them are to:

- Conduct heat from a component mounted on a shelf to a CubeSat external surface.
- Transfer solar load from a sunny side to a shaded side. For example transfer heat from  $-Y$  panel to  $+Y$  panel for spacecraft in position (b) in Fig. 4. The heat pipes are located on the external surfaces and connected to each other.
- Connect an external panel with a deployable radiator.
- Spread heat over radiator to reduce temperature gradients along radiator surface.

There are several requirements associated with the use of a heat pipe including the following:

- (a) Heat transfer liquid and material of the heat pipe should be compatible with each other. Previous work extensively discusses this subject [5].
- (b) Special attention should be paid to the position of the heat pipes relatively to the Earth during TVAC test, namely, heat pipes should be horizontal to the surface of the Earth.

## 6.4 Thermal surface finishes

An increase of CubeSat power intensifies the radiation heat exchanger inside the spacecraft and heat rejection into space. For external surfaces, optical solar reflector

(OSR), white paints and other treatments are used to minimize absorbed solar energy while maximizing heat rejection. If solar arrays are mounted on the spacecraft, the area of the arrays should be treated as having high solar absorptivity ( $\alpha \approx 0.75\text{--}0.8$ ) and high IR emissivity ( $\epsilon \approx 0.85\text{--}0.9$ ). Black paint is commonly used on internal surfaces of the spacecraft to enhance radiative heat transfer among internal components and radiative exchange with the internal surfaces of radiators.

## 6.5 Phase change material (PCM)

PCM absorbs energy during melting and releases the energy during solidification. Both, melting and solidification, occur at the same temperature. The use of PCM-based systems for thermal control is not new [5]. A general application of PCM thermal control is for cyclically operating components that are operating on an ON-OFF cycle. The same is true for environment heating of CubeSats. For example, panels of the spacecraft shown in Fig. 4 are periodically exposed either to a Sun load or are facing space. A PCM accumulator can store solar energy when the radiator is facing the Sun and release solar energy during shadow. Storing energy at the peak load and releasing it later significantly reduces required radiator size.

PCMs are differentiated by melting point and latent heat of fusion. Extensive description of PCMs can be found in Refs. [4,5]. Some PCMs like Octadecane or Eicosane have melting point temperatures around  $40\text{--}60^\circ\text{C}$ , which makes them attractive for thermal control in CubeSats. Paraffin Waxes could be used for CubeSat thermal control systems [6,7]. The toxicity of PCMs should be taken into account, in particular, for CubeSats deployed from the International Space Station due to NASA safety concerns.

Designers of PCM accumulators face two major problems, namely, low heat conductivity of a PCM and changes in PCM volume during the phase change. A solution to the first problem could be the use of fins/fillers to provide low thermal resistance paths through the PCM [5,7]. The container for PCM should be leak-proof and flexible to accommodate the volume change during melt or freezing PCM. It is reported [8] that carbon velvet thermal interfaces are able to accommodate PCM volume change.

## 6.6 Telemetry and commands

A CubeSat should have a sufficient number of temperature sensors and channels to determine the status of critical components and efficiently control heaters from ground. Using an on-board computer for the thermal control system reduces number of telemetry channels that are dedicated to temperature sensors. Typically, temperature sensors are installed on components that

- generate large amounts of heat,
- operate at cryo-level temperatures,
- might have boiling or freezing problems,
- must operate in a narrow temperature range,
- should have a specific temperature difference with other component,
- are sensitive to temperature, like battery.

Flight temperature sensors should be calibrated (typically, during thermal-vacuum testing) over the temperature range that exceeds the expected range of temperature change of a component. It should be noted also that analog-to-digital conversion of temperature reading on the satellite and reverse digital-to-analog conversion on a ground station can lead to a significant loss of accuracy of temperature reading.

A CubeSat can have thermal controls divided into several zones. For example, payload and bus can have separate temperature control zones. Another option would be to group components with similar temperature requirements as one thermal control zone. Components from the same group can be connected to one radiator, which could have the highest temperature and consequently the smallest size. It will reduce complexity of the design and improve thermal control efficiency.

Temperature sensors that are placed inside a component provide information on performance and health of the component. However, additional temperature sensors should be installed to monitor performance and health of the CubeSat. Location and parameters of such temperature sensors should be determined by simulations and verified during a thermal vacuum (TVAC) test.

Temperatures during TVAC tests are monitored by thermocouples placed in areas where the temperatures are indicative to the thermal performance and may be used to make comparisons with simulation results. The thermocouples are usually mounted using adhesive tape to avoid damaging the thermal finish. Positions of test thermocouples are shown in [Table 4](#).

A more comprehensive description of the thermocouple locations at the TVAC test can be found in Ref. [9].

If a CubeSat is designed for LEO and CubeSat crosses shadow/light separation line twice during each 90 min, it might put an additional thermal stress on the CubeSat structure. Existing TVAC chambers cannot simulate such rapid switch from hot to

**Table 4** Thermocouples locations at the TVAC test.

Item	Thermocouple location	Goal
Important electronics component (like battery)	Component baseplate	Verify calibration of flight thermistors
Frame	Near flight thermistors	Verify calibration of flight thermistors
Heaters	Near heater	Track heater activity and verify performance
Thermostats (if applicable)	Near thermostats	Verify thermostats set points
Mounting platform and radiators	Corresponding to nodalization of thermal model	Comparison of thermal model and TVAC test results

cold. Specially designed thermal shock TVAC chambers should be used for such a test. The importance of TVAC testing to validate the thermal models developed for a mission cannot be overstated.

## References

- [1] B. Yendler, How much power is too much for CubeSat, in: 15th Annual CubeSat Developers Workshop, Cal Poly San Luis Obispo, April, 2018.
- [2] NASA, State of the Art Small Spacecraft Technology, Small Spacecraft Systems Virtual Institute Ames Research Center, Moffett Field, California, NASA/TP-2018-220027, 2018
- [3] <https://technology.nasa.gov/patent/GSC-TOPS-40>.
- [4] A.I. Fernández, M. Martínez, M. Segarra, L.F. Cabeza, Selection of materials with potential in thermal energy storage, *Solar Energy Mater. Solar Cells* 94 (10) (2010) 1723–1729. <https://www.sciencedirect.com/science/article/pii/S0927024810003296?via%3Dihub>.
- [5] D.G. Gilmore, *Spacecraft Thermal Control Handbook, Volume I: Fundamental Technologies*, 2nd ed., The Aerospace Corporation; Published by Aerospace Press, 2002. 836 pages, ISBN-10: 1-884989-11-X.
- [6] N. Ukrainczyk, S. Kurajica, J. Šipušić, Thermophysical comparison of five commercial paraffin waxes as latent heat storage materials, *Chem. Biochem. Eng. Q.* 24 (2) (2010) 129–137.
- [7] R. Baby, C. Balaji, Thermal management of electronics using phase change material based pin fin heat sinks, *J. Phys. Conf. Ser.* 395 (2012) 012134.
- [8] C.L. Seaman, T.R. Knowles, Carbon velvet thermal interface gaskets, in: AIAA-2001-0217, AIAA Aerospace Sciences Meeting; Reno, Nevada, 8–11 January, 2001.
- [9] R. Karam, *Satellite Thermal Control for Systems Engineers*, Progress in Astronautics and Aeronautics, vol. 181, AIAA, 1998.

# Part Four

## CubeSat assembly, integration, testing and verification

*Mengu Cho*

Laboratory of Spacecraft Environment Interaction Engineering, Kyushu Institute of Technology, Kitakyushu, Japan

### 1 Introduction

The Kyushu Institute of Technology (Kyutech) inaugurated the Center for Nanosatellite Testing (CeNT) in 2010. CeNT is capable of performing all the tests necessary for nanosatellites whose size is up to  $50 \times 50 \times 50$  cm and weight is up to 50 kg, except radiation. The test facility of CeNT is open to external users. Since its opening, CeNT has been involved in testing of more than 2/3 of the <50kg class of satellites developed in Japan. CeNT has also tested various satellites from abroad, such as satellites from Singapore, Thailand, Vietnam, the Philippine, Egypt, Costa Rica, etc. [Table 1](#) lists the CubeSats tested at CeNT, from year 2012 to June 2019. As of June 2019, CeNT tested 30 CubeSats ranging from 1 U to 6 U. Note that there are many other non-CubeSats tested at CeNT, not listed in [Table 1](#).

Based on the experience gained through the activities at CeNT, the author served as the project lead of ISO-19683, “Space systems—Design Qualification and Acceptance Tests of Small Spacecraft and Units,” which was published in 2017. Kyutech not only tests satellites from external users but also develops its own satellites. From 2012 to 2019, Kyutech launched 18 satellites, among which 14 were CubeSats. According to Bryce Space and Technology. [1], Kyutech is the number one academic operator of satellites, less than 600kg launched since 2012. Among 18 satellites, the author was the principal investigator of 16 satellites, 8 projects. In this chapter, based on this experience, a discussion of how to improve the reliability of CubeSats while keeping the nature of low cost and fast delivery, is presented. ISO-19683 will be described in detail.

### 2 Reliability growth through AITV activities

According to ISO-10795, “Space systems—Programme management and quality—Vocabulary,” “Assembly” is “combination of parts, components, and units that form

**Table 1** List of CubeSat tested at CeNT, Kyutech (as of June 2019).

Launch year	Satellite name	Size	Organization
2012	FITSAT	1 U	Fukuoka Institute of Technology
2014	OPUSAT	1 U	Osaka Prefectural University
2014	KSAT-2	1 U	Kagoshima University
2014	INVADER	1 U	Tama Art University/University of Tokyo
2016	Stars-C	2 U	Shizuoka University
2017	Aoba VELOX-III (AV3)	2 U	Kyushu Institute of Technology/Nanayang Technological University (Singapore)
2017	Freedom	1 U	Tohoku University/Nakashimada Engineering Works
2017	TOKI	1 U	Kyushu Institute of Technology
2017	Ghanasat-1	1 U	Kyushu Institute of Technology/All Nations University College (Ghana)
2017	Mazaalai	1 U	Kyushu Institute of Technology/National University of Mongolia (Mongolia)
2017	BRC Onnesha	1 U	Kyushu Institute of Technology/Brac University (Bangladesh)
2017	Nigeria Edusat-1	1 U	Kyushu Institute of Technology/Federal University of Technology Akure (Nigeria)
2017	VELOX-II	6 U	Nanyang Technological University (Singapore)
2018	Irazu	1 U	Tecnológico de Costa Rica (Costa Rica)
2018	BHUTAN-1 (BIRDS-2)	1 U	Kyushu Institute of Technology/Department of Information and Telecom (Bhutan)
2018	MAYA-1 (BIRDS-2)	1 U	Kyushu Institute of Technology/Department of Science and Technology—Philippine Council for Industry, Energy and Emerging Technology Research and Development (the Philippine)
2018	UiTMSAT-1 (BIRDS-2)	1 U	Kyushu Institute of Technology/Universiti Teknologi MARA (Malaysia)
2018	SPATIUM-1	1 U	Kyushu Institute of Technology/Nanayang Technological University
2018	Stars-AO	1 U	Shizuoka University
2018	AUTcube2	1 U	Aichi University of Technology
2018	KnackSAT	1 U	King Mongkut's University of Technology North Bangkok (Thailand)
2019	Aoba VELOX-IV	2 U	Kyushu Institute of Technology/Nanayang Technological University (Singapore)
2019	Uguisu (BIRDS-3)	1 U	Kyushu Institute of Technology
2019	Raavana-1 (BIRDS-3)	1 U	Kyushu Institute of Technology/Arthur C Clarke Institute for Modern Technologies (Sri Lanka)



**Table 1** Continued

Launch year	Satellite name	Size	Organization
2019	NepalSat-1 (BIRDS-3)	1U	Kyushu Institute of Technology/ Nepal Academy of Science and Technology (Nepal)
–	BIRDS-4	1U	Kyushu Institute of Technology/University of Philippine Diliman/Paraguay Space Agency
–	HSKSAT	3U	Harada Seiki
–	Innosat-2	3U	Astronautic Technology (M) Sdn Bhd (Malaysia)
–	NARSSCUBE-1	1U	National Authority for Remote Sensing and Space Sciences (Egypt)
–	NARSSCUBE-2	1U	National Authority for Remote Sensing and Space Sciences (Egypt)

a functional entity,” “Integration” is “process of physically and functionally combining lower-level products (hardware or software) to obtain a particular functional configuration,” and “Verification” is “confirmation through the provision of objective evidence that specified requirements have been fulfilled”. In other words, assembly is a process to combine satellite components (ISO-19683 uses the word of “unit” for “component”) to make a satellite system or subsystem. Before assembly, each component needs to be “verified” against its requirements. Integration is a process that occurs after the assembly to make the subsystem or the system function as whole. During the assembly and integration processes, the subsystem or the system needs to be “verified” against its higher level requirements. Testing is one verification method out of many verification methods, such as analysis, demonstration, inspection, or review of design (and verification by similarity). Testing can be categorized into environment tests, functional tests, and measurement tests. Although testing is not only the verification method, due to its significance, the system life cycle phase from completion of component development until launch is often referred to as AIT or AITV. It should be stressed, however, that component verification and testing is an important process that should occur before the system AITV, as a defect in a component can stop the entire AITV process if the premature component is integrated into the system without proper verification and testing.

The advantages of CubeSats are low cost and fast delivery. These advantages are gained by the extensive use of commercial-off-the-shelf (COTS) components, parts, and manufacturing methods. COTS components are not meant for use in space. Therefore the advantages are gained by sacrificing reliability of individual satellites against low cost and fast delivery. In fact, several statistics show the poor success rate of nanosatellites including CubeSats. Bouwmeester et al. [2] showed that only 48% of nanosatellite (defined by a weight of less than 10kg) succeeded in mission after the successful launch. The more recent survey by Swartwout et al. [3] shows that only 50% achieved partial or full mission success and 25% fell in dead-on-arrival (DOA) that meant no radio was heard from the satellite.

According to Saleh et al. [4], satellite reliability can be modeled by Weibull statistics. The reliability is defined as the probability of nonfailure from time zero (deployment into orbit) to a given time. The reliability shows a sharp decrease after the launch but approaches an asymptotic decay. The initial reliability decay can be attributed to infant mortality due to mismatch of satellite design or manufacturing against operational (space) environment. The later steady decay of reliability can be attributed to random failure of individual components/parts.

During AITV, a satellite system goes through a series of tests. The tests may detect various defects in design, material, workmanship, etc. Once a defect is detected, it is corrected, and the test resumes or the development process goes back to an earlier phase. The failure rate decreases due to improvement and keeps decreasing as the testing continues until it becomes a steady value indicating the shift to the random failure mode. This is so-called Duane model of reliability growth [5]. According to Duane [5], the failure rate,  $\lambda$ , has the following time dependence, while the reliability grows,

$$\lambda(t) = \frac{\beta}{\alpha^\beta} t^{\beta-1} \quad (1)$$

where  $t$  is the time. The meanings of  $\alpha$  and  $\beta$  are explained later.

According to Crow [6], the failure is modeled by a non-homogeneous Poisson process, where the failure rate,  $\lambda$ , is not constant and decay as the time progresses until it reaches to a steady value. It is referred to as the reliability growth model. Based on the Poisson process, the probability that no failure occurs from time zero to  $t$  is given by the following:

$$R(t) = \exp\left(-\int_0^t \lambda(t') dt'\right) \quad (2)$$

We substitute Eq. (1) into Eq. (2) and integrate over the time. Then, we obtain

$$R(t) = \exp\left(-\left(\frac{t}{\alpha}\right)^\beta\right) \quad (3)$$

This is equal to the Weibull distribution with  $\alpha$  as the scale parameter and  $\beta$  as the shape parameter. Fig. 1 shows an example of Weibull distribution. The smaller the scale parameter  $\alpha$ , the failure rate is higher. The smaller the shape parameter  $\beta$ , the more failure will occur initially.

The fact that the failure of CubeSats in orbit is still modeled by Weibull distribution showing strong infant mortality means that the testing of CubeSats is not performed thoroughly to improve the reliability up to a point where the random failure of individual subsystem/unit/parts dominates.

We can regard the AITV processes as cumulating the time in Eqs. (1)–(3) before the satellite is launched. By cumulating the time the failure rate given by Eq. (1) decreases significantly already when the satellite is launched. Fig. 2 explains this point schematically.

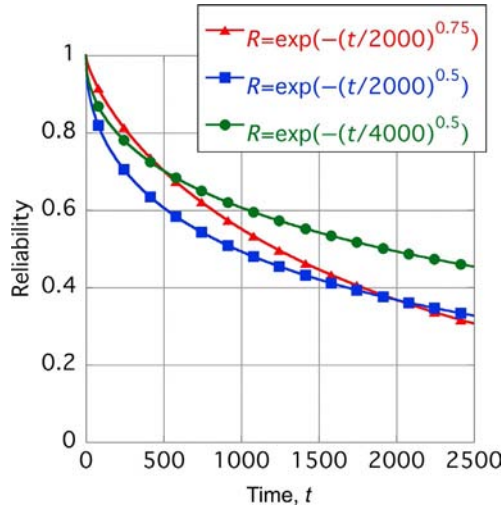


**Fig. 1** Example of Weibull distribution.

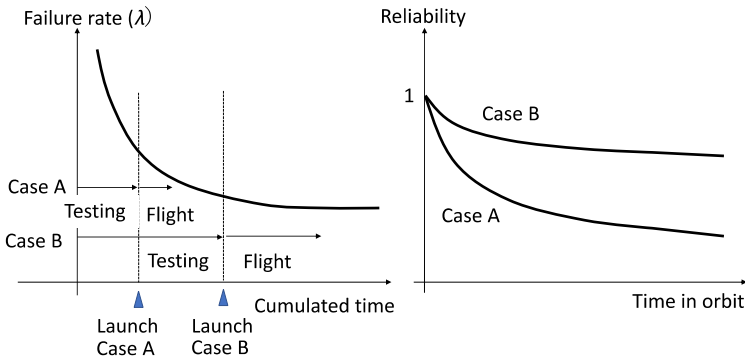


**Fig. 2** Reliability growth and improvement of in-orbit reliability by AITV before launch.

Fig. 3 shows an example of the reliability growth observed in an actual satellite project [7]. We recorded the number of failures observed during AITV process of HORYU-IV that was developed at Kyushu Institute of Technology from 2013 to 2016. Although HORYU-IV was not a CubeSat, it was developed as a typical university-class satellite. Its size,  $30 \times 30 \times 30$  cm, and mass, 10 kg, are equivalent to those of a 6 U CubeSat. The vertical axis of Fig. 3 is the cumulative number of failures observed during AITV process of an engineering model. The time zero is the time when we started to assemble various components into the satellite system. The horizontal axis is the total time spent in AITV. From the beginning to 180 h, numerous failures were observed during structure assembly and electrical performance test. After that the pace of finding new failures decreased. Fig. 3 clearly illustrates the

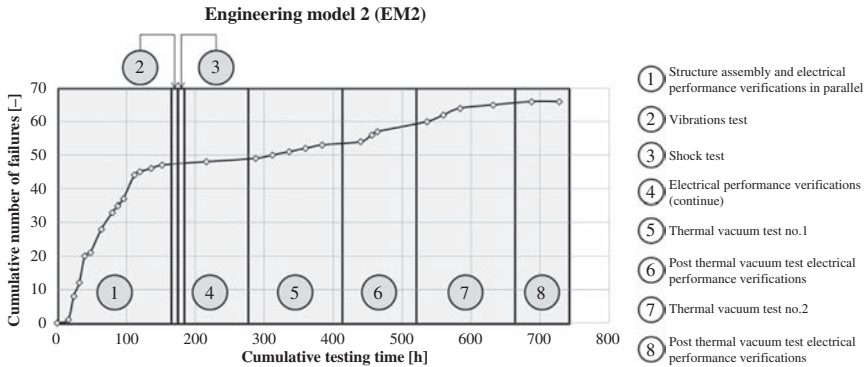


**Fig. 3** HORYU-IV cumulative number of failures against cumulative testing time of Engineering Model [7].

importance of the AITV processes. Even if individual components work, once they are integrated into a system, there are always new problems found. Therefore, when we make the project schedule, a significant amount of time should be allocated to system AITV.

The question is how much time we should allocate to AITV and accumulate testing time to decrease the failure rate before the launch. The reliability certainly grows by cumulating more testing time on the ground. But its growth rate decreases as we accumulate over time. When to stop testing and launching is a very difficult question and has no clear answer. Perhaps, it is determined based on the experience of team members. Based on a 2016 study by Swartout et al. [3], the success rate of the second satellite in university CubeSat projects clearly increases. This increase is described by a simple learning curve, although most likely students who are working on the second satellite are different from those worked on the first satellite. For a constellation program the satellite in-orbit reliability increases generation by generation as improvements are implemented based on the on-orbit results. Although we cannot say how much testing is enough, we can say how much testing is necessary. The international standard ISO-19683 provides the minimum testing criteria. In the next section, we look at ISO-19683 in depth.

## 3 International standard applied to CubeSat AITV activities

### 3.1 ISO-19683

An activity to make an international standard of nanosatellites that included CubeSats was initiated in year 2011. The standard aimed at answering several needs. The first and most significant one was to improve reliability of nanosatellites. It was clear that verification and testing processes needed improvement. There were already several testing standards available, such as ECSS-E-ST-10-03C [8], NASA-STD-7002A [9],

and GSFC-STD-7000 [10]. Even an ISO standard of satellite systems and unit testing existed as ISO-15864 [11]. But applying those standards to CubeSats was not a solution because of the increased cost and time necessary to implement them. There was not a consensus as to what tests were needed, if needed what test levels were appropriate, and what tests were not needed. There was a need for written guidelines related to testing nanosatellites to improve their reliability while keeping the nature of low cost and fast delivery.

The second need was related to trade studies leading to selection of nanosatellite components. In 2011 nanosatellite components were already widely traded on the Internet. To many nanosatellite developers, the components looked attractive in terms of price and the time to be saved by using the commercial product instead of building the components from scratch. There was little guarantee, however, associated with those products. The test history was not transparent to the buyers. Flight heritage did not guarantee that the products sold to the customers were made of the same parts that had been tested. The standards aimed at giving the minimum assurance that the products went through the known environment tests whose test conditions were well documented.

In May 2011 the author proposed the new standard at ISO/TC20/SC14 that encompasses all spacecraft hardware related standards. The first reaction from the community was “CubeSats are a students’ toy. They are polluting orbits with debris. Do something.” There was strong feeling against not only CubeSats but also all kinds of small satellites among the ISO committee members that were made mostly of people from space agencies and big satellite companies. A group was needed to support the initiative. Thanks to the Japanese government’s funding support, the author could host a workshop every year to discuss testing standards. Later, this group grew to discuss wider aspects of small satellites and led to an International Academy of Astronautics (IAA) study of “Definition and Requirements of Small Satellites Seeking Low Cost and Fast Delivery,” which proposed a concept of “lean satellite” in its final report published in 2017 [12]. The testing standard was finally published as ISO-19683 “Space systems—Design Qualification and Acceptance Tests of Small Spacecraft and Units” in July 2017. Although the title of ISO-19683 indicates “small spacecraft,” CubeSats are well within the scope of the standard. This section discusses CubeSats AITV processes based on the standard. Interested readers are encouraged to review the full ISO 19683 [12].

The scope of ISO-19683 is to “provide test methods and test requirements for design qualification and/or acceptance of small spacecraft or units. It provides the minimum test requirements and test methods to qualify the design and manufacturing methods of commercial small spacecraft and their units and to accept the final products.” “Small spacecraft” is used in the standard as a result of compromise made to have the consensus among the ISO member countries. The standard defines “small spacecraft” as one that “utilizes non-traditional risk-taking development and management approaches to achieve low cost and fast delivery with a small number of team. To achieve these two points, low cost and fast delivery, satellite design relies on the use of non-space-qualified commercial- off-the-shelf (COTS) units, making satellite size inherently smaller. The design accepts a certain level of risk associated with the use of COTS.” Fig. 4 shows the target of ISO-19683.

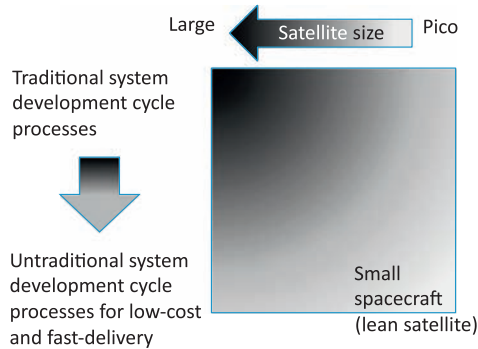


**Fig. 4** Applicability of ISO-19683.

Although the scope indicates “commercial small spacecraft,” the document can be used for any kind of satellites such as academic and civil. The standard can be used as a guideline for the newcomers to the space sector, as a common document in an international satellite project, or for other purposes.

Satellite testing can be categorized into three types, qualification testing (QT), acceptance testing (AT) and protoflight testing (PFT). Generally speaking, QT is done to prove that the design meets the requirements. QT applies more environment stress, that is, margin, than the flight predicted level to a qualification model that is a non-flight item. AT is done to prove that the flight model meets the requirement, and it is free from latent workmanship errors and material defects. AT applies the maximum predicted environmental stress. PFT is done to save the cost of making the qualification model and doing QT. The model used for PFT is called a protoflight model that goes through the same environmental stress level, such as vibration amplitude, as QT for the same duration as AT. In this model the protoflight model is eventually deployed to orbit. ISO-19683 describes the requirements for qualification test (QT), acceptance test (AT), and protoflight test (PFT) at unit (component) level and system level. For system level test the meaning of QT, AT, and PFT are the same as the ones for traditional satellites, which is defined in ISO-15864. For unit level test the meaning of AT and PFT are the same as the ones for traditional satellites, which is defined in ISO-15864.

### 3.2 Satellite system tests

ISO-19683 provides a table of satellite system test items. The table identifies whether each test item is required, optional or not applicable for QT, AT, and PFT.

For QT, the required system tests are the following: electrical interface, functional test, mission test, electromagnetic compatibility (EMC) test, deployment test, physical property measurement test, launcher/spacecraft interface test, random vibration test, and thermal test.

For AT the required system tests are the following, electrical interface, functional test, mission test, deployment test, physical property measurement test,

launcher/spacecraft interface test, random vibration test, and end-to-end mission simulation test.

Between QT and AT the differences are EMC test and thermal test required for QT only and end-to-end mission simulation test for AT only. Annex-D of ISO-19683 provides the selection logic flows whether optional test items, such as sinusoidal vibration test, shock test, and thermal balance test, are necessary or not.

### *3.2.1 EMC test and end-to-end mission simulation test*

The system electromagnetic compatibility (EMC) test is designed to demonstrate satellite's compatibility with the self-induced electromagnetic environment. To properly test for EMC, the satellite should be operated at full power. The test should satisfactorily demonstrate electrical and electronic equipment operation in conjunction with expected electromagnetic radiation and conduction from other internal units in various operational modes. In other words the test should demonstrate that the satellite is free from its own electromagnetic noise. There are several cases in which EMC test becomes important. One is related to reception of uplink data (command) from the ground. The signal from the ground is already very weak when it is received by the satellite, because of the long distance between the ground station and the satellite, so-called free space loss. In the case of 430 MHz UHF signal traveling 400 km distance, the free space path loss is 137 dB, which means the signal strength is weakened by more than 13th orders of magnitude from the original strength at the ground. A slight noise entering into the receiver may jeopardize the signal reception. Another example is an error in the sensor data reading when the noise is coupled to analogue data lines.

Lastly, when a satellite carries a device accompanied with switching of large current and/or high voltage, EMC is a strong concern. If the satellite carries electric propulsion system, especially a pulse discharge type, there is a significant EMC issue. The noise may often interrupt the functionality of digital electronics including micro-processor onboard. It is recommended, for example, to fire the thruster in a vacuum environment while the satellite operates free from external cables, including the power lines. The satellite components including the thruster head may be damaged. Therefore this test should be done at QT phase, and the test results can be reflected to the flight model. A CubeSat is a highly integrated system where so many coupling paths exist between the noise source and the device affected either by radiation or conduction. It is not practical to verify that the satellite is free from EMC issues via analysis. It is the best to demonstrate that the satellite system works in its fully assembled configuration even if all the internal components are working independently. An electromagnetic anechoic chamber may not be necessary as long as the external noise is negligible compared with the internally generated noise. When we need to characterize the minimum power level to succeed in uplink, it is better to perform the test in an anechoic chamber to avoid the external noise influence.

End-to-end tests are intended to verify that the satellite can be controlled and operated by the specified ground network. The emphasis is to verify the flight software onboard the satellite and communication between the satellite, the ground station,

and the ground data system. To verify the flight software, the tests should include simulations of all operational modes in nominal situations (e.g., early orbital operations, mission operations, and decommissioning) within the constraints of what can be simulated on the ground. The nominal operational modes should be tested long enough to detect any latent software error that manifests only after a certain run time. Many CubeSats do power cycling or resets to recover from single events or software hang-ups. The recovery mode from these events should be tested extensively. If there is a command of forced reset to be sent, the command should be sent from the ground station, and the satellite recovery should be confirmed by telemetry sent from the satellite to the ground station.

The compatibility of the RF airlink between the satellite and the ground network should be tested before launch. We can measure the lowest RF power level the satellite receiver or the ground station receiver can decode by directly connecting the receiver and the transmitter (or a signal generator) with variable attenuator inserted between the two. Using the measured value the link budget calculation can be closed with known (or measured) antenna gains. But this is an ideal case. In reality the effective antenna gain, especially the one onboard the satellite, may be different from the design value. The satellite antenna may pick up the radiated noise from the satellite itself. Considering these facts the final check should be done whether the RF air link between the satellite flight model with antennas deployed and the ground station is valid or not. If the license permits, it is recommended to perform the test in open air with a distance far enough to assure the far field of radio propagation. The open-air test has an advantage over the test in an anechoic chamber as the real ground station antenna can be used. Fig. 5 shows a photograph of open-air long distance test of BIRDS-3 (Uguisu), where the satellite was placed at a mountain top of 622 m with the horizontal distance of 6370 m from the ground station at 54 m height.

### 3.2.2 Deployment test

The deployment test verifies that the deployment mechanisms, such as antennas and solar panels, can function according to the design requirements. Antennas and solar panels are the most common deployable components for CubeSats. Their deployment is often critical to mission success. Testing deployment repeatedly may be necessary if the deployment mechanism involves parts whose quality variation is uncertain. The number of repeated deployments should be determined from the viewpoint of securing enough confidence and the cost/schedule associated with the test. The test may be performed in atmosphere. The difference of environment such as vacuum, temperature, and microgravity should be properly assessed during test planning. The worst-case condition should be assumed. Many CubeSats uses synthetic fiber thread to hold the deployable and cut the thread by a resistance heater, for example, nichrome wire. The worst condition is the case in which the heater is not heated to a high temperature high enough to cut the thread. To simulate that condition the deployment should be tested in the coldest temperature, but in an atmospheric condition so that the air can remove the heat away from the heater with the lowest battery voltage condition so that the current to the heater is the minimum. If one uses mechanical parts, such as





**Fig. 5** Photograph of open-air long distance communication test. Actual setup at the mountain (top), closer view of satellite (bottom left) and view of ground station from the mountain (bottom right).

spring and hinge, to release the solar panel and latch after deployment, the worst condition should be tested in vacuum environment at the coldest temperature.

### 3.2.3 Launcher/spacecraft interface test

The Launcher/Spacecraft interface test is the so-called fit-check. The test simply involves inserting an assembled CubeSat into a POD to see whether it can fit into the POD and exit the POD smoothly when it is pushed by the spring at the bottom of the POD. The test should be done with a qualification model before the flight model structure is manufactured. It is common that a CubeSat does not fit into a POD in the first trial. The CubeSat standard indicates that the external dimension should be  $100 \text{ mm} \pm 0.1 \text{ mm}$ . Many machine shops can make CubeSat structural components within the tolerance limit of  $\pm 0.1 \text{ mm}$ . But, once the structure is assembled, slight distortion in three-dimension often prevents the satellite from fitting into the POD. If the satellite does not fit, the structure must be adjusted until it fits into the POD. It is not advised to perform such adjustment during the last minutes of flight model assembly. Therefore the fit test should be done as early as possible in the satellite project once the



**Fig. 6** Photo of fit-check.

structure manufacturer is identified and the initial set of structural parts/components are delivered and assembled. Once the fitting is confirmed with a qualification model, it is advised not to change the structure design nor its manufacturer. Fig. 6 shows a photograph taken during a fit-check test.

### 3.2.4 Thermal test

Thermal tests consist of thermal vacuum tests, thermal cycle functional tests, and functional tests in vacuum. Among the three tests, either thermal vacuum or a combination of thermal cycle function and functional test in vacuum are required. When there is a large temperature distribution within a satellite, thermal vacuum test should be chosen. Thermal vacuum testing is preferred because it is more flight representative. But not all CubeSat developers have access to the test facility as shown in Fig. 7. The difficulty with this test is often the cooling capability of the test facility. Without a cooling capability, finding a vacuum chamber for testing is relatively easy, and even purchasing a chamber large enough to accommodate a CubeSat is not difficult as there is a market of second-hand vacuum chambers that sells unused chambers released from other terrestrial industries, such as semiconductors.

The purpose of the thermal vacuum test is as follows:

- (a) to check the performance at the high-temperature limit in vacuum,
- (b) to check the performance at the low-temperature limit in vacuum,
- (c) to check the susceptibility to the temperature cycle in vacuum,
- (d) to detect latent defects of workmanship and design.

The functional test in vacuum using a simple vacuum chamber without a cooling capability can fulfill item (a). Items (c) and (d) can be partially fulfilled by thermal cycling, although the test article is not in vacuum. The question is whether the performance test

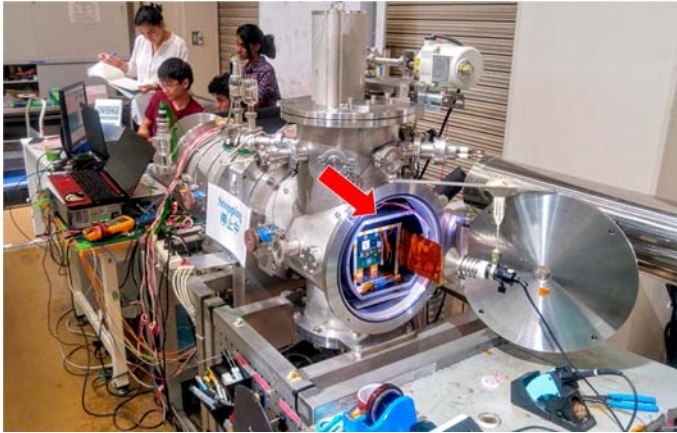


**Fig. 7** Thermal vacuum test facility. There is jacket (pointed by a red (gray in print version) arrow) filled with liquid nitrogen to simulate the cold space environment.

at low temperature in a thermal cycle chamber, that is, atmospheric pressure, can fulfill item (b).

The largest difference between the two environments, vacuum chamber, and thermal chamber, is the presence of air (or nitrogen gas) convection. The convection tends to decrease the temperature difference within the satellite. During the system test the temperature difference should be properly simulated as it can cause a systematic defect that cannot be revealed by functional tests in uniform temperature.

**Fig. 8** shows the temperature distribution of an electrical power control unit measured in vacuum and in atmospheric condition. The unit is operated in the same condition except the ambient environment. We see points where temperature is locally enhanced, where heat dissipation occurs as the power device efficiency is not 100%. The heat spots are more visible in the vacuum as air convection cannot remove the heat away. Although **Fig. 8** is for an electrical power control unit for a 100 W-class satellite, a similar situation **Fig. 8** may arise in CubeSat at a DC/DC converter, a microprocessor, a RF amplifier, and others. If that is the concern, thermal vacuum test should be performed with the lowest and highest temperature extreme expected in orbit plus some margin. In ISO-19683 the QT level is defined as the design temperature and

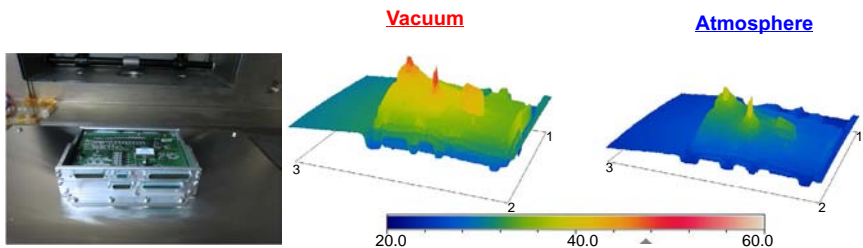


**Fig. 8** Temperature distribution around electrical power system circuit board (left) in vacuum (center) and in atmosphere (right).

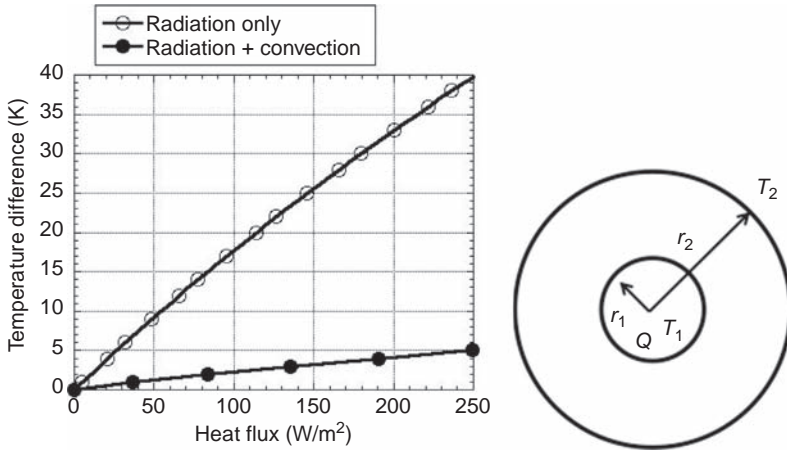


**Fig. 9** Temperature difference between the outer sphere and inner sphere when there is heat transfer due to radiation only and due to radiation and air convection.

qualification margin (minimum  $\pm 5^{\circ}\text{C}$ ) with two cycles or more. For traditional satellites the temperature margin in QT is often  $10^{\circ}\text{C}$  or more [13].

Fig. 9 shows temperature differences calculated for concentric spheres. The inner sphere assumes an internal electric and electronics unit. The outer sphere assumes its surroundings, such as the satellite external surface or the mounting panel. From the inner sphere a heat of  $Q$  is transferred to the outer sphere. The heat flux is given by  $Q/A_1$ , where  $A_1$  is the surface of the inner sphere. Assuming a sphere of 10 cm diameter,  $r_1 = 0.05$  m, 250 K as the outer sphere temperature,  $\epsilon_1 = \epsilon_2 = 0.9$  as the emissivity, the temperature difference  $T_1 - T_2$  was calculated for a given heat flux  $Q/A_1$ . For  $r_1 = 0.05$  m and  $r_2 = 0.06$  m, the area is  $A_1 = 0.0314$  m<sup>2</sup>. Then  $Q/A_1 = 50$  W/m<sup>2</sup> corresponds to  $Q = 1.6$  W, which is comparable with typical 1 U CubeSat power dissipation. If we do the thermal test in atmosphere, the temperature difference is only 1 degree between the outer and inner surfaces. In vacuum the difference is almost 10 degrees. Studies [14, 15] argue that a difference of 10 degrees between the two environments (vacuum and atmosphere) should represent the criteria for exemption of thermal vacuum of electronics units. Therefore, perhaps, a 1 U CubeSat can be tested by thermal cycle. When we consider the heat transfer due to conduction, the temperature difference  $T_1 - T_2$  decreases further. Then, when the power level,  $Q$ , is low, 2U or 3U CubeSat may be also tested by thermal cycle, but not good for a satellite larger than those. Even if thermal vacuum test is replaced by thermal cycle, the functional test in vacuum should be done at least once to make sure that the satellite works in a vacuum environment.

Thermal balance testing is often considered optional for LEO missions and may be required only when enough accuracy in thermal analysis is required or when high power devices or multiple payloads are supported. For LEO CubeSats the main purpose of thermal balance test is to provide the data necessary to verify the analytical thermal model or to verify the thermal control system. The data are designed to derive

the test conditions of subsequent thermal test, especially the lowest and the highest temperature limits. The CubeSat internal units are tightly packed into a small volume. Unless they are intentionally insulated, which is often true for battery but not for other subsystems, the internal units often have more or less uniform temperature except for hot spots inside the units. For a 1U CubeSat, a three node analysis that account for external surfaces, internal units, and battery is often good enough. For a larger CubeSats with deployable solar panels and/or active attitude control, more sophisticated analysis is necessary. Although the combination of thermal balance test and thermal analysis can provide useful information to determine the thermal test conditions, it should be noted that there are many CubeSats already flying in low Earth orbit, and many of them look alike. More than 200 CubeSats have been launched from ISS since 2013. They are flying in the same orbit. Many CubeSats have similar thermal characteristics if they do not have deployables or significant power loads. The surface thermal optical properties are more or less the same as the surface is dominated by solar cell coverglass. Substituting the envelope of flight temperature data of the past satellites into the lowest and highest temperatures of the thermal test is one way to skip the thermal analysis and the thermal balance test. We can also verify the thermal analysis by analyzing the orbit conditions of the past satellites instead of doing the thermal balance test. The flight data should be used more widely. A database of flight temperature data of various satellites in various orbits may be helpful to many CubeSat projects.

### **3.3 Satellite unit tests**

#### **3.3.1 Unit QT in ISO-19683**

In this section unit-level QTs are considered. ISO-19683 assumes that unit QTs are carried out by the unit manufacturer. For any type of subsystem units, functional test, physical property measurement, random vibration tests are required for QT. Except for structural units, either thermal vacuum test or a combination of thermal cycle functional test and functional test in vacuum is required. For an electrical and electronic unit, EMC test and thermal cycle endurance test are required. Total ionization dose and single event tests are optional. They can be done when a manufacturer wants to demonstrate radiation tolerance of the product. For antenna and solar array, deployment test is required if they are deployable units. As they are exposed to outer space, thermal cycle endurance test is required. Each is briefly discussed in the succeeding text. For batteries, leakage tests are required.

ISO-19683 also provides a table that lists the test level and duration for unit QTs. For TID test, 10kRad or higher total dose with 0.01 Gy/s or lower dose rate is given at the test conditions. For a typical CubeSat, the shielding effect of external panels is equivalent to aluminum of 1 mm thickness. We can calculate total dose in orbit using a tool like SPENVIS ([www.spennis.oma.be/](http://www.spennis.oma.be/)). According to SPENVIS, a CubeSat in an orbit of 400km altitude and 51° inclination receives less than 2kRad in 1 year.

The random vibration test level is given as 13.3Grms higher between 20 and 2000Hz. The vibration should be applied once in each orthogonal axis for 1 min.

The test level was derived based on analysis of test data from various 50 kg-class satellites and basic research carried out. For a CubeSat, which is much lighter than 50 kg, the level of 13.3 Grms needs to be increased. In other words, if the CubeSat unit cannot survive this level of random vibration test, it won't survive the rocket launch. It should be noted that if the satellite is launched to ISS, the system random vibration level is 4.4 Grms, which is very low as the satellites are carried as a package inside the cargo vehicle. Then 13.3 Grms as unit QT level may provide margin.

For thermal vacuum testing of an internal unit, the temperature range is specified as  $-15^{\circ}\text{C}$  to  $+50^{\circ}\text{C}$ . The number of cycles is two or more and the test should be done in pressure of  $1 \times 10^{-3}$  Pa or lower. For thermal cycle functional test of an internal unit, the temperature range and the number of cycles are the same as those of thermal vacuum, i.e.  $-15^{\circ}\text{C}$  to  $+50^{\circ}\text{C}$  and 2 cycles or more. At each cold and hot temperature limit, functional tests should be carried out. To derive the temperature ranges, the temperature ranges of internal units on-board various 50 kg-class satellites were investigated. The temperature range of  $-15^{\circ}\text{C}$  to  $+50^{\circ}\text{C}$  corresponds to the coldest and the hottest case of the collected data. If only one cycle is done, there may be some singularities. Therefore, at least two cycles are required. Other standards require four or eight cycles.

The thermal cycle endurance test demonstrates the ability of the test article to withstand the stress imposed by thermal cycles in orbit. A functional test and visual inspection should be performed before and after the cycles. There is no need of doing the functional test during the cycles. The test level is  $-70^{\circ}\text{C}$  (or lower) to  $+100^{\circ}\text{C}$  (or higher) for an external unit such as solar array and  $-25^{\circ}\text{C}$  (or lower) to  $+60^{\circ}\text{C}$  (or higher) for an internal unit. The number of cycles is 24. The temperature range of  $-70^{\circ}\text{C}$  to  $+100^{\circ}\text{C}$  corresponds to a typical temperature range of solar panels at SSO. For an internal unit, the temperature range of  $-25^{\circ}\text{C}$  to  $+60^{\circ}\text{C}$  is the non-operational temperature range. It was derived by adding  $10^{\circ}\text{C}$  margin to the operational temperature range of  $-15^{\circ}\text{C}$  to  $+50^{\circ}\text{C}$ .

### 3.3.2 Battery tests

When we test batteries, we need to consider not only whether the battery functions in space but also whether the battery comply with the safety requirement imposed by the launcher. The major concern about battery safety is leakage and rupture. It is required to expose the battery to a vacuum to check the leakage. Functions to control the hazard leading to rupture need to be tested before and after environmental tests.

When the battery packs are assembled by the satellite developer, screening of individual battery cells may be required. Fig. 10 show the process of battery cell screening required for ISS release. We took an example of BIRDS-2 that used a NiMH battery (Enloop, HR-3 UPT). To verify the individual cells, we followed the flow in Fig. 10. First the battery characteristics were measured for each cell. They were open voltage, battery discharge capacity, mass, and charge and discharge profile along with the temperature, visual inspection, and odor. Among these the battery capacity measurement needed one cycle of charging/discharging test using a DC power supply and an electronic load. Then the batteries were exposed to  $1 \times 10^{-3}$  Pa vacuum for 6h. Then the

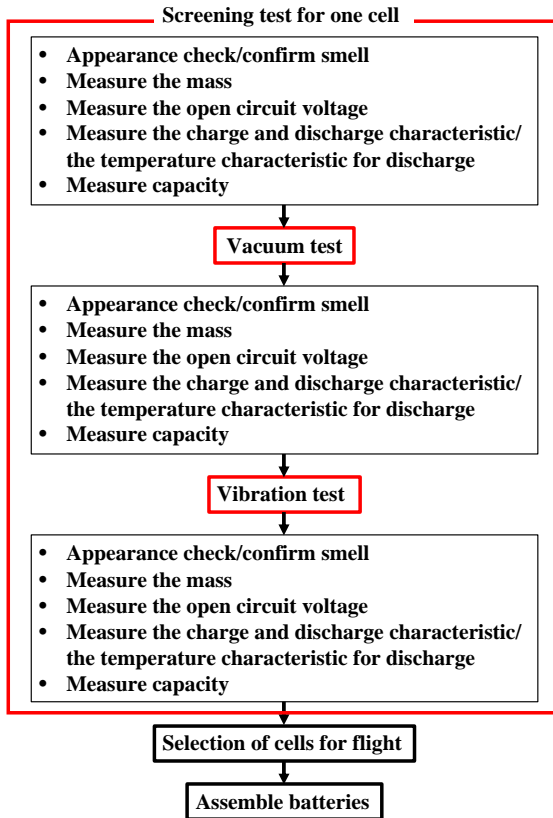


**Fig. 10** Flow of battery screening of BIRDS-2.

characteristic measurement was done again to verify the change of open circuit voltage (less than 0.1%), the battery capacity (less than 5%) and the mass (less than 0.1%) to be within an acceptable range. Then, a random vibration of 6.1 Grms was applied for 1 min to each axis. Cells whose characteristics (open circuit voltage, capacity and mass) change was within the acceptable range were selected as flight batteries and assembled into a battery pack.

If the battery itself has a protection circuit against overcharging, overdischarging and external, short circuit, there is a need to demonstrate that the protection circuit works. The external short-circuit protection, that is, over-current protection, was confirmed by observing that the discharge stops once the current reaches a certain value, as shown in Fig. 11, which was taken from the test data of Aoba VELOX-III (AV3). These tests are very harsh for each battery. Therefore the tests were done using a battery from the same lot as the flight cells, not a flight cell itself.

Nowadays, many CubeSat developers purchase batteries from a component vendor that sells the battery already integrated into an EPS board. If the COTS EPS board is

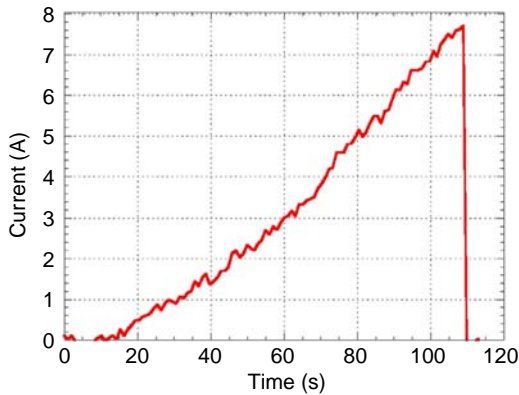


**Fig. 11** Demonstration of overcurrent protection of AV3 battery.

already designed and verified regarding the safety requirements, procuring the COTS EPS instead of developing in-house saves significant amount of time in the safety management. But in many cases, it is not the case.

Kyutech assisted in the safety design and verification of Irazu, which was the first Costa Rican satellite released from the ISS in May 2018 (<https://directory.eoportal.org/web/eoportal/satellite-missions/i/irazu>). Irazu used a commercial EPS that had an integrated Li-ion battery. If the same principle as that for BIRDS-2 and AV3 was applied, each battery cell should have gone through environment tests, and the characteristics should have been measured. As the battery cell was already integrated into the COTS EPS, it was not possible to evaluate the individual cells. Therefore the safety verification of individual cells was done according to the JDX-2017078 “Guideline for safety design and verification for a small satellite using JEM Small Satellite Orbital Deployer with satellite-kit battery cell and EPS.” The battery test report (characteristics measurement, such as open circuit voltage, capacity, and mass before and after vacuum exposure and vibration) conducted by the manufacturer before shipment was used to verify the flight battery cell. Regarding overcharging, overdischarging, and external short circuit, the test data of the battery cells of the same lot were submitted by the manufacturer. The product serial number and the serial number listed in the document submitted by the manufacturer had to clearly show that the batteries are from the same lot. The documents provided by the manufacturer were substituted for the test reports to be otherwise conducted by the satellite integrator. The flight battery pack was verified through the system tests after it was integrated into the satellite system. The tests were vacuum exposure and vibration. The vacuum exposure test was done as part of the thermal vacuum test. The vibration test was done as a part of a protoflight model (PFM) vibration test (6.4 Grms, 1 min). Before and after each test and the charging and discharging characteristics of the battery pack were measured.



## 4 Concluding remarks

CubeSat AITV is a critical process intended to improve the satellite reliability and achieve the mission success. ISO-19683 was published in 2017 to provide the minimum set of CubeSat testing requirements. The standard is a living document. According to ISO regulation, each standard should be reviewed every 5 years. When ISO-19683 was published, a massive constellation was still on the horizon. The standard targeted mostly single satellite projects. One advantage of the CubeSat is its rapid speed of generational change. By experiencing multiple satellite projects and learning lessons from in-orbit results, we can improve ourselves and the mission success rate increases as the generation goes on. It is certainly true for a constellation program. Later generations go through the minimum set of testing on the ground, yet their mission success rate increases. A university project who had a satellite dead on arrival during its first mission often succeeded in getting signals from the satellite in the second mission and achieved the full mission success later. Traditional testing standard, such as ISO-15864 and ECSS also evolved after series of success and failure in early days of space exploration. The AITV processes based on the standards are very mature now and the mission success rate of traditional satellites is high. CubeSat testing standards also can evolve by collecting experiences of the community. For commercial satellite programs, it may be difficult to share the experience and data due to its proprietary nature. But there is little difficulty for university satellite programs to share the information. Looking at the evolving speed of the CubeSat community, if there is an appropriate platform to share the information, it may not be so difficult to have more mature CubeSat testing standards and have drastic improvement in mission success rate in very near future.

## References

- [1] Bryce Space and Technology, SmallSats by the Numbers 2019, [https://brycetek.com/downloads/Bryce\\_SmallSats\\_2018.pdf](https://brycetek.com/downloads/Bryce_SmallSats_2018.pdf).
- [2] J. Bouwmeester, J. Guo, Survey of worldwide pico- and nano-satellite missions, distributions and subsystem technology, *Acta Astronaut.* 67 (2010) 854–862.
- [3] M. Swartwout, C. Jayne, University-class spacecraft by the numbers: success, failure, debris. (But mostly success.), in: *Small Satellite Conference, SSC-XIII-1*, 2016.
- [4] J.H. Saleh, J.-F. Castet, *Spacecraft Reliability and Multi-State Failures, A Statistical Approach*, John Wiley & Sons Ltd, Chichester, UK, 2011.
- [5] J.T. Duane, Learning curve approach to reliability monitoring, *IEEE Trans. Aerospace* 2 (1964) 563–566.
- [6] L.H. Crow, Reliability growth planning, analysis and management, in: *Annual Reliability and Maintainability Symposium*, 2011.
- [7] P. Faure, A. Tanaka, M. Cho, Toward lean satellites reliability improvement using HORYU-IV project as case study, *Acta Astronaut.* 133 (2017) 33–49.
- [8] European Cooperation for Space Standardization, ECSS-E-ST-10-03C – Testing, [http://ecss.nl/get\\_attachment.php?file=standards/ecss-e/ECSS-E-ST-10-03C1June2012.pdf](http://ecss.nl/get_attachment.php?file=standards/ecss-e/ECSS-E-ST-10-03C1June2012.pdf), 1 June 2012.

- 
- [9] NASA-STD-7002A, Payload Test Standard, <https://standards.nasa.gov/sites/default/files/nasa-std-7002a.pdf>, September 2004.
  - [10] GSFC-STD-7000, General Environmental Verification Standard, <https://standards.nasa.gov/standard/gsf/gsf-std-7000>, April 2013.
  - [11] ISO-15864, Space Systems – General Test Methods for Space Craft, Subsystems and Units, (August 2004).
  - [12] M. Cho, F. Graziani (Eds.), Definition and Requirements of Small Satellites Seeking Low-Cost and Fast-Delivery, International Academy of Astronautics, February 2017.
  - [13] D.G. Gilmore (Ed.), Spacecraft Thermal Control Handbook, The Aerospace Corporation, 2002. ISBN 1-884989-11-X.
  - [14] J.W. Welch, MIL-STD.1540E, Thermal test equipment rational as specified in MIL-HDBK-340, in: 26th Aerospace Testing Seminar, Los Angeles, USA, March 2011.
  - [15] SMC-S-016, Test Requirements for Launch, Upper-Stage and Space Vehicles, Air Force Space Command, June 2008.

José Miguel Lago Agra<sup>a</sup> and Alberto González Muíño<sup>b</sup>

<sup>a</sup>Alén Space, AIV & Ground Segment, Nigrán, Spain, <sup>b</sup>Alén Space, CTO, Nigrán, Spain

## 1 Introduction

The ground segment is a key component to the success of any CubeSat mission, whether it is based on a constellation, a swarm, or a single spacecraft. The ground segment gives support to the space segment, relaying payload data to the user segment and managing Tracking, Telemetry, and Command (TT&C) for both the platform and the payload. The increasing demand for high bandwidth and the constant improvement of modulation and codification schemes set the goal of maximum flexibility for the ground segment. The traditional approach of distributed control centers is not generally possible within the budget constraints of a CubeSat mission, and all operations will be usually performed from the same facility. This is another limitation of the situation when there is a need to provide support to several missions and modes using the same ground station (GS).

In this chapter the typical architecture of a modern ground segment will be introduced, using cost-effective, cutting-edge technology and emphasizing flexibility, presenting state-of-the-art solutions that can improve the operations workflow.

## 2 Ground segment overview

The ground segment comprises all the Earth-based elements that give support to one or several spacecraft during the course of a mission (or several, even simultaneously) [1, 2]. The main elements are the ground stations, which provide the communication interface, operation centers from where spacecraft are managed, and ground networks that provide interconnection between the elements. An overview of the typical architecture can be found in Fig. 1.

### 2.1 Functionality

The ground segment enables the management and operation of the involved space segments. It also has to provide access to the required information and science data from the user segment side. In summary, it has to provide the following functionalities to the interested parties:

- TT&C
  - Communication and control
  - Housekeeping and telemetry acquisition and processing to determine the status of the spacecraft

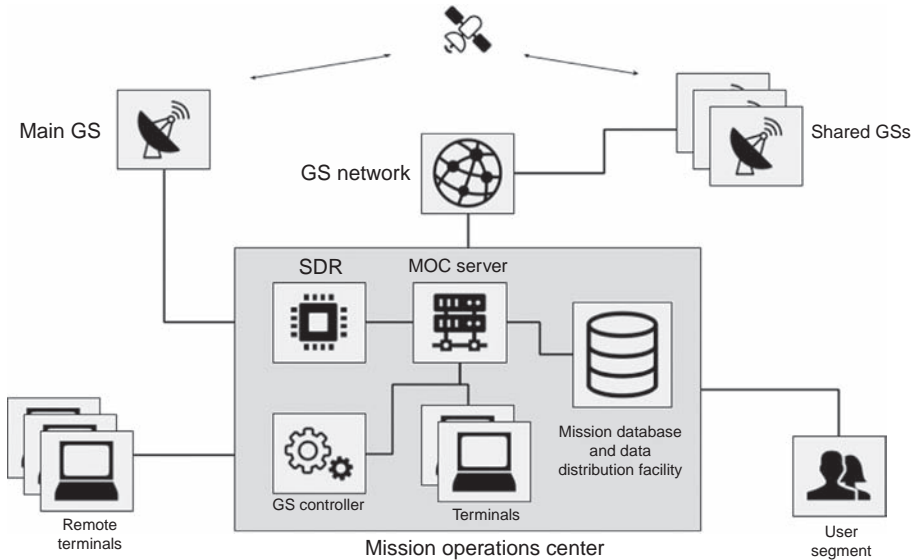


**Fig. 1** Ground segment architecture.

- Forwarding of requests from the user segment
- Scientific/payload data gathering
- Ground station control
  - Configuration for transceivers and radios
  - Doppler corrections in real time
  - Pointing, tracking, and ranging (if required) of spacecraft
  - Management of ground stations network, in case more than one GS is available
- Mission planning
  - Generation of operation plans
  - Operators access to handle conflicts
  - Execution of schedules according to the approved plans
- Operators interface
  - Visualization of the spacecraft status and acquired data
  - Remote access to the ground segment for off-site operations
  - CCTV of the outside facilities for surveillance
- User segment access
  - Access to the scientific/payload data from stakeholders' terminals
  - Requests for scientific/payload operations

## 2.2 Architecture

The traditional approach of distributed facilities like ground station facilities (GSF), flight dynamics facilities (FDF), and mission operations facilities (MOF) is not the usual architecture for the stringent budget-constrained CubeSat missions. More typically a single facility with even a single server is the main topology used to manage all the required hardware, interfaces, and services [3]. One or more ground stations will

be connected to the main facility that is called the Mission Operations Centre (MOC). All the operations are generally managed from this location. The disadvantages of using a single ground station include limits in the ability of simultaneously communicating with more than one spacecraft and restrictions to CubeSats below GEO orbits as they are typically unable to mount far-ranging parabolic dishes owing to their expense and complexity [4].

A network of ground stations can be used to operate the spacecraft or the constellation, using in-house or external services. This is a rising option that provides extended access and can save an important amount of the ground segment costs, monetizing the idle time of the ground stations. However, this generally does not provide the same security, reliability, and latency as classical ground station networks [5].

### 3 Ground station

Space radiocommunications are possible, thanks to the ground stations. The elements of this crucial portion of the ground segment must be wisely selected to attain reliable performance during the operation of a CubeSat. Even a small deviation from the requirements could lead to an unfavorable result. A brief summary of the most important elements (represented in Fig. 2) of a ground station will be introduced to help the reader to make the right choices during the design phase of the ground segment for a CubeSat mission.

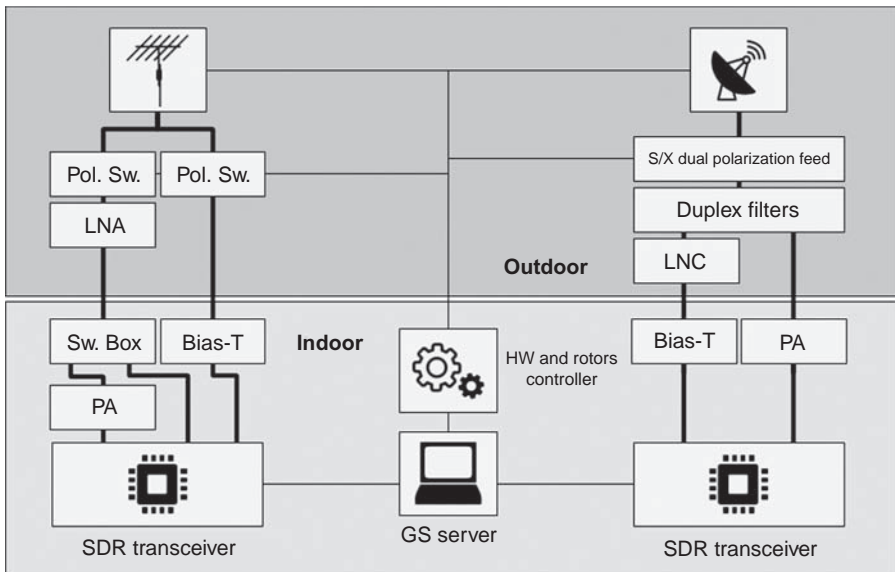


**Fig. 2** Ground station block diagram.

## 3.1 RF hardware

### 3.1.1 Antennas

The main bands for space radiocommunications with CubeSats are VHF, UHF, L band, and S band. Less common but in growing trend are X band and Ka bands [3]. A widely adopted choice for **VHF and UHF** bands is the cross Yagi-Uda antenna, which usually provides great results. Making use of phasing networks, multiple polarizations are available with a single antenna; even remote configuration is possible if a polarization switch is available. The performance depends on the number of elements, at the cost of bigger and heavier antennas. To provide maximum performance on the reception, two antennas can be used for each band, providing **polarization diversity** (simultaneous reception on multiple polarizations), at the expense of having several reception chains, and avoiding the need of an attitude control system aboard the spacecraft that guarantees polarization match with the ground station antennas during contacts. Circular polarization is a common choice for CubeSats, since it guarantees communication regardless of the orientation of the spacecraft with respect to the ground station [3]; if the spacecraft is tumbling, either right-hand circular polarization (RHCP), left-hand circular polarization (LHCP), or linear polarization will be received, with a maximum polarization loss factor of 0.5 (−3 dB).

For L band and higher frequencies, helical antennas or parabolic reflectors are the main options. The decision depends on the requirements of the mission and the link budget; high gain and high data rates generally require a parabolic reflector dish. A parabolic reflector will need a feed system to capture the radio frequency wave and guide it to the transceiver through a coaxial cable or a waveguide or vice versa for the transmission. It is advisable that this dish feed supports configurable polarizations without the need of a setup modification. A complex mission may require support for multiple bands, for example, S band and X band. In this scenario a multiband dish feed is the best choice since it avoids the expensive solution of having multiple antennas. Mounting multiple dish feeds on a single parabolic reflector increases the complexity of the system significantly and does not allow optimization at any frequency, since multiple feeds negatively affect the radiation pattern of the system.

### 3.1.2 Filtering

The use of RF filters in some scenarios is essential. Adjacent commercial services, such as broadband cellular networks, can interfere with the communications. The tight margins of CubeSat communications typically leave little room for extra losses. In the case of full duplex communication using a single band, a duplexer based on ceramic or cavity filters can provide the required channel multiplexing while having a low impact on the overall communication system. If rigorous filtering is required, a carefully designed cavity waveguide filter with walls plated with a thin layer of gold, to improve surface conductivity, provides the lowest losses, high selectivity, and linear group delay [6].

### 3.1.3 Low-noise amplifiers and down-converters

Among many other limitations, power constraints set the pace of CubeSat mission operations. Very low power is available for transmissions; therefore a very weak signal will be captured by the antennas at the ground station, and this will have to overcome the feed line losses experienced in the system before the receiver. To overcome this situation a low-noise amplifier, that is, a variety of electronic amplifiers with low impact in the signal-to-noise ratio, must be placed close to the antennas or reflector feed to keep the overall noise figure as low as possible. The lower the noise figure of the amplifier, the better the signal reception. Numerous commercially available, low-noise amplifiers (LNAs) are suitable for amateur and nonamateur bands routinely used by CubeSats. They often include a voice-operated exchange (VOX) switch, enabling the LNA to switch between transmission and reception detecting the carrier on the feed line and avoiding the need of a push-to-talk (PTT) line from the receiver. Frequently, this switch consists in a RF relay with a higher-than-desired operating delay (plus a bounce period) and a limited life span. Hence a solid-state RF relay activated by a PTT line is preferable, as it will fairly improve the switching time (useful in half-duplex scenarios) and provides practically unlimited life span.

In the case of S band and higher frequencies, the use of a low-noise downconverter is convenient, since it will not only amplify the signal but also convert it to a lower frequency without a severe impact on the signal-to-noise ratio and avoiding high losses during its travel to the receiver through the transmission line, usually a coaxial waveguide. Care must be taken when adjusting the gain of the low-noise amplifier or downconverter to avoid saturation on the reception, particularly with short distances between the antenna and the transceiver. Another important consideration is the impedance of the transmission lines. Some downconverters are designed to work in bands used to feed satellite TV receivers and therefore require transmission lines with a characteristic impedance of  $75\Omega$ .

## 3.2 Transceivers, modems, and software-defined radios

The required architecture to support TT&C in CubeSat missions was commonly built around the robust but outdated combination of a terminal node controller (TNC) (a hardware component designed for packet radio) and a commercial transceiver. This approach has some drawbacks, since the GS can support only the bands allowed by the transceiver (usually VHF, UHF, and L band) and the modulation/codification schemes (MODCODs) and framing modes supported by the TNC, making hard to impossible to support different spacecraft and missions [3]. To overcome these limitations, software-defined radios (SDR) introduce a paradigm shift where transmission and reception chains are fully implemented by software (e.g., filtering, modulation, and mixing). This scheme allows developers to reconfigure the communication system to give support to a wide variety of changing protocols and, hence, multiple spacecraft. Now the only required hardware is a RF front end compatible with the working bands [7, 8]. Typical figures of merit of a modern CubeSat ground station built for amateur bands are included as a reference in [Table 1](#).

**Table 1** Figures of merit of a typical CubeSat ground station.

	Frequency bands (MHz)	Antenna gain (dBi)	Preamplifier gain and NF (dB)	EIRP/G/T	Polarization
UHF uplink	435–438	16.2	–	32.51 dBW	RHCP/LHCP
UHF downlink	435–438	16.2	25 0.7	–3.73 dB/K	RHCP/LHCP
S-band uplink	2400–2450	31.35	–	40.13 dBW	RHCP/LHCP
S-band downlink	2400–2450	31.35	28 0.4	12.90 dB/K	

During the contacts with the spacecraft, Doppler effects must be compensated. When working with SDRs, this operation is easier than ever, since no communication with external hardware is required: just another stage in the transmission/reception chains, as long as the required bandwidth is captured. Monitoring of the spectrum is also a simple task now, without the need of external hardware like a spectrum analyzer connected to the reception chain with a RF splitter that will also cause harm to the received SNR. A single GS can be now part of the ground segment of multiple missions or a ground stations network, that is, a much more cost-effective solution than building several ground stations for a multimission project. The advent of software-defined radios has not fully replaced hardware-based solutions yet, even when it has a smaller footprint than hardware-defined radios, since it tends to be more power demanding. The use of SDRs on the space segment is more challenging, and ground stations for CubeSat missions usually match radios from the space segment.

### 3.3 Mechanical elements and pointing

Ground stations must track the spacecraft during the contacts, precisely pointing the antennas due to the motion of the spacecraft along the orbit. For this purpose a set of rotors mounted over a reliable structure are required. Yagi-Uda antennas are usually mounted over a metal cross boom that in turn is attached to the rotors. This metal cross boom could interfere with the radiation pattern of the Yagi-Uda antennas. As such, a glass fiber-reinforced polymer (GFRP) or carbon fiber-reinforced polymer (CFRP) cross boom is a better option since it will not cause any harm to the radiation patterns. This setup also gives the possibility of mounting a parabolic reflector over the cross boom, increasing the capabilities of a single ground station.

Several commercial rotors are available on the market [3], but this choice should be well pondered. Tracking speed and pointing precision depend on the mission requirements and the orbit selected. Higher-frequency bands (S band, X band, and upper) may require a better pointing accuracy, since a higher gain will be needed to compensate the increase in free-space path loss, and therefore bigger antennas with narrower



beam widths will be used. Meanwhile, very low orbits, mainly under the ISS, will require a very high angular speed for the rotors to keep track of the spacecraft. Precaution must be taken also in harsh environments where adverse weather conditions (e.g., wind and ice) could cause damage or malfunction of the GS. An overzealous estimation of the wind conditions can jeopardize the facilities if the brake torque of the rotors is exceeded or the GS is operated over the nominal wind pressure stipulated by the rotors manufacturer; this requires some calculations for each setup since it depends on the antennas wind surface. Ice loading on the antenna surfaces is definitely also an impediment for the operation of a ground station, particularly in the case of parabolic reflectors. In such locations, extra protection can be provided by a radome, an enclosure that protects the structure and the antennas while being effectively transparent for electromagnetic waves in the radio spectrum.

### **3.4 Considerations for high frequency bands**

X band through Ka-band radiocommunication is gaining more traction in recent CubeSat missions as higher data rates are an indispensable requirement in contemporary complex missions. These bands offer more bandwidth and are arguably quite less congested, but these advantages come with some drawbacks that present a challenge for low-budget CubeSat missions. Atmospheric absorption increases when moving to shorter wavelengths requiring more power, which is a precious resource on board a CubeSat. Other nuances to consider are that higher frequencies antennas offer similar gain with a smaller aperture, making the pointing budget an issue, and RF and baseband hardware required to transmit and receive in these bands are usually too costly for typically budget-constrained CubeSat missions.

## **4 Ground segment software**

It is not an overstatement to say that a massive endeavor in software development is required in any contemporary space project. A thorough study and a wise design of the software architecture are crucial for the success of the mission. Software is the glue that keeps together all the pieces of a modern ground segment for CubeSats, usually backed by open-source frameworks, underpinning the success of the mission providing high automation possibilities and agile development of new features. These aspects ring true for flight software, ground data systems, and software systems. The architecture of a typical ground segment software system is shown in [Fig. 3](#).

### **4.1 Mission control software**

The core of the operations is the Mission Control Software (MCS). This vital piece of the ground segment will provide the required tools for telemetry download, telecommand upload, monitoring of the status of the spacecraft, data distribution and visualization, and operation planning. The MCS serves as the main interface for the

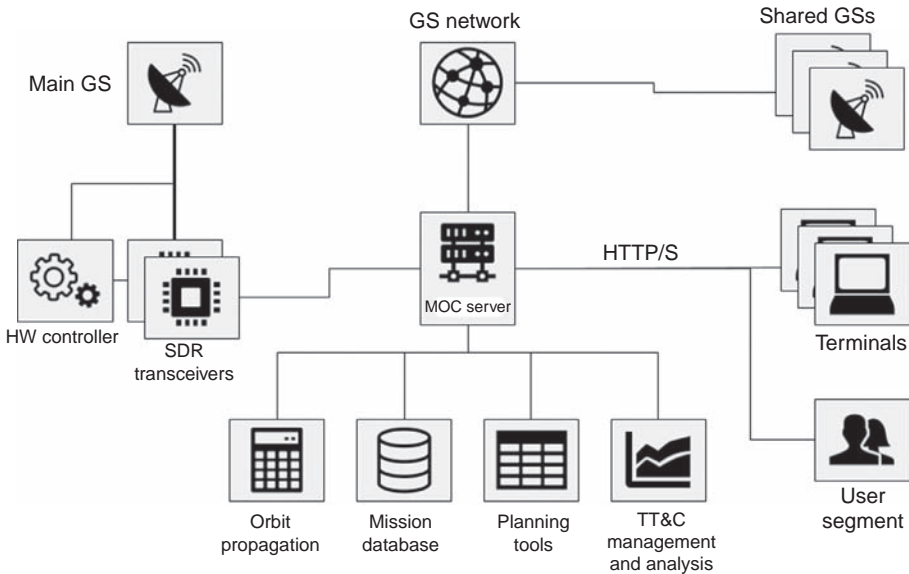


**Fig. 3** Ground segment software architecture.

operators to control the spacecraft and will have to present the information in a condensed and human-friendly way, to allow the operators to take the right decisions quickly and with no place for confusions [1, 2]. A distributed, nonmonolithic, and service-oriented architecture is encouraged. This will allow the service to scale according to the demands, either more spacecraft (constellations and swarms), more operators, or more users consuming data. Another advantage of this scheme is the possibility of remote access to the MCS for off-site operations, giving the maximum flexibility to the operators.

## 4.2 Orbit propagation

An accurate computation of the orbital path of a spacecraft is a requirement of any space mission. Operators need to know the position of the spacecraft days or weeks in advance to plan a schedule of contacts. The ground stations have to allocate the available slots for the selected contacts in accordance with this schedule. During a pass the rotors must perform a precise tracking of the spacecraft to harness the full potential of the antennas and communication systems. Next the Doppler effect, which changes dynamically, must be compensated during a contact, so the transceiver or SDR must ingest this information in real time. The traditional role of the Flight Dynamics Facility has to automate these processes through the use of software systems that provide reliable and updated information to the rest of the ground segment. Several free tools are available for this purpose [9–11].

### **4.3 Ground station control**

During the contacts, all the hardware must work as a perfectly oiled machine. The information provided by the orbit propagation software will be used to interact with the rotors controller to perform a smooth track of the spacecraft [12]. As previously mentioned the Doppler effect must be compensated on the reception chain in real time, and this calculation will be computed also using this information. Before the contact, all systems must be checked to generate an alarm with enough time to take actions. The antennas will be waiting for the spacecraft at the acquisition of signal (AOS) azimuth point. During the tracking phase the strategy of rotors displacement should take into account the limitations of the angular speed. Satellites in LEO orbits and lower, as is the case of many CubeSat missions operating at altitudes lower than the International Space Station, can be difficult to track. After the end of the contact referred to as loss of signal (LOS), the software must take care of parking the ground station in a safe position to prepare for the next track.

## **5 Ground segment operation**

There is little room for improvisation throughout a space mission. All contacts with the spacecraft and every single telecommand sent must be preceded by strict planning and revision. The MCS can be an invaluable tool to simplify the operations and make planning and execution more effective and lower-risk tasks. Software tools often tailored for each mission are a key element of daily operations, supported by strict policies and constant reviews.

### **5.1 Operation planning**

The passage of a CubeSat over a ground station is a precious resource, particularly in LEO orbits where contact windows last for about 10 minutes, a few times per day. The MCS must provide the right tools to simplify the routine operation of mission planning based on orbit propagation computations and contacts prediction [1, 2].

The generation of a schedule by the MCS should ideally be an unattended task, where the operators introduce the inputs (e.g., involved ground stations and spacecraft, time constraints, priorities, and payloads) and the software returns a simplified view (e.g., calendar and Gantt chart) of what is going on during the time frame under revision, how the slots were allocated, and can identify possible conflicts at a glance. The operator's task is to review the schedule and decide how to wisely manage the possible conflicts or hazardous situations. For example, during a multispacecraft mission, two contacts of different spacecraft can overlap at the same time slot, and one of them has to be discarded or reallocated on any other free slot. Information generated by the MCS during the planning phase can be used not only for ground segment management but also for telecommands and schedule generation, ready to upload to the spacecraft.

## 5.2 Contact execution

Following policies and procedures is essential to obtain professional results. Consistency in practices will facilitate effective execution of the space mission. At least two operators are suggested as a best practice for each contact. One should take care of the ground station elements such as rotors, transceivers, controllers, and software status. As a general rule, a low-level overview of the involved hardware is useful to rapidly debug possible issues. Also a plot showing the power spectral density estimation (RTSA-like view) is a very helpful tool to give an insight of what is happening at the physical layer. The other operator will drive the MCS to command the spacecraft. Before each contact opportunity, operators should have a roadmap of the actions to perform (a contact sheet, e.g., with step-by-step instructions) as a sequence of events (SOE). All the decision-making and streamlining must be embodied in the procedures. These guidelines must reflect all possible paths that operators must follow, for example, in case of a contingency; for example, a critical level of a battery could be a no-go decision, making it better to wait until the nominal level is restored. After each successful contact, operators must record in the logbook all the performed actions, the obtained results, and the issues found if an anomaly occurred. This applies to both spacecraft and GS. Future operations, particularly related to anomaly research, will find this information very useful to gain introspection and pinpoint to possible procedural flaws.

## 5.3 Automation

The main aspiration of any ground segment designer should be to make the operators' life as easy as possible. All procedures are susceptible to be automated, with the exception of revision. A human operator should perform tasks associated with exceptions and revisions. As mentioned earlier, ground station planning and spacecraft schedule generation automation provide numerous advantages, since this repetitive task is prone to human errors. Using automation, the ground segment and space segment operations are fully interconnected and can be managed and reviewed using the same tools. If the ground station is fully automated, the operators' primary task is monitoring its status and possible warnings. Low-risk routine operations like periodic housekeeping downloads outside canonical working hours are ideal for automation, allowing the Mission Control Centre to not have to be staffed around the clock. Ground station status can be monitored in the background, sending the appropriate alarms to the operators to be aware of possible issues beforehand and allowing to make a contingency plan for the operations. The level of targeted automation is related to the mission complexity, but most CubeSat missions can greatly benefit from some level of automation.

## References

- [1] Y.J. Kenneth, *Satellite Communications. Network Design and Analysis*, Artech House, 2011.
- [2] J.R. Wertz, D.F. Everett, J.J. Puschell, *Space Mission Engineering: The New SMAD*, first ed., Microcosm Press, 2011.

- 
- [3] Mission Design Division, Ames Research Center, NASA, Small Spacecraft Technology State of the Art, NASA Technical Memorandum, 2018.
  - [4] M. Schmidt, Ground Station Networks for Efficient Operation of Distributed Small Satellite Systems, *Ausgezeichnete Informatikdissertationen*, 2011.
  - [5] T. de Cola, H. Ernst, M. Marchese, Performance analysis of CCSDS file delivery protocol and erasure coding techniques in deep space environments, *Comput. Netw.* 51 (2007).
  - [6] L.A. Belov, S.M. Smolskiy, V.N. Kochemasov, *Handbook of RF, Microwave, and Millimeter-Wave Components*, first ed., Artech House, 2012.
  - [7] T.F. Collins, R. Getz, D. Pu, A.M. Wyglinski, *Software-Defined Radio for Engineers*, Artech House, 2018.
  - [8] GNURadio, <https://www.gnuradio.org>. (Accessed December 2019).
  - [9] Predict, <https://www.qsl.net/kd2bd/predict.html>. (Accessed December 2019).
  - [10] GPredict, <https://github.com/csete/gpredict>. (Accessed December 2019).
  - [11] Space-Track, <https://www.space-track.org/auth/login>. (Accessed December 2019).
  - [12] Hamlib, <https://hamlib.github.io/>. (Accessed December 2019).

Ricardo Tubio-Pardavila and Naomi Kurahara

Infostellar Inc., Network Operations, Shinagawa City, Tokyo, Japan

## 1 Ground segment development for CubeSat missions

The rise of innovative, more complex CubeSat missions calls for new solutions to be implemented in the architecture of the ground segment. The exigency of maintaining the costs low is pushing the evolution of ground architectures toward cloud-based systems, in which the ground stations can be used in a flexible way by multiple users just like a network of sensors on the ground. This leads to the identification of a set of requirements for the operation of different missions, which defines standardized communication protocols. For CubeSats, this idea started within the academic world and is now moving toward the creation of commercial networks operated by private entities.

### 1.1 CubeSat mission overview

CubeSat missions require different types of communications support services from the ground, depending on the number of satellites to be deployed in orbit. These missions can be classified into the following categories, depending on what requirements they imposed on their ground systems:

- (a) **Single satellite missions** for either educational projects (mostly universities) or for scientific and/or technology demonstration purposes (research institutions). Examples of this particular type of missions are the ones led by the PolySat laboratory in CalPoly—like CP8—or others deployed through initiatives like NASA’s ELANA program (see Ref. [1]).
- (b) **Constellation missions** with the objective of deploying multiple satellites to provide global service usually led by private organizations like companies or startups—Spire Inc. is a good example of the latter. Execution of these missions can be further divided into the following stages:
  - i. **Technology demonstration stage** is the initial stage of a mission where a reduced number of satellites are deployed (usually a single satellite) to demonstrate the capacities of the proposed technology.
  - ii. **Service provision stage** is the next stage of the mission, where the constellation is deployed through a set of “batches” or groups of satellites.

For single satellite missions a single ground station satisfies the basic requirements in terms of data downlink and command uplink for most of the use cases. In this sense, most institutions can execute their mission successfully with a single ground station, which can be upgraded or reused for future missions. However, most of the missions that can be included in this category are highly interested in getting more ground stations on the ground to increase the return of the mission.

During the initial technology demonstration stage of constellation missions, a single ground station might also satisfy the necessities of these projects, in terms of amount data to be downlinked. When constellation missions get into the service provision stage, the necessity for developing a connected network of ground stations emerges. Satellite operators like Spire and Planet Labs have developed their own networks, with hardware and software specifically designed for their communications requirements. This way, their ground assets are very cost effective both in terms of development, deployment, and maintenance. The appearance of ground station network service providers has permitted outsourcing this task and eliminated the necessity of owning the ground assets.

## **1.2 Communication requirements**

In terms of communication requirements, most CubeSat missions currently implement either one or more communication channels, for handling payload data separately from commanding and housekeeping/telemetry data. The reason for this is the very different requirements for the required data rate among these types of data. Taking into account the requirements for the communication systems for CubeSat missions as taken from Ref. [2], it is clear that satellite operators mostly choose the UHF band for their commanding and housekeeping/telemetry data and S band for their payload data. X band has become more popular over the last years, due to the emergence of new radio payload communication devices that were not available before. However, the utilization of X band is still reduced to downlinking data, and it is still prohibitive in terms of pointing requirements and power consumption for very small platforms—especially for 1U and 2U CubeSats. A good example of the utilization of X band in CubeSats is GomSpace satellite GOM-X3 (see Ref. [3]), which downlinked more than 115 MB of data in a 5.7-min pass. Planet Labs DOVE satellites have been repeatedly reported to be able to downlink data at a sustained rate of 200 Mbps (see Ref. [4]).

University projects mostly use amateur frequencies that are available for academic purposes (see Ref. [5]). This is a fast and affordable way for universities to get a frequency assigned for their satellite, but this approach does not allow operators to uplink telecommands through unattended remote ground stations. This restriction set by IARU limits the capacity of using remote ground stations for data collecting from satellites, when the data transfer protocols require a bidirectional satellite-to-ground communication.

### **1.2.1 Gain and pointing requirements**

Pointing requirements depend on the selected band, that drives the selection of hardware for the ground station, especially when it comes to choosing the rotators and the mounting system for the antennas. For the VHF and UHF bands, cross Yagi antennas are the main choice for satellite operators, since they are the ones who work the best within this range of frequencies. In the case of Yagi antennas, the half power beamwidth ranges from 60 (VHF band) to 30 degrees (UHF band). In this sense, considering 3 dB of losses due to pointing guarantees the feasibility of the mission in

terms of link budget, even with a drift in pointing of up to 15 degrees for the UHF band. For the UHF Yagi antennas, the gain usually ranges between 12 and 18 dBi (see Ref. [6] as an example of a UHF Yagi antenna). In the case of S band or X band, parabolic dishes are the main solution used at the ground stations. The gain and the half power beamwidth of a dish antenna follow the next well-known expressions:

$$g = e \cdot (\pi d / \lambda)^2 \tag{1}$$

$$\Theta = k\lambda / d = k / d \cdot c / f \tag{2}$$

where  $\lambda$  is the wavelength;  $d$  is the diameter of the dish;  $e$  is the aperture efficiency, ranging from 0.55 to 0.7; and  $k$  is a parameter that characterizes the performance of the antenna, which ranges between 70 and 50 depending on the manufacturing specifics for each antenna. The previous equations are plotted in Fig. 1, using the following reference values: frequencies 2.2, 8, and 27 GHz (S, X, and Ka bands); an aperture efficiency of  $e=0.5$ ; and a performance parameter with value  $k=70$ . Analyzing these plots, we can conclude that the higher the required data rate is, the larger the diameter of the antenna for the same amount of transmitted power. As higher frequencies with higher bandwidth assignments are required to achieve higher data rates, the pointing requirements become more demanding, and the pointing systems become more complex. For S-band systems the pointing requirements can be less than 1 degree of precision, an achievable requirement using open-loop pointing systems for both

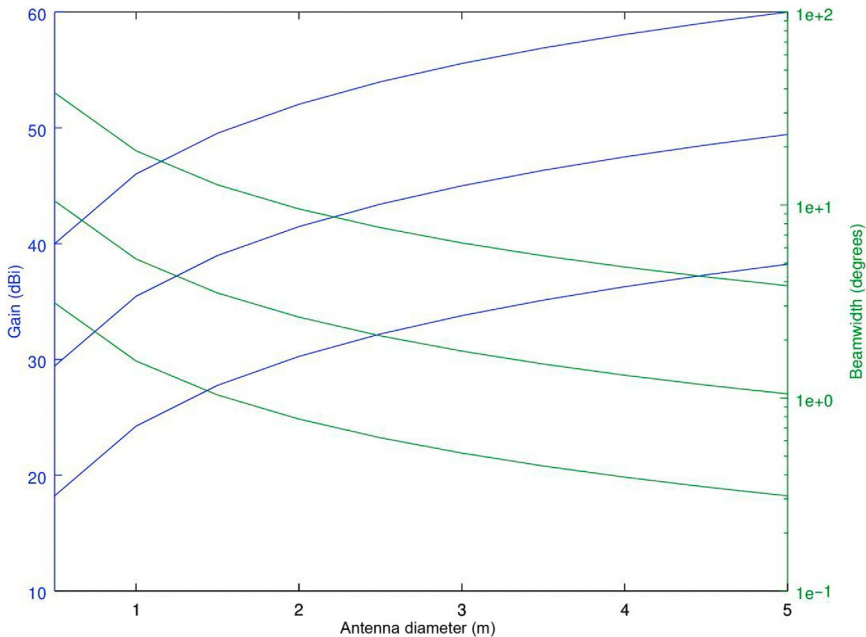


Fig. 1 Gain and beamwidth for S, X, and Ka band dishes.



communication ends. For Ka communication systems the beamwidth of the antenna goes well below 1 degree, potentially requiring closed-loop pointing systems (see Ref. [7]). X-band systems might require autotracking antennas or closed-loop systems for pointing or not depending on the mission.

### 1.2.2 *Link availability and rain fade*

When it comes to higher frequency links, the required system availability needs to be taken into account. It is necessary to include in the link budget the proper amount of attenuation due to rain fade, depending on how often the link with the satellite can be unavailable due to heavy rain. To properly account for this factor, it is recommended to follow the ITU recommendation (ITU P.838; see Ref. [8]). As per that recommendation, rain fade attenuation within the UHF and VHF bands is not a major concern, and its effects can be modeled by adding a fixed attenuation in the link budget calculations for any required system availability (see Ref. [9]). For X band and above the rain fade attenuation needs to be calculated, taking into account the location of the ground station itself and the required link availability. For those use cases in which neither the location nor the hardware cost can be increased, the availability of the link might need to be sacrificed.

### 1.2.3 *Impact at system level*

Taking into account these variables, a 3-m dish operating in S band will achieve around 30 dBi of gain and will require a pointing better than its beamwidth that should be slightly above 5 degrees. The same dish operating in X band will achieve around 45 dBi but requires an accuracy better than 0.5 degrees. It is easy to see that missions limited in terms of budget will easily opt for S-band-based ground assets rather than X-band.

## 2 **Networked ground stations**

Ground stations networks (GSNs) for larger satellites have existed for a longer time; however, their cost and performance are too high—and, therefore not appropriate for small satellite missions. These networks were also usually based on standards for ground station interconnection like SLE (Space Link Extension, see Ref. [10]). Ground station networks for small satellites started being developed, and they were mostly led by people coming from the IT industry. This context permitted the development of software-oriented infrastructures, based on software frameworks and tools coming from the IT industry.

The idea of networking ground stations for CubeSat missions was initially promoted by universities who were seeking to increase the scientific return of their missions. Several projects started in the United States (Mercury, GSN, and SatNet), together with the GSN project in Japan. The Education Office of the European Space Agency started a project called GENSO, which promoted the international cooperation in between different institutions from Europe, the United States, and Japan.

After this initial start as academic projects, several companies (Spire Inc. and Planet Labs) decided to develop their own networks of ground stations. The hardware and software that they use are well adapted to the specific requirements for their missions. Slightly later in time, ground station network providers like RBC Signals, Infostellar, and Leaf Space appeared in the market, proposing novel solutions based on the aggregation of existing resources (RBC Signals and Infostellar) or in the development of ground stations adapted to small satellite missions (Leaf Space). Companies like KSAT who offered products for larger satellites started developing their own solutions for small satellite missions like the KSAT lite network (see Ref. [11]).

## 2.1 University ground station networks

The Mercury (United States), GSN (Japan), GENSO (ESA led project), SatNet (United States and Spain) university-based ground networks are described below.

The Mercury and the GSN ground station networks were originally developed during the early 2000s in the United States and Japan, respectively. The Mercury network (Fig. 2) developed a client/server-based architecture and standardized the message exchange among ground stations through XML. The GSN network (Fig. 3) was composed of two services: the Ground Station Management Service (GMS) and the GS Remote Operation Web Service (GROWS). The GENSO project (Fig. 4) was a

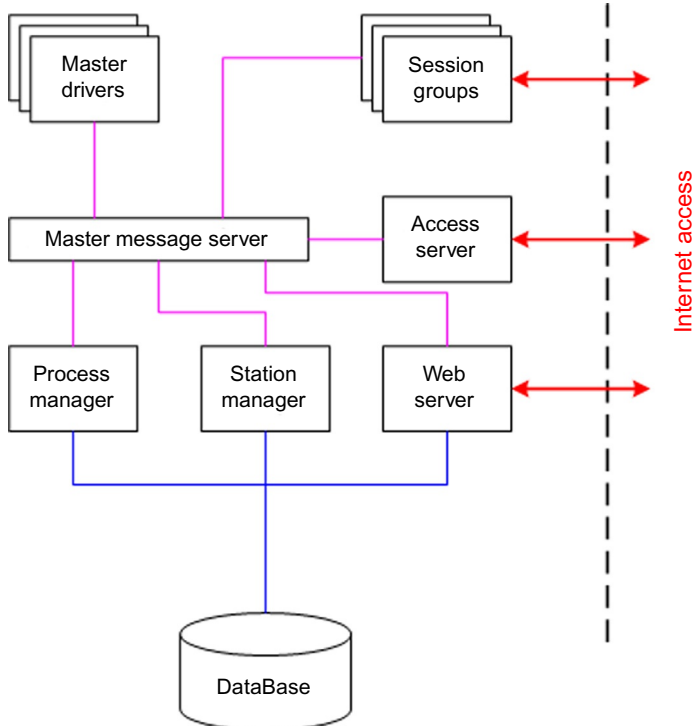


Fig. 2 Mercury GSN architecture.

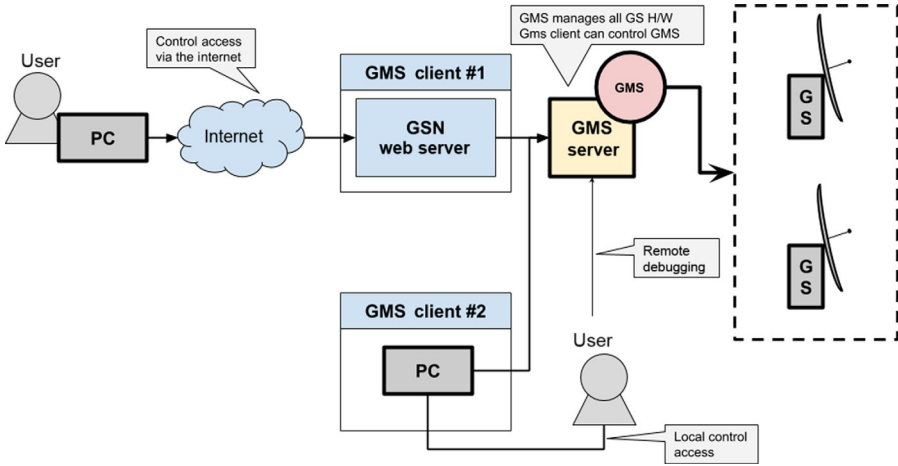


Fig. 3 GSN main architecture.

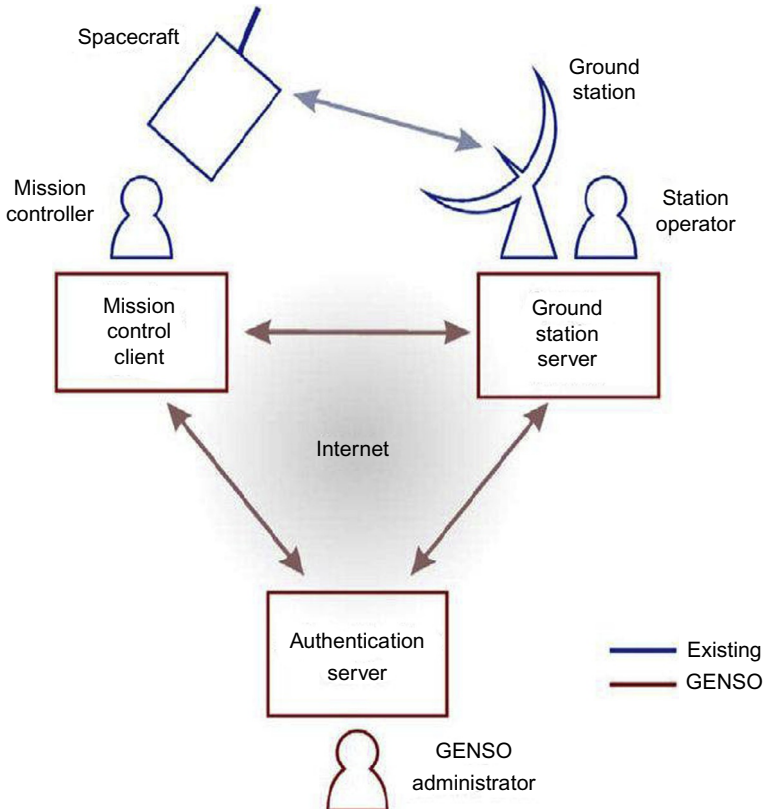


Fig. 4 GENSO architecture.

program of the Education Office of the European Space Agency, which connected several universities from Europe, Japan, and the United States. Its main objective was fostering the development of an educational ground station network to be used for supporting academic, scientific, and educational missions (see Ref. [12]). The implementation of the reference software was led by several universities, and it was based on a peer-to-peer (P2P) network architecture. The SatNet project (Fig. 5) started as a postdoctoral research fellowship granted by the Fundación Pedro Barrié de la Maza. The architecture of this network used IT industry software frameworks (Django, AngularJS, and TwistedMatrix) to develop a distributed server that could aggregate several remote ground stations using software integration only (see Ref. [13]).

Table 1 compares these networks in terms of high level features, from the point of view of the services offered to a satellite operator. In terms of network architecture paradigm, each architecture has been heavily influenced by the dominating network paradigm of its time.

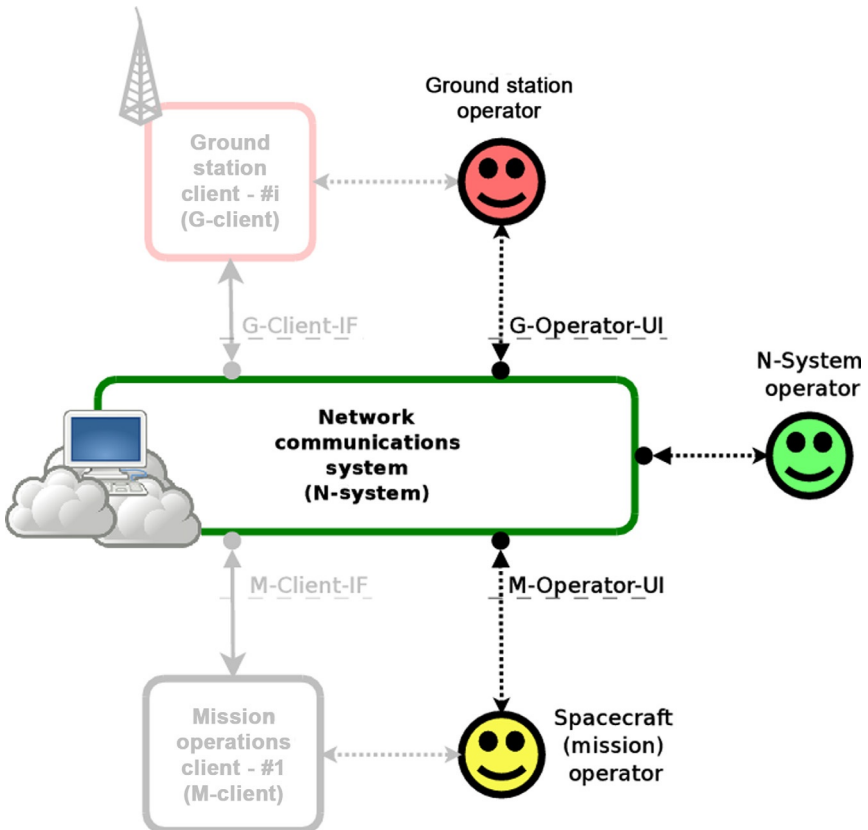


Fig. 5 SatNet architecture.

**Table 1** Feature comparison.

Parameter/ GSN	Mercury	GSN	GENSO	SatNet
Paradigm	Client-server	Client-server	P2P	Distributed
Data transmission	Demodulated bitstream	Demodulated bitstream	Baseband RF in audio format	Demodulated bitstream
Scheduling	Direct usage	Direct usage	Distributed	Distributed
License	GPLv2	–	–	Apache v2

From R. Tubio, et al., Distributed operations network—first deployment results, in: 7th European CubeSat Symposium, doi:10.13140/RG.2.2.26165.99044.

## 2.2 Company ground station networks

The Planet Labs (United States) and Spire (United States) dedicated ground network stations are described below.

Planet Labs Inc. and Spire Global Inc. are two of the pioneering companies from the United States that started developing CubeSat-based constellations for either Earth observation (Planet) or for M2M/AIS/Space weather (Spire). When they started their missions (Planet started in 2010 and Spire started in 2012), there were no ground station network service providers that could meet their requirements in terms of cost and performance.

In this sense, Planet Labs Inc. developed its network to target the specific needs of its own satellites that operate in the UHF, S, and X bands (see Ref. [14]). This network is composed of 32 UHF Yagi stations, 11 × 5 m dishes and 7 × 7.6 m dishes, which allows Planet Labs to downlink around 700 GB of data per day, with a pass failure rate around 30%. In this sense the network of ground stations is deployed to increase the collection capacity from their satellites, which grew from a factor of 1.5 to a factor of 50 from 2015/Q3 to 2016/Q3 (see Ref. [15]).

Spire Inc. started deploying a network for their ground stations in San Francisco in 2012, expanding to more than 30 sites in a few years (see Ref. [16]). As of 2019, Spire is exploring the possibility of integrating their ground segment software with Amazon Web Service (AWS) ground station services. This will allow them to develop all their ground segment infrastructure in a serverless fashion, leaving the ground stations as the only physical assets that they have to manage outside the cloud infrastructure.

To sum up the modern approach for small satellite operators to develop the ground infrastructure is to rely on existing cloud technology. This technology permits satellite operators to write software that can be deployed serverless in the cloud and use all the existing resources of cloud providers like Amazon or Google to transfer and process data. In this sense the advantages of the cloud infrastructure are hard to match by any privately deployed system, especially in terms of cost, storage space, and computational power. On top of this, cloud systems like Amazon WS or Google Cloud provide ready-to-go frameworks that simplify the development and management of software applications for the cloud. At the end of the chain, API development for accessing the results of the processed data permits a fast interconnection with customer's systems (Figs. 6 and 7).

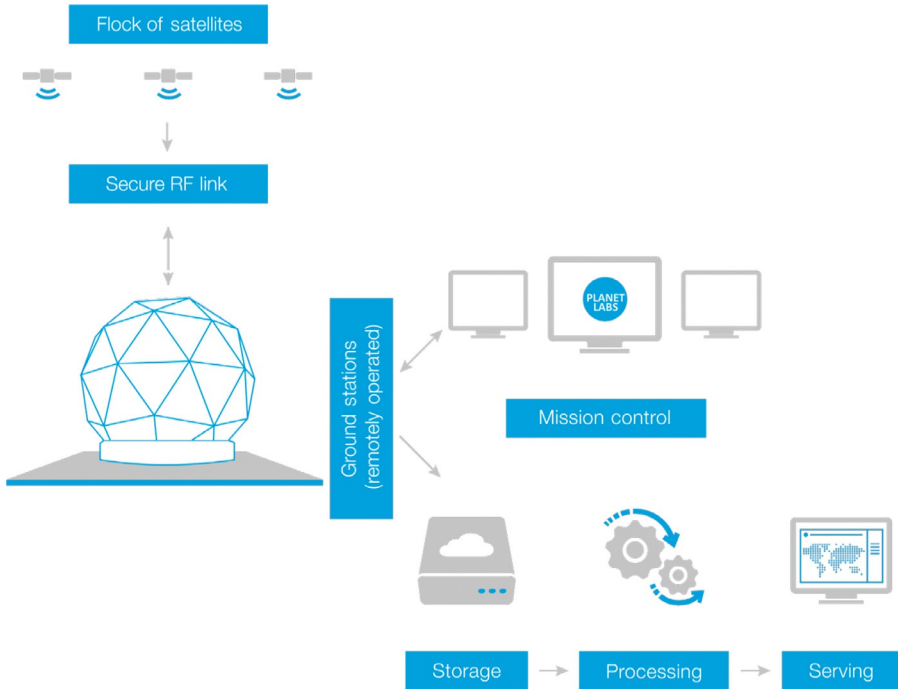


**Fig. 6** Planet Labs ground segment architecture.

Courtesy of Planet Labs, data taken from Planet Labs Specifications: Spacecraft Operations & Ground Systems, version 1.0, June 2015. <http://content.satimagingcorp.com.s3.amazonaws.com/media/pdf/Dove-PDF-Download>.

### 2.3 Commercial ground station networks

The commercial ground station networks- Infostellar, RBC Signals, Leaf Space, KSAT, AWS Ground Stations, and SSC are described below.

Several companies started offering commercial ground station network services for the small satellite operators. These companies can be divided into two groups: companies who already were providing commercial services for larger satellites like KSAT (Kongsberg Satellite Services) or Swedish Space Corporation (SSC) and companies who were created to specifically target the necessities of smaller satellite operators, like Infostellar, RBC Signals, and Leaf Space. AWS Ground Stations started as part of the private space development program of Amazon. Existing ground station networks like KSAT or SSC started developing several products like KSAT lite and SSC Infinity. These products offer access through standard web API interfaces for the transmission of data and the execution of satellite operations. Both solutions standardize the amount of available options for the communications stacks and, at the

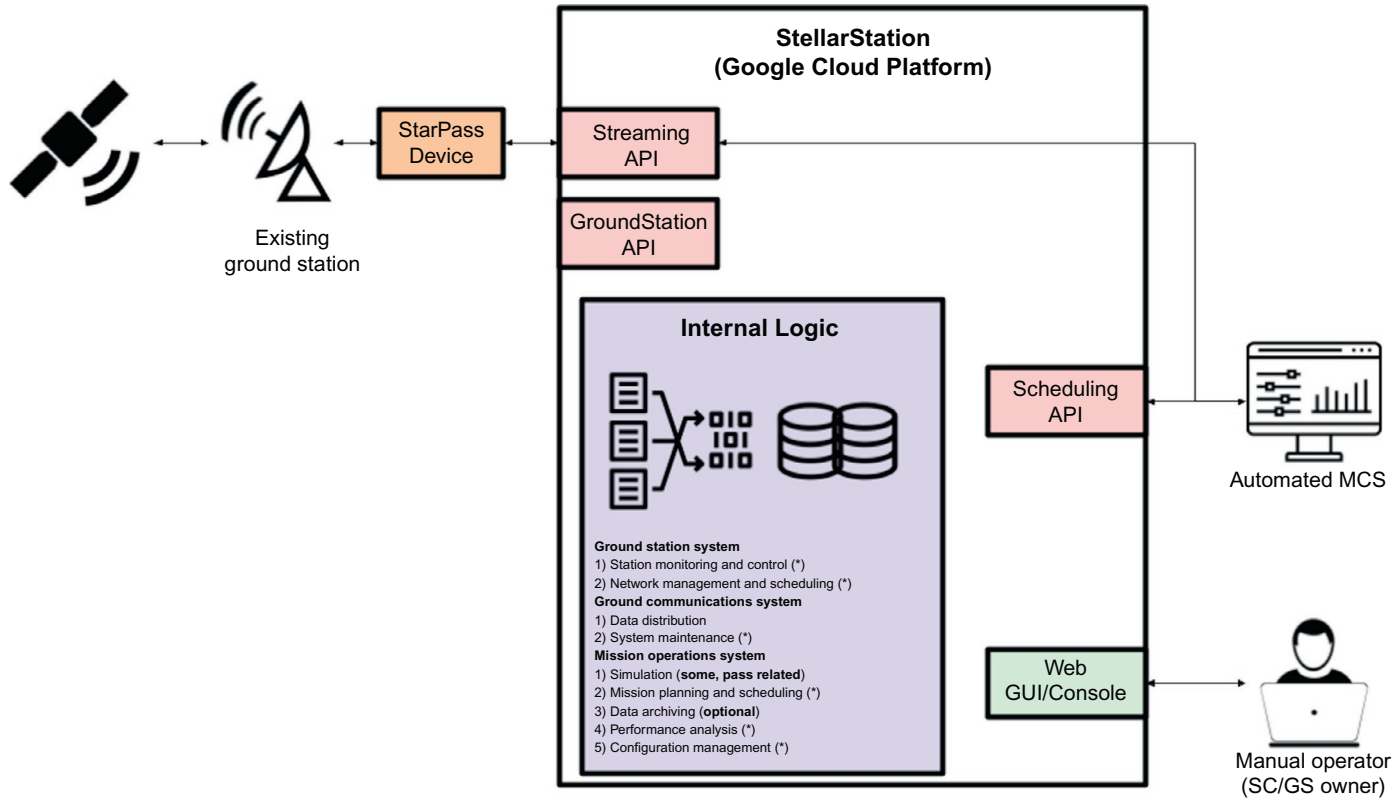


Fig. 7 Infostellar's ground station network architecture.

same time, look for providing standardized testing solutions to ease the satellite-to-ground integration process.

Other companies like Infostellar and RBC Signals started from the business perspective of aggregating existing ground stations and offering their unused capacity through the Internet APIs. Both companies do not develop or own any ground station asset as part of their core business; they only integrate existing ones. In this sense, both companies excel at the speed of integration of ground stations, and they usually look for becoming compatible with as many hardware manufacturers as possible. Leaf Space is a company that started both focusing on services for small satellite operators, and on developing their own ground stations network. In this sense the core of their business is split into creating specific networks for small satellite operators using their own design for the ground stations and offering access to their proprietary-shared low-cost network for fast seamless integration.

These new companies grew their networks using existing cloud infrastructure as the core of their systems. This allows them to integrate third parties API-based mission operation system (MOS) very easily, leveraging the complexity of developing the ground segment for a space mission. Implementing the GSN and MOS bundled within the cloud permits satellite operators to focus on the processing of the payload data and on the development of data-based services. With this approach, satellites and ground stations become commodities, and the focus shifts toward the development of big data and machine learning applications.

### 3 Conclusions

During the last several years, ground station networks have evolved toward cloud-based software systems that come bundled with mission operation systems. Hardware centric-based ground station networks have evolved toward systems that rely on the existing commercial infrastructure for service provision. The integration process relies on the usage of software-defined radios and automated software-based compatibility tests. At the same time, instead of focusing on providing solutions that meet all the specific requirements of the customer, these networks provide standardized communications stacks that ease the compatibility process. Space ground infrastructure is moving toward a service-based business, to which satellites get connected to ground stations like mobile phones seamlessly connect to our current cell telephony networks.

### References

- [1] CubeSat ELaNa Launch on Glory Mission, NASA Facts, NF-2011-01-530-HQ.
- [2] B. Koflas, CubeSat Radios: From Kilobits to Megabits, GSAW, February 2014.
- [3] D. Gerhardt, et al., GOMX-3: mission results from the inaugural ESA in-orbit demonstration CubeSat, SSC 16-III-04, 30th Annual AIAA/USU Conf. on Small Satellites, GomSpace ApS, 2016.
- [4] K. Devaraj, et al., Dove high speed downlink system, in: 31st Annual AIAA/USUS Conference on Small Satellites (SSC17-VII-02), Utah, 2017.



- [5] IARU Mission Planning, <http://www.iaru.org/amateur-radio-satellite-frequency-coordination.html>.
- [6] UHF yagi antenna example, M2 Inc. FG456CP34 model, <https://www.m2inc.com/FG456CP34>.
- [7] R. Mishra, et al., RF tracking test system design for closed loop testing of Ku-band antenna, in: 2016 VLSI-SATA International Conference, 2016, pp. 1–4.
- [8] ITU P.838-3: specific attenuation model for rain for use in prediction models, 03/2005.
- [9] L. Michalek, et al., Analysis of Signal Attenuation in UHF Band, Information and Communication Technologies and Services, 13 April, Dept. of Telecommunications, Electrical Engineering and Computer Science, VSB—Technical University of Ostrava, 2015. <https://doi.org/10.15598/aeee.v13i4.1484>.
- [10] Space link extension—internet protocol for transfer services, CCSDS 913.1-B-2, Recommendation for Space Data System Standards, September 2015.
- [11] K. Monson, KSAT Lite—KSAT Satellite Services, GSAW, Session 11A. 2019.
- [12] Planning the GENSO ground station network via an Ant Colony-based approach, 13th Intl. Conference on Space Operations, 2014, May 2014. <https://doi.org/10.2514/6.2014-1704>.
- [13] R. Tubio, et al., Distributed operations network—first deployment results, 7th European CubeSat Symposium, 2015. <https://doi.org/10.13140/RG.2.2.26165.99044>.
- [14] B. Klofas, Planet labs ground station network, in: 13th CubeSat Developers Workshop, CalPoly, 2016.
- [15] Planet Labs Specifications: Spacecraft Operations & Ground Systems, version 1.0, <http://content.satimagingcorp.com.s3.amazonaws.com/media/pdf/Dove-PDF-Download>, June 2015.
- [16] J. Cappaert, Building, deploying and operating a Cubesat constellation, SSC18-IV-03 Spire Global UK., 32nd Annual AIAA/USU Conf. on Small Satellites, 2018.

# In-space operations

19

Mary Knapp<sup>a</sup> and Kyle Hughes<sup>b</sup>

<sup>a</sup>Massachusetts Institute of Technology, Haystack Observatory, Westford, MA, United States, <sup>b</sup>Jet Propulsion Laboratory, California Institute of Technology, Pasadena, CA, United States

## 1 Introduction

First contact: the moment the whole team has been waiting for and working toward through the long years of development, integration, and testing. The beginning of in-space operations is perhaps the most exciting and nerve-wracking moment of a space mission. Has deployment gone as planned? Will all of the subsystems function properly? Will the payload return the expected science or technical data?

Despite the nerves and sleepless nights, in-space operations can be the most rewarding part of the CubeSat development process. Careful preparation, planning, and training are needed to maximize the likelihood of smooth operations. While it is impossible to prepare for every eventuality or prevent every failure or mistake, this chapter aims at providing useful pointers for CubeSat operators, both new and experienced.

### 1.1 Scope

This chapter will step through preparation for operations, first contact, commissioning, and nominal operations. The future landscape for CubeSat operations and incorporate lessons learned from past missions will also be discussed.

### 1.2 Operational models

Operational models for CubeSats are as many and varied as CubeSats themselves. For the purposes of this chapter, the focus will be on two models: integrated operations, where spacecraft bus and science/payload operations are handled by the same (or overlapping) team in the same physical location, and split operations, where spacecraft operations (everything but the payload) are separated from science and/or payload operations. In the “split” operation case, the bus and payload teams may or may not be colocated and have less personnel overlap than in the “integrated” case. This chapter is written primarily with the “integrated” case in mind but is intended to be general enough to be applicable to both.

If the operation teams are separate or “split,” special care should be taken to develop open lines of communication between the bus operator(s) and the payload/science operations team. CubeSats by their nature are tightly coupled systems that

do not easily lend themselves to the separated bus-instrument model used for larger spacecraft. The instrument or payload will be strongly affected by what the bus is doing and vice versa. For example, reaction wheel speeds above a certain value may generate electromagnetic interference (EMI) that affects the performance of the payload.

The science/payload team should cultivate an understanding of how the bus works and its idiosyncrasies. The bus operator should likewise have a strong grasp of the science or technical mission and function of the payload so that precious time in orbit can be used efficiently. Cross participation in meetings and reviews between the bus and science/payload teams will open these vital lines of communication early in the mission lifecycle, leading to smoother in-orbit operations. Preflight operational readiness tests (Section 2.2) are especially important for split teams so that they can practice working together effectively.

## 2 Preparation for operations

The success of in-space operations depends on the prelaunch (or predeployment) preparation of the team.

### 2.1 Preflight testing and design for operations

Preparation for operations begins during integration and test (I&T). Planning I&T with operations in mind will help avoid last-minute scrambling to develop or refine operations tools and procedures. Personnel overlap from the I&T team to the operations team is desirable, since the I&T team learns the spacecraft's quirks during the testing process. At minimum, I&T personnel should be "on call" during early operations. Elements for consideration for preflight testing and operations design are provided in the following sections.

The spacecraft communications subsystem is, of course, critical to operations as it is the only pathway to command the spacecraft in-orbit and have visibility into spacecraft state and health. As such, radio failures are a common cause of CubeSat "infant mortality" or early loss of mission. Thorough testing of all communication systems is therefore essential to successful in-orbit operations.

#### 2.1.1 Recommended testing

Ground station compatibility tests with flight hardware in the loop are *critical* to successful first contact and operations. The flight radio (or radios) should be tested on site with the ground station(s) that the mission will use in flight. Ideally a full FlatSat<sup>a</sup> with integrated, flight-like radio(s) should be part of compatibility testing. At minimum the flight radio, flight computer (C&DH system), and power subsystem should be in the loop for compatibility testing. On the ground system side, the same set of software tools and user

<sup>a</sup> A FlatSat is a system intended for ground testing of the spacecraft; it has all subsystems, but may not have the same physical/mechanical layout as the spacecraft flight model. In other words, it is all of the spacecraft subsystems and software laid out on a lab bench for the purpose of hardware and software testing.

interfaces that will be used for in-space operations should be used during compatibility testing. Ground hardware, including amplifiers, modems, and computer terminals, should also be the same as what will be used at the ground station(s) for flight operations.

### **2.1.2 Ground station redundancy**

A single ground station represents a single point of failure. If at all possible, multiple ground stations at geographically distributed locations should be included in the spacecraft communications license. Even if the baseline plan is to use just one ground station, others should be licensed for backup in case of an outage. Seasonal weather outages due to high winds, snow, thunderstorms, etc. are common and should be accounted for in operations planning. If the spacecraft will need frequent contact to maintain health, backup ground stations are essential. A backup ground station can also be used to determine whether communications anomalies are due to a problem with the primary ground station or with the spacecraft (see [Section 4.1.1](#)).

### **2.1.3 Real-time telemetry design**

Quickly and accurately assessing the state and health of the spacecraft is essential for timely anomaly response during operations. Real-time telemetry is therefore a critical tool for operations. Real-time telemetry is a set of telemetry points that are streamed to the ground automatically during a ground station contact. A well-chosen set of real-time telemetry points will provide operators with a snapshot of subsystem and overall spacecraft health. Real-time telemetry is often a subset of all spacecraft housekeeping telemetry generated and recorded onboard; the most critical health indicators are selected for inclusion in the real-time stream.

Suggestions for what to include in real-time telemetry:

- spacecraft mode or state (safe, nominal, etc.);
- flight computer boot count and/or uptime;
- temperatures of any components with thermal sensitivity (e.g., batteries and payload);
- solar panel currents/voltages;
- attitude state, including reaction wheel speeds if applicable, voltages/currents, and quaternion from attitude determination;
- radio mode or state, boot count (if applicable), temperature, and currents/voltages;
- fault protection state, including last fault responded to;
- payload state, currents, voltages, and temperatures.

Real-time telemetry channels should be chosen during development and exercised during functional and environmental testing so that the I&T team and operations team become familiar with the telemetry indicators of spacecraft anomalies.

## **2.2 Operational readiness tests**

Operational readiness tests (ORTs) are training scenarios designed to mimic real in-space operations. ORTs are opportunities for the operations team to practice both nominal commanding and anomaly response in a lower-stakes environment than real flight operations. The timing of ORTs will depend on the specific schedule needs of a

mission, but they often take place near the end of the integration and test (I&T) period or soon after spacecraft delivery and before launch or deployment (see [Section 2.2.3](#)).

ORTs last a few days to a week and cover both nominal and off-nominal operational scenarios. During a typical ORT day, the operations team “operates” the spacecraft during several simulated ground contact opportunities.

### *2.2.1 Setup and design of ORTs*

ORTs should strive for the highest level of fidelity to real on-orbit conditions possible given the availability of flight or flight-like hardware and software. Having the real flight unit (if predelivery) or a high fidelity engineering unit or FlatSat (if post-delivery) in the loop is strongly preferred. The ground support software and hardware should also be in the loop. Telemetry playback from preflight testing is also an option if actual flight or flight-like hardware is not available. The operations team should follow the same procedures and use the same tools that will be used for in-orbit operations. ORTs should cover several days of operations so that the operations team can practice the daily decision-making cycle for spacecraft and payload activities and the cadence of contact opportunities.

### *2.2.2 Operational scenarios*

A key goal of ORTs is to “stress test” the operations team and train them to make careful but timely decisions about how to respond to anomalous spacecraft behavior. The project manager, I&T manager, or other team member outside of the operations team design scenarios for both nominal and off-nominal spacecraft behavior. Off-nominal scenarios should be based on issues seen during testing.

Every CubeSat has quirky behavior in one or more subsystems, and ORT scenarios should provide an opportunity to respond to previously observed subsystem misbehavior. For example, if the spacecraft radio has a tendency to freeze or reboot frequently, one ORT scenario should include a radio reboot during a ground station pass. If the attitude control system has known or suspected fault modes that could cause an uncontrolled tumble, the operations team should practice recognizing telemetry indicative of uncontrolled attitude and executing remedies to return the spacecraft to a safe, controlled attitude. ORTs should also include more common anomaly scenarios, like returning the spacecraft to nominal mode from safe mode. If time allows, ORTs should also include off-nominal behavior from the ground station as well as the spacecraft. The ground station team should be included in ORTs as well so that they can exercise procedures to detect faults in their equipment.

The ORT cycle should include several rounds of operations planning, simulated ground contacts with spacecraft telemetry and commanding, and after action debriefs and evaluation. After ORTs the team should assess any gaps in preparation or tools and work to address them before in-orbit operations begin.

### 2.2.3 Timing of ORTs

The delivery schedule and deployment schedule unique to each mission will determine the timing of ORTs. Missions that expect a long delay between delivery and flight could conduct ORTs during that schedule gap. If the CubeSat will be deployed from the International Space Station (ISS), there may be a delay of several months between launch and deployment, providing an excellent opportunity for team training and preparation. Launch and deployment dates are often uncertain however, so it is highly advisable to perform at least a minimal set of ORTs before the flight unit is delivered to the launch provider.

Budget realities often require a CubeSat team to stand down during wait times between delivery and launch or between launch and deployment. A refresher ORT 1–2 weeks before launch or deployment is advisable to dust off operations skills, tools, and knowledge of spacecraft idiosyncrasies. This prelaunch/predeployment ORT is also a final opportunity to shake out bugs in ground tools.

## 2.3 Tools, procedures, and documentation

Successful operations begin during I&T. To the extent possible the team responsible for functional and environmental testing should use the same tools to interface with the spacecraft that the operations team will use during flight. Developing these tools and interfaces early allows debugging before the mission-critical first contact and commissioning phases. Similarly, command sequence generation tools should be developed and used in I&T and then transferred to operations.

Automation of common tasks via scripts is valuable for reducing personnel effort and removing potential sources of human error. In the sprint to assemble and test a CubeSat, automation tasks are sometimes dropped or deprioritized in the interest of getting to the finish line. Including automation of ground tools for command and sequence generation, telemetry parsing and visualization and other routine tasks should be included in the software development schedule and timed to be ready at the beginning of the I&T campaign. Leveraging existing tools and platforms such as Git and GitHub, OpenMCT,<sup>b</sup> COSMOS<sup>c</sup> and AIT<sup>d</sup> and adapting them to the needs of the mission can save considerable personnel effort on ground tool development.

Documentation of software, procedures, and spacecraft idiosyncrasies goes hand in hand with early development of ground tools. The I&T and development teams should collaborate on a “User Guide” for the spacecraft. This living document should include the following:

- basic information about each spacecraft subsystem and interfaces;
- operations block diagram (an example from the ASTERIA mission is shown in Fig. 1);
- command dictionary;
- listing of telemetry channels with typical values;

<sup>b</sup> <https://nasa.github.io/openmct/documentation/>.

<sup>c</sup> <https://cosmosrb.com/>.

<sup>d</sup> <https://ait-core.readthedocs.io/en/master/>.

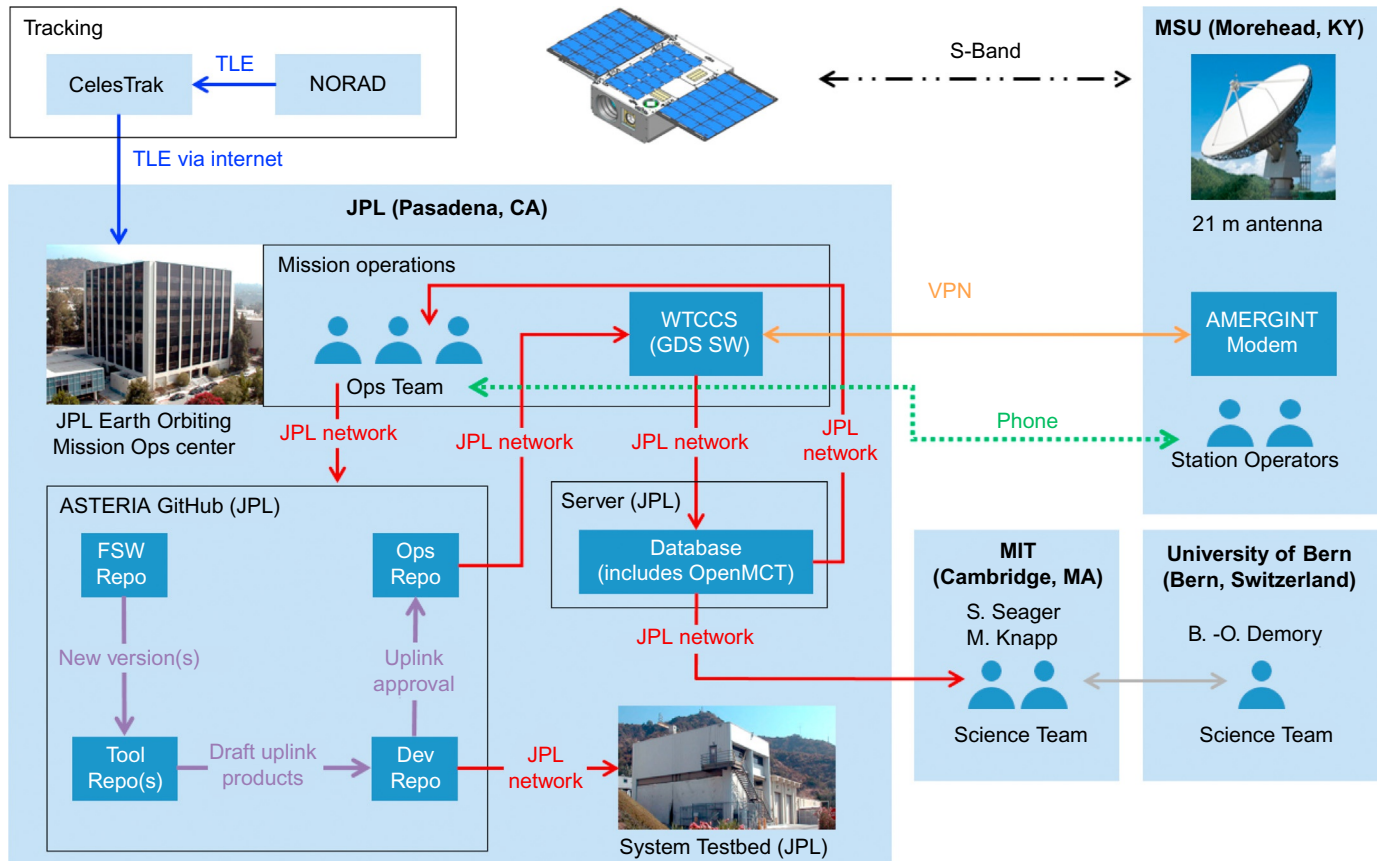


**Fig. 1** Operations block diagram for ASTERIA [1–3]. The various modes of interaction between the ground station at Morehead State University in Kentucky, the operations center at JPL, and other mission stakeholders are shown by *solid and dotted lines*. Sequence generation and approval take place entirely in an institutional GitHub repository.

- Examples of both benign and serious flight software error messages;
- a thorough description of spacecraft and payload modes and a mode transition diagram;
- fault protection tables with descriptions of the responses to each fault;
- a listing of all watchdog timers, their duration, and the response if they trip;
- procedures for generating commands and/or sequences;
- data formats for telemetry and payload data;
- common anomalies seen in I&T;
- responses to correct common anomalies;
- listing and contact information for subsystem or component vendors.

The spacecraft User Guide should exist in a format that can be easily updated, such as wiki, and should be available to the I&T and operations teams. If operations are split between bus and payload, this User Guide should be available to both teams.

Like ground tools, documentation is sometimes, perhaps often, the first casualty of a budget or schedule crunch. One way to avoid this pitfall is to integrate documentation generation into the development process early so that it becomes a habit to update the User Guide regularly. The goal should be to grow documentation organically from many small contributions through mission development rather than to produce it in one chunk at the end of the development cycle.

### 3 First contact

Deployment is the moment of truth. The CubeSat that spent years in development and ground testing has been thrown in the deep end and must sink or swim on its own. It can be a difficult moment for both the development and operations team because there is nothing to be done but wait for a contact opportunity. The success of deployment and first contact rests primarily on preflight preparation and testing, including radio to ground station compatibility testing and fault protection design and testing.

Most CubeSat missions have a series of tasks that they must perform autonomously before ground contact. Many launch providers mandate a waiting period before the CubeSat turns on or releases any deployables. In some cases deployments happen as soon as the CubeSat exits the deployer. After deployment the spacecraft must turn on, charge batteries, and perform any deployments necessary for first contact, such as antennas or solar panels. The CubeSat should boot up into a minimal power mode that can be sustained for a long period of time to give the operations team ample opportunity to make contact and establish commandability.

First contact attempts are high-stress situations for the operations team, so thorough preparation is key. First contact scenarios should be practiced during ORTs so that the operator at the console for in-space first contact has developed a “muscle memory” of how to respond to nominal and off-nominal cases. The operations team should have a plan for the first week of contacts with the spacecraft that includes clearly defined decision gates for moving from one activity to the next. For example, there should be a checklist of telemetry values for commanding the spacecraft to nominal mode from its deployment safe mode. More than one fully trained operator should be present for these critical first contacts.



Personnel from the I&T, flight software, and fault protection teams should be present or on call for first contact and the commissioning phase that follows (Section 4). These are the people who know the spacecraft most intimately and who will be able to recognize anomalous states quickly. If at all possible, members of these teams should be part of the ops team for first contact and commissioning. The ground data system should be able to generate and distribute telemetry summaries and plots quickly so that the operations team and supporting personnel can use that information to assess the state of all spacecraft subsystems.

The stress of first contact can and should be mitigated with careful human factors design. Naturally the whole development team and other stakeholders may want to be present in the control room to experience the excitement of first contact. A crowd of people around the operations console adds considerable stress to the operator whose hands are on the controls. The environment around the operations point person should be kept calm and professional to keep nerves in check, so it is advisable to provide another viewing venue for the rest of the team that removes them from the immediate vicinity of the command console. An essential set of 2–4 subject matter experts should be present to support the operator in evaluating telemetry.

## 4 Commissioning

### 4.1 *Expect the unexpected: dealing with anomalies*

The commissioning phase of the mission is the period of time when each spacecraft subsystem, including the payload(s), is brought online and checked for functionality. It is during this period that the operations team should expect the unexpected, or in other words, anomalies. Each CubeSat is unique and therefore has its own unique anomalies, but we offer some general advice on detecting and responding to unexpected behavior in operations.

#### 4.1.1 *Life signs: interpreting the received signal*

The first “life sign” of the spacecraft is the RF signal itself (or lack thereof). Thorough preflight testing (Section 2.1) should provide the operations team with intuition about how the flight radio behaves with the ground system. During operations, it is helpful to have a live frequency versus amplitude spectrum plot and/or time versus frequency spectrogram available to the operator during ground contacts. The data from these plots should be logged so that it can be viewed or played back at a later time for diagnostic purposes. A constellation plot showing IQ is also helpful for visually assessing the quality of the received signal from the spacecraft. These plots may be generated by either the ground station or the mission operations center (if they are not colocated) but should be available to the whole operations team.

Anomalies may first appear as a change in the strength or shape of the signal on the spectrum or spectrogram plot. The most extreme case is the lack of any detectable signal at all. The operations team should have a clear understanding of the fault scenarios in which the spacecraft is not transmitting when it is expected to be.

The operations team should practice walking through different fault scenarios and identifying other pieces of evidence that can help distinguish one scenario from another.

The following are example set of questions to work through when no signal is detected during a ground contact:

1. Is the ground station functioning properly? Can the ground station verify that it passes its own end-to-end functionality tests?
2. Is the Two Line Element (TLE) defining the orbit out of date or could the spacecraft be misidentified?
3. Could the lack of signal be a symptom of a recent flight computer reboot? How long does the flight computer take to reboot? How long does it take for the radio to be functional and ready to transmit after a flight computer reboot?
4. Does safe mode include a duty cycle for the radio to save power? How long is that duty cycle in each spacecraft mode? How many contact opportunities could be missed in a row in each mode given the duty cycle?
5. In what attitude scenario would the spacecraft transmit antenna be pointed away from the ground station?

Each mission is different, so the aforementioned questions are intended to be representative. Each operations team should know their spacecraft's unique fault tree pathways. If the spacecraft signal is seen by the ground station but its strength or shape is off nominal, there is a different fault tree for the operations team to traverse. In this case it is particularly important to preserve the data for other subject matter experts, like the communications team, to examine after the pass.

A backup ground station, or ground station network, is invaluable for disentangling ground station problems from spacecraft problems (refer to [Section 2.1.2](#)). If the spacecraft can be contacted by the backup ground station but not the primary, the problem clearly lies with the primary ground station. Even if a backup ground station is not included in the communication license, ghost tracks can be used for diagnostic purposes. A ghost track is when a secondary ground station tracks a spacecraft in receive-only mode while the primary ground station is attempting two-way communication. The ghost-tracking secondary station can determine whether the spacecraft is transmitting, whether the spacecraft signal power and spectral shape is nominal, and may be able to record and demodulate real-time telemetry packets. Just a few real-time telemetry packets can be vital for assessing spacecraft health.

#### *4.1.2 Real-time telemetry: Reading the tea leaves*

Real-time telemetry ([Section 2.1.3](#)) received during a ground contact is key to identifying spacecraft anomalies that do not affect the radio. Again the anomalies encountered will be mission specific, but in general, it is important for operators to have a clear understanding of nominal telemetry values so that off-nominal behavior can be identified quickly. The responses to off-nominal behavior will vary, but one frequently used response is to power cycle the offending subsystem or reset the entire spacecraft. The I&T team should thoroughly exercise power cycling of all subsystems and full system resets so that the behavior and timing is well understood. This testing will give the operations team more confidence in commanding subsystem power

cycles or spacecraft resets when or if they are needed. Quick decision-making may be required if, for example, the attitude control system is in a bad state and is not pointing the solar panels at the Sun. An in-pass reset could save the mission in such a scenario.

A flight-like testbed or FlatSat is essential to diagnosing anomalous telemetry. The testbed provides access to all telemetry, not just real-time telemetry, which aids in diagnosing issues. This is especially important if the telemetry received from the spacecraft is severely limited by communication problems. Sequences or commands that led to anomalous behavior can be run on the testbed to reproduce the observed behavior. Fixes can (and should) be run through the testbed before uplink to the spacecraft as well.

## **4.2 Human factors**

### **4.2.1 Operation user interface**

Quickly interpreting real-time telemetry during a ground contact is mission critical, so the way in which that information is displayed is critical as well. The operator's view of incoming telemetry and other data should include color coding of telemetry channels and visual alarms for off-nominal values. The user interface at the operator's station should be iterated during ORTs to minimize distraction and highlight the most important information.

During commissioning, at least two people should be present for ground contacts. The first operator is the point person and is responsible for sending commands. The second operator is a second set of eyes on the telemetry stream and can offer a second opinion if a quick decision is needed. Operator pairs should train together during ORTs to establish a good working relationship.

### **4.2.2 Healthy team, healthy spacecraft**

After first contact the first 1–2 weeks of operations is most stressful for the operations team. Operations staffing should be frontloaded to the extent possible within budget constraints to spread out the work and allow for adequate rest. Many team members may be eager to put in extra hours or skip days off because they are excited that their CubeSat is finally flying, but project management should strongly encourage or require rest days and moderate working hours. Ensuring that operators have sufficient sleep and days off is essential to the safety of the spacecraft—tired operators make mistakes, and mistakes in anomaly situations can end a CubeSat mission prematurely. Underfunding and overworking the operations team are just as risky for the success of a mission as skipping essential preflight testing.

### **4.2.3 Human error**

Human error is inevitable. The human factor considerations discussed in previous sections are aimed at minimizing operator mistakes, but some mistakes will happen anyway. Mitigation for human error has three components: (1) fault protection that

is robust to command or sequence errors, (2) thorough training and documentation, and (3) a solution-focused process for detecting and addressing errors when they do occur.

Fault protection design is complete and tested at the time of launch but should allow for updates as previously unknown fault modes come to light during operations. The second and third components of human error mitigation can be partially addressed by recording ground station contacts. Recording and archiving can be achieved through screen recording and/or video recording. Ground station pass recordings should be available to the operations team and wider support team as necessary. Pass recordings can serve as training tools for new operators; recordings where an anomaly was detected and handled are particularly valuable. Trainee operators can see what experienced operators see, but without the pressure of making split-second decisions.

Recordings of operator errors are valuable as a training tool as well but should not be used to point fingers or shame and blame an operator. Mistakes are an opportunity to uncover weak spots and vulnerabilities in procedures and tools that can then be remedied. The team should avoid questions like “Whose fault is this?” and “Why did you miss that?” and instead ask “What check can be built into our tools/procedure to prevent this from happening again?” and “What can we change in the user interface to avoid this problem in the future?” An increase in operator errors should be a red flag to the team that the operations staff may be overworked or burned out; corrective action should be taken immediately to lighten the load.

### **4.3 Mission assurance during operations**

Members of a small CubeSat development/operations team often wear several hats. During operations, at least one team member should be designated the mission operations assurance manager (MOAM). On large missions the MOAMs are separated organizationally (in terms of their direct reports) from the main project organization so that they can be an independent voice without pressure from project management. A fully separate and independent MOAM is rarely practical on a small CubeSat team, but the role remains critical for maintaining a healthy spacecraft during operations. At minimum the MOAM and the project or mission manager should not be the same person.

The MOAM’s job is to provide the team with risk-informed decision-making guidance. Even if the MOAM is part of the development team, they should strive to provide an independent voice that focuses on maintaining spacecraft health. It is therefore important that the person wearing the MOAM “hat” is free to speak up and slow down or stop actions that he or she deems risky to spacecraft health and that the MOAM’s independence and authority are recognized and supported by project management. If the MOAM says “stop,” the team needs to listen.

The MOAM should take the lead in cross-checking commands and sequences, evaluating automating and other tooling, and overseeing operator training. Additionally, the MOAM should lead anomaly investigations and take responsibility for

tracking anomalies and their resolution. On the ASTERIA mission the MOAM was also in charge of fault protection design and mission assurance during the spacecraft development (see Ref. [4]).

## 5 Prime mission and beyond

### 5.1 Streamlining and optimizing operations for sustainability

As a mission progresses from the commissioning phase to nominal operations, the operations team will shift gears from “firefighting” to “routine maintenance.” In the commissioning phase the primary goal is to ensure that all subsystems, the payloads, and the overall spacecraft are healthy and functioning as intended. During the prime mission the operations team focuses on achieving the program’s key scientific and/or technical goals.

The operations team may shrink due to budgetary or other constraints after the commissioning phase of the mission. *At least one person should remain full time on operations during the prime mission and any mission extensions.* A full time operations lead provides continuity to the mission, training for new operators, and institutional knowledge of the spacecraft and its quirks. Though the operations budget may become increasingly squeezed as the program moves beyond the prime mission, a dedicated operations lead increases the chance that the spacecraft will continue to function and be available for further mission extensions and new experiments and observations if funding is available.

Automation is key to stretching a thin extended mission operations budget. Though ideally automated tools and procedures will already exist, further automating telemetry checks, commanding, and other labor-intensive tasks can reduce or eliminate the need for an operator to be physically present at the operations station during at least some ground station contacts. As operations become routine, longer blocks of sequenced commands can be generated so that the spacecraft can go longer without human-in-the-loop ground contacts.

### 5.2 Rebalancing risk posture

The risk posture of the mission and therefore operations may change if there is a follow-on extended mission after the prime mission ends. During the prime mission the risk posture is relatively conservative because the driving objective is to complete all of the mission goals before the end of the prime mission. Preserving the health of the spacecraft is paramount to that goal. After the prime mission objectives have been accomplished, it may be advisable to relax the risk posture to fully explore the capabilities of the spacecraft. For example, flight software updates are risky and potentially mission-ending so are often not attempted during the prime mission except in dire circumstances. In an extended mission however, a flight software update to fix non-critical bugs and/or add capabilities is a more reasonable risk to take. The MOAM

and project management should be deliberate about defining the extended mission risk posture so that they can provide clear guidance to the operations team.

### 5.3 Training new operators

CubeSat teams are known for high turnover, especially in university settings, so training new operators is necessary for mission longevity beyond the prime mission. Reviewing documentation is the first step in new operator training, so the mission “Users Guide” (Section 2.3) should be complete and up to date. Next, new operators should apprentice with experienced operators by sitting in on ground station contacts and observing. Pass recordings (Section 4.2.3) can also be used for this purpose. After becoming familiar with the workings of the spacecraft and pass logistics, the operations trainee can work through ORT-like simulated passes. If personnel resources for running simulated passes are limited (or nonexistent), playback of telemetry from both nominal and anomalous passes can be substituted. Finally the trainee should serve as the primary operator with an experienced operator observing for several ground contacts.

## 6 Looking to the future

The CubeSat commercial sector is rapidly evolving, as is the range of available operational models. Several CubeSat bus providers are offering ground station and operations support as part of their package, which is nudging the community toward a “split” operations model (Section 2.2.3). The increasing availability of commercial ground station networks is also changing the model for interaction between the mission team and ground station. While the specific implementations will change, thorough testing and documentation, as well as wide-open lines of communication between all parties, will remain the bedrock of successful CubeSat operations.

## References

- [1] L. Fesq, P. Beauchamp, A. Donner, R. Bocchino, B. Kennedy, S. Mohan, et al., Extended mission technology demonstrations using the ASTERIA spacecraft, in: IEEE Aerospace Conference Proceedings, Big Sky, MT, 2019.
- [2] C.M. Pong, On-orbit performance & operation of the attitude & pointing control subsystems on ASTERIA, in: 32nd Annual AIAA/USU Conference on Small Satellites, AIAA/USU, Logan, UT, 2018.
- [3] M.W. Smith, A. Donner, M. Knapp, C.M. Pong, C. Smith, J. Luu, et al., On-orbit results and lessons learned from the ASTERIA space telescope mission, in: Proceedings of the AIAA/USU Conference on Small Satellites, 2018.
- [4] A.J.-N. Donner, P. Di Pasquale, M.W. Smith, C.M. Pong, B. Campuzano, M. Knapp, ASTERIA operations demonstrates the value of combining the mission assurance and fault protection roles on CubeSats, in: 69th International Astronautical Congress (IAC), IAF, Bremen, Germany, 2018.

# CubeSats and orbital debris

20

Kira Abercromby<sup>a</sup> and Chris Ostrom<sup>b</sup>

<sup>a</sup>Department of Aerospace Engineering, California Polytechnic State University, San Luis Obispo, CA, United States, <sup>b</sup>HX5—Jacobs JETS Contract, Orbital Debris Research & Science Operations, Houston, TX, United States

## 1 Introduction

Humans have been sending objects into space since 1957 with the launch of Sputnik. Since all operators of spacecraft share the same space, the US Department of Defense created a central cataloging system called the US Space Surveillance Network (USSSN). The USSSN catalogs objects in low Earth orbit (LEO)  $>10$  cm in diameter and  $>1$  m in diameter in geosynchronous orbit (GEO). As of June 2019 more than 23,000 pieces of orbital debris appear in the catalog, and this number is growing [1]. Of these 23,000 pieces, only about 5% of these are active spacecraft. Scientists believe that  $\sim 500,000$  objects range in diameter of 1–10 cm, most of which are inactive. They believe the total number of objects larger than 1 mm in diameter is  $>100$  million, which includes both cataloged and uncataloged pieces. Due to the increased number of launches each year, the number of payloads housed on a launch, and an increase in fragmentation events, the rise in the number of objects in the catalog has been staggering. Fig. 1 shows the particle environment as seen from outside of GEO with each dot representing an object in the catalog [2]. The dots are not to scale for the size of the particle.

Orbital debris, also known as space debris, is defined as any human-made object in orbit about the Earth no longer serving its useful and/or designed purpose. The Inter-agency Space Debris Coordination Committee (IADC) is an international organization that looks to coordinate efforts dealing with orbital debris. A steering committee exists with four different working groups: measurements, environment and database, protection, and mitigation. This group reports to the United Nations Committee on the Peaceful Uses of Outer Space (UN-COPUOS). One example of the group's efforts is the mitigation working group that determines guidelines for spacecraft operators to follow for mitigation of debris and for limiting debris creation. This chapter introduces the reader to human-made orbital debris and explores areas in which the CubeSat community can be a part of the orbital debris solution.

### 1.1 Orbital debris facts

There are many sources of orbital debris: derelict satellites, upper stages of launch vehicles, debris released during operations, debris created by explosions or collisions (intentional or unintended), solid rocket motor slag, and even paint released during thermal

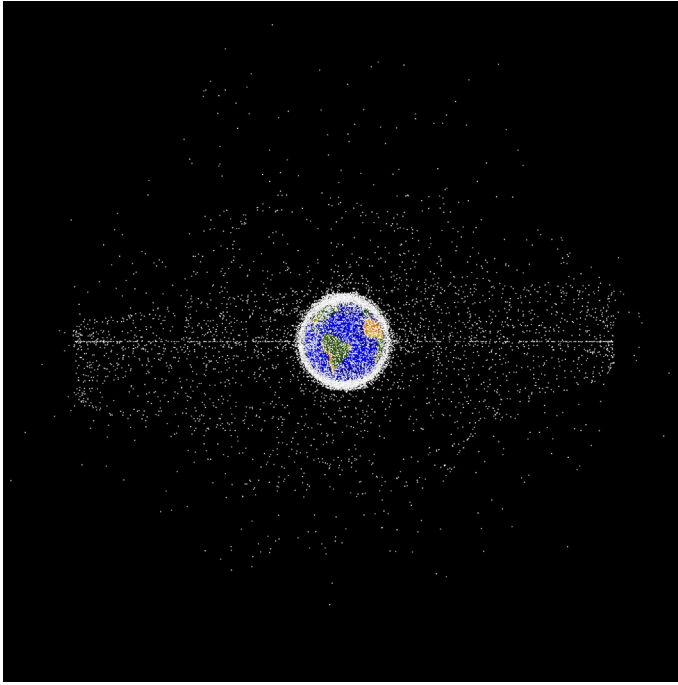


**Fig. 1** Cataloged objects (shown as *dots*) around the Earth.

stress or from small particle impacts. [Fig. 2](#) shows the breakdown of the 23,000 cataloged objects in space [1]. As shown in the figure, fragmentation debris is the largest contributor to the orbital debris environment. Fragmentation debris stems from object explosion or collisions. Prior to 2007 the principal debris source was old rocket body upper stages. However, the intentional collision in 2007 of the Chinese weather satellite Fengyun-1C and the unintentional collision of an American satellite (Iridium 33) and a Russian satellite (Kosmos 2251) in 2009 drastically increased the number of fragmentation objects, accounting for nearly one-third of all cataloged debris.

Because debris travels at the same rate as objects in space, around 7 km/s in LEO, the average impact speed in LEO is close to 10 km/s. [Fig. 3](#) demonstrates the damage caused by a small particle that created a 2 mm in diameter crater in the window of the space shuttle [2]. Collisions with even a small particle will create damage to the spacecraft. Approximately 3–4 times per year the International Space Station maneuvers away from a possible collision with a larger cataloged object. However, objects with no propulsion system have no way of making such maneuvers. In addition, fragmentations usually create many smaller pieces than their original parent objects, which increase the number of smaller objects quickly. Since objects smaller than 10 cm in diameter cannot be tracked reliably, even objects with propulsion cannot always evade collision. While some satellites carry shielding against debris, such shielding creates extra mass and costs money, so shielding is often not an option. Therefore the most important action scientists can take against the growth of orbital debris is to prevent creating more of it, as much as possible.



Monthly Mass of Objects in Earth Orbit by Object Type

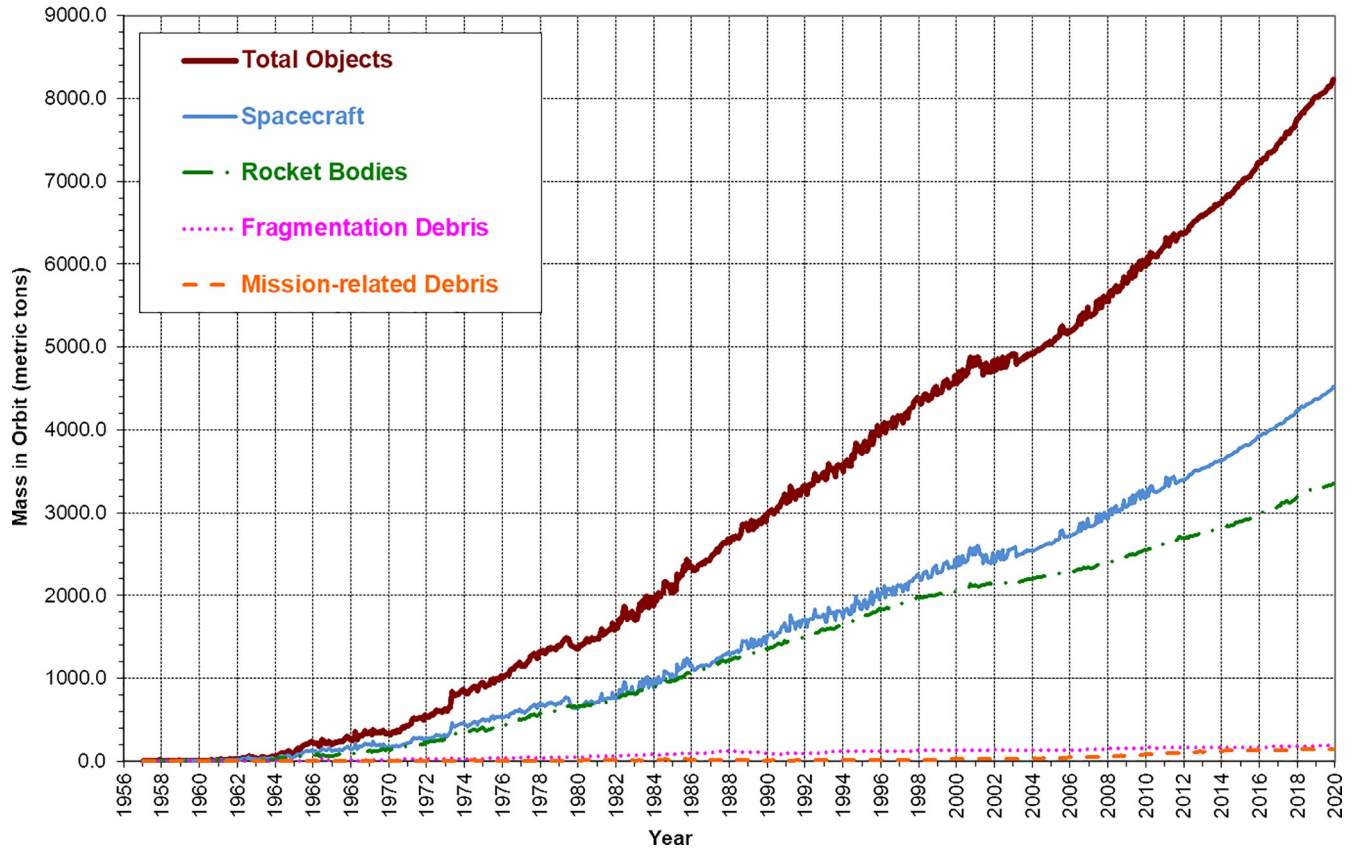
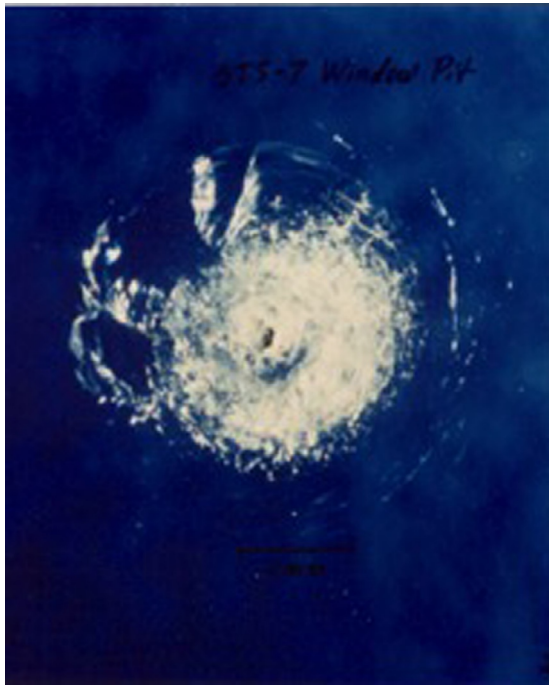


Fig. 2 Number of cataloged Earth-orbiting objects over time.



**Fig. 3** Impact seen on an STS-7 window.

## **1.2 Use of reentry for mitigation**

One method operators use to mitigate the growth of the orbital debris population is to allow the object to reenter the Earth's atmosphere, burning up in the atmosphere at the end of the useful mission. Objects in low Earth orbit (LEO) ( $\sim 2000$  km altitude and lower) are subject to drag from the atmosphere, and most objects will eventually reenter naturally. The time it takes an object to reenter is a function of its size, mass, altitude, and attitude. Further discussion of this method is presented in [Section 2.1](#). However, this mitigation method becomes more effective when satellite operators deorbit their own satellite and rocket body at the end of the mission.

## **1.3 CubeSats**

CubeSats often get into orbit as a secondary payload. In most cases, this means they have less control over the orbit altitude into which they are placed. Due to the variations in CubeSat missions and capabilities, the following sections discuss ways in which CubeSats can meet the orbital debris requirements and potentially be used as a platform to study or remove orbital debris.

## 2 CubeSat mission analysis

### 2.1 Determining a CubeSat's orbit lifetime

A key aspect of a CubeSat mission is the amount of time it spends on orbit; this directly affects the likelihood it will collide with micrometeoroids or orbital debris, potentially making the on-orbit environment worse for future operations, because the longer the on-orbit time, the more the likelihood of a collision. The on-orbit lifetime of a spacecraft is highly dependent on the average altitude of the initial orbit: CubeSats deployed from the International Space Station (~400 km initial altitude) will typically remain on orbit fewer than 3 years, while those deployed in a Sun-synchronous orbit at 700-km altitude may still be on orbit more than 75 years later. These longer times can be contrasted with the typical operational lifetimes of CubeSats of fewer than 3 years, determined by the hardware reliability, the effects of radiation and thermal cycles, and other random failures.

Clearly, even though CubeSats are small in both mass and size (normally 1 kg and 1000 cm<sup>3</sup>), they can produce an outsized effect in the amount of debris in orbit when they are placed in orbits where their lifetimes are longer than expected. The expected lifetime of a satellite can be predicted by computing an area-to-mass ratio (or ballistic coefficient) and using a standard orbit propagator, such as SGP, and propagating forward in time until the perigee altitude drops below 50 km.

A rough calculation of orbital lifetime can be obtained using a high-order Runge-Kutta ordinary differential equation (ODE) solver, like ODE45 in MATLAB. Using initial position and velocity vectors, one can predict the altitude of the object over time in the presence of atmospheric drag by using the equation of motion shown in Eq. (1) and integrating it:

$$a = -\frac{\mu * \mathbf{r}}{r^3} - \frac{1}{2} \rho C_d \frac{A}{m} v_{rel}^2 \frac{\overline{\mathbf{v}_{rel}}}{v_{rel}}, \quad (1)$$

where  $a$  is the acceleration (that is integrated to get velocity),  $\mu$  is the gravitational constant (398,600 km<sup>3</sup>/s<sup>2</sup> for the Earth),  $r$  is the magnitude of the position vector,  $\mathbf{r}$  is the position vector,  $\rho$  is the density of the atmosphere that is a function of altitude,  $C_d$  is the coefficient of drag (usually assumed to be 2.1),  $A$  is the area in the velocity vector direction,  $m$  is the spacecraft mass,  $v_{rel}$  is the speed of the spacecraft relative to the rotating atmosphere, and  $\mathbf{v}_{rel}$  is the velocity vector of the spacecraft. The first half of the formula is the acceleration due to the central body, and the second half is the acceleration due to drag. One can see the dependence the area-to-mass ( $A/m$ ) ratio has on the orbital lifetime of an object. An object with a larger area and a smaller mass, like the case of a solar sail, will greatly reduce the orbital lifetime of an object. With knowledge of the CubeSat's area, mass, position, and velocity, the integration of Eq. (1) over time will give the new position and velocity, and one can determine the estimated orbital lifetime.

## 2.2 Applicable orbital debris requirements

CubeSats that launch with either the NASA Launch Service Program (LSP) or US Air Force or wish to broadcast from orbit to a station in the United States are subject to certain requirements (set forth in Refs. [3–5]). At the international level, similar guidelines were developed by the Interagency Space Debris Coordination Committee (IADC) in 2002 and revised in 2007 [6]. These requirements include quantitative requirements for lifetime and quantity of debris released during mission operations, the likelihood of collision with large objects on orbit, the reliability of end-of-mission maneuvers (if any are planned), and for the expectation of casualty to the human ground population if an atmospheric reentry is planned. Most CubeSat missions will not have pressurized volumes or thrusters onboard, so a large fraction of the orbital debris mitigation requirements is not applicable. In addition, the CubeSat design specifications (1U and 6U; see Refs. [7, 8]) state that if materials other than aluminum are used, “developers should contact the Mission Integrator or dispenser manufacturer.” Stainless steel, titanium, and other materials with high melting point temperatures are likely to survive atmospheric reentry to ground impact, increasing the probability of ground casualty, and so should be avoided if possible.

The final orbit debris mitigation requirements of interest are the maximum orbit lifetime (typically limited to 25 years after end of mission per the guidelines from the IADC) and the large-object collision probability. Satisfying these requirements is strongly dependent on the area-to-mass ratio of the CubeSat; a 3U CubeSat with a mass of 5 kg has an area-to-mass ratio of  $\sim 0.007 \text{ m}^2/\text{kg}$ , which corresponds to an on-orbit lifetime of 80 years when deployed in a 700-km circular orbit at 98.4-degree inclination. A general rule is that an object without propulsion needs to be no higher than 600–700 km in altitude to abide with the 25-year guideline. Since the cross-sectional area of the CubeSat is so small, the probability that any CubeSat will collide with another tracked object during its orbital lifetime is  $< 10^{-6}$ ; however, any decrease in orbit lifetime will reduce the potential effect of the satellite on the future growth of the orbital debris environment.

Operators can reduce the on-orbit lifetime of their satellite in four main ways (summarized in Table 1): increasing area-to-mass ratio by deploying a drag sail, using small chemical thrusters, using electrical propulsion such as ion or plasma thrusters, and by deploying a tether (passive or electrodynamic). Drag sails are perhaps the simplest to understand—these are typically made of a thin film of metal or polymer and

**Table 1** Summary of orbit lifetime reduction methods.

Lifetime reduction method	Residual lifetime	Mitigate casualty risk?
Drag sail	Months to years	No
Chemical thruster	Minutes to years	Only if direct reentry
Electric propulsion	Days to years	No
Passive tether	Days to years	No
Electrodynamic tether	Days to years	No

can increase the cross-sectional area of a satellite by multiple orders of magnitude (and thus reduce the orbit lifetime dramatically). Chemical thrusters can provide enough thrust to perform a controlled reentry (i.e., reduce the perigee altitude to below 50 km) but require a large portion of the mass and volume of the satellite, and many launch providers will not accept CubeSats with chemical propellants onboard. Electrical propulsion, such as ion and plasma thrusters, performs much the same duties as chemical thrusters but has much lower thrust and operates over a much longer period of time than chemical thrusters. These do not typically have the capability of performing a controlled reentry, but can lower the orbit altitude to reduce orbit lifetime, using much less propellant (at the expense of high electrical power requirements). Tethers are simply long cords, made of polymers or conductive materials, depending on the application. Polymer tethers are used similarly to drag sails to increase the area exposed to atmospheric drag. Conductive tethers run a current down the cord and induce a Lorentz force using the Earth's magnetic field. All four of these methods are technically feasible, but each has significant drawbacks: Drag sails and tethers require a deployment at the end of mission, and thus may have reliability concerns, while chemical and electric propulsion may have additional launch safety concerns and restrictions.

If an object cannot reenter within the time, a graveyard orbit is recommended by the IADC. The final altitude must be above 2000 km and below 35,586 km; however, the commonly used 12-h orbit (GPS) altitude should be avoided. Due to the delta- $v$  needed to achieve this requirement, only satellites above 1400-km altitude initially can obtain the desired altitude for graveyard in LEO. CubeSats in GEO will not be able to reenter and thus need to follow different guidelines for end-of-life (EOL) than the LEO satellites. The operators will need to increase the perigee altitude of the spacecraft to  $235 \text{ km} + (C_r * A/m)$ , where the  $C_r$  is the solar radiation pressure coefficient and  $A/m$  is the area related to the mass of the spacecraft. In addition, the eccentricity must be  $\leq 0.003$ .

### 3 CubeSats as measurement and remediation platforms for orbital debris

Thanks to their small size and typically shorter development cycles and lower costs, CubeSats have been used as on-orbit technology demonstration missions. A new area of research interest is in situ measurement of the orbital debris environment, with CubeSats as the base of operation. Three ways of performing these measurements have been proposed (the first two have previous flight heritage, with the NASA Space Debris Sensor and the US Air Force Academy FALCON-ODE mission). The first method is direct measurement of impacts on a surface of known area using changes in resistance in a grid or other electrical measurements and using acoustic sensors to detect impacts.

The second method uses a CubeSat as a deployer for calibration targets for ground-based sensors. Since the 1960s spacefaring nations have placed spheres in orbit to use as objects of known size and electromagnetic and optical properties for calibrating

their assets. These calibration objects have typically been large, ranging from 30 cm to 1 m in diameter. The use of radar and optical assets to survey and track orbital debris, which can be smaller than 1 mm in size, requires the ability to calibrate against smaller objects. Deploying small objects with well-known characteristics from a known initial orbit allows ground-based assets to observe calibration targets that are much closer to the sizes of greatest interest to orbital debris modelers. Finally, CubeSats might be able to detect orbital debris (or meteoroids) passing within a certain distance by using high-power pulsed lasers spread out in a sheet perpendicular to the velocity [9]. This detection method allows for direct observation of orbital debris without interacting with them physically, and if two or more laser frequencies are used, operators may be able to actually determine the material composition of the debris object by comparing spectral responses to laboratory measurements.

CubeSats can also perform active debris removal (ADR) missions. These ADR missions usually entail a CubeSat performing a rendezvous operation with a debris object (whether it is an intact rocket body or spacecraft or some other piece of debris), attaching itself to the debris, and then performing some kind of orbit lifetime-reducing maneuver, such as those described in [Section 2.2](#). The RemoveDEBRIS satellite (having mass 100 kg and approximately a 6-cm cube) was developed by a team at the Surrey Space Center and manufactured by Surrey Satellite Technology Ltd. (University of Surrey) [10] and was successfully launched and deployed in early 2019. This mission conducted three experiments, one of which involved capturing a CubeSat using a net, to demonstrate a new technique for grabbing hold of tumbling debris objects. Future missions may use even smaller spacecraft (such as 6U or 12U CubeSats) as the parent object, which could attach drag sails to spent rocket bodies to mitigate their effect on the on-orbit debris environment.

## 4 Summary

All operators have a responsibility to ensure the sustainability of the on-orbit debris environment, from CubeSats and other small satellites to the massive communications spacecraft in GEO, resulting in every mission minimizing the production of orbital debris during normal operations. Certain launch providers and licensing authorities have requirements that must be fulfilled before receiving permission to launch and operate a CubeSat. These requirements generally deal with on-orbit (production of orbital debris from explosions or collisions) and ground safety (casualty risk to people on the ground from reentering satellites and orbital debris). While CubeSats may not pose a large threat to the orbital debris environment themselves, they may interact with the rest of the on-orbit population (both of active satellites and debris). Ensuring that the on-orbit lifetime is <25 years after the end of the mission (and ideally, no longer than twice the operational lifetime) is a step toward sustainability that any operator can take.

CubeSat operators have a special opportunity: the shorter design-to-launch cycle may allow for innovative uses of space that otherwise would be impossible for a larger, more expensive mission. CubeSats not only can be operated in a way that

minimizes their effect on the debris environment but also can actually serve to improve our understanding of the size, shape, number, and composition of the objects in orbit.

## References

- [1] NASA Orbital Debris Quarterly News, vol. 24 (1), page 4; January 2020. <https://orbitaldebris.jsc.nasa.gov/quarterly-news/pdfs/odqnv24i1.pdf>.
- [2] NASA, ODPO Photo Gallery, <https://orbitaldebris.jsc.nasa.gov/photo-gallery/>, 2019. Retrieved 24 May 2019.
- [3] NASA Technical Standard 8719.14 Revision B, Process for Limiting Orbital Debris.
- [4] Air Force Instruction 91-217, Space Safety and Mishap Prevention Program.
- [5] Title 47 of the Code of Federal Regulations, Part 5—Experimental Radio Service, Part 25—Satellite Communications, and Part 97—Amateur Radio Service Rules.
- [6] IADC, *Space Debris Mitigation Guidelines (IADC-02-01), Revision 1*, Inter-Agency Space Debris Coordination Committee, IADC, September 2007.
- [7] CubeSat Design Specification Rev 13, 2015.
- [8] 6U CubeSat Design Specification Rev 1, 2018.
- [9] J. Bacon, Personal Correspondence.
- [10] University of Surrey, Remove DEBRIS, University of Surrey, 2019. <https://www.surrey.ac.uk/surrey-space-centre/missions/removedebris>. Retrieved 11 September 2019.

# Launching a CubeSat: Rules, laws, and best practice

21

*Joost Vanreusel*

European Space Agency, ESTEC, Strategy Department, Noordwijk, The Netherlands

## 1 CubeSats: A different class of satellites?

Considering their standardized form factor and dedicated technical features and interfaces, from a technical viewpoint, CubeSats form a specific class of satellites, governed by dedicated engineering standards, new or tailored test methodologies, standardized launch adapters, evolved approaches to product assurance, and contributed to a paradigm shift in the launcher sector. Compared with larger, traditional satellites, CubeSats typically have relatively short development cycles, smaller engineering teams, and lower production and operational costs. Additionally, CubeSats often involve players that are relatively new to space activities, including non-governmental actors such as academic institutions and private companies [1].

On the other hand, while some nations have adopted clauses in the national space legislation specifically applicable to pico-, nano-, or microsatellites, from the perspective of public international law, CubeSats are not treated as an individual class or type of satellites. They are bound to the same national and international laws applicable to conventional spacecraft with bigger masses. Bringing a satellite into use, independently from its type or size, is an official national space activity, and it is up to the entities that develop and launch small satellites, including CubeSats, to ensure compliance with the applicable laws. For example, rules and regulations for communication with space objects are legally binding in all member states of the International Telecommunication Union (ITU) [2]. Additionally, those states that have ratified the United Nations space treaties, which are explained in Section 2, must conduct space activities in accordance with applicable binding norms.

In support of a sustainable and responsible use of outer space, it should be recognized that legal and regulatory aspects form an integral part of satellite project management. These legal and regulatory aspects also apply to CubeSats developed by private or public entities. This may create an extra challenge as certain processes may appear to be difficult for less-experienced developers or even for government organizations that are not used to implement the related practice. Due to the typical characteristics of CubeSats, that can be relatively modest in complexity, size, and cost when compared with conventional satellites, they have been the first ever satellite from a given state to be launched into space, in multiple cases [3]. In particular, developers and governments from states new to the cluster of states undertaking space activities may not be fully aware of the applicable legal norms. Those include the



obligation to set up a national register of space objects or the obligation for the state to keep oversight over national space activities undertaken by private parties.

Several important initiatives in this area have been undertaken at an international level, among others, through the World radiocommunication conferences, in the frame of which experts have investigated the dedicated regulations for the assignment of radio frequencies to small satellites. The United Nations Committee on the Peaceful Uses of Outer Space (UNCOPUOS) addresses issues of privatization and commercialization of space activities, which resulted in UN resolutions on the concept of “*launching state*” [4] and in recommendations for states when enacting regulatory frameworks for national space activities [5,6]. For small satellite developers the Secretariat of the UN Office on Outer Space Affairs (UNOOSA) has developed, in consultation with ITU, an information handout on small satellites [7]. Appreciating the relevant legal terminology and being aware of the formal obligations coming forward from applicable rules and laws are key for CubeSat developers. These related processes form an integral part of the project planning and management, and their effective implementation may prevent issues during the final phases of the mission before launch and during the spacecraft operations.

This chapter is organized as follows: [Section 2](#) introduces the main space treaties; [Section 3](#) describes the issues of launch authorization; [Section 4](#) deals with the radio frequencies allocation; [Section 5](#) describes the steps of spacecraft registration; safety aspects of a CubeSat launch are treated in [Section 6](#); [Section 7](#) is dedicated to export issues; [Section 8](#) talks about space debris and collision avoidance; eventually, [Section 9](#) is concerned with third-party liability issues.

## 2 Space law

During the dawn of space exploration, while opposing powers were racing for new accomplishments in space to demonstrate their superiority, the need emerged to regulate the exploration and exploitation of outer space and its celestial bodies. During the 1960s, 1970s, and 1980s, several international treaties and agreements were adopted. They later formed the basis for amendments and clarifications, and the treaty obligations have been specified and implemented through national legal frameworks by several countries around the world. Analogous to the law of the sea that governs the rights and duties of states in maritime waters, a set of internationally legally binding treaties, norms, and principles serve to regulate spaceflight undertakings for scientific, commercial, or other purposes. The underlying principle of the *Outer Space Treaty* [8], which entered into force in 1967, is the prohibition of weapons of mass destruction in space and the limitation to utilize the Moon and other bodies for peaceful purposes only, without appropriation. It furthermore outlines States’ responsibilities in governing national space activities (see [Section 3](#)). The *Liability Convention* [9], which came into force in 1972, establishes liability rules for launchers and spacecraft on ground, during launch and in outer space (see [Section 9](#)), and the *Registration Convention* [10] from 1976 outlines a system to notify, identify, and register space missions (see [Section 5](#)). Other major space treaties are the *Rescue Agreement*, from 1968,

governing the rescue and return of astronauts by any state, and the *Moon Agreement* that entered into force in 1984, overseeing the exploitation of the Moon and other bodies and any stations placed there. While certain activities may be subject to specific requirements, the space treaties apply to any type of satellite as its definitions of space objects make no distinction in type, size, or function [5]. The set of the first three treaties mentioned earlier is crucial, together with any applicable national law, to comprehend the legal framework in which small satellite missions are assumed.

*Space law: Practical recommendations for CubeSat developers*

- Familiarize with the space treaties relevant to the mission, primarily the *Outer Space Treaty*, the *Registration Convention*, and the *Liability Convention*. The treaties are freely available online.
- Verify which of the treaties have been ratified by the State. A list of states party to the space treaties can be consulted on the website of the United Nations Office on Outer Space Affairs (UNOOSA).
- Check if the activity is subject to additional national (space) legislation or regulatory acts and familiarize with the requirements and procedures. A collection of laws relating to exploration and use of outer space is presented on the website of the United Nations Office for Outer Space Affairs.

### 3 Licensing and mission authorization

Placing a satellite in orbit requires a number of subsequent and formal approvals at various levels from different actors, which vary per country. On the side of the developer and customer, the mission is generally submitted to subsequent technical reviews at different stages of development, typically concluding with a flight acceptance review or equivalent, to declare the satellite and its ground segment ready for launch and operations. The launch authority, being the entity overseeing the launcher and offering the launch service to deploy the spacecraft to orbit, has to clear the spacecraft and the launcher-spacecraft combination for launch. In doing so the launch authority relies on a thorough technical, legal, and safety review process that typically starts years or months prior to launch. To obtain final clearance the spacecraft owner/operator and the launch authority will moreover need to obtain certain licenses and approvals by national authorities, irrespective of the size of the satellite, including CubeSats.

Article VI of the *Outer Space Treaty* establishes the provision that states are internationally responsible for national activities in outer space, whether carried on by governmental agencies or by nongovernmental entities. Moreover, state party to the treaty has to ensure adequate and continuous supervision of the activities. Thus, states are under the obligation to authorize private space activities, including CubeSat missions [11]. In the implementation of these obligations, states are free to define whatever practical measures they consider adequate and sufficient to ensure compliance. They can do so by defining licensing processes to be followed by the entity undertaking the space activity or by establishing a national legal framework that regulates the activities, mandating a competent national authority, such as a space agency or ministry, to authorize and supervise those private space activities.

Prior to launching the satellite, the developer must apply for the necessary licenses to obtain authorization from the state to undertake the space activity. Similarly to how driving a lorry loaded with dangerous substances requires a driving license and certain specific permits, operating a satellite requires a license to launch, communication licenses for the usage of uplink and downlink frequencies (see [Section 4](#)), and any additional licenses required for the specific mission, such as a remote sensing license and reentry license. As an integral element of the mission, the ground station and the spacecraft operators need to be licensed to execute the communication activities. The responsible government authority, before granting a license, will verify that the activity proposed by the licensee does not interfere with or by other means causes harm to other ongoing or planned activities and is carried out in compliance to applicable legislation.

Different licenses may require addressing different government authorities, and in some states the authority to be addressed may furthermore depend on the nature of the mission (e.g., low Earth orbit missions vs. geostationary or planetary missions, and commercial vs. academic missions). The processes and conditions for authorization thus differ per country and may depend on the envisaged mission, but they typically cover some or all of the following aspects:

- frequency coordination, out of band emissions and transmitting power;
- technical maturity of the system;
- safety factors;
- orbital lifetime assessment;
- space debris mitigation;
- collision avoidance capability;
- postmission disposal;
- reentry casualty risk;
- dual-use technology and export control;
- recourse for damage, insurance, waivers, and third-party liability;
- financial capacity;
- environmental factors.

#### *Licensing: Practical recommendations for CubeSat developers*

- Identify from the national space law, regulatory acts or practices the licenses to be obtained and additional requirements imposed on the activity (e.g., insurance and maneuvering capability).
- Identify which authorities manage the licensing requests and the requirements to be met by the licensee and the applicable processes to obtain them.
- Consider any relevant requirements in the design and testing of the spacecraft and ground station. For example, the requirement to be able to terminate all transmissions to ground (in case of interference) could result in the implementation of a *silent mode* in the operational architecture.
- Provide the inputs to the relevant authorities following the applicable processes. Once authorized the CubeSat is “ready to go” from an administrative/regulatory point of view. However, this does not represent the last contact with the administrative authorities, and all through the mission’s execution the project team and the administration will have to keep close ties. Ensure that the communication link works well and the project is under the correct regulatory scrutiny.

- Governments or organizations enacting new regulatory frameworks for national space activities are recommended to consult with the United Nations General Assembly Resolution 68/74 of December 11, 2013 on “*Recommendations on national legislation relevant to the peaceful exploration and use of outer space.*”

## 4 Radio-frequency registration

Radio signals from satellites naturally propagate from space into many states, necessitating worldwide frequency coordination among satellite operators. Defining the satellite and ground station operating frequencies during the preliminary design is crucial for the success of a mission, not only because it drives the spacecraft design parameters but also because the frequency spectrum and orbital positions are in fact limited natural resources that must be used rationally, efficiently, and economically [11].

The allocation of the radio-frequency spectrum is managed by the International Telecommunication Union (ITU), a dedicated agency of the United Nations that is responsible for global information and communication issues. Its *Constitution and Convention* [12] and the *ITU Radio Regulations* [13] constitute internationally legally binding rules, according to which also national regulations have to be developed. Subsequently and subject to the law applicable per country, national authorities may need to grant the final spectrum license. For example, in the United States, the Federal Communications Commission manages licensing processes on a first-come-first-served basis or via auction, after the ITU process has been successfully completed [14].

Per the *ITU Constitution*, member states can assign particular frequencies and orbital positions to their respective satellites, but they are obliged to avoid causing harmful interference to the frequency assignments that have been registered earlier, where noncompliance could result in a legal obligation to prematurely end the mission. On the other hand, a state that registers its satellite system using a particular orbital position and certain radio frequencies benefits from international recognition and is protected against harmful interference from latecomers to the registration process (“first-come, first-served rule”). It is in light of this policy that any space station (satellite) shall be fitted with devices to ensure immediate cessation of their radio emissions by telecommand, whenever such cessation is required under the provisions of the Regulations [15].

For CubeSats that are planned to be released to orbit in conjunction with other satellites, it is moreover valuable to set up a communication channel with other operators and to coordinate on the downlink and uplink frequencies. Sharing of information on contacts made with the spacecraft assists in the process to discriminate the different satellites from each other during early operations (see also Section 8.2), and for satellites with the same operating frequencies, it allows operators to request, for instance, to switch off the transmission channel of a copassenger during certain ground station passes to resolve any interference issues that may arise while the satellites fly in close proximity.

## 4.1 Radio amateur frequencies

Contrary to the understanding that many CubeSat developers have shown, satellite systems operating in the amateur-satellite service may be exempt from the full administrative fee that is charged for other filings, but they are not excluded from the frequency assignment notification and recording procedures [16]. Furthermore, when planning to operate in the amateur-satellite service, developers should coordinate additionally with the International Amateur Radio Union (IARU), an international confederation of national amateur radio organizations.

While the usage of radio amateur frequencies has been common practice for CubeSats of a different nature, it should be emphasized that the amateur service is reserved for applications of training, intercommunication, and technical investigations carried out by amateurs, that is, by duly authorized persons interested in radio technique solely with a personal aim and without pecuniary interest [13]. Moreover, transmissions between amateur stations of different countries cannot be encoded for the purpose of obscuring their meaning, except for control signals from ground to a satellite operating in the amateur-satellite service. Instead, with the exception of telecommands for critical satellite functions, all transmissions should be open for use by amateur radio operators worldwide. Practically, that implies that not only CubeSats launched for commercial services, but also CubeSat technology demonstration missions and scientific missions that do not comply with the earlier description, cannot qualify to operate in the amateur-satellite band.

Developers should thus consult the Radio Regulations to identify the frequencies that can both legally and technically be assigned to the mission. As a good practice, consultation with the IARU satellite advisor before initiating further processes allows the mission developer to assess whether or not the proposed frequency will interfere with other planned amateur-satellite services.

## 4.2 Frequency allocation

Frequency allocation and the licensing process are intended for the purpose of avoiding harmful interference between different applications when operative in the same geographic area. The ITU Radio Regulations provide a set of tables that describe the division of the global radio spectrum into bands allocated to particular applications, such as maritime radio navigation, meteorological services, space research services, radio astronomy, intersatellite links, and radio amateur services. For the allocation of frequencies, the world is furthermore divided into three regions, as shown on the map in Fig. 1, where each region has its own set of frequency allocations [13].

Furthermore, two categories of services are set according to the importance and the need for protection of the frequency allocation: primary and secondary. CubeSat missions, in most cases, fall into the category of secondary service. This implies that they can claim protection from harmful interference from other stations in the secondary service, but they cannot cause harmful interference to and cannot claim protection from harmful interference from stations of a primary service, even if assigned at a later date [13].

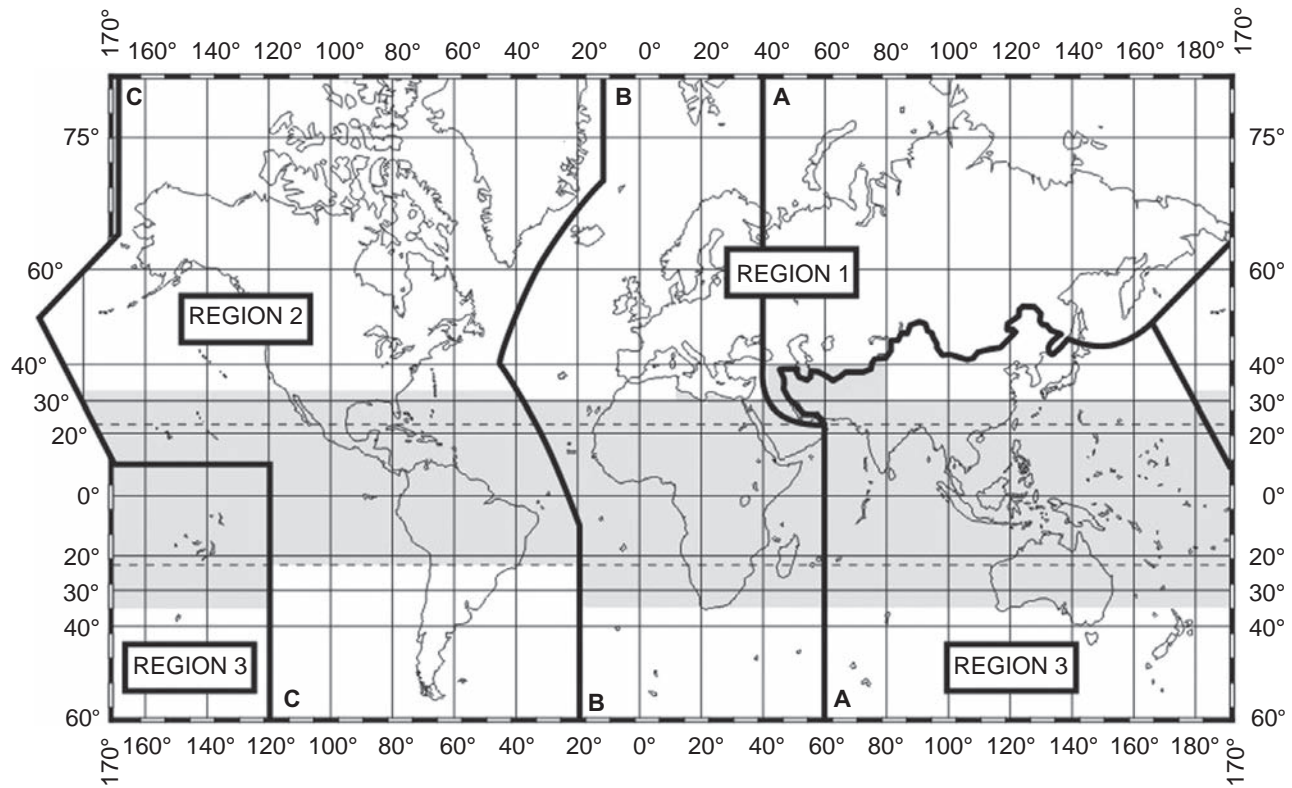


**Fig. 1** ITU regions for the management of the global radio spectrum [17].

### 4.3 Frequency assignment notification and recording procedure

The process to obtain the recording of a frequency assignment in the Master International Frequency Register (MIFR) is described in Article 9 and Article 11 of the ITU Radio Regulations. Fig. 2 outlines the frequency registration timeline, which essentially breaks down into the following key steps [18]:

- coordination with national administration responsible for radio communications,
- coordination with International Radio Amateur Union (in case of radio amateur–satellite service),
- publication in the Advance Publication Information (API) (ITU Radio Regulations Article 9 Section I),
- formal coordination with ITU (ITU Radio Regulations Article 9 Section II),
- notification (ITU Radio Regulations Article 11).

Many CubeSat missions are however exempted from the coordination process (Article 9.2), which only applies if the requirement to coordinate is included in a footnote to the Tables 9.11A-1 and 9.11A-2 of the ITU Rules of Procedure. On the other hand, Articles 9 and 11 are applicable also to the amateur-satellite services, as indicated in Section 4.1.

#### A. Submission of Advance Publication Information (API/A)

Any administration bringing a satellite into use shall provide to the ITU Radio-communication Bureau a general description of the network for advance publication. The characteristics to be provided for this purpose are listed in Appendix 4 of the ITU RR, titled “Consolidated list and tables of characteristics for use in the application of the registration procedures” [13]. Examples of information to be included are the antenna beam characteristics, frequency bandwidth, emission power levels, out-of-band emissions, and ground station descriptions.

The API should preferably be published no later than 2 years before the planned date of bringing the CubeSat into use of, but given the shorter development cycles of CubeSats compared to larger satellites, providing the API at least 1 year before launch can be considered acceptable. It is however recommended to prepare the API as early as possible during the development phase to initiate the process, even if certain details normally included may not yet be known, such as the planned launch vehicle, launch date, and orbital parameters. In such cases ITU generally accepts the API without having these data frozen, and those shall then be communicated no later than upon submittal of the notification request (Step C).

Within 3 months after receipt of the complete information from the national administration, the ITU Bureau shall publish an API/A special section in its biweekly BR International Frequency Information Circular (IFIC).

#### B. Comments from administrations and API/B publication

After publication of the API/A, any administration that believes that unacceptable interference may be caused to its existing or planned satellite networks already registered can provide comments within a period of 4 months, which are published by

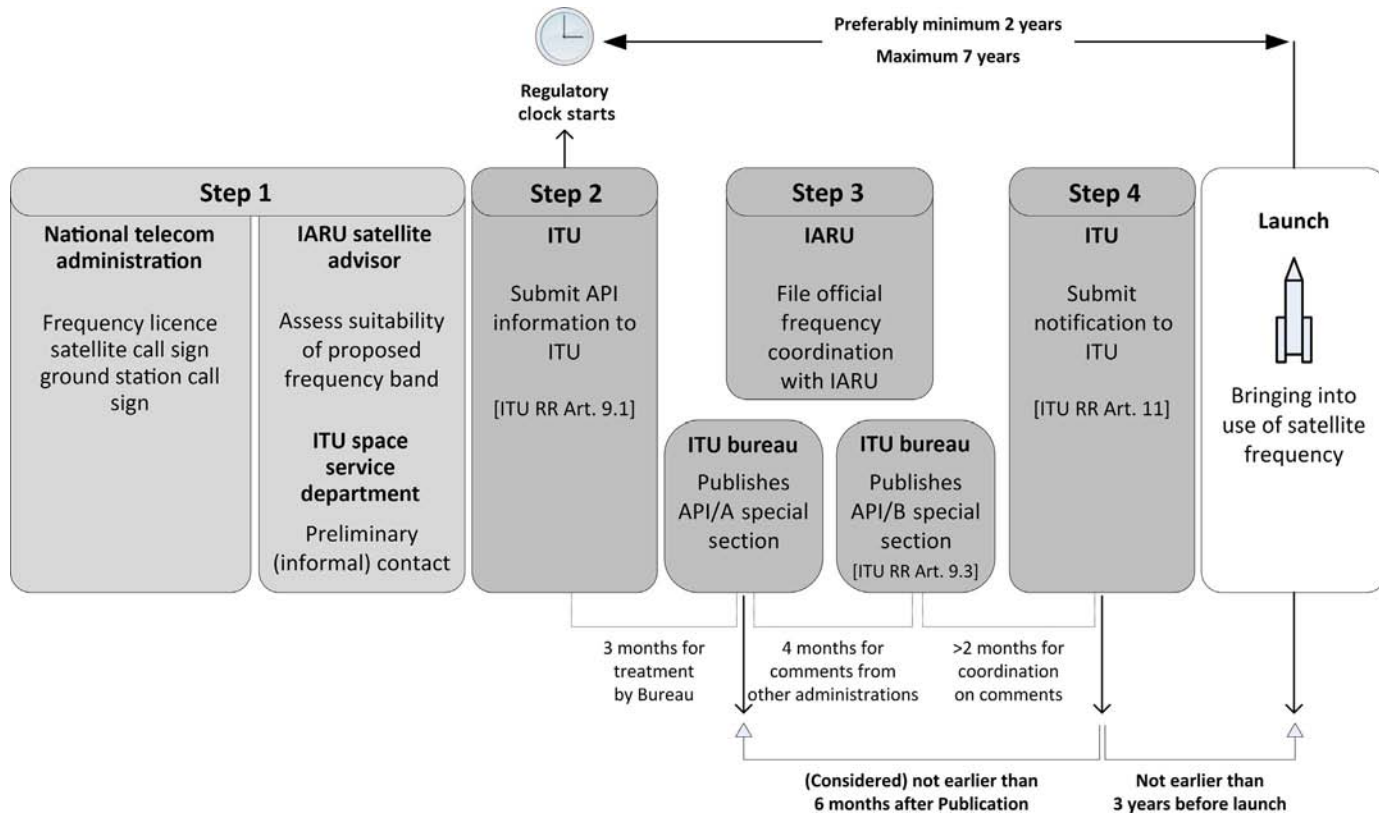


**Fig. 2** Frequency registration timeline.  
*Source:* Author's own figure.



ITU Bureau through an API/B special section. Thereafter, both administrations shall endeavor to cooperate in joint efforts to resolve any difficulties, with the assistance of the Bureau.

### C. Submission of Notification

After the API process is completed and before launch or operations, the frequency assignment of transmitting and receiving satellites and ground stations shall be finally notified to the ITU Bureau, in accordance with Article 11 of the Radio Regulations. This should be done:

- not earlier than 2 months after the date of publication of the API/B (if any),
- not earlier than 6 months after the date of publication of API/A,
- not earlier than 3 years before the first use of the frequencies [13].

The notification information may however also be communicated to the Bureau together with the Advance Publication Information. In that case, ITU will consider the notification as having been received no earlier than 6 months after the date of publication of API/A. Finally, any frequency assignment to a space station provisionally recorded shall be brought into use no later than 7 years from the date of receipt by the ITU Bureau of the API information [13].

Communication with the ITU Bureau shall be performed by the responsible national administration only. If more than one state is involved, one state licensee must be agreed upon between them so that only one administration communicates with the Bureau.

#### *Recommendations for CubeSat developers w.r.t. frequency licensing*

In the case of radio amateur frequency use, developers must:

- Informally consult the satellite advisor of the International Amateur Radio Union (IARU) to assess whether the proposed frequency is not interfering with other planned amateur-satellite services.
- Request an amateur call sign for the spacecraft.
- Ensure that the ground station and operators are licensed and have obtained a call sign.

The coordination request to IARU may be undertaken directly between the licensee (trustee of the ground station) and the IARU satellite advisor.

The latest template of the Frequency Coordination Request can be obtained from the IARU satellite advisor. The template advised the developers to:

- Prepare the Advance Publication Information (API) filing to the ITU Bureau, using the latest version of the ITU Bureau software for the capture and validation of the space notices available on the ITU website.
- Submit, via the national administration, the required data to the ITU Bureau.
- In case of radio amateur frequency use, at the time of submission of the API information to the Bureau, submit the formal Frequency Coordination Request to the IARU satellite advisor.
- Upon completion of the API process, follow the official filing procedure with the national administration to submit the Notification to the ITU Bureau (or communicate it to the Bureau together with the submission of the API).

Satellite developers can consult information considering actual/regulatory status of the API and Notification of their particular or any other satellite networks via the ITU-R Space Network List (SNL).

For an overview of the national Telecommunications Regulatory Bodies, refer to the ITU Global Directory.

## 5 Space object registration

Space object registration forms another important obligation, although here the prime obligation is on the part of the respective state, not on the CubeSat developer. The *Convention on Registration of Objects Launched into Outer Space*, briefly the *Registration Convention*, was adopted by the UN General Assembly in 1975 and entered into force 1 year later. It provides for a legal framework to maintain databases of all man-made objects launched into Earth orbit or beyond.

Firstly, states undertaking space activities shall maintain a registry for all their objects launched into space [10]. Evidently, this requires first and foremost to set up an adequate space object registry at national level—a requirement not yet fulfilled in all states. In particular, when a CubeSat happens to be the very first space object of a state, competences, administrative procedures, and the space object registry need to be established. This includes assigning a governmental body the responsibility over the national registry (usually the national space agency or space office or any other ministerial unit responsible for space activities) [11]. Secondly the secretary-general of the United Nations maintains a register that is openly accessible in which, for each space object, it records the following:

- the name of the launching state (or states),
- an appropriate designator of the space object or its registration number,
- the date and territory or location of launch,
- the basic orbital parameters (nodal period, inclination, apogee, and perigee),
- the function of the spacecraft,
- additional information as provided by the state of registry,
- date of decay/reentry (if applicable, through additional notification).

It is the responsibility of the launching state administration to furnish those data to the UN secretary-general as soon as practicable, using the model registration form that consists of four parts covering (a) information provided in conformity with the *Registration Convention*, (b) additional information relating to a change of operational status, (c) transfer of ownership, and (d) additional voluntary information [10,19]. The notification to the UN is to be sent by the competent authority of the state of registry through a diplomatic mission accredited to the United Nations.

The term launching state, as defined in the *Registration Convention* Art. I, refers to any state that launches or procures the launching of a space object, or from whose territory or facility a space object is launched. By definition, it is likely for CubeSat missions, as for a vast amount of missions, to involve multiple launching states. According to the *Registration Convention* Article II, in such case, it is up to the state parties to jointly determine who should register the object in its national registry and

furnish the data to the UN secretary-general. The state from whose territory a satellite is launched, for example, qualifies as a launching state, but it will typically not register the satellite if it has no obvious relation with the spacecraft other than hosting the launch base. More commonly the state of origin, on whose territory the activity is being undertaken, such as the state where the satellite operator is based, would be the one registering the object. The registration of a space object does not directly trigger liability for damage caused by that object (see [Section 9](#)), but indirectly, there is a clear link: in determining liability, which lies with the launching states, the state of registry will always be considered as only a launching state can register a space object. Certain launch authorities, for instance, those based in Japan, do request evidence prior to launch that the state of origin of the spacecraft is prepared to register the space object after launch. This practice is also being adopted by an increasing number of launch service providers on request of their governments.

International intergovernmental organizations conducting space activities and that have declared acceptance of the *Registration Convention*, such as the European Space Agency, may furthermore act similarly as a state within the context of the *Registration Convention* and may register objects on behalf of its member states [10].

Since the registries must contain details linked to the launch date and orbit parameters, the actual registration in the national registry and the notification to the UN secretary-general are foreseen to take place after launch, as soon as practically possible. It is nevertheless advisable for CubeSat developers and especially those for whom the CubeSat will be the first, or among the first space objects to be launched for that state, to contact the government authorities well before launch to coordinate on and prepare the actual registration. Space object registration not only is an administrative act but also has important legal implications. In particular, through the registration of a space object, a given state will carry jurisdiction and legal control over the satellite [11]. Obtaining a declaration prior to launch on the readiness of the state to register the satellite aids to mitigate the risk of dubiety over the legal status of the satellite after it has been placed in orbit.

#### *Recommendations for CubeSat developers w.r.t. space object registration*

It is recommended that CubeSat developers:

- Familiarize with the UN *Convention on Registration of Objects Launched into Outer Space* (accessible at <http://www.unoosa.org/oosa/en/ourwork/spacelaw/treaties/introregistration-convention.html>).
- Verify which information should be provided in the UNOOSA *Information Form* to be submitted to the UN secretary-general. A model registration forms has been made available in all official languages of the United Nations on the UNOOSA website.
- In case there are multiple launching states, clarify which launching state will register the satellite. Consult with the *United Nations General Assembly Resolution on the "Application of the concept of the 'launching State' (UNGA Res 59/115)* for the identification of all launching States for the mission."
- Identify which is the competent authority in the state, establish contact with the authority during the satellite design or development phase, and share relevant information about the satellite activity.
- Obtain confirmation on the state's readiness to register the space object upon launch in the national and UN registries.

- Upon launch, provide the required information such as exact launch date and orbital parameters, through the appropriate forms and channels, and follow-up with the national authority on the registration of the CubeSat in the national and United Nations registries.
- Upon reentry, whether following a deorbiting maneuver or natural decay, inform the authority to notify the UN secretary-general, as to update the object's status in the registries.

It is noted that states not party to the Registration Convention can still voluntarily provide registration information on their space objects [20].

The *UNOOSA Handout on Small Satellites*, freely accessible online, serves as a good reference for further guidance on the space object registration.

## 6 Safety and cleanliness

The authorization to launch from the state and the acceptance for launch by the launch authority or launch service provider will rely, among other conditions, on a positive outcome of various safety reviews. Not only should the personnel's safety be guaranteed during the spacecraft processing and preparation for launch, but also the launch authority is tasked to reassure that the CubeSat cannot pose a threat to the good integrity of the launch site, of the launcher, and of any other spacecraft onboard the launcher, for instance, through radio-frequency interference, inadvertent activation of the spacecraft, breakup resulting in release of particles or fragmentation, and materials outgassing.

Specific aspects of safety come into play throughout the various program phases, but most of them should be considered starting from the detailed design stage, where they may already have an impact on engineering trade-offs and design choices. Use of pyrotechnics, pressurized vessels, and propulsion evidently leads to more stringent safety procedures and may pose important constraints on the spacecraft handling on ground and in space. But the selection of materials, the type of batteries, and the architecture of the power management system needs to be defined with attention for the environment in which the satellite will need to operate on ground, during launch, and in orbit.

This includes the limitations posed by environmental legislation that limits the use of potentially harmful materials. For example, antenna systems for numerous CubeSats have been made using beryllium-copper alloys, due to their good combination of mechanical and physical properties and formability. The hazardous nature of beryllium, however, requires it to be processed with adequate care for the health risks that it poses if during machining activities particles are inhaled or swallowed. Similarly, Alodine 1200, widely used as conversion coating on aluminum substrates in spacecraft and terrestrial applications, is subject to restrictions that have recently been imposed by certain safety standards due to the associated health risks. It is thus important for CubeSat developers to select materials with awareness on the safety risks they may imply or the constraints they pose with regard to their manipulation and handling. Directives and standards can be consulted to assess the risks in the selection of materials, such as the European registration, evaluation, authorization, and restriction of chemicals (REACH) regulation and restriction of hazardous substances (RoHS) directive.

Other elements that are subject to in-depth safety assessments, in particular by the launch authority, include the configuration of the electrical inhibits to keep the satellite unpowered during launch; the CubeSat's onboard batteries; and any deployables such as antennas, solar panels, or booms must not be deployed prior to deployment of the satellite. A CubeSat is generally not allowed to transmit during launch or soon after its deployment to orbit to minimize the risk of electromagnetic interference to the launcher or other spacecraft. Moreover, the CubeSat should not deploy any appendages until after its release to orbit to avoid mechanical failures.

Battery systems, as they need to withstand extreme temperatures and extremely low pressures, should be equipped with sufficient protection mechanisms and require extensive testing in environmentally representative conditions. Requirements for battery testing differ depending on the type of launch, but in particular for batteries onboard CubeSats that are planned to be launched from or transported to manned space systems, such as the International Space Station, the qualification process is more stringent and may include destructive testing. In relation to the applicable rules on space debris mitigation, certain organizations furthermore require assessments related to the risk for in-orbit explosions and the risk for fragmentation of the satellite or its parts in orbit, and for such assessments the batteries and its protection mechanisms (e.g., overvoltage protections and pressure vents) are typically investigated. It is recommended that the developers select and procure batteries with flight heritage or that have been qualified for the use case by the launch service provider, or otherwise to be aware of the stringent safety and qualification requirements that are typically imposed on batteries.

In selecting materials and components, it is also imperative to consider the extreme temperatures, vibration, and pressures during launch and in orbit. An important aspect to consider is the outgassing of materials, which for any spacecraft must remain below acceptable levels specified by different engineering standards and interface documents. Outgassing is the release of gaseous material from a specimen under high vacuum conditions. It may pose a contamination threat to the satellite itself or to other passengers onboard a shared launch, due to the risk that outgassed material deposits on sensitive surfaces such as optics, with potentially high impact to the mission. For this reason, launch authorities may require evidence of bakeout, a process in which the hardware is placed in a high-temperature environment, usually in vacuum, thus accelerating its outgassing rates to reduce the content of molecular contaminants present in the material. Several major space agencies provide publicly accessible databases of materials, components, and parts that have been tested and for which the outgassing properties are known, which CubeSat developers can consult during the selection process.

Furthermore, due to the rapid pressure drops that the CubeSat faces during liftoff, it is important to enable sufficient venting on the satellite and its deployer to avoid that air traps could result in bursts or explosions with a potentially detrimental impact to the launcher. The minimum venting area depends on the compartment volume, and engineering standards describe requirements on venting that can be readily implemented.

Finally the overall cleanliness of the satellite during ground processing must be guaranteed as good practice to prevent issues at spacecraft or lower level and for similar reasons as above vis-à-vis copassengers onboard the same launch. During storage and assembly, integration, and verification (AIV) activities, the CubeSat should be subjected only to a controlled, clean environment with controlled temperature and

relative humidity. Cleanroom class ISO-8 (class 100,000) or better are generally considered adequate for CubeSats, if no more stringent requirements are imposed by the payload or external factors.

*Recommendations for CubeSat developers: Safety and cleanliness*

- Identify safety requirements applicable to the mission, either imposed by law, by the launch authority, or other, and consider the requirements as of the detailed design stage.
- Obtain access to a cleanroom class ISO-8 or better to process all flight hardware during the assembly, integration, and verification (AIV) phase.
- During manipulation of electronics, ensure operators and hardware are connected to the same electrical ground, among others, by use of antistatic mats and antistatic wrist bands.
- For the transport of flight hardware, make use of antistatic wrapping or bags and place them with the hardware inside a suitable transport container or flight case that limits temperature and humidity fluctuations, and exposure to shocks.

## 7 Export control

States implement export control regimes as part of their foreign policy and national security strategies to control, restrict, or embargo the cross-border transfer of potentially sensitive technology. Export control aims to limit the proliferation of ballistic missiles, weapons of mass destruction, and dual-use technology [21]. Furthermore, economic motivations may play a role in the regulations set forth by governments. Due to its civilian and potential military applications, spacecraft technology and hardware has an inherent dual-use nature. Communications, navigation, and remote-sensing capacities enabling peaceful satellite missions are intrinsically not different from those required for intelligence services and military end use. Their export is bound by restrictions that should be appreciated during the satellite development process, regardless of its size and function and thus also when it concerns a nonmilitary CubeSat mission.

Controls on exports cover the transfer from one entity to another of domestic hardware, software, services, and intellectual property that involves the design, development, use, or operation of the technology in question. Thus the exchange in whatever form and by whatever medium of technical information such as design data, technical drawings, user manuals, or even processes and skills can be subject to export control regulations, the violation of which can lead to significant criminal and civil penalties to companies or individuals [21]. As an example, prior to releasing restricted technical data on launcher interfaces to a foreign customer, US launch service providers and their customers must obtain a technical assistance agreement from the US State Department, and similarly, in the European Union, the transmission of technical data to non-EU launch service providers, for the integration of the spacecraft onto the launcher, requires prior authorization by the competent authorities.

At an international level, nonbinding multilateral instruments are in place, including the Missile Technology Control Regime (1987), the Wassenaar Arrangement (1994), and the Hague Code of Conduct against Ballistic Missile Proliferation (2002). In addition to the multilateral treaties, various states define the implementation of export control regimes through binding domestic legislation, typically based on a periodically updated list of controlled items [22].

Even if most satellite technology is subject to export regulations, not all dual-use items require explicit authorization. Due to the relatively complex nature and the multiplicity of regulations among different states, CubeSat developers are encouraged to seek counsel in the domain as to mitigate cost impacts, schedule overruns or sanctions. A concise description of the practices in the European Union and the United States is provided here as example.

The EU export control regime provides for relatively swift authorization procedures, aiming to stimulate a space industry with a rather high share of export sales [21]. While the final authority is with the EU member states, which may complement or expand them, a set of common rules governs the control of military technology and equipment through the Common Military List. Due to their technical specificities, satellites exported outside the EU for launch from a non-EU territory, regardless of size and function and thus including CubeSats, require prior authorization by the competent member state authorities, which is also needed for the exchange of related technical data. It may moreover be expected that suppliers of parts and subsystems may request a formal declaration on the nonmilitary end use of the ordered items from their customers, as such end use would otherwise impose the supplier to apply for a specific export authorization.

In the United States, various regulations cover items defined by specific categories, i.e., munitions, and the competence to issue export licenses is diffused among different government agencies. Most noteworthy are (a) the International Traffic in Arms Regulation (ITAR) including the US Munitions List, which covers all military spacecraft and of which items cannot be exported to countries under US embargo, and (b) the less-restrictive Export Administration Regulations (EAR) including the Commerce Control List, which nowadays covers most commercial space technology, easing the regulatory burden on many CubeSat operators.

The export of a nonmilitary CubeSat to a non-US territory will usually require the submission of a license application within the scope of ITAR, while at lower level the export of the vast majority of off-the-shelf components (COTS) are subject to the EAR but do not require an actual license, easing their export. EAR licenses cover both hardware and technology; export of ITAR-controlled technology is more burdensome, where hardware export necessitates a license, while the release of technical data or services are regulated via the earlier mentioned Technical Assistance Agreements and Manufacturing License Agreements. Integration of a US satellite under EAR control into a non-US launch vehicle and any related exchange of technical data is always subject to ITAR [21].

## **8 Space debris mitigation, collision avoidance, and reentry casualty risk**

As introduced by Abercrombie and Ostrom in Chapter 20, the paradigm shift toward smaller satellites, the vast increase in the number of satellites launched, together with the numerous large-scale constellations under development have given rise to increased concerns by experts on the threats posed by space debris. In-orbit collisions

or breakups and the eventual manifestation of the Kessler syndrome through a cascade of debris collisions pose significant threats to on-going and planned space activities that call for responsible behavior by all space actors, including CubeSat operators. As indicated in [Section 3](#), compliance to space debris mitigation requirements and safe reentry are part of the safety approvals required to obtain authorization for the mission.

## **8.1 Space debris mitigation**

Space debris mitigation comprises the practices and procedures aiming to

- limit the release into orbit of launcher upper stages and satellite parts during nominal operations,
- avoid intentional destruction of satellites,
- limit the probability of accidental collisions,
- minimize the potential for breakups during operations or after the end of mission,
- limit the long-term presence of satellites and launcher stages in certain protected orbital regions.

By introducing certain basic concepts in the CubeSat design, developers can help in preventing the generation of space debris. As a first step the release of objects or particles larger than 1 mm should be avoided. For the nominal operations, this is achieved by design, by ensuring that no parts such as deployable retainers, lens caps, and separation bolts are intentionally released. This also applies to the burn wire often applied onboard CubeSats as thermal knife in a deployment mechanism.

Release of parts or entire fragmentation of the spacecraft as a consequence of anomalies must also be prevented. This is achieved among other methods through good structural design, adequate selection of fasteners, the use of secondary fastening techniques, and by performing an assessment of the in-orbit breakup risk. Also important to this purpose is the design of the electrical architecture, including the selection of battery boards with adequate protection mechanisms to prevent pressure buildup, battery overcharging, thermal runaway, and short circuits.

Prior to launch the undertaking of a suitable verification program (e.g., testing the battery protection mechanisms in a representative environment) should subsequently provide confidence of the design and the tolerance for failures. Finally, successful disposal at the end of life comprises the deorbiting maneuver or natural orbital decay and spacecraft passivation. Passivation is achieved through the depletion of all energy stored on-board to avoid the satellite undergoing breakup after the end of mission. Propellant tanks can be depressurized by means of venting and depletion burns. Batteries can be discharged and disconnected to prevent explosions as they degrade. Should passivation of the power system not be performed, or safety inhibits fail and pressure buildup does lead to explosion of batteries, physical encapsulation of the batteries inside the spacecraft may further help to prevent in-orbit fragmentation.

In the selection of the launch and orbit, it should be confirmed by analysis that the orbital lifetime will remain below prescribed thresholds and with minimal collision risk. Various standards demand the removal of the spacecraft no more than 25 years beyond the end of the operational mission for satellites in the low Earth orbit protected



region (up to 2000 km). In practice, however, satellites with lower reliability are recommended to start the clock at the launch date. Furthermore, considering also the reliability of utilized parts and depending on the type of application, responsible operators may target far lower orbital lifetimes that approach more closely the operational life span of the satellite. The effective orbital lifetime will depend, among other variables, strongly on the solar activity (that affects atmospheric density and in turn influences orbital drag effects) and the area-to-mass ratio of the spacecraft (and resulting drag). To a much lower effect, the satellite attitude can also play a role as the orientation with respect to the velocity vector can affect the cross-sectional area. As a rule of thumb, disregarding any station-keeping or deorbiting capabilities and assuming circular orbits, one-, three- and six-unit CubeSats can be released at altitudes, respectively, below ca 550 km, 575 km, and 625 km, to comply with the 25-year ruling [23].

If the movement of a space vehicle to nonprotected regions or their reentry does not happen naturally in the space environment, active deorbiting capabilities such as drag augmenting devices or propulsion can be used. The technology associated with such capabilities, however, needs to be highly reliable in order to demonstrate that the mission can comply with the 25-year rule. The effective functioning of an experimental drag sail, for example, should not be vital to the successful timely disposal from the protected region, as the reliability of such experimental sail would be difficult to demonstrate prior to its in-orbit validation.

As the development of large-scale constellations gives rise to increased concern over the risks for in-orbit collisions, commercial operators may play an important role in implementing new practices that could evolve into technical standards over time. This can be expected in the areas of in-orbit serviceability, space traffic management, and possibly other areas. New custom practices will arise beyond the currently adopted guidelines and standards, which may help to mitigate the further growth of debris. Those could include the installation of standardized external fixtures to interface with active debris removal satellites [24], the use of retroreflectors on external surfaces to facilitate tracking, new deorbit and reorbit techniques, and automated collision avoidance maneuvering. In the future a so-called space sustainability rating may also offer an innovative means to encourage the responsible behavior of organizations with respect to debris [25].

While space debris mitigation is not mentioned in the five space treaties introduced in Section 2 and while in some cases the standards may not be legally binding, the sustainability of operations in the protected regions calls for operators to act responsibly and with consideration for the fact that also space is a shared resource in which one's behavior may directly affect current and other future operators.

## **8.2 Collision avoidance**

As part of the mission analysis, collision avoidance should be addressed from various perspectives. First, in selecting the target orbit during the initial mission analysis, developers can take into consideration the probability of impacts with other objects in a given orbit throughout the spacecraft's orbital lifetime. Second and in particular for shared launches with multiple satellites, as usually the case for CubeSats, the

launch authority will perform its own mission analysis to define a deployment scenario that minimizes the risks for cross collisions between different satellites and the launcher during the separation. Third, during the entire orbital lifetime of the satellite, close approach events with other space objects, including other active satellites or inactive objects or other forms of debris, should be handled with maximum care. Collision avoidance processes are generally performed as best practice and are not required by most standards. Recent NASA and ISO standards on space debris mitigation, however, do demand that satellites with maneuvering capability must be operated, for instance, by making use of its limited propellant to maneuver in order to actively limit collision risks during the entire lifetime [26,27].

The world standard provider of space surveillance data is the US Combined Space Operations Center (CSpOC). This center conducts conjunction assessments for all active spacecraft against all catalogued satellite objects within defined threat thresholds [28]. At the same time, CSpOC maintains an operators' contact list and notifies operators of close approach events considered to pose a collision risk.

Prior to launch, operators are strongly encouraged to register with CSpOC. This enables the operators to be contacted in case of conjunction identification, that is, when the satellite is predicted to closely approach another space object. To define the course of action, operators of any involved active satellite subsequently can assess the associated risk—or rely on a commercial or governmental service provider to do so—typically based on the miss distance. When achievable, such action typically consists of a collision avoidance maneuver, using propulsion, or in case of CubeSats sometimes using attitude control systems to adjust the ballistic coefficient and resulting atmospheric drag, to cause a small change to the orbit altitude. Uncertainties related to the miss distance and direction together, however, make the latter less trustworthy. Moreover, the less precise orbital fidelity and often more limited pointing precision makes avoidance maneuvers more challenging [5]. Evidently, in case of two active satellites, maneuvering of either one or the other spacecraft requires direct coordination between both operators. Per the 2019 ISO standard on space debris mitigation [29], having a collision avoidance capability becomes mandatory in certain orbital regimes. However, CubeSats often do not have such capability and in most cases may not implement it in the near future. It is important to note that also if the satellite has no collision avoidance capability, it is valuable to subscribe to the CSpOC service and to share maximum data in case of a notification, if only about the noncapability to maneuver, as any information may prove crucial in the days and hours before a close approach event.

Collision avoidance efforts require first and foremost up-to-date information related to the ownership of active space objects by operators. In particular, when launching and releasing multiple payloads, as often the case for CubeSats, it has proven very challenging to discriminate the satellites from the ground until operators manage to establish contact and notify CSpOC and each other on the successful identification of their satellite. This in turn may help other operators eliminate candidates and point their ground antennas in the right direction on subsequent passes of the batch of objects. There are several cases of cluster launches where it took weeks or even months for all objects to be uniquely identified. Also here, precoordination and

sharing of data during the launch and early operations phase facilitate fewer complications. Additionally, new initiatives are being tested such as the use of either optical (laser) or radio-based “license plates,” being small low-power devices attached to the satellite that regularly transmit an identification beacon, while relying only on their own power generation and transmission system independently from the platform [30].

### 8.3 Reentry casualty risk

Due to atmospheric drag a satellite in low Earth orbit eventually reenters the Earth’s atmosphere at the end of its orbital life. The process subjects the satellite to extremely high temperatures—caused by friction — causing the structure to break up under the extreme loads due to the rapid deceleration. If the disintegration of the satellite is not complete and certain parts survive the extreme temperatures during reentry, they will impact the ground and potentially result in casualties or damage to property, for which the satellite operator can be held liable. Commonly adopted standards require that the risk for serious injury or death due to impact must be demonstrated below 1 in 10,000, which in practice and unless of complete disintegration requires controlled reentry through high-reliability deorbiting maneuvers, guaranteeing that scattered debris will only impact ground over unpopulated regions [31,32]. Software tools and models freely made available by different space agencies can be used to analyze the likelihood of survival of parts, and the risk of casualties in case parts impact the ground. Unless specific mission needs dictate otherwise, CubeSat developers are recommended to design for demise, that is, to design the satellite such that it will be destroyed completely during its atmospheric reentry, thus ensuring compliance without requiring further models and without causing additional operational constraints. Detailed analyses can be performed with different software packages made available by space agencies. For CubeSats up to three units, it is generally considered sufficient to perform a review of design to confirm that all materials will fully burn during reentry. The use of hazardous chemical substances or radioactive materials requires more in-depth safety analyses.

*Recommendations for CubeSat developers w.r.t. collision avoidance and space debris mitigation and reentry*

- Starting from the spacecraft preliminary design, refer to Space Debris Mitigation regulations and incorporate them into the design. As the development matures, provide evidence of compliance through reviews of the design, analyses, and tests. The main points of focus are the following:
  - (1) the overall design and operations that shall not foresee any release of objects;
  - (2) the on-orbit lifetime, which shall remain below 25 years and practically is targeted to remain as short as possible;
  - (3) the risk for in-orbit breakup, which should be demonstrated to be sufficiently low through, for example, battery cell protection features, acceptable operational battery temperatures, and encapsulation reducing the risk for fragmentation;
  - (4) the reentry casualty risk that shall be demonstrated to be lower than  $10E-04$  through an assessment of used materials, the spacecraft configuration, and dimensional features.

- A collection of national space debris mitigation standards can be consulted on the website of the United Nations Office for Outer Space Affairs.
- Prior to selecting the orbit for the mission, make use of one of the freely accessible tools to perform an orbit propagation analysis and to verify how many impacts can be expected in a given orbit. Examples of tools are the NASA Debris Assessment Software (DAS) or the MASTER and DRAMA tools of the European Space Agency. Reentry should be ensured within maximum 25 years.

Repeat the analysis with multiple solar activity models and with both nominal and worst-case cross-sectional area values to decrease the influence of uncertainties.

- Use those same tools to verify the risk for parts of the satellite to survive reentry and the forthcoming casualty risk over certain areas (assumed 0 in case of complete disintegration). For one-, two- and three-unit CubeSats, review of the design can be sufficient and may not require further analysis.
- To be notified of any close approach event, prior to launch register with the Combined Space Operations Center (CSpOC). Any operator not under severe embargo by the United States can sign up for free.
- Prior to launch, define the risk threshold for the miss distance that will trigger a certain action, such as a maneuver (in case of maneuvering capability).
- Establish contacts with operators of other spacecraft on the same launch and maintain a communication channel during early operations. Particular attention should be given to copassengers that are operating in the same or very near frequency bands.
- Upon establishing contact with or identification of the satellite in orbit, notify CSpOC and possibly copassengers to support their efforts to identify other spacecraft in close proximity.

## 9 Third-party liability and insurance

Although a CubeSat is a relatively small and lightweight space object, it cannot be ruled out that it may cause damage, be it to other space objects or, as unlikely as this may be, to objects or people on the surface of Earth or to aircrafts in flight. International space law provides for a unique third-party liability regulation, in particular in relation to damages caused on the surface of the Earth: launching states are absolutely liable for such damages on Earth, or to aircraft in flight, that is, independent of a fault; for damages in outer space, launching states are only liable when at fault (e.g., in the case of wilful misconduct). Although this chapter does not discuss the liability regime of space law including its preconditions and implications in detail, it shall be pointed out that any CubeSat launch automatically triggers the international liability of at least one state (the state of registry) and possibly (and simultaneously) more. As mentioned in [Section 5](#), in the determination of liability, the state of registry will always be considered.

It is therefore vital to clarify the liability framework for a given mission between all involved actors at private, national, and, possibly, international level ahead of launch. Licensed operators must also be aware that, depending on the national regulatory framework under which they operate, they might be required by their government to cover part of a possible compensation of third parties injured or affected by the space object under their control. Likewise, national space laws may require the operator—not at least for that very purpose—to take out insurance and provide evidence of

coverage before granting the mission authorization. Insurance for a small satellite mission is not mandatory in every state, however. Some national frameworks—like the Belgian Space Act—do not provide for an insurance requirement but allow for a governmental decision to impose insurance coverage on a case by case basis. Vice versa, other national space laws—like the Austrian Space Act—go the opposite way, that is, having a general insurance obligation that can be waived if a space mission is in “public interest” (e.g., scientific and educational missions). Whether domestic law requires insurance or not, it is imperative for each small satellite project to be adequately informed about the legal requirements, implications, and, ultimately, consequences of sending a satellite into outer space [11].

*Recommendations for CubeSat developers: Third-party liability and insurance*

- Clarify the liability framework between all involved actors (private, national, and international) ahead of the launch service procurement.
- Coordinate on the obligation status for insurance with the relevant authorities, as a measure contributing to mitigate negative surprises “down the road.”
- Ensure national authorities are fully informed on the mission during the development phase, by contacting the national space agency, or the government administration responsible for space activities.

## Acknowledgments

For the chapter on rules, laws, and what you need to know to launch your CubeSat, the author would like to thank his colleagues for their invaluable and indirect contributions, as the writing has been partially based on work performed through earlier collaborations—Mr. Alexander Soucek, head of the Public International Law Division, for sharing his expertise and helping to tackle all legal aspects of the ESA university CubeSat missions; Mr. Daniel Sagath, academic researcher and space regulations advisor, for the pleasant collaborations on smallsat frequency regulations guidelines and the late-night discussions on the responsible usage of outer space; Mr. Stijn Lemmens, senior space debris mitigation analyst, for his recommendations on spacecraft tracking and collision avoidance; and Mr. Piero Galeone, former head of the ESA Academy and human encyclopedia, for the endless hours of guidance on the engineering and management behind larger and smaller space programs.

## References

- [1] UNOOSA, ITU, *Guidance on Space Object Registration and Frequency Management for Small and Very Small Satellites*, (2015) 2.
- [2] P. Deselding, ‘Spectrum cops advising small-satellite owners of obligations’, in: Space News, 2013 27 September <https://spacenews.com/37411spectrum-cops-advising-small-satellite-owners-of-obligations>. Accessed 12 October 2019.
- [3] United Nations Office for Outer Space Affairs, Online Index of Objects Launched into Outer Space. n.d., [http://www.unoosa.org/oosa/osoindex/search-ng.jsp?If\\_id=](http://www.unoosa.org/oosa/osoindex/search-ng.jsp?If_id=) (Accessed 20 December 2019)
- [4] UN General Assembly, Resolution “Application of the concept of the ‘launching State’”, UNGA Res 59/115, (2004).

- [5] S. Mosteshar, I. Marboe, Authorisation under national space legislation, in: I. Marboe (Ed.), *Small Satellites: Regulatory Challenges and Chances*, Brill Nijhoff, 2016, pp. 131–132.
- [6] UN General Assembly, Resolution “Recommendations on National Legislation Relevant to the Peaceful Exploration and Use of Outer Space”, UN GA Res 68/74, (2013).
- [7] United Nations Committee on the Peaceful Uses of Outer Space, ‘Report of the Legal Subcommittee on its fifty-third session, held in Vienna from 24 March to 4 April 2014’ (A/AC.105/1067, 2014) para 98, (2014) [https://www.unoosa.org/pdf/reports/ac105/AC105\\_1067E.pdf](https://www.unoosa.org/pdf/reports/ac105/AC105_1067E.pdf). Accessed 5 August 2019.
- [8] Treaty on principles governing the activities of states in the exploration and use of outer space, including the moon and other celestial bodies, done 27 January 1967, entered into force 10 October 1967, 610 UNTS 205, (1967).
- [9] Convention on international liability for damage caused by space object, done 29 November 1971, entered into force 1 September 1972, 961 UNTS 187, (1972).
- [10] Convention on registration of objects launched into outer space, done 14 January 1975, entered into force 15 September 1976, 1023 UNTS 15, 14 ILM 43, (1975).
- [11] J. Vanreusel, P. Galeone, D. Sagath, A. Soucek, Supporting the responsible access to space of CubeSat missions, in: 68th International Astronautical Congress: Unlocking Imagination, Fostering Innovation and Strengthening Security, Adelaide, Australia, 25–29 September, 2017, 2017, p. 4 IAC-17-E3.4.8, x40937.
- [12] Constitution and Convention of the International Telecommunication Union, done 22 December 1992, entered into force 1 July 1994, 1825 UNTS 1 (meanwhile repeatedly amended), (1994).
- [13] International Telecommunication Union, Radio Regulations, ITU-R Recommendations incorporated by reference, Edition of 2012, (2012).
- [14] M. Dornik, M. Smith, Small satellite industry and legal perspectives in the U.S.A., in: I. Marboe (Ed.), *Small Satellites: Regulatory Challenges and Chances*, Brill Nijhoff, 2016, pp. 67–82.
- [15] International Telecommunication Union, Radio Regulations, ITU-R Recommendations incorporated by reference, Edition of 2012, (2012) Art 2.1.
- [16] International Telecommunication Union, Radiocommunication Bureau, Circular Letter CR/303, (2009) Art 3.5.
- [17] International Telecommunication Union, Regionally harmonized bands. n.d., <https://www.itu.int/en/ITU-R/information/Pages/emergency-bands.aspx> (Accessed 29 August 2019).
- [18] P. Galeone, D. Sagath, J. Vanreusel, Satellite registration management, in: *Small Satellites: Regulatory Challenges and Chances*, Brill Nijhoff, 2016, pp. 265–285.
- [19] T. Masson-Zwaan, Registration of small satellites: The Netherlands, in: I. Marboe (Ed.), *Small Satellites: Regulatory Challenges and Chances*, Brill Nijhoff, 2016, pp. 174–194.
- [20] United Nations, General Assembly Resolution 1721B (XVI), Adopted 20 December 1961, (1961) [https://www.unoosa.org/oosa/en/ourwork/spacelaw/treaties/resolutions/res\\_16\\_1721.html](https://www.unoosa.org/oosa/en/ourwork/spacelaw/treaties/resolutions/res_16_1721.html). Accessed 28 December 2019.
- [21] M. Trautinger, The impact of technology and export controls on small satellite missions, in: I. Marboe (Ed.), *Small Satellites: Regulatory Challenges and Chances*, Brill Nijhoff, 2016, pp. 286–289.
- [22] C.D. Johnson, Legal and regulatory considerations of small satellite projects, secure world foundation, in: M.V. Alonsoperez, R. Qedar (Eds.), *Small Satellite Program Guide*, first ed., CEI Publications, 2014.

- 
- [23] L. Qiao, C. Rizos, A.G. Dempster, Analysis and comparison of CubeSat lifetime, in: Proceedings of the 12th Australian Space Conference, 2013, pp. 249–260.
  - [24] <https://www.oneweb.world/responsible-space>. Accessed 2 January 2020.
  - [25] H. Knight, A sustainability rating for space debris, MIT Media Lab, 2019. <http://news.mit.edu/2019/space-sustainability-rating-system-mitigate-debris-0506>. Accessed 2 January 2020.
  - [26] Process for Limiting Orbital Debris, NASA-STD-8719.14A (with Change 1), (2012).
  - [27] International Standards Organisation, Space Systems – Space Debris Mitigation, ISO TC 20/SC 14 N 24113:2019, (2019).
  - [28] S. Lemmens, ESA space debris mitigation requirements and small sats, in: Proceedings of the Fly Your Satellite! Selection Workshop, Noordwijk, The Netherlands, 9–13 December, 2019, , pp. 20–55.
  - [29] ISO 24113:2019, Space systems—Space debris mitigation requirements, third ed., (2019).
  - [30] R.M. Holmes, C.T. Weaver, D.M. Palmer, ELROI: A satellite license plate to simplify space object identification, (2018).
  - [31] C.D. Johnson, Secure World Foundation: Handbook for New Actors in Space, (2017) pp. 128–132.
  - [32] S. Frey, S. Lemmens, Status of the space environment: current level of adherence to the space debris mitigation policy, J. Br. Interplanet. Soc. (2017) 118–124.

# Deployers

22

*Nathan D. Fite*

Morehead State University, Space Science Center, Morehead, KY,  
United States

## 1 Deployer overview

An astonishing quantity and variety of CubeSat deployers and configurations have appeared over the past few years. There are in excess of 15 deployer developers that have hardware in space. Nearly every developer has multiple variants of their dispenser (1U, 3U, 6U, 12U, etc.) and varying accommodating features that are available. The accompanying suite of design criteria and attributes per dispenser and dispenser variants can cause a significant amount of uncertainty and prevent progress on the part of the mission. For example, certain deployers can support a 3U z-axis length of 340.5 mm, others can handle 366 mm, and some can support both. Certain deployers can handle the “tuna can” volume; others cannot. Is the protrusion envelope in the x- and y-axes <6.5 mm, <10.0 mm, or some other value? This chapter is intended to act as a transfer function for payload developers to begin thinking through and designing to the dispenser-dependent features and to serve as a pointer to where the latest information not included in this chapter may be obtained.

Boiling things down for simplicity, there are two ways to go about getting a CubeSats manifested to be launched into space. The CubeSat developer can find a dispenser with the features they want and then select a rocket that will get into a desired orbit. This menu approach doesn't completely track, since certain launch vehicles prefer or require certain dispensers or even have contracts with certain launch services companies to handle and coordinate all CubeSat launch opportunities. Alternatively, there are various ride share organizations in which the CubeSat developer can pursue a launch and tailor their design to the dispensers chosen for the ride they would like. Companies such as Spaceflight provide CubeSat to launch vehicle match-making and launch services.

### 1.1 Deployer survey

As is all too frequent in the CubeSat industry, CubeSat developers often need to begin designing and potentially even begin fabrication/procurement prior to knowing which dispenser or launch vehicle they will be using. Very often developers are well into the design and build process without having a formalized vehicle to dispenser/launch vehicle Interface Control Document (ICD). This chapter will attempt to set some general guidelines to allow developers to begin down the path of understanding deployers and the implications to their spacecraft designs. Requisite to a thorough design is an



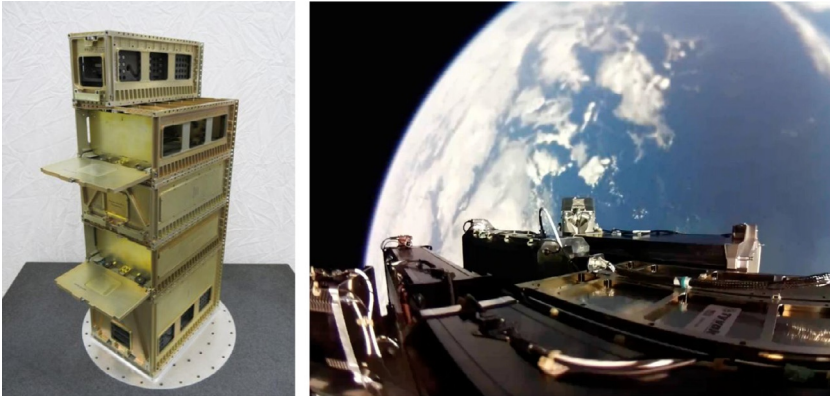


**Fig. 1** (Left) Planetary systems corporation 3U, 6U, and 12U canisterized satellite deployers. (Right) Tyvak 6U NLAS, MK II and 3U RailPOD deployers aboard electron “it’s business time”.

Left: Courtesy Planetary Systems Corporation; Right: Courtesy Rocket Labs.

understanding of what deployers are available and what each offers. Example CubeSat deployers are illustrated in [Fig. 1](#) [1–3].

Getting a payload into space is easier now than ever before. The journey of getting through the proverbial “valley of death” of getting a CubeSat into space is now more of a highway through the desert, due to the infrastructure that has been developed for the CubeSat industry in the form of dedicated launch vehicle and launch service companies. This infrastructure has created a paved pathway of dedicated smallsat and CubeSat launch vehicles, launch service providers, deployer developers, and CubeSat component vendors. The challenge has changed from competing for the very few launch slots on the few deployers to optimizing a CubeSat design to allow for an incredible number of possibilities. The process of solidifying launch opportunities has generated potential revenue opportunities for vendors, spurring the divergence in deployer incompatibility. Referencing [Table 1](#), it may be seen that there are many deployers from many vendors and permutations of available features ([Fig. 2](#)).

## 1.2 Anatomy of a deployer

A dispenser, or deployer, may be thought of as a jack in the box that acts as a mechanical and electrical interface between a CubeSat and the launch vehicle. Boiling the current state of the art down a bit, once the launch vehicle sends the deployment signal to the dispenser, the door actuation mechanism allows the door to open, which permits the spring(s) to extend the pusher plate toward the now open door, pushing the payload along the rails or tabs and ejecting it from the launch vehicle ([Fig. 3](#)).

**Table 1** Partial list of available dispensers.

Descriptions	Country of origin	Launch platform	Rails or tabs	Rails/tabs constrained?	Standards
Astrofein/ECM/EXOLAUNCH PSL-P	Germany	Rocket	Rails	Yes	3U, 3U+, 6U, 12U
Astrofein/ECM/EXOLAUNCH 16U	Germany	Rocket	Rails	Yes	16U
Cal Poly PPOD	USA	Rocket	Rails	No	3U, 3U+
D-Orbit ION	Italy	Rocket	Rails	No	3U, 3U+, 6U, 6U+, 12U, 12U+
ISIS DUO	Netherlands	Rocket	Rails	No	1U–3U, 6U
ISIS ISIPod	Netherlands	Rocket	Rails	No	1U–3U, Custom
ISIS QuadPack	Netherlands	Rocket	Rails	No	1U–3U, 6U, 12U
Jaxa J-SSOD	Japan	ISS	Rails	No	1U–3U
Nanoracks	USA	ISS	Rails	No	1U–6U (1 × 6)
PSC CSD	USA	Rocket	Rails or tabs	Yes	1U–3U, 6U
Rocket Labs Maxwell	USA	Rocket	Rails	No	3U
SFL XPOD Triple	Canada	Rocket	Rails	No	3U
SFL XPOD DUO	Canada	Rocket	Rails	No	16U
Tyvak RailPOD	USA	Rocket	Rails	No	3U, 3U+, 3UXL
Tyvak NLAS, Mk II	USA	Rocket	Rails	No	3U, 3U+, 6U, 6U+
Tyvak 12U	USA	Rocket	Rails	No	3U, 3U+, 6U, 6U+, 12U, 12U+



**Fig. 2** Nanoracks ISS CubeSat deployer.  
 Courtesy Nanoracks.

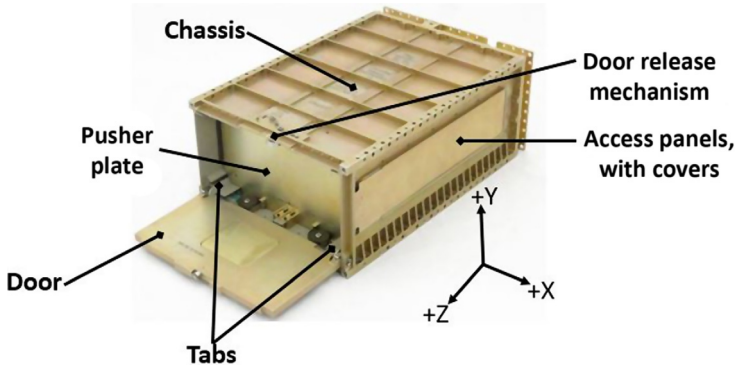


**Fig. 3** Planetary Systems Corporation Canisterized Satellite Dispenser.  
Courtesy Planetary Systems Corporation.

### 1.2.1 Deployer door

The door acts as one of the six faces, most commonly the  $+Z$  face, that fully contain the CubeSat(s) inside of the dispenser. The door in deployers acts as a constraint that prevents the spacecraft from being ejected into space prematurely. Once the deployment signal is sent to the dispenser the door latch releases, torsion spring forces open the door and allow the CubeSat to be deployed. For most deployers the CubeSat  $+Z$  face or rails make physical contact with the door.

### 1.2.2 Deployer pusher plate

The pusher plate acts as the  $-Z$  physical contact location for CubeSats. The pusher plate, as its name implies, pushes the CubeSat along the rails/tabs and out of the deployer once the door has been opened. The pusher plate movement is facilitated by the deployer spring.

### 1.2.3 Deployer springs

The deployment spring, generally a compression spring, is the ejection mechanism that is actuated when the deployer door opens. The springs extend, forcing the pusher plate and CubeSat toward the deployer door. Generally, deployers utilize a single spring per 3U cavity. The ratio of deployment spring force to mass of the CubeSat determines the deployment velocity.

### 1.2.4 Deployer chassis

The chassis of a dispenser consists of the five faces that are not the door. One important consideration for CubeSats is to consider the chassis as an isolation mechanism between the CubeSat and the remainder of the launch vehicle. Most dispensers do not permit contact between the CubeSat payload and the chassis. The deployer chassis is the primary interface and load path between the dispenser and the launch vehicle.

Deployer chassis has access panels along the  $\pm X$  faces that permit limited access to a CubeSat payload once the vehicle has been integrated into the dispenser, but before the access, covers are integrated.

### 1.2.5 *Deployment mechanism*

The deployment mechanism is the device that latches the door to the chassis. It serves to constrain the spacecraft within the deployer and allows it to exit upon command. Once the launch vehicle sends the deploy command, the mechanism actuates and releases the door.

### 1.2.6 *Rails and tabs*

The rails/tabs are the primary CubeSat to deployer mechanical interface. These features constrain the CubeSat in the X-Y plane, and certain dispensers constrain Z-axis movement as well. There are two variants: rails and tabs. The rail system utilizes the four corners of the CubeSat for constraint. The tab systems utilize the +X, -Y and -X, -Y corners to constrain the CubeSat. The deployer tab interface clamps down on the CubeSat tabs to provide an invariant load path and constrain motion in the X, Y, and Z axes.

## 2 **Launch services requirements and documentation**

Launch services have become a viable industry and serve as the intermediary between the payload developer, deployer developer, and launch vehicle developer. There are several companies that offer these services.

There is an adage for developing spacecraft that indicates that required documentation stacked up is taller than the satellite itself. While the data products required for CubeSat missions are generally much less than for larger spacecraft, there is still a considerable volume. The documents required to be provided to the launch service contractor vary considerably and are dependent upon the launch vehicle being utilized. The following list outlines the most common data products required to be provided by the developers:

- mass properties statement
- venting document
- materials list
- orbital debris assessment review (ODAR)
- transmitter survey
- frequency coordination documentation
- thermal vacuum test report
- dynamics (random vibration, sine sweep, sine load vibrate, shock, etc.) test report
- CubeSat electrical requirements report
- CubeSat mechanical requirements report
- CubeSat compliance memo
- day-in-the-life test report

## 3 Deployer characteristics

The CubeSat form factor, now 20+ years from its conception, has grown and formed an entire industry. This industry, as it relates to dispensers, has continued to innovate once the powers that be have become accustomed to the idea of a CubeSat. This innovation has created a variety of different designs from both the private and government sectors. To shed some light on what the standards and features are, it should be noted that deployer developers have followed the spirit, if not the letter of the “CubeSat standard” [1,4].

### 3.1 Deployer to CubeSat energy translation

In the process of getting a CubeSat to space, the integrated CubeSat dispenser system is mounted to a rocket. The process of getting to space and the space environment are not benign. A payload will be shaken and baked during the ascent before being dispensed from the launch vehicle. The launch services provider will provide the anticipated dynamic and thermal environments the dispenser should expect to see. Note that this is not what the CubeSat will experience, but the conditions that the dispenser will experience, most often defined at the launch vehicle to dispenser interface. Every rocket and launch profile is different and will expose the CubeSat to a different environment. The question the CubeSat developer should ask is “Now that we are manifested and have anticipated loads for the deployer, what will the satellite experience? Do the loads published in the ICD have any margin included? If so, how much?” The satellite developer should consider both the thermal and dynamic energy translation through the dispenser to verify that the CubeSat design is adequate.

#### 3.1.1 Thermal translation

When anticipated thermal values are indicated for a mission in a mission-specific ICD, they are generally indicated for the temperatures that the dispenser surface will experience with some amount of margin. Note that these are not the temperatures that the CubeSat will experience. One can think of the thermal mass and the thermal interface between the rocket and the dispenser as a filter or a thermal buffer. The thermal transportation processes in space, once above the Karman line, are limited to conduction and radiation; additionally, the CubeSat should be isolated from short-term temperature radiative effects due to the fact that they are completely encapsulated. If the launch vehicle is intended to BBQ roll, then temperatures will be further muted from the extremes.

The temperatures experienced pre- and short-term postdeployment can vary wildly. Think through the impact of deploying hot or cold, since CubeSats will not likely have an option as to where the rocket deploys the payloads. Generally, in LEO, this is determined by whether the deployment will occur while the dispenser is illuminated by the Sun or eclipsed by the Earth. Deployment mechanisms tend not to function as well if the deployment is actuated while the mechanism is cold. This will depend upon how well the materials comprising the mechanism coefficient of

thermal expansion (CTE) have been matched. Testing deployments at worst-case cold temperatures, building in sufficient deployment margin in movement mechanisms, or including temperature measurements of strategically placed thermal measurement devices in when the mechanism is deployed can buy down the risk of non- or partial deployments.

### ***3.1.2 Dynamic energy translation***

Similar to the thermal load specification, random and static loads are most often specified for the dispenser. This information is not a good indicator of what the CubeSat payload will experience. The deployer will act as an energy translator between the launch vehicle (LV) and payload. Remember that the deployer will have resonant modes as well. Also of note is that many developers have begun to include internal and/or external vibration dampeners to reduce loads applied to the payload.

Through many vibration tests the author has found that railed dispensers tend to dampen sub- 100Hz energy, amplify low-hundred Hz energy, and attenuate in the mid-hundreds to high hundreds of Hertz through low kiloHertz ranges. Keep in mind that this does not take into consideration dispenser or vehicle resonances. Also the slight gap between the CubeSat and dispenser rails permits the rail-based CubeSats to bounce around while exposed to dynamic loads. Tab-based and some rail-based dispensers clamp onto CubeSats, preloading/stiffening the payload to dispenser interface and preventing movement. This causes clamping rail systems to increase resonant mode frequencies, when compared with nonclamping systems.

## ***3.2 CubeSat deployment tip-off rates***

Once the door is opened and the CubeSat is ejected from the deployer, the payload will not come out straight and stabilized. This is due to a number of factors including spring force; LV roll rate, whether tabs or rails are used; CubeSat orientation inside of the dispenser; mass properties; and other considerations. The rule of thumb for most dispensers is that CubeSats should expect a one-sigma rotation rate of 10 degrees per second per axis. There have been several studies conducted of rotation rates in representative environments such as in [5]. This study outlines empirical rotational rates of a payload ejected from a 6U CSD.

The CubeSat developer should consider the first boot order of operations and gauge the impact of imparted dynamics including tumbling and rotation. For example, does the spacecraft have large deployables? If so the developer may want to consider whether these deployables can withstand the given rotational rates. Perhaps the rotational rates could be dampened prior to initializing deployment. If the rotational rates are not well characterized, and the spacecraft contains an attitude determination and control system (ADCS), developers should attempt to get an attitude solution and determine the rotational rates. If they are excessive, attempts should be made to dampen them prior to solar array, antenna, etc. deployments.

### 3.3 Rail and tab considerations

The rails or tabs are meant to be the sole mechanical interface between the dispenser and the CubeSat; accordingly, these areas should be considered keep-out zones. There is generally a deployer-specific exclusion area around these interfaces. The CubeSat developer should consider whether the worst-case bias inside the deployer will interfere with these contact zones.

Rails and tabs are generally required to be either anodized Al 6061-T6 or Al 7075-T7. There have been other flight-verified materials for various deployers such as certain additively manufactured materials such as Windform XT2.0 [6]. Should the developer desire to utilize a previously unqualified material, they should expect to undergo a material qualification regimen that includes the following:

- Verification of the strength of the material
- Verification of CTE and performance analyses of impact to dispenser material
- Verification of material surface roughness
- Verification of size differential pre-/postvacuum testing
- Verification of material outgassing
- Verification that the material is nonconductive

Rails and tabs of both the CubeSat and dispenser are required to be anodized. Historically, this was meant to prevent cold welding between the CubeSat and dispenser. This anodization also results in electrical isolation between the payload and deployer. These areas should be considered critical dimensions by developers. Accordingly, developers should make sure to factor in the dimensional change from anodization after fabrication in the tolerance stackup. Rails for 1U through 3Us are generally required between 100.0 and  $\pm 0.1$  mm in the X and Y planes. Should the structure be designed to 100.0 mm exactly, this requirement could quite easily exceed the requirement, especially when conforming to MIL-A-8625 [7], that generally results in a 0.025–0.05 mm of buildup per surface. Anodizing these areas will cause buildup on each rail, causing twice the effect for any given axis measurement. The buildup for tabbed systems should similarly be verified. The tabbed systems generally are required to be between 2.95 and 3.05 mm, so designing the tabs to be exactly 3.00 mm would almost certainly exceed the requirement, depending upon the machining tolerances.

As the deployer door is opened, the CubeSat will slide along the dispenser rails/tabs. Should the interface be insufficiently smooth, excessive friction between surfaces may cause undesired effects, such as greater than normal rotational rates, slow, or even failed deployments. Rail and tab average surface roughness (Ra) is most often specified as  $\leq 1.2 \mu\text{m}$  postanodization [8]. Another related consideration, generally for unconstrained systems, is that when CubeSats are dynamically tested (random vibrate, sine load vibrate, etc.), developers should expect some wear on the rails. This wear creates small amounts both flaking of the anodization and metal shavings/powder and is most prolific for the rail corners and Z faces. Beyond the hazards of this FOD, the rails may be deformed. Careful sizing and tolerances of the rails may reduce the chance of this occurring.

## 4 CubeSat to deployer testing

CubeSat payloads are expected to undergo a testing regimen that is somewhat variable based upon the launch vehicle. The specific tests outlined in Fig. 4 are common across virtually all missions as they pertain to deployers [7]. Assuming no waivers are required against the CubeSat to dispenser ICD, few other tests are required, again dependent upon mission, to confirm compatibility with the dispenser to be used for the mission.

### 4.1 *CubeSat to deployer fit check and CubeSat acceptance checklist*

The tests that fall under fit check and CubeSat Acceptance Checklist (CAC) cover mechanical measurements such as payload envelope, mass, switch and separation location and functionality, rail size and keep outs, and protrusion envelope. This is something that should be measured early and often with calibrated measurement devices if possible. If calibrated tools are unobtainable, developers should attempt to make the same measurements with multiple sets of measurement devices. The launch vehicle integrator will likely measure the payload prior to integration. If the tools utilized indicate that the payload does not conform, the CubeSat will be rejected. Strictly speaking, any changes to the vehicle at this point invalidate all CubeSat-level tests; therefore the payload may be required to reperform vibration and thermal vacuum tests. The mission-specific ICD will contain the dispenser/launch vehicle restrictions. As is often the case in the CubeSat world, an ICD is not in place until late in the vehicle development flow. If this is the case, developers need to make sure to obtain the dispenser-specific requirements. Alternatively, use the CACs that may be obtained at [CubeSat.org](http://CubeSat.org) until mission-specific details are provided.

Generally the launch service provider will provide a model to developers that will allow them to perform a vehicle to dispenser fit check. If possible, the team should schedule this as early as possible. If no model is provided, developers should attempt to make a simple alternative model, or be very certain of the measurements that indicate compliance. Arriving for integration activities and discover that the spacecraft does not fit will jeopardize the mission's certification of flight readiness.

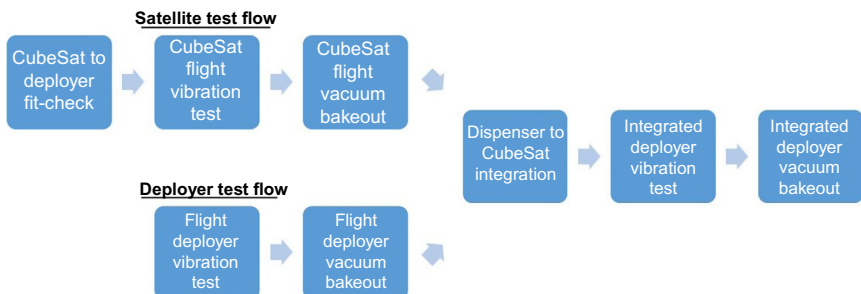


**Fig. 4** General CubeSat to deployer test regimen.



## 4.2 Dynamics testing

Dynamics testing is a rather large umbrella that incorporates a number of tests. It includes everything from low-frequency sine load tests, sine burst, characterization sine sweeps, random vibration, to shock testing. All launch vehicles require random vibration testing and sine sweeps. The loads that the dispenser are anticipated to experience during flight will determine whether a requirement will be levied for the other tests. Tests such as acoustic testing and centrifuge or sine burst static load tests are generally not levied due to the fact that CubeSats are so small.

Most missions will require a standalone CubeSat vibration test of the flight unit, prior to integration into the dispenser. The payload will be required to test the unit to the levels indicated in the mission-specific dispenser to CubeSat ICD. Remember, as is indicated in [Section 3.1.2](#), the levels define the levels for the dispenser to launch vehicle interface and have no bearing upon the payload. The payload may experience more or less energy than the levels experienced by the dispenser, depending upon the design of the payload. CubeSat developers should expect a second and generally lower-level test to be performed once the CubeSat has been integrated into the dispenser.

Test fixtures for dynamics testing are very important. Generally the launch service provider or deployer dispenser will have a dynamic testing system, most often called a TestPOD. In the event that no test fixture is provided, it will be the responsibility of the payload developer to design and fabricate something or obtain a similarly designed test design from another vendor. It is important to keep in mind that all deployers are not created equal. A TestPOD from a different dispenser vendor will likely create a different ride/environment/experience for the payload and is therefore not ideal.

## 4.3 Thermal vacuum testing

Thermal vacuum tests are most often a nonpowered thermal vacuum bakeout process. In other words, they are a process of baking off volatile contaminants that are present from the vehicle assembly and testing processes. The most frequent levels are defined as maintaining a vacuum  $<1 \times 10^{-4}$  Torr and profiles of 60°C for 6h, 70°C for 4h, or 50°C for 24h [7]. Most developers tend to perform this process at the beginning of other thermal vacuum testing such as thermal cycling and thermal balance. Although somewhat rare, additional thermal vacuum tests are levied on the CubeSat by the dispenser ICD. [Fig. 5](#) shows common thermal vacuum bakeout temperature profiles.

## 5 Additional CubeSat design considerations

Satellites are designed to fly in space; however, if developers do not consider the deployer requirements and focus only on those associated with the satellite, the design might not be viable for a specific deployer/launch vehicle or effectively achieve orbit. Experienced satellite developers know that they need to design certain features into their spacecraft such that it may be tested and assembled. Similarly, CubeSat designs

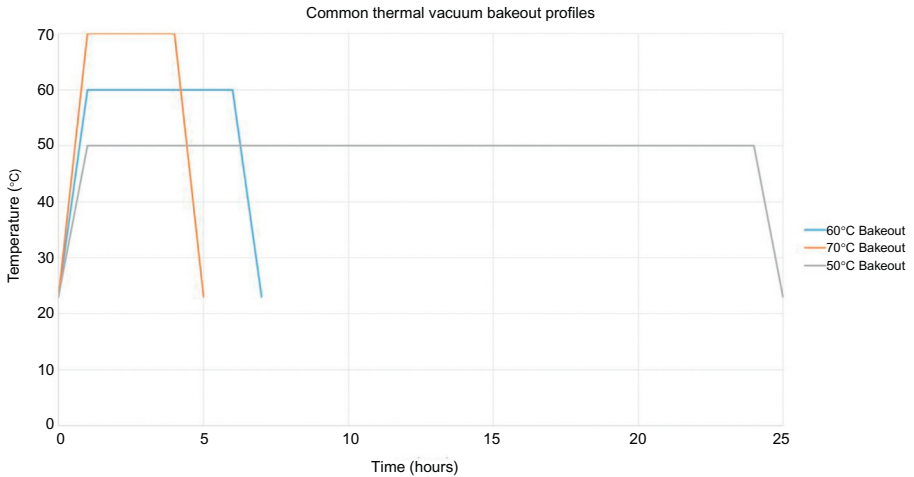


**Fig. 5** Common thermal vacuum bakeout temperature profiles.

should be tailored to the dispenser in which they intend to fly, considering the following elements:

- center of mass/mass properties
- mechanical envelope
- electrical interfaces
- separation springs
- inhibit switches
- remove/insert before flight article locations
- CubeSat to dispenser integration
- CubeSat postintegration and prelaunch delays
- CubeSat venting
- CubeSat initial contact and LEOP concept of operations

## 5.1 Center of mass

Beyond keeping track of the center of mass (CM) for attitude determination and control purposes, the launch service team will need to know where it is located. The premise for launching CubeSats for most launch vehicles is the concept of replacing ballast mass with payload mass and generating additional revenue. The ballast is placed in a manner that corrects the launch vehicle center of mass; therefore the launch vehicle will need to know where the combined CubeSat/dispenser center of mass is located. Since the payload mass is generally equal to the mass of the dispenser, the CubeSat CM factors quite heavily into where the *system* (CubeSat + Dispenser) center of mass is located. The center of mass requirement varies per dispenser, but the boiler plate requirement is between 6.5 [1] and 10 mm [4] of the CubeSat geometric center. Modern-day dispenser requirements can accommodate center of masses of  $\geq$  +/- 20 mm [1,4].

It is incredibly difficult to correct the center of mass with the limited mass and volume inherent to CubeSats. While designing the spacecraft, developers should keep an eye on where the center of mass is located and reserve certain areas to correct X, Y, and Z centers of mass. Developers should attempt to identify which dispenser is being utilized as early in the design process as possible, and utilize the indicated center of mass reference point. Common points are the  $-X$ ,  $-Y$ , and  $-Z$  corner and X-Center,  $-Y$ ,  $-Z$  point. The rationale for the importance is that tracking multiple reference points for attitude determination and control becomes confusing and can become labor intensive to maintain multiple sets of mass properties. It is often a good idea for those maintaining the CAD model to make a box or sphere with zero mass that encompasses the allowable center of mass.

## **5.2 Mechanical envelope**

It is easy to lose track of the mechanical envelope requirements in the midst of designing a CubeSat. There are quite a few to keep in mind. It can be useful to create a max envelope within a CAD model that defines all mechanical envelope requirements. It should include details such as rail or tab maximum allowable dimensions; protrusion envelopes; inhibit switch required locations; separation switch locations; appropriate contact area with the door, pusher plate, and rails/tabs; and access panel locations. Using this in combination with the deployer CAD, if accessible, can prevent designing a satellite that will not conform to requirements. Additionally, developers should keep in mind when using unconstrained deployers that the protrusion envelope needs to be able to accommodate worst-case biasing of the CubeSat in the x and y-axes. In this case, the CubeSat will bounce around inside of the dispenser during ascent and in-orbit maneuvers of the launch vehicle. This effect should be accounted for in the CubeSat design.

## **5.3 Electrical interfaces**

The electrical interface design considerations consist of several facets. The design of many dispensers allows direct access to the CubeSat GSE charge and data ports, remove before flight (RBF), and/or insert before flight (IBF) while the CubeSat is integrated. Most deployer designs do not allow for a direct electrical connection between the CubeSat and dispenser and those that do require precise dispenser to CubeSat connector alignment.

Should the CubeSat developer desire the ability to test or verify the vehicle status once integrated into the dispenser or between axes during dynamic testing, the developer should make sure to place the charge and data ports such that align with the access panels. While performing final integration of the CubeSat into the flight dispenser, designers need to make sure to think through the process to prevent the vehicle from powering ON. One best practice is to design an RBF or IBF article that will allow for integration into the dispenser while these articles are in place, and once integration is

complete, the articles are accessible via one or more of the access panels. Also of note is the very real possibility of launch delays, which means that several months or even years could pass before launch. In situations such as this, it is common for the CubeSat to be allowed to recharge if requested after 3 or 6 months. If the charge port is not within the access port area, then no charging is possible.

#### **5.4 Separation springs**

Separation springs are fairly straight forward. Should there be multiple CubeSats within a given deployment volume, separation spring are used to create separation between the various payloads. Should there be multiple payloads within the same dispenser, one low-cost method of achieving semicontrolled separation is to use calibrated springs to achieve the relative velocity between the payloads. Also of note is the ability to overcome other payloads within the same 3U volume that either prematurely deploy before deployment or have excessively strong magnets. A sufficiently strong separation spring will prevent payloads from being struck together. Most launch service providers will analyze all permanent magnet strengths at the CubeSat external surfaces to verify that will not be stuck together upon deployment; however, CubeSats have been deployed while inadvertently coupled together in flight before. The industry standard separation spring strength is 0.9lbs (4N) [1].

#### **5.5 Inhibit switches**

Inhibit switches are mechanical switches that ensure the vehicle remains powered off while one or more are mechanically closed and while integrated into the dispenser. There are generally several requirements as to their number and location. The switches are generally the only CubeSat articles, other than the rails/tabs and separation springs, that may contact the dispenser or other payloads within the same cavity. Inhibit switches are most often required to be located on the  $-Z$  side of the vehicle and make contact with the pusher plate. Some missions allow roller switches to ride along certain portions of the X or Y faces of the deployer. Generally, two or three independent switches are required.

As has been mentioned previously, the CubeSat moves around within unconstrained deployer systems during vibration tests and during ascent. This and deployment spring movement can allow the inhibit switches to chatter or open and close quickly. CubeSat developers should design their power and computer systems to both allow for this by creating a small time lag between switch actuation and boot and by making certain that any deployment timers to reset in the event of a power on event.

#### **5.6 Vehicle to dispenser integration**

CubeSat developers should think through how their vehicle will be integrated into the dispenser. Should the CubeSat be integrated with the dispenser oriented vertically or horizontally with reference to the orientation of the door? Designers should recall that

unless the dispenser includes a spring locking mechanism, the integrator will be fighting the spring during integration. Integrating horizontally allows for easier initial integration but adds more risk to the payload in the event the integrator loses a handle while integrating. This could potentially push the payloads back out and potentially causing damage. Do the RBF articles have sufficiently low profile to remain within the protrusion envelope, or will they come into contact with the dispenser? If so, is there a way that will allow for a partial integration, ensure deployment switches are actuated before removing the RBF pin, and for the remainder of integration activities? Is there GSE to verify alignment with the dispenser cavity? The dispenser cavity is fairly tightly tolerated and it can be difficult to prevent damage while inserting the CubeSat.

### **5.7 *CubeSat postintegration, prelaunch delays***

Launch delays are very common. Once payloads are integrated into dispensers, developers generally no longer have access to their CubeSat. In the event of a post-integration delay, the CubeSat power supply should have sufficiently low parasitic current consumption that would allow for 6 months of delay and still be able to recover once deployed in space. The industry standard is to allow for spacecraft charging after this period of time; however, it is not guaranteed. This charging opportunity will only be available for those who have placed their charging port in the access panel designated locations. Another alternative is to design the power system such that if the CubeSat were to be launched with dead, it could recover by charging as the CubeSat tumbles, postdeployment. Similarly, stowed deployable mechanisms should be able to be stowed for long periods of time without permanent deformation or compromising the mechanism.

### **5.8 *CubeSat venting***

Venting is rarely a problem due to the size of a CubeSat; but it is something developers will need to address. While a payload is in transit between the launch pad and space, all nonhermetically sealed containers will experience a pressure change of 760 Torr at the launch pad to something along the lines of  $10^{-10}$  Torr in the period of a couple minutes, with the majority of it occurring in a few seconds [7]. If venting is not taken into consideration, pressure concentrations can occur in nonload-bearing structures, causing damage. The industry standards are to design the system to either (1) have an adequate ratio of empty internal volume and pathway to surface area for air to escape, or (2) to have a venting rate above some gas flow rate threshold in pressure versus time ( $\Delta P/\Delta t$ ). The open surface area to volume requirement often used is less than 2000-inch requirement, that is the ratio of empty internal volume in inches<sup>3</sup> to direct pathway surface area for the air to escape in inches<sup>2</sup> should be <2000 inches. Should the requirement be in metric units, the requirement is less than 5080 cm. The volumetric rate calculation can be found in [Chapter 13](#) of reference [2].

## 6 Conclusion

The innovation permitted by the advent of the CubeSat industry ensures an ever-changing list of dispensers that are commercially available with an ever-increasing list of features and accommodations. There are many dispensers not included in this chapter due to the requirement to limit the content. Also not included is the mapping of standards in which each dispenser can support. Some dispensers are capable of supporting a 365.9-mm Z-axis, while others are capable of supporting the more traditional 340.5 mm. Some dispensers are capable of supporting a 10.0-mm protrusion envelope and others 6.5 mm. In an attempt to keep this text relevant to the constant changing state of the art, this content has been intentionally not included. Instead, information has been provided to assist that developers, regardless of experience, will have the background and references needed to pursue the most up-to-date information for the various dispensers and their permutations.

## References

- [1] California Polytechnic State University, CubeSat Design Specification, Vol. 9, The CubeSat Program, San Luis Obispo, CA, 2014.
- [2] C.T. Crowe, D.F. Elger, J.A. Roberson, B.C. Williams, *Engineering Fluid Mechanics*, 9th ed., Wiley, Hoboken, NJ, 2008, pp. 446–447.
- [3] J. Maly, Secondary payload adapters and interfaces, in: 17th Annual Small Payload Rideshare Symposium, 10 June, 2015 Retrieved from, [https://www.sprsa.org/sites/default/files/conference-presentation/Rideshare2015\\_Secondary-Adapters\\_Tech-Committee\\_Maly-Rev0.pdf](https://www.sprsa.org/sites/default/files/conference-presentation/Rideshare2015_Secondary-Adapters_Tech-Committee_Maly-Rev0.pdf). Accessed 10 May 2019.
- [4] Planetary Systems Corporation, Canisterized Satellite Dispenser (CSD) Data Sheet (Rev. F), Planetary Systems Corporation, Silver Springs, MD, 2018.
- [5] S.K. Tullino, E.D. Swenson, J.L. Marshall Tullino, Investigative microgravity deployment tests of the canisterized satellite dispenser (CSD), in: 2018 AIAA SPACE and Astronautics Forum and Exposition, 2018 Retrieved from, <https://arc.aiaa.org/doi/abs/10.2514/6.2018-5121>. Accessed 3 March 2019.
- [6] T. Clements, G. Moore, A. Clements, S. Davis, J. White, D. Wilt, W. Holemans, J. Rexroat, N. Fite, D. Klumpp, B. Malphrus, J. Lumpp, 3D Printed Parts for CubeSats; Experiments from KySat-2 and PrintSat Using Windform XT 2.0. 2014 IAA-AAS, Retrieved from, <https://iaaweb.org/iaa/Scientific%20Activity/conf/dycoss14/IAA-AAS-DyCoSS2-14-09-10.pdf>, 2014. Accessed 10 January 2020.
- [7] NASA Launch Services Program, Program Level Dispenser and CubeSat Requirements Document (Rev. B), NASA, KSC, Florida, 2014 30 January.
- [8] T. Prejean, Nanoracks CubeSat Deployer (NRCSD) Interface Definition Document (IDD) (Rev. 1), Nanoracks, Webster, TX, 2018.

# Launch vehicle overview

23

*Pedro Luiz Kaled Da Cás*

Signal and Telecommunication Department, University of Vigo, Vigo, Spain

## 1 Introduction

One aspect that differentiates CubeSats from conventional spacecraft is the large availability of launch opportunities. This is due to both the interface standardization and containerization [1]. Since the first CubeSat launches in the early 2000s, these satellites have employed the shared payload approach [2] with more than 1000 launched during the following two decades [3]. Only recently have CubeSat clusters become the primary payloads of commercial launch vehicles thanks to the introduction of micro launch vehicles, such as Rocket Labs' Electron [2]. CubeSats have become a frequent element of low Earth orbit launches, although they still compose a small part of the total mass launched to space. Even though PSLV-C37 [4] launched 101 CubeSats, the combined mass of those satellites weighed less than its main payload CARTOSAT 2D (Fig. 1).

Despite the large number of CubeSats launched, the overall participation of nanosatellites in the space launch economy remains small: small satellites (under 500 kg) [5] represented <2%, and CubeSats <0.2% of the overall mass launched between 2013 and 2017. Regardless of that, CubeSats still form a distinctive niche with defined characteristics. The importance of micro payloads (<100 kg), of which CubeSats are the majority both in number and total launch mass, has led to the development of several micro launch vehicles, such as Electron, CZ-11, and Kuaizhou.

The advent of small commercial launch vehicles may well have a deep impact on the design of CubeSat missions, since dedicated launches will allow mission planners to have a considerably greater freedom of design. The participation and importance of micro launch vehicles is expected to increase: until 2017 <1% of all CubeSats were launched on micro launchers; between 2018 and 2019 12% [2] of all CubeSats were flown on micro launch vehicles.

The CubeSat landscape is dominated by the Planet Labs and Spire constellation launches, and this characteristic is reflected in the launch vehicles commonly used and ultimately on the mission planner's choice (Fig. 2).

The rest of this chapter is organized as follows. First the technical characteristics and history of the main launchers employed by CubeSats are presented, grouping them into families of launch vehicles. Then the most important points to be considered when selecting a launch vehicle for a CubeSat mission are discussed.

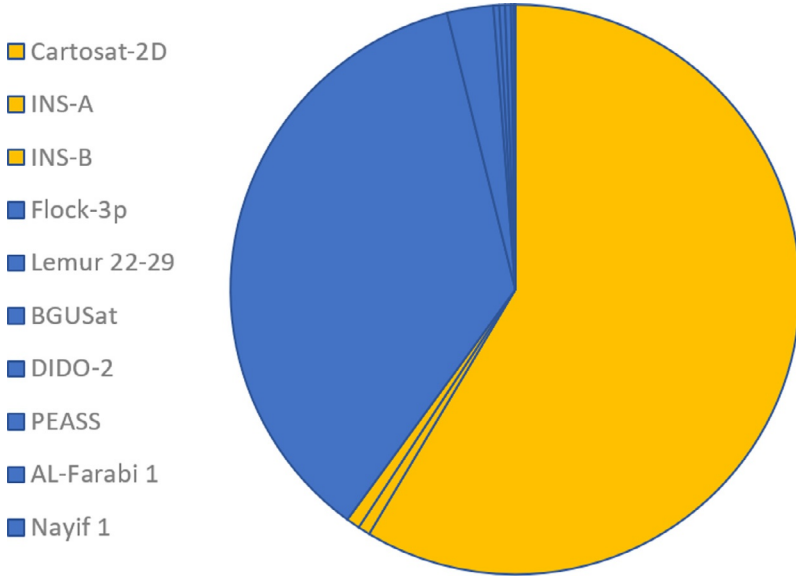


**Fig. 1** PSLV-XL C37 Launch Manifest mass distribution. CubeSats’ mass is shown in *blue* (*dark gray* in print version), and conventional satellite’s is shown in *yellow* (*light gray* in print version).

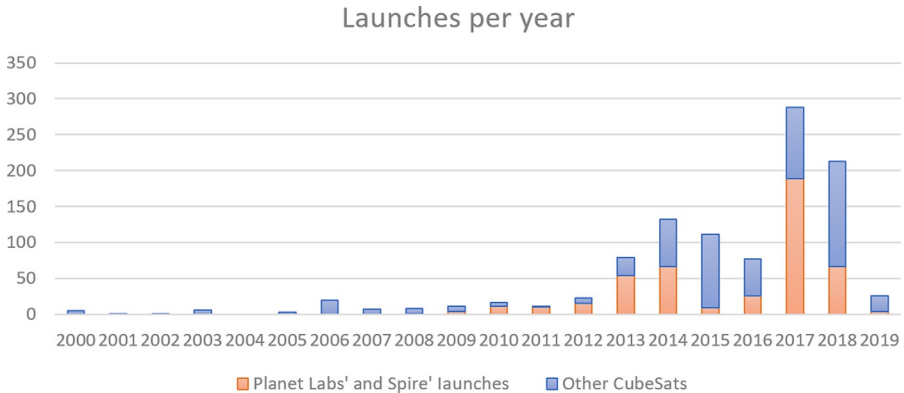


**Fig. 2** Historical launchers of CubeSats from 2000 to March 2019.

## 2 Launch vehicle families

Launch vehicles normally belong to large families as their designers seek to provide optimized performance for several different payload scales, capacities and achievable orbits. Some liberties were taken when considering the families. For example, Minotaur and Antares were consolidated as a single family as they are both manufactured and



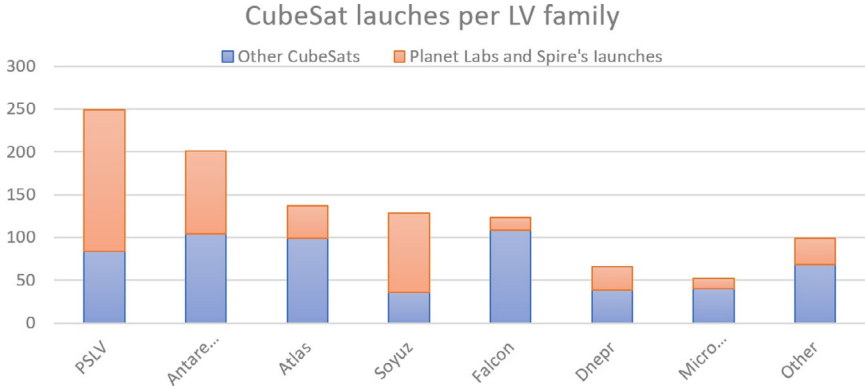


**Fig. 3** Most frequently used launch vehicles for CubeSats from 2000 to 03/2019.

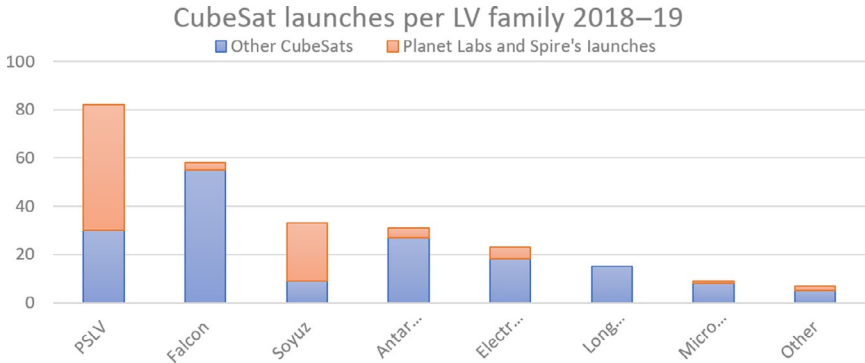


**Fig. 4** Most frequently used launch vehicles for CubeSats from 2018 to 03/2019.

marketed by Northrop Grumman. The typical CubeSat launcher differs from the launch vehicles used on larger satellites, and some very successful vehicles such as Ariane-5 have never launched a CubeSat. The annual number of CubeSats has grown exponentially over the two decades of the standard’s existence, and the launch vehicles employed by them have changed accordingly. Launchers like Soyuz that rarely transported CubeSats have become extremely relevant. Popular CubeSat carriers of the past, like Dnepr, have ceased operations. The landscape of CubeSat launches is set to change again with the consolidation and expansion of micro launch vehicles (Figs. 3 and 4).

### 2.1 Antares/Minotaur

The Antares/Minotaur launch vehicle family combines the launches by Orbital ATK’s (currently Northrop Grumman) Minotaur, Taurus, and Antares rockets. The original vehicles Minotaur, Taurus, and Pegasus were all solid propellant stacks with motors developed by Thiokol and Alliant Techsystems [6]. Following a series of corporate mergers and acquisitions, Northrop Grumman consolidated control over the major subsystems of those vehicles.

**Table 1** Antares 2 information.

<b>Antares</b>	<b>Propellant</b>	<b>Engine/ motor</b>	<b>Thrust</b>	<b>Max G long.</b>	<b>Max G lateral</b>
First stage	LOX/RP1	RD-180	1.92 MN	−1.0, +8.0	±1.5
Second stage	Composite	Castor XL	557 kN		
Payload to ISS orbit	6000–6500 kg (Cygnus capsule)				
Payload at 600 km SSO	3600 kg				
Commercial authority	Northrop Grumman				
Primary launch broker	NanoRacks				
Launch cost [10]	80–85 million USD, 12,880–12,900 USD/kg				
Principal launch site	Wallops Flight Facility				
Most notable flight for CubeSats	CRS Orb-2 08/13/2013, 32 CubeSats launched to ISS				
Greatest strength for mission planner	Frequent low-inclination low-altitude opportunities for CubeSats, direct deployment of release from the ISS				

The Antares/Minotaur family is the second most common launcher for CubeSats (second only to the PSLV family). This is mainly due to NanoRacks' ISS CubeSat Deployment and External Cygnus Deployment with 106 CubeSats deployed from ISS [7] and 30 deployed directly by the Cygnus capsule, which has typically employed Orbital ATK's launchers [7].

Minotaur-C is currently operational with a payload of 1590 kg to low Earth orbit [7]. It operates from four launch centers: US Air Force Western Range (WR) and Eastern Range (ER), NASA's Wallops Flight Facility (WFF), Pacific Spaceport Complex-Alaska (PSCA), and Reagan Test Site (RTS). Because of its many launch sites, Minotaur-C is capable of both polar orbits and low-inclination orbits (28.5 degrees), although commercial launches are only performed from WFF [8]. However, it is unlikely that lower inclinations are available to nongovernmental CubeSat launches as WFF does not serve this type of orbit. The Antares launch vehicle was developed to launch the Cygnus Spacecraft to the International Space Station under the COTS and CRS programs, although it can launch other dedicated satellites or CubeSat clusters. The Cygnus/ISS project has proven to be a reliable and consistent alternative for low-inclination and low-altitude CubeSat launches. Antares only launches from WFF.

Antares' first stage was developed by KB Yuzhnoye and is equipped with a RD-181 produced by NPO Energomash. Antares second stage was developed by Orbital ATK based on the Solid Rocket Motor CASTOR 30XL [9] (Table 1).

## 2.2 Dnepr

The Dnepr is a launch vehicle derived from the repurposing of 150 soviet R-36 ICMBs to serve as space launch platforms. The repurposing and later commercial exploitation of the missiles were tasked to ISC Kosmotras, which still runs the program [11]. Dnepr performed 22 space launches with a unique failure on July 26, 2006, causing the loss

**Table 2** Dnepr information.

Dnepr	Propellant	Engine	Thrust	Max G long.	Max G lateral
First stage	UDMH/NTO	RD-264	4.52 MN	7.5 ± 0.5	±0.8
Second stage	UDMH/NTO	RD-0255	755 kN	7.8 ± 0.5	0.5 ± 0.5
Third stage	UDMH/NTO	RD-864	20.2 kN	-0.3	0.25
Payload to ISS orbit	3000 kg				
Payload to 98° polar at 600 km	1200 kg				
Commercial authority	ISC Kosmotras				
Primary launch broker	Multiple launch brokers				
Principal launch site	Baikonur				
Launch cost [10]	29 million USD, 9063.00 USD/kg				
Most notable flight for CubeSats	19th flight 37 satellites deployed from 26 different organizations				
Greatest strength for mission planner	Talent on planning and managing large and diverse cluster launches				

of 14 CubeSats. Following tensions between the Russian and Ukrainian governments, no Dnepr launch has occurred since 2015.

Kosmotras ISC has shown an exceptional talent for organizing complex and diverse nanosatellite launches, with Dnepr’s 19th launch holding the title of most satellites in a single launch until 2017 when PSLV’s C37 launch surpassed it. Despite the impressive number of 37 satellites launched simultaneously, the most impressive figure of this launch was the participation of 26 independent satellite operators ranging from universities to national space agencies [7] (Table 2).

### 2.3 PSLV

The Polar Satellite Launch Vehicle (PSLV) is the Indian Space Agency’s main low Earth orbit launcher. PSLV was initially developed to support the Indian remote sensing satellite program. PSLV has performed 48 missions [6, 12] with two failures and has performed launches ranging from low Earth orbit to geostationary and lunar orbits.

The PSLV stage configuration is composed of both solid and liquid propellant stages: with the first stage PS1 composed of an S139 and six to nine S12 strap on boosters, the second stage PS2 powered by the hypergolic engine Vikas, the third stage PS3 with solid propellant motor, and the fourth stage PS4 equipped with a pressured-fed hypergolic engine [6].

PSLV currently holds the record for the most satellites launched on a single mission with launch C37 having carried 104 spacecraft of which 101 were CubeSats [4]. PSLV CubeSat payloads are primarily brokered by ISIS [7]. PSLV has currently only performed commercially Sun-synchronous launches for CubeSats with altitudes ranging from 485 to 780 km [2] (Table 3).

**Table 3** PSLV-XL information.

PSLV-XL	Propellant	Engine	Thrust	Max G long.	Max G lateral
Boosters	Composite	6 × S12	6 × 719 kN	5 ± 1	±0.5
First stage	Composite	S138	4.84 MN	5 ± 1	±0.5
Second stage	UH25/NTO	Vilkas	803 kN	4.5 ± 0.2	±0.6
Third stage	Composite	P37.5	240 kN	6.2 ± 0.2	±0.5
Fourth stage	MMH/MON-3	2 × L-2-5	14.6 kN	1 ± 0.2	±0.5
Payload to ISS orbit	5950 kg				
Payload to 600-km SSO	4550 kg				
Commercial authority	Antrix				
Primary launch broker	ISIS				
Principal launch site					
Launch cost [10]	21–31 million USD, 6642.00–9538.00 USD/kg				
Most notable flight for CubeSats	C37 holds the record for largest number of satellites deployed on single launch 104 (101 were CubeSats)				
Greatest strength for mission planner	Low launch cost and frequent access to higher polar orbits for CubeSats				

## 2.4 Soyuz-2

Soyuz-2 and its variants are the current version of the oldest launch vehicle family in history, dating back to Sputnik's launch in 1957. The Soyuz rocket is the most utilized launch vehicle in history, with more than 1700 launches [6]. Historically, Soyuz has launched very few CubeSats, having launched only 18 spacecraft until June 2017. From then on, this changed, and Soyuz has since launched 108 CubeSats on four different missions [7].

Soyuz's main booster is composed of three stages: the first stage, the boosters, is powered by four RD-107A engines; the second stage is powered by a single RD-108A; and the third stage by one RD-0124 [13]. Soyuz also employs the Fregat-M upper stage for launches that need to achieve higher altitudes [14].

CubeSat launches of Soyuz are currently mostly brokered by EXOLaunch and ISIS [7]. Soyuz usually launches CubeSats to high-inclination orbits. Soyuz launches from Baikonur, Plesetsk, Kourou, and Vostochny [13, 14], although CubeSats have never been launched from Kourou (Table 4).

## 2.5 Falcon 9

Falcon 9 is SpaceX's main launch vehicle for geostationary, low Earth orbit, and ISS resupply. Falcon 9 and Falcon Heavy are currently the only partially reusable launch systems in operation. SpaceX successfully lowered the space launch cost by at least two-thirds [10] and is currently developing an interplanetary super heavy launch system and a manned capsule to service the ISS. In 2019 SpaceX announced the first structured rideshare program to allow booking of secondary payloads independently

**Table 4** Soyuz-2-1a information.

Soyuz-2-1a	Propellant	Engine	Thrust	Max G long.	Max G lateral
First stage (boosters)	RP1/LOX	RD-107A	4 × 838.5 kN	4.3 ± 0.7	±1.8
Second stage	RP1/LOX	RD-108A	792.5 kN	2.6 ± 1.2	±0.8
Third stage	RP1/LOX	RD-0124	297.9 kN	2.2 ± 1.5	±0.3
Fourth stage (Fregat)	UDMH/NTO	S5.92	19.6 kN	N/A	N/A
Payload to ISS orbit	5950 kg				
Payload to 98° polar at 600 km	4550 kg				
Commercial authority	Starsem (Soyuz-2-1a)				
Primary launch broker	EXOLaunch				
Principal launch site	Baikonur				
Launch cost [10]	80 million USD, 16,495.00 USD/kg				
Most notable flight for CubeSats	67 CubeSats launched on 07/14/2017				
Greatest strength for mission planner	Possible customized deployment of CubeSat constellations due to Fregat high maneuver capacity				

from the primary; the program also allows for rescheduling of a launch without cost in the event of mission delay [15].

Falcon 9 utilizes RP-1 and liquid oxygen on all its stages. The first stage is equipped with nine Merlin 1D engines, and the second stage is equipped with a single MVac, the Vacuum variant of the Merlin engine [10]. The current version launcher's first stage is also equipped with fast reusability systems: landing legs, titanium grid fins, and nonpyrotechnical actuators.

Falcon 9 operates from Cape Canaveral Air Force Station, Kennedy Space Center, and Vandenberg Air Force Base. SpaceX is currently building a private launch center in Texas. Falcon 9 has launched CubeSats to orbits ranging in inclination from 34.5 to 98 degrees and on altitudes from 245 to 580 km [6]. Falcon 9 CubeSat launches are brokered by several companies: Spaceflight, Tyvak, NanoRacks, and ISIS (Table 5).

## 2.6 Atlas V

Atlas V is the current version of one of the oldest American launch vehicle families with the first launch having occurred in 1959 [6]. Atlas V is manufactured and operated by United Launch Alliance and together with Delta IV handles most US military space launches as part of the National Security Space Launch (NSSL), formerly Evolved, Expendible Launch Vehicle (EELV) [18]. Atlas V has also launched many American interplanetary missions including the only interplanetary CubeSats, MarCO A and B [2].

Atlas V is a two-stage launch vehicle composed of the Common Core Booster (CCB) as its first stage and a Centaur upper stage as its second. CCB is powered

**Table 5** Falcon 9 information.

<b>Falcon 9 Block 5</b>	<b>Propellant</b>	<b>Engine</b>	<b>Thrust</b>	<b>Max G long.</b>	<b>Max G lateral</b>
First stage	RP1/LOX	Merlin-1D	9 × 854 kN	6 (8.5 <sup>a</sup> )	2 (3 <sup>a</sup> )
Second stage	RP1/LOX	MVac	981 kN		
Payload to ISS orbit	8700 kg <sup>b</sup>				
Payload to 98° polar at 600 km	7500 kg <sup>b</sup>				
Commercial authority	SpaceX				
Primary launch broker	Multiple launch brokers				
Principal launch site	Kennedy Space Center				
Launch cost [4]	60.1 million USD, 2864.00 USD/kg				
Most notable flight for CubeSats	Spaceflight SSO-A Sherpa Launch				
Greatest strength for mission planner	Cheapest launcher per kilogram, wide range of inclinations, and SmallSat program could allow better constellation deployments				

<sup>a</sup> Lateral and longitudinal loading for payloads of less than 1814 kg.

<sup>b</sup> Falcon's payload performance is no longer publicly available [16]; the figures presented are from Falcon 9 v1.0 [17].

by a single RD-180 dual-chamber liquid propellant engine [19]. The Centaur is powered by a RL-10 cryogenic engine [19]. Atlas V's performance can be augmented by several configurations of strap-on boosters: from parallel CCB on the HLV variant to solid rocket motors on the 400 and 600 series [19].

Atlas V launchers from both Vandenberg AFB (WR) and Cape Canaveral AFS (ER) provide opportunities for both low-inclination (geostationary and ISS) and high-inclination launches [19]. Following 2014 Antares Accident Orbital ATK has contracted ULA to launch Cygnus. Atlas V CubeSat launches are usually brokered by Tyvak except for the three Cygnus launches, which were majorly brokered by NanoRacks [7]. Atlas V has deployed CubeSats on both ISS and polar orbits on altitudes ranging from 400 km to interplanetary [7] (Table 6).

## 2.7 Micro satellite launchers

Although micro satellite launchers have been in operation since 2006, with the M-5's maiden flight, until recently, none of those vehicles had operated constantly, having performed only proof-of-concept flights or tests. This changed in 2017 with frequent launches of Long March 11, KZ-1A, Epsilon, Electron, and SS-520. From 2018 to 2019, Electron became the fifth most used launcher for CubeSats, and overall micro launchers contributed 12% of the total CubeSat launched on the period [2]. The popularization of micro launchers has opened an unprecedented opportunity for CubeSat mission planners allowing them to design systems where their spacecraft are the primary payloads and where CubeSat orbits can be designed without the burden imposed by ridesharing.

**Table 6** Atlas V-401 information.

<b>Atlas V-401</b>	<b>Propellant</b>	<b>Engine</b>	<b>Thrust</b>	<b>Max G long.</b>	<b>Max G lateral</b>
First stage	RP1/LOX	Merlin-1D	3.82 MN	5	2
Second stage	RP1/LOX	RL-10-A	99.2 kN		
Payload to 28.5° at 600 km	9224 kg				
Payload to SSO polar at 600 km	7434 kg				
Commercial authority	ULA				
Primary launch broker	Tyvak				
Principal launch site	Eastern Range and Vandenberg				
Launch cost [4]	131–179 million USD, 9514.00–12,903.00 USD/kg				
Most notable flight for CubeSats	MarCO A and B, the first interplanetary CubeSats				
Greatest strength for mission planner	Strong utilization by US governmental launches				

**Table 7** Micro launch vehicle launches in 2017–19.

<b>Micro launchers</b>	<b>Launches</b>	<b>Fails</b>	<b>Note</b>
Electron	8	1	Private enterprise, has transported CubeSats
CZ-11	5	0	Chinese, has transported CubeSats
OS-M1	1	1	Chinese Private Enterprise, has transported CubeSats
SS-520	2	1	Has transported CubeSats
Epsilon	2	0	Has transported CubeSats
LandSpace-1	1	1	Chinese Private Enterprise
KZ-1A	5	0	Chinese Private Enterprise
Hyperbola-1	1	0	Chinese Private Enterprise
Jielong-1	1	0	Chinese Private Enterprise

From 2018 to 2019, five different micro launch vehicles transported CubeSats: Electron, OS-M1, Long March 11, Epsilon, and SS-520. Although one SS-520 and one OS-M1 launches failed, the micro launcher trend is persisting (Table 7).

Between 2017 and 2019, nine micro launch vehicles have operated—six of them being Chinese, two Japanese, and one from New Zealand. Six of the nine micro launch vehicles were developed or are operated by private companies. Yet, it is worth noticing that some of the companies are spin-offs of public entities such as China Rocket (Jielong-1's operator), which is a subsidiary of the China Academy of Launch Vehicle Technology (CALT).

The recent increase of commercially available micro launch vehicles opens opportunities for the CubeSat mission planner allowing for freedom both of schedule and orbital design. The micro satellite launchers' payloads vary from the 4 kg on SS-520

**Table 8** Electron information.

Electron	Propellant	Engine	Thrust	Max G long.	Max G lateral
First stage (boosters)	RP1/LOX	Rutherford	$9 \times 16 \text{ kN}$	$\pm 6$	$\pm 0.7$
Second stage	RP1/LOX	Rutherford Vac	22.1 kN		
Third stage (optional)	Monopropellant <sup>a</sup>	Currie	120 N		
Payload to SSO polar at 600 km	142 kg				
Commercial authority	Rocket Labs				
Primary launch broker	Rocket Labs				
Principal launch site	Rocket Lab Launch Complex 1				
Launch cost [4]	4.9 million USD, 32,667 USD/kg				
Most notable flight for CubeSats	14 CubeSats successfully launched by a commercial micro satellite launcher				
Greatest strength for mission planner	Small CubeSat constellation could be deployed as main payload on predesigned orbit				

<sup>a</sup> Green monopropellant.

to 500 kg on Epsilon (500-km SSO). The available range of payloads allow for single CubeSat deployments, although economically ineffective, to consistent cluster launching and constellation building (Table 8).

### 3 Launch vehicle selection: Alternative solutions

Launch vehicle selection is an often overlooked concern on CubeSat missions, mainly due to containerization and lack of influence on the launch provider. In a traditional piggyback launch, CubeSat operators can neither choose nor influence the final orbit, and they are released on the same orbit as the main payload. An exception is represented by launchers with maneuvering final stages, but even in this case, CubeSats do not have control over the destination orbit, since the final-stage maneuvers are performed to protect the main payload. Several missions cannot be launched as piggyback launches, since the typically available orbits (Sun-synchronous orbits and those obtained with the launches from the ISS) do not match the ones needed to accomplish the mission goals. Examples of this are highly elliptical orbits for radiation belt studies, equatorial orbits for high availability communications, and halo orbits for astronomy, among others.

In the case of CubeSat missions, the only alternative usually available for the mission planner is to adapt the mission design to the available launch opportunities or to wait until a bigger mission is scheduled for launch on the same desired orbit. There are several cases of CubeSat missions that have learned to adapt to the available launch opportunities: Planets Labs' agile aerospace method recommends launching as often as possible and on as many launchers as possible [20] to avoid single point failures on



constellation building. Other missions, like Lunar IceCube [21], are completely dependent on NASA's SLS program schedule.

The primary concerns related to launch vehicle selection for CubeSat missions are the availability of the intended orbit, the frequency of launches, and the types of CubeSat deployers that serve the chosen launch vehicle. When it comes to building a constellation, the situation becomes more challenging, because the mission planner must secure not only a single adequate opportunity but also a constant stream of launches.

As seen in the previous section, a recent trend is that of micro launch vehicles, such as Electron and CZ-11. The smaller capacities of micro launch vehicles allow for cluster launches to be easily organized, since a smaller number of CubeSats are required to fully occupy the launch vehicle. Another advantage of micro launch vehicles is the possibility of reaching tailored orbits: a CubeSat customer can contract the entire payload capacity selecting a specific orbit, something previously impossible for CubeSats [22]. This freedom of design allows for great improvements, especially on CubeSat communication constellations [23].

SpaceX's SmallSat and other similar programs under development might also improve the available options for CubeSat launches, in particular for constellation building. Nevertheless, they are less disruptive than micro launchers for the users, since they are still limited to the orbital destinations provided by SpaceX. The SmallSat program provides launches for 150- and 300-kg payloads to be contracted independently of the primary payload [15]. It will give more flexibility since the first scheduling and possible postponement of the main payload will not affect the secondary one and vice versa. The 150-kg payload can also accommodate a small satellite equipped with CubeSat deployers, similarly to GAUSS's UniSat solution [24]. Finally, it is also possible to design a powered space tug to be launched on a SmallSat slot and then perform maneuvers to correctly deploy a constellation of CubeSats on a tailored arrangement [25].

The selection of an available launcher for a CubeSat mission is a complex process. The major drivers and decision points are summarized in the flowchart in Fig. 5. The first point to be considered when selecting a launcher is the desired orbit. As previously stated, there are numerous opportunities for low Earth orbit launches but frequent interplanetary launch opportunities do not yet exist. The alternatives for interplanetary CubeSat missions are either redesigning the mission or waiting for a larger interplanetary mission to piggyback on. One redesign alternative is to fly LEO Proxy missions where not all scientific objectives are met, but the research can move forward. Lunar missions still have the alternative to launch to geostationary transfer orbit (GTO), raise the orbit, and be captured by the Moon; nevertheless, this requires either high  $\Delta V$  from onboard propulsion systems or advanced low- $\Delta V$  trajectories, described in Chapter 1. If no redesign is possible or desirable, the remaining alternative is to wait for an interplanetary mission.

CubeSat missions that require orbits different from the typical ISS or polar orbits have very few launch alternatives at their disposal, nowadays. The situation for these missions is similar to the one experienced by the interplanetary CubeSats. Fortunately, for LEO CubeSats, there is the possibility of launching on a micro launch vehicle. The most frequently launched micro rockets are Electron, CZ-11, and KZ-1A.

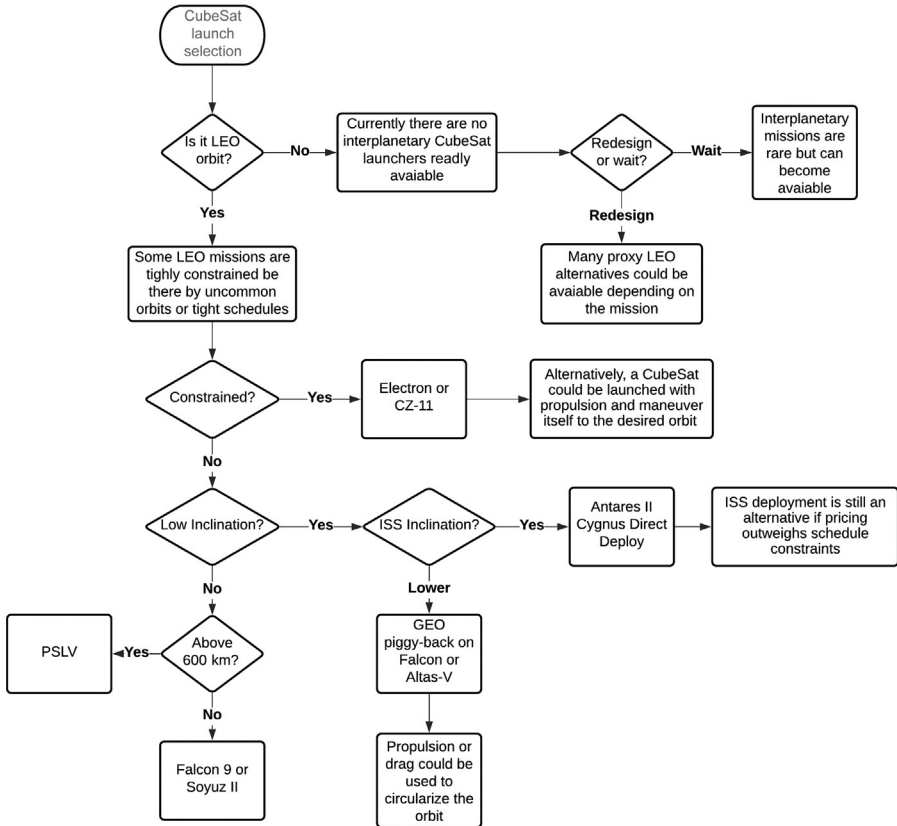


Fig. 5 Flowchart of CubeSat launch vehicle selection.

This alternative is expensive and may not be available to most missions. The SS-520 launcher can deliver a single CubeSat to LEO and might be a viable opportunity for constrained missions; notwithstanding the SS-520 is not planned for serialized production.

If the mission is not constrained by tight schedules or unconventional orbits, more alternatives are possible. Low-inclination missions can be launched from the ISS, but the on-station storage time might be an issue to be considered. The recommended alternative is Cygnus’ direct deployment where the payload is inserted into a near ISS orbit without the storage period. ISS deployment is still interesting, especially to educationally oriented missions since it adds the bonus of interacting with the astronauts and the station itself. ISS launches are described in details in Chapter 24.

There are very few alternatives for rides to low-inclination or equatorial orbits. CubeSat missions requiring these kinds of orbits might have only two options: micro launch vehicles or orbital maneuvers. However, no micro launchers are currently operated from equatorial launch sites and consequently will need to perform highly energetic maneuvers to change the orbital inclination. Henceforth the only remaining

option for a CubeSat to reach equatorial LEO might be to launch to GTO and reduce the orbital apogee to reach LEO. Both passive [26] and active [27] alternatives have been proposed, but these alternatives' have never been tried and would add considerable risk to a mission. Both Atlas V and Falcon 9, however, have frequent opportunities for GTO CubeSat launches.

If the mission targets a polar orbit or Sun-synchronous orbit, it has numerous available alternatives, nowadays. For higher altitudes, PSLV is the recommended launcher for both launch frequency and pricing. For lower-altitude SSO orbits (below 600 km), the recommended vehicles are Soyuz and Falcon 9 also due to the frequency of launches and pricing.

## 4 Conclusions

The CubeSat launcher market is changing rapidly, and new opportunities and challenges will no doubt appear in the future. The consolidation of smaller launch vehicles and new launch arrangements is an important factor to be considered by the mission planner. Identifying a launching strategy and a proper launcher is as important to a CubeSat mission as securing access to space or funding. The process of selecting a launcher is a multidisciplinary process and could be a major mission driver.

## References

- [1] CubeSat Design Specification Rev. 13 The CubeSat Program, Cal Poly SLO, 2014.
- [2] M. A. Swartwout, University of Saint Lois's CubeSat Database, Accessed 15 August 2019.
- [3] M. Swartwout, *Secondary spacecraft in 2016: why some succeed (and too many do not)*, in: *2016 IEEE Aerospace Conference*, IEEE, 2016, March, pp. 1–13.
- [4] Indian Space Research Organization, Publication and Public Relations ISRO Headquarters, Antariksh Bhavan, PSLV-C37 Cartosat-2 Launch Brochure.
- [5] M. Tugnoli, M. Sarret, M. Aliberti, *European Access to Space: Business and Policy Perspectives on Micro Launchers*, Springer Briefs in Applied Sciences and Technology, 2019, ISBN 978-3-319-78960-6. <https://doi.org/10.1007/978-3-319-78960-6>.
- [6] S.J. Isarowitz, J.B. Hopkins, J.P. Hopkins Jr., "International Reference Guide to Space Launch Systems". fourth ed., American Institute of Aeronautics and Astronautics, Reston, VA, 2004. <https://doi.org/10.2514/4.475917> USA.
- [7] Erik Kulu, NanoSat Database, <https://www.nanosats.eu/database>, Accessed 15 August 2019.
- [8] Minitour's User Guide Release 1.0, March 2002.
- [9] Antares User's Guide Release 3.0, August 2018.
- [10] Surplus Missile Motors, Sale Price Drives Potential Effects on DOD and Commercial Providers, United States Government Accountability Office, Washington, DC, August 2017.
- [11] Space Launch System Dnepr User's Guide, Issue 2, November 2001, Surplus Missile Motors, Sale Price Drives Potential Effects on DOD.
- [12] PSLV, User's Manual, ISRO, Issue 3, May 1996.
- [13] Soyuz User's Manual, Issue 2 Revision 0, Arianespace, March 2012.
- [14] Soyuz User's Manual, ST-GTD-SUM-01, Issue 3, Revision 0, Starsem, April 2001.

- 
- [15] SpaceX's SmallSat Program Webpage, <https://www.spacex.com/SmallSat>, Accessed 15 August 2019.
  - [16] Falcon User's Guide, January 2019.
  - [17] Falcon 9 Launch Vehicle Payload User's Guide, Rev 1, 2009.
  - [18] J.L. Buzzatto, The Transition of Space Launch—Heritage to EELV, Space, Long Beach, CA, 2003. 23–25 September 2003.
  - [19] V. Atlas, Launch Services User's Guide, March 2010.
  - [20] M. Safyan, Astronautics Smallsat launch strategy, *Room Space J.* 2 (9) (2016).
  - [21] P.E. Clark, et al., Lunar Ice Cube mission: determining lunar water dynamics with a first generation deep space CubeSat, in: 47th Lunar and Planetary Science Conference, 2016.
  - [22] Payload User's Guide, Version 4.0, December 2016.
  - [23] Nano/Microsatellite Market Forecast, ninth ed., SpaceWorks Enterprises, Inc. (SEI), 2019 Copyright 2018.
  - [24] C. Cappelletti, S. Battistini, F. Graziani, Small launch platforms for micro-satellites, *Adv. Space Res.* 62 (13) (2018) 3298–3304.
  - [25] J. Andrews, Spaceflight secondary payload system (SSPS) and SHERPA tug—a new business model for secondary and hosted payloads, in: 26th Annual AIAA/USU Conference on Small Satellites, 2012.
  - [26] C. Lücking, C. Colombo, C.R. McInnes, Mission and system design of a 3U CubeSat for passive GTO to LEO transfer, in: 63rd International Astronautical Congress, 2012.
  - [27] D.T. Schmuland, C. Carpenter, R.K. Masse, Mission applications of the MRS-142 CubeSat High-Impulse Adaptable Monopropellant Propulsion System (CHAMPS), in: 48th AISS/ASME/ASEE Joint Conference & Exhibit, 2012.

# Launch from the ISS

24

Yuichiro Nogawa<sup>a</sup> and Shigeru Imai<sup>b</sup>

<sup>a</sup>ISS Utilization and Operations Department, Japan Manned Space Systems Corporation (JAMSS), Chiyoda-ku, Tokyo, Japan, <sup>b</sup>Manned Space Systems Engineering Department, Japan Manned Space Systems Corporation (JAMSS), Chiyoda-ku, Tokyo, Japan

## 1 History

To offer more frequent opportunities and moderate environments for small satellite launches into space, a new mission concept capable of deploying small satellites using the Japanese Experiment Module (JEM) Small Satellite Orbital Deployer (J-SSOD) of the International Space Station (ISS) in low-Earth orbit (~400 km) was developed by the Japan Aerospace and Exploration Agency (JAXA).

This capability was first demonstrated by the successful deployment of five CubeSats (four 1U and one 2U satellites) from the J-SSOD on October 4, 2012. These CubeSats, containing pressurized cargo softly stowed in a bag inside an H-IIB Transfer Vehicle (HTV)-3, were launched by H-IIB rocket from the JAXA Tanegashima Space Center. After being installed onto the JEM Remote Manipulator System (JEMRMS) by the ISS crew and positioned by both crew and ground controller commands to the JEMRMS, they were successfully deployed to their planned orbit.

After this success, by 2018, more than 200 microsattellites had been deployed from the JEM using several deployment mechanisms such as the J-SSOD, NanoRacks CubeSat Deployer (NRCSD) developed by NanoRacks LLC, and CYCLOPS [or Space Station Integrated Kinetic Launcher for Orbital Payload Systems (SSIKLOPS)] developed by NASA. Launching microsattellites from the ISS became one of the major launch opportunities for CubeSat developers and users. As a result of the use of the International Space Station, potential developers of small satellites have increased their use of space station deployers, and universities, companies, and other nontraditional space users are realizing affordable access to space.

## 2 Mission overview [1]

As a new way of transferring CubeSats and other small satellites into space, small satellite deployment missions from the JEM by using a robotically manipulated launcher system were developed. Satellite developers or users can exploit this unique capability with the JEM Airlock and JEMRMS (Fig. 1).

The JEM Airlock is a unique feature that moves equipment from inside the ISS to outside space but is not used for the crew's extravehicular activity. There is a slide table in the JEM Airlock, which can be extracted both inside and outside the JPM cabin. The J-SSOD is installed on the Multipurpose Experiment Platform (MPEP)

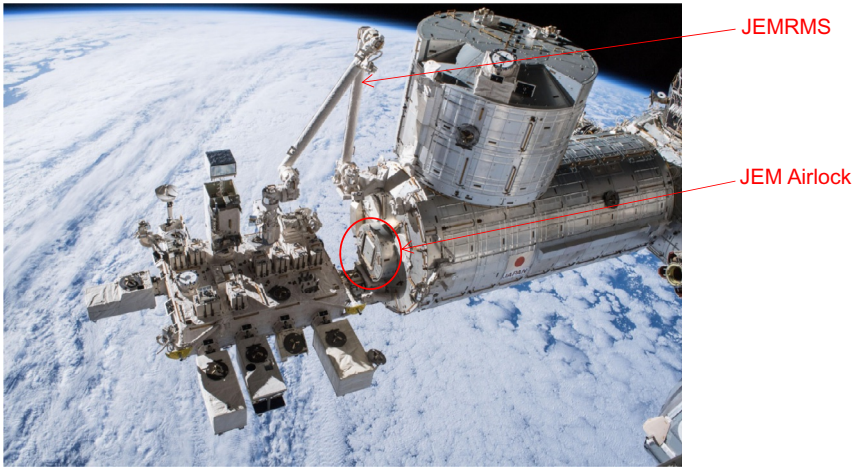


**Fig. 1** JEM outside view.

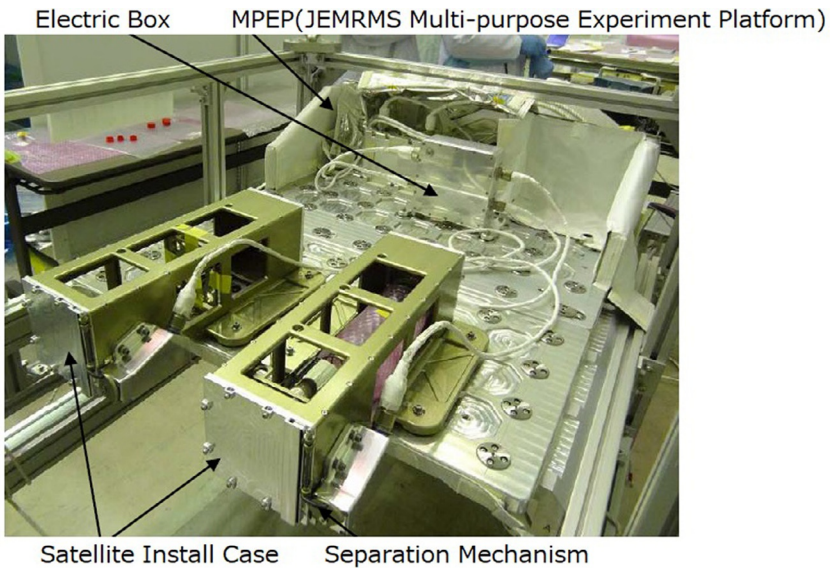


**Fig. 2** J-SSOD and MPEP.

(Fig. 2). The MPEP is a platform that acts as an interface between operations inside and outside the ISS, and the J-SSOD mechanism is installed on this platform.

J-SSOD missions are performed using the following steps as a typical scenario to deploy satellites from the JEM. A typical CubeSat deployment scenario movie can be viewed at: [http://issstream.tksc.jaxa.jp/iss2/video/jssod\\_170530.mp4](http://issstream.tksc.jaxa.jp/iss2/video/jssod_170530.mp4).

1. Satellites are installed into the Satellite Install Case as launched from Earth configuration.
2. The Satellite Install Case is packed in the ISS Cargo Transfer Bag (CTB) with a cushion, launched as a pressurized cargo, and delivered to the ISS by a resupply vehicle like an HTV or other commercial Cygnus or Dragon.
3. In the ISS, once the Satellite Install Cases with prepacked small satellites are received onboard, crew members unpack and install them onto the MPEP, which is already installed onto the JEM Airlock Slide Table, along with other equipment related to the J-SSOD mechanism as shown in [Fig. 3](#).
4. The J-SSOD on the MPEP is passed through the JEM Airlock to outside the ISS and is grappled and handled by the JEMRMS, as shown in [Fig. 4](#).
5. A JAXA robotics specialist ground flight controller team called “KIBOTT” maneuvers the JEMRMS to the appropriate deployment orientation.

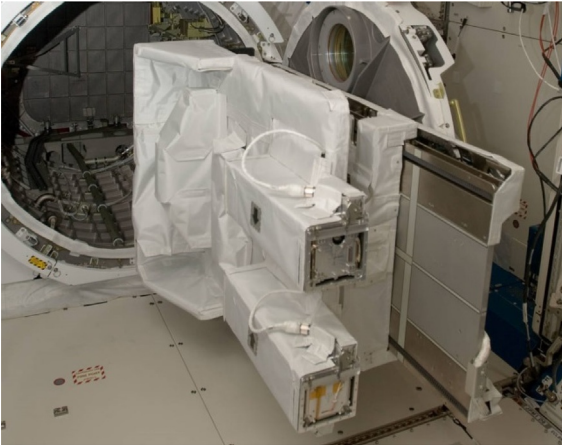


**Fig. 3** J-SSOD installation in the JEM Airlock [\[2\]](#).

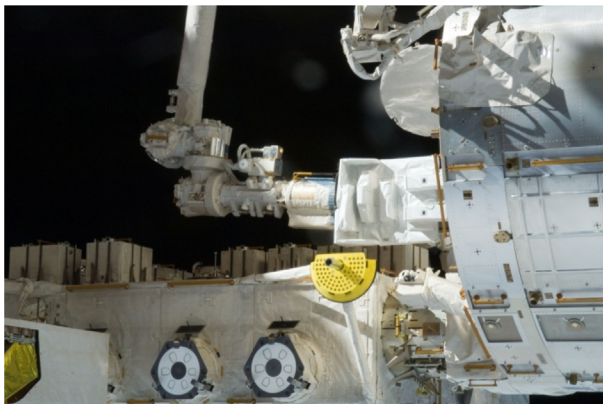


**Fig. 4** The J-SSOD is transferred to the deploy position by the JEMRMS [\[2\]](#).



**Fig. 5** Satellites are deployed into space [2].

6. The satellites are deployed from the Satellite Install Case of the J-SSOD into space using commands from the crew or ground flight controller, as shown in Fig. 5. The Space Station Remote Manipulator System and other ISS cameras may be used to support video monitoring of satellite deployment as necessary. Crew members also monitor the deployed CubeSats and take images as shown in Fig. 6.
7. The J-SSOD is returned to the airlock and stowed inside the ISS.

Deployment of CubeSats or other small satellites requires a specific JEMRMS orientation (i.e., safe deployment cone) to avoid ISS contact. Table 1 shows typical parameters of the deployment orbit [3, 4].

The J-SSOD is capable of deploying not only 1U to 3U CubeSats, but also a 50kg class microsatellite of size  $55\text{ cm} \times 55\text{ cm} \times 35\text{ cm}$ . The J-SSOD is capable of



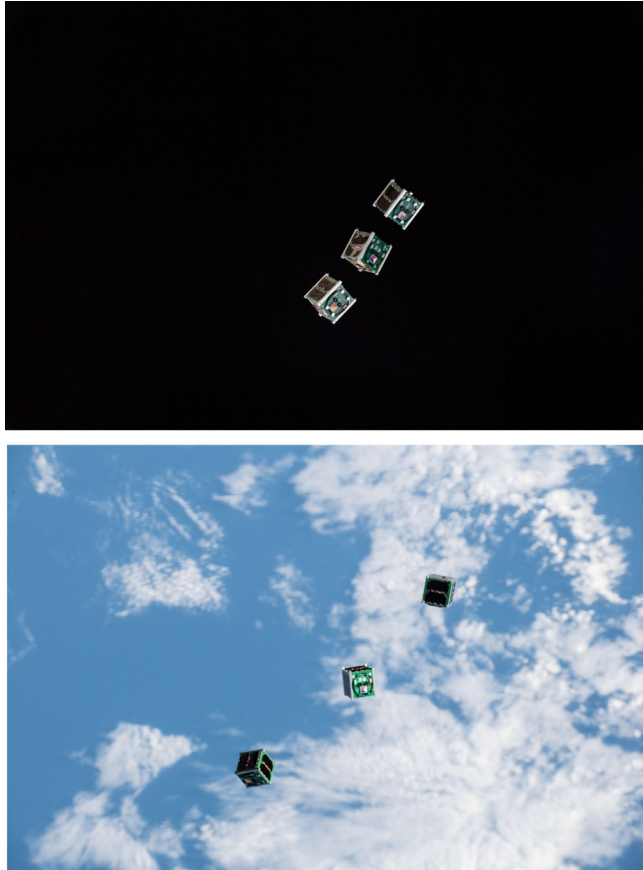


**Fig. 6** Satellites are monitored after deployment.

**Table 1** Deployment orbit parameters (typical).

Parameters	Specification
ISS orbit	1. Altitude at approx. 380–420 km (typically around 400 km) 2. Inclination at 51.6 degrees
Deployment direction	Nadir-aft, 45 degrees from the nadir with respect to the ISS Body Coordinate System
Deployment velocity	1.1–1.7 m/s for 3U satellite
Orbiting lifetime	If the ballistic number (BN) is 100, about 100–250 days depending on the deployment altitude and atmospheric conditions

deploying 12U ( $3U \times 4$ ) in its single mission. Following the J-SSOD, NRCSD, and CYCLOPS were also developed. Details of these other two launch systems will be described in [Section 4](#).

### **3 Advantage of launching from the ISS [1]**

As a result of the use of the International Space Station, potential developers of small satellites have increased their use of space station deployers, and universities, companies, and other nontraditional space users are finding affordable access to space. The major advantages of launching from the ISS using deployers like J-SSOD, NRCSD, and CYCLOPS are described in the following sections.

#### **3.1 More frequent launch opportunities**

Previously, CubeSats or small satellites of a certain class were launched by rockets as piggyback satellites only. If a rocket could launch extra weight in addition to its main satellite, piggybacked smaller satellites were given the opportunity to be placed into orbit after the main satellite was successfully deployed. In a usual piggyback launch, satellite development should be completed on time once its launch schedule is fixed. On the other hand, launch opportunities from the ISS are provided by resupply vehicles like HTV, Cygnus, or Dragon. This means that there is an opportunity to allocate vehicles less than 10 times per year; therefore increased flexibility is expected in selecting the launch vehicle by considering the satellite development schedule. Also, other options are available, e.g., choosing the best timing for the small satellite's ejection without affecting the main satellite's timing.

#### **3.2 Moderate launch environment**

All satellites must pass space environment tests to confirm that they will survive the hard launch environment in space. A vibration test that simulates vibrations experienced during launch subjects the satellite to quite a strong level of vibration. Piggyback satellites are required to pass this severe test. For launch from the ISS, since the satellites are packed in a CTB with cushions and launched in a "pressurized" cargo, the vibration environment is more moderate than a usual piggyback launch. This relaxed condition is more applicable for college students or a less costly satellite project.

#### **3.3 Checkout after launch from Earth and before deployment from the ISS**

One of the issues with piggyback satellites is that once they are launched, it is uncertain whether the satellite is still in good working order after enduring launch vibration. An additional advantage of launching from the ISS is that the satellites can be checked out by the crew in the pressurized ISS cabin to confirm their integrity with additional assessment/coordination to assure compatibility with ISS operation and safety.

## 4 Launch history and lessons learned

As of October 2018, the J-SSOD deployed 34 CubeSats and one 50kg class microsatellite, that were developed in several countries as shown in Table 2 and Fig. 7.

NRCSD development started in February 2014 and NanoRacks LLC has experienced NRCSD operations many times (Fig. 8). Recently, NanoRacks LLC has also

**Table 2** History of J-SSOD satellite deployment.

Mission #	Deployment date	Number of satellites	Satellite size
1	October 2012	5	1U × 4, 2U × 1
2	November 2013	4	1U × 3, 3U × 1
3	February 2015	1	1U × 1
4	September 2015	2	3U × 2
5	April 2016	1	50kg class × 1
6	December 2016 and January 2017	7	1U × 3, 2U × 2, 3U × 2
7	July 2017	5	1U × 5
8	May 2018	3	1U × 2, 3U × 1
9	August 2018	3	1U × 3
10	October 2018	3	1U × 1, 2U × 2

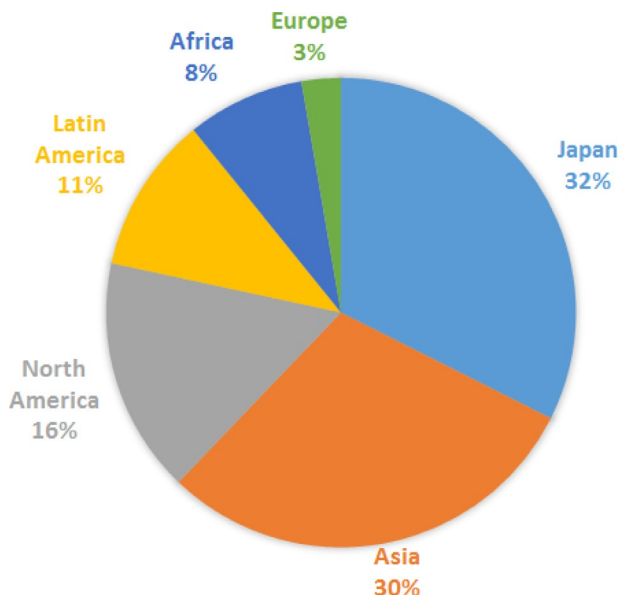


**Fig. 7** History of J-SSOD satellite deployment.

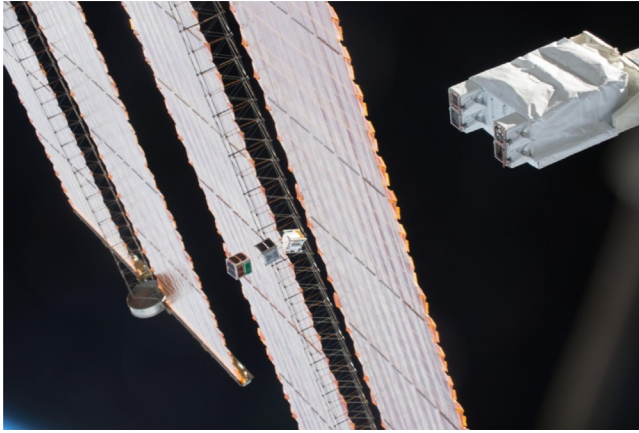


**Fig. 8** Deployment of NRCSD.



**Fig. 9** Deployment of RemoveDebris.

developed a microsat deployer called “KABER” and deployed a European satellite called “RemoveDebris” (Fig. 9) with its size approximately at  $65\text{ cm} \times 65\text{ cm} \times 72\text{ cm}$ . This is the maximum size ever deployed from the ISS through the JEM Airlock, which fully utilized the maximum capable volume of the JEM Airlock. Spinsat was successfully deployed by NASA/CYCLOPS in 2014 using both JEMRMS and Small Fine Arm (Fig. 10).

The lessons learned from these types of launches have identified key requirements that need to be met. It can be seen in Fig. 11 that the design and verification of deployable mechanisms such as antennas and rechargeable batteries are major issues from an ISS safety point of view. Especially for Li-ion rechargeable batteries, screening tests on flight cells to show their integrity are required, such as random vibration and vacuum leak tests. Also the battery circuit requires protection devices for short circuit, overcharge, and overdischarge.



**Fig. 10** Deployment of SpinSat.

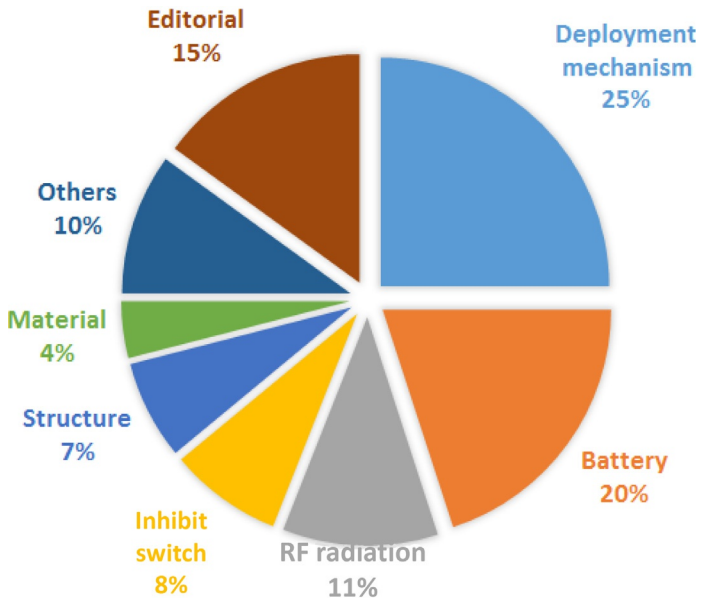


**Fig. 11** Category of typical comments at a safety review for a J-SSOD satellite.

## References

- [1] Y. Nogawa, JAMSS: IAA-CU-13, overview of satellite deployment mission from JEM to provide an opportunity for small satellite/Cubesat users, in: IAA Cubesat Conference, February 2013.
- [2] N. Fujimoto, JAXA: new capability of Kibo utilization—mission on the exposed area, December 2012. APRSAF-19.
- [3] S. Imai, JAMSS: IAA-CU-13-07-01, 1st Cubesat deployment from Japanese Experiment Module of International Space Station, in: IAA CubeSat Conference, February 2013.
- [4] JAXA, JX-ESPC-101132-C, JEM Payload Accommodation Handbook—Vol. 8—Satellite Deployment Interface Control Document, November 2018.

# Index

Note: Page numbers followed by *f* indicate figures and *t* indicate tables.

## A

Accessibility, 53

“Achieving Science with CubeSats”,  
67–68

Acquisition of signal (AOS), 349

ADCS. *See* Attitude determination and  
control system (ADCS)

Administrations and API/B publication,  
398

Advanced algorithms, 218

Advanced coprocessors, 217

Advanced Exploration Systems (AES),  
102–104

Advance publication information (API),  
401–403

Aeolus, 112

Aerogravity assist (AGA) maneuvers,  
45–46

AlamarBlue dye, 158–159

Alodine 1200, 403

Anodization, 422

Anomalies, 372–374

Antares/Minotaur, 432–434

Antennas, 229, 229–230*t*, 344, 403

AOS. *See* Acquisition of signal (AOS)

API. *See* Advance publication information  
(API)

Applications, 54–55

Arizona State University’s Lunar Polar  
Hydrogen Mapper (LunaH-Map),  
75, 75*f*

Arsecond Space Telescope Enabling  
Research in Astrophysics  
(ASTERIA), 56–57, 76, 76*f*

Artemis 1, 85, 101–102

Assembly, integration, and verification  
(AIV) activities, 404–405

Asteroid Impact and Deflection Assessment  
(AIDA), 112–113

Asteroid Probe Experiment (APEX), 111

Asteroids, interplanetary missions, 106–107

Astrobiology, 147, 148–149*t*, 156–157

Astrodynamics

approaches, 35–36

definition, 35

interplanetary missions

ballistic capture, 47–48

dynamical effects, 44

gravity assist (GA) maneuvers, 44–46

high-altitude fly-bys, 46–47

hyperbolic manifolds, 48–50, 49*f*

Interplanetary Transport Network (ITN),  
48–50

Lunar IceCube trajectory, 48*f*

resonant encounters, 46

weak stability boundaries, 47–48

perturbations, 36, 41–44

anomalies of the earth gravitational field,  
42–43

atmospheric drag, 43–44

principles and laws

classical mechanics, 36

empirical, 36

energy and orbital period, 39

Keplerian elements, 39–40, 40*f*

orbit classification, 40–41

two-body problem, 37–38

Astronomy, 56–57, 58*t*

instruments, 76–79, 76*f*, 78*f*

Atlas V, 437–438, 439*t*

Atmospheric absorption, 347

Atmospheric chemistry instruments, 69

Atmospheric drag, 43–44

Atmospheric temperature and humidity  
sounders, 70

Atomicity, consistency, isolation, and  
durability (ACID), 211–212

Atomic oxygen, 171

Attitude determination and control system  
(ADCS), 85–86, 95, 168–169, 169*f*,  
200, 421

actuators

- Attitude determination and control system  
 (ADCS) (*Continued*)  
 control momentum gyro, 268–269  
 fluid dynamic actuator, 269  
 magnetorquers, 269–270  
 reaction wheels, 268  
 spacecraft attitude, 270  
 B-dot algorithm, 277–278  
 classification, 270–274  
 atmospheric resistance and  
 aerodynamical ACS, 272  
 flywheel, 273–274  
 gravity field and gravity-gradient ACS,  
 270–271  
 magnetic field and magnetic ACS,  
 271–272  
 solar radiation pressure, 273  
 spinning and spin stabilization,  
 272–273  
 Earth sensors, 266–267  
 Global Navigation Satellite System  
 (GNSS) -based attitude knowledge,  
 267  
 gyro, 267–268  
 magnetic sensors, 265–266  
 mathematical techniques  
 Kalman filter, 276–277  
 least mean squares algorithm, 275  
 local methods, 274–275  
 spin stabilization, 278  
 star mappers/trackers, 266  
 stellar gyro, 268  
 Sun sensors, 265  
 three-axis stabilization, 278–279  
 Automation, 350, 369, 376  
 Amazon Web Service (AWS) Ground  
 Stations, 361–363
- B**
- Backup ground station, 373  
 Ballast mass, 425  
 Basic input/output system (BIOS), 240  
 Batteries, 307, 407  
 Batch algorithms, 254–255  
 B-dot algorithm, 277–278  
 Beryllium, 403  
 Biological CubeSat missions, 148–149*t*  
 BioSentinel, 158, 159*f*
- Bisat Observations of the Lunar Atmosphere  
 above Swirls (BOLAS), 111  
 Broadband infrared compact high-resolution  
 exploration spectrometer (BIRCHES),  
 72, 72*f*  
 Busek BIT-3 systems, 292, 293*f*
- C**
- Calibrated tools, 423  
 California Institute of Technology (Cal Tech),  
 101*f*  
 California Polytechnic Institute (Cal Poly),  
 353  
 Cape Canaveral AFS, 438  
 Carbon fiber-reinforced polymer (CFRP), 346  
 Cataloged objects in space, 379, 380*f*  
 CCB. *See* Common Core Booster (CCB)  
 Center of mass (CM), 425–426  
 Chariot to the Moons of Mars, 111  
 Checkout after launch from Earth, 450  
 Chemical propulsion system, 284, 288–291,  
 298*t*  
 Chemical thrusters, 289, 384–385  
 ChipSats, 143, 181  
 Circular polarization, 344  
 Circular restricted three-body problem  
 (CR3BP) model, 46–47  
 Cislunar CubeSats, 101–106  
 Clusters, 127  
 CM. *See* Center of mass (CM)  
 Coefficient of thermal expansion (CTE),  
 420–421  
 Cold case, 309–312, 312*t*  
 Collinear libration points (CLPs), 48–50  
 Collision avoidance, 408–410  
 CommCubeSat1, 287–288  
 chemical propulsion system sizing, 291,  
 292*t*  
 electric propulsion system sizing, 292, 294*t*  
 Commercial ground station networks,  
 361–363  
 Commercial launch vehicles, 431  
 Commercial off the shelf (COTS), 253, 283  
 Commercial rotors, 346–347  
 Commissioning, in-space operations,  
 372–376  
 human factors, 374–375  
 life signs, 372–373



- mission assurance, 375–376
  - real-time telemetry, 373–374
  - Common Core Booster (CCB), 437–438
  - Communication licenses, 394
  - Communications, 354–356, 405
    - gain and pointing requirements, 354–356
    - impact at system level, 356
    - link availability and rain fade, 356
  - Communication system layer (CSL), 240
  - Community, 53
  - Company ground station networks, 360
  - Computer on modules (COMS), 217
  - Conceptual design options, 305–306
  - Conductive tethers, 384–385
  - Conic section, 38, 38*t*
  - Constellations, 63, 63*t*, 125–127, 125*f*, 353–354
    - control problems and solutions, 136–138, 138*t*
    - service provision stage, 353
    - technology demonstration stage, 353
  - Consultative Committee for Space Data Systems (CCSDS), 212
  - Contact execution, 350
  - Coordinating Committee for Space Data Standards (CCSDS) protocols, 96
  - Copper strip, 314
  - Cosine loss, 290
  - Coverage analysis, 224–225
  - CubeSat Acceptance Checklist (CAC), 423
  - CubeSat Asteroid Encounters for Science and Reconnaissance (CAESAR), 111
  - CubeSat developer, 415, 421
  - CubeSat energy translation, deployer to, 420–421
    - dynamic energy translation, 421
    - thermal translation, 420–421
  - CubeSat IR atmospheric sounder (CIRAS), 70
  - CubeSats, 382, 386, 391–392, 395, 431
    - active debris removal (ADR) missions, 386
    - calibration targets for ground based sensors, 385–386
    - collision avoidance, 408–410
    - deployment tip-off rates, 421
    - design, 407
    - detect orbital debris, 385–386
    - export control, 405–406
    - landscape, 431
    - launch vehicles for, 433, 433*f*
    - licensing and mission authorization, 393–395
    - measurement and remediation platforms for orbital debris, 385–386
    - missions, 398, 419–420, 431, 440–441
    - on-orbit technology demonstration, 385
    - orbital debris requirements, 384–385
    - orbit lifetime, 383
    - propulsion figures of merit, 285, 286*t*
    - propulsion systems, 288, 288*t*
    - radio-frequency registration, 395–401
      - frequency allocation, 396–397
      - frequency assignment notification, 398–401
      - radio amateur frequencies, 396
      - recording procedure, 398–401
    - reentry casualty risk, 410–411
    - safety and cleanliness, 403–405
    - into space, 416
    - space debris mitigation, 407–408
    - space law, 392–393
    - space object registration, 401–403
    - third-party liability and insurance, 411–412
  - CubeSat UV Experiment (CUVE), 110
  - CubeSat vibration test, 424
  - CubeSat X-ray telescope (CubeX), 111
  - Cupid's Arrow, 110
  - Current and planned CubeSat instruments, 68–79
  - Cyclone Global Navigation Satellite System (CyGNSS) mission, 75
- D**
- Data rates, 95
  - Data volume, 222
  - DCS. *See* Distributed CubeSat systems (DCS)
  - Deep space explorers, 61–62
  - Deep-space maneuvers (DSMs), 46
  - Deep space navigation, 96–98
  - Deep Space Network (DSN), 97
  - Deep Space Station, 61
  - Deployer chassis, 418–419
  - Deployer door, 418
  - Deployer pusher plate, 418
  - Deployers, 415
    - anatomy of, 416–419
    - deployer chassis, 418–419
    - deployer door, 418

- Deployers (*Continued*)
- deployer pusher plate, 418
  - deployer springs, 418
  - deployment mechanism, 419
  - rails and tabs, 419
  - characteristics, 420–422
    - CubeSat deployment tip-off rates, 421
    - CubeSat energy translation, 420–421
    - rail and tab considerations, 422
    - CubeSat to testing, 423–424
    - survey, 415–416
  - Deployer springs, 418
  - Deployment mechanism, 419
  - Deployment orbit parameters, 448
  - Design and verification process, 172–175
    - Sistema Espacial para Realização de Pesquisa e Experimentos com Nanossatélites (SERPENS) mission V-diagram, 173*f*
    - structural analysis, 174–175
    - structural design, 172–174
  - Design validation, 306
  - Deterministic data collection, 201
  - Direct energy transfer (DET), 189–190
  - Distributed CubeSat systems (DCS)
    - clusters, 127
    - constellations, 125–127, 125*f*
    - distributed spacecraft design strategies, 123
    - enabling technologies, 130, 130–131*t*
    - federated CubeSat system concepts, 129
    - fractionated CubeSat system concepts, 128–129
    - series, 127
    - state of the art, 124–129, 125*t*
    - swarms, 128
    - trains, 128
  - Distributed space systems (DSS)
    - definition, 135
    - features, 135–136
  - Disturbance torques, 294
  - Dnepr, 434–435, 435*t*
  - Documentation, 369–371
  - Doppler effect, 346, 348
  - Double Asteroid Redirection Test (DART), 112–113
  - Down-converters, 345
  - Drag sails, 384–385
  - DustCube mission, 253
  - Dynamical systems theory, 50
  - Dynamic energy translation, 421
  - Dynamic loads, 174
  - Dynamics testing, 424
- E**
- Earth observation (EO), 55
  - Earth orbit, 62, 62*t*
  - Earth-orbiting objects, 379–380, 381*f*
  - Earth radiation budget radiometers, 71
  - Earth remote sensing, 55
  - EcAMSat, 155–156, 156*f*
  - Eccentricity, 38
  - Economic motivations, 405
  - Edge computing, 217
  - Electrical interfaces, 426–427
  - Electric power system (EPS), 167–168, 221
    - block components, 185, 186*f*
    - conditioning and distribution, 190–191, 191*t*
    - generation
      - chemical energy, 186
      - nuclear energy, 186
      - photovoltaic effect, 186
      - solar cells, 186–187, 187–188*t*
      - sources, 186
    - power budget, 185
      - average orbital power required, 195, 195*t*
      - energy and solar array, 195, 196*t*
      - orbital parameters, 193, 193*t*
      - primary parameters calculation, 192, 193*t*
      - primary power parameters calculation, 193, 194–195*t*
      - requirements, 192, 192*t*
      - solar array effective area, 194–195, 194*t*
      - solar array power margin and battery capacity, 196, 196–197*t*
      - solar arrays, 192
      - storage, 188–190, 189*t*
  - Electric propulsion (EP) system, 284, 291–293, 298*t*
  - Electronics, 169
  - Energy generation, 312, 313*f*
  - Entrepreneurship, 53
  - Environmental legislation, 403
  - EPS. *See* Electric power system (EPS)
  - Equivalent Isotropic Radiated Power (EIRP), 95

- Europa Clipper, 106–107, 108*f*  
 European Space Agency (ESA)  
   Hera mission to Didymos, 112–113, 113*f*  
   Lunar Volatile and Mineralogy Mapping  
     Orbiter (Lunar VMMO), 114–115,  
     115*f*  
   LUMIO, 114, 114*f*  
   LUNar CubeSats for Exploration, 113–114  
   miniaturized asteroid remote geophysical  
     observer, 115–116, 116*f*  
 ExoCube, 55  
 Exploration Mission-1 (EM-1), 158  
 Export Administration Regulations (EAR),  
   406  
 Export control, 405–406  
 Extended Kalman filter (EKF), 255  
 External heat load on radiator, 309
- F**
- Falcon 9, 436–437, 438*t*  
 Falcon Heavy, 436–437  
 Far-out concept, 91*f*  
 Fault protection, 375  
 FDF. *See* Flight Dynamics Facilities (FDF)  
 Feasible, 68–69  
 Federal Communications Commission, 395  
 Federated CubeSat system concepts, 129  
 Field programmable gate arrays (FPGAs),  
   217  
 First TubeSat missions, 180  
 Flight computer (FCPU), 216–217  
 Flight Dynamics Facilities (FDF), 342–343  
 Flight radio, 366–367  
 Flight software (FSW). *See* Onboard  
   software (OBSW)  
 Flight temperature sensors, 316  
 Flywheel, 273–274  
 Fractionated CubeSat system concepts,  
   128–129  
 Fragmentation debris, 379–380  
 Frequency, 223  
 Frequency allocation, 396–397  
 Frequency assignment notification, 398–401  
   administrations and API/B publication, 398  
   advance publication information, 401–403  
   submission of notification, 400  
 Frequency registration timeline, 398, 399*f*  
 Frequent launch opportunities, 450  
 Full time operations, 376  
 Fundamental space biology, 147
- G**
- Gain and pointing requirements, 354–356  
 Gamma ray bursts (GRBs), 77  
 GeneSat-1, 150–152, 151*f*  
 GEO. *See* Geosynchronous orbit (GEO)  
 Geostationary missions, 308  
 Geosynchronous orbit (GEO), 303–304, 304*t*,  
   379  
 Ghost track, 373  
 Glass fiber-reinforced polymer (GFRP), 346  
 Global Educational Network for Satellite  
   Operations (GENSO), 357–359, 358*f*  
 Global Navigation Satellite Systems (GNSS),  
   253  
 Graphical processing units (GPUs), 217  
 Gravitational mass, 37  
 Gravitational-wave Ultraviolet Counterpart  
   Imager (GUCl) Mission, 77  
 Gravity assist (GA) maneuvers, 44–46  
 Gravity-gradient attitude control system  
   (GGACS), 270–271  
 Gravity instruments, 71  
 Ground hardware, 366–367  
 Ground segment, 341, 353–356  
   architecture, 342–343, 342*f*  
   communication requirements, 354–356  
     gain and pointing requirements, 354–356  
     impact at system level, 356  
     link availability and rain fade, 356  
   functionality, 341–342  
   ground station (*see* Ground station)  
   operation, 349–350  
     automation, 350  
     contact execution, 350  
     planning, 349  
     software, 347–349, 348*f*  
       ground station control, 349  
       mission control software, 347–348  
       orbit propagation, 348  
 Ground station, 221–222, 343–347, 346*t*  
   block diagram, 343, 343*f*  
   compatibility tests, 366–367  
   considerations for high frequency bands,  
     347  
   control, 342, 349

Ground station (*Continued*)  
 mechanical elements and pointing,  
 346–347  
 redundancy, 367  
 RF hardware  
 antennas, 344  
 down-converters, 345  
 filtering, 344  
 low-noise amplifiers, 345  
 transceivers, modems, and software-  
 defined radios, 345–346  
 Ground station facilities (GSF), 342–343  
 Ground stations networks (GSNs), 356–359,  
 358*f*  
 commercial ground station networks,  
 361–363  
 company ground station networks, 360  
 university ground station networks,  
 357–359  
 GSF. *See* Ground station facilities (GSF)  
 GSNs. *See* Ground stations networks (GSNs)

## H

Hardware abstraction layer (HAL), 240  
 Hardware for satellite temperature control,  
 312–317  
 heat pipes, 314  
 highly conductive strips, 314  
 multilayer insulation (MLI), 313–314  
 phase change material (PCM), 315  
 telemetry and commands, 315–317  
 thermal surface finishes, 314–315  
 Heat balance, 309  
 estimation, 307–312  
 Heat pipes, 314  
 Helical antennas, 344  
 Heliophysics, in instruments, 76–79, 76*f*, 78*f*  
 High Earth orbits (HEO), 59, 308  
 Higher-frequency bands, 346–347  
 High-gain antennas (HGA), 229  
 Highly conductive strips, 314  
 High operating temperature barrier IR  
 detector (HOT-BIRD), 70  
 High-resolution optical imagers, 71  
 Hot case, 309–311, 311*t*  
 Human error, 374–375  
 Human factors, in-space operations, 374–375  
 healthy team, healthy spacecraft, 374

human error, 374–375  
 operation user interface, 374  
 Humanitarian Satellite Constellation  
 (HUMSAT), 247  
 Hyperspectral imagers, 71–72  
 Hypervisors, 217

## I

IARU. *See* International Amateur Radio  
 Union (IARU)  
 Icy Moons, 112  
 Imaging microwave radars, 71  
 Imaging multispectral radiometers (Vis/  
 SWIR), 71–72  
 Inertial mass, 37  
 Infeasible, 68–69  
 Infostellar's ground station network  
 architecture, 360, 362*f*  
 Inhibit switches, 427  
 In-orbit demonstration, 60  
 In-space operations, 365  
 commissioning, 372–376  
 human factors, 374–375  
 life signs, 372–373  
 mission assurance, 375–376  
 real-time telemetry, 373–374  
 first contact, 371–372  
 operational models, 365–366  
 preparation, 366–371  
 operational readiness tests, 367–369  
 preflight testing and design for  
 operations, 366–367  
 tools, procedures, and documentation,  
 369–371  
 prime mission and beyond  
 rebalancing risk posture, 376–377  
 streamlining and optimizing operations,  
 376  
 training new operators, 377  
 scope, 365  
 Instrument data processing unit (IDPU), 216  
 Instruments, 67–68  
 for astronomy and heliophysics, 76–79,  
 76*f*, 78*f*  
 current and planned, 68–79  
 future, 79–80  
 remote sensing instruments, 69–75, 70*f*,  
 72–73*f*, 75*f*

- Integrated propulsion system (IPS), 288  
 Integration and test (I&T), 366  
 Interagency Space Debris Coordination  
     Committee (IADC), 379, 384  
 International Amateur Radio Union (IARU),  
     396  
 International space law, 411  
 International Space Station (ISS), 57–58, 404,  
     436–437, 442, 445  
 International Telecommunication Union  
     (ITU), 395  
 International Traffic in Arms Regulation  
     (ITAR), 406  
 Interorbital Systems (IOS), 180  
 Interplanetary missions, 308  
     attitude determination and control systems,  
         85–86  
     ballistic capture, 47–48  
     challenges  
         deep space navigation, 96–98  
         overcoming telecommunication, 94–96  
         propulsion systems, 93–94, 94*t*  
         radiation tolerance and mission duration,  
         93  
     destinations, 86–89  
     developers, 90–92  
     differences, 89  
     dynamical effects, 44  
 European Space Agency (ESA)  
     Hera mission to Didymos, 112–113, 113*f*  
     LUMIO, 114, 114*f*  
     Lunar CubeSats for Exploration,  
         113–114  
     M-ARGO mission, 115–116, 116*f*  
     VMMO, 114–115, 115*f*  
     future opportunities, 116–118  
     gravity assist (GA) maneuvers, 44–46  
     high-altitude fly-bys, 46–47  
     historical perspective, 90–92  
     hyperbolic manifolds, 48–50, 49*f*  
     implementation  
         asteroids, mars, 106–107  
         asteroids, mars and outer Solar System,  
         106–107  
         Cislunar CubeSats, 101–106  
         MarCO A and B, 98–101, 99*f*  
         Venus, 108–109, 109*f*  
 ITN, 48–50  
 low Earth orbit, 85–86  
 Lunar IceCube trajectory, 48*f*  
 NASA  
     Asteroids, 111  
     Earth's Moon, 111  
     Icy Moons and outer planets, 112  
     Mars, 111–112  
     Solar System exploration missions, 109  
     Venus, 110  
     propulsion systems, 85–86  
     resonant encounters, 46  
     telecommunication systems, 85–86  
     weak stability boundaries, 47–48  
 Interplanetary NanoSpacecraft Pathfinder In a  
     Relevant Environment (INSPIRE)  
     mission, 92  
 Interplanetary Superhighway (IPS), 50  
 Interplanetary Transport Network (ITN), 50  
 IPS. *See* Integrated propulsion system (IPS)  
 IR detectors, 307  
 Iris radio, 230–233  
 ISS. *See* International Space Station (ISS)  
 ITAR. *See* International Traffic in Arms  
     Regulation (ITAR)  
 ITU. *See* International Telecommunication  
     Union (ITU)
- J**
- Japan Aerospace and Exploration Agency  
     (JAXA), 445  
 Japanese Experiment Module (JEM), 445,  
     446*f*  
 Japanese Small Satellite Orbital Deployer (J-  
     SSOD), 445–448, 446*f*, 451*t*  
 JEM Airlock, 445–446, 446*f*  
 JEM Remote Manipulator System  
     (JEMRMS), 445  
 Jet Propulsion Laboratory, 103–104, 106,  
     230–233  
 Joint Army, Navy, NASA, Air Force  
     (JANNAF), 285  
 Jupiter Magnetospheric boundary Explorer  
     (JUMPER), 112
- K**
- Ka band, 354–356, 355*f*  
 Ka-band radiocommunication, 347  
 Kalman filter (KF), 255, 276–277  
 Keplerian elements, 39–40, 40*f*

Kepler laws, 36  
 Kongsberg Satellite Services (KSAT), 361–363  
 Kosmotras ISC, 435

**L**

LandMapper-BC satellites, 71–72  
 Launch authority, 393, 404  
 Launch delays, 428  
 Launching state, 401–402  
 Launch Service Program (LSP), 384  
 Launch service provider, 423  
 Launch services requirements and documentation, 419  
 Launch vehicle  
   families, 432–440  
     Antares/Minotaur, 433–434  
     Atlas V, 437–438, 439*t*  
     Dnepr, 434–435, 435*t*  
     Falcon 9, 436–437, 438*t*  
     micro satellite launchers, 438–440  
     Polar Satellite Launch Vehicle (PSLV), 435, 436*t*  
     Soyuz-2, 436, 437*t*  
   integrator, 423  
   selection, 440–443  
 Law of inertia, 37  
 Layered architecture, 239  
 Least mean squares (LMS) algorithm, 275  
 Left-hand circular polarization (LHCP), 344  
 LEO. *See* Low Earth orbit (LEO)  
 LHCP. *See* Left-hand circular polarization (LHCP)  
 Liability Convention, 392–393  
 Libration orbit, 295–297  
 Libration points, 49*f*  
 Licensed operators, 411–412  
 Licensing and mission authorization, 393–395  
 Lidars, 73–74  
 Life sign of the spacecraft, 372–373  
 Lightning imagers, 74  
 Linear energy transfer (LET) spectrometer, 158  
 Linear polarization, 344  
 Linear voltage regulators (LVR), 190  
 Link availability and rain fade, 356  
 LNA. *See* Low noise amplifier (LNA)

Loads, 174–175  
 LOS. *See* Loss of signal (LOS)  
 Loss of signal (LOS), 349  
 Low Earth orbit (LEO), 59, 61, 67, 85–86, 308, 379–380  
 Low-inclination missions, 442  
 Low noise amplifier (LNA), 230–233, 345  
 LSP. *See* Launch Service Program (LSP)  
 Lume-1, 247  
 LUMIO, 114, 114*f*  
 LUNar CubeSats for Exploration (LUCE), 113–114  
 Lunar Flashlight (LF), 73–74, 103–104, 105*f*  
 LunaH-Map. *See* Lunar Polar Hydrogen Mapper (LunaH-Map)  
 Lunar IceCube (L-IC), 102–103, 104*f* trajectory, 48*f*  
 Lunar mission, 294–295, 441  
 Lunar Polar Hydrogen Mapper (LunaH-Map), 105–106  
 Lunar Prospector (LP), 105  
 Lunar Reconnaissance Orbiter (LRO), 95–96, 105

**M**

Machine learning (ML) techniques, 218  
 Magnetometers, 68  
 Maneuver accelerations, 291–292  
 Mars, 88  
 Mars Cube One (MarCO), 85, 92, 98–100, 99*f*  
 MarsDROP MicroProbe concept, 107*f*  
 Mars Reconnaissance Orbiter (MRO), 95  
 Massachusetts Institute of Technology (MIT), 95–96  
 Maximum energy production, 312  
 MCS. *See* Mission control software (MCS)  
 Mechanical elements and pointing, 346–347  
 Mechanical envelope requirements, 426  
 Medium Earth orbits (MEO), 59  
 Medium-gain antennas (MGA), 229  
 Megaconstellations, 63, 63*t*  
 Mercury ground station networks, 357–359, 357*f*  
 Microbiology research, 147  
   EcAMSat, 155–156, 156*f*  
   GeneSat-1, 150–152, 151*f*  
   PharmaSat, 152–154, 153*f*  
   SporeSat, 154–155, 155*f*

- Microgravity, 152
- Micro launch vehicles, 431, 439, 439*t*
- Micro satellite launchers, 438–440
- Miniaturized Asteroid Remote Geophysical Observer (M-ARGO), 115–116, 116*f*
- Miniaturized Electron and Proton Telescope (MERiT), 78
- Minotaur-C, 434
- Mission assurance during operations, 375–376
- Mission authorization, licensing and, 393–395
- Mission control software (MCS), 347–349
- Mission operations assurance manager (MOAM), 375
- Mission Operations Centre (MOC), 342–343
- Mission operations facilities (MOF), 342–343
- Mission operation system (MOS), 363
- Mission planning, 342
- MLI. *See* Multilayer insulation (MLI)
- MOAM. *See* Mission operations assurance manager (MOAM)
- MOC. *See* Mission Operations Centre (MOC)
- Modems, 345–346
- Moderate launch environment, 450
- MOF. *See* Mission operations facilities (MOF)
- Monitoring of spectrum, 346
- Moon, 88
- Moon Agreement, 392–393
- Morehead Rome Femtosatellite Orbital Deployer (MRFOD), 178–179
- Morehead State University Space Science Center, 72, 76, 97, 97*f*, 102–103, 111
- Multilayer insulation (MLI), 313–314  
blankets, 313
- Multiple angle/polarimeter, 74
- Multipurpose Experiment Platform (MPEP), 445–446, 446*f*
- N**
- NanoRacks CubeSat Deployer (NRCSD), 445, 451–452, 452*f*
- Nanoracks ISS CubeSat deployer, 416, 417*f*
- Nanosat Database, 137
- Nanosatellites formation flight control, 138–143  
relative navigation problems, 138–139
- restricted propulsion and control  
approaches without propellant, 139–141  
swarm, 141–143, 141*t*
- NANOSWARM, 68–69, 117
- National Aeronautics and Space Administration (NASA) Ames' Small Satellites Technology Division, 59
- National Aeronautics and Space Administration (NASA) Interplanetary CubeSat missions  
Asteroids, 111  
Earth's Moon, 111  
Icy Moons and outer planets, 112  
Mars, 111–112  
Solar System exploration missions, 109  
Venus, 110
- National Aeronautics and Space Administration (NASA) Ames Research Center, 148–150
- NASA Deep Space Network (DSN), 158–159
- NASA Goddard Spaceflight Center, 102–103, 111
- NASA's Innovative Advanced Concepts (NIAC), 86
- NASA Jet Propulsion Laboratory, 103–104, 106, 230–233
- National Academies of Sciences, 67–68
- National space laws, 411–412
- Navigation, 405
- Near-Earth Asteroids (NEAs), 106, 107*f*
- Networked ground stations. *See* Ground stations networks (GSNs)
- Neutron spectrometers, 75
- New manufacturing technologies, 175–176
- NewSpace, 53–54
- Nonbinding multilateral instruments, 405
- Nonmilitary CubeSat, 406
- North American Aerospace Defense Command (NORAD), 252
- O**
- OBDH. *See* On-board data handling system (OBDH)
- Oberth effect, 44–45
- Ocean color spectrometer, 74
- ODE. *See* Ordinary differential equation (ODE)

- On-board data handling system (OBDH), 199
  - component, 200–209
    - generation, 201–202
    - processing, 207–209, 207–208*f*
    - storage, 202–203
    - time, 206–207, 206*f*
    - transferring, 203–206
  - design process
    - CPU utilization, 210
    - data budget, 209, 209*t*
    - processing budget, 210, 210*t*
    - storage budget, 211
    - transfer budget, 211
  - emerging trends, 217–218
  - functions, 199
  - processors, 199
  - radio aurora explorer (RAX) mission, 212–217, 213–215*f*
  - sinks, 199
  - sources, 199
  - transfer, 199
- Onboard software (OBSW)
  - development process, 242–247
    - analysis, 245
    - design, 245
    - implementation, 245–246
    - planning, 244–245
    - testing, 246–247
  - layers, 240*f*
  - missions, 247–249
  - responsibilities, 238
  - software architecture, 238–242
    - application layer components, 241*f*
    - automation services, 242
    - BIOS, 240
    - command and data handling services, 241
    - CSL, 240
    - HAL, 240
    - layers, 239–240, 240*f*
    - OSAL, 240
    - patterns, 239
    - payload services, 242
    - platform services, 242
    - RTOS, 240
    - service bus, 242
    - telemetry services, 242
- Open Space Network (OSN), 180
- Operating system abstraction layer (OSAL), 240
- Operating systems (OS), 217
- Operational limit, 303
- Operational models for CubeSats, 365
- Operational readiness tests (ORTs), 367–369
  - operational scenarios, 368
  - setup and design of, 368
  - timing of, 369
- Operational scenarios, ORTs, 368
- Operation planning, 349
- Operations staffing, 374
- Operation team, 365–366, 376
- Operation user interface, 374
- Operators interface, 342
- Optical Communications and Sensor Demonstration (OCSD), 95–96
- Optical elements, 307
- Optical solar reflector (OSR), 314–315
- Optical telecommunications, 233–234
- Orbit, 222
- Orbital analysis, 289, 292
- Orbital debris, 379
  - CubeSats as measurement and remediation platforms for, 385–386
  - mission, 383–385
  - mitigation requirements, 384
  - sources of, 379–380
- Orbital determination and control system (ODSC), 169
- Orbital edge computing, 217
- Orbital elements. *See* Keplerian elements
- Orbital lifetime, 407–408
- Orbit determination and control system (ODCS)
  - algorithms, 253–256
    - batch estimation, 254–255
    - filtering, 255–256
  - commands implementation, 258–259
  - ground-based technologies, 252
  - maneuvers, 257–258, 258–259*f*
  - onboard technologies, 253
  - technologies, 257
- Orbit estimation, 252
- Orbit lifetime
  - CubeSat's, 383
  - reduction methods, 384–385, 384*t*
- Orbit propagation, 348
- Ordinary differential equation (ODE), 383



- Organism/Organic Exposure to Orbital Stresses (*O/OREOS*), 150
- ORTs. *See* Operational readiness tests (ORTs)
- OSR. *See* Optical solar reflector (OSR)
- Outer Space Treaty, 393
- Outgassing, 404
- P**
- Parabolic reflectors, 344
- Parallel processing, 217
- Partial list of available dispensers, 416, 417*t*
- Particle filter (PF), 255
- Passivation, 407
- Pass recordings, 375, 377
- Payload interface module (PIM), 214–216
- Payload into space, 416
- Payload Orbital Delivery System (PODS), 78–79
- PCM. *See* Phase change material (PCM)
- Peak power tracker (PPT), 189–190
- Peer-to-peer (P2P) network architecture, 357–359
- Perturbations, in astrodynamics, 36, 41–44
  - anomalies of the earth gravitational field, 42–43
  - atmospheric drag, 43–44
  - perturbed orbits, 41
- PharmaSat, 150, 152–154, 153*f*
- Phase change material (PCM), 309–310, 315
- PICASSO, 69
- Piggyback satellites, 450
- Pipe-and-Filter, 239
- Planetary mission (mars), 297
- Planetary nuclear spectroscopy, 105–106
- Planetary Science Deep Space SmallSat Studies (PSDS3) program, 109
- Planetary Systems Corp., 418*f*
- Planet Labs ground segment, 360, 361*f*
- Plasma Electric Propulsion, 102–103
- PocketQubeSat
  - deployer, 178–179, 179*f*
  - external dimensions, 178
  - Maiden mission, 179–180
- Polarization diversity, 344
- Polar Radiant Energy in the Far-InfraRed Experiment (PREFIRE), 71
- Polar Satellite Launch Vehicle (PSLV), 435, 436*t*
- Polycyclic aromatic hydrocarbon (PAH), 156–157
- Polyether ether ketone (PEEK), 177
- Polymer tethers, 384–385
- Position and time system (PTS), 216
- Power budget, 185
  - average orbital power required, 195, 195*t*
  - energy and solar array, 195, 196*t*
  - orbital parameters, 193, 193*t*
  - primary parameters calculation, 192, 193*t*
  - primary power parameters calculation, 193, 194–195*t*
  - requirements, 192, 192*t*
  - solar array effective area, 194–195, 194*t*
  - solar array power margin and battery capacity, 196, 196–197*t*
  - solar arrays, 192
- Power generation
  - chemical energy, 186
  - nuclear energy, 186
  - photovoltaic effect, 186
  - solar cells, 186–187, 187–188*t*
  - sources, 186
- Power subsystem, 366–367
- Power supply, 428
- Preflight testing, 366–367, 372
  - ground station redundancy, 367
  - real-time telemetry, 367
  - recommended testing, 366–367
- Preliminary analysis, 305–306
- Preliminary orbit determination, 252
- Preparation, in-space operations, 366–371
  - design for operations, 366–367
  - operational readiness tests, 367–369
  - preflight testing and design for operations, 366–367
  - tools, procedures, and documentation, 369–371
- Prime mission and beyond
  - rebalancing risk posture, 376–377
  - streamlining and optimizing operations, 376
  - training new operators, 377
- Propellant system
  - density, 291
  - mass, 291
  - tanks, 407

- Propellant system (*Continued*)  
 types, 285–287, 287*t*  
 volume, 291
- Propulsion system, 257, 284  
 assessment, 285–287  
 for interplanetary CubeSats, 93–94, 94*t*  
 mission applications, 294–299  
   libration orbit, 295–297  
   lunar mission, 294–295  
   planetary mission (mars), 297  
 sizing, 287–293  
   chemical propulsion system, 288–291  
   electric propulsion system, 291–293
- PSLV. *See* Polar Satellite Launch Vehicle (PSLV)
- PSLV-C37, 431, 432*f*
- Push-to-talk (PTT), 345
- Pyrotechnics, 403
- Q**
- Quasi-static loads, 175
- R**
- Radar altimeters, 74–75
- Radiation portion, 306–307
- Radiator heat balance, 309
- Radiators, 307  
 sizing, 303
- Radio, 229–233, 231–232*t*  
 failures, 366
- Radio amateur frequencies, 396
- Radio aurora explorer (RAX) mission, 212–217, 213–215*f*
- Radiofrequency (RF)  
 filters, 344  
 hardware, ground station  
   antennas, 344  
   down-converters, 345  
   filtering, 344  
   low-noise amplifiers, 345  
 registration, 395–401  
   frequency allocation, 396–397  
   frequency assignment notification, 398–401  
   radio amateur frequencies, 396  
   recording procedure, 398–401  
   spectrum, 395
- Radio interferometer, 78–79
- Radio signals from satellites, 395
- Rails and tabs, 419, 422
- RainCube, 70–71, 70*f*
- RaioSat project, 74
- Random and static loads, 421
- RAVAN, 71
- Radiator temperature, 311–312
- Real-time operating system (RTOS), 240
- Real-time telemetry, 367, 373–374
- Rebalancing risk posture, 376–377
- Recordings  
 and archiving, 375  
 of operator errors, 375
- Reentry casualty risk, 410–411
- Reentry for mitigation, 382
- Reentry license, 394
- Remote-sensing capacities, 405
- Remote sensing instruments  
 atmospheric chemistry instruments, 69  
 atmospheric temperature and humidity sounders, 70  
 cloud profile and rain radars, 70–71, 70*f*  
 earth radiation budget radiometers, 71  
 flown on GSFC's 3U IceCube mission, 73  
 gravity instruments, 71  
 high-resolution optical imagers, 71  
 hyperspectral imagers, 71–72  
 imaging microwave radars, 71  
 imaging multispectral radiometers, 71–72
- Light Detection and Ranging (LIDAR), 73–74
- Lightning imagers, 74
- Lunar IceCube's BIRCHES IR spectrometer, 72*f*
- multiple angle/polarimeter, 74
- neutron spectrometers, 75, 75*f*
- ocean color spectrometer, 74
- precision orbit, 74
- PREFIRE, 71
- radar altimeters, 74–75
- scatterometers, 75
- 3D winds, 70
- TROPICS, 73, 73*f*
- Remote-sensing license, 394
- RemoveDebris, 451–452, 452*f*
- Requirements and main characteristics, of  
 structural system, 166–172  
 external requirements, 170–172  
 by the launch vehicle, 170–171

- by the space deployer, 171–172
  - by the space environment, 171
  - internal requirements, 167–170
    - by the bus, 167–170
    - by the mission, 167
  - Rescue Agreement, 392–393
  - Resonance hopping theory, 47–48
  - Reviewing documentation, 377
  - Right ascension of ascending node (RAAN), 136–137
  - Right-hand circular polarization (RHCP), 344
- S**
- Safety and cleanliness, 403–405
  - Satellite Install Cases, 447
  - Satellites, 424–425
    - constellations, 135
    - deployed into space, 448, 448*f*
    - developers, 445
    - monitoring after deployment, 448, 449*f*
    - in orbit, 393
  - SatNet architecture, 357–359, 359*f*
  - Saturn Ring-Diver CubeSat mission concept, 116–117, 117*f*
  - S band, 354, 355*f*
  - Scatterometers, 75
  - Science/payload team, 366
  - SDR. *See* Software-defined radios (SDR)
  - SE-L1 Lissajous orbit, 295–296, 296*f*
  - Semilatus rectum of the orbit, 38
  - Separation springs, 427
  - Series, 127
  - Serpens, 247
  - Service-oriented architecture, 239
  - Service provision stage, 353
  - Short gamma ray bursts (sGRBs), 77
  - Silicon photomultipliers (SiPMs), 77
  - Single satellite missions, 353
  - Size, weight, and power (SWaP), 67
  - Small Innovative Missions for Planetary Exploration (SIMPLEx) program, 91–92
  - Small Next-generation Atmospheric Probe (SNAP), 112
  - SmallSat, 67–68, 221–222, 441
  - SmallSat spacecraft/CubeSats, thermal control system for, 304–306
    - conceptual design, 305–306
    - design validation, 306
    - detailed analysis, 306
    - requirements, 305
  - Snow and Water Imaging Spectrometer (SWIS), 71–72
  - Software-defined radios (SDR), 345–346
  - Solar radiation pressure (SRP), 140, 273
  - Solar System exploration, 85, 87*f*
  - Solid-state power amplifier (SSPA), 230–233
  - Soyuz-2, 436, 437*t*
  - Space-borne experiments, 57–59, 60*t*
  - Spacecraft
    - acceleration, 289, 289*f*
    - vs.* computer, 304*f*
    - heat rejection, 303
    - passivation, 407
    - radio, 366
    - temperature, 311
    - thruster, 289, 290*f*
    - user guide, 371
  - Spacecraft OBDH systems, 200
  - Space debris. *See* Orbital debris
  - Space debris mitigation, 407–408
  - Space Environment Survivability of Life Organisms (SESLO), 156–157, 157*f*
  - Space Environment Viability of Organics (SEVO), 156–157
  - Space exploration, 392–393
  - Spacefaring nations, 385–386
  - Space Launch System (SLS), 102–103
  - Space law, 392–393
  - Space object registration, 401–403
  - Space radiocommunications, 343–344
  - Space Science Center, 59
  - Space treaties, 392–393
  - SpaceX, 436–437, 441
  - Spinning, 272–273
  - Spinsat, 451–452, 453*f*
  - Spin stabilization, 272–273, 278
  - SporeSat, 150, 154–155, 155*f*
  - Sprites, 143
  - SS-520 launcher, 441–442
  - Standardization, 53
  - Star-Planet Activity Research CubeSat (SPARCS) spacecraft, 76–77
  - Static loads, 174
  - Strategic Knowledge Gaps (SKGs), 103–104
  - Streamlining and optimizing operations, 376

- Structural system, 165
    - design and verification process, 172–175
      - SERPENS mission V-diagram, 173*f*
      - structural analysis, 174–175
      - structural design, 172–174
    - materials and manufacturing technologies, 175
    - requirements and main characteristics, 166–172
      - external requirements, 170–172
      - internal requirements, 167–170
    - testing phase, 177–178
  - Sun, 88
  - SunRISE, 78–79, 78*f*
  - Sun-synchronous orbit, 40–41, 41*f*
  - Survival limit, 303
  - Swarm, 128, 141–143, 141*t*
  - Swedish Space Corporation (SSC), 361–363
  - Switching voltage regulators (SVR), 190
  - Synthetic aperture radar (SAR), 68–69, 71
  - Synthetic complete (SC) growth medium, 158–159
- T**
- Tancredo 1 TubeSat, 180
  - Technology, 53
    - demonstration stage, 353–354
    - demonstrators, 59–60, 61*t*
  - Technology readiness levels (TRLs), 285
  - Telecommunication, for interplanetary
    - CubeSats, 94–96
  - Telecommunication, tracking and command (TT&C), 168
    - components
      - antennas, 229, 229–230*t*
      - radios, 229–233, 231–232*t*
    - design
      - component selection, 228
      - coverage analysis, 224–225
      - design finalization, 228
      - Downlink data flow, 223*f*
      - iterative process for designing, 223*f*
      - link analysis, 225
      - requirements, 222–224
    - key factors, 221–222
    - optical communication systems, 233–234
  - Telemetry and commands, 315–317
  - Temperature sensors, 315–316
  - Temporal Experiment for Storms and Tropical Systems-Demonstration (TEMPEST-D) mission, 72–73
  - Terminal node controller (TNC), 345
  - Tethers, 384–385
  - Thermal control system, 303, 312
    - hardware for satellite temperature control, 312–317
      - heat pipes, 314
      - highly conductive strips, 314
      - multilayer insulation (MLI), 313–314
      - phase change material (PCM), 315
      - telemetry and commands, 315–317
      - thermal surface finishes, 314–315
    - heat balance estimation, 307–312
      - example, 310–312
    - management challenges, 306–307
    - power, 312
    - for SmallSat spacecraft/CubeSats, 304–306
      - conceptual design, 305–306
      - design validation, 306
      - detailed analysis, 306
      - requirements, 305
      - workflow of design, 305, 305*f*
  - Thermal resistance of fasteners, 314
  - Thermal surface finishes, 314–315
  - Thermal system, 170
  - Thermal translation, 420–421
  - Thermal vacuum testing (TVAC testing), 306, 316, 316*t*, 424, 425*f*
  - ThinSat, 181
  - Third-party liability and insurance, 411–412
  - Three-axis stabilization, 278–279
  - 3D winds, 70
  - Thruster manufacturing, 289
  - Thrust vector, 290
  - Timing of ORTs, 369
  - Total ionizing dose (TID) tolerance, 93
  - Tracking, telemetry, and command (TT&C), 341, 345
  - Traditional satellite missions
    - astronomy, 56–57, 58*t*
    - earth remote sensing, 55, 56*t*
    - telecommunications, 55–56, 57*t*
  - Trainee operators, 375
  - Training new operators, 377
  - Trains, 128
  - Trajectory, 294
  - Transceiver, 228

- TRIAD algorithm, 274–275  
TRLs. *See* Technology readiness levels (TRLs)  
TROPICS, 73, 73*f*  
TT&C. *See* Telecommunication, tracking and command (TT&C)  
TubeSat, 180  
    Interorbital System, 180  
Two-body problem, 37–38  
Two-line elements (TLE), 252
- U**
- 1U CubeSat, 137, 193–194, 354  
2U CubeSat, 354  
3U CubeSat, 60, 73–74, 77, 98–99, 137, 143, 274, 303–304, 304*t*, 384, 448–450  
6U CubeSat, 70–75, 78–79, 90–91, 94, 99–100, 102–104, 106, 158, 310  
3U HARP CubeSat mission, 74  
UHF bands, 344, 354–356  
UniSat-5, 179  
United Nations Committee on the Peaceful Uses of Outer Space (UNCOPUOS), 392  
University ground station networks, 357–359  
University of Rome (La Sapienza), 178–179  
University of Toronto’s CanX-4&5 mission, 74  
UN Office on Outer Space Affairs (UNOOSA), 392  
Unscented Kalman filter (UKF), 255  
US Combined Space Operations Center (CSPOC), 409  
User segment access, 342  
US Space Surveillance Network (USSSN), 379
- UV degradation, 171  
UV/Vis/IR telescopes, 76
- V**
- Vacuum conditions, 171  
Vandenberg AFB, 438  
Vehicle to dispenser integration, 427–428  
Venting, CubeSat, 428  
Venus, 87–88, 108–109, 109*f*  
Vertically aligned carbon nanotubes (VACNTs), 71  
VHF bands, 344, 354–356  
Vibration test, 450  
Virginia Commercial Space Flight Authority (VCSFA), 181  
Virginia Space and program, 181  
Visible spectral imager for occultation and nightglow (VISION) instrument, 69  
V $\infty$  leveraging maneuver (VILM), 46  
VMMO, 114–115, 115*f*  
Voice-operated exchange (VOX) switch, 345
- W**
- Wallops Flight Facility (WFF), 434  
Waste heat, 306  
Weak stability boundary (WSB), 47–48  
WFF. *See* Wallops Flight Facility (WFF)  
Windform XT 2.0, 176–177, 176*f*  
WREN, 179–180
- X**
- Xatcobeo, 247  
X band, 354, 355*f*
- Y**
- Yagi-Uda antennas, 346